LIGHT REFLECTANCE OF CONCRETE

Angharad Sweeney, BA BAI

A thesis submitted for the degree of Doctor of Philosophy to the University of Dublin, Trinity College.

2013

Abstract

A phenomenon known as the urban heat island (UHI) effect occurs where the air and surface temperatures are hotter than in their rural surroundings (Gartland, 2008). The UHI effect is a direct result of urbanisation whereby the urban fabric comprises mainly of roofs, paved surfaces and less vegetation (Santamouris, 2007). The mitigation of UHI can be achieved by increasing the albedo of surfaces and by planting trees in urban areas (Rosenfeld et al., 1995, Boriboonsomsin and Reza, 2007). Albedo, or solar reflectance, is defined as the ratio of the reflected solar radiation to the incident solar radiation at the surface, over all wavelengths of solar irradiation (Taha et al., 1988, Li et al., 2013). It is a dimensionless fraction and is measured on a scale of 0 to 1, with 0 denoting a perfectly black surface and an albedo of 1 signifies a perfectly reflective white surface. The advantages of improving the albedo of surfaces include the reduced need for air conditioning thus reducing the consumption of energy, and mitigation of the urban heat island effect, as there is an increase in the amount of light reflected back into the universe. The amount of light reflected back induces a negative radiative forcing which can then be converted into equivalent reductions in CO_2. The most widely used material in construction is concrete, and the colour of concrete is principally determined by the colour of the cementitious material. A cement replacement known as ground-granulated blast furnace slag (GGBS) is lighter in colour than normal Portland cement (NPC). Its use as an NPC alternative in concrete at sufficiently high replacement rates results in a concrete that is lighter in colour, thus increasing its albedo.

There has been limited research conducted into the effect of concrete constituents on the albedo of concrete, therefore, the key parameters to be evaluated in this project were determined, namely the aggregate type, cement type, surface finish and age. A total of 96 small concrete specimens were fabricated comprising three different aggregate types, four concentration levels of the cement replacement GGBS, four different surface finishes to represent varying applications and a duplicate of each specimen.

An albedometer was tested to determine whether it could be used to measure the albedo of the small concrete specimens. It was concluded that it is an accurate device which can be used to measure the albedo of large surfaces with an unobstructed horizon, however, caution should be taken in relation to the time of day the reading is taken as the albedo is a maximum value in the morning and afternoon, but a minimum value in-between these times. The instrument could not be used to measure the albedo of small specimens as the lower sensor becomes very insensitive, therefore, this loss in sensitivity would not be acceptable in order to distinguish small differences in albedo between two surfaces. An alternative means of measurement was devised

using a lux meter to measure the reflection of visible light off the small specimens. This proved to be a very reliable and repeatable method of testing as it enabled small differences to be detected between the different specimens.

Thereafter, testing on the specimens was conducted using five principal test methods (namely a sphere spectrophotometer, lux meter, greyness scale, thermal imaging and thermocouple wire) to demonstrate to what degree an increase in GGBS replacement in concrete produces a brighter coloured concrete, with a corresponding reduction in temperature when exposed to solar radiation. Each of the methods demonstrate that there is a significant reduction in temperature/increase in colour between a specimen containing no GGBS and a specimen containing 70% GGBS. It was also concluded that the optimum substitution level of GGBS is 50% as excessive ageing of the 70% specimen was noted by each test method. The order of importance in terms of the influential parameters on the light reflectance of concrete is colour, surface finish, GGBS concentration, age and aggregate type, the latter being of little significance.

On a global scale, research has shown that increasing the albedo of urban roofs and paved surfaces will induce a negative radiative forcing on the earth equivalent to offsetting significant quantities of CO_2 emissions. Consequently, a case study was conducted in Trinity College Dublin and it was estimated that there is a surface area of approximately 33% ($54,434m^2$), where the surface reflectance could be increased. The potential emitted CO_2 which could be offset ranged between 1,040 and 5,620 tonnes for the campus.

Acknowledgements

It would not have been possible to write this doctoral thesis without the help and support of the people around me. In particular, I would like to thank my partner and best friend, Niall, for his continuous support and encouragement throughout the entire project. Your help, advice and good humour have seen me through these last four years. This thesis would not have been possible without the help, support and patience of my supervisor, Prof. Roger West, whose maddening attention to detail drove me to finally learn to punctuate, I hope! Your determination and willingness to help me at every stage was very much appreciated.

I would like to acknowledge the financial, academic and technical support of the University of Dublin, and its staff, particularly in the award of the departmental studentship which provided the necessary financial support for this research. However, the research would not have been possible to complete without the financial and technical support of Ecocem Ltd, for which I am truly grateful. The help and support from Peter Seymour, Ciara O' Connor, John Reddy and John Newall in particular, was an asset towards my work.

I would like to express my sincere thanks in particular to the technical staff in the Civil Engineering Department, namely Dr. Kevin Ryan, David McAuley, and Eoin Dunne. Your willingness to help me throughout my project was truly appreciated, as was your advice. Special thanks to my fellow postgraduate students in the Department of Civil Engineering and the staff of TrinityHaus, in particular Ornagh Higgins, whose contribution to my project was exceptional. I would also like to thank Adrian and Felipe for making an important input towards my project.

Finally, to my parents Adrian and Patricia, for their continuous support and encouragement throughout the past eight years of my education in Trinity College. I really appreciated those early morning and late night lifts to and from the bus more than you know. This thesis would not have been possible without you both. To my sisters Aedamar, Shonagh and Emilia, thank you so much for keeping me sane, especially for those last few months, those GNI's kept me going!

TABLE OF CONTENTS

Table of Figures

List of Tables

List of Appendices

Nomenclature

a = Albedo

Δa = Change in albedo

A = Area, m^2

a* = Red/green colour axis

A_{final} = Final albedo

$A_{initial}$ = Initial albedo

b* = Blue/ yellow colour axis

c = Specific heat, J/kg.K

c = Velocity

CO_2 = Carbon dioxide, t

d = Thickness/ depth

E = Energy radiated, W/m^2

E_i = Incoming solar irradiation, W/m^2

E_r = Reflected solar irradiation, W/m^2

E_{solar} = Irradiance, W/m^2

G_λ = Irradiation, W/m^2

$G_{\lambda, abs}$ = Irradiation absorbed, W/m^2

$G_{\lambda, ref}$ = Irradiation reflected, W/m^2

$G_{\lambda, tr}$ = Irradiation transmitted, W/m^2

h = Heat transfer coefficient, W/m^2K

h = Planck's constant (6.63×10^{-34} J.s)

H_0 = Null hypothesis

h_c = Convective coefficient, W/m^{2}K

I = Intensity

I = Solar flux, W/m^2

k = Boltzmann constant (1.38 x 10^{-23}J/molecule.K)

k = Thermal conductivity, W/mK

L* = Lightness (black and white axis)

m = Mass, kg

M = Momentum

n_i = sample size

P = Critical value for t-test

Q = Heat energy, J/kgK

q_c = Heat transfer rate by convection, W

q_r = Heat transfer rate by radiation, W

q_x = Heat transfer rate by conduction, W

S = Sensitivity, μV/W/m^2

t = T-test statistic

t = Time

T = Temperature, K

T_∞ = Absolute ambient temperature, K (radiation)

T_∞ = Temperature of fluid, K (convection)

T_a = Air temperature, K

T_{black} = Steady state temperature of black surface

T_c = Temperature on cold side, K

T_h = Temperature on hot side, K

T_{max} = Maximum temperature, °C

T_s = Temperature at surface, K

T_s = Temperature of surroundings, K

T_{sky} = Sky temperature, K

T_w = Temperature at surface, K

T_{white} = Steady state temperature of white surface

ΔT = Temperature change, K

$\Delta T/\Delta x$ = Temperature gradient

ΔTCO_2 = Earth's climate sensitivity to radiative forcing caused by CO_2, °C/(W/m^2)

U_{emf} = Output voltage, µV

$\bar{x}_i$ = sample mean

α = Absorption

α = Significance level of t-test

δ = Diffusivity, m^2/s

ε = Emissivity

θ = Angle of incidence/reflection

θ = Direction

λ = Wavelength, nm

μ = Mean or average

μ_λ = Energy density

ν = Frequency, Hz

ρ = Density, kg/m^3

ρ = Reflection

σ = Stefan Boltzmann constant (5.669 x 10^{-8}W/m^{2}K^{-4})

σ_i = Standard deviation

τ = Transmission

1 Introduction

1.1 Background

Warming of the climate system is unequivocal, as is now evident from observations of increases in global average air and ocean temperatures, widespread melting of snow and ice, and rising global average sea level. Changes in the atmospheric concentration of greenhouse gases (GHG's) and aerosols, land cover and solar radiation alter the energy balance of the climate system and are the drivers of climate change as they affect the absorption, scattering and emission of radiation within the atmosphere and at the earth's surface. The resulting positive or negative changes in energy balance due to these factors are expressed as radiative forcings and are used to compare warming or cooling influences on global climate (IPCC, 2007). Akbari et al. (2008b) state that using high solar reflective materials (materials which reflect much of the incoming solar radiation) in urban areas induces a negative radiative forcing on the earth which is equivalent to offsetting CO_2 emissions.

The global atmospheric concentration of carbon dioxide has increased significantly from a pre-industrial value of about 280ppm to 379ppm in 2005 (IPCC, 2007). Responding to concerns that had been recognised regarding increasing concentrations of GHG's in the early 1990's, more than 150 nations signed the United Nations Framework Convention on Climate Change at the earth's summit in Rio in 1992. However, this pledge was voluntary and non-binding, therefore, this was unsuccessful and, as a result, parties to the treaty established a binding protocol for developed nations which was ratified in Kyoto in 1997. The Kyoto Protocol is an international agreement which commits its parties by setting internationally binding emission reduction targets. 15 European Union member states (EU-15), which includes Ireland, are jointly responsible under the Kyoto Protocol's compliance mechanism, for fulfilling the commitment to reduce their collective emissions in the 2008-2012 period to 8% below the 1990 level. Ireland can comply with the first commitment period, however, the next important milestone is to achieve a reduction in emissions of 20% by 2020 (UNFCCC, 2013).

The European building sector is responsible for approximately 40% of the total primary energy consumption (Tommerup and Svendsen, 2006). In addition, the most significant factor contributing to CO_2 emissions from buildings is their use of electricity. In the developed world, buildings are responsible for approximately 70% of the electricity load (USGBC, 2013a). As a consequence of this fact, the need for more efficient building practice is vital. The development of Green buildings is one of the best strategies for meeting the challenge of climate change (USGBC, 2013a). LEED (Leadership in Energy and Environmental Design) is a green building rating system which has been developed by the United States Green Building Council

(USGBC) to assess the environmental performance of a building (USGBC, 2013b). The average LEED certified building uses 32% less electricity and saves approximately 350 tonnes CO_2 annually (USGBC, 2013a). Under the LEED rating system, two credits in a total of 100 available credits can be awarded which correspond directly to the heat island effect. The requirement for achieving these credits specifies that a surface attain a minimum solar reflectance index (SRI) value, which combines solar reflectance (albedo) and thermal emittance of a material into one measurement.

An urban heat island (UHI) occurs where the air and surface temperatures are hotter than in their rural surroundings (Gartland, 2008). The UHI effect is a direct result of urbanisation that creates urban fabric which comprises mainly of roofs, paved surfaces and less vegetation (Santamouris, 2007). Pavements and roofs typically constitute over 60% of urban surfaces (pavements approximately 40% and roofs 20-25%) (Akbari et al., 2008b). The mitigation of UHI can be achieved by increasing the albedo of surfaces and by planting trees in urban areas (Rosenfeld et al., 1995, Boriboonsomsin and Reza, 2007). Albedo, or solar reflectance, is defined as the ratio of the reflected solar radiation to the incident solar radiation at the surface, over all wavelengths of solar irradiation (Taha et al., 1988, Li et al., 2013). It is a dimensionless fraction and is measured on a scale of 0 to 1, with 0 denoting a perfectly black surface and an albedo of 1 signifies a perfectly reflective white surface. The albedo of an asphalt surface is typically between 0.05 (new) or 0.10 (aged) (Santamouris et al., 2011), therefore, absorbing much of the incoming solar radiation. On the other hand, the albedo of traditional concrete is between 0.35-0.40 (new) and 0.25-0.30 (aged) (Bretz et al., 1998), however, this value can be increased significantly through the use of brighter coloured concrete constituents.

The colour of concrete is principally determined by the colour of the cementitious material. As white Portland cement (WPC) is typically much more expensive than grey cement, a cement replacement known as ground-granulated blast furnace slag (GGBS) can instead be used as it is lighter in colour than normal Portland cement (NPC). GGBS is a waste product from the blast furnace production of iron from ore and its use as an NPC alternative in concrete at sufficiently high replacement rates results in a concrete that is lighter in colour, thus increasing its albedo. To date, research on the albedo effect has focused mainly on reflective coatings, however, there has been very little research conducted into methods of increasing the solar reflectance of concrete by altering the composition of the concrete through the use of GGBS. In addition, the choice of aggregate type and surface finish are also factors which may affect the resulting albedo of concrete.

Furthermore, the manufacture of Portland cement is responsible for 5% of anthropogenic CO_2 emissions worldwide. This is due to the sheer volume of cement produced which is approximately 3 billion tonnes per year (Racusin and McArleton, 2012). Therefore as GGBS is a waste material, and is significantly lighter in colour than NPC, it presents natural advantages over the use of Portland cement in terms of both improved albedo and reduced CO_2 emissions. Thus, the primary aims of the thesis are outlined hereafter.

1.2 Aims and objectives

This PhD thesis has set out to meet the following five principal objectives;

1. To investigate the present knowledge surrounding all relevant aspects of physics and engineering to understand the phenomenon of solar reflectivity.
2. To evaluate the sensitivity of an albedometer and determine whether it is possible to measure the albedo of small concrete specimens, thus calibrating the instrument.
3. To design a unique and reliable test method of measuring the light reflectance of individual concrete specimens.
4. To investigate the effect of concrete constituents such as aggregate type, GGBS content, surface finish and age on light reflectance and colour of concrete by utilising a number of instruments to measure either directly or indirectly, the effect of the key parameters on the light reflectance or colour of concrete, and as a consequence, compare the various test methods.
5. To conduct a case study at Trinity College Dublin to assess the possible areas where the albedo of surfaces could be improved, and following this, to calculate the possible emitted CO_2 which could be offset against existing values and compared to existing savings.

1.3 Scope of thesis

This PhD thesis comprises 9 individual chapters. The following is a brief outline of the contents of Chapters 2 to 9.

Chapter 2: Literature Review

This section provides a summary of the existing research conducted into albedo and its effect on the environment. The topics discussed in this chapter include the physics of light and its interaction with materials, solar radiation and the albedo effect. Published albedo values are included in addition to measurement of solar reflectance in accordance with American standards

(ASTM). The urban heat island (UHI) effect is discussed in detail, along with standards and ratings used in association with its mitigation. The influence of concrete constituents on concrete albedo is discussed, and consequently its potential in playing an important role in mitigating the UHI effect.

Chapter 3: Laboratory Methodology

Following on from Chapter 2, this section defines the parameters to be evaluated, the experimental design and the testing regime, which includes the direct and indirect test methods to measure light reflectance. The chapter discusses the experimental work carried out, from the initial phase of manufacturing concrete specimens to the final phase of positioning the specimens on site.

Chapter 4: Instrumentation and Experimental Methodology

This chapter focuses on the various instrumentation and devices which were employed for testing certain properties in relation to sunlight. The section includes the technical specification of each instrument. The calibration of certain instruments will also be outlined in this chapter.

Chapter 5: Light Reflectance Test Methods

The focus of this chapter is on two main light reflectance test methods, namely an albedometer and a lux meter. A number of sensitivity tests were conducted using the instrument, the results of which are outlined here. Furthermore, a number of site visits using the albedometer were conducted and these are detailed in this chapter also. Following the outcome of testing with the albedometer, a lux meter is discussed as a means of an alternative to using an albedometer. An innovative method of testing the light reflectance off a surface is presented, with sensitivity testing included also.

Chapter 6: Preliminary Testing

This section comprises of three preliminary tests performed with the aim of helping to answer some fundamental questions. One of these tests was to determine how different materials behave when subjected to a light source, and the remaining two tests monitor the temperature of a concrete specimen to evaluate how the environmental conditions (sunlight and air) effect the temperature of the concrete specimen, both internally and externally through the use of thermocouple wires.

Chapter 7: Data Analysis and Discussion

Based on the findings from the preliminary tests discussed in Chapter 6, the data acquired during the project is presented in this chapter. The direct test methods are presented first and comprise of the albedometer, sphere spectrophotometer, lux meter and greyness scale. Following this, the indirect test methods are presented and include thermal imaging and thermocouple data. Within each test method, the influence of key testing parameters such as surface finish type and cement concentration and their influence on light reflectance will be evaluated. Following analysis of the data in each individual section, a discussion of the test methods will be presented at the end of the chapter to provide an overall summary of the key findings from each test method.

Chapter 8: The Environmental Impact of Increasing Urban Albedo

Previous research conducted into the environmental impact of increasing urban albedo demonstrates that there is a potential to offset emitted CO_2 through the use of high solar reflective materials. These studies are discussed in this chapter and based on this research, a case study of Trinity College campus is carried out. The potential emitted CO_2 which could be offset as a result of increasing the albedo of roofs and pavements is calculated. This offset is then compared with the current CO_2 emissions from the campus.

Chapter 9: Conclusions and Recommendations

The key objectives of the research will be reiterated in this chapter and a review of objectives accomplished. The principal conclusions of the research will be summarised here and subsequently a number of recommendations for future research will also be presented.

2 Literature Review

2.1 The Physics of Light

The scientific study of light can be traced as far back as the 17th century, when Isaac Newton (1642-1727) regarded rays of light as streams of very small particles emitted from a source of light and travelling in a straight line (Tilley, 2004, Pedrotti et al., 2007). In 1801, the first clear demonstration of the wave theory of light was provided by Thomas Young (1773-1829), who showed that light exhibits interface behaviour. In 1873, James Clerk Maxwell (1831-1879) asserted that light was a form of high frequency electromagnetic wave. He created principles in his set of four Maxwell equations and as a result, from then on, light was viewed as a particular region of the electromagnetic (EM) spectrum of radiation. His theory predicted that light waves should have a speed of approximately $3x10^8$ m/s (Pedrotti et al., 2007, Al-Azzawi, 2007). In 1887, Heinrich Hertz (1857-1894) provided experimental confirmation of Maxwell's theory by producing and detecting EM waves as well as also defining the frequency of a light wave.

In 1900, Max Planck discovered that he was able to derive the correct blackbody radiation spectrum by making an assumption that atoms emitted light in discrete energy chunks rather than in a continuous matter. According to Planck, the energy E, of one of these energy packets, known as a photon, of EM radiation is proportional to the frequency, υ, of the EM wave as in Equation (2-1). Photons have zero rest mass and travel with a constant speed, c, in a vacuum. The energy of a photon is not a function of its speed but of its frequency.

$$E = h\upsilon \tag{2-1}$$

where h is Planck's constant = $6.63x10^{-34}$J.s and v is the frequency of light (Hz).

In 1924, Louis de Broglie published his hypothesis, stating that subatomic particles (i.e. particles smaller than an atom, namely protons, neutrons and electrons) are endowed with wave properties and that a particle with a momentum M had an associated wavelength as described in Equation (2-2).

$$\lambda = \frac{h}{M} \tag{2-2}$$

where h = Planck's constant.

2.1.1 The electromagnetic spectrum

The distribution of energy among the various wave components is called the spectrum of radiation. The various regions of the EM spectrum are referred to by a designated name such as ultraviolet radiation and radio waves, according to the differences in the way in which the regions are produced or detected. These various frequency ranges are illustrated in Fig. 2-1 in which the EM spectrum is displayed in terms of both frequency v and wavelength λ. These terms are related through the velocity, c, as defined in Equation (2-3).

$$c = \lambda v \tag{2-3}$$

The wavelengths of visible light were measured in the first decade of the 19th century and were found to be in the region of 4.0 x10^{-7}m to 7.5 x10^{-7}m (400nm to 750nm). This region is capable of producing a visual sensation in the human eye and is referred to as light. This visible region of the spectrum corresponds to the frequencies of EM radiation that predominate in the output of the sun (Pedrotti et al., 2007). The visible region is bounded by the invisible ultraviolet and infrared regions and these three regions together comprise the optical spectrum and accordingly are the main focus in the study of optics. For the purposes of this literature review, only three aspects of the electromagnetic spectrum will be discussed, namely infrared radiation, visible light and ultraviolet light. The other components of the EM spectrum are irrelevant to this particular study which concerns itself with sunlight.

2.1.1.1 Infrared (IR) Radiation

The infrared region (long-wavelength) of the EM spectrum lies adjacent to the low frequency end of the visible spectrum spanning the region from 770nm to 1mm (Wilson et al., 2007). It is sometimes referred to as 'heat rays' because water molecules readily absorb electromagnetic radiation at frequencies in the infrared wavelength region. As a result, the molecules heat up as their random thermal motion is increased, therefore heating up their surroundings. Infrared radiation is associated with maintaining the earth's temperature through the greenhouse gas effect where visible light is absorbed by the earth's surface which heats up and is reemitted as infrared radiation. This radiation is trapped by the greenhouse gases which are impenetrable to infrared radiation (Wilson et al., 2007). Infrared radiation accounts for approximately 57% of the sun's energy (Gartland, 2008).

2.1.1.2 Visible Light

Visible light has wavelengths in air in the range of approximately 400nm to 700nm and occupies a small portion of the electromagnetic spectrum. It is known as the visible spectrum and comprises different colours from violet (400nm) to red (750nm). This is the only radiation which activates the receptors on the retina of human eyes (Wilson et al., 2007). Visible light accounts for approximately 40% of the sun's energy (Gartland, 2008).

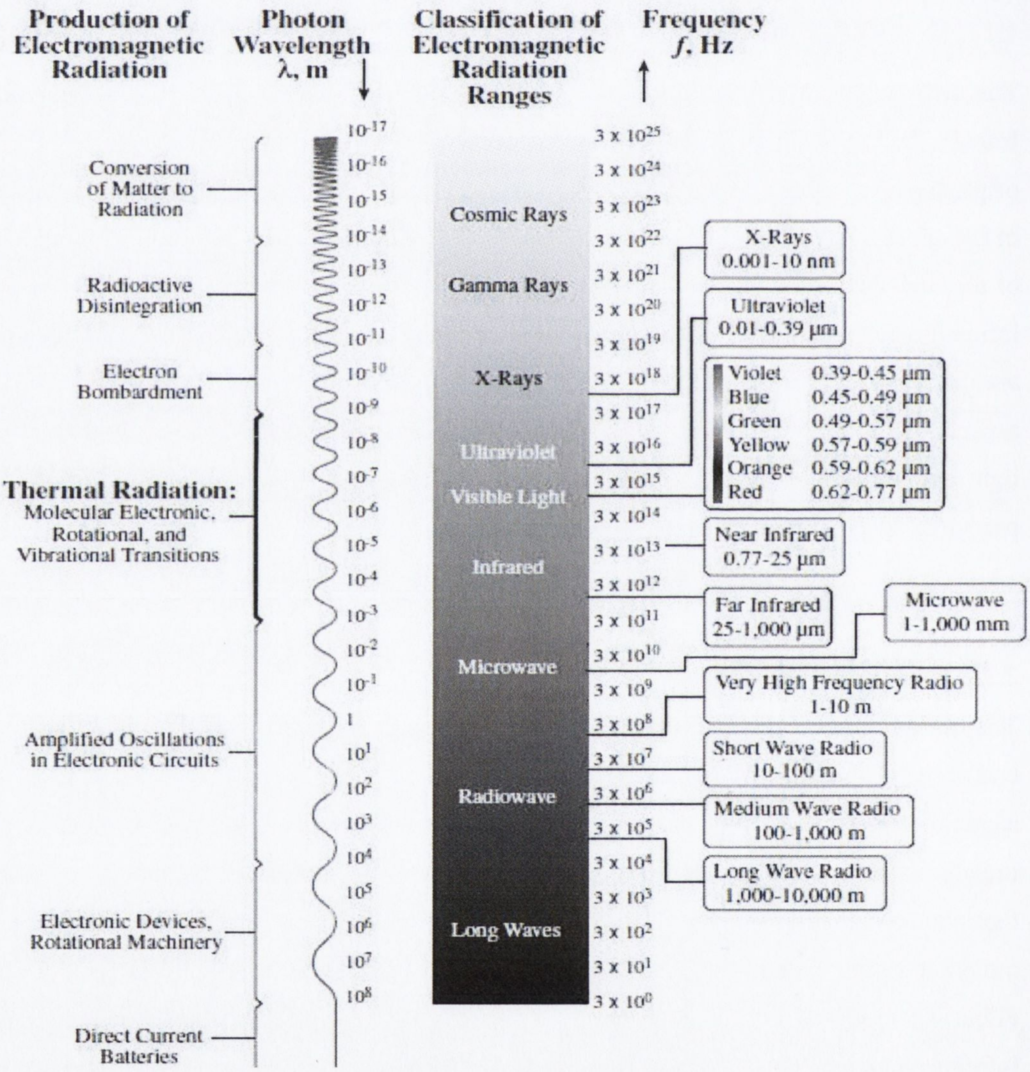

Fig. 2-1 Classification of electromagnetic waves based on the production, wavelength, common names, and frequency (Kaviany, 2011)

2.1.1.3 Ultraviolet (UV) Radiation

The sun's spectrum contains a small component of UV radiation (short-wavelength), which is located beyond the violet end of the visible light and ranges between 10nm to 380nm in the EM spectrum. It is sometimes subdivided into UV-A (380-315nm), UV-B (315-280nm) and UV-C (280-10nm). The sun emits significant amounts of EM radiation in all three of these bands, however, due to absorption in the ozone layer of the earth's atmosphere, most of the UV radiation (99%) which reaches the surface is in the UV-A band (Pedrotti et al., 2007). Ultraviolet radiation is harmful to skin and can cause skin cancer. It is mostly absorbed by the ozone layer in the atmosphere at an altitude of 30-50km and also by ordinary glass. The ultraviolet region accounts for approximately 3% of the sun's energy (Gartland, 2008).

2.1.2 Energy transfer

Heat can be transferred between a system and its environment in three distinct ways; conduction, convection and radiation. The main focus will be on conduction and radiation, however, convection will also be discussed.

2.1.2.1 Conduction

Conduction results from molecular interactions within an object. Molecules at a high temperature region in an object vibrate around their equilibrium position with greater amplitude than normal. This greater vibration causes the molecules to collide with their nearest neighbours, causing them to vibrate more. As a result, these molecules interact with their nearest neighbours passing on this energy as kinetic energy of vibration, thus transferring their energy to the molecules with less energy in a cooler part of the object. The net result of the vibrations is a transfer of thermal energy through a solid. The energy is therefore conductively transferred from a higher temperature region to a lower temperature region resulting in a reduction in the temperature difference. In general, a solid is a better conductor than a liquid or a gas because its molecules are very closely packed, meaning that the energy transfer between the molecules is faster (Ghoshdastidar, 2004).

The rate equation for conduction is given by Fourier's law of heat conduction, as displayed in Equation (2-4) (Holman, 2010, Ghoshdastidar, 2004).

$$q_x = -kA\frac{\Delta T}{\Delta x} \tag{2-4}$$

where q_x is the heat transfer rate (W), k, is the thermal conductivity of the material (W/mK), A is the surface area (m^2) and $\Delta T/\Delta x$ is the temperature gradient in the direction of the heat flow. The minus sign is present so that q is positive. It is measured in units of W/mK, and essentially indicates how fast heat will flow in a given material (see Fig. 2-2).

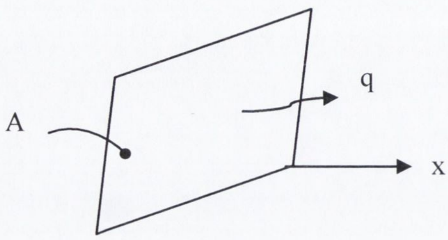

Fig. 2-2 Conduction in the x-direction, normal to area A (Ghoshdastidar, 2004)

By observing a slab of material, the amount of thermal energy conducted through the solid can be determined (see Fig. 2-3). A slab of material of cross sectional area A and thickness, d, is subjected to a high temperature T_h on the hot side and a colder temperature T_c on the other side (Nolan, 2012). It has been found experimentally that the thermal energy conducted through this slab is directly proportional to the following;

1. The area A of the slab. The larger the area, the more thermal energy transmitted
2. The time t, the longer the period of time, the more thermal energy transmitted
3. The temperature difference between the faces of the slab. If there is a large temperature difference, a large amount of thermal energy flows

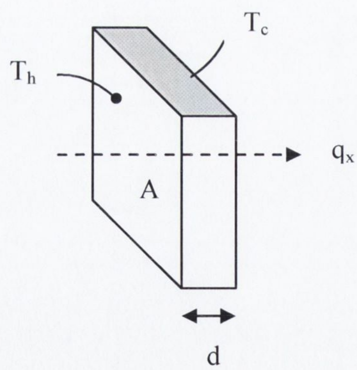

Fig. 2-3 Heat conduction through a slab (Nolan, 2012)

The ratio $(T_h - T_c)/d$ is the temperature gradient $\Delta T/\Delta x$. The thermal energy transmitted is inversely proportional to the thickness of the slab. The thicker the slab, the greater the distance the energy must travel through i.e. a thick slab implies a small amount of energy transfer and a thin slab implies a larger amount of energy transfer

Similarly to Equation (2-4), the amount of thermal energy transferred by conduction is displayed in Equation (2-5).

$$q_x = \frac{kA(T_h - T_c)t}{d} \tag{2-5}$$

Thermal conductivity, k, is a measure of the rate at which heat is transferred through a material. Some typical values are given in Table 2-1. The thermal conductivity of concrete is small, therefore only a small amount of thermal energy will flow through the material, and it is therefore a poor conductor, or a good insulator. A typical value for concrete ranges between approximately 0.4 and 1.6, with general concrete having a value of 1.3 (Nolan, 2012).

Table 2-1 Typical thermal conductivity values (Wilson et al., 2007)

Material	Thermal conductivity (W/mK)
Aluminium	240
Iron/Steel	46
Concrete	**1.3**
Wood (oak)	0.15

2.1.2.2 *Convection*

Convection is a process whereby thermal energy is transferred between a solid and a fluid flowing past it (Ghoshdastidar, 2004). If the fluid motion in the process is induced by an external means such as wind, the process is called forced convection. In order to express the overall effect of convection, Newton's law of cooling is used, where a solid surface is cooled by the fluid, thus:

$$q_c = hA(T_s - T_\infty) \tag{2-6}$$

where q_c is the rate of heat flow by convection (W), h is the heat transfer coefficient (W/m^2K), (T_s-T_∞) is the temperature potential difference for heat flow away from the surface (K) where T_s is the surface temperature and T_∞ represents the fluid temperature, and A is the surface area (m^2).

The process of convection from a surface is displayed in Fig. 2-4. The convection heat transfer coefficient, h, depends on many factors such as the space, time, geometry, orientation of the solid surface and flow conditions (Ghoshdastidar, 2004). Typical values of h for forced convection involving gases and liquids are 25-250W/m^2K and 50-20,000W/m^2K respectively.

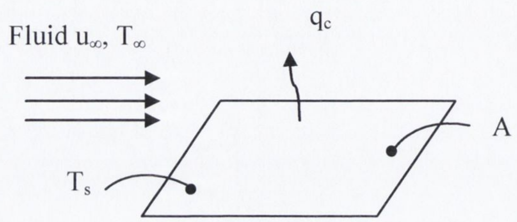

Fig. 2-4 Convection from surface area A at T_s to cool flowing fluid at T_s (Ghoshdastidar, 2004)

2.1.2.3 Radiation

The method of transfer by which an object and its environment exchange energy as heat via EM waves, is referred to as thermal radiation (Wilson et al., 2007). Thermal radiation refers to the EM radiation emitted by a body, as a result of its temperature, and is generally detected by heat or light (Al-Azzawi, 2007). These EM emissions are due to the molecular electronic (energy associated with the molecule's electrons), rotational (rotation of the whole molecule), and vibrational (vibration of chemical bonds within the molecule) energy transitions of the matter (Kaviany, 2011). Thermal radiation has significant energy in the wavelength range of 2 x 10^{-7} to 10^{-3}m which comprises of the visible range, infrared range and a small portion of the ultraviolet range (Kaviany, 2011). However, for low to moderate temperature applications, thermal radiation is dominated by the infrared wavelengths and by molecular rotational and vibrational transitions (Kaviany, 2011).

By considering the thermal radiation of a gas, the principles of quantum-statistical thermodynamics can be applied to derive an equation for the energy density of radiation per unit volume and per unit wavelength, u_k, as in Equation (2-7)):

$$u_\lambda = \frac{8\pi hc\lambda^{-5}}{e^{hc/\lambda kT} - 1} \tag{2-7}$$

where k is Boltzmann's constant = 1.38x10^{-23}J/molecule.K, h is Planck's constant = 6.63x10^{-34} J.s as previously, and T is the temperature (K) (Holman, 2010, Al-Azzawi, 2007).

When the energy density, which is defined as the energy radiated from a surface per unit time and per unit area, is integrated over all wavelengths, the total energy emitted is proportional to the absolute temperature to the fourth power, which is known as the Stefan-Boltzmann law as in Equation (2-8):

$$E_b = \sigma T^4 \tag{2-8}$$

where E_b is the energy radiated in W/m^2, T is the temperature (K) and σ is the Stefan-Boltzmann constant = $5.669 \times 10^{-8} W/m^2K^4$.

The subscript b in the equation denotes that it is radiation from a blackbody. It is referred to as blackbody radiation because materials which obey this law appear black to the eye as they do not reflect any visible radiation (Holman, 2010). The total energy radiated by a surface increases rapidly with temperature. By observing the spectrum of blackbody radiation at different temperatures, also known as Planck's distribution (see Fig. 2-5), the energy is found to lie within the infrared regions of the spectrum, where wavelengths are longer than visible light.

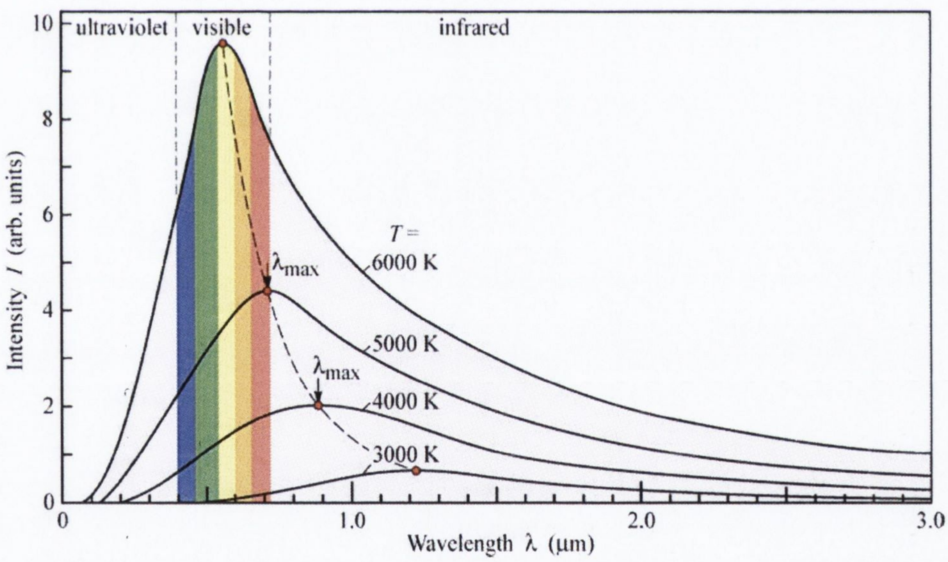

Fig. 2-5 Spectral intensity distribution of Planck's black-body radiation as a function of wavelength for different temperatures (Van der Pol, 2012)

The wavelength of peak emission λ_{peak} (nm) decreases as temperature (T) increases, and is inversely proportional to the temperature in Kelvin. This is known as Wien's displacement law (Equation (2-9)) where

$$\lambda_{peak} T = 2.898X10^{-3} mK \tag{2-9}$$

The radiation heat loss from a hot surface to the cool air can be described by Equation (2-10) and this process is displayed in Fig. 2-6.

$$q_r = \sigma \varepsilon A({T_s}^4 - {T_\infty}^4) \tag{2-10}$$

where q_r is the rate of heat flow by radiation (W), ε is the emissivity of the surface (=1 for a blackbody, < 1 for a non-black body), σ is the Stefan-Boltzmann constant as previously, A is the surface area (m^2), T_s is the absolute surface temperature (K), and T_∞ is the absolute ambient temperature (K).

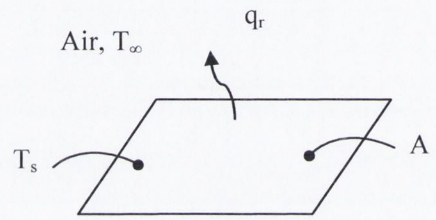

Fig. 2-6 Radiation heat loss from a hot surface at Ts to cool air at T∞ (Ghoshdastidar, 2004)

The three processes of heat transfer (conduction, convection and radiation) are summarised in Fig. 2-7, where T_s is the temperature of the surroundings, T_w is the surface temperature, and T_∞ is the fluid temperature.

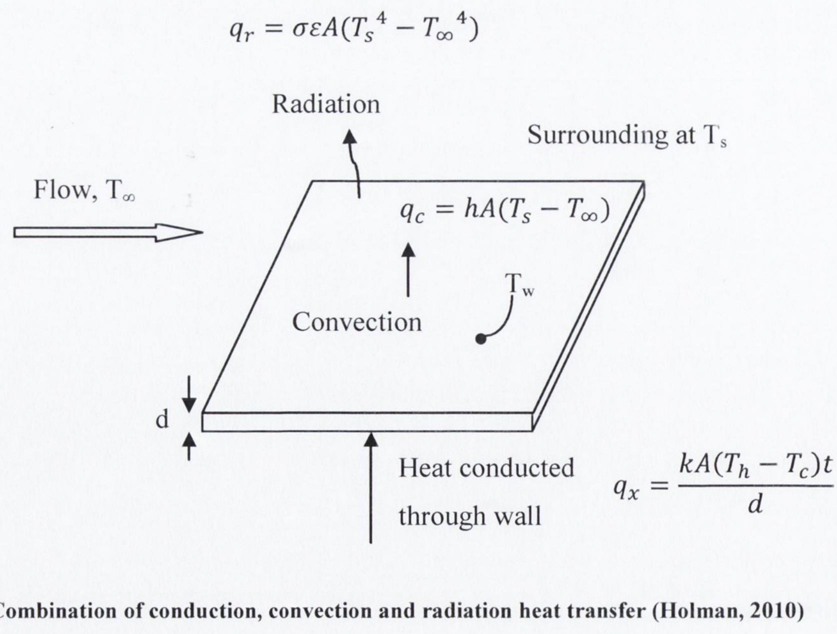

Fig. 2-7 Combination of conduction, convection and radiation heat transfer (Holman, 2010)

2.1.2.4 *Surface emissivity*

The emissivity of a surface, ε, is defined as the total radiation emitted (E) divided by the total radiation that would be emitted by a blackbody (E_b) at the same temperature (see Equation (2-11)).

$$\epsilon = \frac{E}{E_b} \tag{2-11}$$

so that:

$$\epsilon = \alpha \tag{2-12}$$

as the ratio of the emissive power of a body to the emissive power of a blackbody at the same temperature is equal to the absorptivity of the body (α). Equation (2-12) is known as Kirchhoff's identity.

A real body (or real surface), such as concrete, will emit less radiation than ideal black surfaces as measured by the emissivity value. The emissivity of a surface is always between zero and unity (Newton, 1990). A blackbody is characterised by the following (Bergman et al., 2011):

1. A blackbody absorbs all incident radiation, regardless of wavelength and direction.
2. For a prescribed temperature and wavelength, no surface can emit more energy than a blackbody.
3. Although the radiation emitted by a blackbody is a function of wavelength and temperature, it is independent of direction. That is, the blackbody is a diffuse emitter.

The spectral radiation emitted by a real surface differs somewhat from Planck's distribution (see Fig. 2-5). Also, the directional distribution may be other than diffuse (see Fig. 2-8).

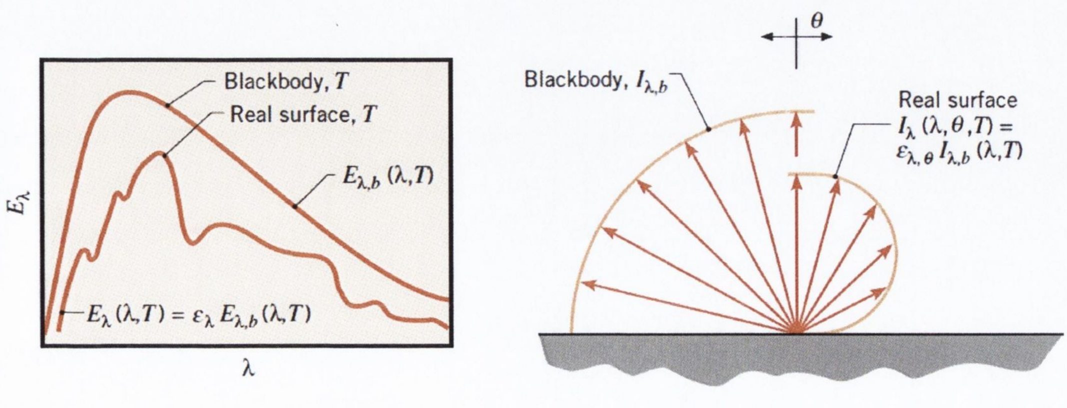

Fig. 2-8 Comparison of blackbody and real surface emission: spectral distribution (left) and directional distribution (right), where I is defined as the intensity and θ the direction (Bergman et al., 2011)

2.1.3 Absorption, reflection and transmission from real surfaces

The total irradiation on a surface, G (W/m^2), encompasses all spectral components and when it is incident upon a medium, depending on whether the surface is semi-transparent (such as glass) or opaque (such as concrete), this radiation may be absorbed, reflected and transmitted. For a radiation balance on a medium, it follows that:

$$G_\lambda = G_{\lambda,ref} + G_{\lambda,abs} + G_{\lambda,tr} \tag{2-13}$$

Where the medium is opaque, such as concrete, $G_{\lambda,tr}$ will equal zero and the remaining absorption and reflection processes are treated as surface phenomena i.e. they are controlled by processes occurring within a fraction of a micrometer from the irradiated surface. It is therefore appropriate to refer to irradiation being absorbed and reflected by the surface, with the relative magnitudes of $G_{\lambda,abs}$ and $G_{\lambda,ref}$ dependant on the wavelength (λ) and the nature of the surface material. There is no net affect of reflection on the medium, however, absorption has the effect of increasing the internal thermal energy of the medium (Bergman et al., 2011), that is light is converted into heat and the materials temperature rises. The processes of radiation incident upon a medium can be seen in Fig. 2-9.

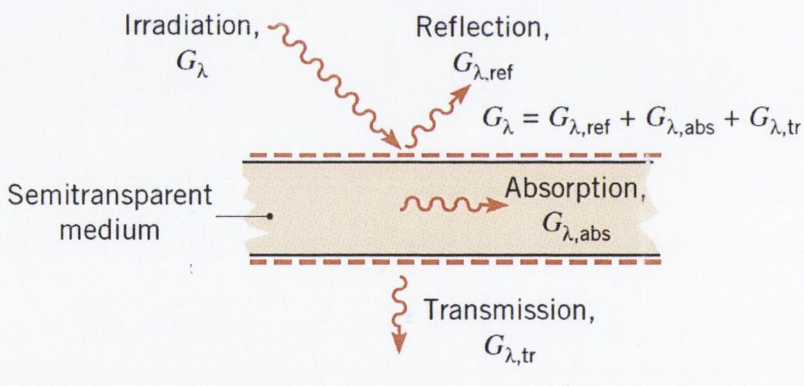

Fig. 2-9 Spectral absorption, reflection and transmission processes (Bergman et al., 2011)

In most solids and liquids, radiation emitted from interior molecules is strongly absorbed by adjoining molecules. Accordingly, radiation that is emitted from a solid or a liquid originates from molecules that are within a distance of approximately 1 μm from the exposed surface and for this reason, emission from a solid or a liquid into an adjoining gas can be viewed as a surface phenomenon (Bergman et al., 2011).

Surface absorption and reflection are responsible for the perception of colour. Colour is due to selective reflection and absorption of the visible portion of irradiation that is incident from the sun or an artificial source of light. A surface appears "black" if it absorbs all incident visible radiation, and it is "white" if it reflects this radiation. However, for a given irradiation, the "colour" of a surface may not indicate its overall capacity as an absorber or reflector, since much of the irradiation may be in the IR region. A "white" surface such as snow, for example, is highly reflective to visible radiation but strongly absorbs IR radiation, thereby approximating blackbody behavior at long wavelengths. The following subsections focus on the absorption, reflection and transmission processes. However, it is important to note that these properties depend on the surface material and finish, surface temperature, and the wavelength and direction of the incident radiation.

2.1.3.1 Absorption

The radiation incident on a solid surface is referred to as irradiation and when photons interact with the electronic or crystal structure of a material, absorption may occur whereby photons give up their energy to the material (Askeland and Phule, 2006). The total absorption, α, is defined as the fraction of the total irradiation absorbed by a surface:

$$\alpha = \frac{G_{abs}}{G} \tag{2-14}$$

The absorptivity depends on the spectral distribution of the incident radiation, as well as the directional distribution and the nature of the absorbing surface. Electrons in matter occupy energy levels called orbits. Fig. 2-10 displays both absorption and emission of a photon by an atom. If a photon is incident on the electron in the atom, the photon gives up its energy to the electron which, having increased in energy, moves to a higher level (away from the nucleus).

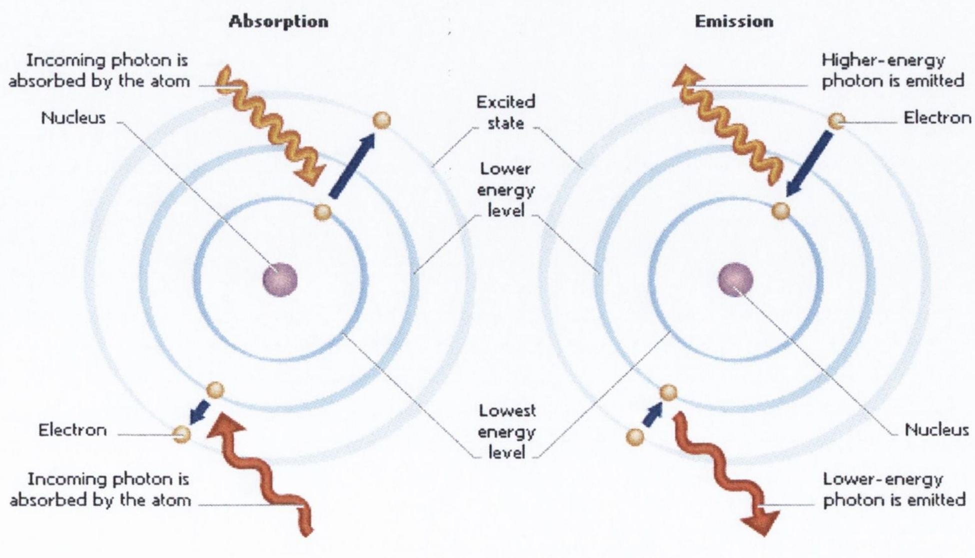

Fig. 2-10 An electron in an atom absorbing and emitting a photon (Simmonds, 2012)

Similarly, the electron in the upper level moves to the lower level by giving up energy by emitting light (Beeson and Mayer, 2008). The energy of a photon is equal to the difference between energy levels (Newton, 1990). For light of a frequency v, the energy of a photon, E, is given by Equation (2-1).

2.1.3.2 Reflection

Reflection is a property that determines the fraction of the incident radiation reflected by a surface. It is dependant on the direction of the incident radiation and the direction of the reflected radiation. Reflection is the process of incident radiation being redirected away from the surface, with no effect on the medium i.e. when radiation is incident on a medium, photons may give up their energy but photons of identical energy are immediately emitted by the material (Askeland and Phule, 2006). The total reflection, ρ, is defined as the fraction of the total irradiation reflected by a surface:

$$\rho = \frac{G_{ref}}{G} \tag{2-15}$$

Two types of reflection occur when radiation strikes a surface. When a ray of solar light is reflected at an interface dividing two optical media (a material through which EM waves propagate), the angle of the incoming light ray on a surface is described as the angle of incidence (θ_1) and this angle is measured relative to a line perpendicular to the reflecting surface which is known as the normal. The angle of the reflecting ray is described by the angle of reflection (θ_2) also measured from the normal (see Fig. 2-11) . The angle of incidence is equal to the angle of reflection and this is known as the law of reflection as displayed in Equation (2-16).

$$\theta_1 = \theta_2 \tag{2-16}$$

When the incident rays, which are parallel to each other, strike a perfectly smooth and flat reflecting surface, the corresponding reflected rays are also parallel to each other. This is called specular or regular reflection. If the surface is rough, however, the reflected rays are no longer parallel due to the irregular nature of the surface. This type of reflection is called diffuse or irregular reflection (see Fig. 2-11). The law of reflection still applies to each individual ray impacting on a surface inclined at θ_r to the normal to that surface (Kingslake and Thompson, 2011).

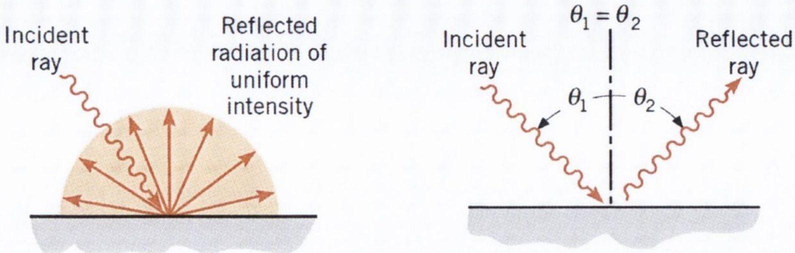

Fig. 2-11 Reflection of light: diffuse (left) and specular (right) reflection (Bergman et al., 2011)

2.1.3.3 *Transmission*

Transmission refers to radiation passing through a medium, and occurs when a layer of water or a glass plate is irradiated by the sun or artificial lighting. When transmission occurs, the photons do not interact with the electronic structure of the material (Askeland and Phule, 2006). Instead, the wave travels from one transport medium into another, causing refraction to occur. Refraction is defined as a change in direction of a wave at the surface boundary (Wilson et al., 2007). The change of direction is due to the fact that light travels at different speeds in different media. The refraction of light, as it enters one medium from another, is described by Snell's Law. The total transmission, τ, is defined as the fraction of the total irradiation transmitted by a surface:

$$\tau = \frac{G_{tr}}{G} \quad \textbf{(2-17)}$$

However, as concrete is an opaque material, this particular property is irrelevant to this study.

2.1.3.4 *Summary*

Reflectivity may be defined as the fraction of the irradiation that is reflected, absorptivity as the fraction of the irradiation that is absorbed, and transmissivity as the fraction of the irradiation that is transmitted (Bergman et al., 2011). As all of the irradiation must be reflected, absorbed, or transmitted, it follows that:

$$\rho_\lambda + \alpha_\lambda + \tau_\lambda = 1 \quad \textbf{(2-18)}$$

A medium that experiences no transmission ($\tau_\lambda = 0$) is opaque, in which case:

$$\rho_\lambda + \alpha_\lambda = 1 \quad \textbf{(2-19)}$$

A summary of the key surface radiation properties are displayed in Fig. 2-12. Surface radiation consists of emission, absorption, reflection and transmission. As concrete is an opaque material, the transmission component can be disregarded. Emission from a surface is temperature, wavelength and direction dependant in all cases for a real body such as concrete. Similarly, absorption and reflection are dependent on many factors such as temperature, wavelength, direction and angle.

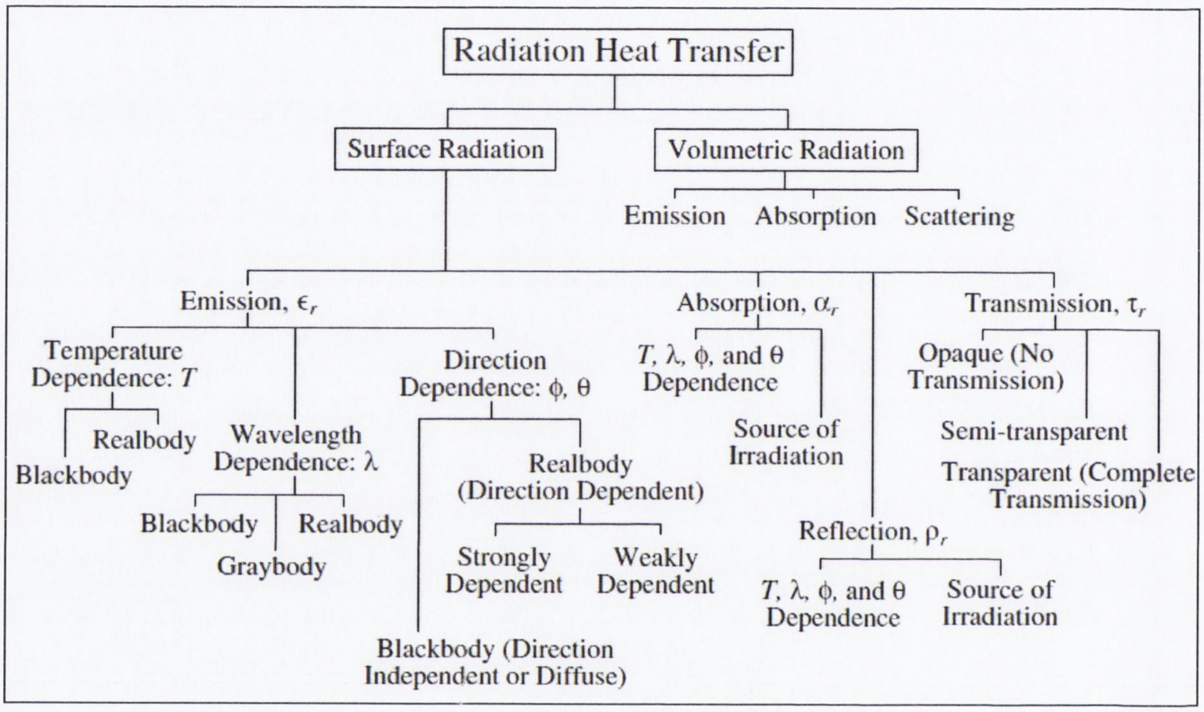

Fig. 2-12 Summary of surface-radiation properties and volumetric radiation (Kaviany, 2011)

Both absorption and reflection are also influenced by the source of radiation i.e. the energy received at the earth from the sun is subject to variations due to the following; variations in distance and tilt of the earth relative to the sun, variations in atmosphere scattering by air molecules of water vapour, gases and dust particles and variations in atmosphere absorption.

2.1.4 Thermal properties of materials

2.1.4.1 Specific Heat

A calorie is defined as the amount of energy necessary to raise the temperature of one gram of a specific substance, water, by one degree and that amount is 4.186J. The amount of energy required to raise the temperature of a particular substance by 1°C varies, as each substance requires a different amount of energy per unit mass to change the temperature by 1°C (Giancoli, 2009). Askeland and Phule (2006) define the specific heat, or heat capacity, of a material as the energy required to change the temperature of a unit mass of that material by one degree Kelvin/ one degree Celsius) and is calculated using Equation (2-20). In particular, the specific heat of a substance is the heat energy required to raise the temperature of 1kg of a material by one degree Kelvin.

$$Q = mc\Delta T \tag{2-20}$$

where Q is the heat energy required (J/kgK), m is the mass of the material (kg), c is the specific heat of the material (J) and ΔT is the change in temperature (Kelvin).

Therefore, it can be concluded that, if two materials had the same surface colour and were the same mass, the material with the higher specific heat would remain cooler if both samples were subjected to identical heat loads.

The common range for the specific heat of ordinary concrete is 840-1170 J/kg.K, however, specific heat increases with an increase in temperature and with a decrease in the density of the concrete (Neville, 1995). Some specific heat values are shown in Table 2-2. These values are valid at 1atm constant pressure and 20°C.

Table 2-2 Typical values of specific heat for common substances at 20°C (Giancoli, 2009)

Substance	Specific Heat, c (J/kg.K)
Water	4186
Wood	1700
Concrete	**840-1170**
Asphalt	920
Aluminium	900
Glass	837
Iron/Steel	488
Copper	385

2.1.4.2 Volumetric heat capacity (VHC)

The volumetric heat capacity (VHC) is the heat capacity per unit volume rather than mass and is equal to the specific heat capacity times the density of the material (Bergman et al., 2011).

$$VHC = c\rho \tag{2-21}$$

where c is the specific heat (J/kgK) and ρ is the density of the material (kg/m^3).

2.1.4.3 Thermal diffusivity

The thermal conductivity, k, of a material is related to the thermal diffusivity, δ, as described by Equation (2-22). Thermal diffusivity represents the relative ability of the material to conduct heat by thermal conductivity (k) as compared to its ability to store heat by its volumetric heat capacity (cρ). The larger the value of δ, the faster the propagation of heat into the material. Thermal diffusivity represents the ability of the material to respond to changes in the thermal environment. The larger the value, the quicker the material will come into equilibrium with the surroundings (Thirumaleshwar, 2006). It is defined as follows:

$$\delta = \frac{k}{c\rho} \tag{2-22}$$

where c is the specific heat (J/kgK) and ρ is the density of the material (kg/m^3). The larger the value of δ, the faster heat will diffuse through the material. Thermal diffusivity has units of m^2/s.

Concrete with k, c and ρ of 1.3W/mK, 840J/kgK and 2,400kg/m^3 respectively, for example, will result in a thermal diffusivity value of $0.64x10^{-6}$ m^2/s, which demonstrates a slow energy transfer rate in the material. However, steel with k, c and ρ of 46W/mK, 488J/kgK and 8,000kg/m^3 respectively, for example, will result in a thermal diffusivity value of $11.8.x10^{-6}$ m^2/s, which demonstrates a higher energy transfer rate in the material. Aluminium has an even higher thermal diffusivity of approximately $97.5x10^{-6}$ m^2/s (Thirumaleshwar, 2006).

2.2 Solar Radiation and Albedo

2.2.1 Solar radiation

Solar radiation is a form of thermal radiation having a particular wavelength distribution. (Holman, 2010). As previously outlined in Section 2.1, the energy from the sun is transferred to the earth in the form of photons moving at the speed of $3x10^8$m/s, and this energy can be converted into many types of energy such as heat energy. This heat energy received by the earth through photons is responsible for much of the earth's temperature. The amount of solar radiation reaching different parts of the earth varies with location and season (Solanki, 2008).

The sun emits energy in a wide range of wavelengths, however, the radiation of particular importance, which constitutes 99% of solar energy, is made up of ultraviolet, visible and infrared radiation. The amount of solar radiation received by a planet depends on its distance from the sun, which is approximately 1.5×10^{11}m for earth. Extraterrestrial radiation refers to the amount of radiation falling on the earth outside its atmosphere which is constant and is often referred to as the solar constant. The solar constant is defined as the average radiation intensity received per unit area perpendicular to the earth's surface at the mean sun-earth distance and it is taken as 1367W/m^2 (Solanki, 2008).

2.2.1.1 Radiation at the earth's surface

Solar radiation passes through the earth's atmosphere before reaching the earth's surface where it is subjected to absorption and scattering. This occurs due to the presence of the ozone layer, water vapour, CO_2, O_2, dust particles etc. present in the atmosphere. The solar radiation intensity (irradiation) as a function of wavelength is represented in W/m^2/nm. The extraterrestrial solar radiation and radiation reaching the earth's surface is displayed in Fig. 2-13.

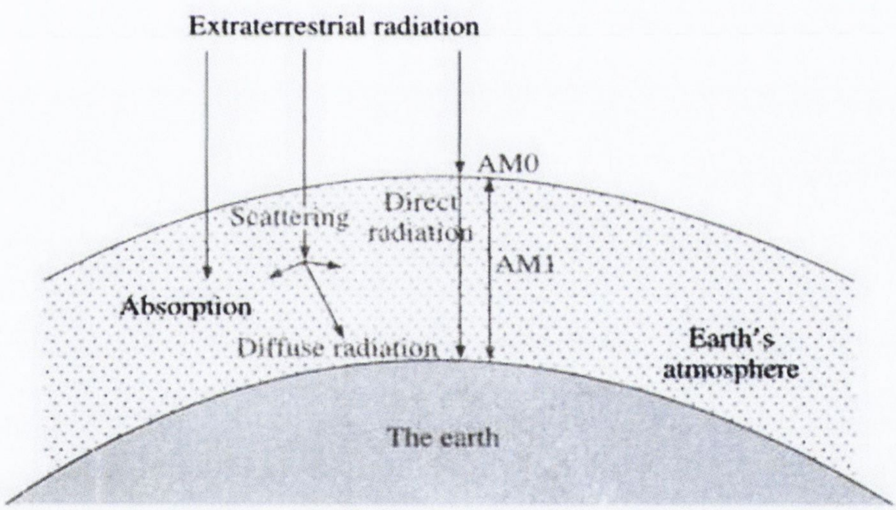

Fig. 2-13 Diagram of earth and the atmosphere demonstrating extraterrestrial , direct and diffuse radiation and Air Mass (Solanki, 2008)

The amount of attenuation of solar reflectance depends on the distance the solar reflection travels through earth's air mass. The thickness of the earth's atmosphere is referred to as Air Mass (AM). When radiation is measured outside the earth's atmosphere it is referred to as AM0 radiation as the air mass travelled by the sun's rays is equal zero (see Fig. 2-13). At the earth's surface when the sun is exactly at an overhead position, this is called AM1 as the rays reaching the earth's surface have travelled a distance equivalent to one air mass. However, when the sun is at an angle to the overhead position, the rays need to travel a longer distance within the earth's atmosphere to reach the surface. Therefore, AM1.5 is the distance travelled by the radiation if it is 1.5 times that of AM1 (Solanki, 2008).

2.2.1.2 Direct, diffuse and global radiation

When solar radiation passes through the earth's atmosphere it undergoes several interactions (absorption and scattering) with gaseous molecules and particles in the atmosphere. The absorption interaction is a loss of radiation, as the energy of the solar radiation is given to the gaseous molecules and the atmosphere, amounting to approximately 20% of the radiation (Solanki, 2008). The scattering interaction involves the direction of the sun rays changing and this is known as diffuse radiation. The radiation which is neither absorbed nor scattered, reaches the earth's surface directly and is known as direct radiation. Therefore, the total radiation reaching the earth's surface is called global radiation and is the sum of the diffuse and direct radiation (see Equation (2-23)).

$$Global\ radiation = Direct\ radiation + Diffuse\ radiation \tag{2-23}$$

On a sunny day, the diffuse radiation is approximately 15-20% of that of the direct solar radiation and on a cloudy day, the percentage of diffuse radiation increases with respect to direct radiation. The amount of solar radiation at a given location at a given time is dependant on many parameters such as; latitude and longitude of location, time of day and day of year. These parameters are key to calculating the sun's position, thus the available solar radiation. The chart displayed in Fig. 2-14 is the sun's global radiation (blue line) and direct radiation (red line) which was obtained from ASTM G173 - 03 (2012) for AM 1.5.

The radiation for AM1.5 represents an overall yearly average for mid-latitude locations (which is between approximately 23° and 66°N) which includes Ireland at 53°N, and is used by the solar industry for all standardised testing. The radiation for AM0 is also displayed in the plot and it is the extraterrestrial radiation i.e. the spectrum outside of the atmosphere.

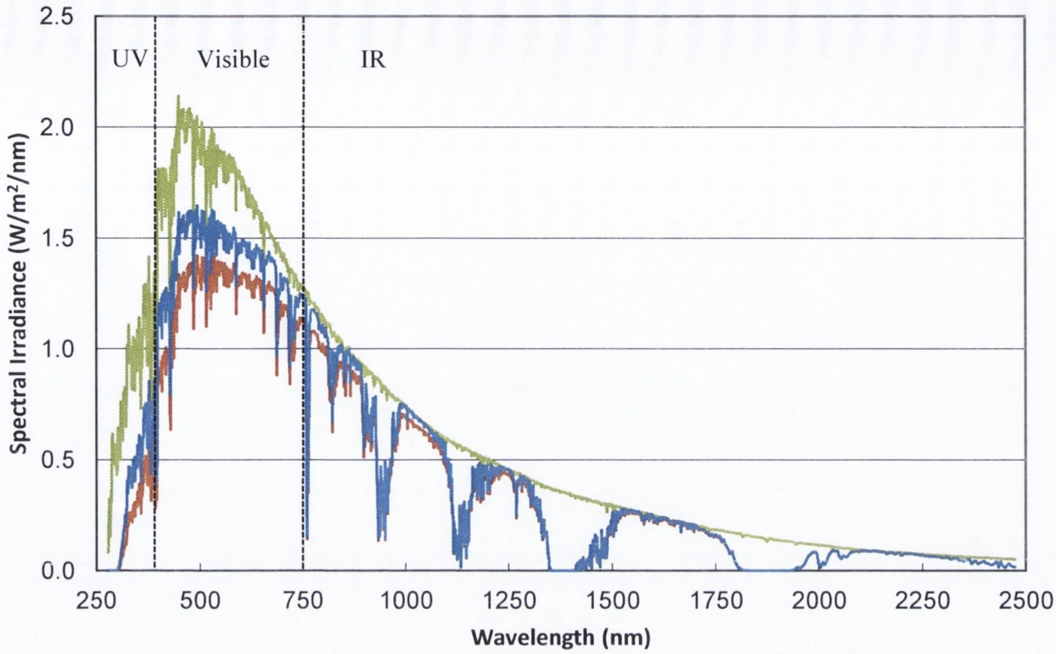

Fig. 2-14 Global radiation (blue line) and direct radiation (red line) for AM1.5 (ASTM, 2012) and AM0 (green line) (ASTM, 2006)

2.2.2 Definition of Albedo

Albedo is defined as the ratio of the reflected solar radiation to the incident solar radiation at the surface, over all wavelengths of solar irradiation (Taha et al., 1988, Li et al., 2013). Albedo is a dimensionless fraction and is measured on a scale of 0 to 1. An albedo of 0 denotes no reflecting ability of a perfectly black surface (zero reflectance, total absorbance), and an albedo of 1 signifies a perfectly white surface (total reflectance). In other words, if a surface is white then the solar radiation is reflected back out into the atmosphere. However, if a surface is dark then the solar radiation is absorbed by the surface. When energy is absorbed, it raises the temperature of the substance which absorbs it e.g. the earth, and this causes the earth to radiate this heat in the form of infrared radiation. This infrared radiation results in the warming up of the earth's lower atmosphere and surface.

As indicated in Fig. 2-15, the incoming solar radiation which is shown in yellow, consists of ultraviolet, visible and a limited portion of infrared energy (shortwave radiation) and the outgoing infrared (longwave) radiation is shown in red. The earth's global mean energy budget is discussed in detail in Section 8.1 (where the potential for CO_2 to be offset is discussed) and is displayed in Fig. 8-1. It is the balance between incoming shortwave solar radiation and the emission of longwave radiation to space in order to achieve equilibrium. The earth's atmosphere receives an average of 341W/m^2 of incoming solar radiation which is approximately one quarter of the solar constant (1367W/m^2), and 102W/m^2 of this radiation is reflected or scattered back into space by clouds and the atmosphere (79W/m^2) and the surface (23W/m^2). This ratio is known as the global albedo which is close to 31% or 0.31 (Zdunkowski et al., 2007), or 0.30 according to Taha et al. (1988). The objective of this research is to increase the radiation reflected off a surface (23W/m^2 here) and to reduce the absorbed radiation by the surface (161W/m^2) which is relevant as it would reduce the amount of infrared radiation emitted from the surface (the reader is referred to Fig. 8-1 for the figures).

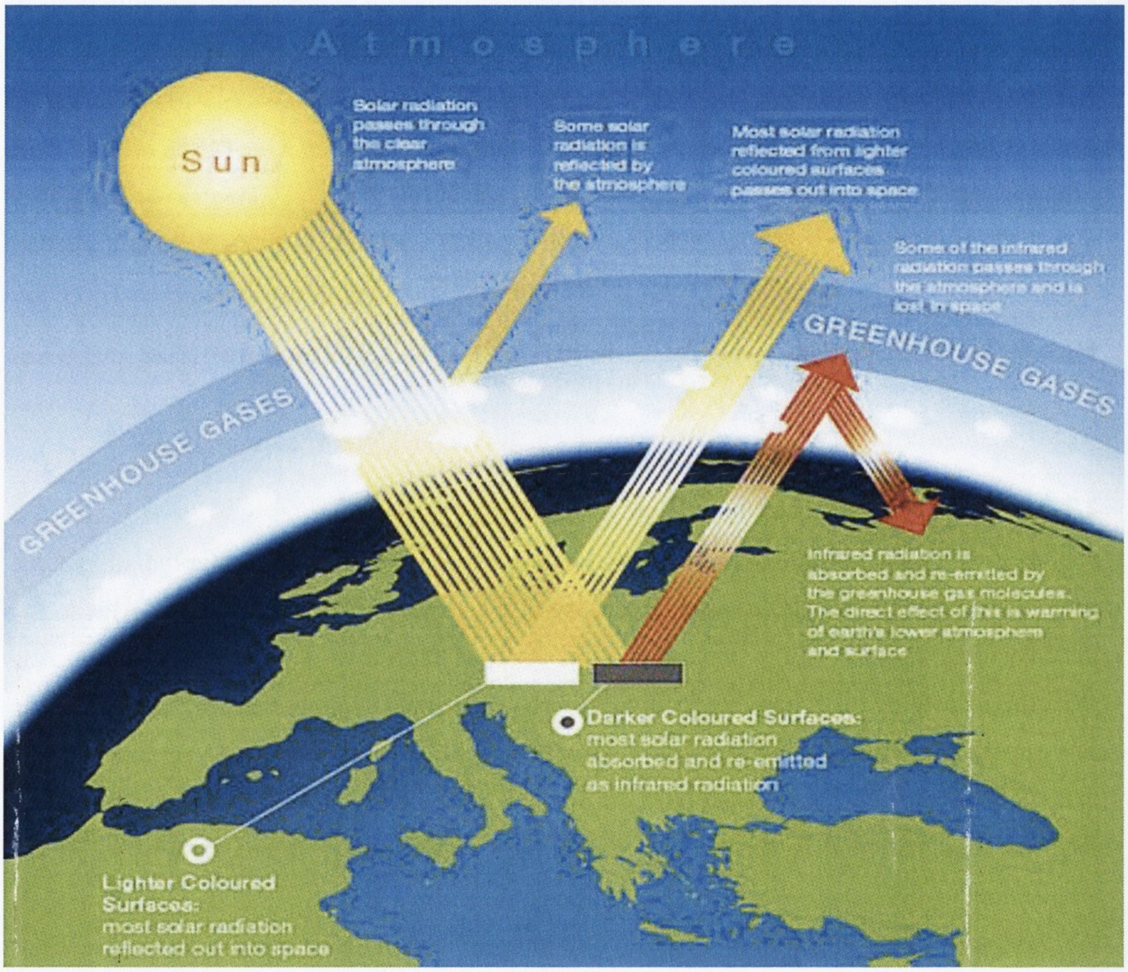

Fig. 2-15 The Albedo Effect (ECOCEM, 2011)

2.2.3 Published values of albedo and emissivity

2.2.3.1 Published albedo values

The published values of albedo for a variety of different surfaces will be outlined in this section. The albedo values have been divided into two main categories; albedo values for urban areas and building materials (see Table 2-3) and albedo value for natural and vegetative surfaces (see

Table 2-4), with the reference source included. In Table 2-4, the most reflective natural surface is new snow, having an albedo of between 0.75 and 0.95.

The author consulted a wide range of references, as displayed in Table 2-3 and Table 2-4, from which it may be observed that there is no universal agreement on values of different materials. In some cases significant variability exists for different materials.

Table 2-3 Albedo value for urban area and building materials

Surface	Material	Albedo	Source
Urban area	Streets	0.14	(Oke, 1987, Stull, 2000)
		0.15	(Stull, 2000)
	Building surfaces light	0.60	(Solanki, 2008)
	Building surfaces dark	0.27	(Solanki, 2008)
	Urban area (average)	0.15	(Santamouris, 2001)
	Urban area	0.15-25	(Solanki, 2008)
Asphalt	Asphalt (aged)	0.15-0.20	(Martien et al., 1989)
		0.09-0.18	(Santamouris et al., 2011)
	Asphalt (new)	0.05-0.10	(Martien et al., 1989)
		0.04-0.06	(Santamouris et al., 2011)
Concrete	Concrete (new)	0.35-0.40	(Bretz et al., 1998)
	Concrete (aged)	0.25-0.30	(Bretz et al., 1998)
		0.22	(Solanki, 2008)
	Concrete (white cement)	0.68-0.77	(Levinson and Akbari, 2002)
Paint	Black paint	0.02-0.15	(Santamouris, 2001)
	White paint	0.50-0.90	(Santamouris, 2001)
Other	Wood (freshly planed)	0.40	(Santamouris, 2001)
	Wood (oak)	0.10	(Santamouris, 2001)
	Red Brick	0.30	(Santamouris, 2001)
	Gravel	0.72	(Santamouris, 2001)
	Bituminous and gravel roof	0.13	(Solanki, 2008)

Table 2-4 Albedo value for natural and vegetative surfaces

Surface	Material	Albedo	Source
Snow	Snow (new)	0.90	(Taha et al., 1988)
		0.75-0.95	(Stull, 2000)
	Snow (old)	0.40-0.70	(Oke, 1987)
		0.35-0.70	(Stull, 2000)
	Ice caps	0.80-0.90	(Taha et al., 1988)
	Ocean	0.06-0.10	(Taha et al., 1988)
		0.03-0.10	(Solanki, 2008)
Vegetated area	Average soil	0.30	(Santamouris, 2001)
	Soil, dark wet	0.06-0.08	(Stull, 2000)
	Soil, light dry	0.16-0.18	(Stull, 2000)
	Deciduous plants	0.20-0.30	(Santamouris, 2001)
	Deciduous forests	0.15-0.20	(Santamouris, 2001)
		0.10-0.25	(Stull, 2000)
		0.18	(Solanki, 2008)
	Coniferous forest	0.05-0.15	(Stull, 2000)
		0.16	(Solanki, 2008)
	Grass	0.23	(Solanki, 2008)
		0.25	(Reagan and Acklam, 1979)
		0.26	(Stull, 2000)
		0.30	(Santamouris, 2006)

2.2.3.2 Published emissivity values

A number of emissivity values are outlined in Table 2-5 for some common building materials. The emissivity value of particular importance is that of concrete which ranges between 0.85 and 0.95. The emissivity is dependant on two main factors; composition and surface geometry. It is related to reflectance or colour. Dark materials absorb more and therefore emit more energy than light materials. Moreover, smooth surfaces have lower emissivity values than rough surfaces (Gupta, 2003, Myers, 2006). In general, rough concrete has an emissivity of between 0.92-0.95.

Table 2-5 Emissivity values for some common materials (Anderson, 2006)

Material	Emissivity
Aluminium (polished)	0.03-0.06
Aluminium (dull/rough polish)	0.18-0.30
Asphalt/bitumen pavement	0.90-0.98
Brick	0.85-0.95
Concrete	0.85-0.95
Steel (polished)	0.074-0.097
Wood	0.82-0.94

2.2.4 Solar reflectance and thermal emittance

As previously outlined in Section 2.2.2, albedo, or solar reflectance, is defined as the ratio of the reflected solar radiation to the incident solar radiation at the surface, over all wavelengths of solar irradiation. Emissivity is defined as the fraction of energy radiated by a body compared to that radiated by a black body at the same temperature (McMullan, 2007). A material which is able to radiate heat away from it to stay cool has a high thermal emittance whereas a material with a low thermal emittance traps energy at long wavelengths between 5-40μm (Infrared Radiation) (Gartland, 2008). Infrared emittance is measured on a scale from 0 to 1. A true black body has an emissivity value of 1 and the more reflective or shiny the material is, the lower the emissivity value e.g. polished silver has a value of 0.02. In general, the colour and texture of a material's surface control its emissivity, as darker and duller surfaces tend to have a value close to 1 than more polished and brighter surfaces (Wang et al., 2012). A material with a higher thermal emittance has the ability to radiate away any collected heat. The thermal emittance of most materials is greater than 85 per cent, but bare metallic surfaces tend to have emittance values ranging between 0.20 and 0.60 (Gartland, 2008).

2.2.4.1 Cool material

A 'cool' material is defined as a material which has both high solar reflectance and high thermal emittance. These two properties combined affect the surface temperature (see Fig. 2-16). If a surface with a high solar reflectance and infrared emittance is exposed to solar radiation, the surface temperature will be lower compared to a surface which has a lower solar reflectance and thermal emittance value. This parameter can be determined by calculating the solar reflectance index (SRI) of the material which incorporates both the solar reflectance and infrared emittance in a single value.

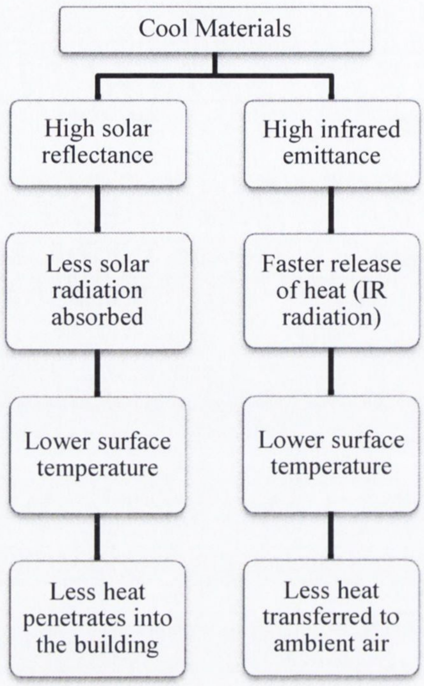

Fig. 2-16 The basic principles of a cool material (Santamouris et al., 2011)

2.2.4.2 *The Solar Reflectance Index*

The solar reflectance index (SRI) is a value which combines solar reflectance and thermal emittance of a material into one measurement expressed as a fraction (from 0.0 to 1.0) or as a percentage (from 0 to 100) and represents a material's performance in the sun. Materials with relatively high SRI values are referred to as cool materials.

To determine the SRI value of a material, ASTM E1980-11 (2011) is the standard which defines SRI calculation methods. The SRI value quantifies how hot a flat surface would get relative to a standard black and a standard white surface (see Table 2-6). The calculation is based on a set of equations where the solar reflectance and thermal emittance of a material are required, for specific environmental conditions. The SRI has a value of 0 for a standard black surface and 100 for a standard white surface.

Table 2-6 Solar Reflectance Index-a standard black and white surface (Mulvaney, 2011)

	Albedo	Emissivity (ε)	SRI (%)
Standard black material	0.05	0.90	0
Standard white material	0.80	0.90	100

For a surface exposed to the sun, when the conduction into the material is zero, the steady-state surface temperature is obtained iteratively using the Equation (2-24) (see Equations (2-6) and (2-10)).

$$\alpha I = \epsilon\sigma\left(T_s{}^4 - T_{sky}{}^4\right) + h_c(T_s - T_a) \tag{2-24}$$

where:

α = solar absorptance = 1 - solar reflectance

I = solar flux (W/m^2)

ε = thermal emissivity

σ = Stefan Boltzmann constant, 5.667 $\times 10^{-8}$ (W/m^2K^4)

T_s = steady state surface temperature (K)

T_{sky} = sky temperature (K)

h_c = convective coefficient (W/m^2K)

T_a = air temperature (K)

In the ASTM E1980-11 standard, SRI is defined using the Equation (2-25);

$$SRI = \frac{(T_{black} - T_{surface})}{(T_{black} - T_{white})}.100 \tag{2-25}$$

where T_{black} and T_{white} are the steady state temperatures of black and white surfaces. Under the standard solar and ambient conditions, Equation (2-25) can be regressed to Equation (2-26), which is used to calculate the SRI.

$$S.R.I = 123.97 - 141.35X + 9.655X^2 \tag{2-26}$$

Equation (2-27) is employed to calculate X, which is then substituted into Equation (2-26).

$$X = \frac{(\alpha - 0.029\varepsilon)(8.797 + h_c)}{9.5205\varepsilon + h_c} \tag{2-27}$$

Typical standard solar and ambient conditions for the purpose of a calculation are defined in ASTM E1980-11 (2011) and are as follows;

$I = 1000W/m^2$ (equal to AM1.5 at 48°)

$T_a = 310K$

$T_{sky} = 300K$

$h_c = 5$, 12 and $30W/m^2K$

The SRI of a test surface varies with two material properties, namely the solar reflectance and thermal emittance, and four environmental conditions, namely the solar flux, convection coefficient, air temperature and sky temperature. SRI is calculated for three convective coefficients of 5, 12 and $30W/m^2K$, corresponding to low, medium and high wind conditions, respectively.

2.2.5 Measurement of solar reflectance and thermal emittance

There are three main standard test methods for determining solar reflectance of a surface in order to determine a material's SRI;

1. ASTM E1918-06 Standard Test Method for Measuring Solar Reflectance of Horizontal and Low-Sloped Surfaces in the Field
2. ASTM C1549-04 Standard Test Method for Determination of Solar Reflectance near Ambient Temperature Using a Portable Solar Reflectometer
3. ASTM E903-12 Standard Test Method for Solar Absorptance, Reflectance and Transmittance of Materials Using Integrating Spheres

The method by which thermal emittance is determined will also be discussed briefly in this section.

2.2.5.1 ASTM E1918-06 (Pyranometer test method)

This test method covers the measurement of solar reflectance of various horizontal and low sloped surfaces and materials in the field, using a pyranometer. The test method is intended for use when the sun angle at the normal from a surface is less than 45°. This method requires an area of approximately $10m^2$ and is best applied to large surfaces that may also be rough and/or non-uniform.

Levinson et al. (2010a) reviewed this technique for measuring solar reflectance and stated that the solar reflectance measured using the conventional pyranometer method will equal the global solar reflectance if; (a) the surface reflects diffusely (b) the pyranometer casts no shadow on the surface and (c) the pyranometer sees only the target surface when measuring the reflected solar irradiance. They state that there are a number of restrictions when using this test method:

1. The sky must be clear, particularly around the sun as haze or cloudiness can alter the spectral power distribution of sunlight, and the passage of cloud across the sun can lead to serious error.
2. The spectral distribution of the incident solar irradiance and the irradiance angle of the solar beam both vary with hour of day and day of year which restricts the daily time window for testing.
3. The target must be large enough to ensure that nearly all reflected radiation collected by a downward facing sensor comes from the target and not its surroundings.
4. The technique will always slightly underestimate the global solar reflectance as the shadows cast by the pyranometer and its support reduce the reflected solar irradiance.
5. The pyranometer responsitivity is a strong function of the angle of incidence.

Levinson et al. (2010a) concluded that the need for a large testing surface makes the method suitable for characterising roofs, pavements and other large surfaces but inconvenient to apply to small samples such as product prototypes.

Similarly, recent research was conducted by Li et al. (2013) with the aim of determining the albedo values of commonly used materials such as asphalt and concrete using a dual pyranometer method. This method is essentially an albedometer which contains two pyranometers, one to measure incoming radiation and another to measure reflected radiation. Li et al. (2013) examine the diurnal variation of albedo, whereby the solar reflectivity was continuously monitored on three consecutive clear days on an asphalt surface (see Fig. 2-17). Their research discovered that measured albedo changes over time during the course of one day. It is high in the early morning and then low and relatively constant around the middle of the day, and then relatively high again in the late afternoon, when there is a low incident angle of solar radiation as in the early morning.

The same trend was observed for the concrete pavement, whereby the solar reflectivity was continuously monitored over time on one clear day on a concrete pavement (see Fig. 2-18). This result implies that the albedo should be measured in the middle of the day to obtain a constant and conservative value. Otherwise, if the albedo is measured in the early morning and late afternoon, the value obtained will tend to be larger than that measured in the middle of the day.

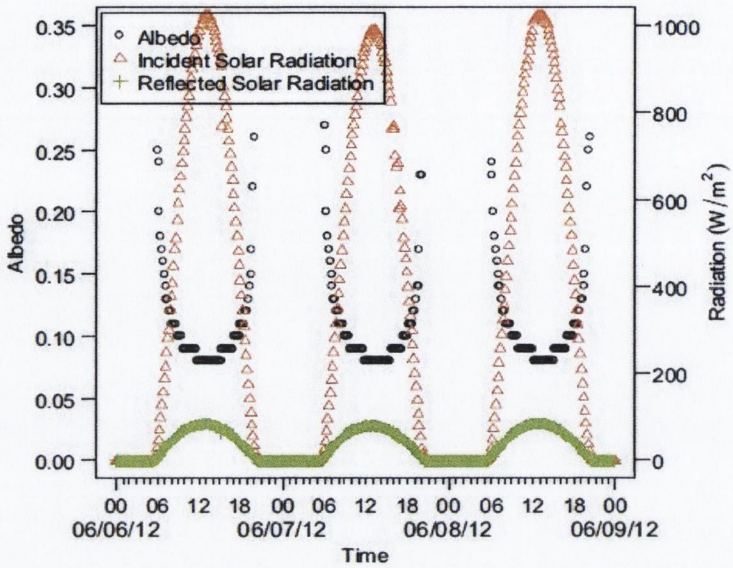

Fig. 2-17 Variation of solar reflectivity for an asphalt surface for three consecutive days (Li et al., 2013)

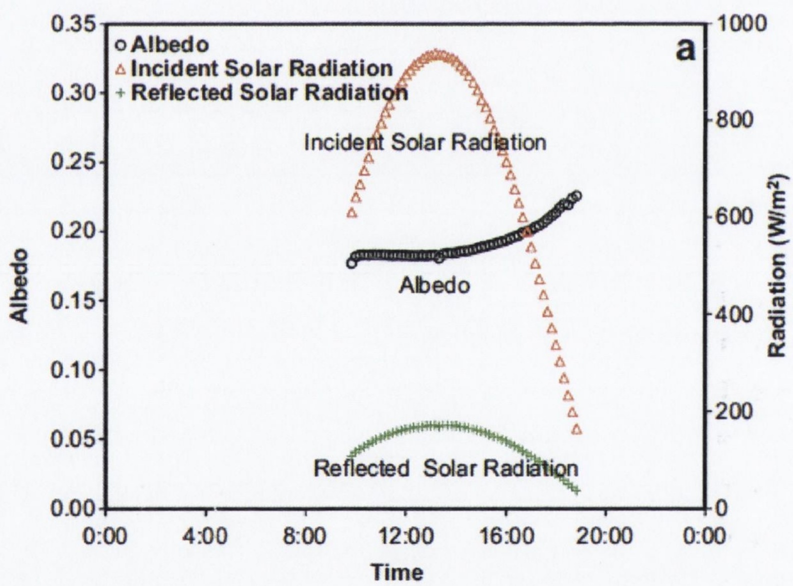

Fig. 2-18 Diurnal variation of solar reflectivity in one day for a concrete pavement (Li et al., 2013)

They also concluded that there is no significant seasonal variation in albedo, however, cloud cover will negatively influence the value of albedo.

The findings from the study conducted by Levinson et al. (2010a) and Li et al. (2013) will be compared to the primary results of albedo measurements which were carried out during this project. These results will be discussed in detail in Chapter 5.

2.2.5.2 *ASTM C1549-09 (Portable solar reflectometer test method)*

This test method determines the solar reflectance of flat opaque materials in a laboratory or in the field using a portable solar reflectometer. The portable solar reflectometer is calibrated using specimens of known solar reflectance to determine solar reflectance from measurements at four wavelengths in the solar spectrum: 380nm, 500nm, 650nm, and 1220nm. This test method is applicable to specimens of materials having both specular and diffuse optical properties and is particularly suited to the measurement of the solar reflectance of opaque materials. The portable solar reflectometer measures the reflectance of a flat and uniform surface of approximately $5cm^2$.

The instrument is calibrated using a black body surface with a reflectance of zero and one or more surfaces of known solar reflectance provided by the manufacturer. The surface to be evaluated is placed against the 2.5 cm diameter opening on the measurement head and maintained in this position until constant readings are displayed. In Europe, the use of portable reflectometer methods for measuring solar reflectance is not widespread apart from their use in the measurement of colour (Hutchins, 2009).

2.2.5.3 *ASTM E903-12 (Solar spectrophotometer test method)*

A solar spectrophotometer illuminates a surface with monochromatic light at near-normal incidence and measures the light reflected into an integrating sphere. A series of such measurements at wavelengths spanning the solar spectrum (300–2500 nm) yields the surface's solar spectral reflectance. A properly calibrated solar spectrophotometer can accurately measure the spectral reflectance but there are several limits to its use. Levinson et al. (2010a) stated these restrictions to include the sample having to be flat, to ensure that any specularly reflected light is captured by the integrating sphere; small enough (typically not larger than 10-15cm) to fit in the instrument's sample port and, if the instrument has a vertical sample port, sufficiently cohesive to be mounted vertically. Also, the beam only illuminates $10mm^2$ of the sample, with each measurement taking several minutes, therefore, the instrument is best utilised on a uniform surface where minimal readings are required. A solar spectrophotometer is a large, immobile and expensive instrument to which samples must be brought.

2.2.5.4 *Measurement of emissivity*

As discussed in Section 2.1.2, emissivity is a relative measure on a scale of 0 to 1 of heat (radiation) emitted by a material's surface compared to the energy radiated by an ideal black body at the same temperature and at the same solar angle. In general, the higher the emissivity, the lower the reflectance value of the material. A material's emissivity is measured using a determined temperature and a predetermined angle. An emissivity of 1 would suggest the material absorbs all the energy and heat and an emissivity of 0 suggests a perfect reflector of heat (Postell and Gesimondo, 2011). Infrared emittance of a surface can be measured using a portable emissometer as described in ASTM C1371-04a (2010) and ASTM E408-71(2008). There are many uncertainties that are involved in the measurement of emissivity as several factors affect the measurement such as the sample temperature and the surface geometry.

2.2.6 Albedo and the environment

By increasing the reflectance of surfaces using 'cool' materials, this would contribute to lowering surface temperatures when exposed to sunlight (Bretz et al., 1998, Berdahl and Bretz, 1997). Creating cool communities requires lowering the average surface temperature, for example, a city so that there is less surface-to-air heat transfer. For building and pavement surfaces in the sun, surface characteristics such as albedo and emissivity are highly relevant. Albedo is an indicator of the reflecting power of a surface and is a key thermal characteristic. The thermal characteristics (such as albedo, heat capacity and thermal conductivity) interacting with solar radiation are the causal factors affecting the urban heat island (UHI) phenomenon (Li et al., 2013). Therefore, as albedo plays an important role in the thermal behaviour of pavements, roofs and other ground surfaces, it consequently has an impact on humans and the environment.

Increasing the urban albedo results in more of the incoming solar radiation being reflected, and this effectively counteracts to some extent the effects of global warming. Akbari et al. (2008b) and Menon et al. (2010) have quantified this in terms of offset CO_2 emissions. This will be discussed in detail in Chapter 8.

Furthermore, the impact of albedo on the environment is also relevant in terms of the transmission of heat through conduction into buildings. For example, when heat is generated on the surface of concrete, some of the heat will be emitted as IR radiation, however, some of the heat will be conducted down through the depth of the slab. Where there is reasonable insulation in the roof of a building, this prevents the heat from transferring to the room below. This results in the heat being given off upwards. In conclusion, the albedo effect is not just a surface phenomenon as it is important what the material comprises of below the surface.

2.3 The Urban Heat Island Effect

The urban heat island effect was first discovered by a British meteorologist Luke Howard in 1818 who was also known for the classification of clouds (Santamouris, 2009). He studied London's climate by measuring the temperatures at several sites within and outside the city and found that the temperature within the city was noticeably warmer than its rural surroundings. Following this discovery, the urban-rural temperature contrast was termed the 'urban heat island' by Manley (1958) and this term has since been widely used across various areas of research.

An urban heat island is a 'reverse oasis' where air and surface temperatures are hotter than in their rural surroundings (Gartland, 2008). Fig. 2-19 is a thermal image of a midday surface urban heat island in Salt Lake City, Utah which was taken on July 13 1998. The warmer urban surfaces are on the left of the image (at a maximum of 70°C) while the dark blue areas (at 30°C) are the cooler surfaces (Akbari et al., 2008a). The urban heat island effect is now considered as one of the most serious urban environmental problems.

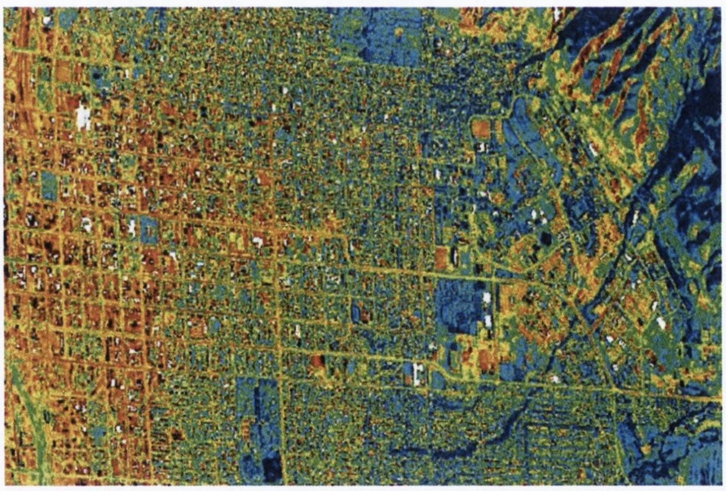

Fig. 2-19 Thermal image of a surface urban heat island in Utah (Akbari et al., 2008)

The urban heat island effect is a direct result of urbanisation that creates urban fabric which comprises mainly of roofs, paved surfaces and less vegetation (Santamouris, 2007). Heat islands occur both on the surface and in the atmosphere. They differ in a number of ways including the way they are formed, the methods used to identify them, their impacts and mitigation techniques (Akbari et al., 2008a). Surface urban heat islands are a direct result of the sun heating up dry urban surfaces such as roofs and pavements to temperatures which are hotter than the surrounding air. They can be identified through remote sensing and this data is collected to produce thermal images (see Fig. 2-19). Surface urban heat islands are present both during the day and at night and tend to be most intense on a hot clear summer's day.

Atmospheric urban heat islands occur when the air temperature in an urban area is higher than that in the nearby rural surroundings. These differences in temperature can be small or non-existent during the day and are most intense at night or predawn. This is due to the slow release of heat from buildings. They are measured directly with fixed weather stations and the data is displayed on an isotherm map or temperature graph (Akbari et al., 2008a). There are two major atmospheric types of urban heat island; the urban canopy layer heat island (UCL) which is the air between the ground and the tops of trees and roofs, and the urban boundary layer heat island (UBL) which is situated above the UCL.

Extensive research has been carried out into characterising the fabric of an urban environment by Rose et al. (2003) by using high-resolution aerial digital orthophotos covering selected areas in each city. The study focused on the fabric of Sacramento, Salt Lake City and Chicago, examining four major land use types; commercial, industrial, transportation and residential. Of approximately 900km^2 of urban area in Sacramento, 49% was residential, about 59% of 620km^2 urban area in Salt Lake City was residential and 53% of 2520km^2 urban area in Chicago was residential. The data in Table 2-7 displays a comparison of the fabric of these three cities.

Table 2-7 Comparison of the percentage of the horizontal fabric of Salt Lake City, Sacramento and Chicago (Rose et al., 2003)

City	Vegetation	Roofs	Pavements	Other
Above the canopy	%	%	%	%
Metropolitan Salt Lake City	40.9	19.0	30.3	9.7
Metropolitan Sacramento	28.6	18.7	38.5	14.3
Metropolitan Chicago	30.5	24.8	33.7	11.0
Residential Salt Lake City	46.6	19.7	25.3	8.5
Residential Sacramento	39.2	19.4	25.6	15.8
Residential Chicago	44.3	25.9	25.7	4.1
Under the canopy				
Metropolitan Salt Lake City	33.3	21.9	36.4	8.5
Metropolitan Sacramento	20.3	19.7	44.5	15.4
Metropolitan Chicago	26.7	24.8	37.1	11.4
Residential Salt Lake City	38.6	23.9	31.6	6.0
Residential Sacramento	32.8	19.8	30.6	16.8
Residential Chicago	35.8	26.9	29.2	8.1

This research demonstrates that impervious surfaces such as roofs and pavements make up a significant fraction of an urban area and that characterisation of the urban fabric is very important in order to be able to design and implement heat island reduction strategies.

Gartland (2008) and Bhatta (2010) suggest that there are two main causes of the heat island effect. The first of these is that most urban building materials are impermeable and watertight and therefore there is no available moisture to dissipate the sun's heat. The second cause is the use of dark materials which absorb and retain the sun's energy. Gartland (2008) and Taha et al. (1988) believe that other factors, such as an increase in anthropogenic heat released from buildings and vehicles and increased city roughness (slower wind speeds), also contribute to its formation. It is important to look at the energy balance at the earth's surface in order to understand the origin of the energy and how it is transferred. This is done by evaluating the energy balance equation.

2.3.1 Energy balance equation

The energy balance equation illustrates how energy is transferred to and from the earth's surface and is based on the first law of thermodynamics which states that energy cannot be lost (Gartland, 2008). The energy balance equation is represented by Equation (2-28);

$$\text{Convection} + \text{Evaporation} + \text{Heat storage} = \text{Anthropogenic heat} + \text{Net radiation} \tag{2-28}$$

- Convection is energy which is transferred from a solid surface to a fluid, in this case from the earth's surface to the air above it, and it increases with higher wind speeds.
- Evaporation is energy which is transmitted away from the earth's surface by water vapour, and includes the process of evapotranspiration. Both processes increase when there are higher wind speeds and when the air is drier and warmer, and also when there is more moisture available.
- Heat storage depends on two properties of a material; thermal conductivity (a high value indicates an increased ability of the material to transmit heat into its depth) and heat capacity (a high value indicating a material can store more heat in its bulk). These properties are outlined in Section 6.2.
- Anthropogenic heat is heat which is generated by buildings, machinery or people. In dense urban areas this term is larger and can have a significant effect on the formation of heat islands.

Net radiation (see Equation (2-29)) consists of four separate radiation processes taking place at the earth's surface with each term defined below;

Net radiation = Incoming solar radiation – Reflected solar radiation + Atmospheric radiation – Surface radiation **(2-29)**

where:

- Incoming solar radiation is the amount of energy reaching earth as radiated by the sun and is dependent on the season, time of day, cloud cover and atmospheric pollutant levels.
- Reflected solar radiation represents the amount of solar energy reflected off the earth's surface and is represented by the albedo value.
- Atmospheric radiation is heat which is emitted by particles present in the atmosphere such as water vapour droplets and clouds.
- Surface radiation is heat which radiates from the earth's surface and is dependent on the temperature of the surface and the surroundings.

2.3.2 Factors which Influence the UHI Effect

There are many factors which can influence the heat island effect. Akbari et al.(2008a) and Gartland (2008) focuses on five main causes;

1. Reduced evaporation
2. Increased heat storage
3. Increased net radiation
4. Increased anthropogenic heat
5. Reduced convection

2.3.2.1 Reduced evaporation

Urban areas evaporate less water which contributes to elevated air and surface temperatures (Akbari et al., 2008a). Trees and vegetation provide shade which keeps surfaces cooler, reducing the amount of heat transferred to the air above them and reducing the energy use of buildings below (Gartland, 2008). In addition, this vegetation helps to reduce temperatures through evapotranspiration, which is the process whereby the plants release water to the surrounding air, dissipating ambient heat (Solecki et al., 2005). When there is no energy outlet of evaporation available, urban and suburban areas store more energy during the day which is subsequently released back into the atmosphere at night (Gartland, 2008). Shade from trees intercept sunlight before it warms a building or pavement. They also decrease the wind speed and shelter buildings from cold winter breezes (Akbari et al., 2001). Taha (1997b) studied the impacts of evapotranspiration on the near surface climate through numerical simulations. These results indicated that increasing vegetation cover in urban areas can result in approximately 2°C decrease in air temperature. Taha et al. (1988), Bretz et al. (1998) and Rosenfeld et al. (1995) also believe that reduced vegetation cover, in addition to exposed dark exterior surfaces, lead to the increase in urban air temperatures.

2.3.2.2 Increased heat storage

Properties of urban materials determine how the sun's energy is reflected, emitted and absorbed, in particular, solar reflectance, thermal emissivity, thermal conductivity and heat capacity (Akbari et al., 2008a). Thermal diffusivity (as previously discussed in Section 2.1.4), represents the ability of the material to respond to changes in the thermal environment. The larger the value, the quicker the material will come into equilibrium with the surroundings Urban areas tend to have lower thermal diffusivity due to manmade materials such as concrete and asphalt pavements. Materials such as concrete and asphalt have a higher heat capacity than natural materials found in the environment and as they absorb and retain solar radiation, the stored heat is released slowly at night time from the urban surface. Thus, the urban heat island intensity peaks several hours after sunset as the urban surfaces are still warm.

2.3.2.3 Increased net radiation

The difference in net radiation between urban and rural areas is mainly due to factors such as the low albedo value of urban materials, urban geometries and the higher air pollution levels in cities (Gartland, 2008). Most urban materials have a low albedo value and as a consequence reflect less of the incoming solar radiation. A typical example of this is asphalt which has an albedo of approximately 0.05 when new compared to grass, for example, which has an albedo of 0.25.

Urban geometry refers to the dimensions and spacing of buildings within a city (Akbari et al., 2008a). It influences wind flow, energy absorption and the ability of a surface to emit long-wave radiation back to space. A surface at ground level, which is surrounded by buildings, radiates heat diffusely or evenly in all directions and this heat is captured by building walls instead of escaping to the atmosphere (Gartland, 2008). Urban geometry can be simulated through urban canyon models which study a configuration of buildings surrounding a street. The model is based on energy balance equations that represent the heat transfer between pavements and building walls. The model takes into account wind patterns, solar loads and shading of certain areas throughout the day and can help evaluate how urban geometry affects urban climate (Gartland, 2008). The effects of urban geometry are assessed using a 'sky view factor'(SVF) which is the visible area of the sky from a given point on the surface and this factor ranges from 0 to 1 with close to 0 being a low SVF typically in urban areas where there are tall closely spaced buildings and 1 being a high SVF such as in a field (Akbari et al., 2008a). The SVF value in urban environments is calculated by using one of three methods; analytical, photographic or video imagery (Emmanuel, 2005). An analytical method is one whereby the SVF is calculated once the angles from the planar surface to the tops and sides of the surroundings are known. A photographic method is one where a fish eye lens photograph is used to project the hemispherical radiating environment onto a circular image plane and a photographic method is one where a video camera with a fish eye lens is digitalised and analysed to distinguish the relative areas covered by sky and buildings.

2.3.2.4 Increased anthropogenic heat

Anthropogenic heat refers to heat produced by human activities (Akbari et al., 2008a, Gartland, 2008) and it comes from many sources such as cars, buildings, industrial processes and people. The importance of each source depends on the city itself but in general there are three major sources; intensity of energy use, power generation and transportation systems (Taha, 1997b, Shahmohamadi et al., 2011). Anthropogenic heat is calculated by computing the sum of all energy use (commercial, residential, industrial and transport) and dividing it by the region's area. It is typically larger in winter than in summer due to the larger heating load in winter. The average value of anthropogenic heat for most major U.S cities ranges between 20-40W/m^2 in summer and 70-200W/m^2 in winter (Taha, 1997b).

2.3.2.5 Reduced convection

Urban heat islands require calm winds and clear skies to form. This is due to the fact that less heat is convected from the surface to the air when wind speeds are low. The decreased wind speeds increase heat storage during the day which is released slowly at night time. As buildings within cities act as wind breaks, cities tend to have slower wind speeds than rural areas (Gartland, 2008).

2.3.3 Characteristics of an UHI

Gartland (2008) suggests that the heat island effect is characterised by hotter surface temperatures, hotter air temperatures, larger effects during clear, calm weather, and it increases with development and thermal inversions.

2.3.3.1 *Hotter surface temperature*

During the daytime, urban surfaces heat up by absorbing the incoming solar radiation from the sun and at night-time these surfaces release the heat, eventually cooling down to the air temperature. Areas containing vegetation, however, contain moisture which evaporates and keeps the surfaces cool (Gartland, 2008, Sabnis, 2012). The surface temperature of the earth was first visualised from satellites in the late 20th century and it was possible to map the temperatures on the earth's surface. The Explorer Mission 1 was one of the first satellites used to observe urban heat in 1978. For example, a heat capacity mapping radiometer was used to measure surface temperatures in Buffalo, New York. This means of visualization clearly showed warm regions both in urban areas and surrounding them all over the world (Gartland, 2008).

2.3.3.2 *Hotter air temperatures*

The difference between the urban and rural air temperatures is used to measure the heat island effect. The heat island effect is usually largest at night time as urban surfaces continue to release heat. Heat island intensity varies in its magnitude and the timing of its peak for each city. These peaks usually occur 3-5 hours after sunset (Oke, 1987). Cities built of materials that release heat quicker reach peak heat island intensity sooner after sunset whereas a material, such as concrete which releases heat more slowly, may not reach the peak until sunrise (Gartland, 2008). The air temperature in a typical city on a summer afternoon can be 2.5 degrees higher than in the surrounding rural areas (Rosenfeld et al., 1995, Akbari et al., 2001). Gartland (2008) describes a phenomenon known as the 'oasis effect' which has been recorded in the desert city of Phoenix in Arizona. This is where urban daytime temperatures are cooler than the surrounding rural desert as a result of more landscaping and irrigation. However, the night-time air temperatures are warmer than the surrounding rural area, therefore, the heat island is still a factor here. Similarly, in cold northern climates, a 'cool island' can be created whereby the urban-rural air temperature difference during the day is less than zero as a result of the low sun casting long building shadows. Consequently the city is cooler than its surroundings and this cool island consequence can be seen in Reykjavik in Iceland. Surface temperatures have a significant effect on air temperatures, especially in the canopy layer, which can be seen in Fig. 2-20.

The peak in surface temperature during the day is located directly at the location of the buildings, with the minimum value of surface temperature occurring in vegetated areas. The diagram also shows that the pond area is cool during the day and warm at night time, which is due to its high heat capacity. The increase of surface temperature during the day consequently has an effect on the night time temperature which also reaches a peak where the buildings are situated.

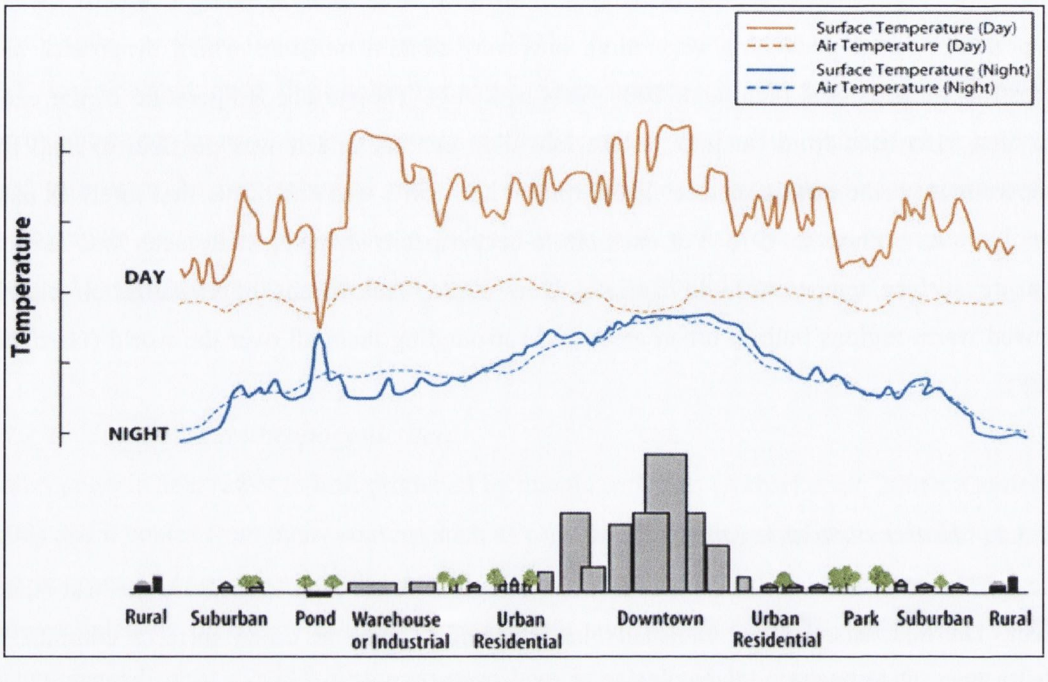

Fig. 2-20 Variations of surface and air temperatures (Akbari et al., 2008)

2.3.3.3 Larger effects during clear, calm weather

The heat island effect is weakest during cloudy, windy weather and is strongest during calm clear weather. The main reason for this is that calmer winds remove the heat at a slower rate and also more solar energy is received on clear days.

2.3.3.4 Increases with development

As urban areas expand over time, the heat island also expands and tends to be more intense. Brazel et al. (2000) studied the effect of increasing urbanization in two urban locations in Phoenix, Arizona, as well as urban Mesa and compared them with suburban Tempe, Arizona. The maximum and minimum temperatures in these cities are compared to temperatures in Sacaton, a rural area in the Arizona desert. Maximum temperatures in the urban and suburban areas have not changed relative to the temperature in Sacaton, but minimum temperatures at night time have increased by 4°C in Phoenix, Mesa and Tempe relative to the temperatures in Sacaton. This study would imply that the cities are storing more heat due to parameters outlined in Section 2.3.2 such as urban geometry, reduced vegetation and anthropogenic heat, and releasing the heat at night-time which is increasing the intensity of the heat island effect.

2.3.3.5 *Thermal inversions*

The effect of the heat island can also be seen at the boundary layer, which is the lowest 2000 metres of the earth's atmosphere. As the earth's surface heat up during the day by solar energy, this heats the air above it. This warm air expands and becomes lighter, therefore rising into the atmosphere. This can often result in a thermal inversion of warm air over cool air, thus inverting the usual condition in which air becomes cooler with altitude (see Fig. 2-21). Urban and suburban areas tend to heat up more than rural areas, and this extra heat gives rise to thermal inversions which trap warm air and pollution near the ground (Gartland, 2008, Thorpe, 2009). This could have adverse effects on health such as asthma and an increase in lung cancer.

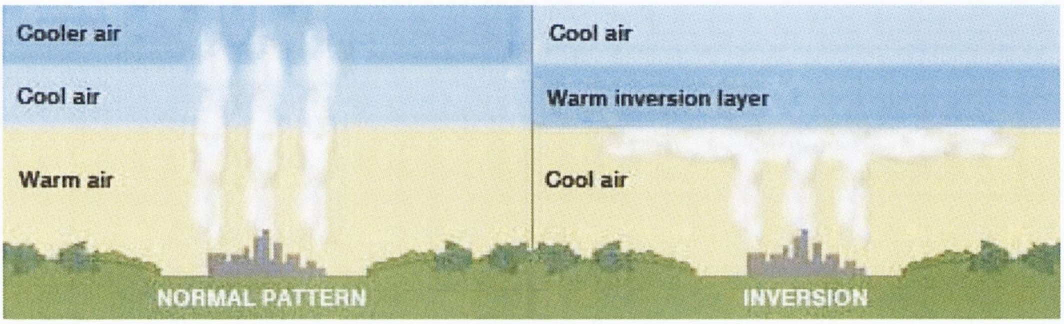

Fig. 2-21 Normal pattern of air flow and thermal inversion (Rohrer, 2013)

They are influenced by the presence of clouds, wind, length of the night and the condition of the ground (Ackerman and Knox, 2012, O'Hare et al., 2005). Clouds are made up of tiny water droplets which absorb outgoing thermal energy from the surface and can reradiate such energy back to the surface. Winds are the mixers of the atmosphere, therefore, if a thermal inversion exists and the winds increase suddenly then the inversion will be destroyed. Winter nights are longer than summer nights, therefore, the surface has more time to cool down and form an inversion. Finally, the condition of the ground is a factor, for example, the presence of ground snow cover. Snow has many air filled pockets which prevent the heat being conducted from the surface of the ground to the air above. Also, snow has a high solar reflectance value, therefore, by not absorbing much solar radiation, the surface can remain cold. The presence of snow cools the air immediately above much more effectively and for longer than if there was no snow present (Ackerman and Knox, 2012, O'Hare et al., 2005).

Radiation (nocturnal) inversion is the most common form of surface inversion and occurs nightly as land cools rapidly by emitting thermal infrared radiation. During the day, the land also emits thermal infrared radiation, but this loss is exceeded by a gain in solar radiation. At night, thermal infrared emissions cool the ground, which in turn cools the molecular layers of air above the ground, creating an inversion. The strength of a radiation inversion is maximized during long calm cloud free nights where the air is dry (as dry air minimizes absorption of thermal IR energy by water vapour). Radiation inversions also form in the winter during the day in regions that are not exposed to much sunlight. They do not form regularly over the ocean as the ocean water only cools slightly at night-time (Jacobson, 2012, Ahrens et al., 2012). This phenomenon is demonstrated in some preliminary experiments, which are discussed in Chapter 6.

2.3.4 Effects of the urban heat island

The urban heat island effects are most severe during days and nights with limited cloud cover and light winds, when temperature differences between urban areas and surrounding rural areas tends to be at a maximum (Solecki et al., 2005). Taha et al. (1988) categorize the effects of albedo on building energy use as either local or global. The local effects of albedo, or direct effects, refer to those due to modifications in the absorptive and reflective characteristics of the envelope of a building. Global or indirect effects refer to micro climatic changes i.e. the change in the climate of a small, specific place within a larger area, mainly in air temperature, which result when the meso-scale (100-km order) urban albedo is altered.

As previously stated in Section 2.3.3, the air temperature in a typical city on a clear summer's day is as much as 2.5°C higher than in surrounding rural areas. This elevated summertime temperature in cities increases the energy demand for cooling. Akbari et al. (1992) have found that peak urban electric demand in six American cities (Los Angeles, CA; Washington, DC; Phoenix, AZ; Tucson, AZ and Colorado Springs, CO) rises by 2-4% for each 1°C rise in daily maximum temperatures above a threshold of 15-20°C. The additional air conditioning use caused by the urban air temperature increase is responsible for 5-10% of urban peak electric demand costing several billion dollars annually.

In cold climates, the effect of the heat island is considered a mild asset as it reduces the heating loads in buildings. However, in warm or hot climates, the urban heat island contributes to the discomfort of the urban population. Air conditioning is used to maintain a comfortable indoor environment, however, where air conditioning is not used, there is discomfort and even death, as transpired in the high profile heat wave in Chicago in 1995 (Bretz et al., 1998, Solecki et al., 2005). The heat wave resulted in the death of more than 700 people (Klinenberg, 2002). In 2003, the extended heat wave in Western Europe caused over 14,800 deaths in France alone (Pirard et al., 2005). Solecki et al. (2005) identify a potential link between the urban heat island effect and heat waves which is a concern, particularly during summer months.

The use of air conditioning to compensate for the heat island effect has a number of drawbacks. It can be expensive to both buy and use. It represents one-sixth of electrical energy demand in the United States, totalling to an annual cost of $40 billion (Rosenfeld et al., 1997). In order to meet this demand for energy, a large amount of fossil fuels are burned. The combustion of these fuels results in the emissions of air pollutants from power plants including sulphur dioxide (SO_2), nitrogen oxides (NOx), particulate matter (PM), carbon monoxide (CO) and mercury (Hg) which are ozone precursor chemicals. A precursor chemical is a compound such as carbon monoxide that, in the presence of solar radiation, will react with other chemical compounds to form ozone (Cleveland and Morris, 2009). These pollutants are harmful to human health and sulphur and nitrogen oxides are associated with acute and chronic respiratory diseases (Solecki et al., 2005). The burning of large amounts of fossil fuels also releases greenhouse gases such as carbon dioxide (Solecki et al., 2005, Akbari et al., 2008a, Bretz et al., 1998) , which contributes to global climate change.

Shahmohamadi et al. (2011) conducted an analysis of the urban heat island effect in Tehran, Iran. Their research focused on the relationship between the urban heat island effect and human health. The urban heat island effect is due to a number of contributing factors including materials and on-going activities within a city which are responsible for anthropogenic heat release and air pollution as outlined in Section 2.3.2. As a result, the urban heat island exerts a direct or indirect effect on human health.

The elevated temperatures associated with the heat island effect accelerate the formation of smog (Bretz et al., 1998, Taha, 1997b, Rosenfeld et al., 1997) . Akbari et al. (1990) shows that the probability of smog increases by 6% per °C in maximum daily temperature, above a threshold of 22°C. Decreasing the near surface air temperature can lead to a reduction in the depth of the mixed layer potentially resulting in higher ozone concentrations (Rosenfeld et al., 1995, Taha, 1997b). Rosenfeld et al. (1995) and Bretz et al. (1998) state that as well as accelerating the formation of smog, higher air temperatures are associated with increased emissions of reactive organic hydrocarbons in addition to ozone precursors from automobiles and vegetation.

Surface urban heat islands also degrade water quality by thermal pollution. Pavements and roofs can reach excessive temperatures, higher than air temperature, and this excess heat is transferred to storm water, which drains into storm water sewers and eventually rivers. This rapid temperature change affects aquatic life (Akbari et al., 2008a).

2.3.5 Adaptation to and mitigation of urban heat islands

A response to the urban heat island effect may be described as either adaption or mitigation. Adaption of the urban heat island is defined as an adjustment to moderate the harm caused by it, while mitigation of the urban heat island may be defined as an intervention to reduce the extent of it (Solecki et al., 2005). A number of adaptive measures in response to urban heat islands have been studied by Solecki et al. (2005). The primary objective of these measures is to reduce night time sleeping temperatures as temperatures higher than the normal body temperature can induce stress on the human body. Traditional measures include:

- Wearing light coloured clothing
- Reducing indoor cooking/ increasing outdoor cooking
- Use of fans and wet clothes by windows
- Finding places to sleep outside

However, the most recent adaptive measure to heat islands is the use of indoor air-conditioning.

2.3.5.1 A cool material

A 'cool material' is characterised by having a high solar reflectance value and a high thermal emittance value as previously mentioned in Section 2.2.4. The use of materials presenting these two characteristics, contribute to increasing the urban albedo which is considered to be one of the more promising techniques to mitigate the heat island effect (Santamouris et al., 2011). Cool surfaces (cool roofs and cool pavements) along with urban trees can have a significant effect on urban air temperature, therefore reducing cooling energy use and smog (Akbari et al., 2001, Taha, 1997a). Urban trees can improve urban air quality through the direct uptake of pollutants (Taha, 1997a). The effects of modifying the urban environment in this way are quantified in terms of 'direct' and 'indirect' contributions (Akbari et al., 2001). The direct effect of planting trees around a building or using reflective materials on roofs is to alter the energy balance and cooling requirements of that building. Indirect effects are as a result of albedo modified throughout an entire city producing city-wide changes in climate. Cool materials can be divided into two main categories; cool roofing materials and cool paving materials.

Fig. 2-22 illustrates the methodology used to analyse the impact of heat island mitigation measures, such as shade trees, cool roofs and cool pavements, on energy use and urban air pollution. The mitigation of urban heat islands can be achieved by increasing the albedo of the surface and by planting trees in urban areas (Rosenfeld et al., 1995, Boriboonsomsin and Reza, 2007). The implementation of these strategies could have a number of positive effects such as reducing the need for air conditioning and reducing health problems.

The incorporation of higher albedo surfaces into the urban environment could be achieved by using lighter coloured roofing materials on new developments or by painting roofs and shingles lighter colours as used in the USA (Solecki et al., 2005). Pavements can be made lighter in colour by the use of white or light coloured aggregate in an asphalt binder such as quartz, white stone or white marble (Bretz et al., 1998).

In addition to aggregates, the use of a lighter cement in concrete is more important than the aggregate as the aggregate tends not to be exposed, and in particular white cement is more likely to produce a concrete which is lighter in colour. A concrete containing white cement will have an approximate albedo of between 0.68-0.77 when new (Levinson and Akbari, 2002).

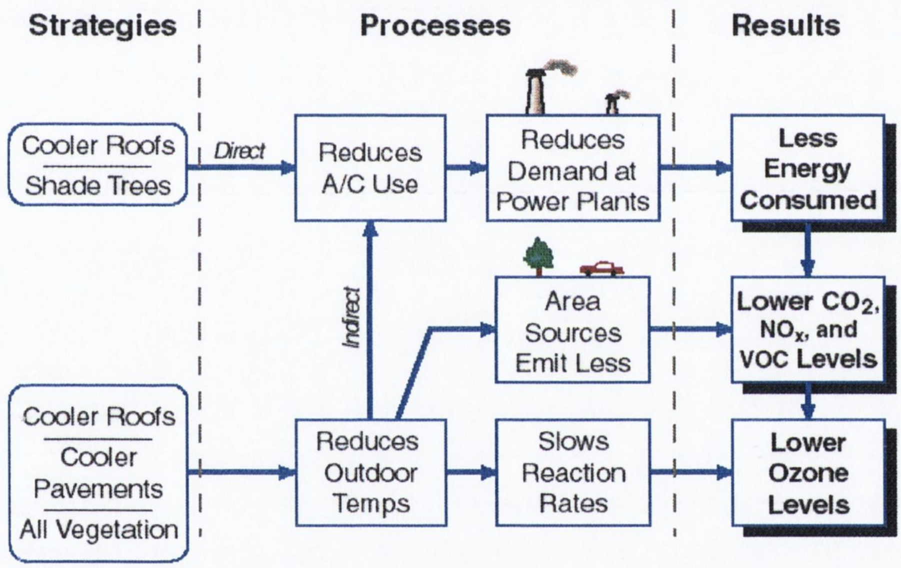

Fig. 2-22 Methodology used to analyse the impacts of heat island mitigation measures on energy use and urban air pollution (Akbari et al., 2001)

2.3.5.2 Cool Roofs

Cool roofs can lower the energy flux which enters into the building through the roof. This is governed by three factors, namely the solar reflectance, infrared emittance and thermal insulation of the roof (Boixo et al., 2012). The insulation in a roof defines how much energy will go through the roof as a result of the heat absorbed by the roof from the sun. Insulation is quite expensive as this factor depends on the physical constitution of the material, however, the solar reflectance value can be altered by the utilisation of highly reflective materials.

Cool roofing involves using materials which have both high solar reflectance and high thermal emittance. These properties are outlined in Section 2.2 and 2.1.2 respectively. There are two types of cool roofing; a low slope roof and steep slope roof. A low slope roof has a slope of no more than one in twelve and is generally used for industrial buildings such as warehouses. A steep sloped roof has a slope greater than one in twelve and is found on residential buildings using materials such as composite shingles and metal roofing in the USA and roofing tiles or slates in Ireland.

There are two options for low-slope roofs; these include coatings and single-ply membranes. Cool coatings are surface treatments with the consistency of paint, however, with superior characteristics such as their ability to 'self wash' and high durability. The two main types are elastomeric and cementitious which are both bright white in colour with a solar reflectance of 0.70 or higher when new and a thermal emittance greater than 0.8 (Santamouris et al., 2011). The coating has no effect on the roof's insulation and in general the cementitious coatings tend to be more problematic when it comes to sticking to the roof due to their brittle nature under thermal movements (Gartland, 2008). Single-ply roofing is a material which comes in a prefabricated sheet and is applied in one layer to the roof. Such cool single-ply products include thermoplastic polyolefin (TPO), polyvinyl chloride (PVC), ethylene propylene diene monomer (EPDM) and copolymer alloy chlorosulphonated polyethylene (CSPE).

Steep sloped roofs are visible in comparison to low sloped roofs, therefore contributing to the visual architecture of a building. The easiest option for a cool roof is to make it bright white by applying a cool coating, for example, which is more desirable in hot dry climates.

Research carried out by Levinson et al. (2007) indicates that non-white surfaces can be made cool by maximising reflectance in the near infrared (NIR) spectrum which does not affect the colour, and this is equivalent to maximising the solar reflectance. They state that the solar reflectance can be maximised by establishing high reflectance's in the visible and in the NIR spectra which comprise 95% of incident solar radiation. The reflectance in the NIR spectrum is maximised by colouring a topcoat with pigments which weakly absorb NIR radiation, in addition to adding a NIR reflective basecoat. A grey-cement concrete tile has low NIR reflectance, but by applying coatings of NIR scattering pigments, a NIR reflectance of 0.60 was achieved. This could be further increased by using a white basecoat, increasing the NIR reflectance to 0.85.

Xu et al. (2012) conducted research into the benefit of cool roofs using data collected from a field study in Hyderabad, India. The objective of this study was to develop a new field-based analytical method in addition to a building simulation, and to quantify the direct cooling energy savings by applying cool roof technologies to buildings. The results are displayed in Table 2-8. The data from the field-based analysis was used to estimate the potential carbon emission reductions associated with the cooling energy savings. Two side by side commercial buildings in Hyderabad, India were used for the study, both buildings having similar use and a flat 700m^2 concrete roof. The reflectance of the roofs were altered by applying various coatings to the roof of each building in different phases over the course of one year and these are highlighted in Table 2-8. There is essentially three phases over the duration of the project. The west building had a concrete roof (0.3) initially in phase 1 and a white roof coating (0.7) in phase 2 and 3. The east building also had a concrete roof initially in phase 1 (0.3), painted black (0.1) in phase 2 and then a white coating (0.7) applied in phase 3.

A number of parameters were measured including indoor and outdoor air temperatures, roof surface temperatures, roof heat fluxes, solar radiation and electricity use for the building's cooling systems. For the west building, the maximum roof temperature decreased from 54.7°C in phase 1 to 41.2°C in phase 2 following the application of the white coating on the concrete roof. It decreased to a further 38.3°C in phase 3, where the white coating remained on the roof, with the outdoor temperature decreasing to approximately 27°C. For the east building, the maximum roof surface temperature increased from 54.7°C to 71.3°C after the black coating was applied to the concrete roof in phase 2 and decreased to 39.6°C once the roof was coated white in the final phase (see Table 2-8).

Table 2-8 Results of buildings monitored in Hyderabad, India (Xu et al., 2012)

Parameters and performance metrics	West building	East building
Roof Coatings and corresponding solar reflectance value for each phase	Concrete roof **(0.3)** to white roof **(0.7)** to white roof **(0.7)**	Concrete roof **(0.3)** to black roof **(0.1)** to white roof **(0.7)**
Roof area (m^2)	700	700
Maximum roof-surface temperature	**(°C)**	**(°C)**
Phase I (Jan-March)- (Pre-coating)	54.7	54.7
Phase II (March-July)- (Post-coating)	41.2	71.3
Phase III (August-Dec)- (Post-coating)	38.3	39.6
Roof heat flux	**(W/m^2)**	**(W/m^2)**
Phase I - Peak	12.8	11.0
Phase II - Peak	12.6	21.9
Phase III - Peak	7.6	8.6
Phase I – Average between 9am-5pm	2.2	2.8
Phase II – Average between 9am-5pm	3.6	9.7
Phase III – Average between 9am-5pm	0.1	0.8
Daily air-conditioning energy use	**kWh/day**	**kWh/day**
Phase I	219	200
Phase II	285	280
Phase III	215	187

The cooling energy use was monitored from 9am to 5pm on weekdays and, when the surface reflectance changed from 0.10 to 0.70, the measured energy savings were approximately 46-50kWh/day per 700m^2 of roof area (20-22kWh/m^2 of roof area per year). By changing the roof from concrete (0.3) to white coated (0.7), the savings of approximately 31-34kWh/day for 700m^2 of roof area (13-14kWh/m^2 per year) were observed. The annual direct CO_2 reductions associated with cool roofs was estimated between 11-12kg/CO_2/m^2 of flat roof area per year by changing a concrete roof to a white coated roof. There were additional factors affecting the daily cooling energy demand, such as the total area of the west-facing windows in the west building which were larger than that of the east building, therefore, higher solar heat gains into the air-conditioned space in the west building were expected than that of the east building in all phases. This intensified the demand for more cooling energy use in the west building compared to that of the east building. However, this study indicated that cool roofs which have a higher surface reflectance can significantly reduce cooling energy use for buildings compared to roofs with a lower surface reflectance.

Akbari et al. (2003) conducted field research on two small non-residential buildings (14.9m^2) in Nevada, US during the summer of 2000. The roof surface albedo was measured using a pyranometer. The albedo of the concrete roof which was painted grey-green was 0.26. The roof was then painted with a white coating with a reflectance of 0.80, however, this decreased by 10% to 0.72 after only two months. The roof surface temperature was monitored in addition to temperature in the attic space and inside the building. Before the roof was coated white, the roof surface temperature was approximately 14-19°C higher than the ambient air temperature. After the coating was applied, the average daily roof surface temperature was approximately 19-22°C cooler than the pre-retrofit conditions. In both buildings, the results of the hourly data collected indicated savings of about 0.5kWh/day (33Wh/m^2). The daily air conditioning energy use for each of these buildings is about 35–40 kWh, therefore, savings as a result of implementing the reflective roofs amount to about 1% of the total air conditioning use. As the buildings were air conditioned for over 250 days of the year, the annual energy savings were estimated at approximately 100-125kWh/year equating to an annual saving of \$10-\$12.50 or \$0.67-0.84/m^2 per year. Akbari et al. (2003) acknowledge that it costs significantly more than this amount to apply the reflective coating, however, since the prefabricated roofs are already painted before arriving onsite, painting them a white (reflective) color would bring no additional cost, therefore, a reflective roof saves energy at no incremental cost.

Further research on monitoring the effects of cool roofs was carried out by Akbari et al. (2005). A total of 6 buildings in California were monitored in three different sites; a retail store in Sacramento, a school in San Marcos, and a four building cold storage facility in Reedley. The albedo of the roof areas was measured using ASTM E1918-06 (1997). The retail store in Sacramento (1400m^2) was a single story concrete building with a plywood deck roof covered with grey mineral cap sheet which has an albedo of 0.21. The albedo increased to 0.80 following the covering of the roof with a white elastomer coating. The elementary school in San Marcos (570m^2) was a single storey wood frame building with a roof covered with a grey mineral cap sheet measuring an albedo of 0.25. The roof had a white PVC single-ply membrane installed which increased the albedo to 0.79, however, this dropped to 0.65 in two months. The cold storage facility (9300m^2) was mostly covered with a black membrane with an albedo of 0.04 with the remainder of the roof area consisting of metal with an albedo of 0.30. All of the roofs were coated with a white elastomeric coating with an albedo ranging between 0.63 and 0.70. A number of parameters were monitored, including the roof surface temperature, indoor and outdoor air temperatures, air conditioning and electricity energy use. All buildings had recorded a reduction in the daily peak roof surface temperature to between 33-42°C after roof coating. In the retail store, the savings in average air conditioning energy use was approximately 70Wh/m^2/day of conditioned area (52%). In the school building the measured savings in average air conditioning energy use was approximately 42-48Wh/m^2/day of conditioned area (17-18%) and the cold storage facility in Reedley measured savings in average chiller energy use of about 57-81Wh/m^2/day of conditioned area (3-4%). Depending on the climate zone, the value of annual air conditioning savings ranged between \$0.6-2/m^2.

Some research was carried out by Synnefa et al. (2012) to estimate the impact of a cool roof on energy performance and thermal behaviour of a non-cooled school building in Athens, Greece. The building was 410m^2 and was non-insulated with an initial solar reflectance of 0.20. This value increased to 0.89 once the white elastomeric cool coating was applied. Results of onsite measurements of air temperature, relative humidity and surface temperature were combined with a numerical analysis using dynamic building simulation software to assess the thermal comfort conditions and the energy performance both before and after the application of the cool roof. The results show that after the cool coating was applied, the indoor temperature was reduced by 1.5-2°C during summer and by 0.5°C during winter. The annual energy load reduction was 40% with a heating penalty of 10%. There was a significant surface temperature reduction reaching up to 25°C during the summer.

Similarly, recent research into the high-scale implementation of cool roofs in Andalucía, Spain was carried out by Boixio et al. (2012). An estimated potential saving of 295,000kWh/year (2% of the overall residential electricity consumption) could be achieved by considering only residential areas with flat roofs, which amounts to €59m per year in electricity. A saving of 136,000 tonnes of CO_2 could potentially be avoided by a reduction in this electricity production. The numbers are calculated assuming that all of the houses use electrical heating. Boixio et al.

(2012) conclude from this research that the economical savings are significant at approximately €1/m^2/year. In addition, if radiative forcings are considered, installing cool roofs in Andalucía could potentially offset 9.44-12Mt of CO_2. Radiative forcing is reported in the climate change scientific literature as a change in energy flux in the tropopause (the boundary between the troposphere and stratosphere) and is calculated in units of W/m^2 (National_Research_Council, 2005). A negative radiative forcing (corresponding to more outgoing energy) essentially results in a cooling of the climate system. This phenomenon will be discussed in detail in Chapter 8.

The cost of applying a cool coat depends on the condition of the roof. If the roof is well conserved the cost ranges between 9 and €11/m^2 including labour costs and materials. The cost of the white paint ranges between €2.9/m^2 and €6.5/m^2 depending on the application. However, during construction or upgrade of the roof, the marginal cost of a cool roof is negligible (between 0 and €1/m^2) for a certified reflective paint (Boixo et al., 2012). Cool roofs incur no additional cost if a solar reflective surface is chosen at the time of installation (Rosenfeld et al., 1995, Bretz et al., 1998, Akbari et al., 2001), therefore a reflective roof saves energy at no incremental cost.

Some of the principal benefits of cool roofs are as follows (Gartland, 2008);

1. Improved building comfort
2. Energy and utility bill savings
3. Peak electricity demand reductions
4. Reduced air pollution
5. Reduction in the heat island effect

The possible disadvantages of implementing a cool roof are;

1. Heating penalty during winter
2. It does not negate the need for good insulation, and they cannot be compared in terms of energy savings

In general, the cooling energy savings outweigh the heating penalties since the effects of albedo in winter are smaller because of low sun angles, shorter day lengths, cloudy weather and snow on the roof (Bretz and Akbari, 1997).

The use of cool materials can also increase the lifetime of the roof as the degradation of some materials is associated with chemical reactions which increase with higher temperatures. As a consequence, the roof will experience less thermal fatigue (Berdahl et al., 2008, Santamouris et al., 2011). An example of cool roofs in Bermuda is displayed in Fig. 2-23.

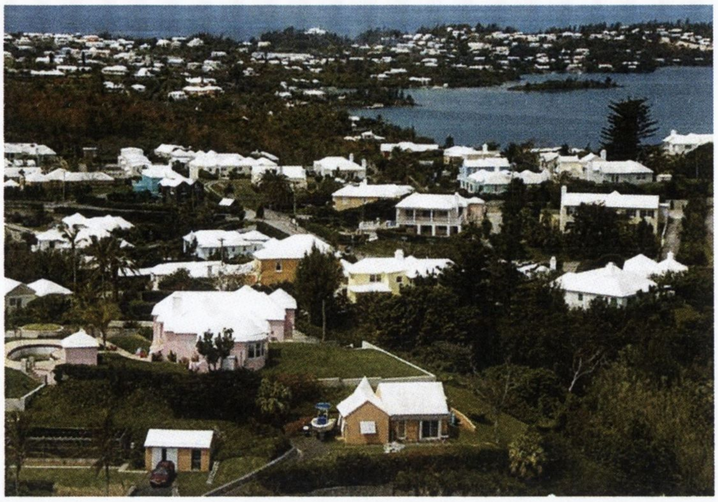

Fig. 2-23 Cool roofs in Bermuda (Boixo et al., 2012)

2.3.5.3 Cool Pavements

Pavements are essential for transportation and account for a significant percentage of the urban fabric which was evident from Table 2-7 . As with roofing materials, paving materials can reach approximately 65°C or more during a summer's day, with this excess heat radiating into the air in the UCL during the day and at night (Sabnis, 2012). Boriboonsomsin and Reza (2007) and Gartland (2008) examine the concept of cool pavements as a mitigation strategy. Cool pavements do not require new materials and can be constructed with existing paving technologies. In order to reduce the surface temperature of the pavement it is necessary to:

1. Increase the solar reflectance: There are a number of options to achieve this. The use of conventional concrete or concrete with a light coloured cement, white topping, asphalt concrete and asphalt chip seals with light coloured aggregate as used in the USA.

2. Increase permeability: Permeable pavements can be constructed from concrete or asphalt, open celled stones and gravel, the main difference being that they are mixed in such a way as to create an open cell structure. The purpose of this is to allow air and water to pass through. This can lower the temperature of the pavement through the evaporation of water.

There are two main types of pavements, namely asphalt cement concrete (ACC) or simply asphalt, and Portland cement concrete (PCC) or simply concrete. An asphalt pavement is black in colour when new, with a solar reflectance value of approximately 0.05. However, it lightens with age and this value increases typically to 0.10. An asphalt pavement absorbs solar radiation and heats up due to its dark colour. This heat is stored until it is eventually given off as the pavement cools down in the afternoon and evening (Gartland, 2008). Asphalt pavements can be lightened using light pigment or light coloured aggregates in an asphalt binder, increasing the solar reflectance by 30%. Light coloured aggregates that are suitable for asphalt pavements include high silica gravel, quartz, white stone, white marble and certain types of granite (Bretz et al., 1998). Asphalt pavements can also have white-topping applied whereby a thin layer of concrete is used to cover the existing pavement to increase the reflectance.

Concrete pavements are light grey in colour with a solar reflectance ranging from 0.35 to 0.40 when new. The pavement becomes dirty over time, reducing the solar reflectance to between 0.25-0.35. A comparison of the solar reflectance of asphalt and concrete pavements can be viewed in Fig. 2-24. Concrete can be also be applied over existing asphalt pavements through processes called white-topping or ultra-thin white-topping (Gartland, 2008). Although both the concrete and asphalt pavements age over time, the concrete pavement remains more reflective and, therefore, cooler than asphalt pavements as they store less heat in the morning and do not release as much heat back into the air in the afternoon. Concrete pavements have a higher initial cost than asphalt pavements but typically last longer and with less maintenance costs. They are especially suited to parking areas and driveways where access to underground utilities is not necessary (Bretz et al., 1998).

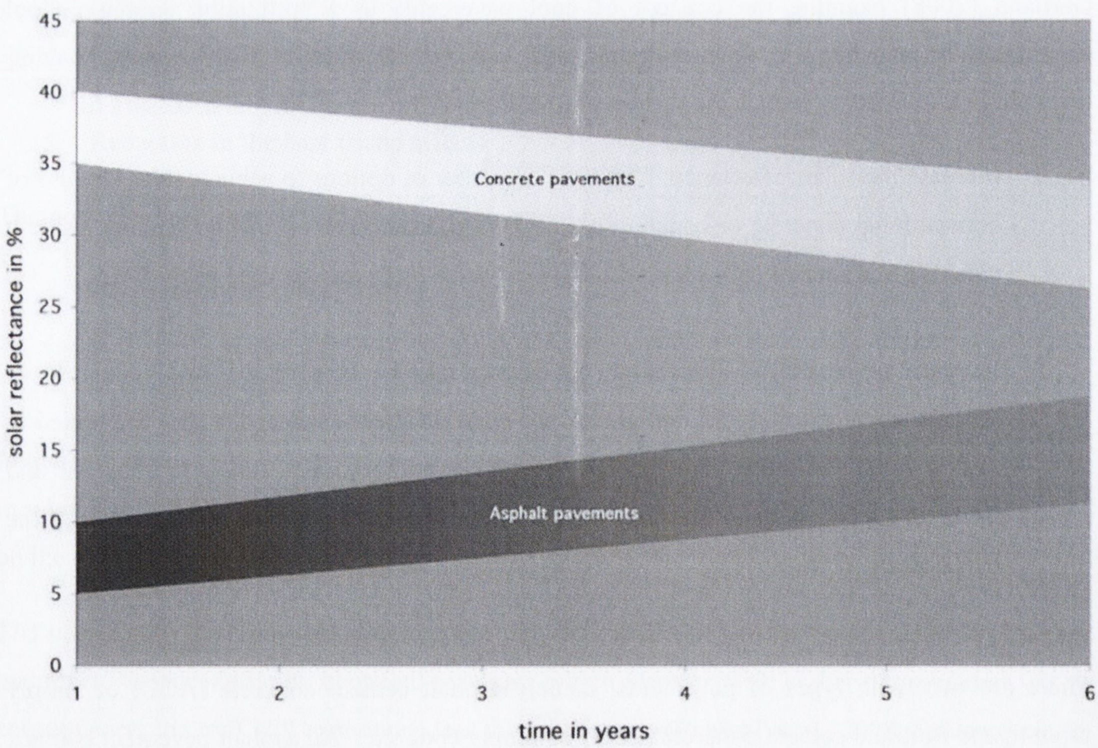

Fig. 2-24 Variation of the solar reflection of asphalt and concrete pavements over time (Gartland, 2008)

An additional method to cool either an asphalt or concrete pavement is to have permeable pavements which allow rainwater to pass through the pavement and this is stored in the layers and soil below. The water evaporates and cools the pavement on sunny days. Asphalt and concrete pavements are made permeable by excluding the fines of sand and rock from the mix creating space between the larger stones that allows the water to pass through (Gartland, 2008).

Block pavers are another type of cool pavement and these comprise lattice blocks made of plastic, metal or concrete. The blocks are laid in place over a prepared base and filled with rocks or filled with soil and planted with grass or flowers. The blocks allow water to drain, be stored and evaporate in addition to providing structural support (Gartland, 2008). They are used in low traffic areas such as car parks and driveways. Resin-based pavements use tree resin, which is clear in colour, to bind the pavement as opposed to cement or asphalt binders. Resin pavements are generally lighter in colour than other pavements and as they are clear in colour they adopt the colour of the rocks and sand that form the remainder of the pavement mix. They are used mainly as hiking and biking paths in parks (Gartland, 2008). A summary of the various pavement types is displayed in Table 2-9.

Akbari et al. (2001) carried out research into the relationship between pavement temperature and albedo at two locations in California, namely Berkeley and San Ramon. The data was recorded at about 3pm in Berkeley on new, old, and light-colour coated asphalt pavements. The data from San Ramon was taken at about 3pm on four asphalt concrete and one cement concrete pavements. The data demonstrated a linear relationship between temperature and albedo, with a 10° decrease in temperature for a 0.25 increase in albedo.

Table 2-9 Summary of pavement types (Gartland, 2008)

Material	Pavement Type	Colour/ Solar Reflectance
Asphalt	Asphalt	0.05 (new), 0.1 (old)
(ACC)	Chip Seals	0.40-0.50 (dependant on aggregate)
	Pavement texturing	
	Coloured asphalt seals and seal coats	Designed to be black
	Open-graded asphalt pavement	Dependant on aggregate used
Concrete	Portland cement concrete	0.35-0.40 (new), 0.25-0.35 (old)
(PCC)	White topping	Up to between 0.40-0.60
	Interlocking concrete pavers	Tinted with pigment
	Porous cement concrete	Wide range of solar reflectance
Other	Resin based pavement	Resin is clear in colour
	Porous block pavement	0.30-0.50 if using light colour aggregate

Research conducted into the use of reflective coatings on the building envelope, including other surfaces such as pavements and footpaths was carried out by Synnefa et al. (2006). A total of 14 types of reflective coatings applied to concrete tiles were assessed to investigate their thermal performance on a 24h basis by using temperature sensors on the surface of the sample. A spectrophotometer was also used to measure the spectral reflectance, in addition to an emissometer and infrared camera. It was demonstrated that the use of a cool coating can reduce a white concrete tiled surface under hot summer conditions by 4°C and during the night by 2°C. Similarly, Wan et al. (2009) conducted research into the effectiveness of dark coloured pavement coatings with high albedo (near infrared reflection of 81%), low conductivity of 0.252W/mK and high emissivity of 0.828. Field measurements demonstrated a reduction in surface temperature of asphalt to 38°C (a reduction of 17°C). Similarly for concrete, there was a reduction of approximately 5°C in peak surface temperature. The difference in the pavement temperature of concrete in comparison to asphalt is demonstrated clearly in Fig. 2-25. The digital photo on the L.H.S can be compared with the corresponding thermal infrared image on the R.H.S, with the asphalt pavement having a much higher temperature (pink/red) than the adjacent concrete pavement (yellow/green) on a sunny day.

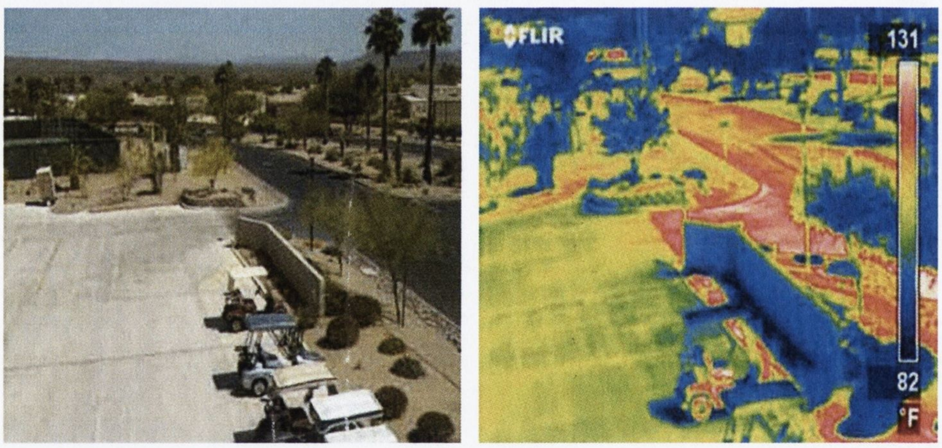

Fig. 2-25 Digital image of a concrete pavement adjacent to an asphalt pavement (left) with the corresponding thermal image demonstrating the surface temperature difference (Chao, 2010)

The benefits of cool pavements are as follows;

1. Cooler urban and suburban air temperatures
2. Better management of water run-off
3. Increased pavement durability
4. Better night-time illumination and lower lighting energy use
5. Less road noise
6. Greater flexibility and beauty in urban design

The possible disadvantages of implementing a cool pavement;

1. Concrete has a higher initial cost than asphalt
2. Concrete pavements generally have lower life cycle costs than asphalt pavements
3. For a pavement to have a high solar reflectance, lighter coloured components must be used which might not be readily available
4. Increased glare in sunshine when driving

The increased night-time illumination is evident in Fig. 2-26 where photographs were taken in Springfield Illinois at night-time of two similar malls with the same amount of lighting outside. The main difference between these images is that the left image has an asphalt surface and the right image has a concrete surface which appears much brighter as it is reflecting the light. The brighter surface does two things; it increases visibility especially at night time, and this leads to greater security and reduced lighting costs by approximately 30% (SCA, 2003).

Fig. 2-26 The albedo effect at night time demonstrating the difference between an asphalt pavement (left) and a concrete pavement (right) (SCA, 2003)

Colour has the largest influence on solar reflectance, therefore, the lightest coloured pavements are generally the coolest. However, a large increase in the albedo has the ability to create a glare and visual discomfort for drivers if not maintained at a reasonable level which in turn could also increase the amount of traffic accidents (Akbari et al., 2001). There is on-going research into cool coloured pavements which absorb in the visible part of the spectrum in order to appear darker in colour, but will reflect in the near infrared part of the solar spectrum (Santamouris et al., 2011).

On a global scale, Akbari et al. (2008b) estimate that by increasing the world wide albedo of urban roofs and paved surfaces (having a net albedo increase for urban areas of 0.1) will induce a negative radiative forcing on the earth equivalent to offsetting approximately 44Gt of carbon dioxide emissions (as discussed in detail in Chapter 8), without allowing for the carbon cost of reducing the albedo.

2.3.5.4 High Solar Reflectance Concrete

A method in which the albedo of concrete can be increased is to alter the composition of the concrete through suitable choice of cement and aggregate. Levinson and Akbari (2002) examined the correlation between the albedo of smooth concrete and cement. The albedo was measured using a solar spectrum reflectometer. They manufactured 32 concrete mixes using two types of cement, four types of sand and four types of rock. The cements used were white cement and normal Portland cement, which is medium grey. Unfortunately, as 24 of the 32 mixes had surface finishes which tended to crumble easily, their study focused only on the 8 remaining mixes. The four most reflective unexposed samples were constructed using white cement with albedo values ranging between 0.68 and 0.77. The four remaining samples which were the least reflective had results ranging between 0.44 and 0.52 and were made with grey cement.

As white cement is typically more expensive than grey cement, a cement replacement known as ground-granulated blast furnace slag (GGBS) can be used as it is lighter in colour than normal Portland cement (NPC). GGBS is a waste product from the blast furnace production of iron from ore and its use as an NPC alternative in concrete at sufficiently high replacement rates results in a concrete that is lighter in colour, thus increasing its albedo. Limited research carried out by Boriboonsomsin and Reza (2007) using 30, 60 and 70% GGBS replacement gave early indications which seem to suggest that they have increasingly higher albedo values than the conventional mix and that the albedo of concrete consistently increases as the percentage of slag increases. The samples containing 70% slag achieved an albedo of 0.58 at 14 days which is approximately 70% higher than typical conventional concrete.

2.3.5.5 Thermochromic material

A thermochromic material is one which responds thermally to the environment and changes in colour, with the process being reversible. As a result, the material is highly absorptive (when dark in colour) during the winter and highly reflective (when light in colour) during the summer which contributes to both the heating and cooling needs of the building (Santamouris et al., 2011). This reversible transformation is based on organic leuco dye mixtures with the components comprising of a colour former, which determines the colour of the material in its coloured state, the colour developer, which is a weak acid that allows the colour change, and the solvent whose melting point controls the transition temperature for the change in colour. Photodegradation is a big problem for thermochromic materials as the solar radiation causes the breaking of the polymer chains leading to loss of the reversible thermochromic effect. The cost of this material is also very high. There have been tests carried out using this material, however, this is outside the scope of this thesis report and will not be discussed further.

In summary, global climate change, in addition to the heat island effect, increases the temperature of the urban environment, and materials play an important role in determining at large the thermal balance in the environment. The use of materials containing high solar reflectance and high thermal emittance values contributes significantly to the reduction of the convective and radiative thermal gains in the environment, and as a consequence, mitigation of the heat island phenomenon (Santamouris et al., 2011).

2.4 Standards and Ratings

The use of surfaces with high solar reflectance is internationally recognised through various energy rating systems. These rating systems award credits for implementation of highly reflective surfaces and three of these will be discussed in this section, namely LEED, BREEAM and Green Globes.

2.4.1 LEED Green Building Rating System

Leadership in Energy and Environmental Design (LEED) is a green building rating system which has been developed by the United States Green Building Council (USGBC) to assess the environmental performance of a building (USGBC, 2013b). LEED certification provides "independent, third-party verification that a building, home or community was designed and built using strategies aimed at achieving high performance in key areas of human and environmental health: sustainable site development, water savings, energy efficiency, materials selection and indoor environmental quality" (USGBC, 2013b). Developed by the USGBC in 2000, LEED has evolved and is currently in its fourth version, which consists of a total of nine ratings systems. These nine ratings are grouped to form five major categories, namely Green Building Design and Construction, Green Interior Design and Construction, Green Buildings Operations and Maintenance, Green Neighbourhood and Development and Green Home Design and Construction (see Fig. 2-27).

LEED is a credit-based system whereby points are awarded relative to performance under the aforementioned categories. There are 100 base points distributed across five major credit classifications: Sustainable Sites, Water Efficiency, Energy and Atmosphere, Materials and Resources, Indoor Environmental Quality and an additional 6 points for Innovation in Design as well as 4 additional points for Regional Priority. Ratings are determined by the total number of points recorded in each category and a given building can qualify for four potential levels of LEED certification as follows: Certified (40-49 points), Silver (50-59 points), Gold (60-79 points) and Platinum (greater than 80 points).

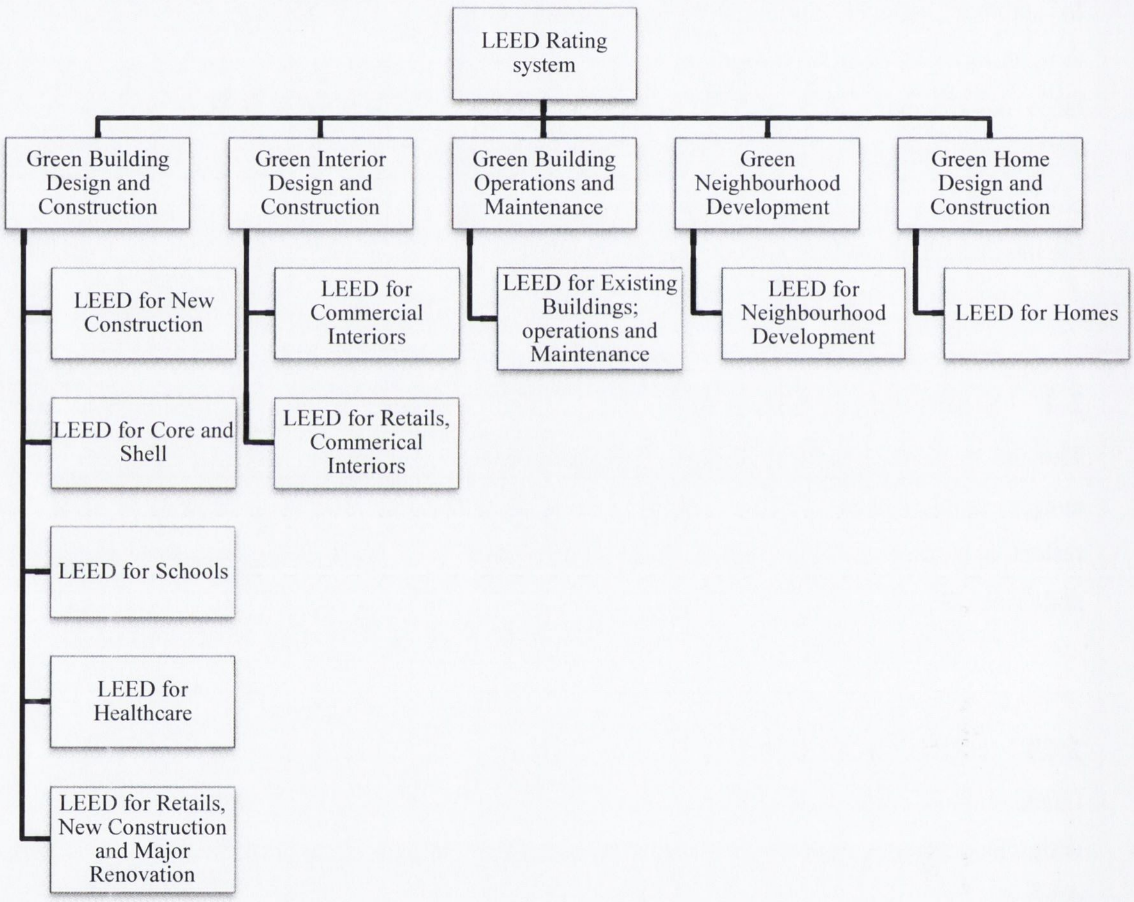

Fig. 2-27 The main categories and sub categories under the LEED rating system

2.4.1.1 LEED and Solar Reflectance Index (SRI)

The use of concrete in construction can increase the number of LEED points achieved, in particular, the two relevant credits to note are credit 7.1 and 7.2, which correspond to the heat island effect for a roof and non-roof. These credits can be achieved as follows;

- The non-roof credit is worth 1 point and involves the use of hardscape materials having an SRI required value of at least 29.
- The roof credit is worth 1 point and involves using roofing materials with an SRI value equal to or greater than the required value calculated (which is dependant on the slope and the calculation is outlined in the standard), for a minimum of 75% of the roof surface.

2.4.2 BREEAM

BREEAM (Building Research Establishment Environmental Assessment Method) is the most widely used environmental assessment method for buildings in the world and was first launched in the U.K in 1990 (BRE-Global, 2012). BREEAM has been regularly updated over the years and can be applied to a range of building types and designs. It is now applied in its various forms in over 50 countries. There are 5 main schemes for BREEAM (see Fig. 2-28). BREEAM Communities is the main category of relevance as it is concerned with the social and economic impacts of development. It contains 5 main categories plus a sixth category for innovation.

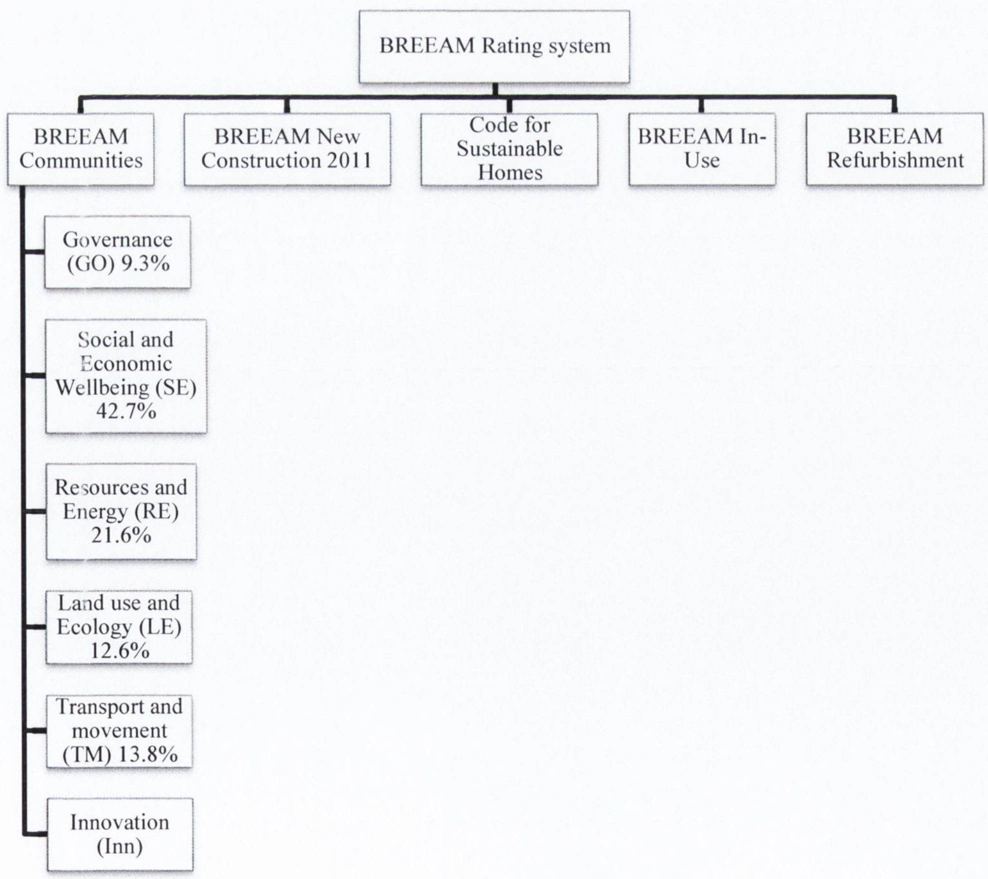

Fig. 2-28 The main categories and sub categories (for BREEAM Communities) under the BREEAM rating system including the percentage weighting of each category

Credits are awarded in the listed categories according to the assessed performance of the building against the assessment criteria. These credits are totalled to produce a single overall score. The BREEAM rating benchmarks for the BREEAM Communities 2012 scheme are as follows; outstanding (≥85%), excellent (≥70%), very good (≥55%), good (≥45%), pass (≥30%), unclassified (<30%). An additional 1% can be added to the final category score to which the innovation is most relevant. The maximum number of 'Innovation credits' that can be awarded for any one development proposal assessed is 7. Therefore, the maximum available score achieved for innovation is 7%.

2.4.2.1 BREEAM and the heat island effect

Within the social and economic wellbeing (SE) category, there is a subcategory "SE10: Adapting to climate change" and there are 3 credits available here (with an overall weighting of 2.7%). The aim of this category is to ensure a development is resilient to the known and predicted impacts of climate change.

- Credit 1 requires that evidence has been used from the local authority and statutory bodies to understand the known and predicted impacts of climate change for the site. An impact of climate change which should be considered is increased temperatures (including the heat island effect), or changes in ground conditions.
- To obtain up to 3 credits, the masterplan takes account of the evidence of impacts of climate change on the site and demonstrates in the design plans how the risks will be reduced through the use of 'win-win' measures. A win-win measure delivers benefits in addition to climate change adaptability and these could include;
    - Reducing more than one impact of climate change. For example, helping to reduce the heat island effect whilst also reducing flood risk.
    - Reducing the contribution of the development to climate change. For example, reducing the need for electric cooling and therefore reducing carbon emissions.

One such method specified for adapting to or reducing the heat island effect includes providing external finishes that are designed to avoid heat absorption. The standard, however, does not specify a minimum SRI value for surfaces.

2.4.3 Green Globes

The Green Globes system was introduced by The Green Building Initiative (GBI) in the United States in 2004. It was adapted from a Canadian protocol of the same name, which evolved through an iterative process from BREEAM Canada (G.B.I, 2013). Green Globes is a web-based program for green building guidance and certification and assesses the overall environmental performance and sustainability of commercial buildings. The Green Globes system provides higher levels of achievement based on the number of points a building acquires. Those buildings that achieve 35% or more of the 1,000 points possible in the Green Globes rating system are eligible candidates for a certification of one, two, three, or four Green Globes as follows; 85-100% (4 globes), 70-84% (3 globes), 55-69% (2 globes) and 35-54% (1 globe). There are three main categories (see Fig. 2-29), however, the category of relevance to this research is Green Globes for New Construction as it contains the sub heading 'site'. The Green Globes for existing buildings or the Green Globes continual improvement of existing buildings for healthcare do not contain this category.

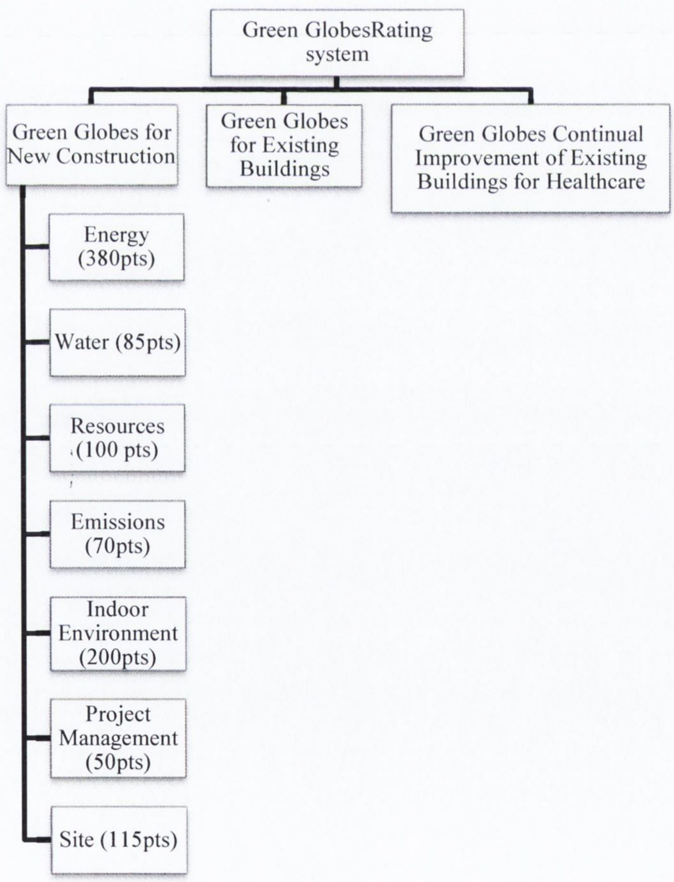

Fig. 2-29 The main categories and sub categories under the Green Globes rating system including the points awarded for each category

Under the 'site' category, there is an opportunity to attain up to 7 points by reducing the heat island effect. These credits are under the category of 'Minimization of ecological impact' and the requirement is;

1. Specify measures to reduce heat build-up on the roof, either by using high-albedo roofing materials (reflectance of at least 0.65 and emissivity of at least 0.9) for a minimum of 75% of the roof surface, or by constructing a green roof, or by a combination of both high-albedo materials and a green roof.

A further 7 points may be obtained by carrying out the following criterion which also has an indirect affect on the heat island effect;

2. Ensure at least 35% of impervious surfaces be shaded - preferably with trees, shrubs or vines

In conclusion, each of the three aforementioned rating systems provide an incentive for owners of buildings to reduce the heat island effect by utilising surfaces that are designed to avoid heat absorption i.e. a surface which has a high SRI value. The individual credits awarded for the implementation of these strategies is small when the entire rating system is considered, however, the impact on the environment could be quite significant in terms of a reduction in surface and air temperatures.

2.5 Concrete and Ground-Granulated Blast Furnace Slag (GGBS)

2.5.1 Normal constituents of concrete

Concrete is a composite material made from cement, water and aggregate. Portland cement was invented in 1892 by Joseph Aspdin of Leeds and it took this adjective as it resembled Portland stone (Tilley, 2004). It comprises approximately 80% limestone and 20% clay/shale. To make cement powder, the raw materials are ground together with water to form a slurry which is then heated in a kiln to 1500°C, firstly to dry off the water and secondly to decompose the calcium carbonate. The reaction products partly melt to produce clinker, which is then ground finely when it is cooled. Finally 2-5% gypsum is added to produce the grey cement powder best known as the binder in concrete.

2.5.2 Ground Granulated Blast Furnace Slag (GGBS)

Ground-granulated blast furnace slag (GGBS) is a by-product from the blast furnaces used to produce iron. Blast furnaces are fed with a controlled mixture of iron-ore, coke and limestone, and when these components melt (at approximately 1500°C), both molten iron and molten slag are produced. The process of granulating the slag involves cooling the molten slag through high pressure water jets which rapidly quench the slag and form granular particles. The granulated slag is further processed by drying and grinding in a rotating ball mill to a very fine powder called GGBS (Siddique and Khan, 2011).

The colour of concrete is principally determined by the colour of the cementitious material. GGBS is an off white powder and its use, particularly at levels of 50% or above, lightens the colour of concrete (The_Concrete_Society, 2011). GGBS can be used as a direct replacement for ordinary cement on a one-to-one basis by weight (Siddique and Khan, 2011), with replacement rates varying from 30-85%. In general, 50% is used in most applications and high replacement rates of 70% in Ireland are used in specialist applications, such as structural concrete, where the need to reduce the heat of hydration is necessary. As a waste material and as the embodied CO_2 of Portland cement is so high (1 tonne of cement produces approximately 800kg of CO_2 (Neville, 1995)), there are natural advantages to using GGBS. However, the slower hydration rate means curing times have to be longer, which does not suit the precast concrete industry. But, the subsequent lower peak temperatures in GGBS concrete make thermal cracking much less likely. In addition, the contrast in colour between GGBS and ordinary concrete is evident in Fig. 2-30 which has obvious advantages for albedo.

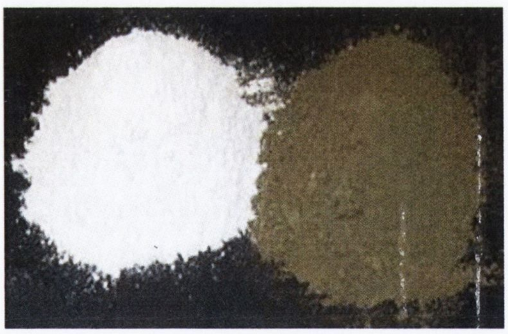

Fig. 2-30 Colour contrast of GGBS (left) and ordinary cement (right) (Ecocem, 2009)

The albedo of concrete containing various cement substitutions is displayed in Table 2-10. Traditional concrete, when new, has an albedo ranging between 0.35-0.40, however, this value decreases with age. It is evident that concrete containing GGBS in sufficiently high concentrations yields a higher albedo, however, this is based on one limited study. The albedo of concrete containing white cement ranges between 0.68-0.77.

Table 2-10 Albedo values for varying concrete surfaces

Surface	Material	Albedo	Source
Concrete	Concrete (new)	0.35-0.40	(Bretz et al., 1998)
	Concrete (aged)	0.25-0.30	(Bretz et al., 1998)
		0.22	(Solanki, 2008)
	Concrete (30% GGBS)	0.36	(Boriboonsomsin and Reza, 2007)
	Concrete (60% GGBS)	0.54	(Boriboonsomsin and Reza, 2007)
	Concrete (70% GGBS)	0.58	(Boriboonsomsin and Reza, 2007)
	Concrete (white cement)	0.68-0.77	(Levinson and Akbari, 2002)

2.5.3 The influence of mix constituents, finish type and age on concrete albedo

2.5.3.1 The influence of cement type on albedo

As mentioned previously in Section 2.3.5, Levinson and Akbari (2002) conducted a study where the variation with composition and environmental exposure of the solar reflectance of Portland cement concrete pavements was investigated through laboratory fabrication and exposure of concrete. The cement types used in this study were white Portland cement and grey Portland cement. The values of solar reflectance were recorded using a solar spectrum reflectometer. However, as stated previously, due to improper casting, 24 of these mixes were substandard and consequently rejected. Of the remaining eight mixes, the four most reflective unexposed concretes were made with white cement (0.68-0.77) and the four least reflective unexposed concretes were made with grey cement (0.44-0.52). Levinson and Akbari (2002) concluded that the albedo of white cement concrete was significantly higher than grey cement concrete. The albedo of the most reflective white cement smooth concrete was 0.18 to 0.39 higher than that of the most reflective grey cement smooth concrete. White cement, however, is typically twice as expensive as grey cement (Levinson and Akbari, 2002, Bretz et al., 1998).

A similar study carried out by Boriboonsomsin and Reza (2007) in Ohio focused on methods of creating high albedo concrete for use in pavement applications by making concrete whiter through the replacement of cement with whiter constituents. The study focuses on fly ash (which is a darker pozzolanic binder, a waste product of the coal-fired electricity generation industry) and slag in particular. The levels of GGBS replacement used were 30, 60 and 70% and the levels of fly ash were 24, 30 and 60%. The top surface of the samples were measured for albedo at 14 days in accordance with ASTM C1549 (2009), using a portable solar reflectometer. Results showed that concrete mixes containing fly ash all had lower albedo values than conventional concrete, but with no consistent trends. The mixes containing GGBS, however, recorded a higher albedo than the conventional concrete mix and the albedo value consistently increases with the increase in the level of GGBS replacement. The samples containing 30, 60 and 70% GGBS recorded albedo values of 0.36, 0.54 and 0.58 respectively. The albedo of the 70% mix (0.58) is an increase of approximately 70% in comparison with conventional concrete which recorded an albedo of approximately 0.34. Thus, concrete containing substantial percentages of GGBS, is lighter in colour than concrete made with conventional Portland cement, particularly with higher levels of GGBS (Neville, 1995).

It is the significant contrast in colour of the cement which is of particular interest to this research. As outlined in Section 2.2 and 2.3, the implementation of a material with a higher solar reflectance, is a mitigation technique for the urban heat island effect. In terms of concrete, the colour of the concrete can be made brighter by using cement which is whiter in colour such as GGBS. Substitution rates of up to 70% GGBS will be used for this research project.

2.5.3.2 The influence of aggregate type on albedo

Asphalt is a widely used material in the construction of roads and has a very low albedo of 0.05 when new. As it wears over time, the aggregate in the road becomes exposed and oxidation causes the binder to fade, resulting in an albedo increase which is evident from the published albedo values presented in Section 2.2.3 (Bretz et al., 1998). One technique for light coloured pavements is to use white or light coloured aggregates in an asphalt binder. Light coloured aggregates that are suitable for asphalt pavement mixtures include high silica gravel, quartz, white stone, white marble and some types of granite (Bretz et al., 1998).

Similarly, Santamouris et al. (2011) state that in order to increase the solar reflectance of a pavement, amongst a number of methods, one such method is the use of white or light coloured aggregate (gravel, white stone) or pigment in the asphalt mix to increase the solar reflectance by approximately 0.3. The research carried out by Boriboonsomsin and Reza (2007) examined conventional concrete made with white sand and also with latex which are both off white ingredients. It was found that these both increase the albedo of concrete. The albedo of white sand and latex individually are 0.46 and 0.39 respectively.

There has been limited research conducted on the effect of aggregate type on albedo, however, since it has shown that the aggregate type does alter the albedo, this parameter will be investigated in this research.

2.5.3.3 *The influence of surface finish on albedo*

A rough surface is less reflective than a smooth flat surface of the same material since part of the light reflected from the rough surface returns to the rough surface and dispersed light tends to be less intensive than direct reflected light (Levinson et al., 2010b). Research carried out by Levinson et al. (2010b) involved creating solar reflective non-white concrete tile and asphalt shingle roofing materials, where analysis of surface roughness effects were performed using a spectrophotometer. They estimated that the probability for a photon reflected from a coated shingle to return to its surface is about 33.3% and that surface roughness reduces the spectral reflectance of a coated shingle by approximately 0.10.

A rough surface can result in a smaller albedo value because of geometrical effects and because air-borne particles can accumulate in depressions on the surface thereby darkening the overall surface (Bretz and Akbari, 1997). A clean smooth and solar-opaque white surface strongly reflects both visible and near infrared radiation, achieving a solar reflectance of approximately 0.85. By smoothing rough surfaces, reflectance at all wavelengths can be increased (Levinson et al., 2007).

Similarly, research was conducted into the effect of surface roughness on albedo by Berdahl et al. (1997) who state that if a surface is rough rather than smooth, a photon which is reflected once is likely to require one or more additional reflections before it escapes, therefore, the probability of absorption is increased. They demonstrated this by measuring the reflectance of a white coating which was applied to both a smooth glass substrate, and on a rough asphalt shingle (which was covered in granules). The exposed surface area of the shingle was estimated to be approximately twice its nominal area. The study demonstrated that the rough surface had only 75% of the reflectance of the smooth surface, therefore, from their results they concluded that that the roughness of the asphalt shingle contributed significantly to the low surface reflectance.

Taha et al. (1992) measured albedo on a number of samples which were painted white. Although the paint was highly reflective, it was applied to a rough surface, consequently reducing the albedo, due to geometrical effects of the surface (multiple reflections). They concluded that for the same material/colour, a rough texture decreases the albedo compared to that of a smooth texture, because a rough surface increases the possibility that a reflected beam strikes the same surface again and is absorbed. In general, a rough surface will have a higher temperature than a smooth one. The dispersion of the light rays when reflected off a rough surface is demonstrated in Section 2.1.3 which displays the difference between specular and diffuse reflection. The finish of concrete surfaces is thus assumed to have an effect on albedo and heat development, therefore, this parameter will also be investigated in this research.

2.5.3.4 *The influence of weathering and age on albedo*

The albedo of a surface changes over time due to the effects of weathering and wearing. Building surfaces are exposed to many external factors such as solar radiation, humidity, frost, dust, dirt and rain. Urban surfaces (roads, footpaths and car parks) are subject to wear effects from pedestrians and vehicles in addition to the aforementioned factors. By sloping a roof for example, this minimises the effect of dirt accumulation, water ponding and biological growth (Taha et al., 1992). In general, asphalt surfaces tend to increase in albedo over time due to asphalt oxidation. In contrast, solar reflective surfaces decrease in albedo as dirt collects on the surface (Bretz and Akbari, 1997, Taha et al., 1992).

Bretz and Akbari (1997) examined high albedo coatings on roofs at various stages of exposure to determine the magnitude of this effect. The change in albedo over time depends on factors such as the coating itself, the absorption and texture of the surface, the slope of the surface and nearby sources of dirt and debris. From the roofs monitored in this study, they estimate an average decrease of 0.15 in the first year and a more gradual decline after the first year (approximately 2%). In most cases, washing the high albedo roof coatings returns the albedo to 90-100% of the estimated original value.

Weathering is caused by surface contamination (atmospheric pollution, biological growth) and/or other alterations such as UV radiation, sudden temperature changes or moisture penetration. Synnefa et al. (2006) examined the thermal performance of 14 types of reflective coatings. Some of these coatings showed degradation in the thermal performance after a relatively short period of exposure (2.5 months), with one coating in particular becoming warmer during the second and third month of the experiment (acrylic elastomeric coating). The study concluded that coatings with good weathering and 'dirt pick up' resistance should be chosen.

Similarly, Li et al. (2013) conducted research involving the measurement of albedo on 9 test surfaces over a period of time. These comprised of three different pavement surfaces, namely interlocking concrete pavers, open graded asphalt concrete and Portland cement concrete. The colour of the pavement surface tends to change over time due to weathering and traffic (the duration of the experiment is approximately 9 months). The 9 surfaces were not exposed to any type of traffic. The albedo of the concrete pavements generally tend to decrease over time and in contrast the albedo of asphalt pavements increase slightly with time. The change in the albedo occurs mostly in the first month just after construction of the test surfaces, due to weathering. Under both continued weathering and trafficking, the change of albedo is expected to be larger, and for concrete and especially asphalt, traffic will wear the binder (cement or asphalt) off of the surface aggregate which will result in the albedo being influenced by the reflectivity of the aggregate. The effect of ageing on concrete albedo is the final parameter to be investigated in this research.

2.6 Conclusions

It is evident from the foregoing literature review that there are significant gaps in knowledge in relation to how solar reflectivity or albedo, as a phenomenon, is affected by different types of concrete constituents, and in particular, the amount of work done on the surface finish types, aggregate types, and how albedo relates to GGBS concentration and ageing. These are all areas where there is a significant absence of in-depth research. The restricted studies that have been conducted to date are not in any way comprehensive and, hence, due to rating systems, such as LEED, there is a demand coming from the infrastructure owners, particularly in sunny climates, to try to take advantage of the additional benefit of using GGBS as a consequence of its improved solar reflectance. This is the topic of this thesis, hence the objectives, as described in Chapter 1 are as follows;

1. To investigate the present knowledge surrounding all relevant aspects of physics and engineering to understand the phenomenon of solar reflectivity.
2. To evaluate the sensitivity of an albedometer and determine whether it is possible to measure the albedo of small concrete specimens, thus calibrating the instrument.
3. To design a unique and reliable test method of measuring the light reflectance of individual concrete specimens.
4. To investigate the effect of concrete constituents such as aggregate type, GGBS content, surface finish and age on light reflectance and colour of concrete by utilising a number of instruments to measure either directly or indirectly, the effect of the key parameters on the light reflectance or colour of concrete, and as a consequence, compare the various test methods.
5. To conduct a case study at Trinity College Dublin to assess the possible areas where the albedo of surfaces could be improved, and following this, to calculate the possible emitted CO_2 which could be offset against existing values and compared to existing savings.

3 Laboratory Methodology

3.1 Introduction

The following chapter is concerned with the methodology that outlines the primary objectives of the work, and as a consequence, the parameters to be evaluated. Following this, an experimental design was created based on the testing parameters and a subsequent testing regime produced, which outlines the various instrumentation utilised to examine the parameters of the concrete specimens. The chapter also concerns itself with the manufacture and placement of the concrete specimens. Extensive laboratory work was carried out, from the initial concrete design stage to the final stage of placing the finished specimens prior to being tested.

3.2 Methodology

3.2.1 Primary objectives

The objectives of this experimentation are as follows;

1. To calibrate and use an albedometer to record albedo of small scale concrete specimens.
2. To compare direct methods of recording light reflectance from the following instruments; a lux meter, an albedometer, a sphere spectrophotometer and a greyness scale.
3. To determine whether indirect methods of testing light reflectance are a viable alternative as an indicator of concrete albedo, for example, thermocouples and an infrared camera.
4. To investigate the effect of parameters such as the cement type, aggregate type, surface finish and age on concrete albedo.
5. To collect data over a number of years using various instruments to measure temperature and light reflectance of the specimens.

3.2.2 Parameters to be evaluated

An important component of this research which was outlined in the primary objectives, is to investigate the principal parameters affecting concrete albedo. There are many properties that affect the colour of concrete such as formwork type and segregation. However, there are other factors that influence the colour variation of concrete which are principally due to workmanship, and are outside the scope of this study, for example, mould oil, grout loss, laitance, curing regime, striking time and compaction (Deegan et al., 2012, Newman and Choo, 2003). Based on the findings from previous research conducted in this area, as was presented in Section 2.5, the key parameters which will be evaluated are as follows;

1. Aggregate type
2. Surface finish type
3. Cement type
4. Age

The effect of age on concrete albedo will only be discussed by virtue of a comparison between the data sets collected over the course of the project which is of 3 years duration. The three primary parameters are numbers 1-3, which will be the main emphasis in the experimental design.

3.2.3 Experimental design

Based on the objectives outlined for the project, and consequently the key parameters to be assessed, an experimental design was created and is illustrated in Fig. 3-1. It was decided that small scale concrete specimens would be manufactured, having dimensions of 300x300x60mm. As the surface is the only area of relevance for measuring albedo, the specimen did not require a large depth, therefore, they needed to be deep enough to provide sufficient rigidity and strength but also light enough to be lifted for testing purposes. The surface area was sufficiently large at 300x300mm as the specimens would be too heavy if they were made larger but also the restriction of placing them on a rooftop, their destination for testing, needed to be considered in terms of both loading and the space available. For each of these specimen types, a duplicate specimen would be created for repeatability purposes. These duplicate specimens were placed apart to determine whether there were significant microclimatic influences on the specimens.

Three aggregate types were chosen, namely crushed limestone, partially crushed limestone and sandstone. Crushed limestone is readily available in Ireland and is typically dark grey in colour. It comes directly from a quarry source where it has been blasted from the rock. It was sourced from Cement Roadstone Holdings (CRH) in Belgard. Partially crushed limestone is used very frequently in Ireland also, and was sourced from Cemex in Tullamore. This aggregate type is from a natural deposit, for example, a river or glacial deposit, that crushes down the oversize stone allowing the more rounded smaller stones to pass through. In general, the crushed limestone contains more flaky/elongated shapes whereas the partially crushed limestone is smaller and contains more rounded stones. Sandstone is a much lighter aggregate and was sourced from John A Wood in Cork. These three aggregate types are typically light in colour when compared to basalt, for example, which is not used in Ireland and is dark grey in colour.

There were four concentrations of GGBS chosen, namely 0, 30, 50 and 70%. The substitution rate of 0% was used as a baseline against which other concentrations could be compared. A substitution rate of 30% was chosen as it is used in applications where the development of strength will not be affected and is slowly becoming the normal rate of substitution due to the environmental advantages of using GGBS. Similarly, a substitution rate of 50% was chosen as it is used in applications where the development of strength will only be affected marginally and it is the most common substitution rate used in Ireland at present. A concentration of 70% was chosen as it is the maximum allowable rate of GGBS and is specified for bridges in particular.

The four surface finishes chosen are cast, screed, tamp and brush. The cast surface finish was used as baseline against which other finishes could be compared. Although a cast finish will never normally see the sun, it was chosen as the baseline finish as it is easier to control and is expected to be the surface with the smoothest finish. Similarly, the screed finish is also expected to be a smooth surface and its typical application is for a roof slab. As a contrast, a tamped finish was chosen as it is typically used for a pavement. A brush surface finish was also chosen as it is typically used on footpaths.

Therefore, the total number of specimens to be fabricated is as follows;

2 (duplicate) x 3 (aggregate type) x4 (GGBS concentration) x4 (surface finish) = 96 specimens

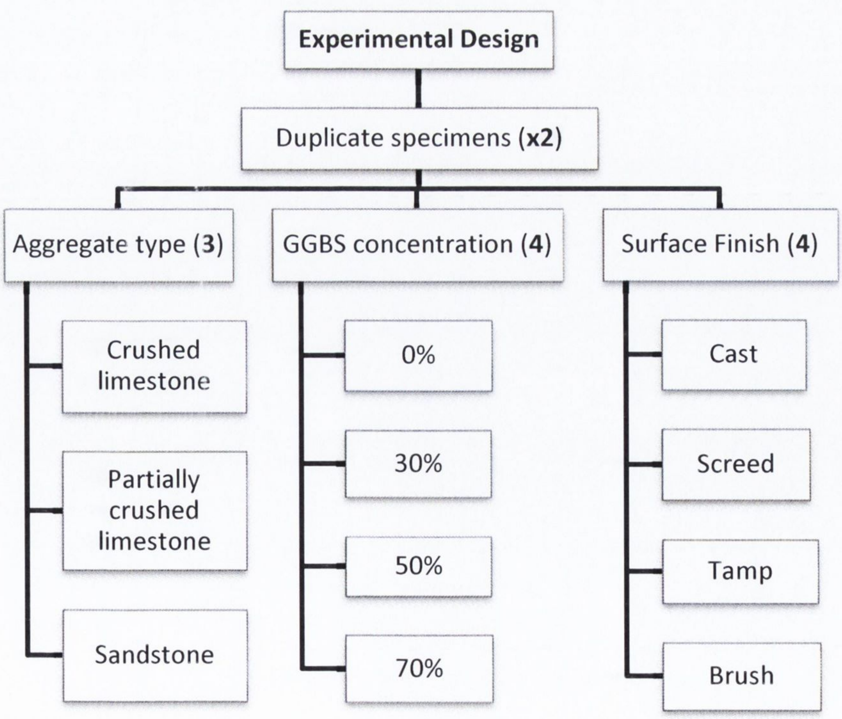

Fig. 3-1 Experimental design demonstrating all testing parameters

3.2.4 Testing regime

A test regime was established following the fabrication and placement of the concrete specimens (see Fig. 3-2). The regime can be categorised into three main groups, namely direct test methods, indirect test methods and other tests. Three of the direct test methods involve using the albedometer, sphere spectrophotometer and a lux meter, to directly measure an aspect of light reflectance off the specimens. The fourth test method is a greyness scale index which indicates the concrete 'colour'.

Similarly, the indirect test methods measure the effect of the parameters on the internal temperature of the specimens using two mechanisms, namely a thermal imaging camera and a thermocouple wire. A thermal imaging camera measures infrared emissions given off from the surface of the specimens and a thermocouple wire measures, for example, the internal temperature of the concrete and is placed prior to the specimen being cast.

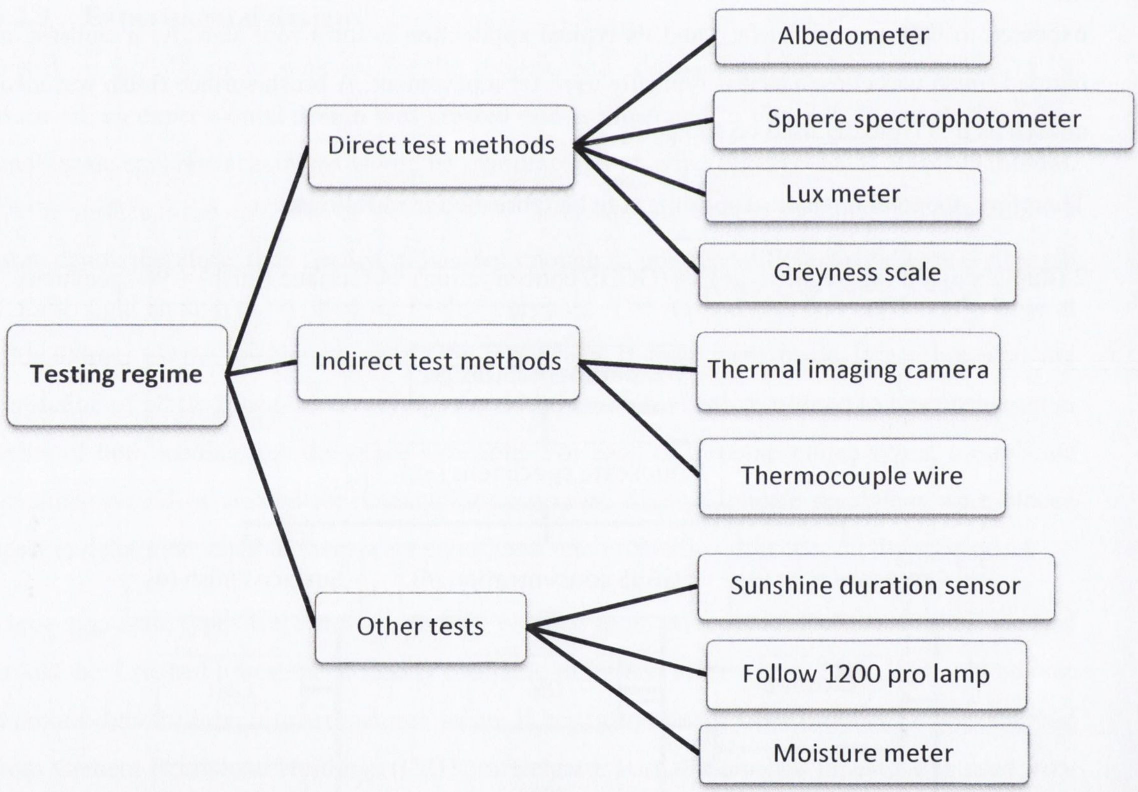

Fig. 3-2 Testing regime demonstrating direct and indirect test methods, and other tests

The other tests comprise of using a sunshine duration sensor, a heat lamp (Follow 1200 pro lamp) and a moisture meter. The sunshine duration sensor will be used in tandem with the thermocouple wires to monitor the sunshine intensity and duration, which will be compared with the temperature change in the specimens. The heat lamp will be used on a small scale preliminary experiment to demonstrate some key physical characteristics relating to the thermal properties of materials. The moisture meter will be used to determine the moisture present on the surface of the specimens at the time of testing, as moisture content of damp concrete can affect its greyness.

3.3 Concrete Mix Constituents

The primary focus of this study is to demonstrate enhanced albedo of GGBS concretes compared to a reference concrete with no GGBS present, for a variety of different concrete constituents, finishes and at different ages. Therefore, the established testing parameters for the concrete mix design are the aggregate type, cement type and surface finish.

3.3.1 Aggregate type

There are three different types of aggregates used; crushed limestone, partially crushed limestone and sandstone. It is not believed that the aggregate type will significantly affect the surface albedo, however, it was included in the study to justify the elimination of this parameter to ensure consistency throughout all test samples. There is, however, a clear differentiation in colour between, for example, limestone and sandstone (see Fig. 3-3), so the extent, if any, of the effect of aggregate type on albedo needs to be clearly determined. The limestone is a dark grey colour and sandstone is a light yellow colour.

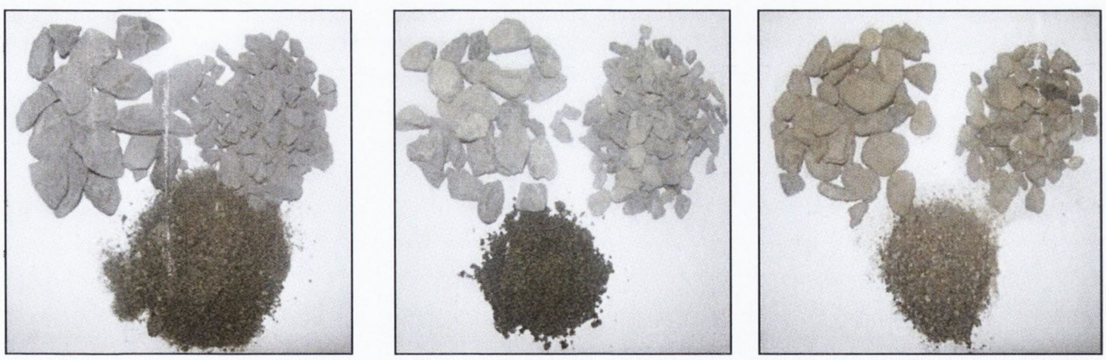

Fig. 3-3 Coarse and fine aggregates used in concrete mix: crushed limestone (left), partially crushed limestone (middle) and sandstone (right)

The coarse aggregate sizes are 20mm and 10mm and both aggregates were taken from the one batch for consistency in the concrete mix. The moisture level of the fine aggregate (sand) was measured using the 'Speedy Test' (see Section 3.4.2) in order to ensure that the same amount of free water was present in each concrete mix.

3.3.2 Cement type

There are two types of cements which are used in the concrete mixes; Normal Portland cement blended with a small percentage of limestone powder known as a (CEM II A-L) to I.S EN 197-1(2011) and the supplementary cementitious material ground granulated blast furnace slag (GGBS). There is a significant difference in colour between these two cements, with GGBS being significantly lighter in colour than CEM II A-L (see Fig. 2-30). GGBS when used as a partial replacement for CEM II A-L, at sufficiently high replacement rates, results in a concrete that is much lighter in colour, thus increasing its albedo. The substitution rates were chosen based on replacement rates in established concrete practice, as reflected also in previous research which was carried out by Boriboonsomsin and Reza (2007), who used 30, 60 and 70% GGBS replacement. The substitution rates chosen for testing were 0, 30, 50 and 70% GGBS.

3.3.3 Surface finish

Previous research carried out by Taha and Sailor (1992) measured the albedo of certain roofing materials and they concluded that for the same material or colour, a rough texture effectively decreases the albedo compared to that of a smooth texture. Based on the very limited existing research into the effect of surface roughness on solar reflection, surface roughness is investigated here. In total, four different surface finishes were chosen; generally, two rough and two smooth finishes. These surface finishes represent different application types and were achieved as follows:

- Cast (smooth) – achieved by exposing the underside (cast face) of the slab
- Screed (semi-smooth) – using a steel float to smooth and seal the surface of the concrete
- Tamp (rough) – crudely, a piece of timber is used to tamp the surface, resulting in an undulating surface
- Brush (semi-rough) – carried out by using a brush over the surface prior to final set, sweeping in one direction

3.4 Concrete Mix Design and Formwork

A concrete mix design form was completed (see Appendix A) and the concrete was specified with a characteristic strength of 35MPa at 28 days. A summary of the resulting quantities is displayed in Table 3-1. The GGBS replaced CEM II A-L, one-for-one, by percentage weight. The chosen slab size (which will be discussed further in chapter 4) was 300x300x60mm (having a volume of $0.0054m^3$) and each concrete pour consisted of fabricating a total of 8 slabs with 4 concrete cubes (of side 100mm). An additional 15% volume was added to account for the loss of material in the mixer. Therefore the mix volume for one pour is as follows;

$$[8 \text{ slabs } (0.0432m^3) + 4 \text{ cubes } (0.004m^3)] + 15\% \text{ (waste)} = 0.0543m^3$$

As there were 48 different types of specimens to be manufactured (96 in total including duplicate specimens), each consisting of a different aggregate type, cement type and surface finish, a detailed schedule of mixing was outlined to demonstrate what each pour contained (see Appendix B). There was a total of 12 pours to be completed over the duration of 3 weeks. The 8 slabs and 4 cubes were made in the morning, followed by stripping of the previous pour's slabs and cube moulds in the afternoon, in preparation for the following day.

Table 3-1 Concrete mix design quantities (per kg/m^3)

	Unit weight of mix (kg/m^3)	Pour weight per $0.0543m^3$ of mix
Cement (CEM II A-L)	410	22.26
Water	225	12.24
Fine aggregate	615	33.40
Coarse aggregate (10mm)	380	20.60
Coarse aggregate (20mm)	760	41.24

3.4.1 Trial mix

In order to establish whether the specified concrete mix design would conform to the standards required, a trial mix was conducted. The volume of water needed for the mix was calculated based on the Speedy test result. The Speedy test determines the amount of moisture present in a granular material. The sand had 5.5% water present for the trial mix, therefore, the actual water added to the mix was calculated as follows;

$$12.24L - [(5.5/100) \times 33.4kg] = 10.4L$$

This procedure of water content adjustment was carried out for the 12 pours to follow (see Appendix C for the moisture content results). It was important to ensure that all of the concrete pours had equal amount of water present as the water/cement and aggregate/cement ratios may affect the resulting colour of the concrete. All of the cement and GGBS came from one batch from the manufacturers.

3.4.2 Concrete tests

3.4.2.1 The "Speedy" Test Procedure (BS 812-109:1990)

The "Speedy" test is a method of measuring the moisture content of a material and gives accurate results in approximately three minutes. In the case of these experiments, the moisture content of the sand was required in order to account for the excess water in it as sand with a saturated surface dry condition is assumed in the concrete mix. The details of how to conduct the test are contained in the supplier's instructions or the standard BS 812-109:1990. A sample of sand and a reagent, calcium carbide, is added into the Speedy pressure chamber which is shaken when closed to ensure that the reagent reacts fully with the water in the sand. Consequently a gas is produced which increases the pressure in the chamber and the calibrated reading on the gauge on the front of the device displays a moisture content reading for a given quantity of sand.

3.4.2.2 The Slump Test (I.S EN 12350-2)

The purpose of performing a slump test is to test the workability of fresh concrete on site. The slump test was carried out for each pour of concrete in accordance with I.S EN 12350-2 (2009c). The details of how to conduct the test are contained in the standard and the results of the tests are presented in Appendix C.

3.4.2.3 Cube strength testing (I.S EN 12390-3)

The procedure for testing the cubes for the concrete's compressive strength was carried out in accordance with I.S EN 12390-3 (2009b). The details of the test procedure can be found in the standard and the results are presented in Appendix C. The range in average strength of the cubes at 28 days is between 35.4 and 47.5MPa, with the higher concentrations of GGBS content, in particular 70% GGBS, having lower cube strength due to the slower rate of strength development associated with using GGBS. One cube strength result was discarded as the range in strength divided by the average cube strength result was greater than 15% (see Appendix C).

It can also be noted that the partially crushed limestone aggregate is weaker than the crushed limestone aggregate. This result can be explained by the fact that the crushed limestone aggregate is more angular in shape, therefore, it increases the cube strength as there is better interlocking of the aggregates and increased surface area for the cement to bond with the aggregates.

3.4.3 Formwork Manufacture

3.4.3.1 Design of formwork

The formwork for the slabs was constructed according to the chosen dimensions of 300x300x60mm. A total of 18 slab forms were required to allow for consecutive days of pouring (8 slabs each day), taking into account the stripping of the moulds, and also having two supplemental forms on standby. The base of the formwork was manufactured using marine plywood which was a requirement in order to produce a smooth finish on the underside of the slab to represent a cast surface finish. The sides of the formwork consisted of a standard rough timber measuring 60x60mm in cross section which were cut to the required length.

Before the sides were fixed onto the base of the formwork using screws, a hole was drilled for the thermocouple wire to enter through the side of the slab (highlighted in red in Fig. 3-4). The thermocouple wire is set to be 20mm from the top surface for all specimens (see location highlighted in blue in Fig. 3-4). However, as one quarter of the slabs would be turned upside-down to produce a cast finish, 4 forms were manufactured especially for the cast finish slabs and marked appropriately, with the hole drilled 40mm from the top of the formwork (equivalent to 20mm from the bottom).

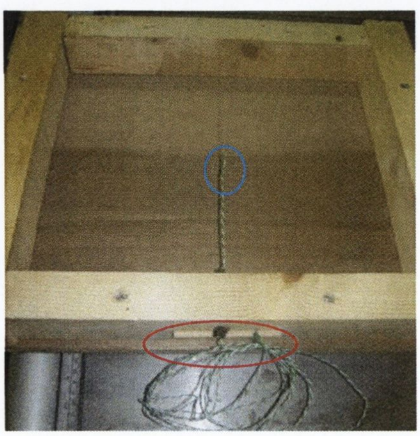

Fig. 3-4 Thermocouple wire placement in formwork

The sides of the formwork were screwed tightly into the marine plywood base to prevent any gaps allowing concrete grout to escape. This was important as surface discolouration due to grout loss had to be avoided. Following this, a piece of masking tape was placed over each screw to prevent concrete setting into it. This procedure allowed the formwork to be easily disassembled for cleaning and reuse. The formwork was prepared with de-moulding oil both on the inside and outside surfaces prior to the placement of fresh concrete, to aide in the removal of the formwork once the concrete was set.

Similarly, the plastic cube moulds (100x100x100mm) had a small hole on the bottom surface which was covered with masking tape to prevent air entering or fresh grout from escaping through it. The cube moulds were prepared with de-moulding oil both on the inside and outside surfaces prior to the concrete being placed in them. The oil made the removal of the cubes and their cleaning easier after they had set.

3.4.3.2 Thermocouple placement

Each slab required internal temperature monitoring using a thermocouple wire. Each thermocouple wire (96 in total) was cut to approximately 2.5m length from a 25m roll. This is to allow adequate distance between the slab and the data logger. Each end of the wire was stripped back by approximately 10mm to expose the thermocouple wire underneath. At one end, the two wires were twisted to make a secure connection between them. This is the location where the temperature is measured. Once it was twisted, the connection was also welded to add further security to the connection before being placed into the formwork. The other end of the wire is later inserted into a channel in the data logger which will record the temperature reading over a set period of time.

It was necessary for the thermocouple wire to be situated exactly in the centre of the slab, 20mm below the top surface as highlighted in blue in Fig. 3-4. As mentioned previously, a small hole was drilled into the side of the formwork to allow the wire to pass through. However, to overcome the problem of how to maintain the thermocouple in position while the concrete was being poured and compacted in the formwork, a fishing line was used to secure the wire in place. The fishing line was tied to a small wooden peg (circled in red in Fig. 3-4). The line was inserted into one side of the formwork and out through the other side where another peg was used to wrap the fishing line around and create tension in the line. A staple gun was then used to hold the peg in place at the side of the formwork. Once this procedure was completed, the thermocouple wire was inserted into one side of the formwork and was placed over the fishing line, with the welded part of the wire at the very centre of the slab. A couple of small pieces of additional fishing line were used to tie the thermocouple wire onto the fishing line, thus holding it in position. A glue gun was used at a number of locations along the wire for added security and it was also placed over the two holes at the sides of the formwork to act as a sealant. The wire outside the formwork was then wrapped up in a coil to avoid being accidentally pulled during casting.

To ensure this method of placement of the thermocouple wires was successful, it was tested on the trial mix specimen. One of the specimens was cut down the centre using a concrete saw to locate the thermocouple wire. As demonstrated in Fig. 3-5, the thermocouple wire can be seen in the section entering the slab on the left and running through to the centre of the slab at a depth of almost exactly 20mm (circled in red). This test confirmed that the chosen method of placing the thermocouple wires worked to the required accuracy.

Fig. 3-5 Section of concrete slab to determine location of thermocouple wire

3.5 Concrete Specimen Manufacture

3.5.1 Concrete mixing procedure

The concrete mixer was prepared for each mix firstly by pouring water in, rotating the drum, and subsequently pouring it out. The purpose of this was to prevent the mixer surface from absorbing the water from the designed concrete mix. The fine and coarse aggregates and the cement were weighed out on a scales correct to 0.001kg and the water was measured in a plastic graduated cylinder. The aggregates were previously batched out in plastic bags in advance of a pour taking place.

The batched aggregates were placed in the mixer in order according to their size- the 20mm aggregates, 10mm aggregates and sand. The lid on the mixer was closed before being turned on for approximately one minute to briefly blend the aggregates together. Following this, the cement was added and combined again until such a time as it was uniformly distributed throughout the mix. The Speedy test was carried out beforehand and an adjustment to the water was made. The water was then slowly added to the contents of the mixer through a small lid on the top of the mixer which allowed the concrete to mix continuously while the water was being added. The concrete was blended for a further 5 minutes. The finished concrete was left to stand for a further fifteen minutes. Following this, the slump test was carried out to assess the workability of the concrete (see Section 3.4.2). The slab forms and two cube moulds were placed on the vibrating table (see Fig. 3-6) ready for the placement of the concrete.

Fig. 3-6 Formwork on vibrating table (right)

3.5.2 Concrete placement

3.5.2.1 Placement of concrete in cube and slab formwork

1. The cube moulds and the slab formwork (two forms) were placed on the vibrating table (with demouling oil applied first), and half filled with concrete. Care was taken when placing concrete into the slab forms so that the thermocouple wire in the centre was not damaged. This could be easily determined as the wooden peg on the outside of the formwork which was holding the fishing line in place, would drop if the wire had broken.
2. The specimens were vibrated for 10 seconds to eliminate air voids. The vibrating time was recorded and was the same for all of the specimens. It was important not to over vibrate the concrete as this would have caused segregation of the aggregates.
3. The forms were then filled to the top before being vibrated again.
4. The cube moulds were finished off with a steel trowel to obtain a smooth finish on the surface.

3.5.2.2 *Surface finishes*

The method by which the surface finishes were obtained was important as it needed to be consistent throughout each pour. The slabs were finished off as outlined in Section 3.3. The cast surface finish was attained simply by using the underside of the slab. The top of the slab was finished off with a wood float finish. A screeded finish is normally achieved by vibrating the concrete over a 6m span. However, the screeded finish was achieved here by vibrating the concrete beforehand using a vibrating table and by using a steel trowel to seal the top surface of the concrete and to mimic this surface finish type as found on a ground floor slab or a roof slab. The width of the steel float was greater than the width of the slab which was important so that the finish could be achieved in one continuous motion. The screed surface finish (see Fig. 3-7 (a)) could be applied as soon as the concrete was compacted.

The rough surface finishes, however, could not be achieved immediately following the placement and compaction of the concrete, therefore, the specimens were initially finished using a wood float finish before being left to set for one hour. This enabled the concrete to become less workable and for initial set to occur, therefore, maintaining the surface finish. The brushed finish was achieved by dragging a brush over the surface in one direction only once. The tamped surface was attained by using a piece of timber to tamp the surface resulting in an undulating surface finish. For all of the surface finishes, the bleed water comes to the top after the concrete is finished and evaporates off the surface. (see Fig. 3-7 (c) and (d)).

(a) (b) (c) (d)

Fig. 3-7 Different surface finishes (a) Cast (b) Screeded (c) Tamped (d) Brushed

3.5.2.3 *Curing of the specimens (I.S EN 12390-2)*

The cubes were left to set and harden overnight, covered in wet hessian and a sheet of plastic to provide an optimum level of moisture to the concrete. They were removed from the moulds using an air pump (after 24 hours), labelled appropriately then placed in the curing tank of ambient temperature in accordance with I.S EN 12390-2 (2009a) for the remainder of the 28 days. These are ideal conditions for curing concrete as the water is at ambient temperature and all sides of the concrete are in contact with water.

The slabs were left for 48 hours under wet hessian and plastic (without touching the surfaces of the specimens) before being removed from the formwork (see Fig. 3-8). Following this, the slabs were covered with wet hessian and plastic for the remainder of the 4 weeks curing. These curing conditions were ideal as the concrete specimens were in a moist environment allowing comparisons to be made between the specimens.

Fig. 3-8 Slab specimens before curing

3.5.2.4 Labelling and storing of the specimens

Before the slabs were placed on the rooftop, where they would remain for the duration of the project, they were stored in the laboratory. Each slab was labelled with chalk on one side immediately following the removal of the formwork. Once the slabs were fully cured, this chalk was replaced by industrial paint (see Fig. 3-9) so that it would not wear away and so that each specimen was easily identifiable. The labelling system was as follows; initial of aggregate type, percentage of GGBS and surface finish. For example, the label of the slab at the top of the stack displayed in Fig. 3-9 (C-70-T) represents a slab containing crushed limestone aggregate with 70% GGBS and a tamped surface finish. The slabs were stacked using two pieces of timber between each one to allow them to breathe. The cast and screed surface finishes were placed at the bottom of the stack and brushed and tamped at the top. The purpose of this particular order was due to the nature of the surface finish (the undulating rough finishes could be damaged at the bottom of the stack).

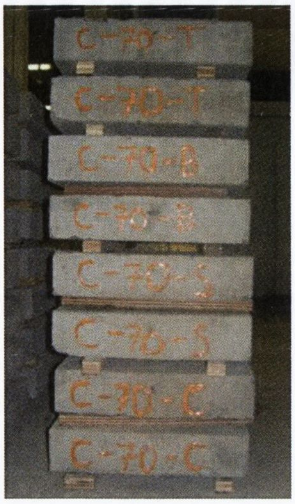

Fig. 3-9 Labelling system for slab specimens

3.6 Placement of specimens in an exposed area

A flat rooftop with low parapets was identified on campus to expose the specimens to the environment in Dublin city centre. The location of the 96 specimens to the rooftop required planning as they would be placing an additional load on the roof of the building. Normally this would not be a concern but in this instance the roof was a lightweight insulated metal deck. The following steps were carried out in order to complete this task;

1. The additional load imposed by the concrete slabs was calculated. If the imposed load was below the permitted design live load, a detailed procedure for laying out the specimens on the rooftop along the lines of the steel joists below would be necessary.
2. The method by which the slabs would be transported from the laboratory onto the roof and placed in position would require a detailed method statement as normal access to the roof was through a ceiling hatch over a stairwell which was not considered to be a safe route.

3.6.1 Loading calculation

The specimens were to be placed on plywood boards (1.2x2.4m) and based on this size, 16 specimens could be placed onto one board.

Therefore, the imposed loading on one plywood board due to 16 specimens was calculated to be 0.72kN/m^2, where the concrete density was assumed to be 24kN/m^3. As the design snow load on the roof was 0.75kN/m^2, it was thought prudent to position the boards in line with the steel joists below.

3.6.2 Layout of specimens

An image of the civil engineering building under construction was obtained (see Fig. 3-10) to assess where the columns and beams were located in the building. The purpose of this was to determine where the beams were spanning on the rooftop (see image on right in Fig. 3-10) so they could be marked out using tape on the roof. This task was necessary in order to distribute the imposed load of the specimens directly over the beams.

Fig. 3-10 Trinity College Civil Engineering building under construction (left) and roof of the building where the concrete specimens are placed

A plan of the rooftop is displayed in Fig. 3-11. For health and safety reasons (a fall hazard existed due to the low parapet wall), a 2m wide area around the parapet of the roof was identified and marked out as a no entry zone and a fall arrest system was put in place in case of an accident. On the top of the drawing, the area where an air handling unit is situated was also marked out. Therefore, after the exclusion of these two main areas, there were just 7 remaining possible areas to locate the boards where the beams below existed, 6 of which are clear in Fig. 3-11.

The air handling unit is located to the north side of the roof and the parapets are only 0.9m high, therefore, even in winter the specimens were never in shadow. However, microclimates could exist locally on the roof and pairs were placed as far apart as possible on the roof to establish if this was a cause for concern.

From this, based on the size of the chosen plywood boards (1.2x2.4m), 16 specimens could be placed on one board, making a total of 6 boards, as displayed in Fig. 3-11. The slabs were situated around the perimeter of the plywood boards, with the centre of the board being left free for the data logger to be placed when the temperature is being measured.

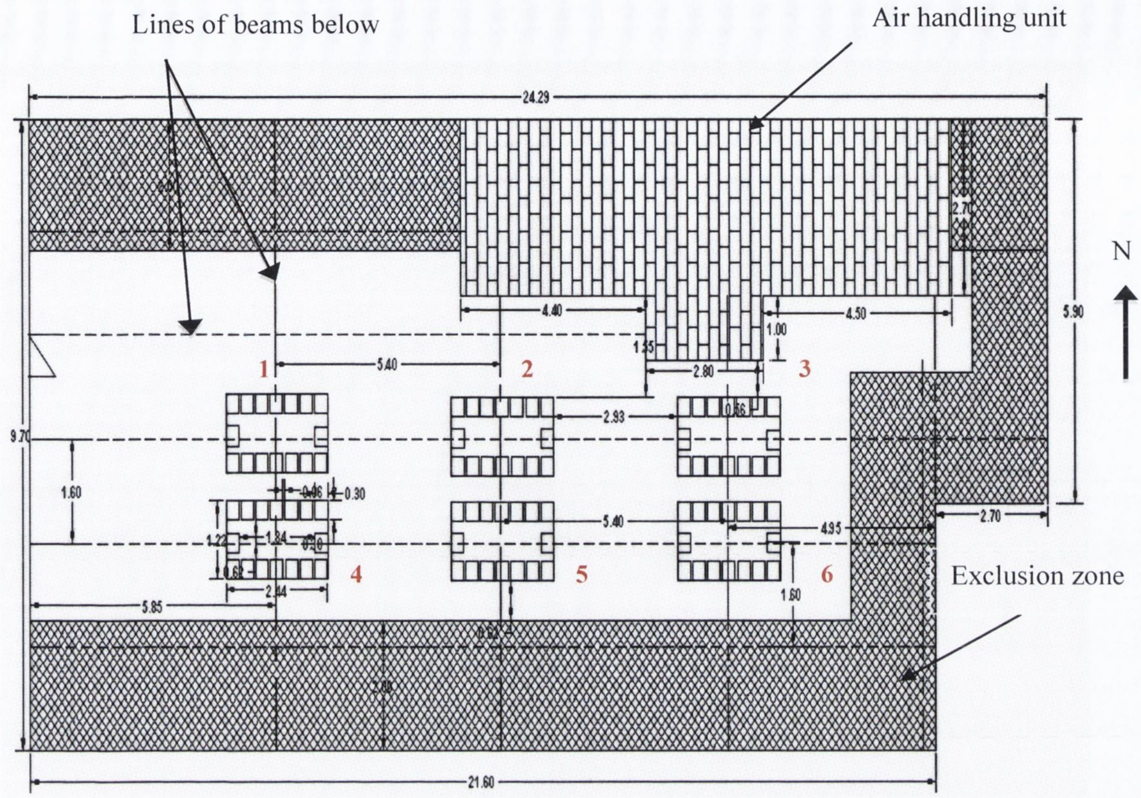

Fig. 3-11 Drawing of roof to assess location of specimens including board numbers 1-6

3.6.3 Procedure for placing the specimens on the roof

Following the establishment of where the specimens would be situated on the roof, it was necessary to decide which specimens would be located on which boards, labelled 1 to 6. Based on the knowledge that 16 specimens could be placed on one board, it was decided that the samples would be placed in situ according to aggregate type. There are three different aggregate types, with duplicate specimens, therefore, this would comprise of 6 boards in total. The duplicate aggregate boards were not placed beside one another in order to assess whether there were microclimatic differences which would affect the weathering of the samples over time.

Initially the striations on the slab surfaces were random but when the initial readings were taken, when it was realised that the reflectance off the surface varies depending on what the orientation of the slab was for the rough surfaces, they were consistently put in the one direction, that is, the striations were parallel to the direction of North-South.

The board specimens were comprised as follows (see Fig. 3-11);

1. Board 1-Limestone aggregate
2. Board 2-Partially crushed limestone aggregate

3. Board 3- Sandstone aggregate
4. Board 4- Sandstone aggregate
5. Board 5-Limestone aggregate
6. Board 6-Partially crushed limestone aggregate

A method statement was drawn up detailing the method by which the concrete slabs would be put in place on the roof. This was submitted for safety approval before permission was granted. The following steps were carried out;

1. Plastic sheeting was cut to size (1.2x2.4m) to be placed under the timber boards
2. A cherry picker was used to bring the 6 plywood boards onto the roof to put them in place with the plastic sheet being placed underneath each board.
3. The slabs were loaded onto the cherry picker, taking 8 at once. These were offloaded on the roof and were placed on the relevant boards.
4. The specimens were placed around the perimeter of the boards (see Fig. 3-12) with the thermocouple wire facing inwards towards the centre (where the data logger would be situated), the label of the slab facing outwards, and the relevant surface finish facing upwards.
5. Wooden boxes (manufactured from timber and felt) were placed in the centre of the boards to protect the thermocouple wire connectors from the environment. These had concrete cubes placed on top to prevent the wind from moving or overturning them.

Fig. 3-12 Image of concrete specimens in place on the rooftop, with the thermocouple connectors being stored in the centre

In conclusion, based on the parameters to be evaluated, a detailed experimental design was fabricated. This comprised of manufacturing appropriate concrete mixes and finishes to investigate a number of key parameters on the effect of concrete albedo including aggregate type, GGBS concentration, surface finish and ageing.

The concrete specimens were manufactured in a laboratory where parameters such as curing, compaction, moisture content and striking time remained constant. This was important as the aforementioned factors would affect the resulting colour of the concrete. Following the manufacture of the specimens, placement in an exposed area was conducted, with careful consideration as to their precise location. The next procedure following their placement in situ is to utilise some of the test methods for measuring light reflectance off the specimens, which is the topic of the next chapter.

4 Instrumentation

4.1 Introduction

This chapter focuses on the various devices which were employed/designed for testing certain properties of the specimens in relation to sunlight. The technical specification of each of the instruments is included in addition to calibration procedures for the relevant instruments. The instrumentation to be discussed in this section is as follows;

Direct (Primary) measurements:

1. Albedometer to measure the albedo/solar reflectance of a surface
2. Spectrophotometer to measure colour values of a surface
3. Lux meter to measure the incoming visible light and its reflectance from the specimen
4. Greyness scale to measure the colour or greyness of a surface

Indirect (Secondary) measurements:

1. Thermal camera to detect infrared emissions from a surface
2. Thermocouple wire and data logger to measure internal temperature of the specimens

Other measurements:

1. Sunshine duration sensor to measure intensity and duration of sunshine
2. Follow 1200 pro lamp to be used as a light source to heat up specimens
3. Moisture meter to measure the level of moisture in a concrete specimen

4.2 Albedometer

An albedometer measures the true albedo of a surface and consists of two components, an upper dome (pyranometer) to measure the incoming solar radiation and a lower dome (albedometer) to measure the reflected solar radiation (see Fig. 4-1). It measures albedo from a recommended height of 1.5m above the reflective surface. It is also a requirement that the upper dome has an unobstructed horizon. The lower sensor has a field view of 170°, so, again, a large unobstructed surface is usually sought to give an accurate reading.

As the concrete specimens are 300mm square, it is necessary to scale down and calibrate the instrument by restricting the field view of the lower dome. This is discussed in detail in Section 5.2 in addition to the sensitivity tests carried out on the albedometer. A stand was designed and manufactured specifically for the albedometer in the laboratory in Trinity College in order to support and keep the instrument level for taking albedo measurements. A timber box with handles was also manufactured to improve portability.

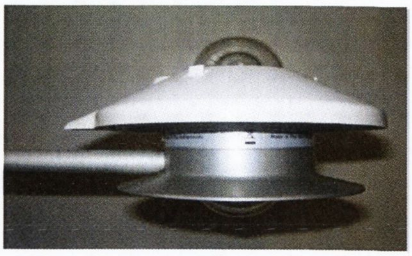

Fig. 4-1 Albedometer model CMA11 series containing upper dome (pyranometer) and lower dome (albedometer)

4.2.1 Specification of Albedometer – CMA11 series

The albedometer has the following technical specifications and was calibrated by the supply company following the manufacturing of the instrument. It complies with the relevant ISO standard (ISO 9060:1990) and is supplied with a calibration certificate traceable to the World Radiation Centre, with the device being very sensitive to irradiance change.

- Spectral range from 285-2800nm
- Sensitivity: 7 to 14 μV/W/m²
- Maximum solar irradiance: 4000W/m^2
- Field of view: Pyranometer 180°, albedometer 170°

A bubble level is fitted in the albedometer and a screw-in drying cartridge keeps the interior free from humidity.

The calibration coefficient, known by the suppliers as sensitivity (S) of the instrument, was attained at the calibration stage which was carried out by the manufacturer and the values are as follows:

- Upper dome (pyranometer) S = 8.39μV/W/m^2
- Lower dome (albedometer) S = 8.72μV/W/m^2

Accordingly, the irradiance (E_{solar}) is calculated in W/m^2 for both the pyranometer and albedometer, using the aforementioned sensitivity values, as per Equation (4-1);

$$E_{solar} = \frac{U_{emf}}{S} \tag{4-1}$$

where E_{solar} (W/m^2) = irradiance, U_{emf} (μV) = output voltage and S (μV/W/m^2) = sensitivity

For example, if the output voltage for the pyranometer and the albedometer is 5.3×10^3 μV (5.3mV) and 1.7×10^3 μV (1.7mV), the incoming solar irradiance E_i and reflected solar irradiance E_r are 631W/m^2 ($5.3 \times 10^3/8.39$) and 195W/m^2 ($1.7 \times 10^3/8.72$) respectively. The albedo value is calculated from these two resulting irradiance values.

Some typical values of incoming sunshine irradiance are as follows:

- Fully clouded (50-120W/m^2)
- Sunny partly clouded (120-500W/m^2)
- Clear and sunny (500-1000W/m^2)

These values are dependant on the degree of cloud cover, time of day, season and location.

4.2.1.1 Calculation of albedo value

Once the irradiance is calculated individually for the pyranometer and albedometer, the albedo value (between 0 and 1) is calculated as per Equation (4-2).

$$Albedo = \frac{E_r}{E_i} \tag{4-2}$$

where E_r (W/m^2) is the total reflected solar irradiation and E_i (W/m^2) is the total incoming solar irradiation. From the example above, the albedo is 0.31 (195W/m^2/631W/m^2).

4.2.1.2 Meteon voltmeter

The output voltage (U_{emf}) is measured using a voltmeter (see Fig. 4-2). Meteon is a highly accurate hand-held display unit and data logger for the measurement of solar irradiance. The specification of the Meteon voltmeter is as follows:

- Input range: ± 6.25 to ± 200 mV
- Inaccuracy: < 0.1 %

Fig. 4-2 Meteon voltmeter

4.2.1.3 *Stand for the albedometer*

For the purpose of taking readings with the albedometer, an instrument height of 1.5m and an unobstructed horizon are necessary. As the instrument weighs 1.2kg, a stand was designed and manufactured from steel (see Fig. 4-3). This stand contained a wide base for support in addition to a bracing bar under the main horizontal member to hold the instrument firmly in place. The stand can be disassembled allowing it to be transported for site measurements. There is also a sliding vertical bar which allows for lower height readings for smaller specimens if required.

Fig. 4-3 Stand for the albedometer which is necessary to keep the instrument level and the view largely unobstructed

4.3 Sphere Spectrophotometer

A spectrophotometer is the most commonly used instrument for measuring colour. It measures the amount of light energy reflected from an object at several intervals along the visible spectrum. A colour has its own unique appearance based on three attributes; hue, chroma and value (lightness). Hue is how an object's colour is perceived e.g. red, green, blue etc. Chroma describes a colour's vividness or dullness. Lightness describes the luminous intensity of a colour and the degree of lightness is called its value. Colours can be classified as either light or dark when comparing their value.

Three things are necessary in order to observe and measure a colour; a light source, an object or sample, and an observer or processer. The CIE (Commission Internationale de l'Eclairage, or the international commission on illumination) is the body responsible for international recommendations for photometry and colourimetry. One such method which the CIE recommends to measure colour and express it numerically is CIE (L*a*b*) or CIELAB.

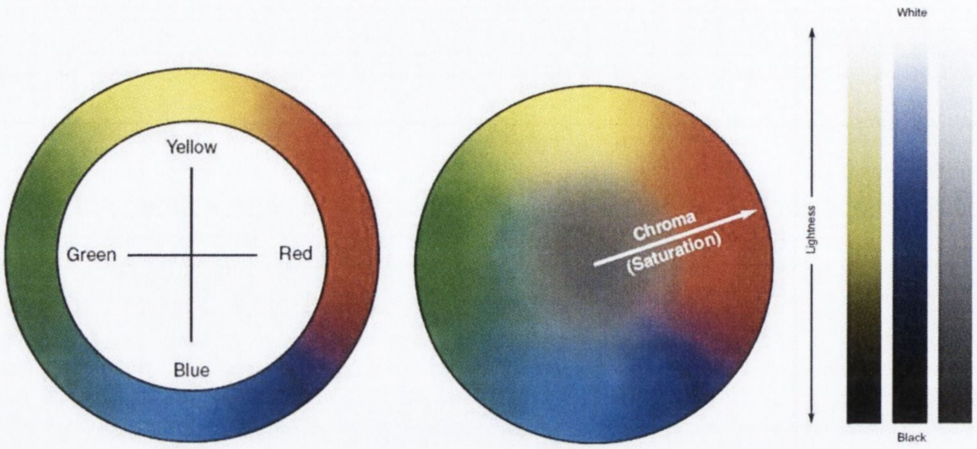

Fig. 4-4 Hue (left), chromaticity (middle) and lightness (right)

4.3.1 CIELAB method

When a colour is expressed in CIELAB form, L* defines lightness, a* denotes the red/green value and b* the yellow/blue value. Fig. 4-5 and Fig. 4-6 display the colour plotting diagrams for L*a*b*. A colour measurement in the +a* direction depicts a shift towards red and –a* towards green. A measurement in the +b* direction represents a shift towards yellow, and –b* towards blue. The centre axis (perpendicular to the page in Fig. 4-5) is represented by L*. An L* value of zero represents black or total absorption, and a value of 100 represents white, or total reflection.

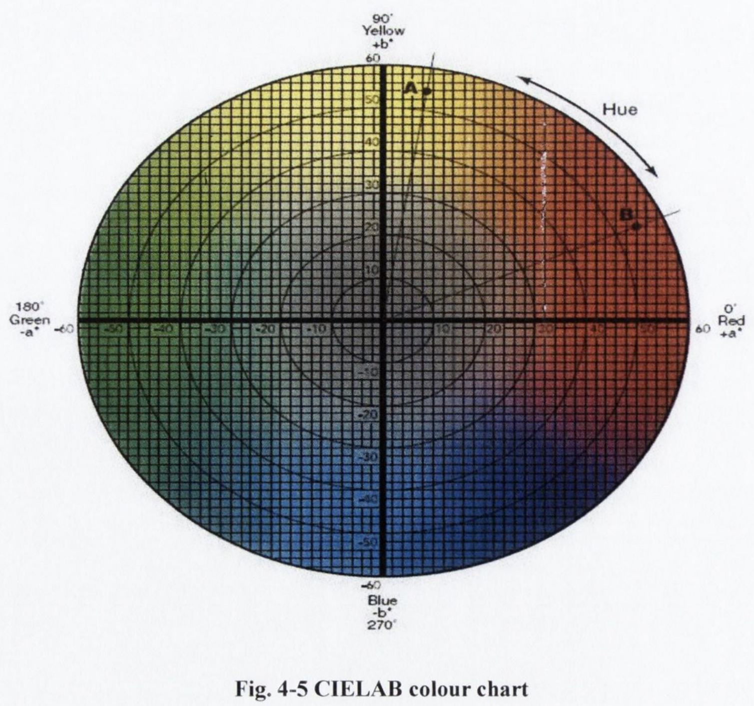

Fig. 4-5 CIELAB colour chart

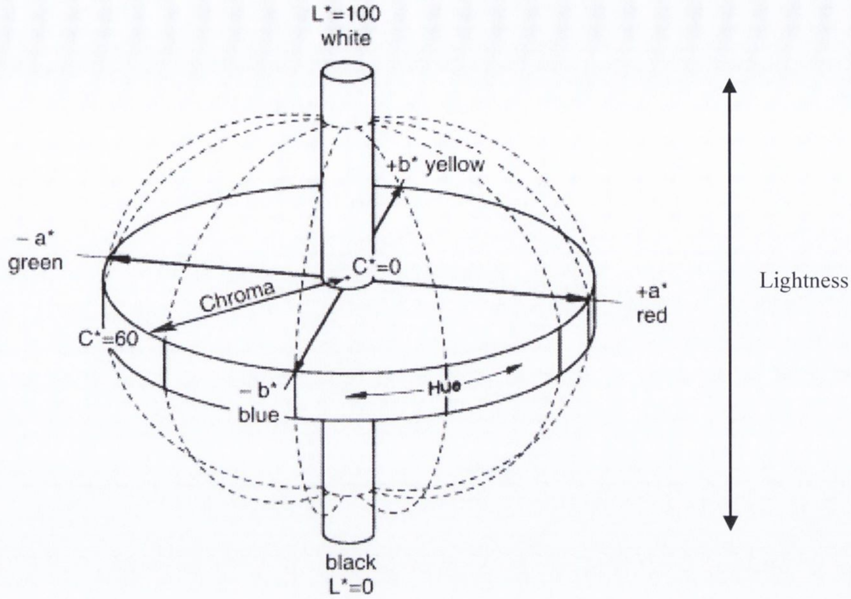

Fig. 4-6 The L* is represented on the central vertical axis and the a* and b* axes are located on the horizontal plane

4.3.2 Specification of Sphere Spectrophotometer Model SP62

A spectrophotometer measures spectral data, the amount of light energy reflected from an object at several intervals along the visible spectrum. The relevant details of the sphere spectrophotometer's specification (Fig. 4-7) are as follows;

- Spectral range: 400-700nm
- Range for L*, a* and b* readings: -60 to +60 (a* and b*), 0 to 100 (L*)
- Accuracy: 0.02

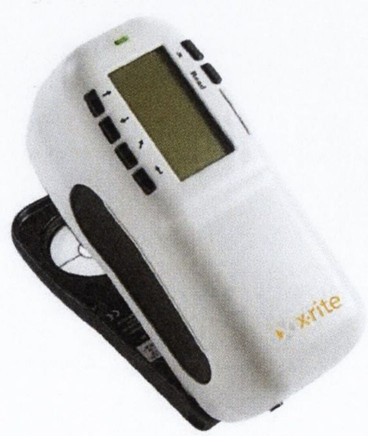

Fig. 4-7 SP62 sphere spectrophotometer

4.3.2.1 Process of taking a reading

The spectrophotometer is calibrated first before readings of L*, a* and b* values can taken. The calibration option is selected from the menu. Calibration is carried out by defining dark and light references; the instrument is placed onto the black reference surface provided with the instrument. The top surface of the instrument is then pushed down firmly against the shoe until the light is issued from the device onto the surface and the reading appears on the screen. This process is repeated for the white reference surface and the instrument is then calibrated.

In order to take a reading of L*, a* and b* values for a surface, the instrument must be placed on the surface and the mode 'analyse' is selected from the menu. The top of the instrument is placed firmly down against the shoe of the instrument and this position is held for a couple of seconds until the light is issued onto the testing surface and the reading appears on the screen. The readings for L*, a* and b* are noted at this point.

4.3.2.2 The spectral output produced by the sphere spectrophotometer model SP62

A spectrometer is an instrument used to measure properties of light over a specific portion of the electromagnetic spectrum. It was used to measure the exact output of light emitted from the sphere spectrophotometer SP62 in terms of the spectral intensity. The spectrometer used to determine this (see Fig. 4-8) has a wavelength range of 200-1100nm which encompasses the ultraviolet, visible and infrared wavelengths (StellarNet_Inc, 2013). The device has a accuracy wavelength < 0.25nm, repeatability wavelength < 0.05nm and resolution of <0.75nm.

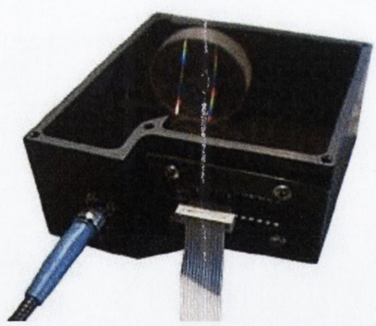

Fig. 4-8 Black comet spectrometer model C-SR-50 for UV, VIS and NIR (StellarNet_Inc, 2013)

The spectral data for the sphere spectrophotometer is displayed in Fig. 4-9 (blue line) along with the sun's direct global radiation (red line) which was obtained from ASTM G173 - 03 (2012) for AM 1.5. The AM represents air mass and 1.5 refers to the length of the path through the atmosphere in relation to the shortest length if the sun was in the apex (see Section 2.2.1 for description on Air Mass). The spectral intensity will change depending on the season, time of day and location.

As shown by the dashed lines in Fig. 4-9, a wavelength of between 10-400nm represents the ultraviolet radiation component of light. Visible light ranges between 400 and 750nm and a wavelength of between 750nm and 1mm represents the infrared component of light. The direct global radiation from the sun (red line) ranges over all three components of light as expected, with the highest intensity from the visible light. The spectrophotometer, however, produces light that primarily falls in the visible section as indicated in the specification of the instrument. This information is relevant, in particular, for Section 6, which focuses on results from a physical test carried out, where the L* was measured on a number of different materials.

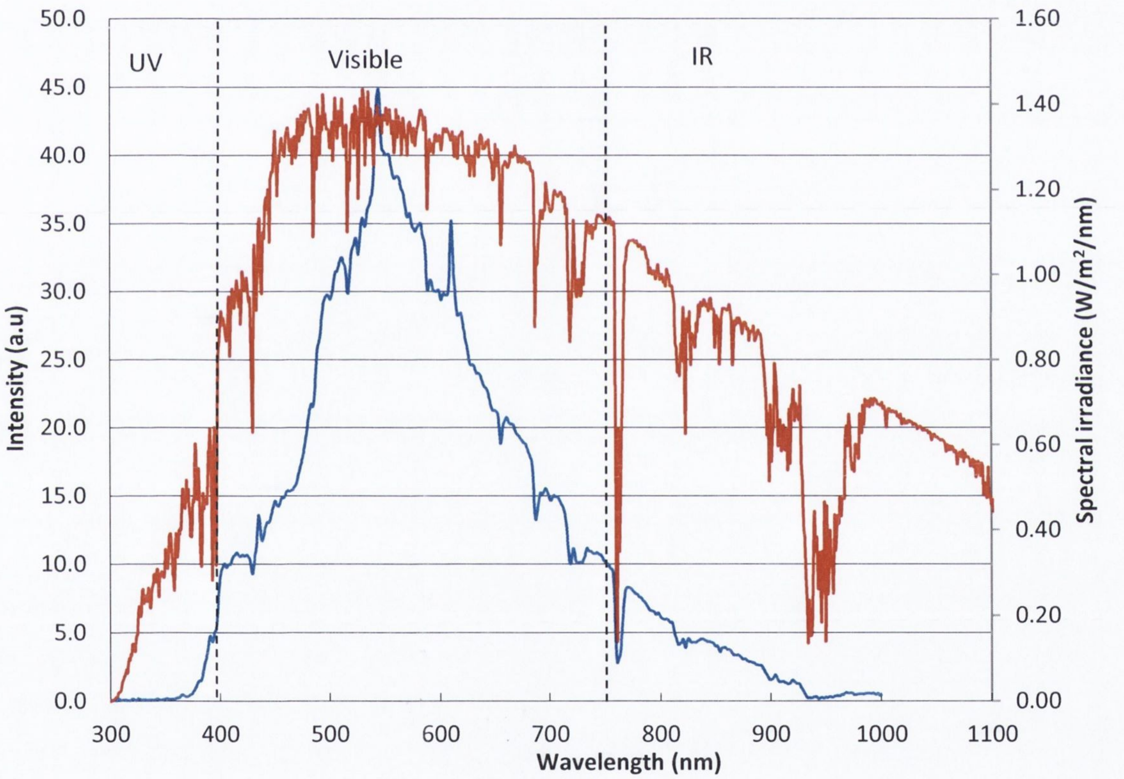

Fig. 4-9 Spectral information from a sphere spectrophotometer (blue) and direct global radiation (red) for air mass 1.5 (ASTM, 2012)

4.4 Lux meter

A lux meter is a device which measures visible light in units of lux (lumens/m^2), which is the unit of illuminance. It is frequently used by cricket umpires, photographers and lighting engineers. The digital lux meter (model LX 1330B) has a range of 0.1 to 200,000 lux and an accuracy of ±3% when reading up to 20,000 lux and ±5% thereafter (see Fig. 4-10). A typical value of incoming lux at midday in the summertime in Dublin with sunny weather conditions is between approximately 50,000 and 80,000 lux. The photo detector consists of one silicon photo diode with a filter.

When using a lux meter for reflectance off a surface, like the albedometer, it is very sensitive to background light interference, thus, as shall be shown, for the purposes of testing, it is used in conjunction with a black box specifically designed for this project to measure the visible light reflectance off a concrete slab (see Chapter 5) without such interference. The design and initial testing process are carried out to determine whether the lux meter can be used as a discerning and reliable indirect means of calculating the albedo value, and thus distinguish between different specimen reflectance characteristics.

Fig. 4-10 Digital lux meter to measure visible light

4.5 Greyness scale

As the colour of a surface has an effect on the amount of light reflected off it, it is important to examine and evaluate this parameter. This can be carried out by characterising the 'greyness' of the concrete slabs surface by using a greyness index card. A greyness scale was utilised in order to give an indication of the level of ageing of the slabs over time through subjective visual evaluation. The greyness scale (Fig. 4-11) ranges from 0% (white) to 100% (black) in increments of 5%. It is placed on the exposed surface of the slab and the percentage of greyness which matches the concrete's colour segment of the chart is evaluated and recorded (Sweeney and West, 2013).

As albedo ranges from 0% (black) to 100% (white), the greyness scale is converted to an albedo index value using Equation (4-3) as follows;

$$\text{Colour Albedo Index} = (100 - \text{greyness value})/100 \qquad \textbf{(4-3)}$$

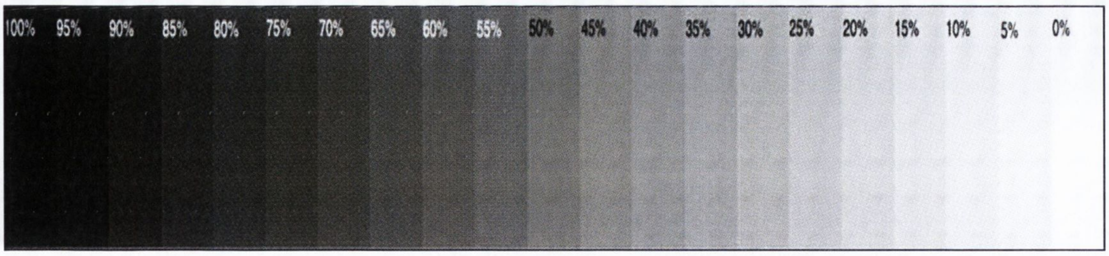

Fig. 4-11 Greyness card (Sweeney et al., 2012a, Sweeney and West, 2013); Source: (Resnik, 2013)

Concrete surface measurements using a grey scale ranging from a very light grey to a very dark grey is simple in principle, however, is problematic due to the subjectivity of the human eye and the different optical properties of concrete and paper (Lemaire et al., 2005). Although this is a colour albedo 'index', it is not a representation of the true albedo of a surface as it is a subjective visual examination, whereas the true albedo of a material factors into account the reflectance of different frequencies off the surface, which are dependant on a number of parameters such as surface roughness and the nature of the material. However, it is a quick and free means of assessing the relative values of the colour albedo index.

4.6 Thermal Imaging Camera: FLIR InfraCAM SD

A thermal image is a representation in colour of infrared radiation differences in objects. Hotter objects emit more infrared radiation for a given emissivity and so appear brighter and this can be used to demonstrate differences in a material's temperature. An infrared thermal imaging camera (see Fig. 4-12) is being used to measure surface heat development and differences between the slabs (Sweeney et al., 2012a). As the concrete slabs absorb sunlight, this is converted into heat and is reemitted as infrared radiation. Two parameters which are expected to have an effect on the radiation observed are the GGBS content and surface finish (see Section 7.5 for results).

Fig. 4-12 Thermal imaging camera; FLIR InfraCAM SD

It is a requirement to input the emissivity of the surface to be tested into the thermal camera before a thermal image can be taken. For the concrete specimens, the emissivity (ε) was set to an average constant value of 0.94 (Baehr and Stephan, 2011). In general, the emissivity of concrete ranges between 0.85 and 0.95, with a rougher surface finish having a slightly higher emissivity value (Anderson, 2006). Thermal images were recorded only when there was sufficient sunshine to allow the slabs to heat up. The thermal imaging camera has a spectral range of 7.5-13μm and an accuracy of ±2°C or ±2% of reading.

4.7 Thermocouple wire and data logger

The internal temperature of the slabs is being measured using thermocouples which were placed in the slab 20mm from the top or bottom surfaces (as appropriate) during the manufacturing process. They measure the increase in temperature inside the slab when the surface is exposed to natural sunlight and this is being used to indirectly evaluate the solar light absorption. A data logger is used to collect results (see Fig. 4-13).

The thermocouple wire used is a type K thermocouple (the most common general purpose thermocouple). A thermocouple is available in different combinations of metals or calibrations. The four most common calibrations are J, K, T and E. The type K combination of metals provides a range in temperature of approximately -200 to 1250°C.

Each slab's thermocouple is connected to one channel on a data logger. The Datascan 7220 is a 16 channel data logger with a maximum sample rate of one sample per second.

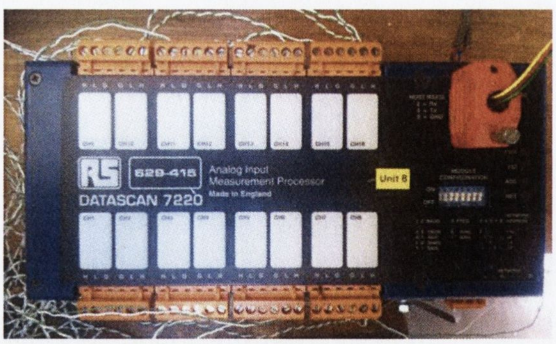

Fig. 4-13 Data logger containing 16 channels

4.7.1 Calibration of thermocouple wires

The thermocouple wires were connected to a data logger, which was in turn connected to a laptop. The software enables the user to observe real-time changes in values across all channels in the data logger. Two tests were carried out using 6 thermocouple wires. The simplest and most effective method to check the accuracy of the thermocouple wires is to measure two known temperatures of water, ice melt water, which is 0°C and steam, which is 100°C.

The first test involved placing ice cubes in a beaker and allowing the ice to melt slightly. As soon as melt water is produced, all thermocouple wires are placed in this melt water together and the temperatures were recorded. The results are displayed in Table 4-1 and are approximately 0°C.

The second test involved boiling water in a kettle and placing the wires at the nozzle where steam is produced. As soon as the kettle boiled the results were noted and the outcome of the tests are displayed in Table 4-1. The results of both tests demonstrate that all thermocouples agree well, having a temperature of approximately 100°C. Results from both the melt water test and steam test indicate that the thermocouple wires are accurate in taking measurements with the data sets having a reasonably low standard deviation.

Table 4-1 Calibration results for thermocouple wires

Wire	Melt water test (°C)	Steam test (°C)
1	-0.03	100.20
2	-0.35	100.13
3	0.38	100.16
4	0.49	100.44
5	0.57	100.20
6	0.65	100.50
μ	0.30	100.27
σ	0.38	0.16

4.8 Sunshine Duration Sensor

Sunshine duration is defined by the World Meteorological Organization (WMO) as the time during which the direct solar radiation exceeds the level of 120 W/m². The sunshine duration sensor CSD 3 operates from a 12VDC (Voltage Direct Current) power source and has built-in heaters to dissipate rain, snow and frost. The sensor is required to be mounted in the vertical plane at an angle equal to the angle of latitude within ±1° and in the direction of the nearest pole within ±5°. For the purpose of testing in Trinity College, the sensor was pointed in the direction of the north pole at an angle of 53.34°N. An unobstructed horizon is also required so the sensor was placed on the paraphet on the roof of the civil engineering building where the sample specimens are located.

Fig. 4-14 Sunshine duration sensor CSD 3

4.8.1 Specification of Sunshine Duration Sensor – CSD 3

The sunshine duration sensor has the following technical specifications and was calibrated by the company following the manufacturing of the instrument.

- Spectral range: 400-1100nm
- Sunshine signal: 1 ±0.1 V (direct radiation > 120 W/m^2)
- Analogue output signal: 1 mV/Wm^2
- Accuracy of sunshine hours: > 90% in monthly total

Some typical values of sunshine hours per day and corresponding direct irradiance values are indicated in Table 4-2 for summer and winter on midlatitude (the Earth's temperate zones between the tropics and the Arctic and Antarctic polar regions). As expected, there is significantly less sunshine hours and intensity of sunshine in winter due to the sun's altitude.

Table 4-2 Typical values for clear and sunny conditions on midlatitude (Kipp_and_Zonen, 2013)

Summer half year	12-16 hours sunshine	500-1000W/m^2 direct irradiance
Winter half year	6-12 hours sunshine	300-900W/m^2 direct irradiance

4.9 Follow 1200 Pro lamp

The Follow 1200 Pro lamp (see Fig. 4-15) was used as part of a physical test to demonstrate some key reflectance and absorption properties of materials when subjected to a light source. The results from this test can be found in Chapter 6. The lamp produces light over the three wavelengths of light; visible, infrared and ultraviolet, and mimics daylight. The exact quantities of each component of light were measured using a spectrometer (as discussed in Section 4.3). It was necessary to obtain this information so that the temperature increase on exposure to light could be interpreted correctly.

Fig. 4-15 Follow 1200 Pro heat lamp

The Follow 1200 Pro contains a 1200W HTI lamp. It contains a variable colour temperature; 3200K (tungsten light), 5600K (daylight) or 6000K (daylight), with a motorized focus and movement of pan (360°) and tilt (90°). The colour temperature of a light source is determined by comparing its hue with a theoretical perfect black body radiator. The colour temperature of the light source is the same as the thermal temperature that the black body must be heated to in order for the two to emit radiation with the same hue. The apparent colour temperature of a light source does not refer to the thermal temperature (Malpas, 2007).

4.9.1.1 The spectral output produced by the Follow 1200 Pro light

A spectrometer was used to measure the exact output of light emitted from the Follow 1200 Pro lamp in terms of the spectral intensity. This result was then plotted (see Fig. 4-16) against the sun's direct global radiation which was obtained from ASTM G173 - 03 (2012) for AM 1.5. The global radiation from the sun (red line) ranges over all three components of light as expected, with the highest intensity from the visible light. The lamp, however, which is represented by the blue line, produces light that primarily falls in the visible section with little contribution from the ultraviolet or infrared section. This information for the lamp will be useful when clarifying the cause of the resulting temperature changes in materials which are exposed to this light source for a period of time.

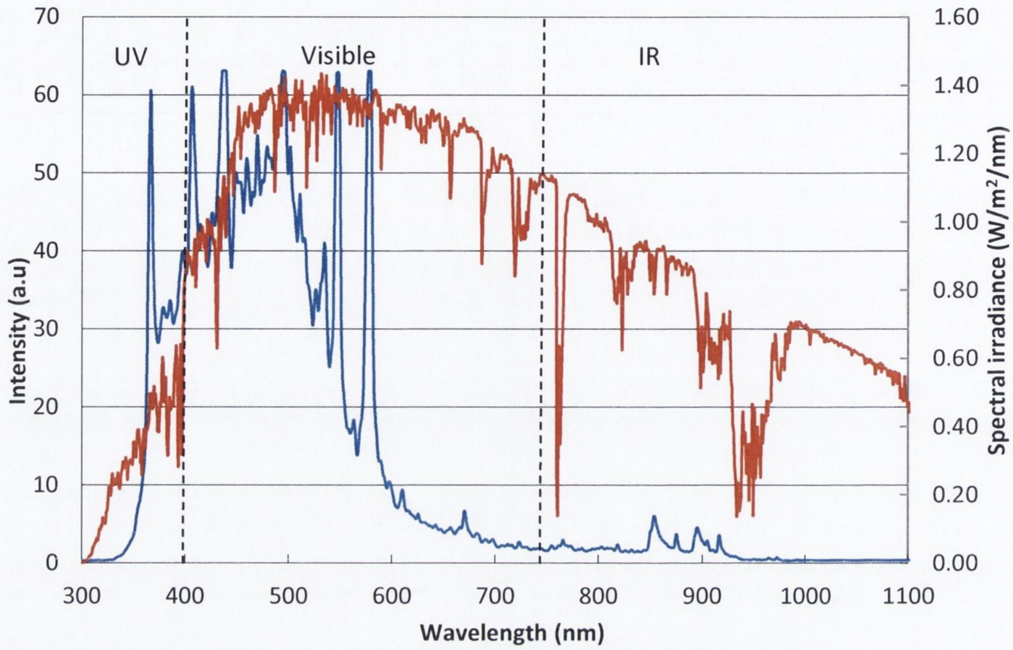

Fig. 4-16 Spectral information from Follow 1200 pro lamp (blue) and direct global radiation for air mass 1.5 (red) (ASTM, 2012)

4.10 Moisture meter: Tramex concrete moisture encounter

The Tramex Concrete Moisture Encounter is a meter which is placed directly on the surface to measure moisture in concrete. The Concrete Moisture Encounter operates on the principle of non-destructive impedance measurement. Parallel coplanar electrodes fitted with spring-loaded contacts are mounted on the base of the instrument. During operation, a low frequency signal is transmitted into the concrete or floor screed to measure the change in impedance caused by the presence of moisture (Wan et al., 2009). The device measures the near-surface moisture condition and is calibrated to measure between 2 and 6% moisture content.

Research by Levinson and Akbari has shown that wetting the surface of the concrete strongly depressed the albedo of the concretes by virtue of a darker surface colour, which pertained until their surfaces were dried (Sweeney and West, 2013). Therefore, as the slabs are exposed to the environment, the moisture level on the surface will change depending on weather conditions. The surface moisture is recorded using a moisture meter (see Fig. 4-17) before taking readings of light reflectance as the moisture level has an effect on the colour of the concrete slabs (Sweeney and West, 2013). A reading greater than 4.5% moisture content would be considered to be significant, therefore, as the cast surface finish was always the slowest to dry out, moisture readings were taken on this finish to ensure that the surface was relatively dry.

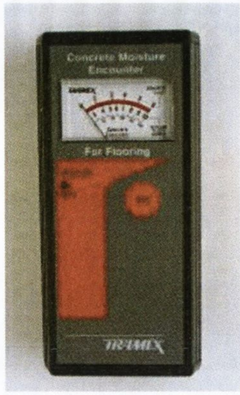

Fig. 4-17 Tramex concrete moisture encounter

To demonstrate the resulting decrease in light reflectance and colour with increase in surface moisture, a small test was conducted using a lux meter in conjunction with a greyness scale card to assess the change in light reflectance and colour, both before and after wetting the surface of the slab. The details of this test are discussed in Section 7.3.4.

In conclusion, the principal instruments to be used to test the prepared specimens for their solar reflectance have been described. An examination of the light reflectance methods follows.

5 Light Reflectance Test Methods

5.1 Introduction

This chapter focuses on two of the direct methods of testing light reflectance, namely an albedometer and a lux meter. As outlined previously in Chapter 4, an albedometer measures solar reflectance over three wavelengths (visible, infrared and ultraviolet radiation), whereas a lux meter measures only visible light. These test methods will be investigated in this chapter to establish whether they can be employed to measure the light reflectance from small concrete specimens.

5.2 Albedometer

5.2.1 Introduction

An albedometer is the primary means of measuring the solar reflectivity or albedo value of a surface. The apparatus is levelled over the chosen surface at the recommended height of 1.5m and a voltmeter is used to measure the solar radiation of both the upper (pyranometer) and lower (albedometer) sensor/dome. The albedo value is calculated as a ratio of the reflected to the incoming light from the readings of the upper and lower dome, taking into account the calibration factor for each sensor. The principal objective of the testing here is to determine whether the instrument can be calibrated (by carrying out a number of sensitivity tests) to measure the albedo of the small (300x300mm) concrete specimens which were manufactured. To calibrate the albedometer in this way, it was necessary to restrict the field view of the lower dome (normally 170° field of view), which was achieved by attaching a black cardboard cone to the lower dome.

Initially, the normal operation of the albedometer is established through its use on three different sites in which new concrete had been poured. Then, using a restricted view, sensitivity test parameters are performed to establish:

1. The change in albedo over time on one day
2. Albedo on different days in similar circumstances
3. The effect of changing the height of the instrument
4. The consequences of employing a black cone to restrict the field view of the lower sensor
5. The relationship between albedo readings with and without the cone.

5.2.2 Testing at St James Gate Brewery on an aged concrete slab

5.2.2.1 Introduction

The objective of this site testing is to examine the normal use of the albedometer in practice and to assess the solar reflectivity, or albedo, of a concrete pavement with 30% GGBS cement replacement of ordinary Portland cement, and with a brushed surface finish, using an albedometer. The concrete slabs are approximately 12 months old and are subject to heavy trafficking at St. James Gate Brewery (see Fig. 5-1). Following the tests, the solar reflectance index (S.R.I) can be established in accordance with ASTM 1980-11 (2011). By obtaining a minimum S.R.I value of 29 for a surface (0 and 100 being the SRI values for a standard black and standard white surface respectively), it is possible to obtain points in an environmental rating system under the LEED incentive (see Section 2.4 for details). A typical published albedo value for traditional concrete when new is generally between 0.30-0.40 and aged concrete has a value of between 0.20-0.30 (Bretz et al., 1998). However, by using 30% GGBS, as a partial replacement for grey Portland cement, one can reasonably expect slightly higher albedo values to be obtained for new concrete due to GGBS's whiteness (Boriboonsomsin and Reza, 2007). This value would be reduced for aged concrete as discolouration and dirt accumulation due to exposure to the environment can substantially increase greyness.

Fig. 5-1 Satellite image of St. James Gate site with three site locations indicated in red (Google_Earth, 2008)

5.2.2.2 Process of taking measurements

The testing was carried out in November 2012 and the locations of the two sites are displayed in Fig. 5-1 labelled 1 and 2 (with James Street at the north of the image beside the river Liffey). The third site location will be discussed in Section 5.2.3. Prior to gaining access to the site, a safe pass course was completed and an extensive method statement was developed. Two different site locations were chosen: both locations have a brushed surface finish (see Fig. 5-2 and Fig. 5-3). This was to obtain a comparative result of albedo for this type of concrete slab surface. Barriers were erected around the two different site locations during testing for safety purposes. The surfaces were dry and the sun was shining for the duration of testing. A procedure was formulated in order to determine the variability and repeatability in the albedo readings (see Appendix D). The testing was carried out as follows;

1. The pavement to be evaluated (see Fig. 5-2) had four different random spot locations marked out with chalk (labelled A, B, C and D) with approximately 2 metres between each location.
2. At location A, three reading of albedo were recorded, one taken every minute.
3. The albedometer was moved to locations B, C and D in turn and the process was repeated.
4. The cycle of taking readings at locations A-D was repeated to ensure small variability.
5. The albedometer was relocated to site 2 (see Fig. 5-3), where processes 1-4 were again carried out as appropriate.
6. Site 2 was divided into 2(a) and 2(b) where site 2(b) consisted of a rougher brushed surface finish in comparison to site 1 and site 2(a). This is evident from the relevant photographs in Fig. 5-4 and Fig. 5-5. A full set of 4 readings were taken at both site 2(a) and 2(b).

Fig. 5-2 Photograph of Site 1 at St. James Gate Brewery

Fig. 5-3 Photograph of Site 2 at St. James Gate Brewery

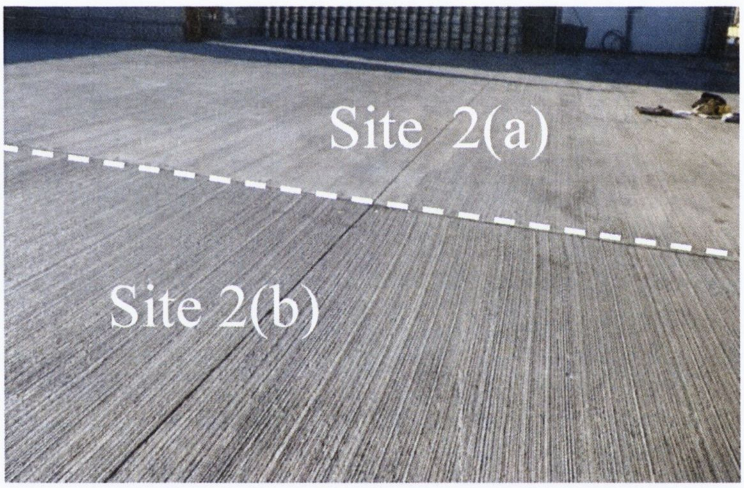

Fig. 5-4 Photograph of site 2 divided into site 2(a) and site 2(b)

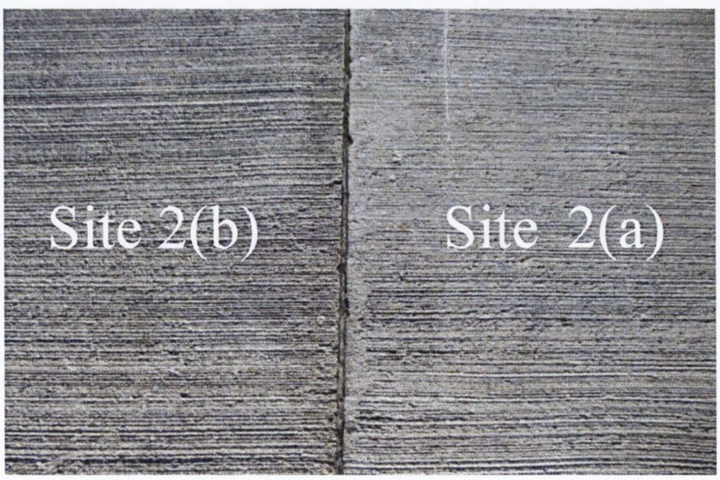

Fig. 5-5 Photograph demonstrating difference in surface finish between site 2(a) and site 2(b)

5.2.2.3 *Results of albedo measurement*

The detailed results of albedo for each of the site locations can be found in Appendix D. For each of the four locations on the three sites, an average reading was calculated for three albedo readings, with little variability evident between these readings. This is demonstrated clearly in Table 5-1 with the standard deviation (σ) being very low. Upon returning to the same location, there is also little change in the albedo which is evident by the results shown in Table 5-2, which outline the second cycle of readings recorded at the same site location. This would verify the reasonable repeatability of the testing. A summary of these results is shown in Table 5-3.

Table 5-1 Cycle 1 of readings at site 1 demonstrating the variability in albedo

Location	Reading	Albedo		
A	1	0.242		
	2	0.241	μ_3	0.2413
	3	0.241	σ_3	0.0006
B	1	0.230		
	2	0.232	μ_3	0.2310
	3	0.231	σ_3	0.0010
C	1	0.226		
	2	0.226	μ_3	0.2270
	3	0.229	σ_3	0.0017
D	1	0.245		
	2	0.243	μ_3	0.2450
	3	0.247	σ_3	0.0020

Table 5-2 Cycle 2 of readings at site 1 demonstrating the variability in albedo

Location	Reading	Albedo		
A	1	0.253		
	2	0.253	μ_3	0.2527
	3	0.252	σ_3	0.0006
B	1	0.242		
	2	0.242	μ_3	0.2417
	3	0.241	σ_3	0.0006
C	1	0.235		
	2	0.231	μ_3	0.2337
	3	0.235	σ_3	0.0023
D	1	0.248		
	2	0.247	μ_3	0.2473
	3	0.247	σ_3	0.0006

For site 1, albedo values ranging between 0.23 and 0.25 were recorded. These readings were slightly higher at location 2(a) where the albedo ranged between 0.25 and 0.26. This may be explained by the fact that there were some shadows present at the periphery location 1 due to the low elevation of the sun early morning. The albedo at site 2(b) was marginally the lowest (between 0.23 and 0.24). This can be expected as this surface had a rougher surface finish which produces more diffuse radiation and the surface was visibly slightly darker than site 2(a) (see Fig. 5-5).

Table 5-3 Summary of average albedo results at three site locations

Site	Cycle no.	Location	Average albedo	Range in albedo readings
1	1	A	0.241	0.231-0.253
		B	0.231	
		C	0.227	
		D	0.245	
	2	A	0.253	
		B	0.241	
		C	0.233	
		D	0.248	
2(a)	1	A	0.246	0.241-0.264
		B	0.252	
		C	0.261	
		D	0.254	
	2	A	0.241	
		B	0.248	
		C	0.264	
		D	0.254	
2(b)	1	A	0.240	0.226-0.241
		B	0.226	
	2	A	0.241	
		B	0.227	

The albedo values obtained from this testing were used in accordance with ASTM 1980-11 (2011) to evaluate an approximate S.R.I value (see Section 2.2.4 for details of equations). This calculation assumes standard solar and ambient conditions. Three convective coefficients of 5, 12 and 30W/m^{2}K, corresponding to low (0 to 2m/s), medium (2 to 6m/s) and high-wind (6 to 10m/s) conditions respectively, were evaluated for their effect on S.R.I but made less than approximately 2% difference in the results. The reason why the wind affects the result is because the surface temperature reduces under high winds, thereby reducing the emissions from the concrete.

By using emissivity values of 0.90, 0.95 and 1.0, for example, the corresponding S.R.I values range between approximately 25 and 31. The emissivity of the concrete was estimated at 0.94 for a rough finished concrete (Baehr and Stephan, 2011), yielding an S.R.I value of 29.

5.2.2.4 *Conclusions*

- The range of albedo values for the two sites ranges between 0.23 and 0.26. This corresponds to a range in S.R.I. of between 25 and 29 (assuming $h_c = 5W/m^2K$). By using the average albedo value of 0.25, an S.R.I. value of 28 was obtained. However, in order to meet the LEED requirements, an S.R.I. value of 29 is necessary. By assuming an emissivity of 0.94 for a brushed surface finish, a minimum albedo value of 0.26 is required to achieve the required S.R.I. of 29.
- If one wished the tested slabs to qualify for the LEED credits, a higher S.R.I. value may be attained by cleaning the surface of the concrete on a regular basis. Alternatively, it is suggested that a new concrete topping could be applied to the slabs with a significant GGBS content, to ensure degradation of whiteness over time does not disqualify the slab from being awarded this credit within a reasonable period.

5.2.3 Testing at St James Gate Brewery on a new concrete slab

5.2.3.1 *Introduction*

The objective of this additional survey is to assess the albedo of a new concrete surface (one week after casting) with 30% GGBS cement replacement and a brushed surface finish using an albedometer at St. James Gate Brewery. The location of the test (site 3) is at the site entrance at Victoria Quay (as labelled in Fig. 5-1).

5.2.3.2 *Process of taking measurements*

The testing was carried out on 16th April 2013. The surface was apparently dry and the sun was shining for the duration of testing. Using a method statement derived for the purpose, as previously, a total of 10 readings of albedo were taken at this location.

It is important to note that the albedo values measured will be conservative due to the presence of some shadow in the periphery of the testing surface, as evident in Fig. 5-6.

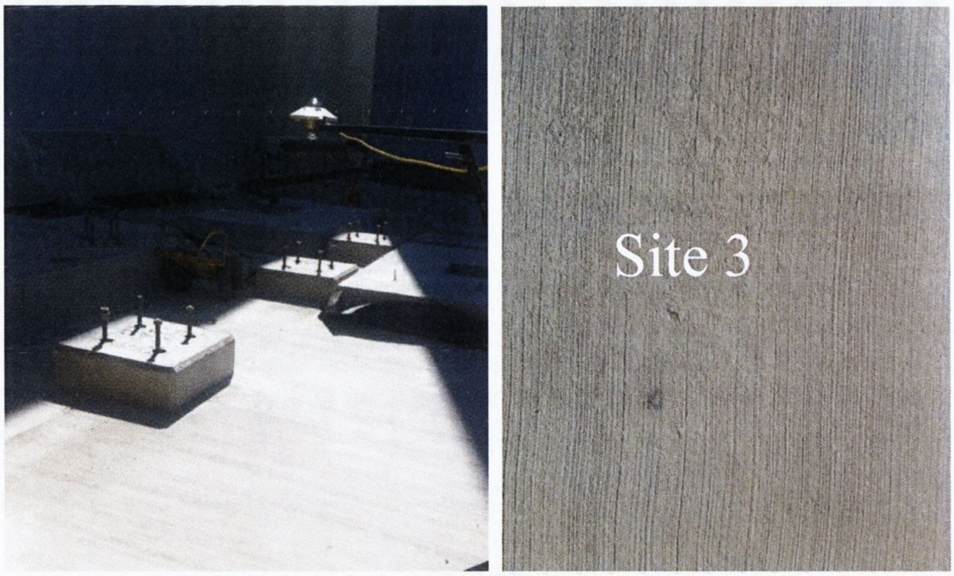

Fig. 5-6 Albedometer set up (left) and testing surface containing a brush finish with 30% GGBS (right)

5.2.3.3 Results of albedo measurement

The results of albedo are displayed in Table 5-4, with the pyranometer (upper dome) and albedometer (lower dome) showing consistent readings, and the average albedo for the surface is 0.285. There is very little variation over the 10 readings with a coefficient of variation (CoV) of 0.88%, indicating the results are accurate and repeatable.

Table 5-4 Albedo results for new 30% GGBS concrete containing a brushed surface finish

Reading	Pyr (W/m^2)	Alb (W/m^2)	Albedo
1	740	211	0.285
2	737	208	0.282
3	741	212	0.286
4	741	211	0.285
5	740	210	0.284
6	738	208	0.282
7	751	216	0.288
8	746	213	0.286
9	742	208	0.280
10	750	216	0.288
		μ	**0.285**
		σ	0.002
		CoV (%)	0.878

The albedo values obtained from this testing were used in accordance with ASTM 1980-11 (2011) to evaluate an approximate S.R.I value (see Section 2.2.4 for details of equations). This calculation assumes standard solar and ambient conditions. The albedo value for the site is 0.285 which corresponds to an S.R.I of 32 (assuming h_c = 5W/m^{2}K and an emissivity of 0.94 for a rough finish surface (Baehr and Stephan, 2011).

Similarly, by using emissivity values of 0.90, 0.95 and 1.0, for example, the corresponding S.R.I values range between approximately 30 (ε =0.90) and 34.5 (ε =1.0).

5.2.3.4 Conclusion

- In obtaining the albedo reading of 0.285 for the site, the corresponding S.R.I value is 32. Therefore, the S.R.I value of the surface of 32 at this location in St. James Gate Brewery exceeds the minimum S.R.I requirement of 29 for LEED accreditation.
- The albedo reading of 0.285 is lower than would be expected, as a new concrete surface has a published albedo of approximately 0.35-0.40 (see Table 2-3). The measured albedo is a conservative albedo value as the testing surface was relatively small, in addition to the periphery of the test area being in shadow, with some obstructions.
- The S.R.I value of a new concrete surface containing 30% GGBS is 32 compared to a similar but aged concrete surface which had an S.R.I of 28. Therefore, in order for a surface to maintain the minimum S.R.I requirement of 29, a higher GGBS content is recommended to allow for ageing with time.

5.2.4 Testing at Father Collins Park Donaghmede on a 2 year old slab

5.2.4.1 Introduction

The objective of this site testing is to assess the solar reflectivity, or albedo, of a concrete pavement with 70% GGBS cement replacement of ordinary Portland cement, and with an exposed aggregate finish, using an albedometer. The concrete slabs are approximately 24 months old and are subject to light trafficking by pedestrians as they are located within Father Collins Park in Donaghmede, Dublin (see Fig. 5-7). An additional concrete surface containing no GGBS at the same site will be tested for comparison. Following the tests, the solar reflectance index (S.R.I) can be established in accordance with ASTM 1980-11 (2011).

As already stated, a typical albedo value for traditional concrete when new is generally between 0.30-0.40 and aged concrete has a typical albedo value of between 0.20-0.30 (Bretz et al., 1998). However, by using 70% GGBS, as a partial replacement for grey Portland cement, one can reasonably expect an appreciably higher albedo value to be obtained for new concrete due to GGBS's whiteness (Boriboonsomsin and Reza, 2007). Research suggests that a concrete sample containing 70% GGBS has an albedo of approximately 0.58 after 14 days (Boriboonsomsin and Reza, 2007), which is an increase of 71% in comparison with conventional concrete, which has an albedo of approximately 0.34 at the same age. This value would be lower for aged concrete as ageing due to pollution from the environment can substantially decrease albedo.

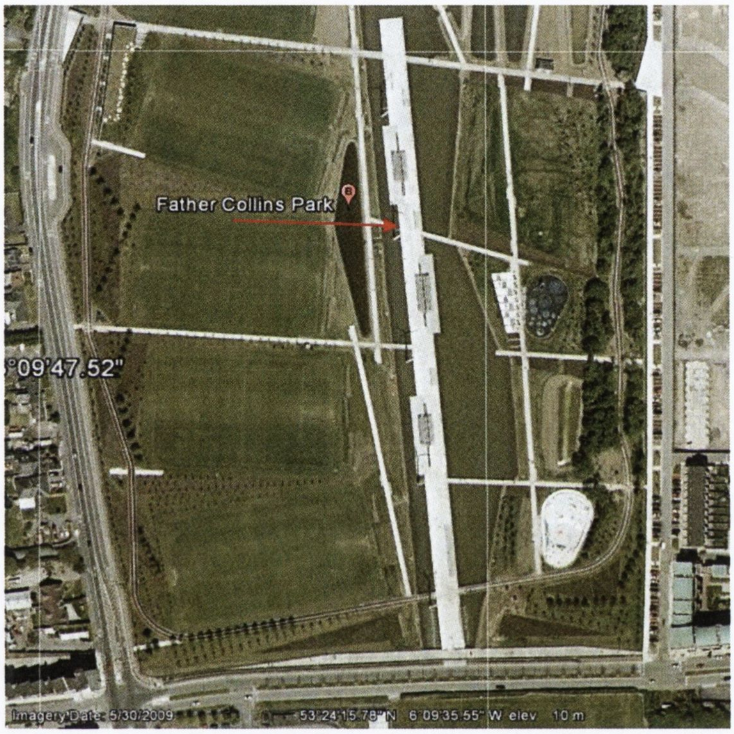

Fig. 5-7 Satellite image of Father Collins Park with the site location indicated (Google_Earth, 2009)

5.2.4.2 Process of taking measurements

The testing was carried out in March 2013. The two testing surfaces containing 0 and 70% GGBS are displayed in Fig. 5-8. For the 70% GGBS surface, three site locations in close proximity to one another were tested, and for 0% GGBS surface two different site locations adjacent to one another were tested. The purpose of the multiple site testing is to assess the variability across the surface. The surfaces were dry for the duration of testing and the sun was shining.

The testing was carried out as follows;

1. The albedometer was set up directly above the 70% GGBS surface, and three readings were recorded (see Fig. 5-8).

2. A lux meter was used on the same location approximately 300mm above the surface to measure the incoming and reflected lux, with three readings recorded.
3. A sphere spectrophotometer was used to measure the L* value of the surface. A total of 5 readings were taken and the purpose of this was to assess the variability in colour due to the exposed aggregate on the surface which is evident from the photograph in Fig. 5-8.
4. A greyness chart was used to measure the colour of the surface.
5. The albedometer was relocated to Site 2 and Site 3 in turn, where processes 1-4 were again carried out as appropriate.
6. The processes 1-5 were repeated for the 0% GGBS surface for both selected sites.

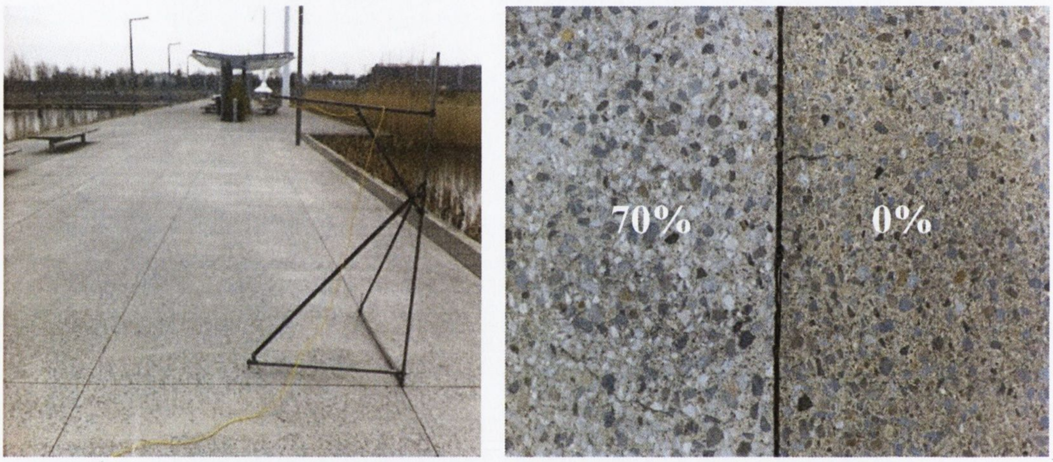

Fig. 5-8 Digital image of site (left) and image of the two testing surfaces containing different levels of GGBS (right)

5.2.4.3 *Results of albedo measurement*

The results of albedo are displayed in Table 5-5 with the pyranometer (upper dome) and albedometer (lower dome) showing consistent readings, and the average albedo for the 0 and 70% surfaces are approximately 0.24 and 0.33 respectively. There is very little variation over the readings with the coefficient of variation (CoV) ranging between 0.05-0.80% indicating the results are accurate and repeatable.

The albedo values obtained from this testing were used in accordance with ASTM 1980-11 (2011) to evaluate an approximate S.R.I value. A value of $5 W/m^2K$ was input for the convective coefficient and the emissivity of the concrete was estimated at 0.94.

Table 5-5 Results of testing albedo at Father Collins Park

Surface	Site	Albedo				
		Pyr	Alb.	Albedo		
70%	1	242.4	83.1	0.343	μ_3	**0.34**
		244.8	83.2	0.340	σ_3	0.003
		245.4	82.8	0.337	CoV (%)	0.80
	2	244.4	79.6	0.326	μ_3	**0.33**
		241.5	78.5	0.325	σ_3	0.001
		238.4	77.4	0.325	CoV (%)	0.16
	3	210.5	67.1	0.319	μ_3	**0.32**
		208.8	66.5	0.318	σ_3	0.000
		207.7	66.2	0.319	CoV (%)	0.05
0%	1	217.4	53.6	0.247	μ_3	**0.25**
		219.5	53.8	0.245	σ_3	0.001
		221.2	54.3	0.245	CoV (%)	0.31
	2	229.6	56.1	0.244	μ_3	**0.24**
		230.8	56.5	0.245	σ_3	0.000
		232.3	56.8	0.245	CoV (%)	0.10

The albedo for 0% GGBS ranges between 0.24-0.25, which is a typical result for aged concrete containing no GGBS. However, the surface containing 70% GGBS is significantly higher, having an albedo ranging between 0.32-0.34. The albedo is still lower than might be expected of a surface containing 70% GGBS from published literature. There are two reasons for this; the exposed aggregate surface finish results in much of the aggregate being exposed and the concrete surface is approximately 2 years old. Both of these factors would decrease the albedo of the concrete. This albedo value yields an S.R.I result of between 36.7 and 39.3 which is considerably higher than the LEED requirement of 29 (see Table 5-6). The 0% surface, however, does not meet this criterion as a value of approximately 27 is obtained.

Table 5-6 Summary of results at Father Collins Park

Surface	Site	Albedo	S.R.I
70% GGBS	1	0.34	39.3
	2	0.33	38.0
	3	0.32	36.7
0% GGBS	1	0.25	27.9
	2	0.24	26.6

5.2.4.4 *Conclusions*

- The albedo of 0% GGBS surface ranges between 0.24-0.25 which is typical of an aged concrete surface. The 70% GGBS surface is approximately 36% more reflective having an albedo ranging between 0.32-0.34.
- The albedo readings have a coefficient of variation (CoV) ranging between 0.05-0.80% indicating the results are accurate and repeatable.
- The resulting albedo of the 70% GGBS surface would confirm that ageing has occurred to some extent as the albedo should be higher given the high level of GGBS present. The surface finish would also have a significant effect on the resulting albedo as the aggregate, which is exposed at the surface (see Fig. 5-8), would reduce the overall reflectance.
- The albedo value for 70% GGBS yields an S.R.I result of between 36.7 and 39.3 despite the presence of aggregate on the surface, which is considerably higher than the LEED requirement of 29. The 0% surface does not meet this criterion.

This section demonstrates the normal satisfactory use of an albedometer when large surface test areas are available. It also shows that the device is accurate and reliable.

5.2.5 Sensitivity testing using the albedometer

The objective of the sensitivity tests conducted using the albedometer, were established to determine whether the albedo value changes over the course of a day or if it is a constant value, irrespective of the varying external conditions. Moreover, as the lower dome of the albedometer has a large field of view, further testing was conducted to verify whether this field view could be reduced in order to test the albedo of small concrete specimens.

5.2.5.1 *The change in albedo over time on one day*

Testing with the albedometer was carried out on a number of different surfaces, one of which was located in Trinity College. The chosen surface, which was in sunshine just inside the Civil Engineering Building, was adequate as is a spacious old concrete surface (see Fig. 5-9). The data displayed in Fig. 5-10 was recorded in April 2010 and displays the output voltage for the pyranometer and albedometer starting at approximately 11:30 and finishing at 15:30. The incoming sunshine recorded by the pyranometer at 11:30 was 4.5mV which is equivalent to approximately 530W/m^2, confirming that it is sunny with no clouds present. This intensity value increases to a maximum of 5mV (600W/m^2) at approximately 15:30, before decreasing to 4mV (480W/m^2) at 16:00 in the afternoon. The corresponding reflectance from the surface as measured by the lower dome, the albedometer, is significantly lower in magnitude, as would be expected, at approximately 0.55mV in the morning. This value increases marginally as the incoming intensity increases, reaching a peak of 0.76mV at 13:30. This value of reflectance is maintained throughout the remainder of the day. The corresponding albedo is displayed in Fig. 5-11 which is calculated by dividing the albedometer result by the pyranometer result.

It is important to note that the corresponding albedo plots hereafter factor in the calibration coefficient for the upper and lower dome (as described in Section 4.2), therefore, the resulting albedo will be modified very slightly to accommodate this.

Fig. 5-9 Concrete testing surface at Trinity college

The albedo recorded at approximately 11:30 is 0.12, however, this increases broadly linearly reaching a value of 0.17 by 15:30 in the afternoon. Upon linear regression, the coefficient of correlation (R^2) is 0.98 which confirms that there is a strong correlation between the resulting albedo and time. The plot demonstrates the change in albedo over time as there is a significant change in the incoming sunlight throughout the day (across a range of 475-600W/m^2). It can be noted that the albedo of the surface is low (0.12-0.17) as the concrete is in a heavily trafficked area and is approximately 15 years old.

Although it would be simpler in this research project if the albedo was a constant value at a given point in time for a given surface, this appears not to be the case. This is supported by the view of Li et al. (2013) who found similar results, whereby the albedo is high in the early morning and then low and relatively constant around the middle of the day, and then relatively high again in the late afternoon, when there is a low incident angle of solar radiation as in the early morning (see Fig. 2-17). Similarly, Levinson et al. (2010a) also verify that there are a number of restrictions when using an albedometer as the spectral distribution of the incident solar irradiance and the irradiance angle of the solar beam both vary with hour of day and day of year which restricts the daily time window for testing. They concluded that the technique will always slightly underestimate the solar reflectance as the shadows cast by the pyranometer and its support reduce the reflected solar irradiance and also that the pyranometer responsitivity is a strong function of the angle of incidence. In conclusion, as the height of the sun changes throughout the course of the day, the dispersion of the surface may vary (even if the surface appears smooth to the eye i.e. at a macro level) depending on the time at which a reading is taken.

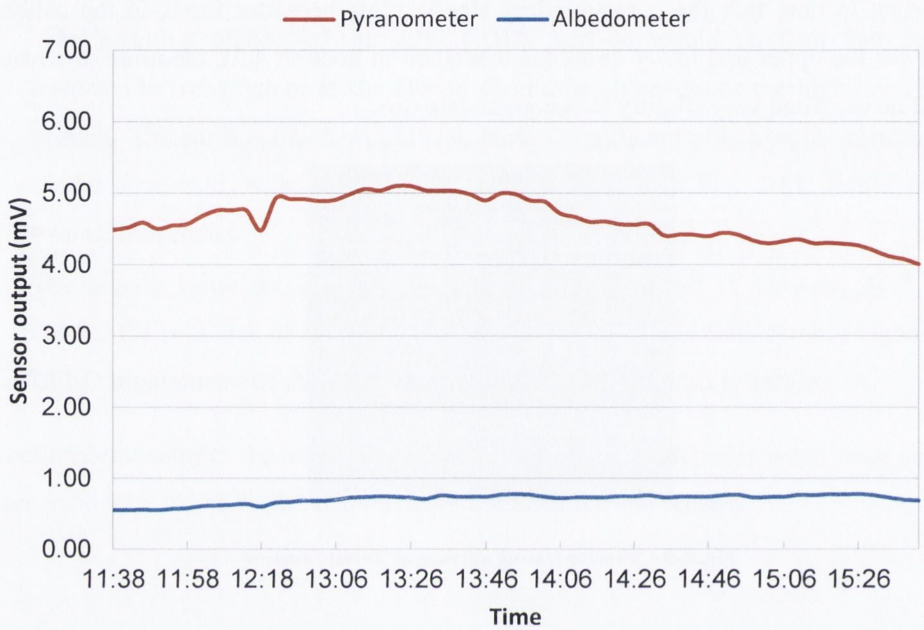

Fig. 5-10 Pyranometer and albedometer output on testing surface in Trinity College (21st April 2010)

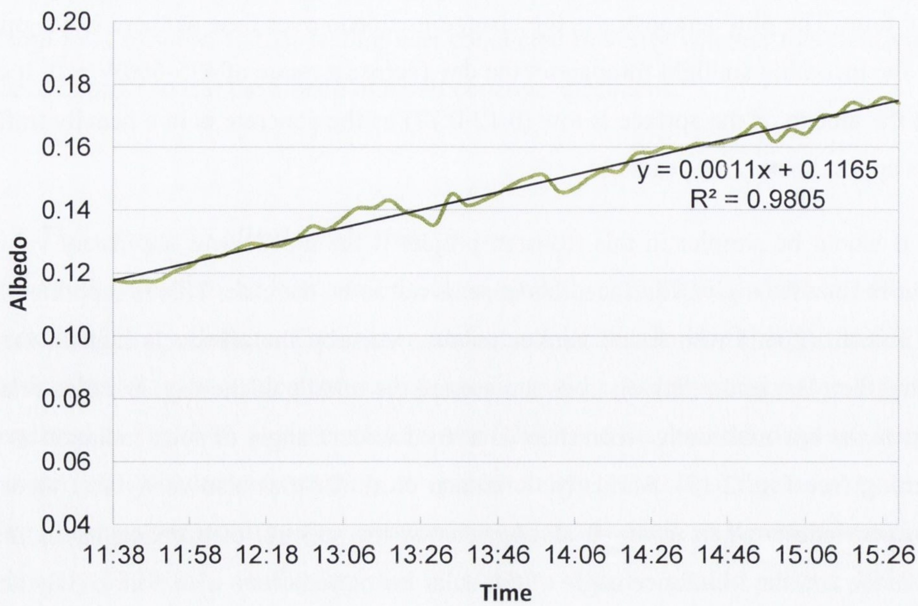

Fig. 5-11 Resulting albedo of testing surface in Trinity College (21st April 2010)

To confirm the results from the testing carried out in April, an additional test was carried out on the same surface in May 2010. The new data is displayed in Fig. 5-12 giving the output voltage for the pyranometer and albedometer. The testing commenced at 12:20 when there was a high level of incoming sunshine, recorded at approximately 5.5mV which equates to 650W/m^2. It is evident from the plot that this level of sunshine intensity is not constant with time, as it increases to 5.85mV (700W/m^2) at approximately 13:30. Following this peak, the intensity decreases to approximately 4.78mV (570W/m^2) in the late afternoon. This result is not consistent with the albedometer which remains at a broadly constant value of approximately 1mV, reaching a maximum, albeit marginally, of 1.17mV at 13:30.

The resulting albedo is displayed in Fig. 5-13 where it is evident once more that there is a linear relationship between albedo and time with an initial value of 0.18. As the incoming sunshine intensity changes throughout the day, this results in an increase in the albedo to 0.20 at approximately 15:40. This confirms the surprising result that the time of day at which the albedo is recorded is important as it affects the resulting albedo value. The R^2 value for the plot is 0.96 which confirms that there is a strong linear relationship between albedo and time.

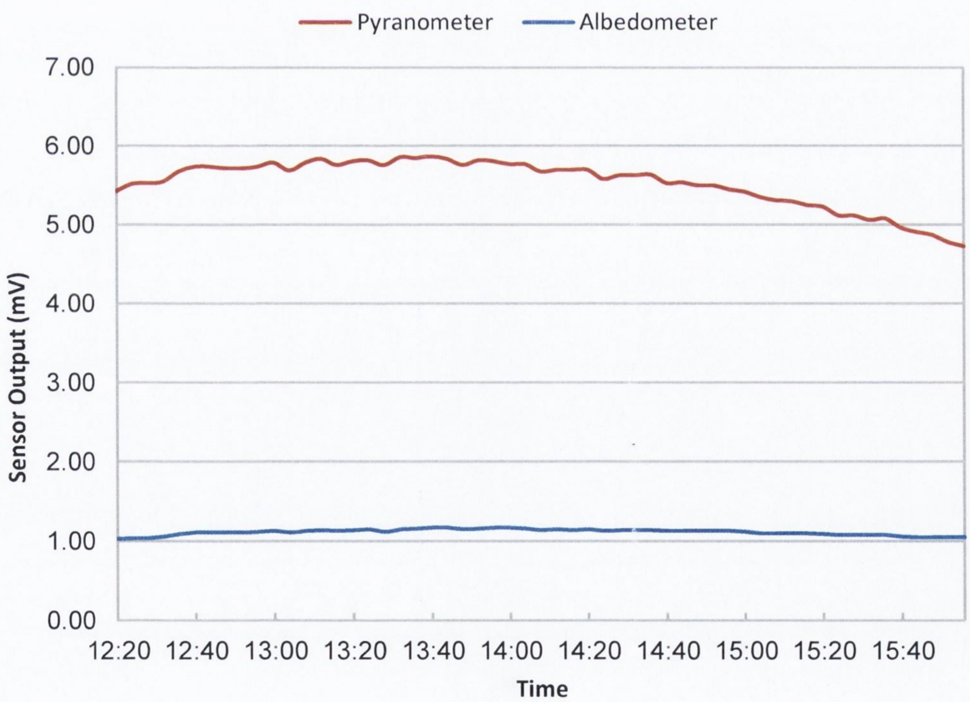

Fig. 5-12 Pyranometer and albedometer output on testing surface in Trinity College (4th May 2010)

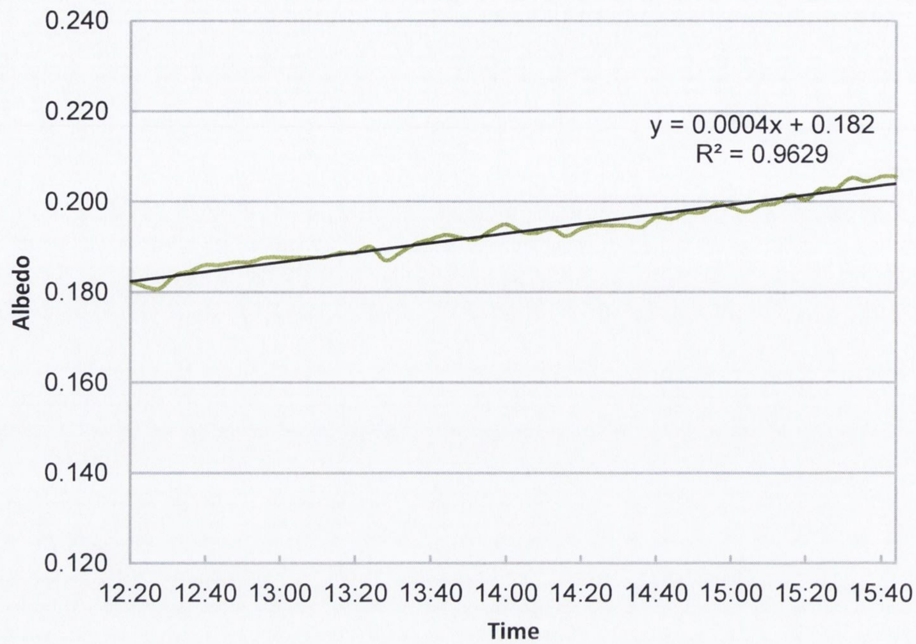

Fig. 5-13 Resulting albedo of testing surface in Trinity College (4th May 2010)

In conclusion, the albedo reading does indeed depend on the time of day at which it is recorded. As demonstrated from the albedo results, it increases linearly from about midday to mid afternoon. This is a relatively short duration of testing, and had the albedo been recorded over a longer duration, the expected result would indicate that the albedo is high in the early morning and then low and relatively constant around the middle of the day, and then relatively high again in the late afternoon, as confirmed by Li et al. (2013).

The method of testing solar reflectance using an albedometer was evaluated by Levinson et al. (2010a), who state that as the spectral distribution of the incident solar irradiance and the irradiance angle of the solar beam both vary with hour of day and day of year, this restricts the daily time window for testing i.e. as the height of the sun changes throughout the course of the day, the dispersion off the surface may vary.

5.2.5.2 Albedo on different days in similar circumstances

In order to ascertain whether measuring albedo of a single surface on different days would yield different results, two data sets will be presented, one from April 2010 and another from June 2010. These results were taken on the same surface at the same location in Trinity College (see Fig. 5-9) and at the same time of the day. However, these tests were conducted 2 months apart, therefore, there are a number of parameters to be noted. The elevation of the sun is slightly different in April as compared with June, and the intensity of the sun would be different in June with the earth being closer to the sun. In addition, there will be a small variation included from taking a reading for albedo from one day to the next.

The data displayed in Fig. 5-14 represents the pyranometer and albedometer output for the testing carried out in April 2010. The pyranometer recorded ranges between approximately 4-5mV (475-600W/m^2) over a period of 3 hours, while the albedometer remains constant at approximately 0.75mV. This result corresponds to an albedo ranging between 0.14 at 13:00 to approximately 0.165 at 16:00 (see Fig. 5-15).

This outcome can be compared with the result from June which is displayed in Fig. 5-16. There is a higher sunshine intensity on this day which is evident by the higher range in the pyranometer readings of between 5-6.5mV (600-785W/m^2). The reflectance from the surface recorded by the albedometer remains at a constant 1mV. As seen in the previous results of incoming and reflected light in Fig. 5-10 and Fig. 5-12, the reflected light (detected by the albedometer) remains broadly constant. This recurring trend is once again as a result of the spectral distribution of the incident solar irradiance and the irradiance angle of the solar beam both varying with hour of day and day of year i.e. the change in the elevation of the sun with time.

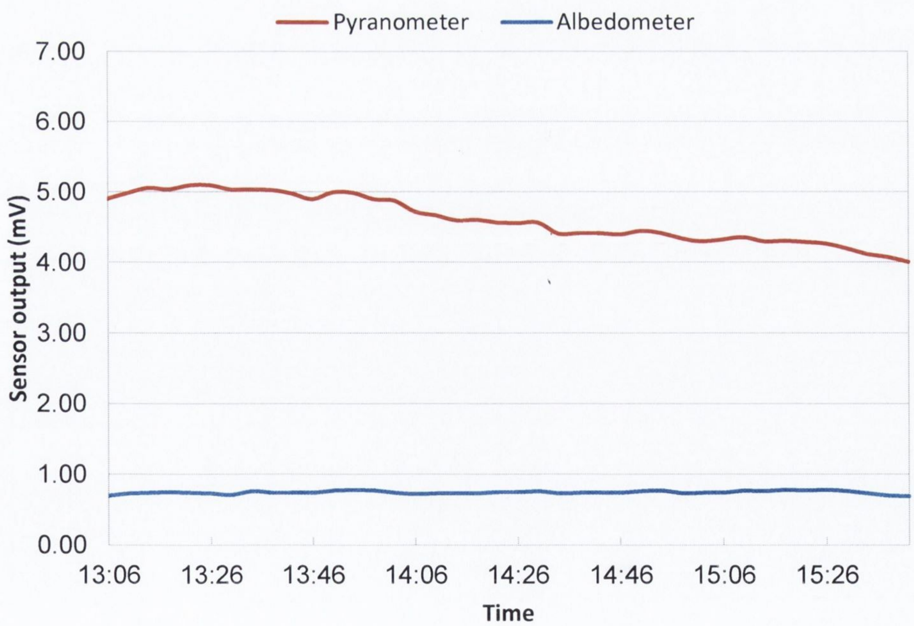

Fig. 5-14 Pyranometer and albedometer output on testing surface in Trinity College (21st April)

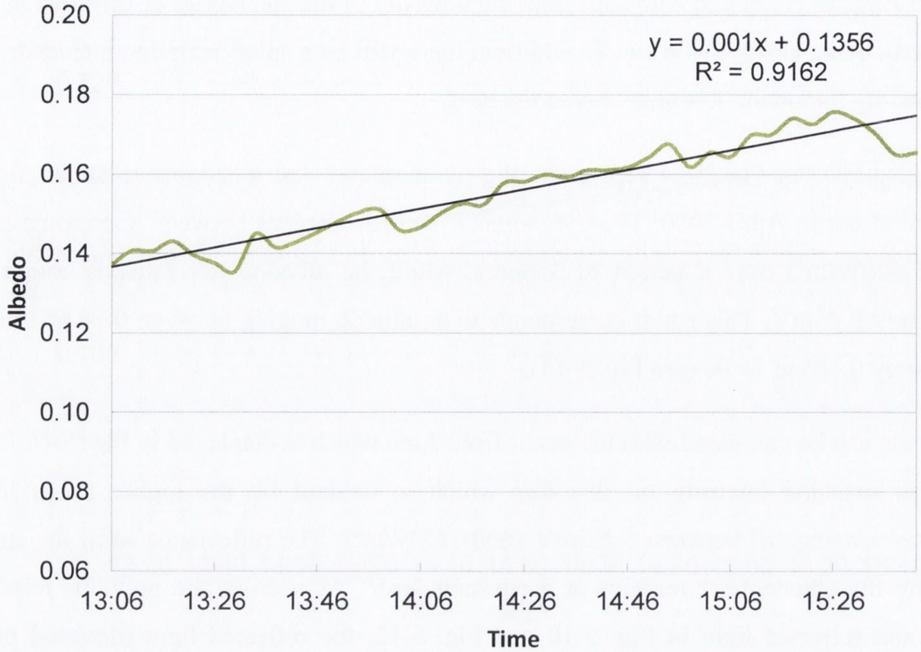

Fig. 5-15 Resulting albedo of testing surface in Trinity College (21st April)

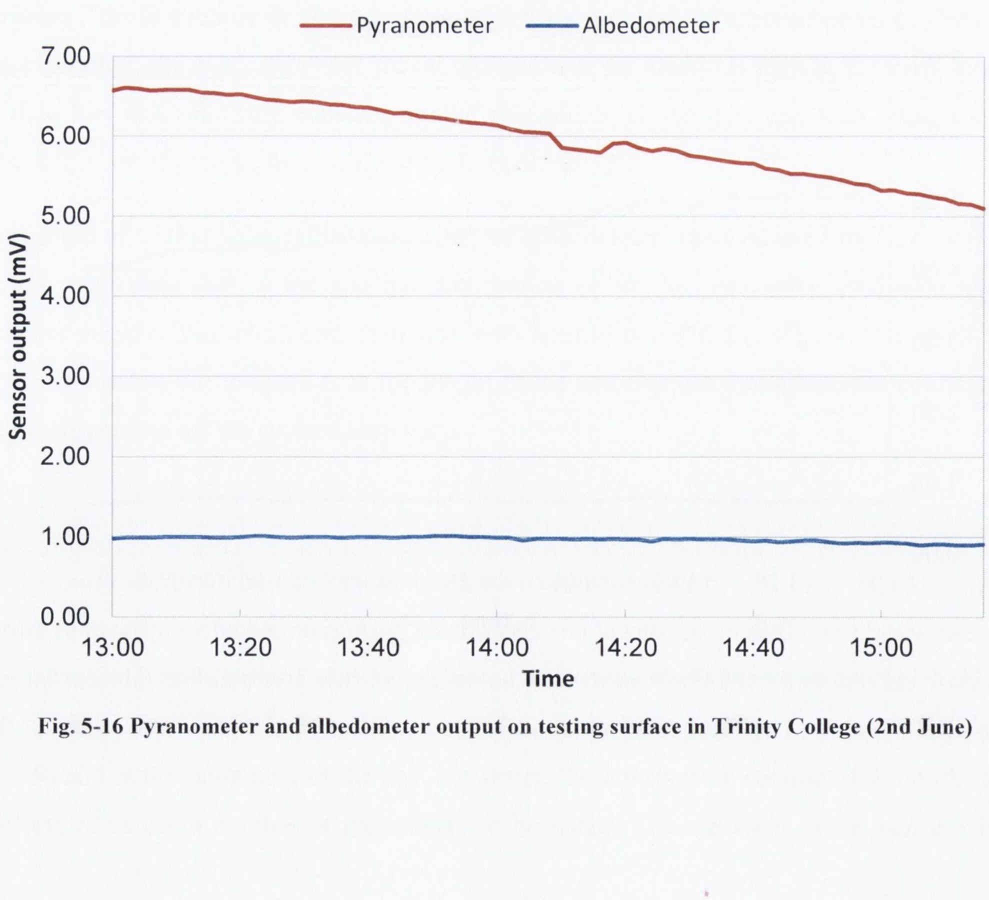

Fig. 5-16 Pyranometer and albedometer output on testing surface in Trinity College (2nd June)

The resulting albedo from testing carried out in June is presented in Fig. 5-17. The albedo ranges between 0.14 at 13:00 and increases linearly to approximately 0.17 at 15:30. A comparison of these results is displayed in Table 5-7 for every half hour between 13:30 and 15:30. It is evident that the albedo is almost identical at each time interval, with a marginal difference in some cases.

Table 5-7 Comparison of albedo for May and June 2010 on the same concrete surface in Trinity College

	13:30	14:00	14:30	15:00	15:30
May	0.140	0.150	0.160	0.165	0.175
June	0.150	0.155	0.160	0.168	0.172

In conclusion, although there is a significant difference in the incoming sunshine intensity between the two days of testing, the resulting albedo is approximately the same for the surface when taken at the same time of day, despite being 2 months apart. This result also reconfirms the effect that the time of day at which the reading is taken has as there is a 0.035 difference in albedo over just 3 hours. This figure would appear small, however, in order to determine the difference in albedo of concrete specimens which may only differ very slightly in colour (such as in specimens described here in), this difference in albedo is quite substantial. Therefore, this test would suggest that the albedometer cannot be used easily to establish accurate results of albedo for small scale concrete specimens.

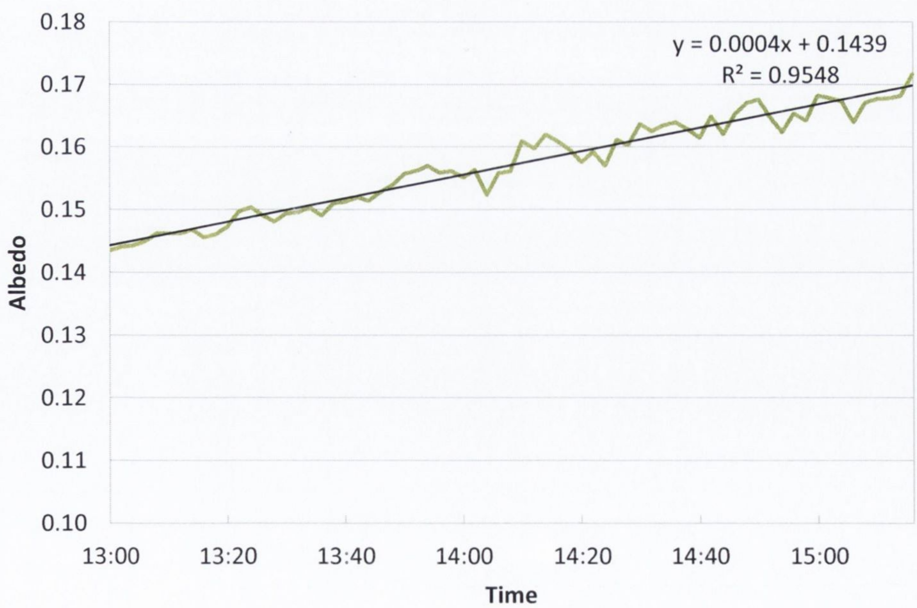

Fig. 5-17 Resulting albedo of testing surface in Trinity College (2nd June)

5.2.5.3 *The effect of changing height of the instrument*

The recommended height at which the albedometer is positioned to take a reading is 1.5m above the surface, with an unobstructed horizon, however, this parameter was tested with the intention of measuring the albedo at a lower height due to the small surface area to be tested. Therefore, establishing the effect of changing the height at which albedo is measured is important, to establish whether it is possible to obtain comparable and sensitive readings when one modifies this variable. An assessment of this parameter was carried out by placing the instrument on a testing surface using the accompanying stand. The chosen surface was the testing surface at Trinity College (see Fig. 5-9), using two different heights of 1.5m and 0.50m (see Fig. 5-18).

The results were recorded at the same time of the day to eliminate this parameter having an effect. The albedo recorded at the recommended height ranges between approximately 0.145 to 0.170, however, by reducing the height of the instrument there is an appreciable difference of approximately 28%, with the albedo ranging between approximately 0.185 to 0.20. The albedo value increases when the instrument is closer to the surface. This outcome can be explained by the fact that there is less background interference from the surroundings when the instrument is closer to the testing surface, as suggested by Levinson et al. (2010a). This result verifies that the height of the instrument does affect the resulting albedo value and, in conclusion, this parameter would need to remain constant in order to exclude this variable.

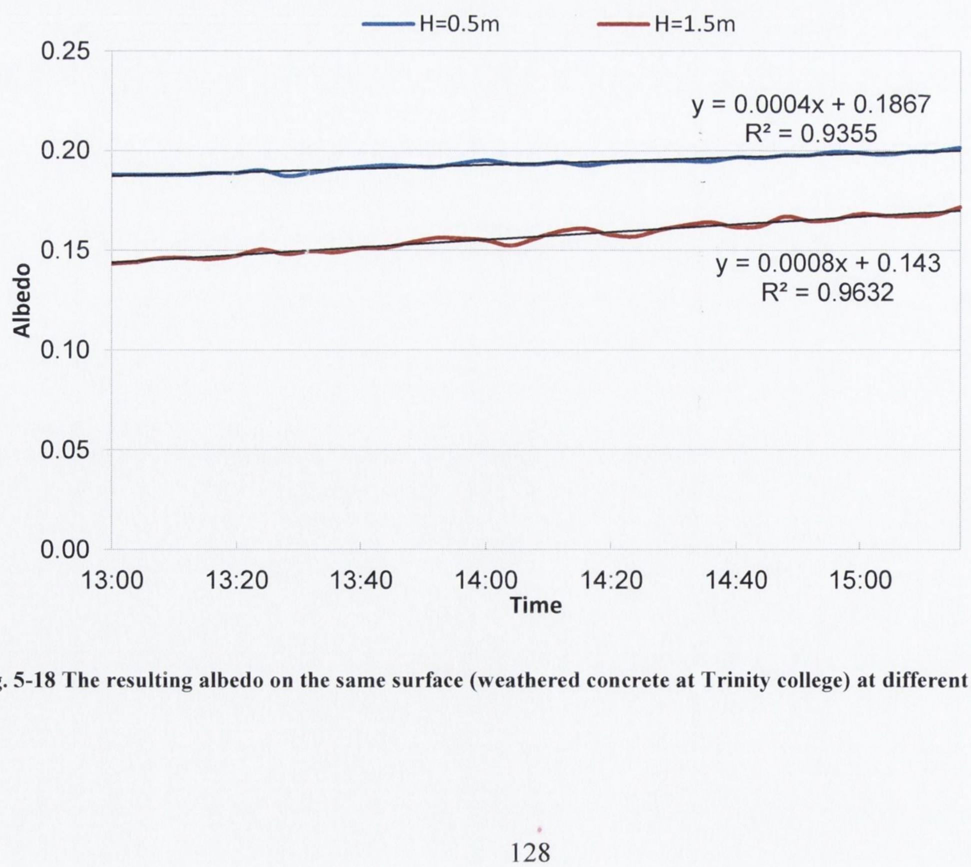

Fig. 5-18 The resulting albedo on the same surface (weathered concrete at Trinity college) at different heights

5.2.5.4 *The consequences of employing a black cone to restrict the field view of the lower sensor*

The field view of the albedometer is 170°, therefore, when the instrument is positioned at a height of 1.5m above the surface, a large surface area for testing is required, otherwise the instrument will take the reflectance reading from the surroundings as well as the testing surface. To overcome this issue for the purposes of testing smaller concrete specimens, the field view of the albedometer would need to be restricted. Thus to enable meaningful comparisons, calibrating the instrument to factor in the restricted reflected light would be essential. Restricting the field of view to the surface of a 300mm square slab 1.5m below the albedometer requires a cone to be manufactured from black card and fixed onto the lower sensor (see Fig. 5-19). The dimensions of the cone are 200mm in height and 200mm in diameter at the base.

A test was carried out at Dun Laoghaire east pier in Dublin on a concrete surface over a duration of four hours and the output for the individual sensors is displayed in Fig. 5-20 both with and without the cone restriction. The pyranometer reading is identical for both cases as there was no restriction placed on this sensor. However, not surprisingly the results for the albedometer show otherwise. The output voltage without the presence of the cone is approximately 2mV, however, with the cone, a significantly lower value of approximately 0.6mV is observed.

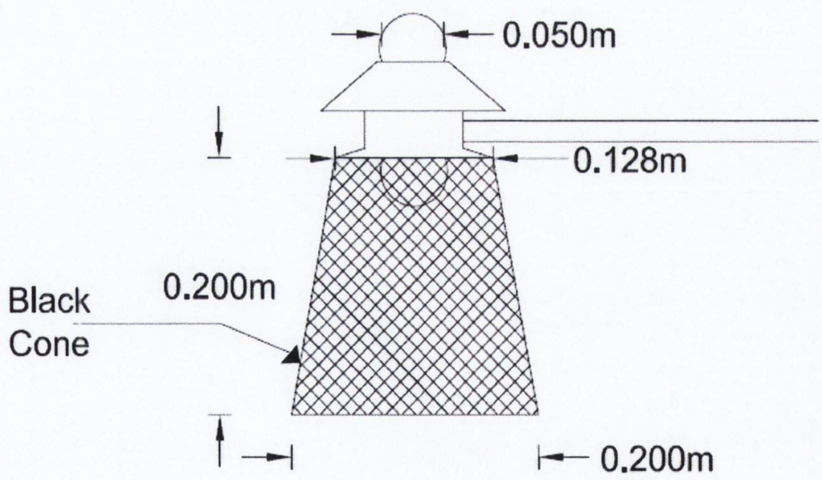

Fig. 5-19 The black cone used to restrict the field view of the lower sensor

The corresponding albedos are displayed in Fig. 5-21 for testing both with and without the cone restriction. The albedo of the surface is approximately 0.27, which is typical of such a concrete surface, however, by using the cone, an albedo of approximately 0.09 is recorded, a difference of 67%. Not unexpectedly, the presence of the cone greatly reduces the amount of light detected as reflecting off the surface.

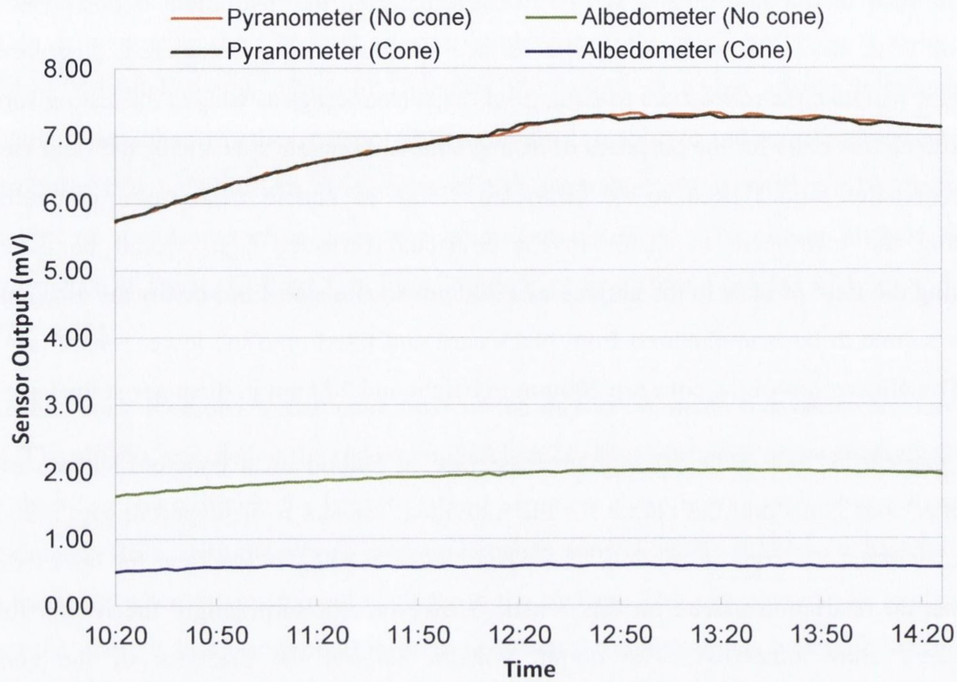

Fig. 5-20 Testing at Dun Laoghaire on concrete surface both with and without the black cone (June 2010)

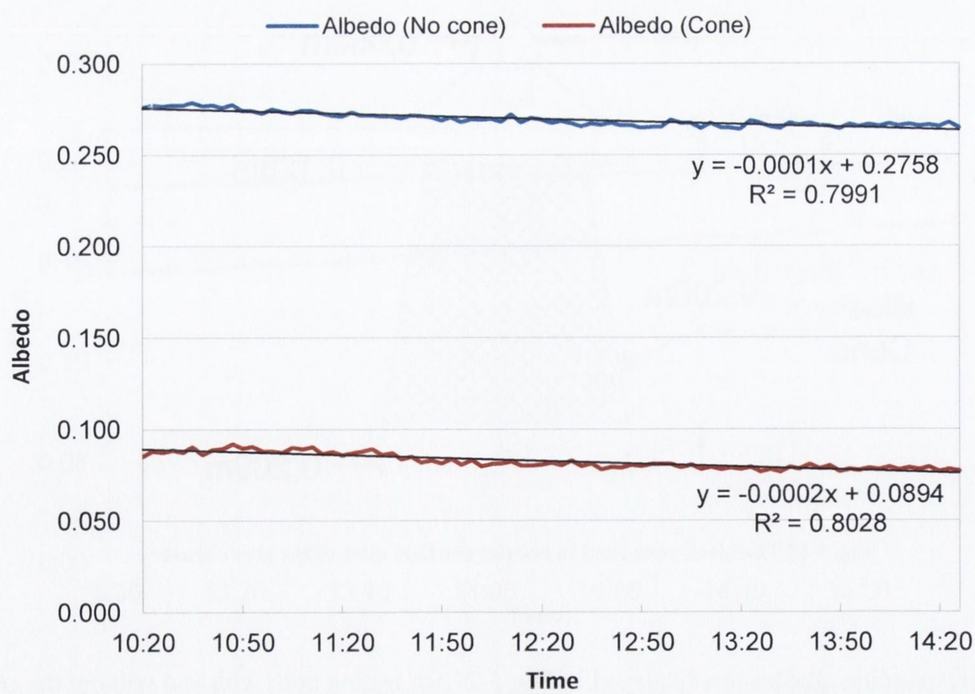

Fig. 5-21 Resulting albedo of testing surface at Dun Laoghaire (June 2010)

It should be noted that the albedo is decreasing linearly, however, in previous results it was increasing, for example, in Fig. 5-18. It was concluded in the first sensitivity test that the time of day at which the albedo is recorded is important, and this is evident here once more. This test was conducted earlier in the morning when compared with the previous tests, and from the published work conducted by Li et al. (2013), who verify that albedo is at a maximum in the morning and afternoon, and is lower in the middle of the day, it is possible to conclude from this test that the albedo is decreasing here as the result was recorded earlier in the day.

5.2.5.5 *The relationship between albedo readings with and without the cone*

To identify whether the cone would be a viable solution to the problem of how to get the true albedo of small specimens, albedo results were analysed. A test carried out at Trinity College in June 2010 (see Fig. 5-22) demonstrated that the albedo, without the presence of the cone, increased linearly from 0.14 to 0.17, while the addition of the cone reduced the albedo by about half (0.07), in addition to remaining constant. This difference in slope would suggest that the results are not correlated because the device loses its sensitivity once the cone is in place.

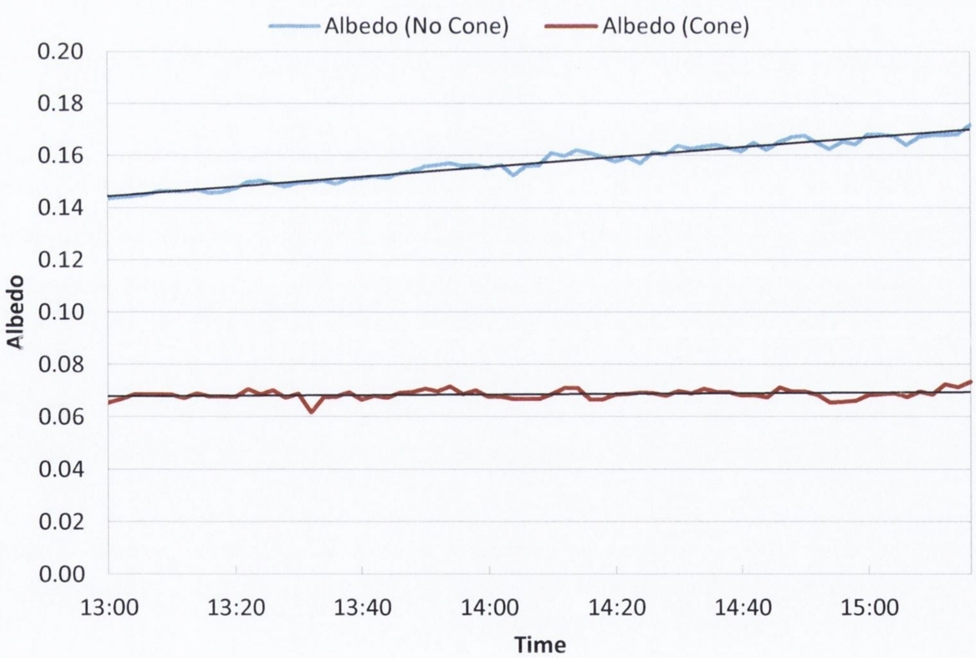

Fig. 5-22 Resulting albedo of testing surface at Trinity College (June 2010)

The correlation for albedo between the cone being present and absent for this test is displayed in Fig. 5-23, with an R^2 value of 0.12. Although the R^2 value would suggest that there is no correlation present between the cone being present and absent, it is misleading as the scale is very small, and there is a small range of albedo. This results in a very small range having a very shallow slope. In order to establish whether there is a good correlation, the data points need to be over a wider scale.

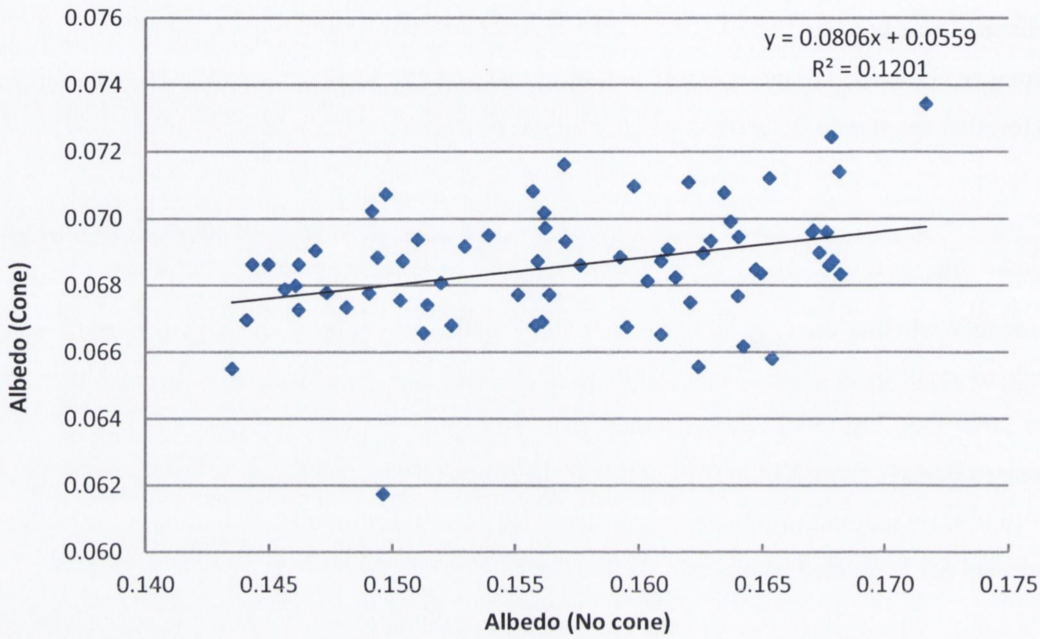

Fig. 5-23 Relationship between albedo for cone and no cone (June 2010)

To confirm this important result, this relationship was investigated for a second test also carried out at Trinity College (see Fig. 5-24). The albedo result where there is no cone present, yields a linear relationship once more, ranging from 0.12 to 0.18. Where the cone is present, this range is between 0.06 to 0.08, confirming that the device has lost some considerable sensitivity.

The results from this second test are displayed in Fig. 5-25 with an R^2 value of 0.88. There is a reasonably good correlation here but it is not acceptable as it needs to be accurate and reliable enough to detect small changes between two concrete specimens containing different surface finishes, for example. As there is too much variability in the curve, it can be concluded that the device cannot be calibrated using the cone given that its presence results in the sensor becoming less sensitive.

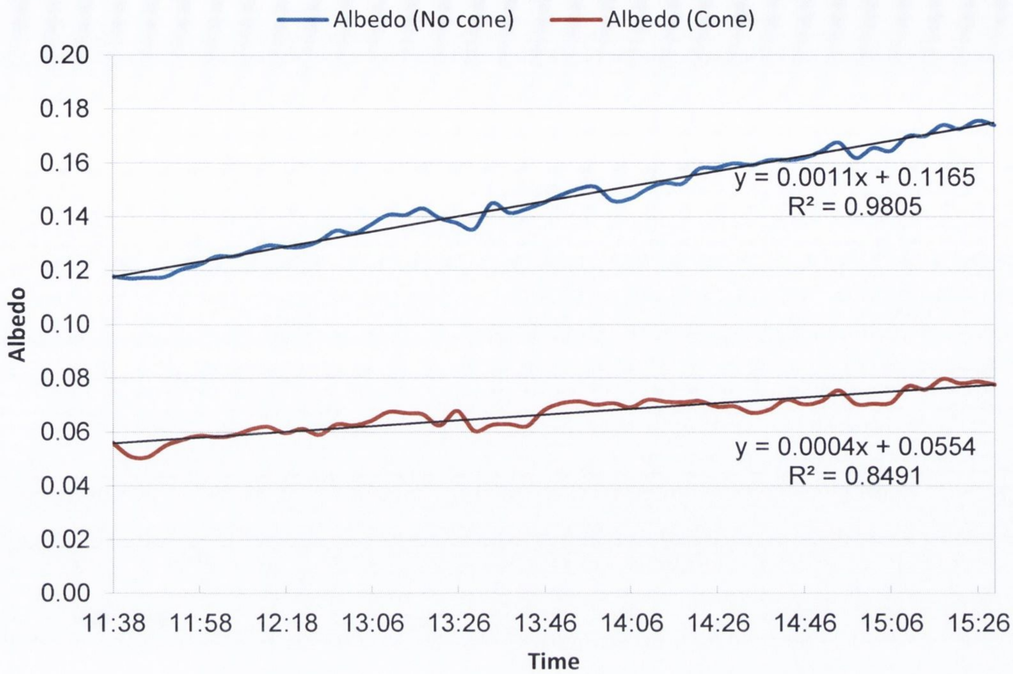

Fig. 5-24 Resulting albedo of testing surface at Trinity College (April 2010)

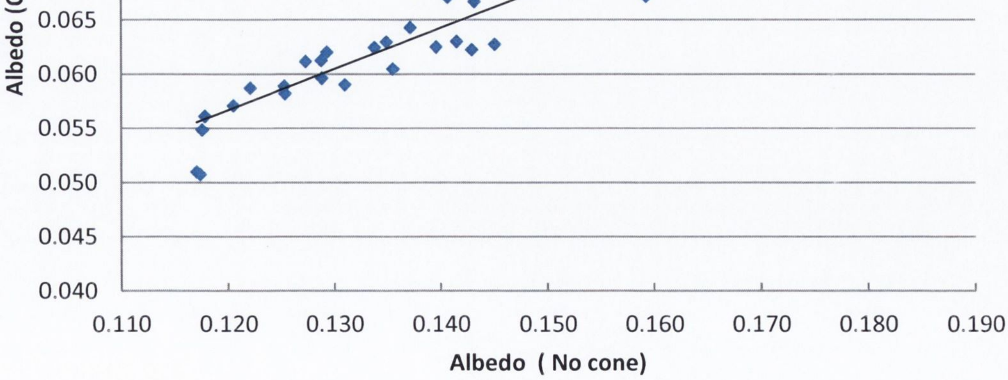

Fig. 5-25 Relationship between albedo for cone and no cone (April 2010)

5.2.5.6 *Conclusions*

- The results indicate that the incoming solar radiation increases throughout the day until it reaches a peak, before reducing again. This is due to the change in position of the sun and thus would also depend on latitude and the time of the year. The albedo changes with time over the course of one day as a consequence of getting different amounts of light being dispersed off the surface. This would suggest that the time of day at which albedo is recorded is important. The results from these tests would support previous work carried out whereby the albedo is at a maximum in the morning and afternoon, but it decreases to a minimum during the middle of the day, as the elevation of the sun changes throughout the course of the day.
- Although the incoming sunshine intensity is slightly different depending on the day, the resulting albedo is approximately the same for the same surface, provided that the reading is taken at the same time of day. In addition, the season is important as the sunshine intensity would be different as the sun is higher in the sky in the summer and lower in the sky in winter.
- The recommended height of the albedometer is 1.5m, however, this parameter was tested with the intention of measuring the albedo at a lower height due to the small surface area to be tested. The result demonstrated that the height of the instrument does affect the albedo reading, with the albedo increasing as the height of the instrument is reduced. This parameter would need to remain constant in order to exclude this variable.
- The use of a cone to restrict the field view results in a significant reduction in the reading of the lower dome. It is also evident that the albedometer is not at all sensitive when the cone is used as the rate of change in albedo is not the same as when there is no cone present. This would strongly suggest that the device cannot be calibrated using the cone given that its presence results in the sensor becoming so insensitive.
- The height of the cone was reduced significantly in order to determine whether this would compensate for a reduction in albedo with the cone, however, it was found that this made the lower sensor even less sensitive as the area over which the light is being reflected reduced even further.

5.2.6 Conclusions

- The overall range in S.R.I values for St James Gate Brewery on the first site is between 25 and 29. By taking an average albedo reading of 0.25 for the site, the corresponding S.R.I value is 28 which is just below the LEED requirement of 29. The average albedo value obtained for the second site at St James Gate Brewery containing new 30% GGBS concrete is 0.285, with a corresponding S.R.I value of 32, which exceeds the minimum S.R.I requirement for LEED accreditation. This would suggest that with age, 30% GGBS does not seem to be sufficient, therefore, it could either be cleaned or replaced, however, if it is to be replaced, a higher percentage of GGBS content would be advisable.
- The albedo of 0% GGBS surface at Father Collins park ranges between 0.24-0.25 which is typical of an aged concrete surface and the 70% GGBS surface is significantly more reflective having an albedo ranging between 0.32-0.34. These albedo readings correspond to S.R.I values on average of between 27.2 and 38 respectively. The 70% GGBS surface is considerably higher than the LEED requirement of 29, however, the 0% surface does not meet this criterion.
- The albedometer works well in the field provided there is a large unobstructed area available, however, it is inconsistent when one is testing small specimens. The albedometer can be used reliably for calculating the approximate albedo of a large surface, such as was carried out at the three site locations (St. James Gate Brewery and Father Collins Park).
- The albedometer is a very sensitive instrument, however, it is not possible to adjust it so that it can be used to measure albedo of small specimens. The results from the sensitivity tests performed indicate that there are a number of parameters which affect the albedo value. These include; the time of day the reading is taken, the time of year, the location, the height of the instrument, the influence of cloud cover, and an unobstructed horizon is required.
- The albedometer (lower) sensor is not as sensitive when the cone is present as the rate of change in albedo is not the same as when there is no cone present. This would verify that the device cannot be calibrated using the cone, so that it can be used on small concrete specimens, given that its presence results in the sensor becoming so insensitive.

5.3 Lux meter box development

5.3.1 Introduction

An accompanying black box was required to obtain lux meter readings from the small concrete samples in order to eliminate background light and to obtain a reading of visible light reflectance solely from the concrete specimen under test. Since no such device exists, a prototype needed to be designed and constructed for this purpose. The prototype to be developed needed to be a device which holds a lux meter in a suitable position over a concrete slab so readings of reflected light could be taken from the concrete surface. The following points were taken into consideration before and during the design process:

1. The maximum exposure of the concrete slab to sunlight is necessary so as to obtain adequate reflectance of visible light.
2. As the sun moves throughout the day, it is necessary for the box device to rotate horizontally as well as vertically. This is necessary because the incoming light needs to be hitting the surface of the slab at an incident angle which ensures the maximum reading at the lux meter and also without the device casting a shadow on the surface of the specimen, which would reduce reflected lux values.
3. The background light must be eliminated (light reflecting from building etc.) as this would affect the overall result. It is important that only direct sunlight is being reflected from the slab in order to reduce the effect of variability of surroundings on the readings.
4. The inside surfaces of the device needs to be matt black in colour so as not to allow any light to reflect off it into the sensor. The outside of the box is also painted black for appearance, however, this will not affect the reading of light reflectance.

One of the first aspects of the design process which needed to be determined was the optimum angle at which the sun's rays should hit, and be reflected off, the concrete surface (assuming a smooth surface, at which the angle of incidence equals the angle of reflection, that is, ignoring dispersion).

5.3.2 Lux meter box prototype development stages

A test was devised to determine an optimum angle of inclination of the specimen to the incoming rays and to assess light reflectance from small prisms containing different contents of GGBS. A test model was designed to demonstrate light reflection from a small concrete specimen and was fabricated first from cardboard (before being manufactured from aluminium) to determine the optimum angle at which the specimen should be placed at the back of the apparatus (see Fig. 5-26). The light source was placed at a height in such a way that it was pointing towards the surface of the specimen. By rotating the specimen, small variations in the angle, α, were created, and the results of lux for the varying angles are outlined in Table 5-8. By taking the geometry of the design into account, α is equal to 44°.

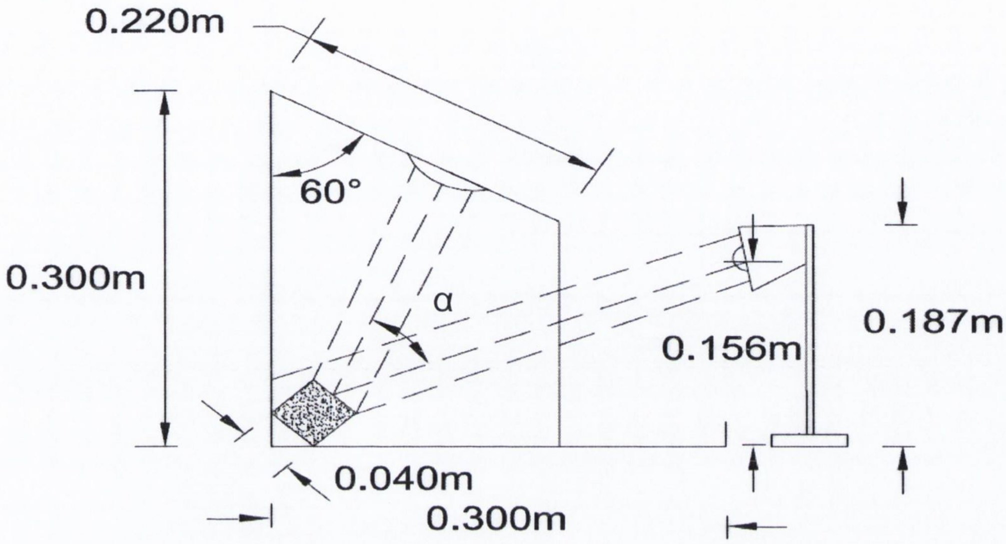

Fig. 5-26 Sketch of test setup to determine optimum angle of specimen inclination

Table 5-8 Results from varying the angle of the prism (50% GGBS) to the horizontal

Angle to horizontal (°)	Lux
30	36.8
35	38.6
40	40.0
45	**42.4**
50	42.0
55	41.4
60	41.2

When the optimum angle of approximately 45° was confirmed, the apparatus was then constructed using aluminium so that samples of concrete with varying percentages of GGBS (0, 50, 70 and 90%) could be tested with a lux meter to determine whether there was a discernable difference in lux reflected by the different samples. Rectangular prisms (160x40x40mm in size) were placed in the apparatus, as illustrated in Fig. 5-27. The lux meter was placed on top of the apparatus which previously had a circular hole cut that was the exact diameter of the lux meter receiver so that it protruded through but also to exclude peripheral light entering from above, around the edge of the hole. The apparatus' surfaces are black inside to absorb any background or reflected light. Artificial or natural light enters the front open face of the apparatus and is reflected off the surface of the sample and up towards the lux meter where a reading is taken.

This apparatus demonstrated that for each increase in the percentage of GGBS, there was a corresponding and identifiable increase in the amount of light reflected off the surface as established by the varying readings on the lux meter. The reflected lux readings from the experiment are displayed in Fig. 5-28. These values ranged from approximately 30 to 60 lux which indicates a small range but discernable trend, despite the relatively small reflective surface of the prism and the low intensity (60Watt bulb) of the incoming light (Sweeney et al., 2010).

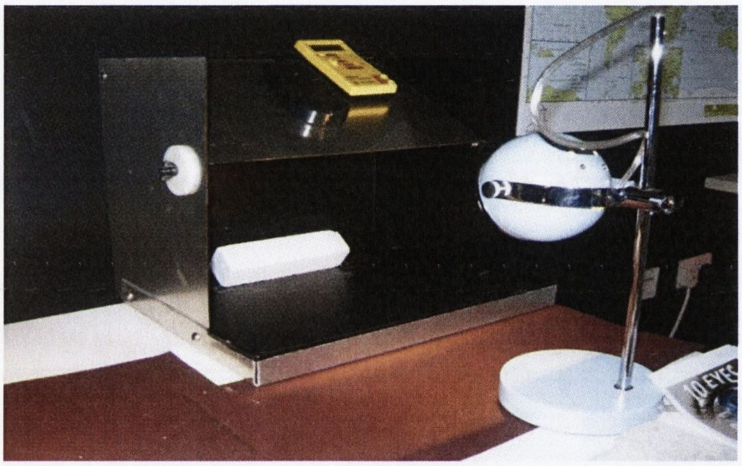

Fig. 5-27 Test apparatus for demonstrating light reflection (Sweeney et al., 2010)

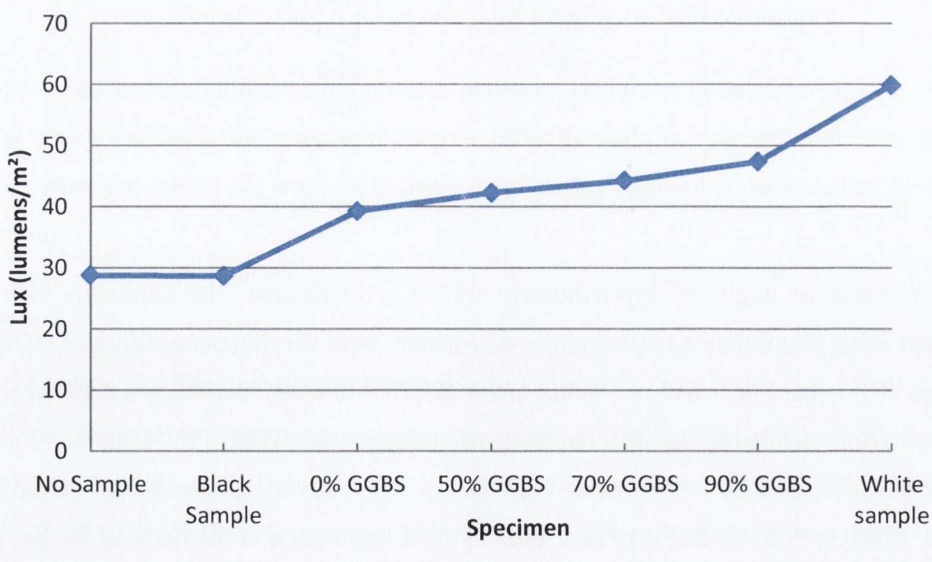

Fig. 5-28 Results from test apparatus for demonstrating light reflection

5.3.2.1 Prototype number 1

Based on the four requirements which the device has to meet (see start of Section 5.3), a prototype was designed, as displayed in Fig. 5-29. This model was proposed to be fabricated from metal and the base of the apparatus was to be placed onto the concrete slab specimens planned to measure 400x400mm at that time. The quarter-spherical component is independently free to rotate around the cut out circular shape on the surface of the slab so that the slab does not need to be moved as the sun moves across the sky, while still exposing the circular plan of the slab to incoming rays.

A pointer device is attached to the top of the plate, as indicated in Fig. 5-29, the purpose of which is to determine the degree of tilt in the slab in the vertical direction so as to align the pointer with the incident radiation, i.e. position the pointer in the direction of the sun such that there is no shadow cast by the pointer. This ensures that the light rays hit the slab at an identical angle every time and are reflected back up perpendicularly towards the lux meter which is situated at the back of the spherical component.

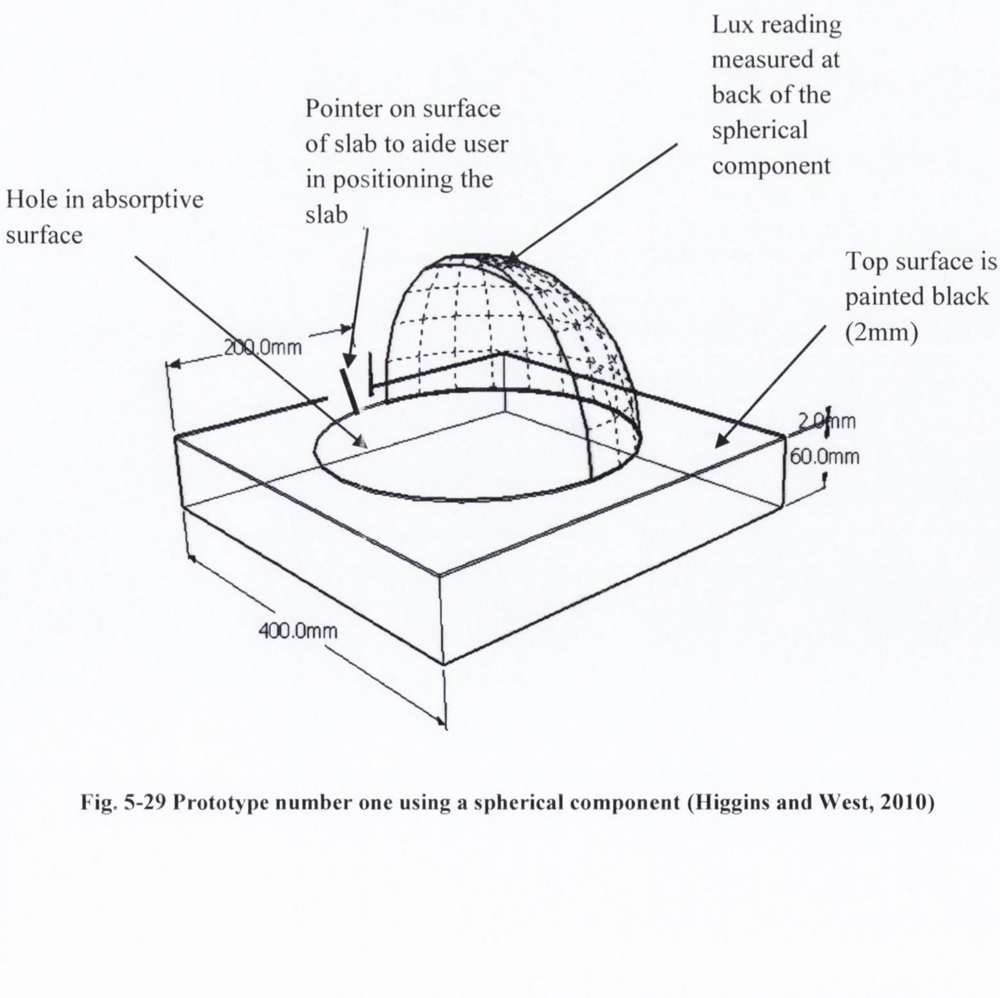

Fig. 5-29 Prototype number one using a spherical component (Higgins and West, 2010)

There are a number of advantages and disadvantages to this design. The advantages are as follows:

1. The spherical component allows for the device to rotate with the sun as it moves throughout the day in the horizontal plane. This is very practical compared with the alternative of lifting and rotating the slab in order to achieve the correct horizontal angle.
2. The vertical angle of the sun in relation to the slab can be found using the small pointed device which rotates with the quarter-sphere. The slab is rotated in the vertical direction until the point where there is no shadow cast by the pointer.

The disadvantages of this design;

1. The circular shape results in a significant reduction of surface area which is exposed to the sun's rays.
2. Although the device allows for rotation through the horizontal plane, it does not allow for vertical rotation. This would require the slab to be lifted and unfortunately it would be pivoting about a corner which is more awkward.
3. The design does not eliminate all background light from reaching the concrete slab's surface, nor all background light from the lux meter.
4. Construction of the spherical component using metal would also be difficult.

From critiquing this design, it was necessary to create a new design, which would expose more of the surface area to the incoming light. It was also important to incorporate the elimination of background light in this prototype in addition to making the design easier to fabricate.

5.3.2.2 Prototype number 2

Noting that horizontal rotation is only possible by using spherical shapes, and that the slab needs to be tilted in the vertical plane by lifting, a separate device was manufactured for the slab specimens to allow for rotation in the vertical and horizontal plane (see Fig. 5-30). There are two vertical bars (one at each corner of the device) which allow the change in the vertical angle and there are two wheels on the apparatus to reduce the amount of lifting involved. The tilting device is placed beside the board where the slab is located and the slab can slide onto the base of the lifting device. This simplifies the overall design of the apparatus for measuring light reflectance and allows the focus to be on maximizing the exposed surface area and limiting the entry of background light.

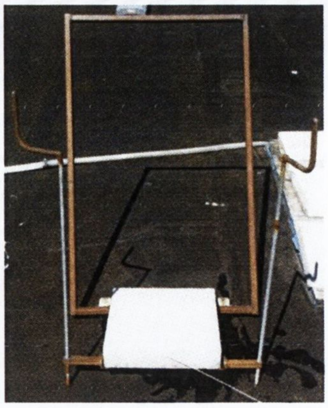

Fig. 5-30 Tilting device allowing rotation of the specimen in the vertical and horizontal direction

The second model which was designed took these factors into account, and can be seen in Fig. 5-31. This design is largely based on the apparatus shown in Fig. 5-27 but where there is an increase in the exposed surface area and the angle of reflected visible light is at 45° when the back of the slab is lifted while pointing towards the sun. There is a further addition to the design, whereby a lip has been included at the top part of the prototype to prevent, as much as possible, direct incoming light from reaching the lux meter, as illustrated in Fig. 5-31. The inside of the apparatus would have to be matt black as mentioned previously, to absorb background and unwanted reflected light.

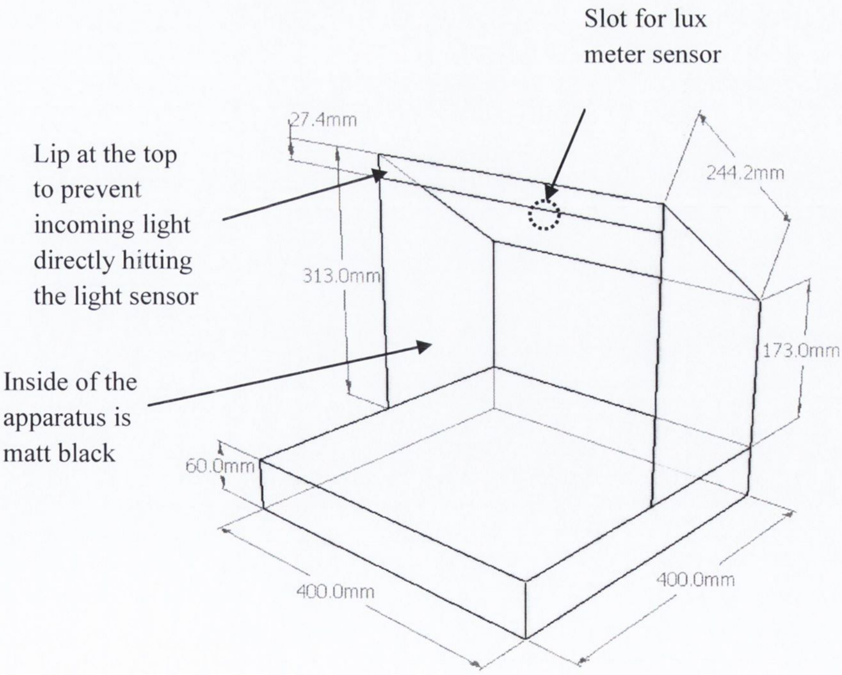

Fig. 5-31 Prototype number 2 (Higgins and West, 2010)

The prototype is illustrated in Fig. 5-32, with the specimen in place. In order to take a reading, the apparatus is tilted in the vertical direction (θ) so the surface of the slab is in full sunshine (with no shadow cast on the surface). Once this is carried out, the apparatus is designed in such a way that the incoming sun rays are entering the apparatus and are perpendicular to the lux sensor at the back of the device.

The advantages of this design are;

1. The shape of the device is simple making the fabrication easier.
2. The lip at the top of the device stops any direct sunlight shining onto the lux meter.
3. The depth of this lip is designed to aide the user to determine the angle of the sun relevant to the slab i.e. the shadow cast by the lip is on the intersection between the slab and the back wall. In this position the sun's rays are approximately at a 45° angle.
4. The horizontal positioning is easily determined by ensuring the front edge of the sides do not cast a shadow onto the concrete's surface.

The disadvantages of the design;

1. There is still a considerable amount of exposure to background light from the front region although it is partially excluded from the sides.

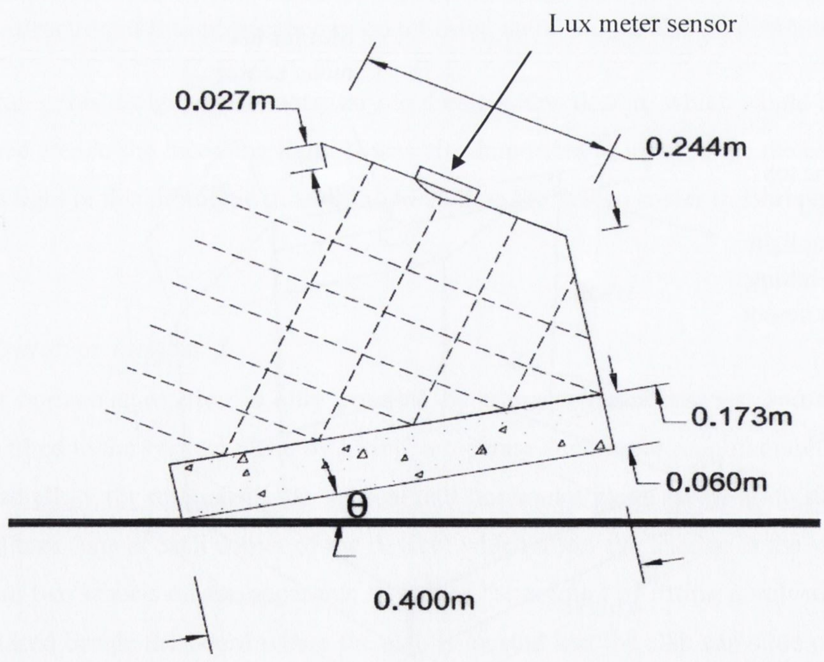

Fig. 5-32 Sketch of specimen tilted using prototype number 2 where the incoming sun rays are entering the apparatus and are perpendicular to the lux sensor at the back of the device

5.3.2.3 *Prototype number 3*

In order to overcome the disadvantage of having excessive exposure of the slab to background side light, a final design was proposed which allows for sunlight to be channeled onto the slab as shown in Fig. 5-33 and Fig. 5-34. The design acts in a similar way to the previous design (prototype number 2) but also eliminates background light.

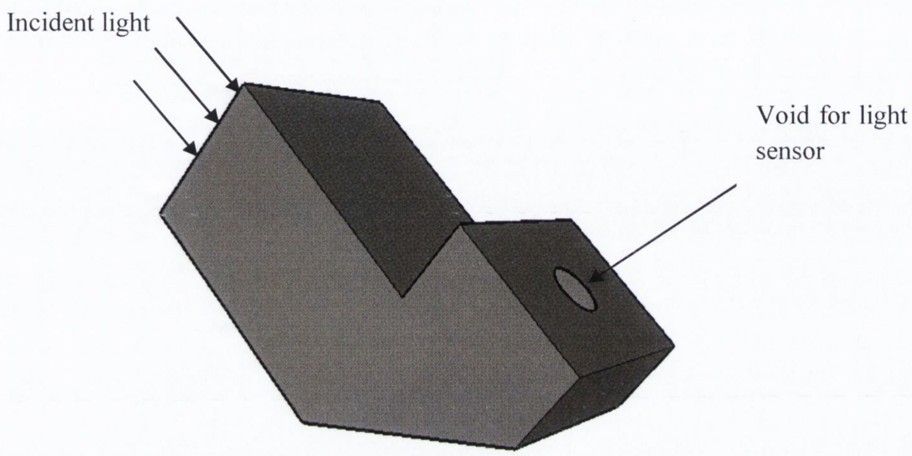

Fig. 5-33 Prototype number 3

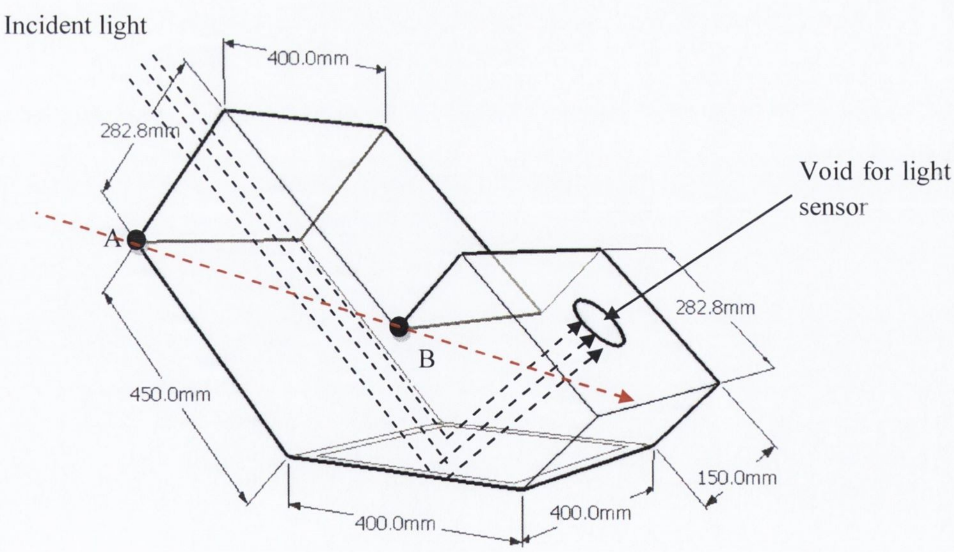

Fig. 5-34 Design of prototype number 3 (Higgins and West, 2010)

In this design, the box is placed on top of the slab and they are rotated in a horizontal plane so that the tunnel points towards the incoming sunlight. Both the slab and the box are then tilted on the front edge (or back edge depending on the sun's position) in the vertical plane until there is no shadow cast on the surface of the slab, at which point the incoming rays are parallel to the entrant sides of the tunnel. Firstly, the incoming incident light is measured orthogonal to the ray at the slab surface then, secondly, the reflected light is measured through a circular hole at the back of the box. This hole is fully blocked to prevent ambient light leakage during data collection. The chosen length of the tunnel is 450mm as shown in Fig. 5-34, the reason being that no light that passes from point A to point B can impact directly on the lux meter sensor (see red dashed line in Fig. 5-34). Therefore, only light reflected off the slab specimen is measured at the lux meter sensor and, as the box is painted black internally, very little of this reflected light is further reflected off the walls onto the lux meter.

In choosing this design, the accompanying mechanical device with wheels can hold the concrete slab (weighing 13kg) in place and which, essentially, enabled the user to rotate the specimen easily in both a horizontal and vertical direction until there was no shadow cast upon the surface of the concrete slab (see Fig. 5-30).

5.3.2.4 Manufacture of prototype

A prototype made from cardboard was manufactured and covered in black plastic as seen in Fig. 5-35, the purpose of which was to test the effectiveness of the prototype before proceeding to the manufacturing stage. By placing the prototype over black and white surfaces and taking readings using the lux meter, a significant difference in the lux was measured which indicates that the prototype is capable of accurately testing reflectance off a surface as designed.

Fig. 5-35 Manufacture of prototype number 3

5.3.3 Preliminary testing using the prototype lux meter box

In order to understand the outcomes of the light reflectance measured in the lux meter box, a number of preliminary tests were devised. These tests were carried out using two concrete slabs, both with equally flat surfaces which were finished off in the same manner. The slabs which measured 400x400mm in plan dimension, contained 0% and 70% GGBS. Five sensitivity tests were devised as described herewith (Higgins and West, 2010).

5.3.3.1 *A comparison of reflected lux meter readings on slabs containing both 0 and 70% GGBS*

This test was conducted in order to identify the extent of the difference in reflected lux meter readings between the two specimens, with one containing 0% GGBS and one containing 70% GGBS, for two different weather conditions, namely cloudy or diffuse conditions (Fig. 5-36) and sunny or direct conditions (Fig. 5-37). The readings of reflected lux were recorded at the back of the lux meter box prototype for each slab specimen and were taken at 5 second intervals. The magnitude and range of reflected lux readings in Fig. 5-36 is small (130-300 lux) due to the presence of clouds. Conversely, the data in Fig. 5-37 displays a larger range in reflected lux readings (8,000 to 10,500 lux) which are much more consistent due to clear-sky conditions.

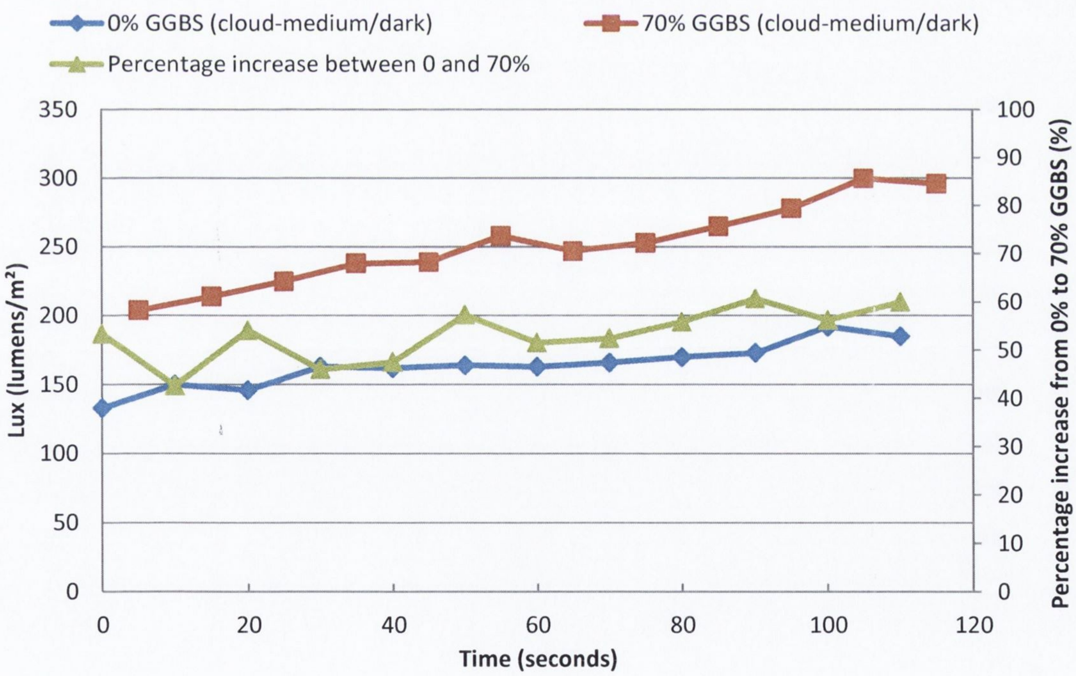

Fig. 5-36 Change in reflected lux reading for 0 and 70% GGBS slab in medium/dark cloud conditions

There is an increase observed in the reflected lux readings with time due to a change in the cloud conditions in Fig. 5-36. There is also a measurable difference between the reflected lux readings for the slab containing 0% GGBS and the slab containing 70% GGBS despite the cloudy conditions, with 70% being noticeably more reflective. It can also be noted that the difference in lux between the two slabs is relatively low (70-110 lux), although this outcome results in a relatively high percentage increase from 0 to 70% GGBS of approximately 50%.

In sunny conditions, the reflected lux for both specimens is relatively constant due to the clear-sky conditions, and there is a significant difference between the two specimens of approximately 2,260 to 2,620 lux. However, as the lux readings are higher in sunny conditions by a substantial amount, this results in a lower percentage increase from 0 to 70% GGBS of approximately 30%. This could be a significant improvement in terms of CO_2 reductions.

In conclusion, there is a discernable difference between the amount of lux reflected off a 0% GGBS specimen when compared with that of a 70% GGBS specimen, and this difference is evident in both sunny and cloudy weather conditions. However, the lux reading in cloudy conditions is not constant, therefore, a more reasonable comparison can be made between the 0 and 70% GGBS specimens in sunny conditions as there is a smaller variability in the readings of reflected lux over time.

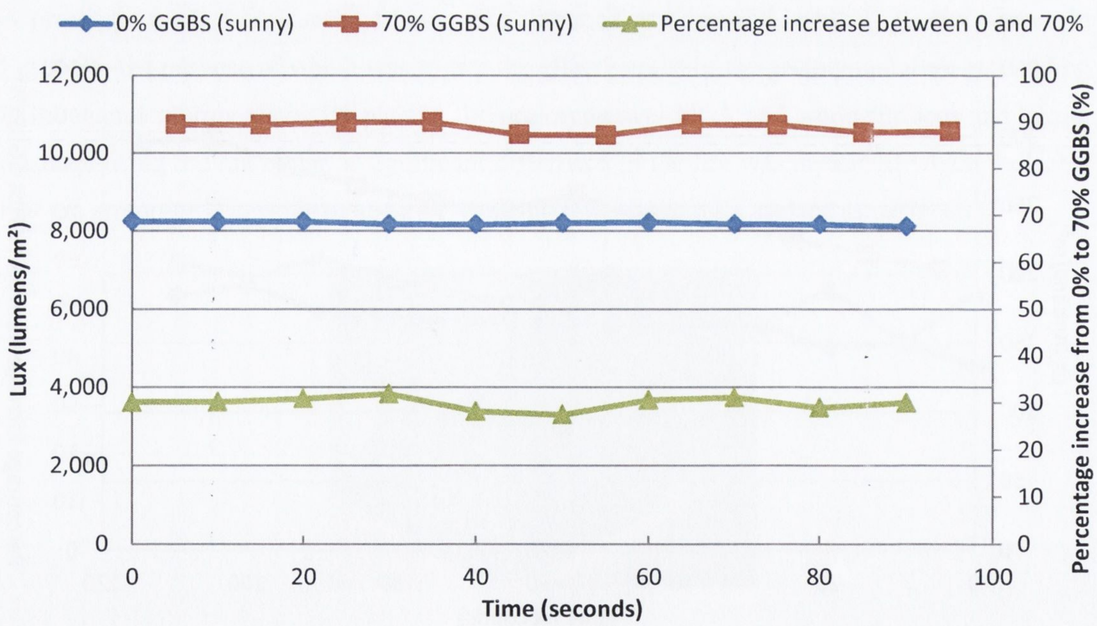

Fig. 5-37 Change in reflected lux reading for 0 and 70% GGBS slab in sunny conditions

5.3.3.2 *The change in reflected lux over time*

This test records reflected lux readings at the back of the lux meter box at thirty second intervals over a ten minute period to assess the variability in the readings. The specimen containing 0% GGBS was tested in conditions varying from cloudy to sunny. The aim of this test is to determine the consistency of reading taken and to investigate the effect of cloud cover on a lux meter reading. The plot in Fig. 5-38 demonstrates the change in the reflected lux and there were three tests carried out on different occasions for repeatability purposes. There is little variability in the readings, indicating that on a clear sunny day, uniform results can be achieved within the sensitivity of the lux meter. As the results were recorded on different days, there is a difference in the light intensity, therefore, the reflected lux values will be different, as evident from the outcome in Fig. 5-38.

Furthermore, from additional sensitivity testing conducted at a later stage, the results verified that the day on which the lux readings are recorded will not affect the resulting percentage of lux reflected but absolute values may vary considerably depending on incoming light intensity.

In conclusion, the results are uniform over 10 minutes provided there is no cloud cover. The reflected lux value is dependant on the incoming light intensity. It is also evident that the percentage reflected does not vary much between different days

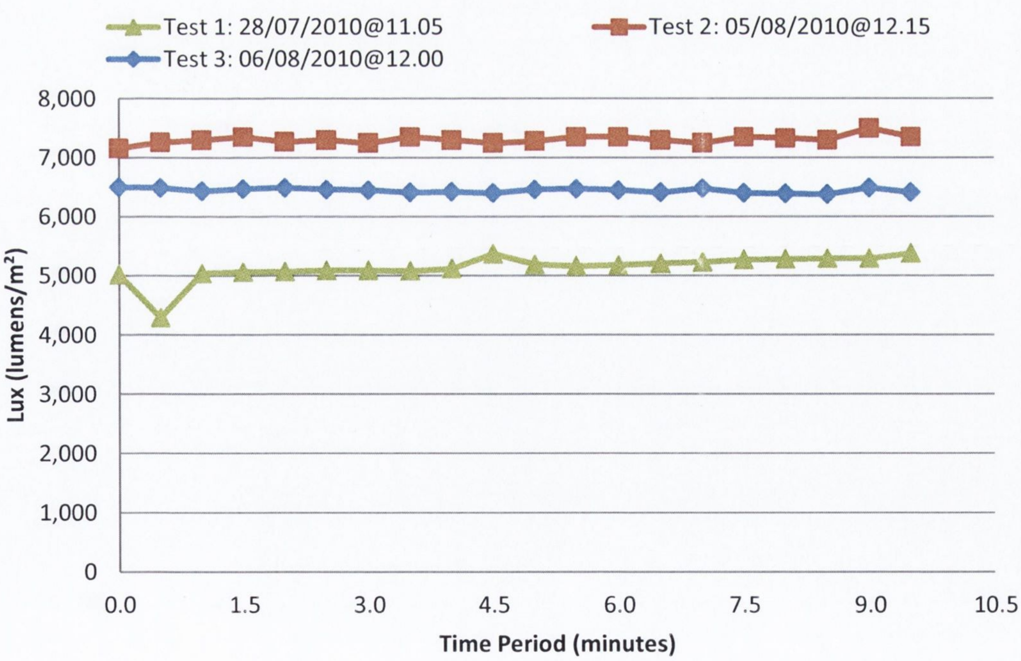

Fig. 5-38 Readings of three tests recording reflected lux taken over a 10 minute period of one slab containing 0% GGBS

Similar testing was carried out in varying cloud conditions. These results are displayed in Fig. 5-39 for 0% GGBS. These results demonstrate how the presence of cloud cover adds a significant variability to the results. The inconsistency of these results indicates that it would be difficult to carry out accurate testing in overcast conditions as there is a wide range in lux readings over a short period of time. For example, the test carried out on 03/08/2010 at 11.30am in medium cloud conditions displays a large variability in lux readings, ranging from 350 lux at 3 minutes to 900 lux at 7.5 minutes. During testing it was also noted that the readings taken when white clouds were in close proximity to the sun were higher than the readings taken in direct sunlight. In this case, the increase in lux readings was due to two contributions of incoming light; the direct incident light from the sun and the light reflecting off and being dispersed by the clouds. This indicated, firstly, that, as expected, it is not possible to completely eliminate background light from reaching the slab and, secondly, that care should be taken when testing in sunshine to ensure that the clouds are not in close proximity to the direct sunlight so as not to influence the readings of light reflectance i.e. ideal reading conditions are in uninterrupted sunshine with clear skies. Two of tests in Fig. 5-39 were carried out on the same date (03/08/2010) but at 20 minutes apart, by which time the cloud conditions had changed to dark, with a corresponding significant decrease in the reflected lux readings.

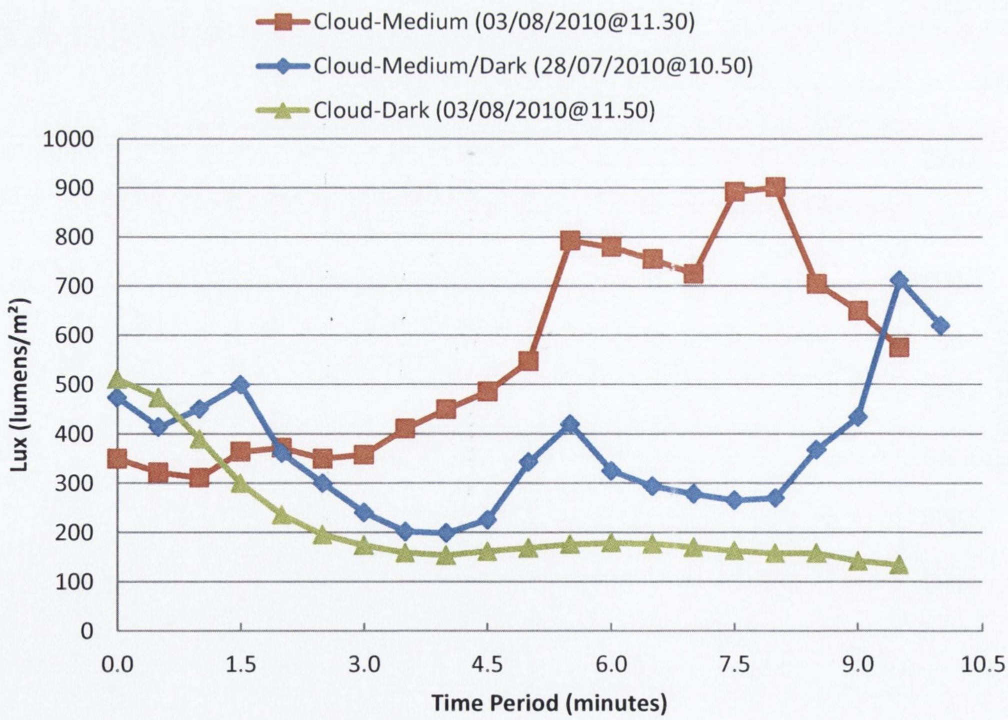

Fig. 5-39 Readings of reflected lux on a 0% GGBS slab in different cloud conditions

In conclusion, there can be a large variability in the lux readings depending on the type of cloud conditions as illustrated in Fig. 5-39. There are also extreme values of lux where readings vary by more than 550 lux over a period of less than ten minutes. Thus, due to the large variability in these results brought about by the presence of clouds, it is recommended that direct and unimpeded sunshine should be a requirement for taking consistent readings of light reflectance.

5.3.3.3 The change in reflected lux as a result of changing the surface area

The aim of this test is to determine how a change in the exposed surface area will affect a reflected lux meter reading. The area of the slab is decreased from the maximum (370x370mm) and readings are taken at each increment in exposed surfaces. The change in area is achieved by placing a matt black non-reflective material over the slab at the perimeter effectively reducing the cross sectional area but maintaining a perfect square surface area in the centre. The reduction of the cross sectional area is outlined in Fig. 5-40 indicating both the initial and final areas, where 4 reductions were imposed in 30mm side reduction increments. The angle of the incident rays were kept constant in these tests as the entire surface area is enclosed with light but only the edges of the slab were covered to effectively reduce the surface area reflecting light.

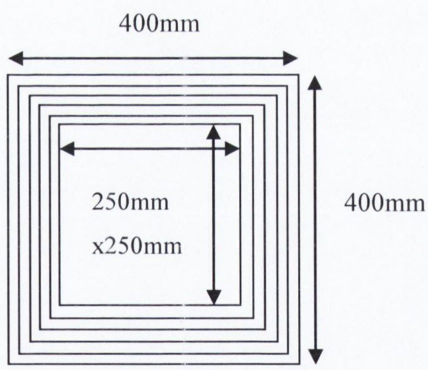

Fig. 5-40 Reduction in cross sectional area of slab specimen

The data displayed in Fig. 5-41 represents results of lux which were taken when the test area of the slab was changed for both 0% and 70% GGBS slabs respectively. These results were taken in sunny conditions and the areas to be used ranged from 250mmx250mm to 370mmx370mm. The lux reading values range between 4,000 and 6,500 lux for the 0% GGBS slab and there is a broadly linear relationship between the area of exposed slab and the corresponding lux reading. As the 70% GGBS slab is more reflective, the range of lux readings increases to between 6,000 and 10,000 lux also with a broadly linear relationship. There is on average approximately 50% increase in reflected lux for 70% GGBS when compared with that of 0% GGBS.

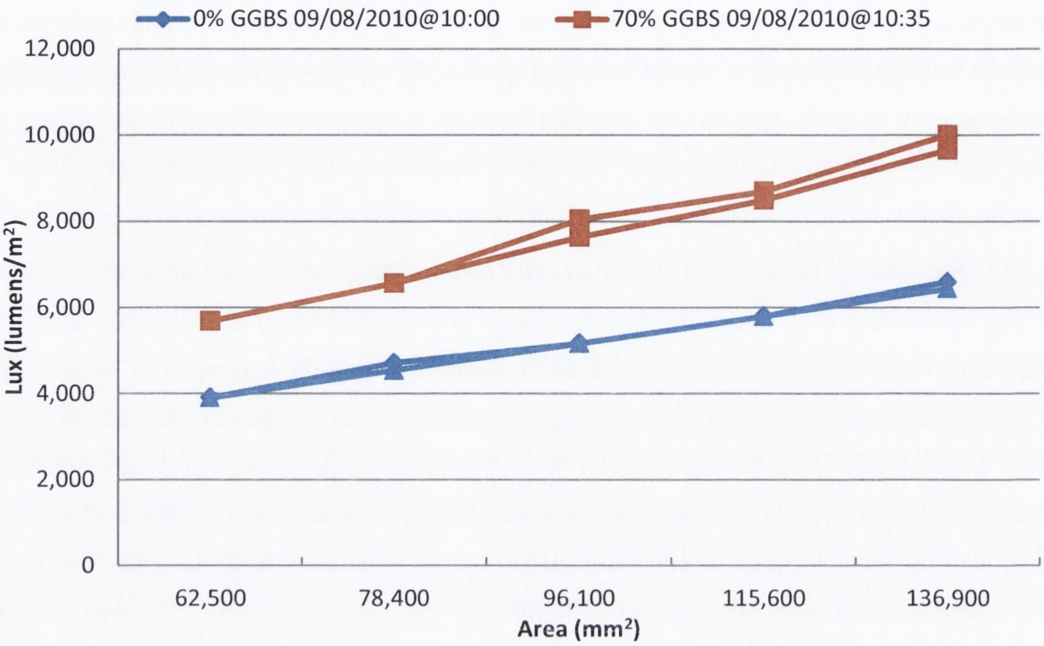

Fig. 5-41 Change in reflected lux readings resulting from change in surface area exposed for a 0% and 70% GGBS slabs

This test was carried out in order to evaluate the sensitivity of results to the area exposed. In conclusion, as the area of the slab increases, there is a proportional increase in the reflected lux reading. This result is explained by the fact that there is more light reflected from a larger surface area and that this should be a factor to take into account when making a decision on the size of the concrete specimens to be tested. Once an area is chosen, this must be maintained in order to be able to make a comparison between readings of reflected lux. It can also be concluded that the sensitivity of the test results are well within the range of the lux meter sensitivity. As the resulting ratio of reflected light depends on the size of the specimen, it can be concluded that the lux meter cannot be used to measure the true albedo of a surface.

5.3.3.4 The change in reflected lux as a result of changing the vertical angle

This test was carried out to determine how a change in the angle at which the slab is tilted from the horizontal affects a lux meter reading. This is carried out whereby the slab angle was varied in intervals of 6° starting from an initial position where the entire slab is exposed to sunlight (angle of 0°). The slab was tilted in the vertical orientation until a maximum angle of 24°, at which point there was little light reflectance from the surface. The results from this test are displayed in Fig. 5-42 and represent the change in lux reading for both the 0 and 70% slabs.

Both 0 and 70% GGBS demonstrate a common trend, whereby the maximum value of lux is obtained only where there is 100% exposure of the slab, as expected. Full exposure of the 0% GGBS specimen at an angle of 0° (where the entire surface is in sunshine) produces a reflected lux of approximately 7,300 lux, however, this is reduced to approximately 900 lux when the slab is cast in shadow, a reduction of approximately 88%. The same trend is observed for 70% GGBS, whereby the maximum lux reading occurs when the slab is completely exposed to sunlight at 0° (10,000 lux) and the minimum occurs when the slab is at its greatest angle of 24° (1,200 lux), corresponding to a reduction of approximately 88% also. This is due to the simple fact that the shadow is being cast on the surface as a result of the specimen being tilted in the vertical direction, and this shadow reduces the resulting lux reading by a significant amount. It can also be observed that the rate of change reduces so that any deviation from the angle of 0° results in a sudden change.

In conclusion, the slab is required to have full exposure to the sunlight in order to get the maximum reading of reflectance, as any presence of shadow cast upon the surface gives rise to substantial changes in reflected lux. When small trends in albedo exist due to mix constituents or surface finish, controlling such gross changes will be important.

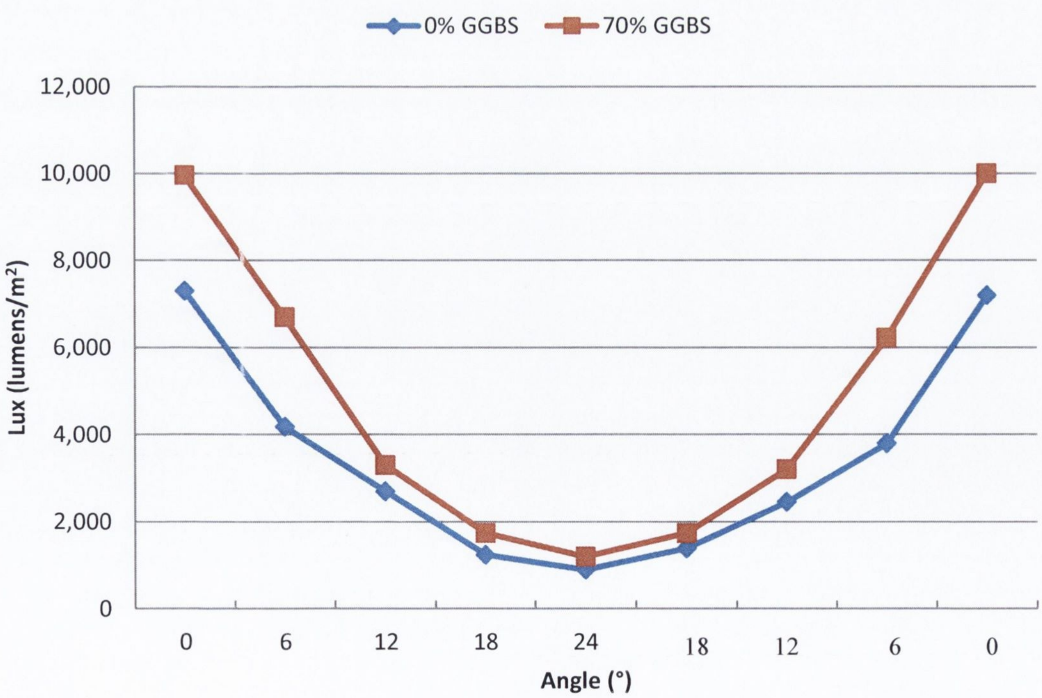

Fig. 5-42 The change in reflected lux reading as a result of changing the vertical angle of the slab

5.3.3.5 *Comparing 'relative albedo' with published albedo values*

The aim of this test is to calculate a 'relative albedo' value. The lux meter is positioned in the centre of the slab at an angle of 45° to the slab surface with the sensor pointing out of the tunnel in the direction of sunlight, and the reading of incoming lux is recorded. A reading of reflected lux is taken immediately afterwards at the recessed hole of the lux meter box. It should be noted that normally an albedo value is calculated as the reflected solar radiation divided by the incoming solar radiation over all wavelengths of solar rays. However, the 'relative albedo' is calculated as the ratio between the incoming and reflected lux readings. The resulting 'relative' albedo values will be compared with published albedo values. A number of readings for each slab were recorded for comparison purposes. This test was carried out in full sunshine conditions only, as the presence of cloud results in readings with very high variability and are, therefore, not reliable.

From the results obtained in Table 5-9 (which display the incoming lux, reflected lux and relative albedo) there is a detectable difference in the relative albedo of these two concrete specimens. However, the values calculated from this test are much lower than published albedo values for concrete. This is due to the sample size as it was demonstrated previously in this chapter (see section 5.3.3.3) that the surface area has a significant impact on the resulting reflected lux. As the surface area is restricted, this reduces the overall reflectance ratio. For the slab containing 0% GGBS an expected albedo value would be in the region of 0.35 to 0.40 for new concrete and for the slab containing 70% GGBS, an expected albedo value would be approximately 0.60. However, the relative albedo values for 0 and 70% slabs based on visible light reflectance are 0.0583 and 0.0747 with corresponding standard deviation values of 0.000362 and 0.000750 respectively.

Table 5-9 The 'relative albedo' test for 0 and 70% GGBS slab

0% GGBS			**70% GGBS**		
Reflected Lux	Incoming Lux	Relative Albedo	Reflected Lux	Incoming Lux	Relative Albedo
7,900	135,000	0.0585	10,000	132,000	0.0758
7,800	134,900	0.0578	10,100	134,000	0.0754
7,800	134,400	0.0580	9,900	134,000	0.0739
7,900	134,500	0.0587	10,000	134,100	0.0746
7,800	134,700	0.0579	10,100	133,900	0.0754
7,900	134,800	0.0586	9,900	134,300	0.0737
7,900	134,900	0.0586	10,100	134,200	0.0753
7,800	134,800	0.0579	10,000	133,900	0.0747
7,900	134,900	0.0586	9,900	133,800	0.0740
7,900	134,900	0.0586	9,900	133,800	0.0740
Average		0.0583			0.0747
St. Dev		0.000362			0.000750

The relationship between the incoming lux and relative albedo was also investigated in Fig. 5-43 for the 0 and 70% GGBS specimens. It is evident from this plot that there may be a correlation between these two parameters, however, two sets of points is not sufficient to determine this. However, the plot demonstrates a clear differentiation between the 0 and 70% GGBS specimens, with 70% GGBS resulting in a higher 'relative albedo'.

In conclusion, the 'relative albedo' value for both specimens is not comparable to the published albedo values as the restricted surface area and the restricted light frequency (only visible light) do not produce a true albedo, however, the lux meter prototype has shown that it is a very good mechanism for comparing results as it is very sensitive. It can only be used for comparative studies as it has been demonstrated that the prototype apparatus can distinguish very clearly between different surfaces finishes and different percentages of GGBS as the device is sensitive. However, 'relative albedo' values enable a comparison to be made between different slab surfaces for identical surface areas. Hereafter, the parameter 'relative albedo' will be presented as a percentage which is calculated by dividing the reflectance of the specimen by the incoming light.

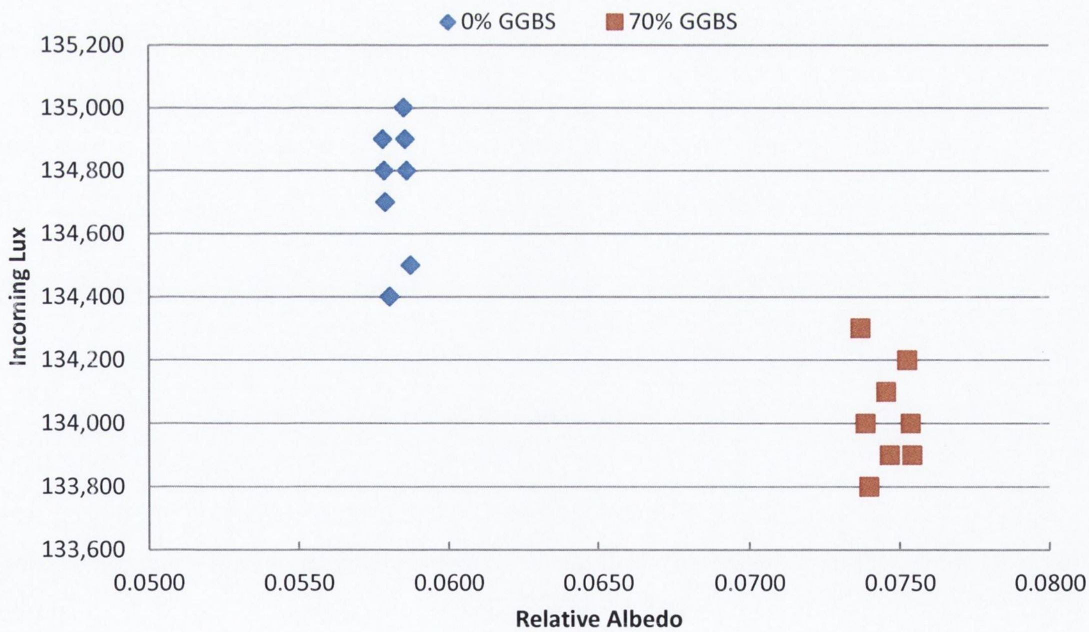

Fig. 5-43 Relationship between relative albedo and incoming lux for 0 and 70% GGBS specimens

5.3.3.6 Conclusions from using the prototype lux meter box

- The replacement of cement by GGBS increases the reflectivity of the concrete, with the 70% GGBS specimen producing a higher reflected lux reading. There was a significant increase in the reflected lux of the 70% GGBS specimen by approximately 30% (from a baseline of 0% GGBS) in clear sunshine.
- Readings taken in overcast conditions are extremely variable and cannot be carried out reliably in these circumstances, however, readings recorded when there is sunshine with no clouds in close proximity to the sun i.e. when there is no light dispersion from the clouds, result in very consistent and reliable readings.
- There is a clear trend where the change in reflected lux is proportional to the change in surface area, with the relationship being broadly linear. The device is very sensitive to this parameter, therefore, the size of the surface area must be a constant in order to be able to compare results of reflected lux.
- In order to achieve a maximum reading for lux, the entire concrete slab must be exposed to sunlight i.e. with no shadow present on the surface of the slab. Where there is any shadow present on the surface, there is a sudden decline in the result, demonstrating that the device is also very sensitive to this parameter.
- The results of 'relative albedo' were not consistent with published albedo values which is due largely to the size of the testing surface. It would suggest that lux meter readings using the black box cannot be used as a direct method of testing albedo, however, the instrument is sufficiently sensitive to detect a small difference between the two slab types, indicating that it could be used as an indirect means of testing albedo where comparisons are desirable. In conclusion, 'relative albedo' values enable a comparison to be made between different slab surfaces provided the area remains constant.

5.3.4 Manufacture of final lux meter box

Following testing using the prototype, the final lux meter box for measuring visible light reflectance was fabricated. As mentioned in Section 5.3.2, the material for the device was originally proposed to be thin sheet metal, however, as there was a risk of the metal distorting due to the self weight of the device, the chosen material was changed to timber. It should be noted that the final design was reduced from 400x400mm to 300x300mm in surface area in order to reduce the weight of the specimens (from 23kg to 13kg).

The joints were filled with silcone to seal the apparatus, thus preventing any stray light passing into the chamber. Following this it was painted internally using matt black paint to prevent any light reflecting from the inside surfaces of the device. The outside was also painted black for aesthetic purposes only. The reflectance off a matt black surface was conducted to determine if there was any light reflectance from the inside of the black box, and the resulting lux was zero. Fig. 5-44 illustrates the finished prototype.

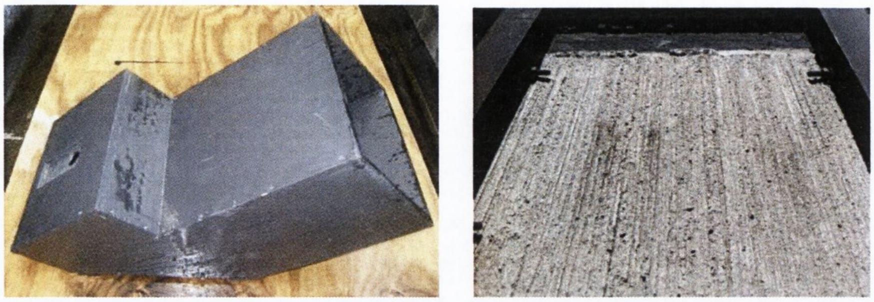

Fig. 5-44 Black box to measure visible light reflectance (left) and view of inside the box from the opening where the lux meter is placed to measure the reflected light off the surface (right) (Sweeney et al., 2012b)

5.3.5 Sensitivity tests using lux meter box

In order to have confidence in results obtained using the lux meter and black box, a number of tests were carried out, the main objective of which was to assess the sensitivity of the device. The tests were conducted on two slabs, one with a rough surface finish (brush with 50% GGBS) and one with a smooth surface finish (cast also with 50% GGBS). A single GGBS content was chosen to facilitate comparison between the finishes. All tests were conducted when, ostensibly, the sun was shining with little if any, cloud cover. The tests can be described as follows:

1. Large area test- to determine the approximate lux readings using the device without the black box present.
2. Repeatability test- to assess whether a variability in a reading is due to the instrument or is a result of a process error.
3. Orientation test- to determine whether the orientation of the slab gives different results of light reflectance, particularly for samples of brush and tamp finishes.
4. Time of day test- to assess how the sun elevation (sun intensity) impacts on light reflectance.
5. Day test- to determine whether the particular day has an effect on light reflectance including the effect of cloud cover (testing within the same season, a couple of days apart and at the same time of day).

5.3.5.1 Large area test (no lux meter box)

The lux meter is used in conjunction with the designed black box for measuring the light reflectance off the small slab specimens, however, a test was conducted without using the black box. The objective of this test is to determine the approximate overall percentage of lux reflected if the lux meter was used in a similar manner to an albedometer. The lux meter was held in position over a concrete surface at a height of 1.5m and the incoming and reflected lux were recorded by facing the sensor upwards for the incoming reading and downwards for the reflected reading (see Table 5-10 for results). This was performed for four locations over the same surface.

During the test, it was observed that the readings were difficult to take, with large variations in the resulting lux, and this was due to the surroundings having an impact on the sensor. Although there was sunshine with no clouds present, the incoming lux was in the region of 18,000-20,000 lux. This is a significant reduction when compared with the incoming lux measured using the lux meter box in the aforementioned sensitivity tests. The range of incoming lux was between 70,000-80,000 for these tests and this would suggest that when the black box is used, only direct sunshine is measured, with the impact of the surroundings removed completely. Accordingly, a low value of percentage reflected lux is obtained (≈6%).

It is also important to note that the lux meter is parallel to the concrete surface in this test, and is not pointing directly at the sun unlike testing with the lux meter box. This would reduce the incoming lux reading significantly.

Table 5-10 Testing on a concrete surface using the lux meter without the black box at four locations (1 –4)

Location	Incoming Lux	Reflected Lux	% Lux	Average
1	16,250	5,310	32.7	28.3
	17,800	4,730	26.6	
	18,930	4,880	25.8	
2	18,600	4,020	21.6	21.5
	19,400	4,110	21.2	
	18,200	3,960	21.8	
3	16,210	4,130	25.5	22.4
	17,380	4,080	23.5	
	23,500	4,320	18.4	
4	17,830	5,290	29.7	29.9
	15,900	5,230	32.9	
	20,500	5,540	27.0	

In conclusion, the average reflected lux results ranges between approximately 21 and 30% (0.21-0.30 in 'albedo' terms) when the lux meter box is not used, for a concrete surface. However, there is fluctuation in the reading of the lux meter as the surroundings have an effect on the result. There is no strong correlation between the incoming and reflected lux using this method, hence a loss in the sensitivity of the device is observed. Accordingly, this method is not used to measure the reflectance off surfaces due to the unreliability of the test method.

5.3.5.2 *Repeatability test*

There were a total of 10 readings recorded over one hour (one reading every 6 minutes). As each reading was taken, the lux meter box apparatus was removed from the slab and reassembled between each reading. The purpose of this was to determine whether there was any error present through carrying out the process of recording a reading assuming the incoming light did not vary much. The results for the brushed slab are displayed in Table 5-11, while the results of the readings taken for the cast finish slab are displayed in Table 5-12. The values for the average (μ), standard deviation (σ) and coefficient of variance (CoV) are provided in both cases.

Table 5-11 Result of repeatability test for brush 50% slab

	Reading No.	Incoming lux	Reflected lux	% lux
Brush 50%	1	75,500	4,720	6.25
	2	74,400	4,620	6.21
	3	74,800	4,680	6.26
	4	76,200	4,740	6.22
	5	76,100	4,700	6.18
	6	74,000	4,540	6.14
	7	66,600	4,180	6.28
	8	67,100	4,170	6.21
	9	72,200	4,510	6.25
	10	70,500	4,370	6.20
			μ	**6.22**
			σ	**0.042**
			CoV	**0.70%**

When the readings were recorded there was no cloud cover, however, there is a small fluctuation in the incoming light. This results in a corresponding change in the result for the reflected light. The average light reflectance ratio for the brush finish slab was 6.22% with a standard deviation of 0.042. Similarly, the average reading of light reflectance for the cast finish slab was 5.12% with a standard deviation value of 0.074. As the computed values of the coefficient of variation are low (0.70 and 1.45% respectively), it can be concluded from this test that there is low variability as a result of the instrument accuracy and due to the process of taking a reading.

The data for a brush and cast finish slab respectively, is also displayed in Fig. 5-45 in order to demonstrate the relationship between incoming and reflected lux. The plot verifies that the reflected lux does depend on the incoming lux, and over a relatively small range of lux readings, the ratio of reflected to incoming lux is approximately a constant. There is some variability, in particular for the cast finish specimen, however, there is the value for R^2 for each of the specimens is very high. The slope of the line is calculated as y/x, or reflected/incoming, which is approximately a constant.

It is also evident from the plot that the brush specimen is more reflective than the cast specimen. This can be explained by the fact that the colour of the finish has more predominance in terms of outcome, rather than the nature of the surface finish, with a cast finish having a slightly darker colour than a brush finish, therefore reflecting less light.

Table 5-12 Result of repeatability test for cast 50% slab

	Reading No.	Incoming lux	Reflected lux	% lux
Cast 50%	1	77,400	3,940	5.09
	2	73,300	3,690	5.03
	3	74,600	3,840	5.15
	4	76,100	3,950	5.19
	5	76,000	3,860	5.08
	6	75,200	3,760	5.00
	7	64,400	3,270	5.08
	8	64,700	3,360	5.19
	9	67,800	3,530	5.21
	10	70,300	3,650	5.19
			μ	**5.12**
			σ	**0.074**
			CoV	**1.45%**

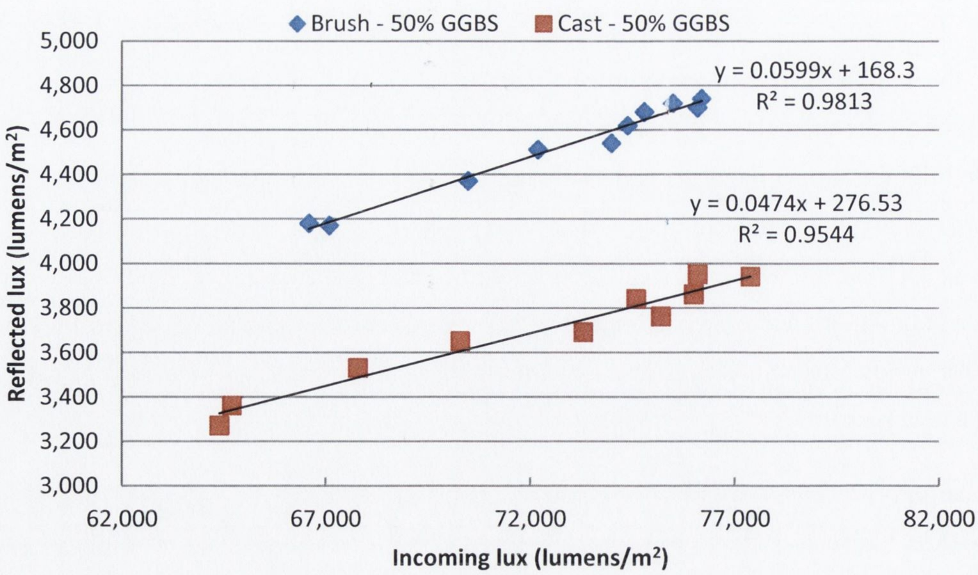

Fig. 5-45 Repeatability test for cast and brush specimens containing 50% GGBS

5.3.5.3 Orientation test

As there are two surface finish types which are undulating, the objective of this test was to determine whether the orientation of the slab has an effect on the light reflectance of the slab, and the brushed case is used to demonstrate this. For comparison purposes, this test was also carried out on a smooth surface finish (cast).

The first orientation of the slab was set up so that the vertical component of the lines of the rough finish are parallel to the vertical component of the incoming rays (inclined to the vertical). A total of three readings were taken for each orientation. Then the slab was rotated in a clockwise direction by 90° so that the lines of the surface finish were perpendicular to the incoming light (horizontal). This process was repeated twice, whereupon the slab was back in its original orientation. The average of the three readings was taken to give one result of light reflectance for each orientation. The results are presented for both brush and cast surface finishes in Table 5-13 and Table 5-14 respectively.

Table 5-13 Orientation test using brush 50% slab

Orientation	Incoming	Reflected	% Refl.	Average
0° (vertical)	79,800	4,930	6.18	6.18
	79,000	4,890	6.19	
	79,200	4,890	6.17	
90° (horizontal)	79,000	4,410	5.58	5.58
	79,200	4,410	5.57	
	78,900	4,400	5.58	
180° (vertical)	76,600	4,750	6.20	6.19
	77,300	4,780	6.18	
	76,300	4,710	6.17	
270° (horizontal)	78,400	4,390	5.60	5.57
	78,500	4,400	5.61	
	78,200	4,300	5.50	

The results for a brushed finish slab illustrate that there is more light reflected from the surface of the slab where the lines run in the vertical direction. The average readings for this orientation are 6.18 and 6.19% respectively. However, when the slab is orientated with the lines running in a horizontal direction, there is less light reflected from the surface even though the incoming light is constant with marginal fluctuation. These results give a reflectance ratio of 5.58 and 5.57% respectively. The difference in the percentage of reflected light between the two orientations is, on average, approximately 10% (0.60/5.57). This difference can be attributed to the enhanced dispersion of light from the surface when the incident light impacts on horizontal striations.

The results for a cast finish slab are displayed in Table 5-14 and although the slab was rotated in the same manner as the brushed finish slab, the average light reflectance remains the same, at approximately 5.1%. This result is due to the slab having a smooth surface finish, with the incoming light being reflected to the some degree regardless of the orientation. In conclusion, this test has demonstrated that the orientation of a concrete slab with an undulating surface finish has an effect on the resulting light reflectance, with the vertical orientation giving a higher light reflectance ratio by approximately 10%, while there is practically no difference in albedo with orientation for slabs with a smooth finish.

Table 5-14 Orientation test using cast 50% slab

Orientation	Incoming	Reflected	% Refl.	Average
0° (vertical)	76,100	3,800	4.99	5.0
	76,100	3,820	5.02	
	77,200	3,850	4.99	
90° (horizontal)	77,700	3,880	4.99	5.0
	77,500	3,880	5.01	
	77,200	3,870	5.01	
180° (vertical)	78,000	3,930	5.04	5.07
	75,600	3,850	5.09	
	77,000	3,910	5.08	
270° (horizontal)	77,000	3,950	5.13	5.09
	78,000	3,950	5.06	
	77,400	3,940	5.09	

5.3.5.4 *Time of day test*

As the sun elevation changes throughout the course of one day, so too does the incoming intensity and angle of incidence to the ground. This variable is examined by measuring the percentage lux reflected off the two specimens at different times throughout the course of one day, when the sunshine is present. The data presented in Table 5-15 represents the cast finish and the data from Table 5-16 represent the brush finish specimen. The coefficient of variation (CoV) is presented for both data sets. The readings were taken every hour between 10:00 and 14:00, with three readings recorded each time.

The results displayed in Table 5-15 confirm that the incoming lux changes throughout the course of the day, starting at approximately 66,000 lux and increasing to approximately 80,000 lux at 14:00. However, this increasing trend is also present for the reflected lux and as a consequence, the percentage of lux reflected from the specimen remains approximately constant at 4.8%, having a low CoV of approximately 0.46%. Similarly, the brush finish slab (see Table 5-16) was also recorded at the same time interval. The incoming lux at a particular time is approximately the same as a result. However, the reflected lux is marginally higher for this specimen due to the nature of the surface finish. The average percentage of lux reflected remains relatively consistent when it is recorded each time, therefore, the CoV is low at 0.25%.

Table 5-15 Time of day sensitivity test results using cast 50% slab

Time	Reading	Incoming Lux	Reflected Lux	% Lux	Average
10:00	1	66,600	3,200	4.80	4.83
	2	65,800	3,150	4.79	
	3	66,000	3,230	4.89	
11:00	1	74,900	3,630	4.85	4.84
	2	72,800	3,510	4.82	
	3	73,600	3,580	4.86	
12:00	1	75,000	3,600	4.80	4.80
	2	75,100	3,600	4.79	
	3	74,800	3,590	4.80	
13:00	1	76,100	3,660	4.81	4.79
	2	76,400	3,630	4.75	
	3	75,700	3,650	4.82	
14:00	1	79,900	3,840	4.81	4.80
	2	80,500	3,860	4.80	
	3	80,500	3,860	4.80	
				μ	4.81
				σ	0.022
				CoV (%)	**0.46**

Table 5-16 Time of day sensitivity test results using brush 50%

Time	Reading	Incoming Lux	Reflected Lux	% Lux	Average
10:00	1	65,800	3,430	5.21	5.21
	2	65,600	3,430	5.23	
	3	66,000	3,430	5.20	
11:00	1	73,200	3,820	5.22	5.22
	2	73,200	3,820	5.22	
	3	73,300	3,830	5.23	
12:00	1	78,500	4,090	5.21	5.19
	2	77,200	3,990	5.17	
	3	78,000	4,040	5.18	
13:00	1	76,300	3,970	5.20	5.20
	2	75,700	3,940	5.20	
	3	75,600	3,930	5.20	
14:00	1	73,300	3,850	5.25	5.20
	2	78,000	4,030	5.17	
	3	79,100	4,100	5.18	
				μ	5.20
				σ	0.013
				CoV (%)	**0.25**

The data from Table 5-15 and Table 5-16 which represents a cast and brush finish respectively, is presented in a plot in Fig. 5-46. It is clear from this plot that there is a linear relationship between the incoming and reflected lux readings with very high values of R^2, therefore, it can be concluded that time of day at which the reading is taken is not important given that the outcome will be a constant value.

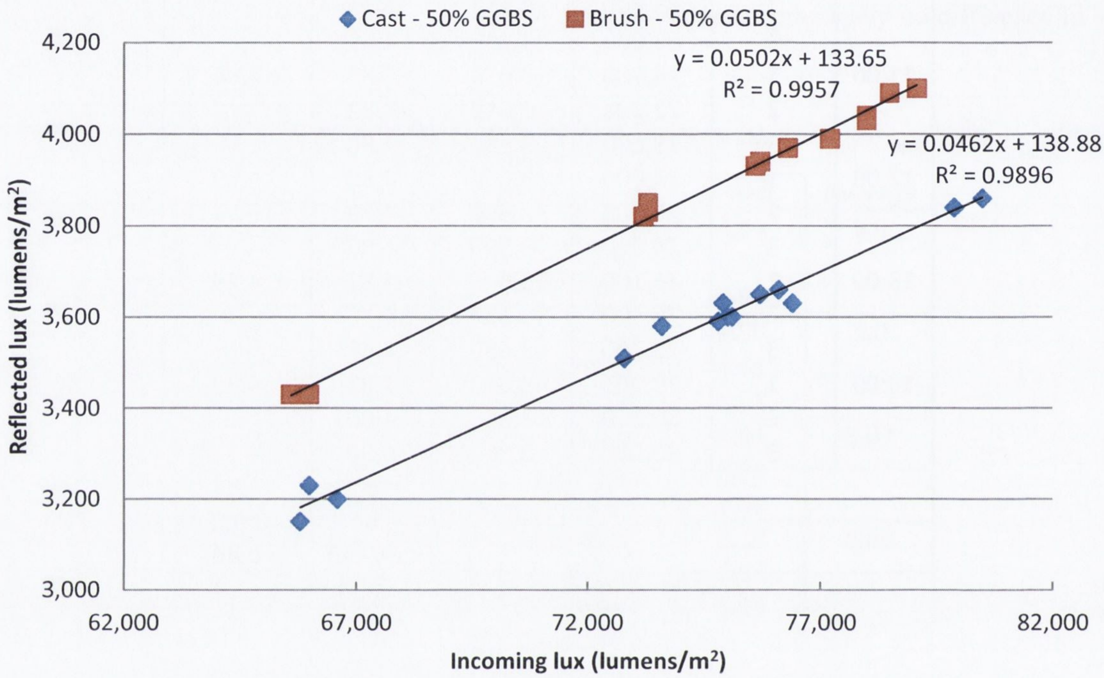

Fig. 5-46 Time of day test for cast and brush specimens containing 50% GGBS

In conclusion, the incoming lux changes during the day as a result of the change in the sun's elevation. However, this change is also evident in the amount of light reflected by both specimens, which confirms that the time of day at which the reading of lux is recorded will not significantly alter the overall reflected lux result, provided that there are no clouds present.

In the albedo test as discussed previously, it was concluded that there was variation in the albedo value during the day and this was as a result of the testing surface being fixed at a horizontal position. Therefore, as the sun's position changed throughout the course of the day, the dispersion properties also changed. However, in the case of the lux meter test method, the slab is rotated such that it is always pointing towards the sun and although the intensity changes throughout the day, the dispersion properties do not. As a result, there is no variation during the course of one day. This method is therefore a superior method of testing over the albedometer.

5.3.5.5 *Day test*

The previous sensitivity test (time of day) was repeated to evaluate whether the reflected lux ratio is identical on a different day as one clear day may be different to another clear day (close to the previous day). There were readings recorded every hour between 10:00 and 14:00, with three readings recorded each time for the two specimens, as previously. The data presented in Table 5-17 represents the cast finish specimen and the data from Table 5-18 represents the brush finish specimen.

The important value to note is the average of the three percentage lux readings recorded at each time interval and this value ranges between 4.80 and 4.84%, with an overall average of 4.82% for the cast finish specimen. The CoV is very small at 0.30%. If this outcome is directly compared with the results which were taken on the different day one week previously (see Table 5-15), a very similar average of 4.81% is observed. This would confirm that the day on which readings are recorded does not affect the resulting percentage reflected lux reading, provided the readings are taken close to each other in time.

Table 5-17 Day sensitivity test results using cast 50% slab

Time	Reading	Incoming Lux	Reflected Lux	% Lux	Average
10:00	1	68,100	3,290	4.83	4.84
	2	68,200	3,300	4.84	
	3	67,900	3,290	4.85	
11:00	1	71,300	3,450	4.84	4.82
	2	71,200	3,420	4.80	
	3	71,300	3,440	4.82	
12:00	1	73,600	3,520	4.78	4.80
	2	73,500	3,520	4.79	
	3	73,600	3,560	4.84	
13:00	1	75,700	3,660	4.83	4.82
	2	76,400	3,680	4.82	
	3	75,800	3,650	4.82	
14:00	1	78,500	3,790	4.83	4.84
	2	78,700	3,820	4.85	
	3	78,700	3,800	4.83	
				μ	4.82
				σ	0.014
				CoV (%)	**0.30**

Similarly, the brush finish specimen results (see Table 5-18) have an average percentage reflected lux ranging between 5.18-5.23%, with an overall average of 5.21%, and a low CoV of 0.41%. When this average is compared to the previous result recorded on a different day (see Table 5-16), the average lux recorded was 5.20%. This result reaffirms the conclusion that the day on which a specimen is tested will not alter the resulting reflectance, provided the time interval between the two days is not sufficiently big to allow the specimens time for ageing to occur, the season does not change and there are no clouds present, as all of these parameters may result in a different percentage of lux being reflected.

Table 5-18 Day sensitivity test results using brush 50% slab

Time	Reading	Incoming Lux	Reflected Lux	% Lux	Average
10:00	1	68,300	3,560	5.21	5.22
	2	68,400	3,580	5.23	
	3	68,300	3,570	5.23	
11:00	1	71,700	3,710	5.17	5.19
	2	72,000	3,730	5.18	
	3	72,200	3,760	5.21	
12:00	1	73,800	3,820	5.18	5.18
	2	73,700	3,810	5.17	
	3	73,700	3,830	5.20	
13:00	1	75,200	3,920	5.21	5.23
	2	75,500	3,950	5.23	
	3	75,600	3,960	5.24	
14:00	1	78,000	4,070	5.22	5.21
	2	78,300	4,090	5.22	
	3	78,800	4,100	5.20	
				μ	5.21
				σ	0.021
				CoV (%)	**0.41**

5.3.5.6 Conclusions from sensitivity tests

- When the lux meter box is not used, the incoming lux is significantly lower due to the impact from the surroundings. There are fluctuations in the lux meter reading using this test method as the instrument loses its sensitivity. The overall percentage of reflected lux ranges between 21-30% for a concrete surface containing 30% GGBS and a brush surface finish using this method. In conclusion, a box apparatus is necessary to detect small changes due to aggregate type, GGBS content, surface finish or age.
- The repeatability test demonstrated that the use of the lux meter with the black box is a reliable test method. There is neither significant variation as a result of the instrument nor in the process of taking a reading.
- The orientation of the rough surface finish is important as it effects the percentage of light reflected by approximately 10%. The amount of light reflected is higher when the lines of the surface finish are vertical with respect to the sides of the black box. The orientation of a smooth slab does not impact on the resulting light reflected.

- The incoming lux changes during the course of one day due to the sun's position, however, the amount of light reflected by the specimen increases accordingly. Therefore, it can be concluded that the time of day at which the reading is recorded will not affect the overall percentage of reflected lux, provided there are no clouds present, unlike the albedo readings. This is because the angle of the slab can be changed so that the sunlight always comes in at the same angle and, therefore, the dispersion is a constant.
- The time of day sensitivity test was repeated within a few days on the same two slab specimens. The same average percentage reflectance was obtained on both days. Therefore, it was concluded that the day on which the specimen is tested does not affect the result, provided that the slab has not aged, it is roughly at the same time of year, and there are no clouds present to obscure the reading.

5.3.6 Conclusions

- It has been demonstrated that the lux meter box apparatus works well in that it can distinguish very clearly between different surfaces finishes and different percentages of GGBS. The sensitivity tests also confirm that the device is sensitive and produces uniform readings over a short period of time, for a given specimen size which is fully exposed to sunlight.
- The lux meter box readings are restricted in two ways; the surface area is small and the light frequency being measured is visible light only, therefore, a true albedo is not attained. However, the apparatus and lux meter are a very good mechanism for comparing results as it is very sensitive, so it can be used for comparative studies.
- The lux meter test is a superior test to the albedo test as a lux reading is not dependant on the time of day at which a reading is recorded. In addition to this, the apparatus for the lux meter eliminates background light, whereas the albedometer has a large field of view. The lux meter is about one hundredth the cost of an albedometer and so is more universally accessible.

5.4 Conclusions

The albedometer works reasonably well in the field provided there is a large unobstructed area available. It can be used reliably for calculating the approximate albedo of a large surface, such as was carried out at the three site locations (St. James Gate Brewery and Father Collins Park).

It is a very sensitive instrument, but has proven to be problematic in terms of its ability to measure the albedo of small specimens accurately. The results from the sensitivity tests performed indicate that there are a number of parameters which affect the albedo value. These include; the time of day the reading is taken, the time of year, the location, the height of the instrument, the influence of cloud cover, and the ability to obtain a 170° unobstructed horizon. In addition, the lower sensor is not as sensitive when the field view is restricted as the rate of change in albedo is not the same as when there is no restriction present. This would verify that the device cannot be calibrated so that it can be used on small concrete specimens, given that its presence results in the sensor becoming much less sensitive.

An alternative means of measuring the light reflectance from the small concrete specimens was devised using a lux meter. A lux meter reading is not the same as an albedometer reading as there is a restricted wavelength - the lux meter measures across the visible range only. The lux meter cannot be used to take direct albedo readings, however, it enables the user to distinguish between the specimens containing different parameters such as GGBS content and surface finish. It provides consistent results which are repeatable and reliable. Unfortunately the lux meter cannot be used to measure the visible light reflectance off small surface areas without the use of a black box which excluded the surrounding light. The slab and the black box were tilted together, rotated and pointed in the direction of the sunlight, which would be impossible to do for a large surface area.

6 Preliminary Testing

6.1 Introduction

There were three preliminary tests carried out which will be discussed in detail in this chapter. These tests are as follows;

1. Physical tests on materials; aluminium, concrete and timber.
2. Test to determine the influence of external ambient air temperature on internal temperature of concrete specimens in the absence of other heat sources.
3. Test to determine the air temperature distribution in the vicinity of a concrete slab compared to the internal temperature.

The objective of the physical tests is to determine how different materials behave (in both their natural state and when they are painted on the surface), when they are subjected to a light source. This experiment will aide in understanding how heat generated from light and is transferred through a material as both the top and bottom surface of test specimens will be monitored.

The primary aim of the second test is to establish the relationship between the air temperature (on the roof where the slab specimens are located) and the concrete specimens, both during the day and at night time.

The final preliminary test conducted involves monitoring the temperature of one slab both internally and externally on the surface at a number of locations. In addition to this, the temperature of the air will be measured at different heights with respect to the slab.

6.2 Physical test on materials: Aluminium, concrete and timber

As part of an extensive literature review, research was conducted into the physics of light and its interaction with materials (as described in Section 2.1), however, some fundamental questions remained unanswered. One particular question is as follows; if two different materials, which are the same size, are both painted with the same colour paint and are subjected to a light source, is the dominating factor for the temperature change the parent material itself or is it as a result of the light's reaction with the surface that has been painted. A physical test was devised to answer this key question. Three materials were chosen for this experiment, namely aluminium, concrete and timber.

6.2.1 Test configuration

A total of 9 specimens were manufactured for this experiment; three solid aluminium prisms (6061 aluminium alloy), three concrete prisms (using CEM II A-L) and three timber prisms (red deal timber), each 160x40x40mm in size for comparison purposes. For each of these three materials, one specimen was painted matt black, one matt white and the remaining specimen left in its natural colour. In order to measure the temperature of the materials, thermocouple wires would be fixed to both the top and bottom surfaces of each of the 9 specimens so as to measure the temperature change as a result of heat being generated at the surface by a light source and transmitted through the material.

6.2.1.1 Calibration of thermocouple wires

The thermocouple wires were calibrated before being placed on the surface of the specimens and the results are displayed in Table 6-1. The wires were placed in steam from a kettle at boiling point and the maximum temperature was recorded using a data logger. The average temperature was 98.9°C with the coefficient of variation (CoV) calculated at 0.78% which is satisfactory. This calibration procedure is important to ensure that the thermocouple wires are accurately measuring temperature so that accurate and reliable comparisons can be made between the temperatures recorded on each channel.

Table 6-1 Calibration of thermocouple wires for the physics test using steam on aluminium, concrete and timber

Channel no.	Temp (°C)	Channel no.	Temp (°C)
1	99.9	12	98.6
2	99.8	13	97.9
3	98.4	14	98.9
4	99.0	15	98.0
5	99.5	16	98.7
6	99.6	17	97.9
7	98.7	18	98.4
8	99.4	19	98.9
9	97.9	μ_{19}	98.92
10	97.9	σ_{19}	0.776
11	98.0	CoV(%)	0.784

6.2.1.2 Placement of thermocouples and painting of the specimens

Once the thermocouple wires were calibrated, the surfaces of each of the specimens were cleaned to ensure no dirt was present before placing the thermocouple wire on the surface. The thermocouple wires were fixed to the centre surface (ensuring the wire made good contact with the surface) using silicone (as this would not affect the temperature reading and would provide a good adhesive bond with the surface of the specimens). Following the placement of the thermocouple wires top and bottom, the designated samples were then painted, each having two coats of paint applied to the surface. The 9 specimens are displayed in Fig. 6-1, with three aluminium samples on the left, three concrete samples in the middle and three timber samples on the right as demonstrated. The thermocouple wires can be seen on each surface of the specimens and these are all connected to the data logger which is shown on the right in Fig. 6-1. The samples were fixed on timber supports and an additional thermocouple wire was situated beside the test set up to measure the air temperature of the laboratory.

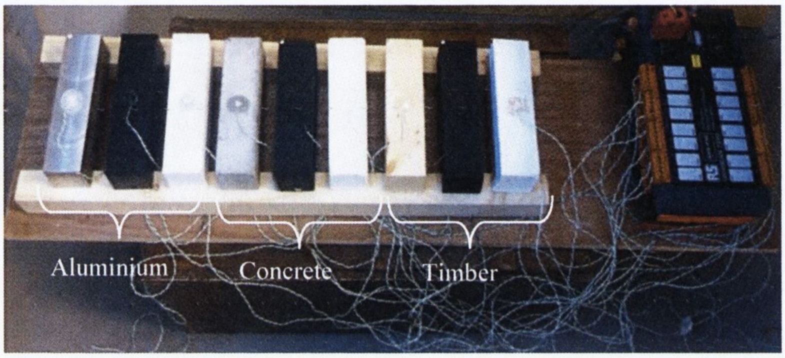

Fig. 6-1 Aluminium, concrete and timber specimens with data logger

6.2.1.3 Test procedure using heat lamp

The heat lamp (see Section 4.9 for the specification of this instrument) was configured to shine light evenly on three samples in one test. The lamp and test set up is displayed in Fig. 6-2. The lamp could not be used to test all 9 specimens concurrently because there was a large range of irradiation intensity across the spot light which the lamp produces. For consistency purposes, it is necessary to have equal intensity across all of the specimen's surfaces so that the results are comparable. The contours of light across the specimens were examined and were found to be broadly uniform (within 5%) across all specimens once the testing area was reduced to three specimens. The average light intensity was measured across the spotlight prior to testing all specimens and was found to be approximately 380W/m^2±20W/m^2 as measured using a pyranometer.

Three separate tests were conducted; one test per material type. The specimens were propped on timber for two purposes;

1. This inclined the specimens at an angle of approximately 50° so that their surfaces were parallel to the lens of the lamp in order to obtain optimum light intensity.

2. The surface below the specimens did not affect the temperature recorded on the underside of the specimens.

Once the test specimens were set up on the timber supports as per Fig. 6-2, the data logger was set up to record temperature at one minute intervals. The heat lamp was then switched on (on the white light setting to produce all components of visible light) and the specimens were left under the lamp for a period of 2 hours. Thereafter, the lamp was switched off and the data logger continued to record the temperature for a further 1.5 hours to monitor the cooling rate of the specimens. This method was repeated for the remaining two tests with the lamp set up remaining unaltered throughout testing.

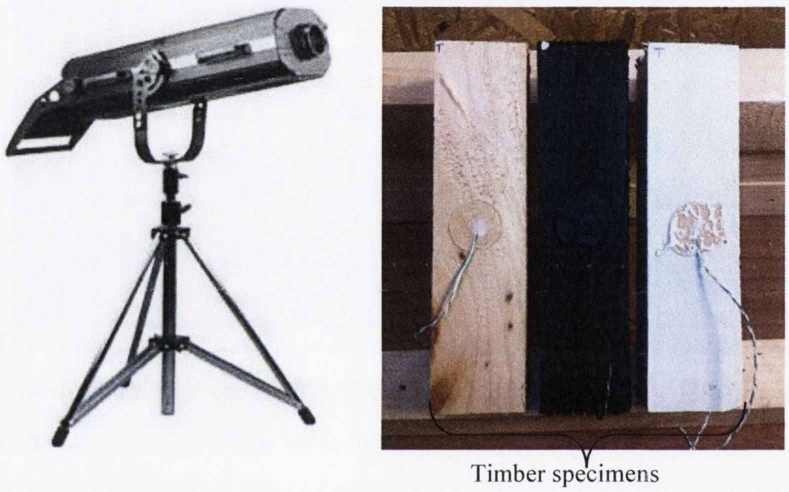

Fig. 6-2 Heat lamp (left) and test set up of three samples at once with natural, black and white (right)

6.2.1.4 Thermal properties of aluminium, concrete and timber

Knowledge of the thermal properties of the three materials is necessary to aide in understanding the behaviour of the materials when subjected to heat. The mass, volume and density of each material was acquired (specimen size:160x40x40mm), which along with the published values of specific heat, c, thermal conductivity (k) and emissivity (ε) are displayed in Table 6-2.

The volumetric heat capacity (VHC) of the three materials was calculated also (VHC = cρ). The reader is referred to Section 2.1 for a detailed description of these properties. The specific heat, c, of a material is the energy required to change the temperature of that material by one degree Kelvin (or one degree Celsius). The VHC is a measure of the amount of heat a material can store. Thermal conductivity, k, is a measure of the rate at which heat is transferred through a material. Emissivity, ε, is defined as the ratio of the total radiation emitted divided by the total radiation that would be emitted by a blackbody at the same temperature.

Table 6-2 Physical and radiative properties of aluminium, concrete and timber (Wilson et al., 2007, Askeland and Phule, 2006)

Material	Mass (kg)	Volume (m^3)	Density (ρ)	c (J/kg.K)	VHC = $c\rho$ (MJ/m^3K)	k (W/mK)	ε
Aluminium	0.64	0.000256	2500	900	2.25	240	0.05
Concrete	0.57	0.000256	2226	840-1170	1.87-2.6	1.3	0.85
Timber	0.13	0.000256	508	1700	0.86	0.15	0.90

6.2.2 Results of physical test

6.2.2.1 Results of L for aluminium, concrete and timber*

The colour of the 9 specimens was measured first using a sphere spectrophotometer (see Section 4.3 for specification of this instrument), where L* defines lightness, a* denotes the red/green value and b* the yellow/blue value. A colour measurement in the +a* direction depicts a shift towards red and –a* towards green. A measurement in the +b* direction represents a shift towards yellow, and –b* towards blue. An L* value of zero represents black or total absorption, and a value of 100 represents white, or total reflection.

The objective of this test is to aide in understanding the temperature changes which arise when the samples are subjected to a uniform light source. Each prism sample had three spot readings recorded, with each specimen having a low coefficient of variation that is, CoV (< 1.31%). The average L* readings (μ_{L*}) are displayed in the chart in Fig. 6-3 and also highlighted in bold in Table 6-3. The standard deviation for the three L* readings (σ_{L*}) are also displayed in Table 6-3. The a* and b* values were also noted but are small and do not contribute to the temperature change of the materials and so will not be discussed further.

For the case of the natural specimens, that is those which were not painted, the order of decreasing L* is as follows; aluminium (88.05), timber (80.08) and concrete (68.20). Once painted black, the three different materials have an average L* value of approximately 25.70 and are within 5.3% of one other. The average L* value of the three specimens painted white is approximately 94.21 and the results are within 0.4% of one another. In conclusion, if a surface is painted black or white, the L* value recorded will essentially be the same when measured using a sphere spectrophotometer, irrespective of whether the material is aluminium, concrete or timber, not surprisingly.

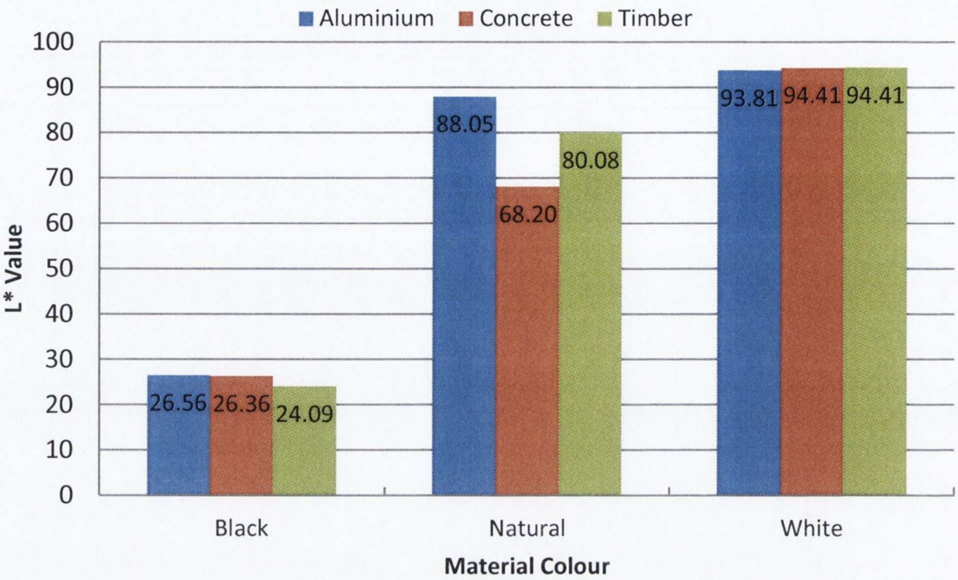

Fig. 6-3 Results of L* for aluminium, concrete and timber

Table 6-3 Results of L*, a* and b* for aluminium, concrete and timber specimens

Material	Reading	L*	a*	b*		
Aluminium: natural	1	88.74	0.09	1.97	μ_{L*}	**88.05**
	2	87.07	0.08	2.58	σ_{L*}	0.870
	3	88.33	0.2	2.26	CoV (%)	0.988
Aluminium: black	1	26.34	-0.02	-1.34	μ_{L*}	**26.56**
	2	26.40	-0.04	-1.52	σ_{L*}	0.330
	3	26.94	0.04	-1.16	CoV (%)	1.244
Aluminium: white	1	93.39	-0.81	2.10	μ_{L*}	**93.81**
	2	93.97	-0.84	1.76	σ_{L*}	0.364
	3	94.06	-0.81	2.05	CoV (%)	0.388
Concrete: natural	1	68.38	-0.44	4.88	μ_{L*}	**68.20**
	2	67.36	-0.36	5.25	σ_{L*}	0.770
	3	68.87	-0.28	5.01	CoV (%)	1.129
Concrete: black	1	26.69	-0.02	-1.06	μ_{L*}	**26.36**
	2	26.40	0.01	-0.85	σ_{L*}	0.346
	3	26.00	-0.01	-0.92	CoV (%)	1.314
Concrete: white	1	94.72	-0.44	2.94	μ_{L*}	**94.41**
	2	94.06	-0.49	1.90	σ_{L*}	0.332
	3	94.45	-0.47	3.05	CoV (%)	0.351
Timber: natural	1	80.33	5.32	19.20	μ_{L*}	**80.08**
	2	79.71	5.74	18.71	σ_{L*}	0.327
	3	80.20	5.35	18.92	CoV (%)	0.408
Timber: black	1	24.20	0.08	-0.27	μ_{L*}	**24.09**
	2	23.89	0.06	-0.35	σ_{L*}	0.176
	3	24.19	0.09	-0.21	CoV (%)	0.731
Timber: white	1	94.33	-0.37	2.44	μ_{L*}	**94.41**
	2	94.36	-0.43	2.79	σ_{L*}	0.119
	3	94.55	-0.45	2.89	CoV (%)	0.126

6.2.2.2 Results of temperature change for each material type; aluminium, concrete and timber

The data recorded for aluminium, concrete and timber are plotted in this section, with three different colour surfaces included, namely natural, black and white. The scale on the y-axis represents the temperature change from that of the ambient air temperature. This was calculated by subtracting the air temperature at that time from each data point. The 'T' descriptor denotes the top surface temperature (this thermocouple is fully exposed to the light) and 'B' denotes the bottom, or underside temperature of the sample which is not in direct light.

The temperature change for aluminium is displayed in Fig. 6-4. The sample which is painted black increases in temperature at a higher rate, with the underside of the sample increasing at the same rate. This would suggest that aluminium is a highly conductive material. The thermal conductivity value, k, of aluminium is high at 240W/mK which would explain the very small temperature difference between the top and bottom surface of the sample. The sample absorbs the light on the top surface and, as it is a highly conductive material, the subsequent heat generated is conducted through the material very quickly and it is also dissipated from the material in every direction. The specimen painted black is significantly higher in temperature than the natural specimen, by approximately 4°C.

There is approximately a 1°C difference in temperature between the natural sample and the sample which is painted white. The difference in L* values would account for the small temperature difference between the natural coloured specimen and the specimen which was painted white. In other words, as the natural colour of aluminium is closer to the white specimen than to black, there is little difference in their temperatures. The L* value for the natural specimen is approximately 88.1 and the L* for the sample painted white is approximately 93.8. As aluminium has a high L* value in its natural state, painting the surface white only increases its value very slightly.

As soon as the lamp is switched off, after approximately 2 hours, the natural and white specimens decrease in temperature at the same rate, however, the sample painted black loses heat more quickly. There are two reasons for this, as the temperature obtained by the black specimen is higher, it naturally gives off heat quickly due to a higher temperature differential with the air and also as it is black in colour, it is naturally more radiative. It can also be observed that when the lamp was switched on, there was a measurable difference between the top and bottom surface of each of the specimens. However, as soon as the light is switched off, the temperatures at the top and bottom are almost identical, suggesting that the material is very conductive as heat is transferred rapidly across the material.

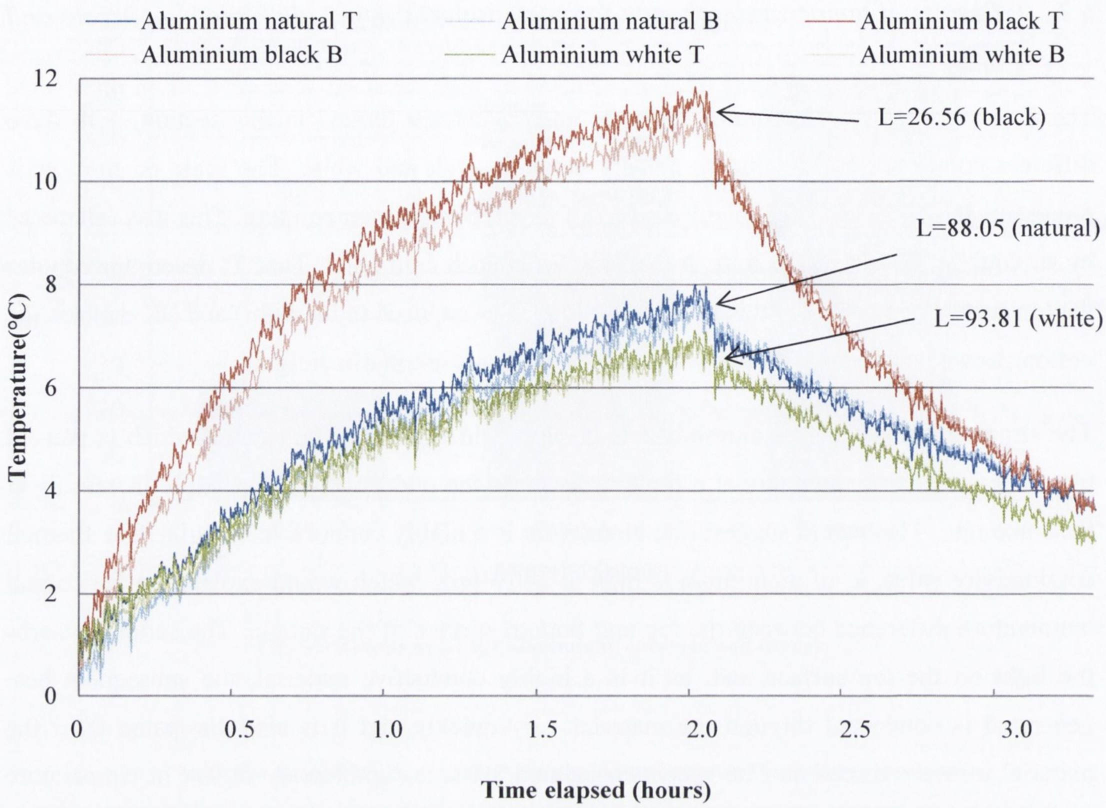

Fig. 6-4 Time vs. temperature for aluminium specimens under heat lamp (11th January 2013)

The temperature change in the three concrete specimens is displayed in Fig. 6-5. These samples experience a higher change in temperature than that of aluminium due to concrete having a particularly high VHC (see Table 6-2). The black sample reaches a peak of approximately 13°C on the top surface and 11°C on the underside. As concrete has a low thermal conductivity value (1.3W/mK), this temperature difference is expected as concrete is less conductive than aluminium. The natural coloured specimen has a peak top surface temperature of approximately 9.4°C and a bottom peak surface temperature of 8°C. The peak temperature of the white sample is approximately 7.3°C on the top and 6.2°C on the bottom. A more discernable distribution in temperature between the samples is observed in the concrete when compared with those of aluminium. The corresponding L* values for natural, black and white are 68.2, 26.36 and 94.41 as outlined in Fig. 6-5. This would explain the distribution in temperature as there is a better distribution between the L* values of the specimens.

There is radiative heat being generated on the surface due to the light source and this heat is transmitted through to the bottom of the specimen through thermal conductivity. As concrete is somewhat insulative, as soon as light switched off after 2 hours, the heat on the top surface dissipates upwards very quickly (in particular for the black specimen due to its colour), therefore, there is a sudden change in temperature. The temperature reduces until it reaches the ambient temperature of the specimen itself. The temperature of the 3 specimens decreases gradually as heat is lost from both top and bottom surfaces, a characteristic of concrete's well known thermal mass.

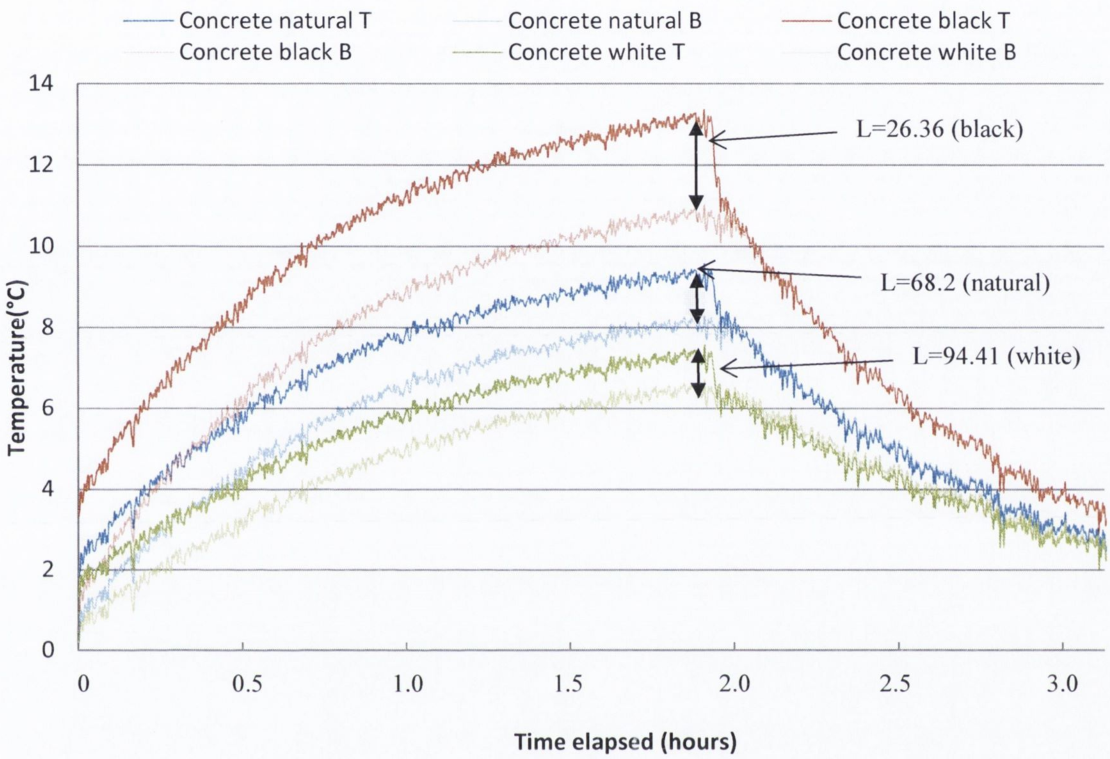

Fig. 6-5 Time vs. temperature for concrete specimens under heat lamp (10th January 2013)

The results of the test conducted on three timber specimens are outlined in Fig. 6-6. For this material, the first observation to note is that timber reaches its peak temperature quickly before reaching a plateau. The top surface of the black specimen reaches a peak temperature of approximately 20°C above ambient, with the bottom surface reaching only 8°C. This would suggest that timber is a good insulator, with a low thermal conductivity value of 0.15W/mK to confirm this. Therefore, as timber is a good insulator, the heat generated at the top surface remains at the top surface, and this would explain why the temperature reaches a plateau very quickly. The top surface of the natural sample reaches a peak of approximately 10.5°C and the bottom surface 5°C. This temperature difference between the top surface of the black sample and natural sample of almost 10°C is very significant and quite different to the aluminium and concrete. The white specimen is only slightly lower in temperature than that of the natural coloured specimen, having a top surface temperature of 10°C and a bottom temperature of approximately 6°C. The corresponding L* values of natural, black and white timber are 80.08, 24.09 and 94.41 are shown in Fig. 6-6. The large change in temperature between the black specimen and natural or white specimen is primarily explained by the large difference in L* value of approximately 55.

There is heat being generated on the top surface of the specimens due to the light source and when the light is switched off after approximately 2 hours, there is a rapid decrease in the top surface temperature of all three specimens due to the timber being a very good insulator. There is less heat going downwards, therefore, when light is switched off, the heat at the surface primarily dissipates upwards. This contrasts with the aluminium samples as shown in Fig. 6-4 where there is no sudden drop in temperature when the light is switched off due to aluminium being highly conductive, therefore, the heat is uniform throughout its depth.

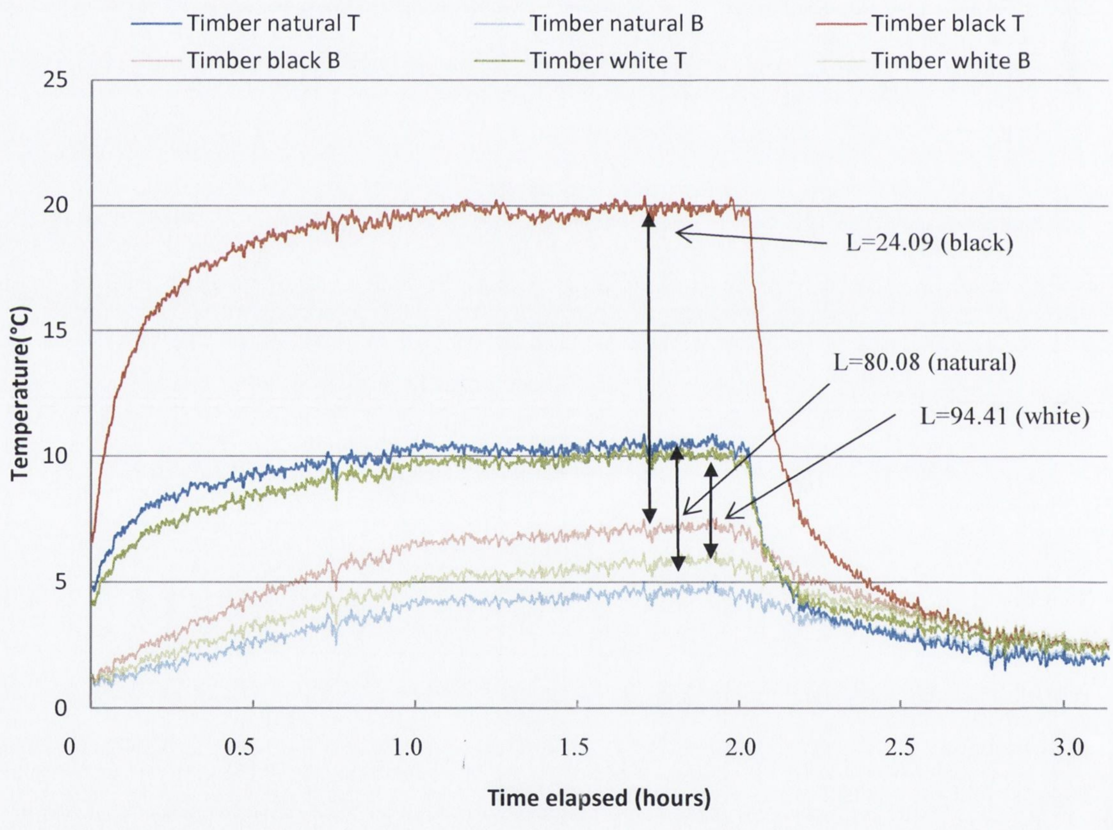

Fig. 6-6 Time vs. temperature for timber specimens under heat lamp (14th January 2013)

6.2.2.3 Results of temperature change for each colour; natural, black and white

The temperature change data for the three specimens with no paint on the surface i.e. natural colour, is re-displayed in Fig. 6-7. The timber specimen demonstrates an interesting result because it reaches the highest top surface temperature (10.5°C) and also at the fastest rate. The corresponding bottom surface has the lowest temperature (5°C). This is due to timber being a very good insulator as heat generated at the top surface is not conducted downwards and so the temperature increases on the surface. The concrete specimen increases in temperature at a steady rate, and as concrete is neither a good conductor nor a good insulator, there is a difference in temperature between the top and bottom surface of approximately 1.5°C. The sample continues to increase in temperature as it has quite a high VHC of approximately 1.87-2.6 MJ/m^3K, compared with timber which has a value of $0.86 MJ/m^3K$. Aluminium remains the lowest in temperature as is a very good conductor, therefore, the heat is transferred through the depth of the material very quickly and it is also dissipated from the material in every direction. The maximum temperature reached by the specimens is also due to their emissivity values, with timber having the highest emissivity (0.90) which is similar to concrete (0.85), and aluminium the lowest (0.05).

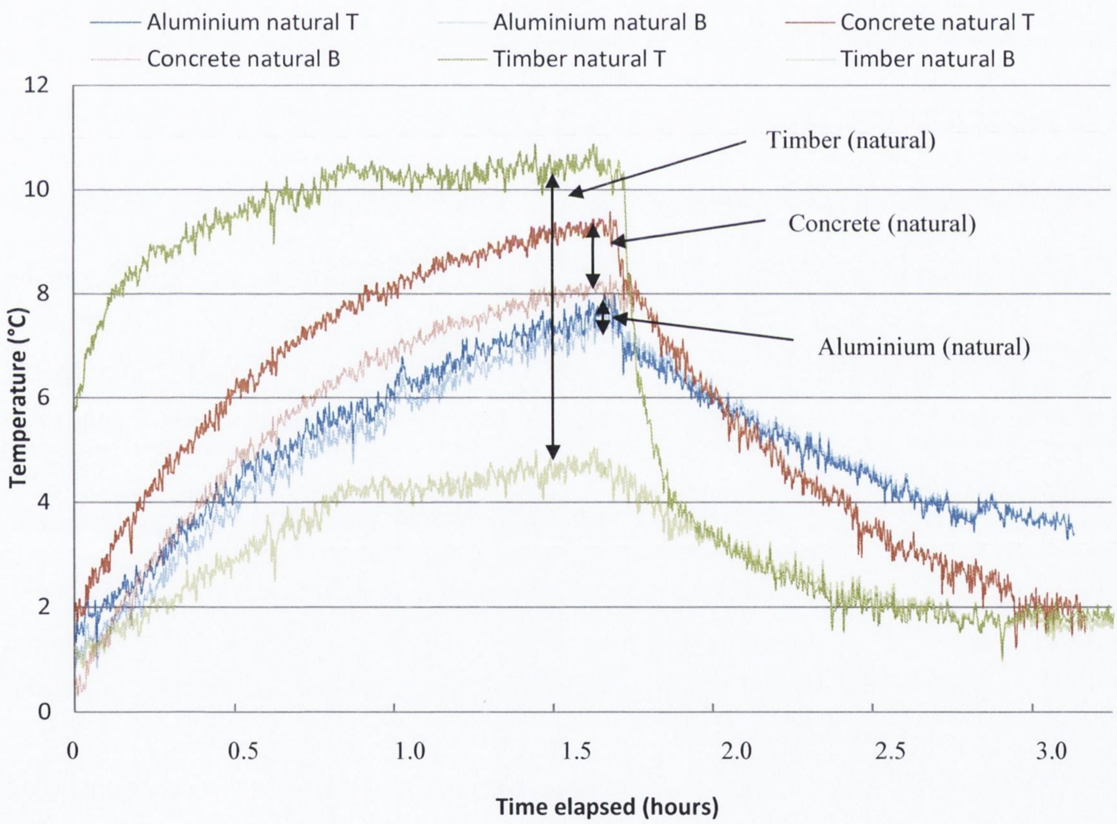

Fig. 6-7 Time (over 3.5 hour period) vs. temperature for aluminium, concrete and timber specimens under heat lamp with no paint (January 2013)

In conclusion, the maximum temperature in the natural specimens is primarily due to the colour and conductance or dissipation of heat. Furthermore, an insulation effect is very evident, particularly for the timber specimen. When the light source is switched off, it is clear that the specimens lose heat at different rates. The timber specimen drops suddenly as it is a very good insulator and once the heat at the top surface is given off, the temperature just below the surface will be cooler. This results in top surface temperatures reducing rapidly to match that of the bottom surface. In contrast to this, the aluminium has a very slow rate of cooling as the temperature is uniform throughout the depth of the material due to its high thermal conductivity. The rate of cooling for the concrete specimen is in between that of timber and aluminium, which is due to heat dissipating downwards as well as upwards.

The colour of the three different materials, when painted black, is virtually the same when measured with the sphere spectrophotometer ($L^* \approx$ 24-26) as expected. The temperature gain which was measured by the thermocouple wire, however, was different although the top surfaces are all exposed to very similar heat loads (see Fig. 6-8). By painting the specimens black, it appears to make a difference with regards to the peak temperature obtained by the material. The timber specimen remains the highest in temperature, however, it has increased significantly to 20°C. It also reaches a plateau as there is a limited amount of energy coming in from the light source, therefore, it heats up very quickly and reaches an equilibrium. As the material is dissipating little heat downwards, the temperature reaches a peak very quickly on the surface. The bottom surface of the specimen has only increased marginally.

The concrete sample has increased by approximately 3°C from its natural state, as has the aluminium sample. This result would confirm that by painting the surface of a material black, the paint will heat up and as a consequence the material underneath will also heat up as heat is transferred by conduction between the paint and the material. The temperature gain is also due to the thermal properties of the material itself particularly the thermal conductivity, where heat is dissipated downwards in the more conductive materials, thus keeping the surface cooler.

Once the light source is switched off, the timber sample loses its heat almost immediately, while the concrete and aluminium retain heat and cool at a much slower rate. This is due to the difference in radiative properties between the three different materials, with timber having the lowest VHC of 0.86MJ/m^{3}K (see Table 6-2 for the full set of radiative properties), therefore, timber does not have much ability to store heat. It can also be observed that the most conductive material (aluminium) is the slowest to return to equilibrium, due to it having a relatively high VHC (2.25 MJ/m^{3}K). In conclusion, the black paint and the nature of the material below it, both contribute to the temperature gain of the material. The temperature difference between the top and the bottom surface of each of the materials indicates the conductive ability of the material.

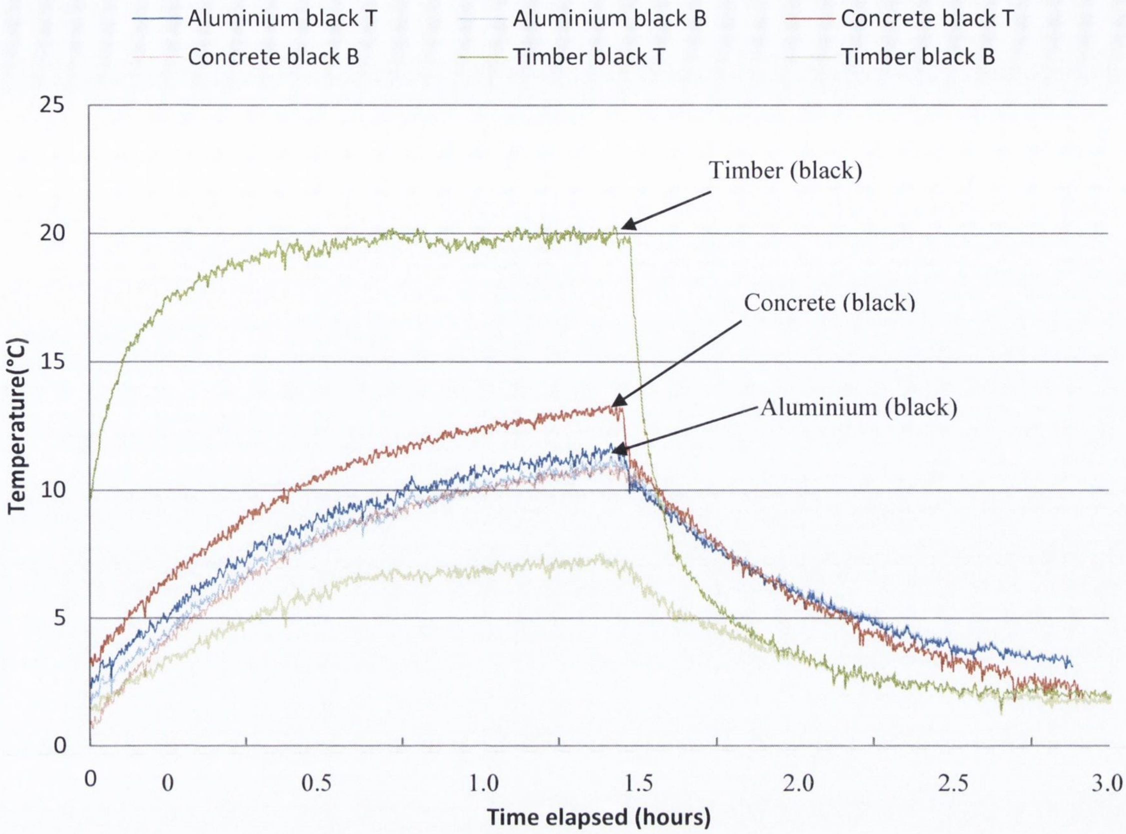

Fig. 6-8 Time (over 3.5 hour period) vs. temperature for aluminium, concrete and timber specimens under heat lamp with black paint on the surface (January 2013)

A similar overall result is observed for the prism samples which have been painted white (see Fig. 6-9). The spectrophotometer recorded an approximate L* value of 94 for all 3 samples. The temperature of the specimens, when compared to the natural specimens, shows that there is a small reduction in temperature as a result of the white paint, therefore, it is true to say that there is relationship between L* and the peak temperature, however, this particular behaviour depends on the material's conductance and not the surface colour (as they are all white). The timber sample has not changed in temperature from its natural state, however, the concrete sample is approximately 2°C lower and aluminium is 1°C lower. This result would suggest that by painting the materials white, there is only a small reduction in the temperature of the material as compared to its natural surface colour, given all three materials are naturally on the white end of the greyness spectrum. It can also be noted that there is virtually no difference in temperature between the top and bottom surface of concrete as the generation of heat on the top surface is slower due to the greater reflectance of the white surface.

The plot also shows concrete behaving very similarly to aluminium more so than timber, even though, the k value of concrete is closer to timber than it is to aluminium. This would suggest that although thermal conductivity of a material is relevant, the VHC value is equally as important in terms of the heat that is retained in the material. As timber has a low k value (0.85W/mK), illustrating that the heat is confined to the top surface, the temperature drops very quickly when the heat source is removed. However, the VHC value is equally important as the ability to retain and store heat is better for concrete and aluminium due to their higher density (see Table 6-2 for material properties).

When the light is switched off, it was evident that the top surface of the specimens dropped below that of the bottom surface. This may be explained by the possibility of a small microclimate being created under the specimens upon cooling where the heat is being dissipated downwards, therefore, slightly increasing the temperature of the bottom surface.

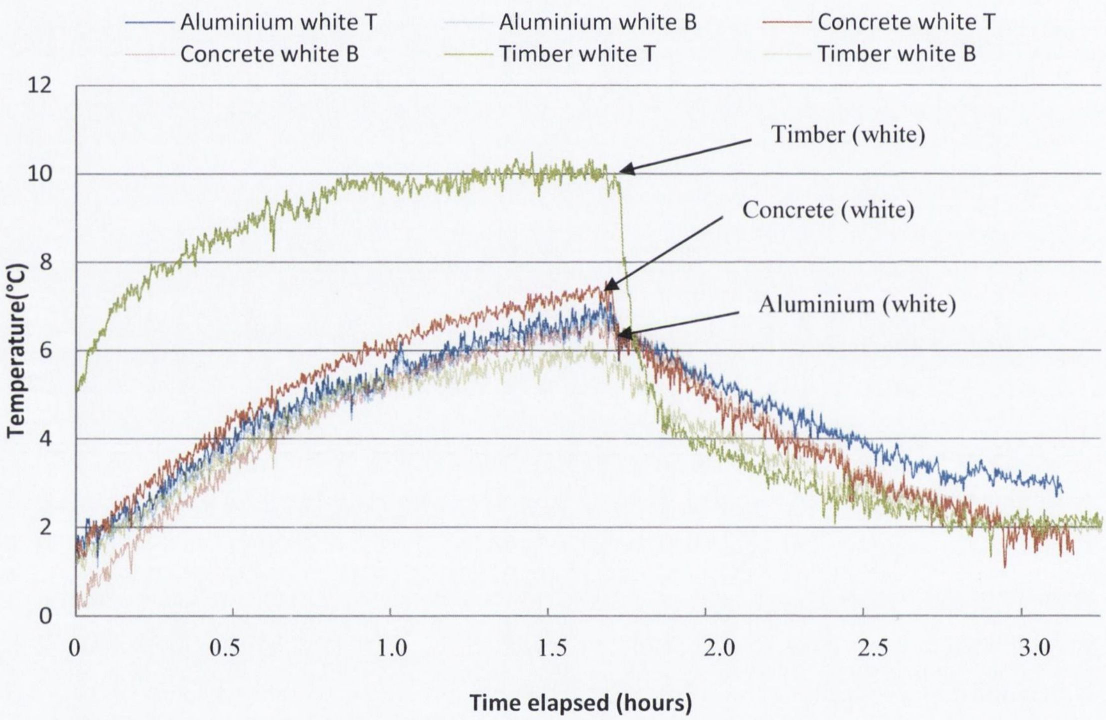

Fig. 6-9 Time (over 3.5 hour period) vs. temperature for aluminium, concrete and timber specimens under heat lamp with white paint on the surface (January 2013)

A summary of all results for this test are outlined in Table 6-4 including L* and peak temperature values on the top surface for the 9 specimens. By changing the natural surface to black or white, the percentage increase or decrease in L* and peak temperature were also calculated. There is a relationship between L* and the peak temperature, however, this behaviour is heavily influenced by the material's conductance and the surface colour. It is also evident that painting the surface of the material black has a far greater effect on the colour and surface temperature than painting the surface white, as the specimens are originally more white in colour than black. The results indicate that where there is an increase in L* value, there is a corresponding decrease in peak temperature and vice versa. The data in Table 6-4 demonstrates that there is a clear and consistent relationship between the change in surface colour (L*) and the corresponding peak temperature. The concrete specimen, for example, experiences the greatest reduction in peak temperature by painting the surface white (22.3%), and this corresponds directly with the highest increase in L* value.

In conclusion, it is a combination of the surface colour and the materials' radiative properties which affect the resulting temperature changes. For example, in Fig. 6-9 the specimens are all the same colour (white), but the difference between the temperature is due to the different conductive and insulative properties of the individual materials. When the light is switched off, the heat in the timber specimens has been confined to the surface and heat dissipates from the surface very quickly. As a consequence, the top surface temperature decreases to match the temperature below the specimen. It is also evident that the aluminium specimen, which is the most conductive, is the slowest to return to equilibrium and this is due to the temperature remaining constant throughout the depth, in addition to having a relatively high VHC (2.25 MJ/m^3K) in comparison to concrete or timber.

Table 6-4 Summary table of results of physics test demonstrating change in absolute L* and change in peak temperature (on the top surface) from the natural specimens

	L*	Peak temp. (°C)	Surface colour change	Change in L* from natural (%)	Change in peak temp. from natural (°C) (%)
Aluminium	88.05	7.90			
(white)	93.81	6.90	Natural to white	+6.5	-12.6
(black)	26.56	11.6	Natural to black	-69.8	+46.8
Concrete	68.20	9.40			
(white)	94.41	7.30	Natural to white	+38.4	-22.3
(black)	26.56	13.2	Natural to black	-61.0	+40.4
Timber	80.08	10.3			
(white)	94.41	10.0	Natural to white	+18.0	-2.9
(black)	24.09	20.0	Natural to black	-70.0	+94.2

Similarly, a summary table of the results is presented in Table 6-5 demonstrating the difference in peak temperature between the top and bottom surface of the specimens. The thermal conductivity (k) is also displayed here. In general, as the aluminium specimens have a high k value, the temperature difference between the top and bottom surface is minimal (0-0.5°C) as it is a highly conductive material. On the other extreme, timber has a very low k value, therefore the temperature range between the top and bottom surface is between 4.3-12.8°C as timber is a good insulator. The VHC value is better for concrete and aluminium due to their higher density which is the reason why concrete behaves more like aluminium than timber, despite concrete and timber having closer k values (see Table 6-2 for material properties).

Table 6-5 Summary table of results of physics test demonstrating the difference in peak temperature between the top and bottom surfaces of the specimens

	L*	Peak temp. (°C) (Top)	Peak temp. (°C) (Bottom)	Thermal conductivity (W/mK)	Difference in peak temp. between top and bottom (°C)
Aluminium	88.05	7.90	7.40	240	0.50
(white)	93.81	6.90	6.90	240	0.00
(black)	26.56	11.6	11.1	240	0.50
Concrete	68.20	9.40	8.20	1.30	1.20
(white)	94.41	7.30	6.40	1.30	0.90
(black)	26.56	13.2	10.8	1.30	2.40
Timber	80.08	10.3	4.51	0.15	5.79
(white)	94.41	10.0	5.70	0.15	4.30
(black)	24.09	20.0	7.20	0.15	12.8

By measuring the spectral output from both the lamp used to heat the specimens and the sphere spectrophotometer to measure L* values, the results outline that both devices produce light predominately in the visible range of the spectrum, but more importantly there is very little infrared present. The information from both of these instruments is displayed in Fig. 6-10 with the Follow 1200 Pro lamp represented by the green line and the sphere spectrophotometer by the blue line. The contribution from infrared and ultraviolet is negligible for both devices. The direct global irradiation on the earth's surface is also displayed illustrating light across the three wavelengths for comparison purposes (ASTM, 2012).

The spectral irradiance from the direct global radiation is measured in $W/m^2/nm$, however, the two instruments have a level of intensity measured in arbitrary units (a.u). The measurement from the spectrometer is a photon count reading and not an intensity as such, as it measures the number of photons produced by the lamp. It is a relative wavelength measurement and not a measurement of intensity. Arbitrary units are often used in spectroscopy to express spectral intensity, however, a comparison may be made between the intensity of the two instruments, as measured by the spectrometer. The wavelength (nm) is the factor of particular importance as it displays the distribution of light across the spectrum. The purpose of the plot in Fig. 6-10 is to demonstrate that the two instruments produce light predominately in the visible range, when compared with the global radiation. Despite this fact, the Follow 1200 pro lamp produces ample amounts of light necessary in order to heat the samples and consequently detect the fundamental differences in the thermal properties between each of them.

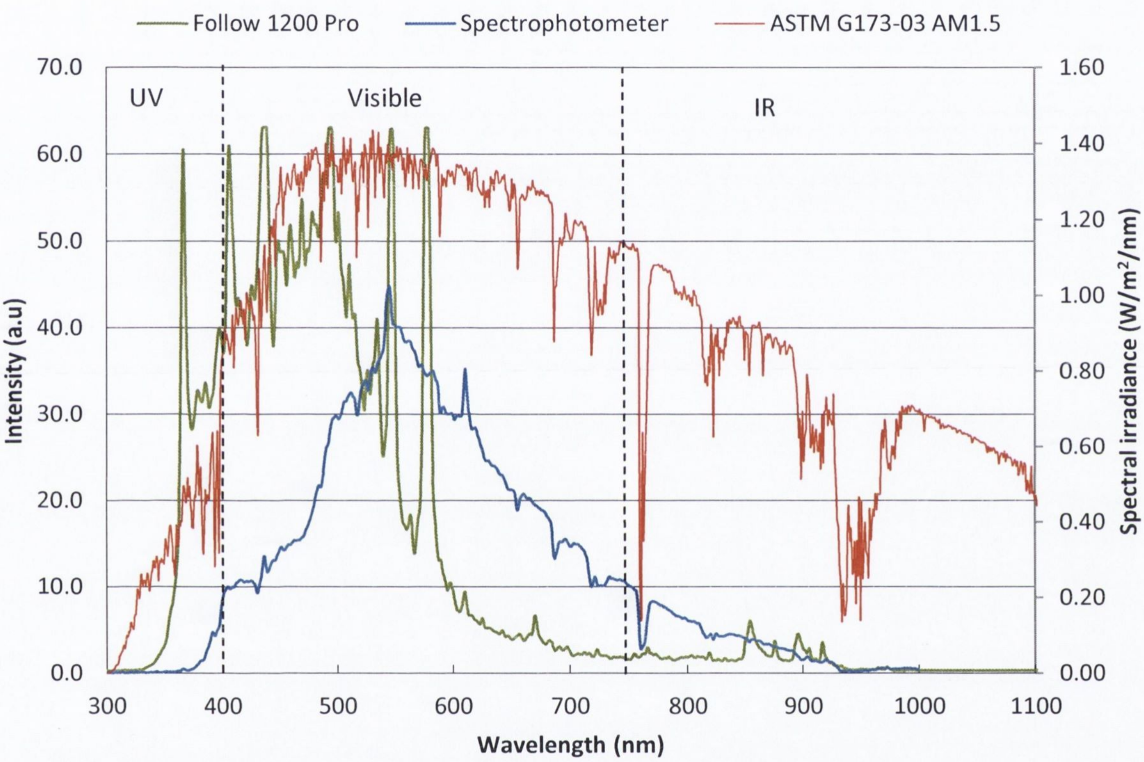

Fig. 6-10 Spectral information from Follow 1200 pro lamp (green), sphere spectrophotometer (blue) and direct global radiation for air mass 1.5 (ASTM, 2012)

6.2.3 Conclusions

6.2.3.1 Temperature change for each material

- The data demonstrated that aluminium is a highly conductive material, with heat being transferred from the top surface to the bottom surface very quickly. The k value of aluminium is 240W/mK which explains the very small temperature difference between the top and bottom surface of the sample.
- Painting aluminium black greatly increases the temperature of the specimen and reduces the L* value from 88 to 26, however, painting the specimen white does not have a

significant influence in the temperature as the colour was originally relatively light to start with. It was observed that when aluminium is painted black, it loses heat more quickly once the light source is removed. This is as a result of the peak temperature being higher, therefore, it naturally gives off heat quickly and also as it is black in colour, it is naturally more radiative.

- The concrete specimen is slower to transfer heat through the depth of the material, therefore, it is a less conductive material than aluminium. It is clear from the data obtained that the peak temperature of concrete is not as high as aluminium and the heat is transmitted downwards, with a clear temperature difference between the top and bottom surface. However, the temperature of aluminium is broadly uniform throughout the depth as the heat is transferred quickly through the material.
- By painting concrete white (L=94.4), there is little difference in the temperature as the concrete was close to the white sample to start with, however, painting the concrete black has a strong influence on the temperature due to the lower reflectance from the black surface and also since the colour of the black surface (L=26.4) is further away in terms of colour from the parent natural material (L=68.2). The heat is generated on the surface of the material by virtue of the colour, and the colour is important in terms of the light reflected or absorbed. Once this heat is generated, whether or not it is emitted out into the atmosphere or whether it is conducted down through the material depends on the properties of the material.
- The results from the timber specimen show that it is a good insulator and that there is only a small amount of heat being transferred through the material. The surface of the material heats up considerably as the material does not permit the heat to travel down through its depth, therefore, the heat is mostly dissipated upwards from the top surface.
- Timber reaches its peak temperature and plateaus very quickly (within approximately 30 minutes) as there is a certain amount of energy coming in from the light source, therefore, it heats up very quickly and reaches an equilibrium. As the material is not dissipating much heat downwards, the temperature reaches a peak very quickly on the surface.

6.2.3.2 Temperature change for each colour

- The plot of the three natural specimens shows the true properties of the materials. Timber is a good insulator and reaches the highest temperature with an L* of 80. The poor conductivity of timber is confirmed by the result when the bottom surface of the specimen has a very low temperature. Concrete heats up at a slower rate than aluminium and has an L* value of 68. If the heat source had been left on another hour, it is possible that the temperature of concrete would have surpassed that of timber as the L* value for concrete is lower than that of timber. Aluminium remains the lowest in temperature of all three specimens due its low emissivity value (0.05), with concrete and timber being significantly better emitters of radiation, having emissivity values of 0.85 and 0.90 respectively.

- All of the materials have almost identical L* values when painted black (24-26) or white (94). However, despite the L* values and the heat input from the lamp remaining the same, there is still temperature differences between the different specimens which is clear from the results. This is due to the nature of the material e.g. whether or not the material conducts heat downwards. For example, aluminium is a very good conductor , therefore, the temperature is constant throughout the depth. On the other hand, timber is a very good insulator, therefore, the heat cannot easily transmit down through the material, and this results in the surface temperature reaching a plateau very quickly and dissipating the heat upwards, with a large temperature difference existing between the top and bottom surface of the material.
- Timber increases significantly in temperature when painted black and this heats the near-surface of the timber only. This is evident from the results, where it is clear that when the heat is switched off, the material cools down extremely quickly until the top surface temperature is more or less the same as the bottom surface temperature. This would imply that the material has not transmitted the heat throughout its depth and that the heat remained at the surface only. On the other hand, concrete and aluminium are significantly lower in temperature and this would confirm their superior conductive properties as they allow the heat to transmit through the depth of the material.

6.3 Monitoring the correlation between air temperature and the temperature of concrete

6.3.1 Test to determine the influence of external air temperature on internal temperature of the concrete specimens in the absence of other heat sources

6.3.1.1 Introduction

The following is a summary of results from a test carried out in December 2011, with the aim of determining the influence of the external ambient air temperature on the internal temperature in the concrete specimens. The concrete samples used in this test were manufactured using partially crushed limestone aggregate both with screed and brush surface finishes. The GGBS contents of the slabs were 0%, 30%, 50% and 70%. Each concrete specimen on one board, containing a total of 16 slabs, has a thermocouple located at the centre of the plan of the slab at a depth of 20mm from the top surface which was placed prior to the concrete being cast. An additional thermocouple was situated in the centre of this board and was fixed to a stand, which was above the level of the specimens and measured the ambient air temperature. All thermocouple wires were connected to a data logger to record the natural temperature change in the specimens as well as the air temperature. The objectives of this test were as follows;

1. To establish the influence of air temperature with respect to changes in the temperature of the interior of the concrete slabs
2. To identify the behaviour of the ambient air temperature over time

6.3.1.2 Results and observations

The results for the screed and brush finish specimens are displayed in Fig. 6-11 and Fig. 6-12. The variations of the temperatures for the screed finish slabs ranging from 0% to 70% GGBS with the external air temperature readings are observed in Fig. 6-11. The sun was not shining for the duration of this test, therefore, eliminating the influence of the sunshine on the temperature. The slabs begin to increase slowly in temperature at the start of Day 1 to a maximum temperature of 10°C at approximately 11am, with the external air temperature reaching a peak of approximately 11°C approximately one hour earlier. The chart indicates that the rate of change of temperature in both media is approximately the same, however, there is a lag in the temperature gain in the concrete. This is due to the thermal mass of the concrete, which regulates the heat observed inside the slab. Accordingly it takes the external heat longer to induce a temperature change at a depth of 20mm into the concrete (where the thermocouple wire is located). In the afternoon there is a sudden drop in the ambient air temperature which may be due to the passing of a cold front, for example, and this produces a corresponding drop in the temperature of the specimens, however, the drop off in temperature occurs approximately 40 minutes after the ambient air temperature drops off.

As these results were recorded in December, the temperatures reached were not substantial enough to observe a difference between the peak internal temperatures of the slabs comprising different GGBS contents. However, there are small differences in temperature due to different GGBS contents, and this could be attributed to thermal conductivity changes or different emissivity values, or possibly as a result of different changes in the surface colour i.e. the thermal properties of concrete with GGBS may be slightly different to that of Portland cement. As the specimens cool down in the evening, the air temperature and temperature of the slabs remain in close proximity until about 18:00 such that at midnight, the air temperature remains at a temperature of 2°C, and the slab has decreased further to between 0°C and -1°C. This is a significant difference (of approximately 3°C) between the air temperature and temperature of the specimens.

On the second day, the slab specimens slowly increases in temperature in the morning and reaches a peak of 4°C around midday. The air temperature is marginally higher at this point at approximately 5°C, with evidence of a lag occurring between the air temperature and the temperature of the concrete slabs. There is a noticeable difference between the temperature of the slabs on this day, with 0% and 30% recording a discernibly higher temperature than 50% and 70%. This is resulting from the greater light reflectance from the brighter surface of the specimens containing a higher concentration of GGBS. Similarly, on this day the slabs cool down at night time reaching a minimum temperature of -2°C and the air temperature is approximately 1°C, a difference once more of 3°C at night time. This reoccurring trend is due to a phenomenon known as a radiation inversion (described in Section 2.3.3), whereby the surface temperature falls because the land cools by emitting thermal infrared radiation. The strength of a radiation inversion is maximized during long calm cloud free nights where the air is dry. This results in the surface (and hence internal temperatures of an object) falling below that of the surrounding air temperature at night-time. It can also be noted that there is no lag in temperature at night time between the air and the concrete as they have reached an equilibrium temperature.

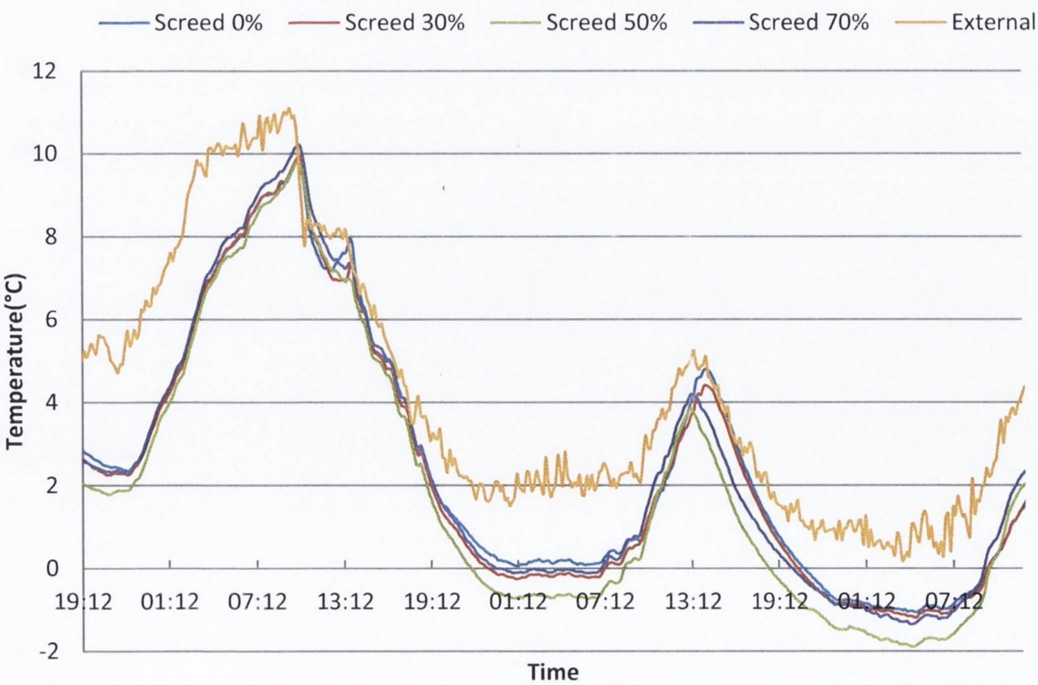

Fig. 6-11 Time vs. temperature for a screed finish slabs (0-70% GGBS) and external air temperature

Similar observations to those made for the screed finish slabs are recorded in the brush finished specimens also in Fig. 6-12. The trend in the patterns of the lag periods is consistent with the screed finish (Fig. 6-11) which would confirm that the surface finish does not affect the resulting outcome. It may be observed once again that as soon as the air temperature decreases relatively quickly due to for example the passing of a cold front, the concrete loses its heat relatively quickly and therefore the temperature of the air is almost the same as the temperature of the concrete.

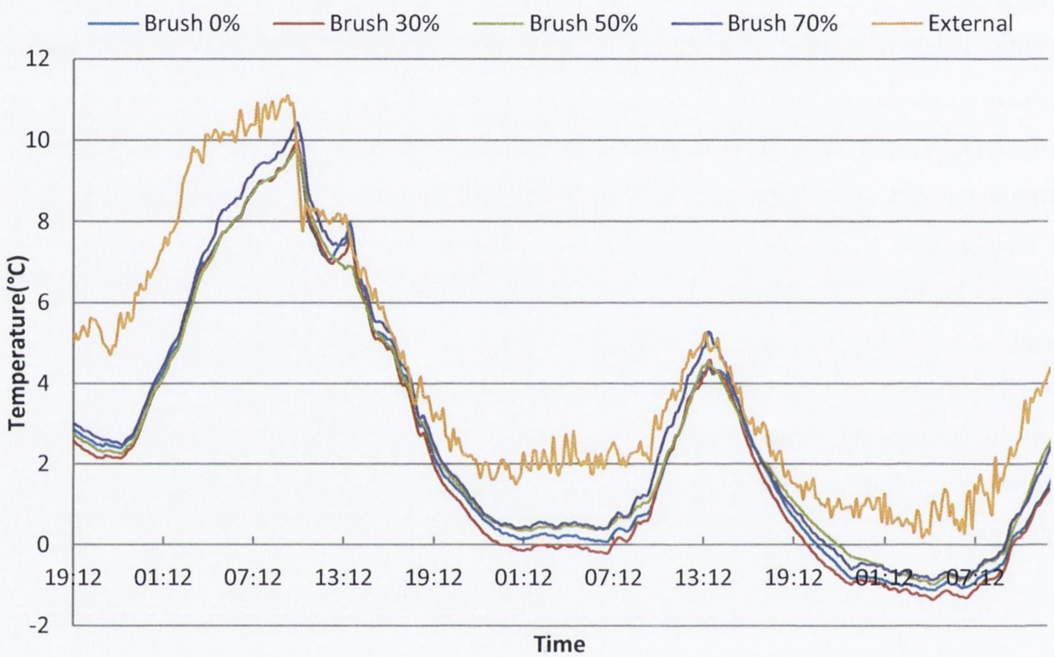

Fig. 6-12 Time vs. temperature for a brush finish slab (0-70% GGBS) and external air temperature

6.3.1.3 Conclusions

- The external air temperature is consistently higher than the temperature of the slabs by between 2 and 3°C at night-time due to a radiation inversion.
- The internal temperature of the slabs lags behind the air temperature when the concrete is increasing in temperature. This outcome is due to the low thermal conductivity value of concrete i.e. it takes time for a change in the ambient air temperature to influence the temperature in the concrete at a depth of 20mm below the surface, and this is dependant on the thermal conductivity.
- There is no significant difference in the temperature of the slabs containing different levels of GGBS as the test was carried out when there was no sunshine on this particular

day. The effect of GGBS concentration on the temperature change within the specimens will be discussed in detail in Section 7.6.

- There are identical trends present for both the screed and the brush surface finish which would suggest that the behaviour of the air temperature with the temperature of the specimens is entirely independent of the surface finish type.

6.3.2 Test to determine the air temperature distribution in the vicinity of a slab compared to the internal temperature

6.3.2.1 Introduction

This was an independent test which took place in February 2012 in order to further explain slab behaviour arising from the test outlined in Section 6.3.1. The purpose of this test was to monitor the variation in the surrounding air temperature as well as that of the slabs. The sunshine intensity is also recorded to study its effect on the air temperature change. The screed finish specimens which were utilised in the previous external air temperature measurement test were used in this experiment.

The objectives of the experiment are as follows;

1. To monitor the temperature of a slab both internally and externally on the surface at a number of locations.
2. To monitor the temperature of the air at different heights with respect to the slab, in order to assess how the local air temperature behaves.

6.3.2.2 Test configuration

The experiment involved the use of seven thermocouple wires which were set up as per the layout in Fig. 6-13 to record temperature changes of the air and slab over a period of 2 days. The slab chosen for this setup had a screed finish with 50% GGBS. One thermocouple was placed on the top centre of the slab (No. 1), one was previously cast inside the slab 20mm from the top surface (No. 2) and one was placed beneath the slab in the centre (No. 3). A thermocouple was also placed on the side of the slab at mid-depth (No. 4). Three thermocouples were set up beside the specimen to measure air temperature on a thermocouple stand (fabricated from concrete cubes), which the thermocouple wires were fixed onto using tape. One was placed at a height of 120mm above ground to monitor the ambient air temperature (No. 5), one at a height of 60mm which is the level of the top of the slab (No. 6) and one at the ground level (No. 7) located just above the roof, without making contact with the surface. The thermocouple wires were protruding out from the surface of the cube by approximately 30mm, ensuring the measurement of the air temperature and not the temperature of the concrete cubes.

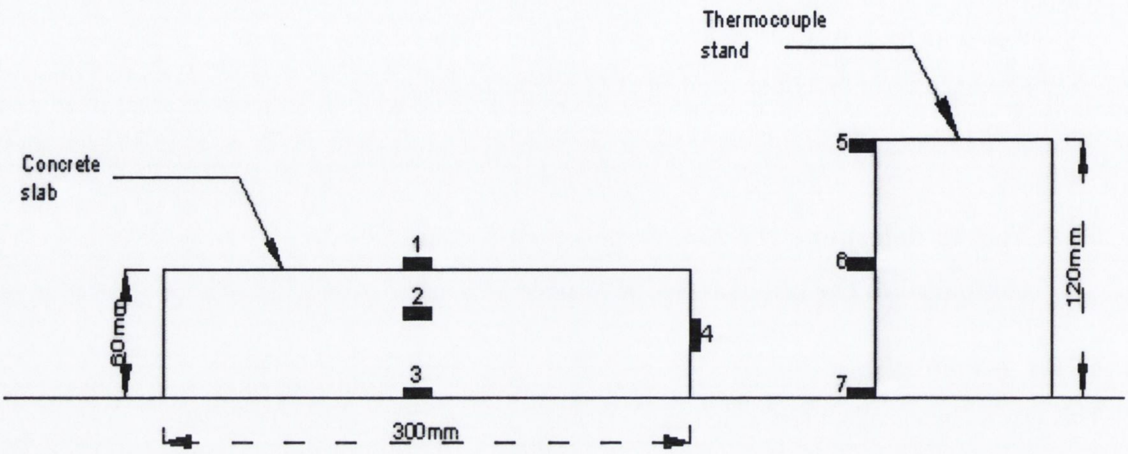

Fig. 6-13 Thermocouple configuration for test on roof to measure air temperature, internal and external temperature of a concrete slab, with thermocouple locations numbered 1-7

6.3.2.3 Results and observations

The results for air temperature variation are displayed in Fig. 6-14 and these are plotted with the sunshine intensity superimposed on the chart. This plot focuses on the change in air temperature as a result of the change in level of direct irradiance (W/m^2) and the natural change in the ambient temperature over a period of 2 days. It is evident from the graph that the sunshine intensity ranges from a low peak value on Day 1 to a high peak reading on Day 2. On Day 1 of the test, an initial air temperature of approximately 11°C is recorded, which then increases to a peak of 15°C. A low intensity of sunshine is also observed (<$100W/m^2$), significantly below the threshold value of $120W/m^2$ indicating that cloudy conditions were noted on this day. This would suggest that the increase in air temperature at the three different heights occurs due to the natural increase in the air temperature throughout the day. The thermocouple at a height of 0mm (No. 7) experiences the highest temperature due to its close proximity to the black roof. As the incoming solar radiation, albeit low, is absorbed by the black roof, it is reemitted as heat, therefore warming the near-surface air temperature, resulting in a marginally higher air temperature reading. On both days, the highest air temperature is the surface temperature at a height of 0mm, and the temperature at 60mm (No. 6) and 120mm (No. 5) are very close together. It is also important to note that there is only a very slight lag in temperature as the sudden change in air temperature is a direct consequence of the change in sunshine intensity.

The results from Day 2 in Fig. 6-14 demonstrate the effect of sunshine intensity on the resulting air temperature. The data from Day 2 can be seen more clearly in Fig. 6-15 where there is a large increase in the level of sunshine intensity, reaching a maximum of 850W/m^2 which indicates that the sky was clear and it was sunny on this day. The peaks in the temperature of the air correspond directly to the peaks in sunshine intensity with a slight lag. The increase in sunshine intensity gives rise to a change in the air temperature from 11°C to a maximum peak of 20°C at approximately 1.30pm. Although the temperature of the air would naturally increase as a result of the ambient temperature (see Fig. 6-14), it has increased significantly as a result of the presence of direct sunshine.

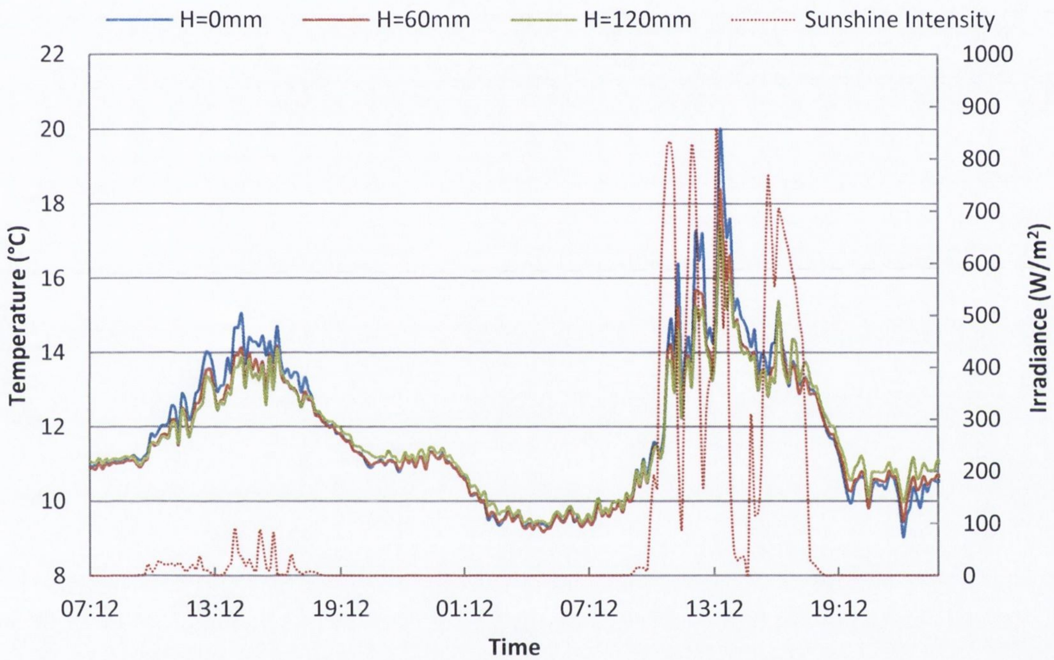

Fig. 6-14 Air temperature at three different heights vs. sunshine intensity over two days

There is a clear differentiation in the peak temperature of the air; for example, the maximum peak occurring at approximately 13:30, shows the air temperature close to the roof (No. 7) was recorded at 20°C, while the thermocouple at a height of 60mm (No. 6) and 120mm (No. 5) recorded lower temperatures of 18°C and 17°C respectively. The large increase in temperature experienced by thermocouple No. 7 is due to the heat radiating off the black roof. When the sunshine is incident on the black roof, it absorbs the sun's energy and heats up as a consequence. This heat is dissipated from the surface due to the high thermal emittance of the roof. As thermocouple No. 5 and No. 6 are further away from the radiating source, they consequently experience a lower temperature as expected. It is also important to note that the last peak in temperature at approximately 16:30 recorded a sunshine intensity of approximately 700W/m^2, however, the corresponding air temperature is significantly lower than previously, at 15°C. This is due to a noticeable drop in the ambient air temperature at this time of the day, resulting in an overall reduction in the air temperature recorded.

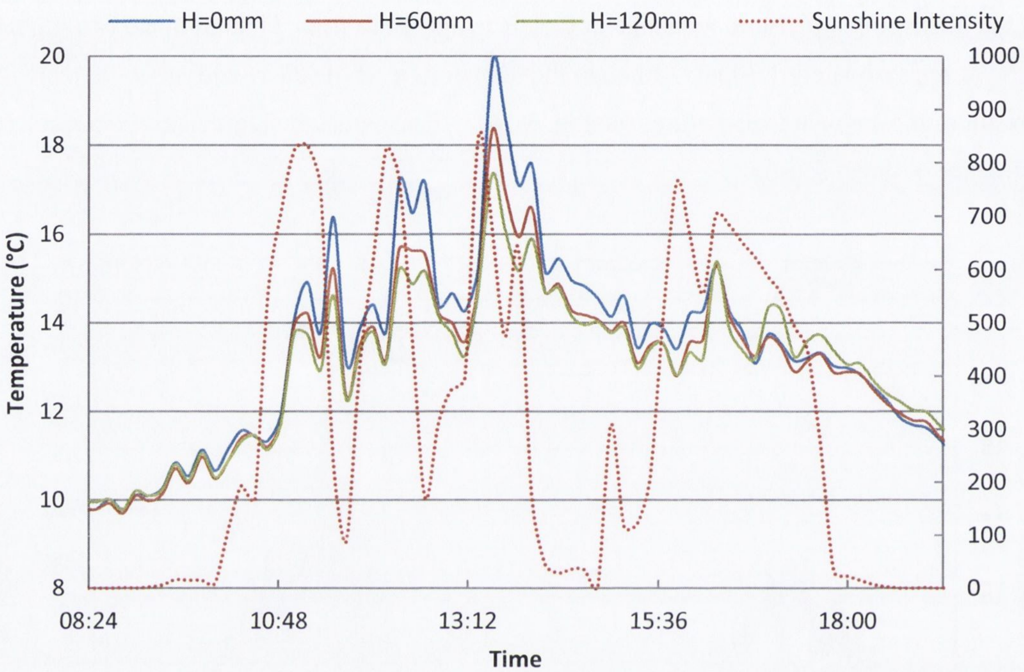

Fig. 6-15 Air temperature at three different heights vs. sunshine intensity (Day 2)

In conclusion, the presence of sunshine has a significant influence on the temperature of the air, however, this is dependant on the location of the air temperature being recorded. The black roof contributes significantly to the results, as it heats up considerably when it is exposed to direct sunshine. This heat is emitted from the black surface (having a high emissivity value) which directly affects the air above the surface as expected, with the thermocouple close to the heat source recording the highest temperature. The data would also suggest that the ambient air temperature is important, in addition to the presence of sunshine intensity, as they both contribute to the resulting temperature recorded, with a slight lag evident between the sunshine intensity and the air temperature.

Fig. 6-16 illustrates the results recorded by the thermocouple wires located both on the surfaces of and inside the specimen already stated, in addition to the sunshine intensity. As it was cloudy on Day 1, there was a gradual increase in the temperature of the slab, very similar to that of the air temperature in Fig. 6-14, reaching a peak of 15°C. The temperature at the top surface of the slab increased at the greatest rate as it is exposed directly to sunshine, as expected. This was followed closely by the temperature inside the specimen, however, the curve is smoother as the temperature change within the slab is more gradual due to the thermal conductivity of the concrete. As the other thermocouple wires were exposed but somewhat sheltered from the environment (side and underneath), the change in temperature occurred at a more gradual rate. The side of the slab (No. 4) is exposed to the environment, therefore, decreasing in temperature at a faster rate. The temperature beneath the slab (No. 3) lagged as it took some time before the heat transmitted through to the bottom of the slab due to thermal conductivity.

The data recorded over 2 days demonstrates the influence of sunshine on the behaviour of the specimens, and the resulting influence is evident on Day 2 in particular, recording a high level of sunshine intensity.

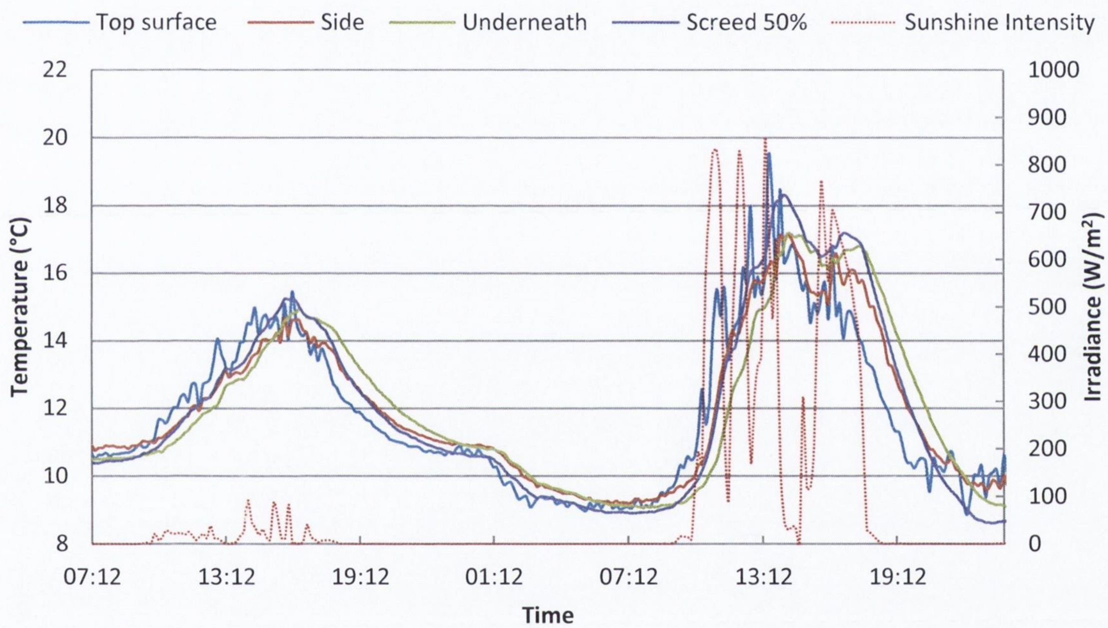

Fig. 6-16 Internal (depth =20mm) and external surface temperature of slab with sunshine intensity

The results from Day 2 can be seen clearly in Fig. 6-17. At approximately 11:00, the sunshine intensity recorded is a maximum of 833W/m^2, and this incident radiation on the surface of the specimen causes the top surface to experience a significant increase in temperature as there is heat being generated on the surface of the slab. This trend is consistent throughout the day, with a slight lag occurring of between approximately 15-30 minutes. The internal temperature of the specimen increases in temperature at a slower rate due to the thermal conductivity of the specimen. The heat generated at the surface takes some time before a change is experienced at a depth of 20mm in the concrete. It can also be observed that when the sunshine intensity suddenly decreases, for example, at 11:10, the top surface temperature decreases suddenly also. As the sunshine decreases, the heat is lost from the surface very quickly.

The internal temperature peaks at 14:10, approximately 40 minutes following the last peak in sunshine intensity. Once the sunshine intensity drops off, the heat is radiated from the specimen, however, due to the thermal mass of the material, this process takes some time, as the change in internal temperature is gradual. The side temperature follows the internal temperature very closely, with approximately 1.3°C between their peak temperatures. As the side thermocouple is sheltered from the environment somewhat, it would not receive as much direct sunshine as the top surface. The underneath temperature is lower than the side temperature during the heating up stage by approximately 1°C, as the thermal mass of the concrete means that the temperature at the bottom surface takes longer to register a change, with an additional lag present of approximately 20 minutes. It also has the slowest rate of cooling which is explained by the fact that it is kept warm by the specimen above it. Also, as there is timber below, this insulates the thermocouple, therefore, the heat travels predominately upwards, resulting in this thermocouple having the highest temperature upon cooling.

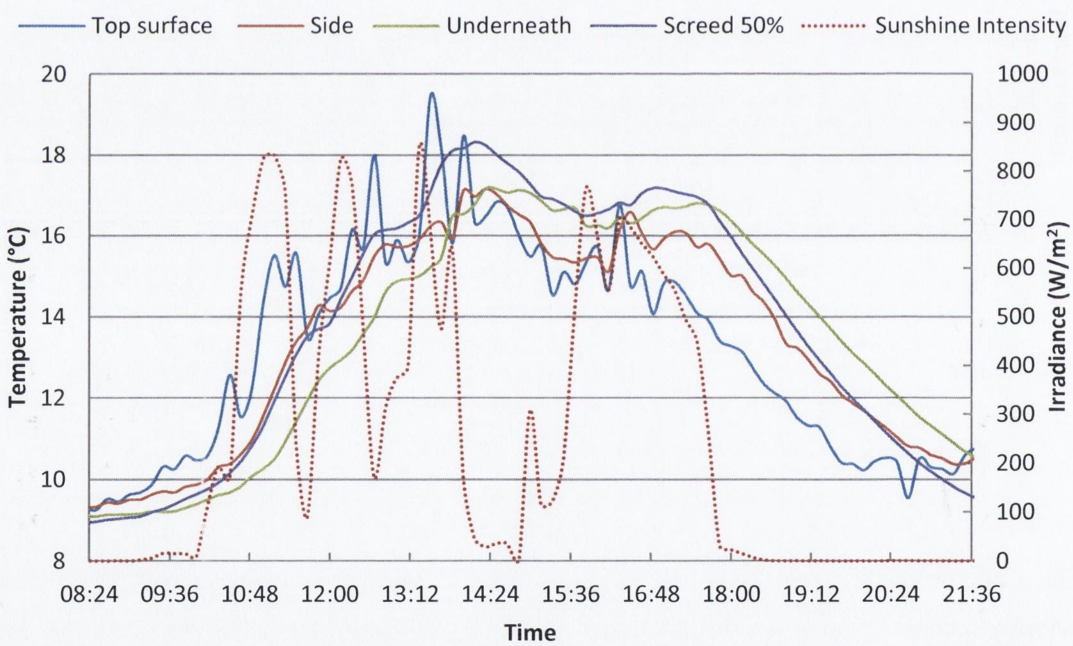

Fig. 6-17 Internal (depth =20mm) and external surface temperature of slab with sunshine intensity (Day 2)

In conclusion, the temperature profile is as expected, with the order of decreasing temperature as follows; top surface, internal (screed), side and underneath. However, this order is not maintained throughout the day, for a number of reasons relating to external factors. The ambient air temperature plays an important role, and this is evident in particular in the evening time when the specimens drop in temperature, with the top surface temperature decreasing first, suggesting that the specimens are losing their heat to the environment. The sunshine is also important as it affects the temperature of the specimen, in particular, at the top surface where the heat is generated, with a slight lag present. The conductance of heat through the depth of the slab is evident by the lag in the internal temperature, with the change in temperature being very gradual. The side and underneath temperatures are sheltered by the environment, therefore, experiencing a further lag in temperature. The outcome demonstrates that external factors such as sunshine and the ambient air significantly affect the temperature of the slab, and the thermal properties of concrete are very distinctive, with the rate of change of temperature occurring some time after the change in the external conditions occur.

6.3.2.4 Conclusions

- The thermocouple which is placed closest to the roof (No. 7) recorded the highest air temperature for both days due to its close proximity to the black roof. The roof absorbs solar radiation and reemits this in the form of heat, which in turn warms up the near-surface air temperature.
- There is a significant difference in the air temperature at different heights which is due to the distance away from the roof which is a radiative source of heat. However, as there is timber beneath the concrete specimen, the heat from the roof below would be minor as timber is a very good insulator, as was demonstrated in the physical test on materials in Section 6.2.
- The peak in sunshine intensity corresponds directly with the peak in air temperature, with a slight lag of approximately 20 minutes. Although the sunshine intensity directly affects the resulting air temperature, the ambient air temperature is also important as it contributes to the gain/loss of heat in the specimens also. For example, in the afternoon, when the sunshine intensity remained high ($800W/m^2$), the temperature of the air did not reach as high as would normally be expected, which is due to the natural decrease in the ambient air temperature in the afternoon.
- The internal and external temperature of the slab, where there is no sunshine present, shows a general trend in the temperatures, and these fluctuations are as a result of the ambient air temperature. These trends are seen more clearly where there is a high level of sunshine intensity in particular, at the top surface where the heat is generated, with a slight lag present. The temperature profile is as expected, with the order of decreasing temperature as follows; top surface, internal (screed), side and underneath, however, this

order is not maintained due to external factors. The ambient air temperature plays an important role, for example, in the evening time when the specimens drop in temperature, with the top surface temperature decreasing first, suggesting that the specimens are losing their heat to the environment, as expected.

- The conductance of heat through the concrete is evident by the lag in the internal temperature, with the change in temperature being gradual. This is clear from the result whereby the internal temperature peaks approximately 40 minutes following the sunshine intensity peak. The side and underneath temperatures are sheltered by the environment, therefore, experiencing a further lag in temperature. It was also noted that the underneath temperature remained the highest upon cooling in the evening. This is explained by the fact that the thermocouple is insulated from the environment and that due to the ability of concrete to store heat, the heat generated in the specimen is retained and is released very slowly.
- The overall outcome from this test demonstrates that external factors such as sunshine and the ambient air significantly affect the temperature of the slab, as expected. The thermal properties of concrete are very distinctive, with the rate of change of temperature with depth occurring some time after the change in the external conditions arise.

6.4 Conclusions

- The colour of a material is important in terms of white and grey, but equally if not more important is the thermal behaviour of the material i.e. its emissivity or ability to shed heat from the surface, and the thermal conductance allowing the transfer of heat down through the depth if the material.
- Although thermal conductivity of a material is relevant, the VHC value is equally as important in terms of the heat that is retained in the material. As timber has a low k value (0.85W/mK), the heat is confined to the top surface, therefore, the temperature drops very quickly when the heat source is removed. The VHC value is better for concrete and aluminium due to their higher density.
- There is relationship between the L* and the peak temperature, however, this behaviour is heavily influenced by the materials' conductance and the surface colour. It is also evident that painting the surface of the material black (for aluminium, concrete and timber) has a greater effect on the surface temperature than painting the surface white, as the specimens are originally more white in colour than black. The results indicate that where there is an increase in L* value, there is a corresponding decrease in peak temperature and vice versa.

- There are identical trends for both the screed and the brush surface finish for the second test, which would suggest that the behaviour of the temperature of the specimens with respect to the air temperature is entirely independent of the surface finish type.
- The overall outcome of the third test demonstrates that external factors such as sunshine and the ambient air significantly affect the temperature of the slab but in different ways. The thermal properties of concrete are very distinctive, with the rate of change of temperature occurring some time after the change in the external conditions arise.

7 Data Analysis and Discussion

7.1 Introduction

This chapter examines the data acquired by the following test methods as described in detail in Chapter 4 and 5, three of which are direct test methods.

1. Sphere spectrophotometer
2. Lux meter
3. Greyness scale
4. Thermal imaging
5. Thermocouple wire

Following analysis of the data obtained, a discussion of the test methods will be presented at the end of the chapter, with the aim of giving an overall summary of the findings from each process, thereby explaining the influence of aggregate type, GGBS content, surface finish and age on the solar reflectance of concrete.

A standard t-test was used to analyse and compare some of the data presented in this chapter so that it could be established whether there are systematic or random variability's between two data sets being compared. For comparing two independent population averages, a hypothesis testing procedure such as the t-test can be employed. A null hypothesis is a hypothesis to be tested and is denoted by H_0 (Weiss, 2008). The null hypothesis is that the two population means are the same i.e. that the difference in the means of the entire populations is equal to 0. The notation for the null hypothesis is $H_0:\mu_1=\mu_2$ where μ_1 represents the mean of the first population and μ_2 represents the mean of the second population. The test statistic variable in Equation (7-1) is the basis for deciding whether or not to reject the null hypothesis of two samples of the populations:

$$t = \frac{(\bar{x}_1 - \bar{x}_2)}{\sqrt{\frac{\sigma_1{}^2}{n_1} + \frac{\sigma_2{}^2}{n_2}}} \tag{7-1}$$

where $\bar{x}_i$ represents the sample mean, σ_i represents the standard deviation and n_i is equal to the sample size (i = 1, 2). The degree of freedom (DF) is defined as (n_1+n_2-1) for this test.

The probability of rejecting a true null hypothesis is called the significance level, α, of a hypothesis test. If the hypothesis test is conducted at a high significance level (e.g. α=0.05), the chance of rejecting a true null hypothesis will be very small. For the purpose of the t-tests conducted hereinafter, α=0.05. Once the t-statistic value is calculated using Equation (7-1), and the DF is determined, the percentiles of the t-distribution table are used to determine if the t-statistic value is greater than or equal to the critical P value obtained in the significance table (see Appendix E). If this is the case, one reject H_0. This demonstrates that the two sets of data are significantly different such that there is a systematic reason for their difference. Otherwise, the differences in the mean must be random, not systematic.

7.2 Sphere Spectrophotometer

As outlined in Section 4.3, a sphere spectrophotometer is an instrument which is used to measure colour. Colour is an important parameter when it comes to the albedo of a surface. The L* value, which a sphere spectrophotometer produces, concerns itself solely with the scale of black and white (L*=100=white, L*=0=black) which is most relevant to the colour of concrete. The concrete specimens that were fabricated for this project contain cement blends of CEM II A-L with GGBS ranging between 0 to 70% GGBS. The following tests were carried out using the sphere spectrophotometer to assess the difference in L* values between different cement blends, and subsequently different concrete specimens;

1. Sensitivity tests to determine the accuracy and variability of the instrument
2. Testing L*,a* and b* values of varying cement blends (WPC, GGBS, CEM II A-L)
3. Testing L*,a* and b* values of concrete specimens containing varying substitution rates of GGBS and different surface finishes

7.2.1 Sensitivity tests

A number of tests were devised to assess the sensitivity of the sphere spectrophotometer before any initial testing could begin on the cement powder blends and the concrete slab specimens. The chosen surface for this test was a plain white A4 sheet of paper.

The first of these tests was to determine the accuracy of the instrument by testing its repeatability. This was carried out by taking a reading in the same location on the white sheet of paper 8 times. A reading for L*, a* and b* were recorded each time and the instrument was not moved between each reading. The second test was carried out to assess the variability of taking a reading on a uniform surface at 12 random locations on the same sheet of white paper. Similarly, a reading for L*, a* and b* were recorded at each location. Both of these tests were then repeated on a second white sheet of paper to ensure the results were applicable on a different specimen, recognising that although the paper appeared highly uniform, and that sheets were identical, they may not be.

7.2.1.1 Test for accuracy and variability of the spectrophotometer using a white sheet of paper

The readings, which were obtained for L*, a* and b* for the first test are displayed in Table 7-1. The average value for L* is 93.75 and is not unexpected given it is a white surface. The value for a* is very small at 1.77 and would suggest there is a hint of red present. The b* value of approximately -6.19 would suggest there is a small percentage of blue present. However, for the purposes of the sensitivity tests and the further tests carried out using the spectrophotometer, these values of a* and b* are insignificant unless stated otherwise. The value for L* is the one of most importance as it is the axis concerned with the scale of black and white.

Table 7-1 Results for L*, a* and b* on first white sheet of paper in the same location

Reading	L*	a*	b*
1	93.63	1.73	-6.19
2	93.66	1.72	-6.16
3	93.76	1.77	-6.12
4	93.81	1.79	-6.13
5	93.80	1.79	-6.12
6	93.80	1.78	-6.11
7	93.80	1.78	-6.10
8	93.77	1.79	-6.10
μ_L	93.75		
σ_L	0.070		
CoV	0.074%		

The standard deviation between the L* values is very small at 0.070, giving rise to a coefficient of variation of 0.074% which is very low. This result is evidence that the instrument is very sensitive and accurate.

The second test, to determine the variability in L* reading across an apparently uniform white sheet of paper was performed and the corresponding results are outlined in Table 7-2. The average reading of L* is almost identical at 93.76, however, the standard deviation for the 12 readings is marginally bigger at 0.109, which results in a bigger coefficient of variation of 0.12%. This result is still acceptably small and confirms the accuracy and sensitivity of the instrument. It also signifies that there is little variability in a reading taken over a visibly uniform surface in different locations across that surface, and also that the white paper is highly uniform in colour. This increase in CoV could be due to the very small variations in whiteness across the sheet.

The first test was repeated on a second sheet from the same batch of white A4 paper with 8 readings being recorded on the same point without moving the instrument (see Table 7-3). This time the average value of L* has decreased marginally to 93.63 from 93.75 on sheet one. The standard deviation has also increased from 0.07 to 0.085, which results in an increase in the coefficient of variation to 0.09%. This remains an extremely low result and reaffirms the accuracy and reliability of the instrument. The instrument is highly sensitive and can detect very small changes in colour between two sheets of white paper that appear identical to the naked eye.

Table 7-2 Results for L*, a* and b* on first white sheet of paper in different locations

Reading	L*	a*	b*
1	93.67	1.70	-6.04
2	93.72	1.74	-6.08
3	93.71	1.79	-6.09
4	93.79	1.79	-6.08
5	93.69	1.77	-6.1
6	93.73	1.78	-6.05
7	93.62	1.78	-6.13
8	93.73	1.76	-6.09
9	93.72	1.80	-6.12
10	93.87	1.85	-6.08
11	93.93	1.83	-6.05
12	93.98	1.84	-6.01
μ_L	93.76		
σ_L	0.109		
CoV	0.116%		

A t-test was performed between the results from sheet one (see Table 7-1) and sheet two (see Table 7-3) where the reading was taken on the same location 8 times to assess whether the two data sets are significantly different. The t-test statistic was calculated to be 3.09 and the critical P value was obtained from the t-distribution table (see Appendix E). The critical P value (where DF=15) was 1.753 at a significance level (α=0.05), therefore, as the test statistic is greater than the critical P value the null hypothesis is rejected. It can be concluded that the test results are statistically significant at the 95% level. This result illustrates that the data is statistically not from the same data set, and would reconfirm the sensitivity of the instrument and the non-uniformity of the paper sheets.

The second test was also repeated on the second sheet of white paper with 12 readings being recorded at random locations across the sheet (see Table 7-4). The average value of L* is almost identical to the first two tests carried out (see Table 7-1 and Table 7-2) with a value of 93.70. The standard deviation is 0.093, which results in a coefficient of variation of 0.09%. This value remains very low and demonstrates the accuracy and reliability of the instrument.

Table 7-3 Results for L*, a* and b* on second white sheet of paper in the same location

Reading	L*	a*	b*
1	93.69	1.71	-6.01
2	93.67	1.72	-5.96
3	93.57	1.73	-5.97
4	93.46	1.74	-5.96
5	93.71	1.74	-5.98
6	93.68	1.72	-5.97
7	93.65	1.73	-5.98
8	93.57	1.72	-5.95
μ_L	93.63		
σ_L	0.085		
CoV	0.091%		

In conclusion, the two tests carried out on the two seemingly identical sheets of white paper result in an almost identical result in L* each time (<0.1% change). The standard deviation is very small for each test (< 0.109) as is the corresponding coefficient of variation (< 0.12%). These results suggest that the instrument is highly sensitive and produces readings with minimal variability when taken across a highly uniform white surface.

Table 7-4 Results for L*, a* and b* on second white sheet of paper in different locations

Reading	L*	a*	b*
1	93.65	1.73	-5.98
2	93.66	1.67	-6.01
3	93.65	1.70	-6.02
4	93.57	1.73	-6.05
5	93.70	1.73	-6.05
6	93.67	1.72	-5.98
7	93.62	1.73	-6.01
8	93.71	1.74	-6.02
9	93.71	1.73	-6.04
10	93.77	1.76	-6.01
11	93.80	1.78	-6.06
12	93.92	1.79	-6.03
μ_L	93.70		
σ_L	0.093		
CoV	0.099%		

7.2.1.2 Sensitivity test using plastic sheet over white paper

As the spectrophotometer is to be used to take readings on cement powder blends, a clear plastic sheet was selected to cover the powders to prevent the powder from entering the aperture where the reading is taken, while also providing a uniform surface from which readings could be taken. The two sensitivity tests were repeated again, however, a clear plastic sheet was placed on top of the white sheet of paper first, to identify whether the clear plastic sheet had an impact on the readings. The first test indicated that the average L* value reduced from approximately 93.7 previously to 92.6 (see Table 7-5). This is an overall reduction of approximately 1.3%. The standard deviation and corresponding coefficient of variation are very small which suggests that the instrument is very accurate and that the test is repeatable even with a plastic sheet in place, although there is a slight drop in the L* reading taken.

Table 7-5 Results for L*, a* and b* on white sheet of paper in the same location using a clear plastic sheet as a cover

Reading	L*	a*	b*
1	92.56	1.42	-4.73
2	92.53	1.45	-4.69
3	92.62	1.46	-4.70
4	92.62	1.48	-4.72
5	92.64	1.48	-4.71
6	92.60	1.48	-4.70
7	92.61	1.48	-4.71
8	92.64	1.47	-4.70
μ_L	92.60		
σ_L	0.038		
CoV	0.042%		

The t-test was performed on the results from sheet two (see Table 7-3) and the results using the plastic sheet (see Table 7-5) to investigate whether the two data sets are significantly different. The t-test statistic was calculated to be 31.2 and the critical P value was obtained from the t-distribution table (see Appendix E). The critical value (where again DF = 15) is 1.753 at the 95% significance level. Therefore, as the test statistic is significantly greater than the critical P value the null hypothesis is rejected. It can be concluded that the test results are statistically significant at the 95% level. This result illustrates that the two sets of data are not from the same data set, which is an expected result given the high accuracy of the device and the presence of the clear plastic sheet.

The second test was also repeated, with the clear plastic sheet placed on top of the white sheet of paper. The data obtained from this test are displayed in Table 7-6. The average L* value is almost identical to that of the previous test (Table 7-5). The standard deviation of 0.054 is very low and this results in a low coefficient of variation of 0.058%. This result leads to the conclusion that by using the clear plastic sheet on top of the white paper, although there is a minor reduction in the measured L* value, the result will not vary across the surface of the plastic sheet and so a clear plastic sheet may be used to obtain L* values of cement blends. In other words, the results of L* for cement powders will be slightly underestimated, but the readings are repeatable to a very low variability.

Table 7-6 Results for L*, a* and b* on white sheet of paper in different locations using a clear plastic sheet as a cover

Reading	L*	a*	b*
1	92.5	1.49	-4.68
2	92.41	1.49	-4.70
3	92.54	1.49	-4.67
4	92.53	1.48	-4.72
5	92.58	1.52	-4.78
6	92.51	1.53	-4.71
7	92.58	1.52	-4.80
8	92.49	1.50	-4.67
9	92.47	1.50	-4.70
10	92.47	1.50	-4.68
11	92.42	1.54	-4.72
12	92.52	1.56	-4.73
μ_L	92.50		
σ_L	0.054		
CoV	0.058%		

7.2.2 Testing of cement blends for L* value

The colour of the cement is one of the primary characteristics which determines the colour of concrete. It is therefore important to examine the difference between the L* values of the cement before looking at the difference in L* values between the different concrete specimens. In order to measure the L*(also a* and b*) values of a number of different cements, a clear plastic sheet, as mentioned in Section 7.2.1, is necessary to protect the spectrophotometer from damage. This plastic sheet is placed over the compacted cement blend and the sphere spectrophotometer is placed directly onto the plastic sheet for a reading to be taken. A total of 5 readings (the maximum amount given the sample dimensions) were recorded at random locations over the surface of the cement sample.

7.2.2.1 Results of L values for some typical cements*

A number of typical cements were tested for L* value to obtain an overall picture of the colour of the various cements and the order in which they would be placed in a list of descending greyness. The average L* value for each of the cements are summarised in Table 7-7 and are in order of increasing L* value (see Appendix F for the full set of results). The data illustrates that the CEM I and CEM II cements are in the order of 63.6 and 65.7. By making a 60:40 blend of CEM III/A (containing 60% GGBS and 40% CEM I), an increase in L* up to 77.1 is evident.

Table 7-7 Summary of L* values for some typical cements

Cement type and source	L*
CEM II A-V (Quinn)	63.57
CEM II (Ecocem)	64.78
CEM I (Spanish cement)	65.32
CEM II A-L (Irish cement)	65.65
CEM II A-V (Lagan)	65.71
60:40 CEM III A-L	77.06
GGBS (Sweden)	81.39
GGBS (Ecocem)	88.20
White cement (WPC)	90.72

A CEM II A-V cement contains pulverised fuel ash (PFA), which is naturally dark in colour (up to 20% PFA may be present but generally 10%). It is interesting to note that there are two different sources of this cement (Quinn and Lagan), however, there is a difference in the colour of the cement. This would suggest that Quinn uses either a darker PFA or a higher percentage of PFA in the cement as the colour is darker. A CEM II A-L cement contains limestone powder, and similarly, up to 20% of the cement can contain limestone powder, however, in general approximately 10% is used.

It is important to note from Table 7-7 that the GGBS from Ecocem as used in this research, had the closest L* value (88.2) to white cement (90.7). This summary of results for the typical cements on the market demonstrate the significant difference in colour between a standard CEM I/CEM II cement and that of GGBS or white cement. The colour difference between these various cements is displayed in Fig. 7-1.

Fig. 7-1 Digital image of cement powders from left to right: CEM 1, CEM II A-L, CEM II A-V,60:40 CEM III A,GGBS, WPC

7.2.2.2 Results of L values for various cement blends*

The L*, a* and b* value of a number of GGBS powder blends mixed with CEM II A-L in various proportions (0-100%) were measured along with a number of GGBS with different WPC powder blends ranging between 0-100%. For comparison purposes, the L*, a* and b* value of a number of WPC powder blends mixed with CEM II A-L in various proportions (0-

100%) were also measured. For a detailed set of results for the cement blend mixes containing GGBS and CEM II A-L, GGBS and WPC, and WPC and CEM II A-L, the reader is referred to Appendix G, Appendix H and Appendix I respectively. In these results, the average L* is denoted by μ_L and the standard deviation of the L* values is denoted by σ_L. The coefficient of variation (CoV) for the L* values is also displayed for each cement blend variation which is of particular interest. The CoV values for the sets of results are all less than 1% which confirms that the cement blends are very uniform and well blended. The readings of a* and b* range between approximately -1.72 to 0.30 and 4.01-6.35 respectively. The range of possible a* and b* parameters is between -60 and +60, therefore, as these results are within a small range and do not vary significantly, they will not be discussed as the L* value is the axis of colour which has the greatest significance here.

A summary of the average L* value readings is outlined in Table 7-8 and these results are displayed in graph format in Fig. 7-2. The three cement powders before any blending occurs show interesting results. The L* value for 100% WPC (90.72) is very similar to that of 100% GGBS (87.92). As expected, the L* value of CEM II A-L (64.78) is significantly lower as it is dark grey in colour. The mixing of WPC and GGBS (in the ratios 70:30, 50:50 and 30:70) produce the highest range in L* values of the cement blends, ranging from between 88.0 to 89.6.

Table 7-8 Summary of average L* values for cement blends containing different percentage quantities of WPC, GGBS and CEM II A-L cement powders

WPC	GGBS	CEM II A-L	L*
100	0	0	90.72
0	100	0	87.92
0	0	100	64.78
70	30	0	89.59
50	50	0	88.94
30	70	0	87.96
0	70	30	76.31
0	50	50	72.80
0	30	70	68.28
70	0	30	75.61
50	0	50	71.65
30	0	70	68.55

There is a very small range in these L* values due to the close proximity in the colour of the two parent cements. The blend containing GGBS and CEM II A-L (in the ratios 70:30, 50:50 and 30:70) have a range of L* values between approximately 68.3 and 76.3. By adding 70% GGBS to 30% CEM II A-L (76.3), there is an approximate increase of 18% in the L* value from that of 100% CEM II A-L (64.78). The cement mix between WPC and CEM II A-L (in the ratios 70:30, 50:50 and 30:70) produced a range of results in L* between 68.6 and 75.6. These values are very similar to those of GGBS mixed with CEMII A-L.

In conclusion, this test indicates that the cement mixes were well blended and uniform across the surface and that the accuracy of the instrument is such that it can detect small changes in colour which the human eye could not differentiate between. The results in Fig. 7-2 confirm that there is little difference in the colour produced by using GGBS with CEM II A-L and WPC with CEM II A-L. However, as one adds WPC/GGBS to CEM II A-L, the colour becomes significantly lighter.

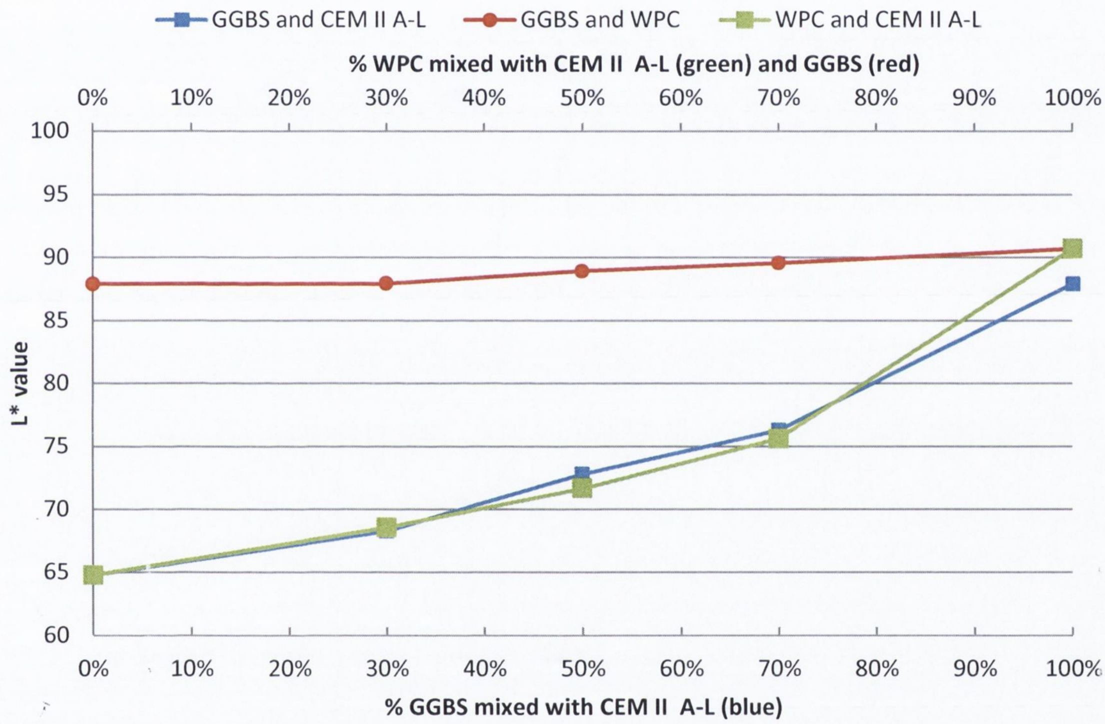

Fig. 7-2 Average L* value for cement blends using GGBS, CEM II A-L and WPC

7.2.3 Testing concrete specimens for L*, a* and b* values

The sphere spectrophotometer was utilised in order to determine the colour of the slab specimens containing the 3 aggregate types, 4 different surface finishes and 4 levels of GGBS substitution (after approximately 2.5 years of exposure). The specimens were tested when the surface was dry as the moisture level would have an effect on the colour. The level of near-surface moisture was measured, using a moisture meter and noted for each specimen and these ranged between 2.5 and 4.5%. This suggests that the near-surface concrete is relatively dry (greater than 6% indicates that the concrete is still highly moist).

For each specimen, a total of 9 readings of L*, a* and b* were recorded (a matrix of 3x3 on a notional grid on the surface) with the aim of determining the approximate uniformity of the surface. The result of a* on average ranged between 0.69 and 2.45, with b* having an average reading of between 6.05 and 9.1. These readings are nominal with respect to the overall scale of colour, therefore, only the L* values will be discussed in the results to follow.

For the 9 readings of L*, the average (μ_9) was calculated along with the standard deviation (σ_9). Following this, the coefficient of variation (CoV) was calculated. For each of the 96 specimens, the CoV was less than 5% which confirms both the accuracy of the device and the uniformity of the surface being tested. The CoV was found to be lower for the smooth surfaces and higher for the undulating surfaces in general. This result is due to the light being diffused off the rough surface leading to a larger variation of L* values over the surface of the slab, depending on where precisely the reading is taken.

As there are duplicate specimens present, having almost identical L* values, the readings were collated to derive one average L* reading (μ_{18}). A detailed set of these results can be found in Appendix J. A summary of these L* readings are outlined in Table 7-9 for each specimen type. The GGBS concentration (%) is displayed along the left column with aggregate type (limestone, partially crushed limestone and sandstone) alongside it. The four surface finishes are displayed at the top of the table columns. The following will be discussed in detail;

1. The effect of aggregate type on L*
2. The effect of surface finish on L*
3. The effect of GGBS content on L*
4. Testing 0 and 70% GGBS concrete surfaces (at the Father Collins Park location)

Table 7-9 Average L* value for slab specimens for different surface finish type, aggregate type and % GGBS (in February 2013)

GGBS	Agg.	Cast	Screed	Tamp	Brush
0	L	58.59	64.06	55.00	61.08
	PCL	60.00	64.51	51.69	57.52
	SS	58.84	61.17	46.57	52.07
30	L	60.44	65.64	54.26	56.31
	PCL	59.18	62.72	57.71	54.70
	SS	57.52	62.01	49.41	58.32
50	L	59.88	64.48	58.12	60.16
	PCL	59.47	67.01	57.56	62.10
	SS	57.28	64.36	56.40	62.99
70	L	60.83	66.71	61.79	65.31
	PCL	61.91	66.89	58.81	61.65
	SS	57.76	64.62	55.84	60.87

7.2.3.1 *The effect of aggregate type on L* value*

The effect of aggregate type on colour is evident from the L* value readings in Table 7-9. The specimens have been exposed to the environment for just over 2 years at the time of these readings, with the aggregate visibly exposed on many of the cast finish specimens. The effect of the aggregate type on the L* values will be studied in detail, for each of the surface finishes individually, focusing on the four concentrations of GGBS . The cast surface finish readings are displayed in Fig. 7-3 and, as suggested by the results, there is a small difference in L* between each of the aggregate types for the four GGBS contents. The range in L* values across the aggregate types is between approximately 1.4 and 4.15. This low range would suggest that the aggregate type does not significantly affect the colour of the concrete. It can also be observed that the SS aggregate has the lowest L* value consistently for the cast finish. This would indicate that the presence of SS aggregate results in a concrete which is marginally darker in colour than concrete containing LS or PCL aggregate. However, the cause for this difference in aggregate colour may be due to the finish type. As a cast finish exposes aggregates at the surface, this would contribute to the dissimilar L* values.

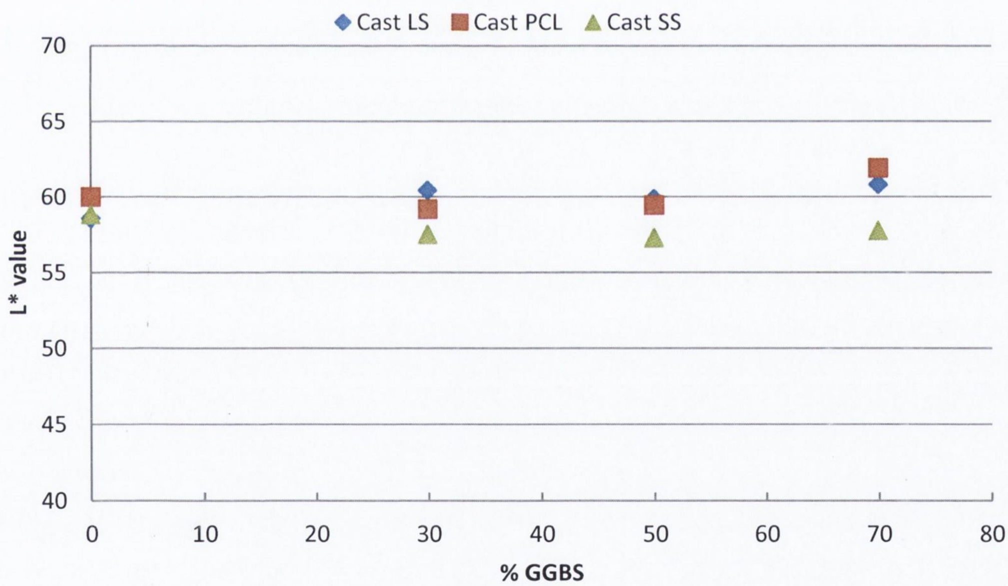

Fig. 7-3 The effect of aggregate type on L* value for a cast surface finish containing 0, 30, 50 and 70% GGBS

A similar observation can be made for the screed surface finish displayed in Fig. 7-4. The L* values of LS and PCL interchange as they are almost identical in colour, however, the sandstone aggregate is the lowest L* value. The range in L* value across the three aggregate types for the screed finish is between 2.27 and 3.63. This is a small range in L* value, therefore, it can be concluded that the aggregate type does not make a considerable difference in the colour of the concrete.

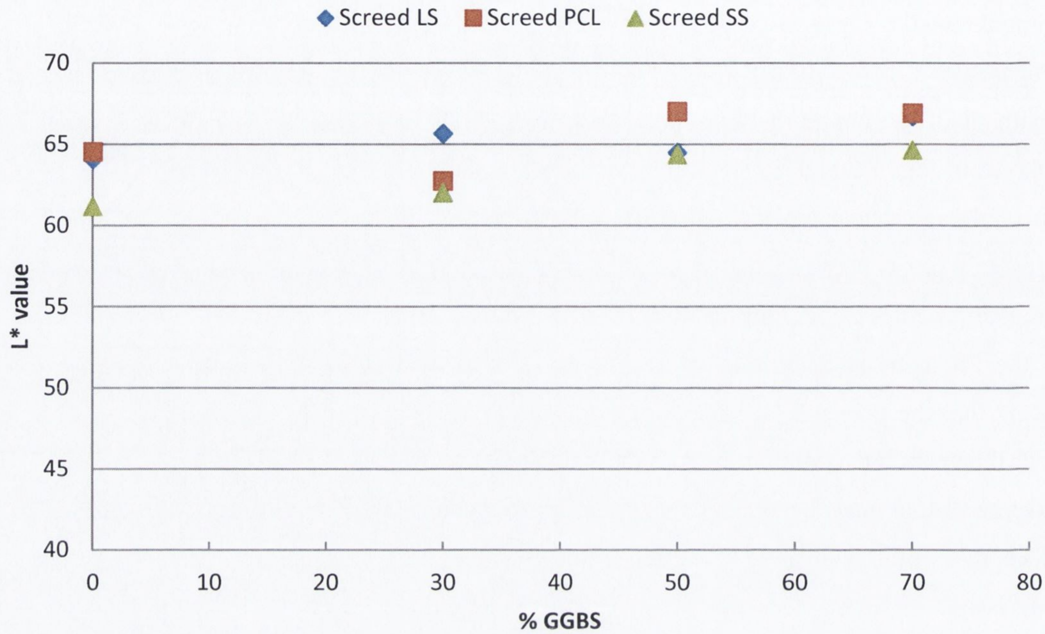

Fig. 7-4 The effect of aggregate type on L* value for a screed surface finish containing 0, 30, 50 and 70% GGBS

The trends observed for the rougher surface finishes (tamp and brush) are illustrated in Fig. 7-5 and Fig. 7-6 respectively. It is evident from the data that there is a larger range in the L* values across the surface of the specimens. The range in L* values in terms of the aggregate type across the tamped finish is 1.72 and 8.43, and similarly, the range for the brush finish is between 2.83 and 9.01. This is a marginally higher range when compared with the smoother surface finishes, however, the cause for this is due to the process of taking a reading over a rough surface finish. The instrument is accurate and produces very consistent and reliable results, however, when it is employed to measure the L* of an undulating surface, there is a wider range in readings. This can be seen very clearly by observing the coefficient of variation (CoV) values for the rough surface finishes (see Appendix J). The CoV ranges between 3.47 and 6.73 for the tamp finish, and between 1.42 and 5.06 for the brush finish. This increase in variability results in a wider range of L* values for the specimens with a rough surface finish.

By examining the effect of aggregate type for each of the surface finishes in turn, it can be concluded that there is no perceptible difference in L* values for the specimens containing different aggregate types. The SS aggregate was observed to have a marginally lower L* value, however, the difference in L* value is not substantial. Therefore, the subsequent sections will disregard the effect of aggregate type, and derive one result in order to examine the effect of GGBS and surface finish type on the L* value of concrete.

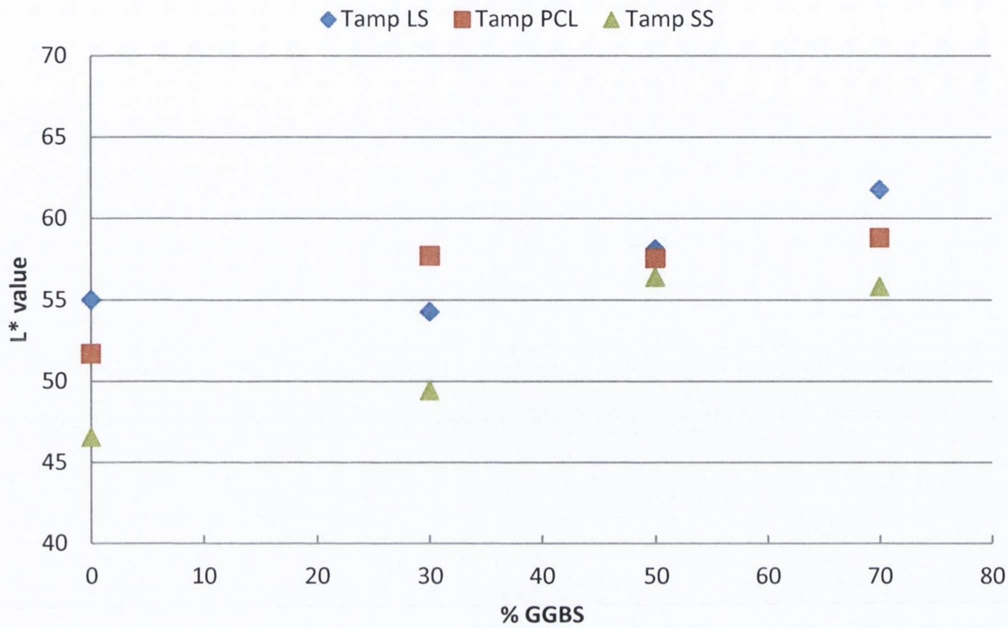

Fig. 7-5 The effect of aggregate type on L* value for a Tamp surface finish containing 0, 30, 50 and 70% GGBS

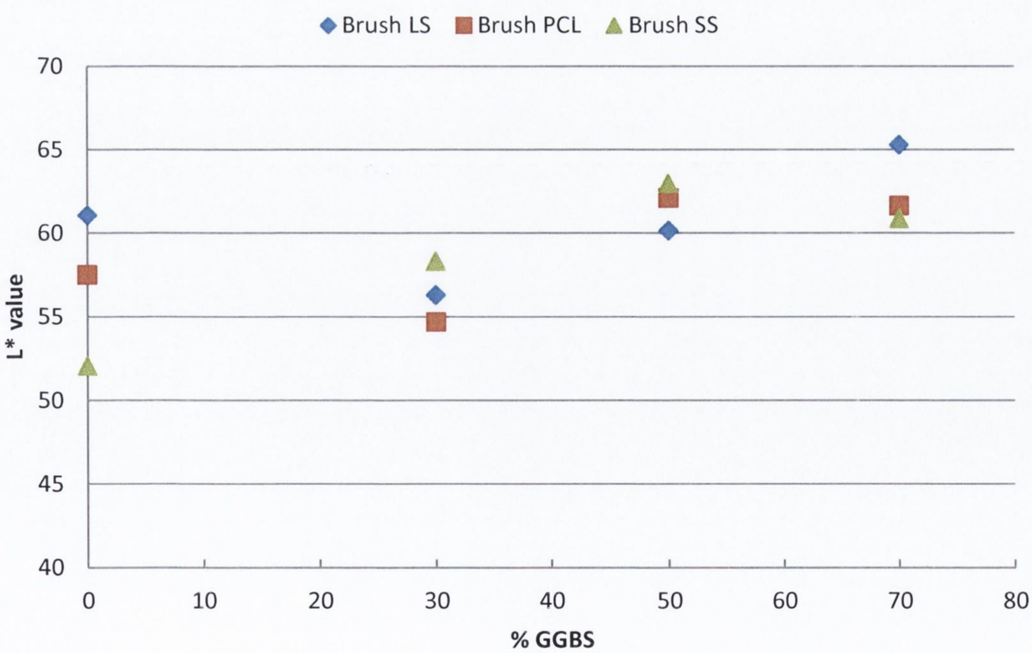

Fig. 7-6 The effect of aggregate type n L* value for a brush surface finish containing 0, 30, 50 and 70% GGBS

7.2.3.2 The effect of GGBS content on L value*

The data displayed in Fig. 7-7 demonstrates the effect of GGBS concentration (from 0 to 70%) on the L* value of concrete for the four different surface finishes. There is a broadly linear progression in terms of L* value, from 0 to 70% GGBS, in particular for the screed finish (maximum L*) and tamp finish (minimum L*) specimens. The smooth screed finish has the highest L* value as it is visibly the brightest in terms of colour, with cast having the lowest value of the smoother surface finishes as it is the darkest. The two undulating finishes overlap somewhat, in-between the two smooth finishes in terms of colour. This outcome is due to the nature of the surface finish, which accumulates dirt over time. However, it is interesting to note that the undulating surface finishes do not have as clear a progression, which is due to the larger variability in the L* reading. Nonetheless, there remains a strong correlation between the increase in L* value with a corresponding increase in GGBS content.

The general increase in L* with increased concentration of GGBS is evident in Fig. 7-8. The error bars denote the range at the 95% significance level. The error bars are large as they encompass the effect of the surface finish type, however, despite this fact it may still be concluded that the addition of GGBS to concrete increases the L* value by a measurable amount. The slope of the line is approximately 1.56 which would signify a small increase in L* with percentage GGBS and the relationship between L* value and % GGBS is approximately linear.

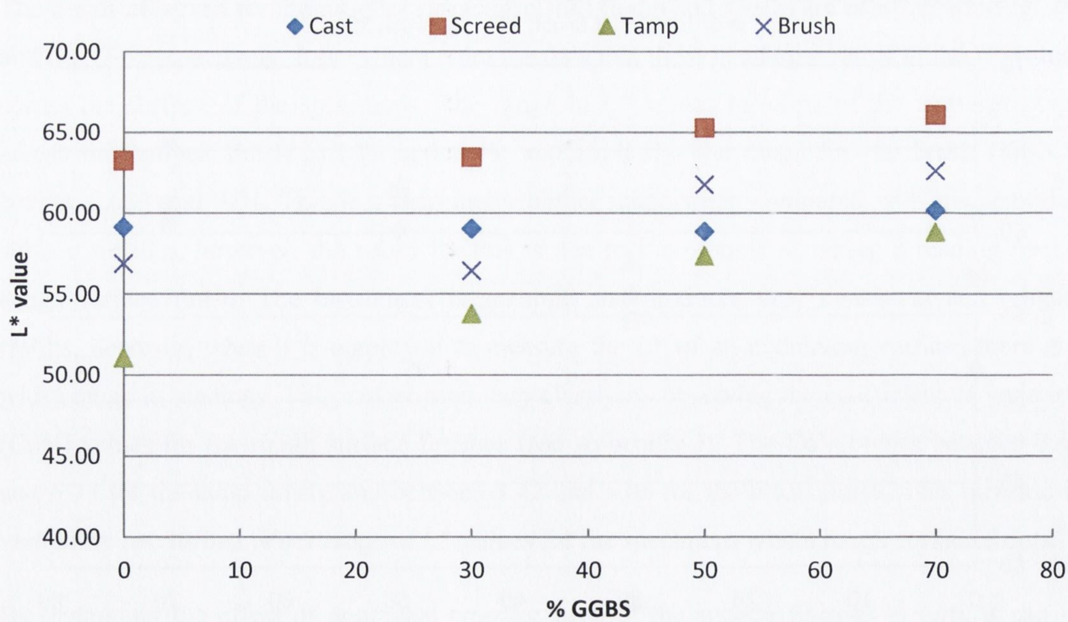

Fig. 7-7 The effect of GGBS concentration on L* value for specimens containing varying surface finishes

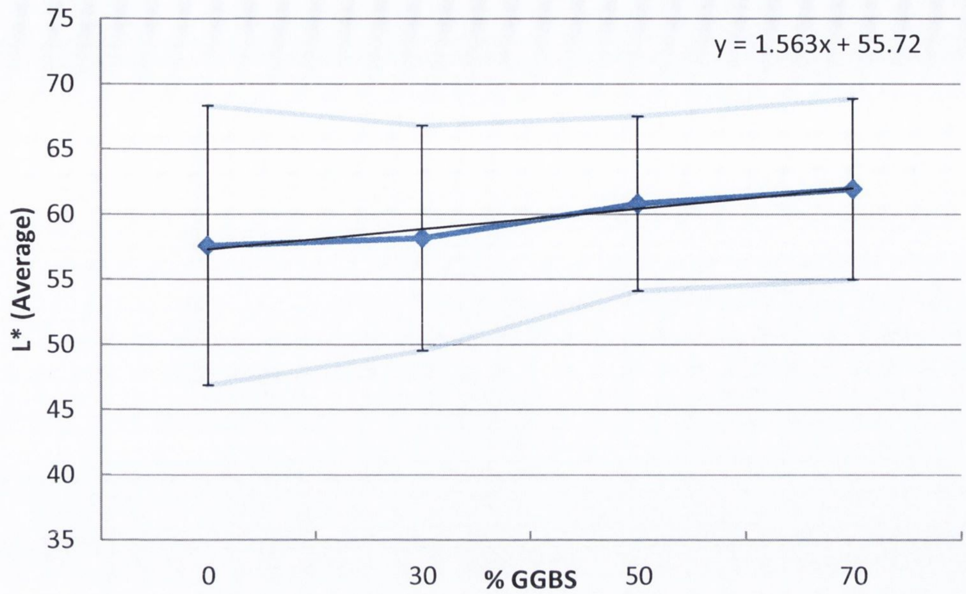

Fig. 7-8 Average L* value vs. % GGBS for concrete specimens with standard deviation at the 95% level (2xS.D)

7.2.3.3 The effect of surface finish on L value*

The data produced in Fig. 7-9 demonstrates the clear effect which surface finish has upon the L* value of concrete. As the points are closely positioned for the four GGBS concentrations, and there is significant difference between the four clusters, this would confirm that the surface finish is the prevailing factor over the effect of aggregate type and the effect of GGBS concentration. The order of decreasing L* value in terms of surface finish is screed, brush/tamp and cast. There is very little difference in the colour measured between the two rough surface finishes, which is due to dirt accumulation on the surface in addition to the larger variability incurred with taking a L* reading on a rough surface. It can also be observed that the 70% GGBS specimens have the highest L* reading in each case, which reconfirms the sensitivity of the instrument as it has the ability to differentiate between two seemingly identical surfaces.

The influence of both the percentage GGBS and surface finish on the L* of concrete are evident in Fig. 7-10 by means of a bar chart. The effect of GGBS is investigated by taking an average of each of the GGBS concentrations, for all of the surface finishes. Similarly, the effect of surface finish is established by obtaining an average for each, including for every GGBS concentration. This process conceals the true trends present, however, it gives an indication as to the overall effect of surface finish and GGBS content on the L* value. The aforementioned trend of GGBS (blue bar) is clearly demonstrated here having a linear relationship, with the increase of GGBS resulting in a marginal increase in L* value. Moreover, this chart allows the influence of the two parameters to be seen clearly. The surface finish type (red bar) has a stronger influence on

L* as there is a significant difference between the various surface finish type L* values. The order of decreasing L* value in terms of GGBS concentration and surface finish type is 70, 50, 30 and 0% GGBS, and screed, brush/cast and tamp respectively.

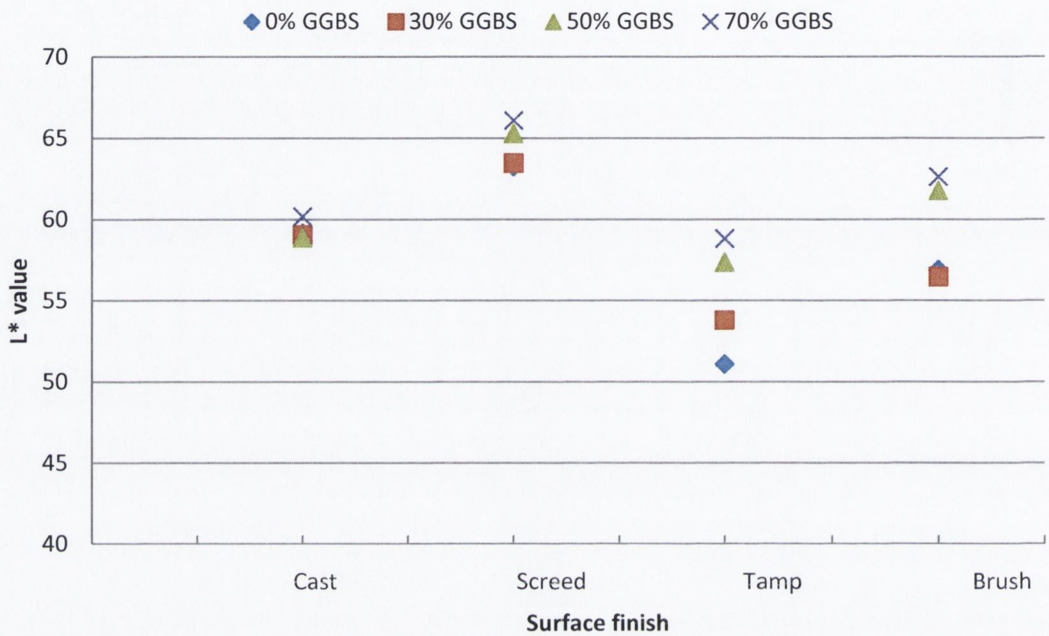

Fig. 7-9 The effect of surface finish on L* value for specimens containing 0 to 70% GGBS

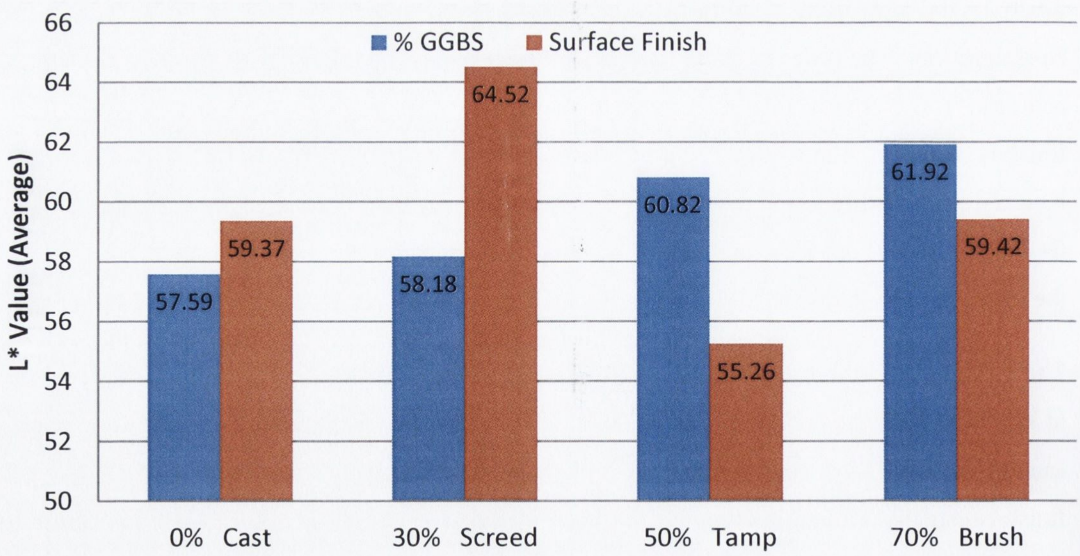

Fig. 7-10 Average L* value vs. % GGBS and surface finish type for concrete specimens

7.2.3.4 Testing 0 and 70% GGBS concrete surfaces (at Father Collins Park location)

The sphere spectrophotometer was used to measure the L* value of two aged concrete surfaces located at Father Collins Park containing 0 and 70% GGBS (see Section 5.2.4 for details of site location). A total of 5 readings were taken at random site locations across the test surfaces. The CoV in each case is acceptably low demonstrating the low variability of the readings. The variability due to differences in L* values between the 5 readings for a given location, is due to the surface having an exposed aggregate finish and not as a result of instrument error. The L* value is dependant on colour of the exposed aggregate, therefore, obtaining a wider range in L* values than normally expected.

The L* of the 0% surface ranges between approximately 53.0 and 58.9 (an average of 54.9), with the 70% surface having a higher L* range between approximately 59.0 and 63.4 (an average of 61.2). These L* results are very similar to the L* measured on the concrete specimens in Trinity College, with a 0% cast surface yielding a result of approximately 56-60 and a 70% cast surface yielding a result of between 60 and 62.

Table 7-10 Sphere spectrophotometer results recorded at Father Collins park for 0 and 70% GGBS concrete containing an exposed aggregate surface

Surface	Site	L*		
70%	1	60.08	μ	**61.18**
		62.50	σ	1.211
		59.73	CoV	1.98
		61.58		
		61.99		
	2	62.96	μ	**60.86**
		59.36	σ	1.686
		58.97	CoV	2.77
		61.09		
		61.90		
	3	59.23	μ	**61.50**
		59.80	σ	1.903
		61.94	CoV	3.09
		63.36		
		63.17		
0%	1	56.57	μ	**56.78**
		56.37	σ	1.264
		58.91	CoV	2.23
		56.54		
		55.52		
	2	53.04	μ	**52.92**
		54.57	σ	1.597
		50.33	CoV	3.02
		52.89		
		53.79		

7.2.4 Conclusions

- The sensitivity tests carried out on the sphere spectrophotometer demonstrate its high accuracy level. By testing the L* of a uniform white sheet of paper, a CoV of 0.1% is obtained which signifies that there is very little variability in a reading taken over a highly uniform surface in different locations across that surface.
- By using a clear plastic sheet on top of the cement powders to take a reading of L*, there was an overall reduction of approximately 1.3% in L*. Similarly, by using the clear plastic sheet on top of white paper, there is a minor reduction in the L* measured, but this result will not vary across the surface of the plastic sheet (CoV is 0.058%).
- The L* value of some typical cements displayed a range of values from 63.6 to 90.7. The CEM I and CEM II cements tested were in the order of 63.6 to 65.7. The L* of GGBS and white cement were of similar magnitude (88.20 and 90.72 respectively), with white cement having a higher L* than GGBS by approximately 2.8%. These results demonstrate an important and discernible trend.
- The L* of WPC, GGBS and CEM II A-L before blending occurs is 90.7, 87.9 and 64.8 respectively. By blending WPC with GGBS (in the ratios 70:30, 50:50 and 30:70) ranges between 87.9 and 89.6 result which is the highest range of L* in the cement blends.
- The cement blend of GGBS and CEM II A-L (in the ratios 70:30, 50:50 and 30:70) have a range of L* between 68.3 and 76.3. This range of L* is close to that of the cement blend between WPC and CEM II A-L which yields a range between 68.6 and 75.6.
- The L* of the concrete specimens confirmed that although there is a minor difference in L* between the three aggregate types (with SS having the lowest L* value), on a whole the aggregate type does not have a significant affect on the colour of the concrete, as there are very small ranges in L* across the three aggregate types.
- There is a general increase in L* with increased concentration of GGBS [0(57.59), 30(58.18), 50(60.82) and 70% (61.92)]. This influencing parameter, however, is much less significant when compared to that of the surface finish type.
- The order of decreasing L* in terms of the surface finish type is screed, brush/cast and tamp. The t-test result shows that the surface finish type has a definite influence on the L* of the specimens. The only exception, however, is that there is virtually no difference in colour between cast and brush. Therefore, it is possible to conclude that the surface finish is the key determinant.
- There is a significant increase from 0 to 70% GGBS concrete in terms of colour (approximately 11.5%), as measured at Father Collins Park. The L* value of 0% and 70% GGBS are similar to the L* of the cast 0% and cast 70% concrete specimens in Trinity College, with the age of both samples being approximately the same (2.5 years).

7.3 Lux Meter Results

7.3.1 Introduction

A number of sets of lux meter results were recorded over the duration of this project using the designed apparatus as outlined in Section 5.3. Apart from calibration and sensitivity testing, a full set of results on all 96 specimens were taken in March 2011, July 2011 and March 2012, 12 months following the first set of readings. There were three readings taken on each specimen in quick succession so as to assess any variability of the individual instantaneous readings. A summary of the results is presented in this section and the full set of lux meter readings can be found in Appendix K, Appendix L and Appendix M. The level of GGBS is indicated along with aggregate type along the left hand side of the table, where L denotes limestone, PCL is partially crushed limestone and SS refers to sandstone. The surface finish is indicated at the top of each column, along with a column indicating the coefficient of variance (CoV) for each set of data. The mean and standard deviation values are also displayed. Each entry has 6 readings as there are two identical slabs, each of which have had three readings taken.

There are a number of parameters which influence the reflectance of light which will be considered individually as follows;

1. Duplicate specimens
2. The effect of aggregate type
3. The effect of GGBS concentration
4. The effect of surface finish type
5. Ageing

7.3.2 Analysis of lux meter results

7.3.2.1 Duplicate specimens

As discussed previously in Chapter 3, there were a total of 96 concrete specimens manufactured for the purposes of testing, however, as there was a duplicate of each testing parameter included, there were 48 unique specimens. Therefore, before conducting an analysis on the lux meter readings (percentage reflected lux ratio) to determine the influence of key properties on lux reflectance, a t-test was carried out between the "identical" slabs with the objective of determining whether these duplicate specimens were producing different amounts of reflected lux.

The number of DF for this t-test is low as it is a comparison between two sets of readings in a pair, with each set containing three readings (where DF= [3*2]-1= 5). Three results from each slab were recorded to eliminate any gross errors but as there are a large number of concrete slabs, these readings were not always taken on the same day. However, unlike readings of albedo, the lux meter test can be carried out on any day at any time, with broadly the same percentage of reflectance obtained, with the readings taken only where there is consistent sunshine (no cloud cover). The reader is referred to Section 5.3.3 for a discussion on a sensitivity test on lux meter readings taken on different days.

The full data set for this particular test can be found in Appendix N, Appendix O and Appendix P and a sample of these results is displayed in Table 7-11. The four surface finishes are shown at the top of the table, with the three aggregate types in rows, as indicated along the left side of the table. These results are for 0% GGBS and are based on data recorded in March 2011.

Table 7-11 Sample of duplicate t-test March 2011 – 0% GGBS

DF=5
>2.015
<2.015

GGBS	0%	Cast	Screed	Tamp	Brush
L	μ_{a3}	4.81	8.25	6.78	5.20
	σ_{a3}	0.05	0.07	0.06	0.25
(a)	μ_{a3}	4.65	8.21	6.91	5.18
	σ_{a3}	0.04	0.08	0.03	0.22
	t(aa)	4.58	0.66	3.41	0.12
PCL	μ_{b3}	4.60	7.92	6.24	5.59
	σ_{b3}	0.35	0.28	0.37	0.08
(b)	μ_{b3}	5.11	8.25	6.14	5.45
	σ_{b3}	0.10	0.05	0.04	0.17
	t(bb)	2.44	2.02	0.48	1.31
SS	μ_{c3}	4.88	8.11	5.82	5.12
	σ_{c3}	0.01	0.08	0.15	0.24
(c)	μ_{c3}	4.91	7.53	5.46	4.38
	σ_{c3}	0.05	0.09	0.44	0.06
	t(cc)	1.09	8.27	1.37	5.28

The mean (μ_3) and standard deviation (σ_3) values are given for each data set containing three values. Accordingly, each aggregate type has been given a label of a, b and c which have been included in the subscript for comparison purposes. These values are then used to carry out the t-test, to determine whether the two data sets are statistically the same or otherwise. For example, t(aa) denotes the t-statistic from a t-test carried out between the two limestone aggregate slabs i.e. the duplicate specimens each containing limestone aggregate, for a given surface finish. The critical P value for the significance level (α=0.05) is shown at the top right-hand corner of Table 7-11, for DF=5. The calculated t-value is highlighted accordingly, indicating whether the value is greater (red) or less (green) than the t-value statistic. For example, the t-test for a cast surface finish containing limestone aggregate and 0% GGBS yielded a result of 4.58 suggesting the two duplicate specimens are statistically different, however, this contrasts with the screed surface finish for the same aggregate type and GGBS content, having a result of 0.66 suggesting there is no difference between the duplicate specimens. It should be noted that the value of the standard deviation for each of the data sets is very low which greatly impacts the resulting t-test statistic. This indicates there is small variability in the test process rather than variability in the specimens, therefore, based on the variability of the test, there appears to be a difference between the two duplicate specimens.

In conclusion, this test would indicate that there is statistically a difference between the duplicate specimens based on the lux meter test method, however, this can be attributed to the very low values of standard deviation (σ). Moreover, the difference between the individual specimens is small in comparison to the differences between GGBS content and surface finish, therefore, the data are sufficiently close to about half, enabling one to combine the data for the duplicate specimens and compute an average. The succeeding sections will use the duplicate average when analysing the results.

7.3.2.2 The effect of aggregate type

The 6 boards on which the specimens were placed, each containing 16 slabs, were divided according to aggregate type and as a consequence, there were two identical boards for each aggregate type (see Fig. 3-11 for layout of the boards). These identical boards were randomly placed on the roof of the Civil Engineering building in Trinity College. A t-test was conducted on the visible light reflectance results to compare and contrast the three aggregate types. A sample of these results can be viewed in Table 7-12 for 0% GGBS and Table 7-13 for 70% GGBS and the full set of t-test results can be found in Appendix Q, Appendix R and Appendix S. The results of the two duplicate specimens have been collated and an average obtained. As each slab has three readings and there is a duplicate of each slab, the DF is 11 for this t-test (DF= [6*2]-1= 11). The mean and standard deviation are denoted by μ_6 and σ_6 and are displayed in Table 7-12 and Table 7-13.

A t-test is carried out between each of the aggregate types within the same level of GGBS, and for a given surface finish. For example, the t-test result is given by t(L,PCL), denotes a t-test conducted between the data set obtained for the specimens containing limestone and the specimens containing partially crushed limestone (for a given surface finish and GGBS concentration) in order to determine whether the light reflectance data for limestone and partially crushed limestone specimens are different. The calculated t-value is then highlighted accordingly, indicating whether the value is greater (blue) or less (yellow) than the t-value statistic. The result for the cast finish specimens for t(L, PCL) in Table 7-12 is 0.82 (highlighted yellow), which would suggest that there is statistically no difference in the data between these two specimens containing different aggregate types. However, for the most part, the results are significant (highlighted in blue) which suggests that the aggregate type does in fact make a difference. The standard deviation value is low for each of the individual data sets (due to the accuracy of the test methods and closeness of the duplicates) and this affects the resulting t-test value quite significantly despite the individual results being close to one another.

Table 7-12 Sample Aggregate t-test March 2011 – 0% GGBS

DF=11
>1.796
<1.796

GGBS	0%	Cast	Screed	Tamp	Brush
L	μ_6	4.73	8.23	6.84	5.19
	σ_6	0.10	0.07	0.08	0.21
	t(L,PCL)	0.82	1.35	6.23	3.15
PCL	μ_6	4.85	8.09	6.19	5.52
	σ_6	0.36	0.26	0.24	0.14
	t(PCL,SS)	0.31	1.58	3.11	4.13
SS	μ_6	4.90	7.82	5.64	4.75
	σ_6	0.03	0.33	0.36	0.43
	t(SS,L)	4.14	3.03	8.05	2.25

Table 7-13 Sample Aggregate t-test March 2011 – 70% GGBS

DF=11
>1.796
<1.796

GGBS	70%	Cast	Screed	Tamp	Brush
L	μ_6	5.91	8.84	6.26	6.43
	σ_6	0.22	0.48	1.08	0.44
	t(L,PCL)	0.93	1.87	0.62	0.99
PCL	μ_6	6.05	7.92	5.94	6.25
	σ_6	0.28	1.10	0.61	0.06
	t(PCL,SS)	0.66	0.66	3.81	19.99
SS	μ_6	5.97	8.22	7.05	5.29
	σ_6	0.07	0.18	0.37	0.10
	t(SS,L)	0.61	2.93	1.70	6.21

Similarly for 70% GGBS, the aggregate type t-test demonstrated that there were a number of results which were statistically significant. However, when one observes the individual readings and the very low values of standard deviation, it is possible to conclude that there is virtually no difference between the lux readings for the differing aggregate type specimens. The results for 30 and 50% GGBS show broadly similar results in Appendix Q. The t-test conducted on the aggregate types shows that this parameter is statistically significant, however, the individual differences are small. Therefore, the data is sufficiently close to enable one to combine them and compute an average of the three aggregate type results.

The effect of aggregate type on light reflectance can also be viewed in Fig. 7-11 for a cast (smooth) surface finish and in Fig. 7-12 for a brush (rough) surface finish. These plots display both 0 and 70% GGBS with each of the aggregate types plotted individually. The results for 0% are in a cluster and are circled with a black line, and the 70% GGBS results are presented in the same manner with a dashed black line.

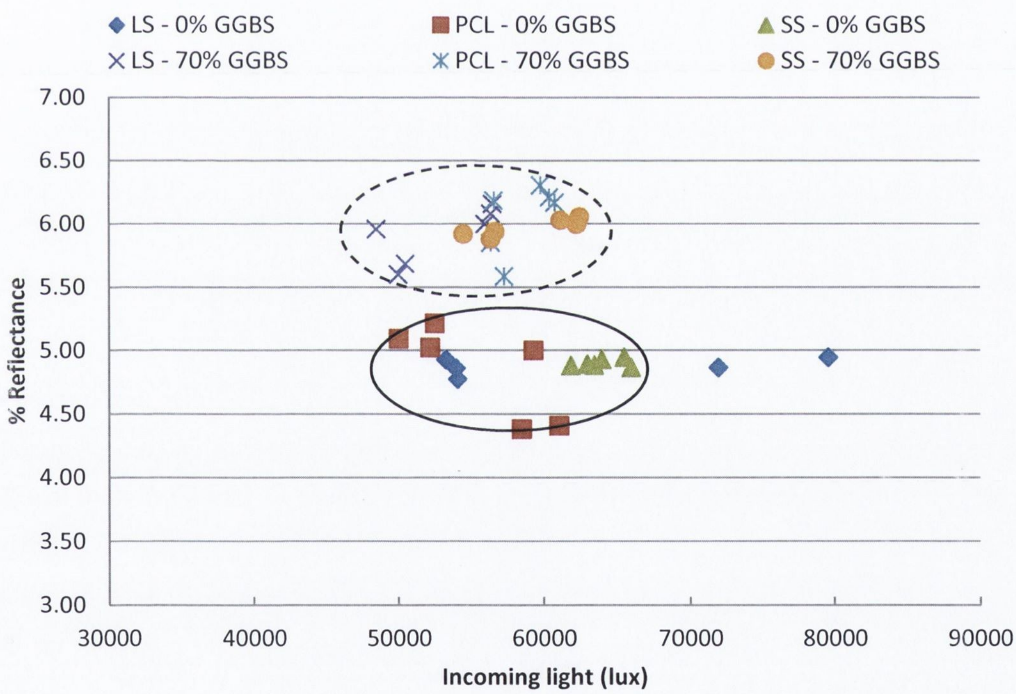

Fig. 7-11 The effect of aggregate type on light reflectance for a cast surface finish containing 0 and 70% GGBS

The typical rough and smooth surface graphs would strongly suggest that as the data points are closely grouped together and span in the horizontal direction as opposed to the vertical direction, therefore, the aggregate type does not have a significant influence on the lux reflectance despite the t-test results showing otherwise. This trend reconfirms the process of combining the three aggregate type results together to compute an average result. The plots for screed and tamp surface finishes can be found in Appendix T which display broadly similar results.

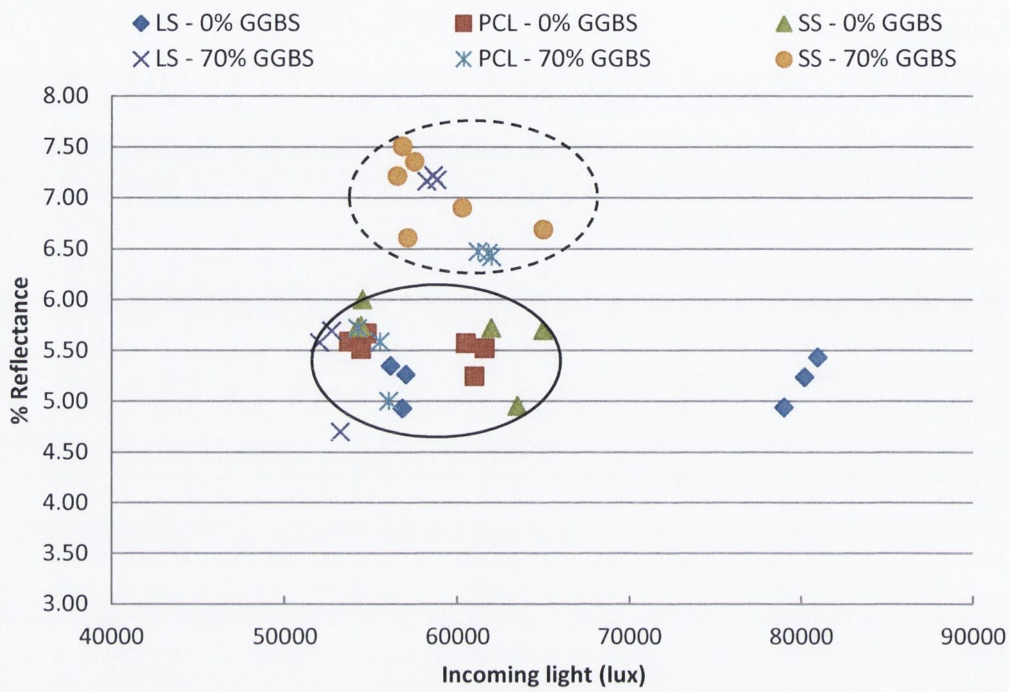

Fig. 7-12 The effect of aggregate type on light reflectance for a brush surface finish containing 0 and 70% GGBS

7.3.2.3 The effect of GGBS concentration

The effect of GGBS concentration on the amount of light reflected off a concrete specimen is clearly evident in Fig. 7-13. The plot displays results for a cast surface finish and the aggregate types have been included in each of the data points. There is a clear progression from 0 to 70% GGBS with minor overlapping evident for the individual GGBS concentrations. It is evident from the plot that there is overlapping occurring in particular for 50 and 70% GGBS results. Some of the variability evident is due to including all of the aggregate types together, yet the trends are discernable.

A t-test was conducted on these results to determine whether there was statistically any difference in lux reflectance between each of the GGBS concentrations, with the number of parameters considered being 18, as there are three readings, with 2 duplicate slabs and including 3 aggregate types (3 x 2 x 3=18). This is denoted by the subscript of μ_{18} and σ_{18} in Table 7-14. The top of the columns denote the GGBS concentration and the DF is 35 [(18+18) -1], with the t-statistic shown as before. The t-test t(0,30) for example, demonstrates the test is conducted between 0 and 30% GGBS, and if the result is greater than the t-statistic obtained from the percentiles of the t-distribution table, it is highlighted in blue (otherwise it is highlighted in yellow). As evident from Table 7-14, each t-test result is highlighted in blue, which confirms the significant difference in the lux reflectance between each of the concentrations of GGBS. The order of decreasing reflectance in terms of GGBS concentration is as follows; 70, 50, 30 and 0% GGBS, as would be expected.

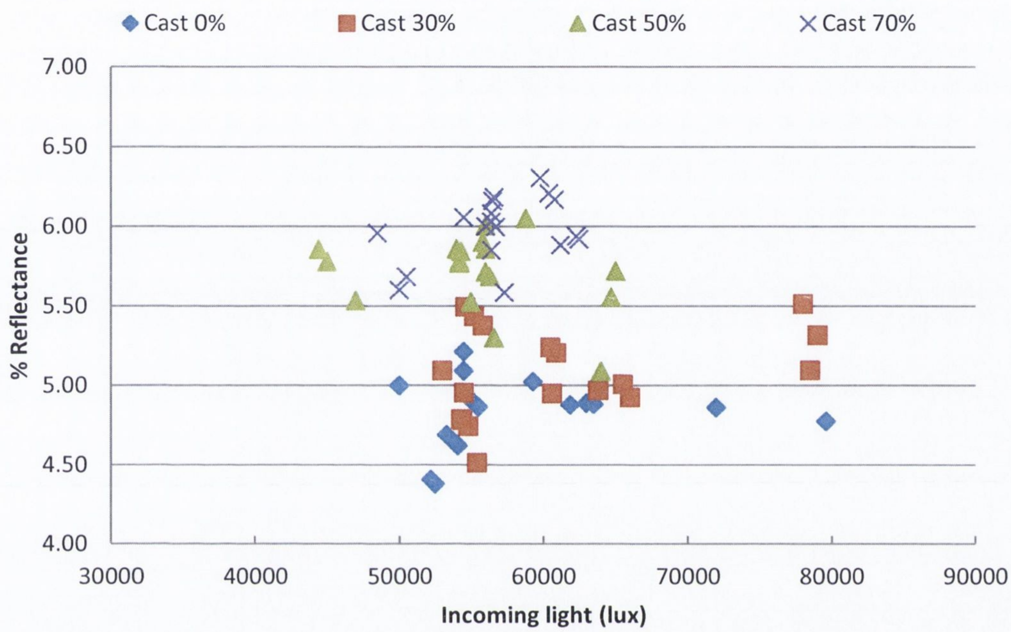

Fig. 7-13 The effect of GGBS content on light reflectance for a cast surface finish (including all aggregate types) – March 2011

Table 7-14 T-test on cast surface finish for March 2011 (all aggregates included)

DF=35
>1.6905
<1.6905

	0%		30%		50%		70%
$\mu_{0,18}$	4.83	$\mu_{30,18}$	5.08	$\mu_{50,18}$	5.71	$\mu_{70,18}$	5.98
$\sigma_{0,18}$	0.224	$\sigma_{30,18}$	0.2823	$\sigma_{50,18}$	0.2395	$\sigma_{70,18}$	0.2038
t(0,30)	2.942	t(30,50)	7.22	t(50,70)	3.643		
t(0,50)	11.38	t(30,70)	10.967				
t(0,70)	16.103						

As mentioned previously, there is variability of the results evident in Fig. 7-13 which is due partly to the aggregate type. Therefore, one may consider the data for only one aggregate type, only to see if the trends are clearer. To observe the effect of GGBS on light reflectance for the cast surface finish, only one type of aggregate is considered (LS) and this plot is displayed in Fig. 7-14. The chart demonstrates a very clear progression from 0 to 70% GGBS as before, however, there is some overlapping between 50 and 70% GGBS specimens. Furthermore, a t-test was conducted on this data and the results are displayed in Table 7-15. The number of parameters has now been reduced from 18 to 6 (as there are 3 aggregate types), and this in turn reduces the DF from 35 to 11. It is evident from the t-test results that one result is highlighted yellow, indicating that the result lies below the t-test statistic. This signifies that there is virtually no difference between the results for 50 and 70% GGBS, which was previously noted from the scatter plot.

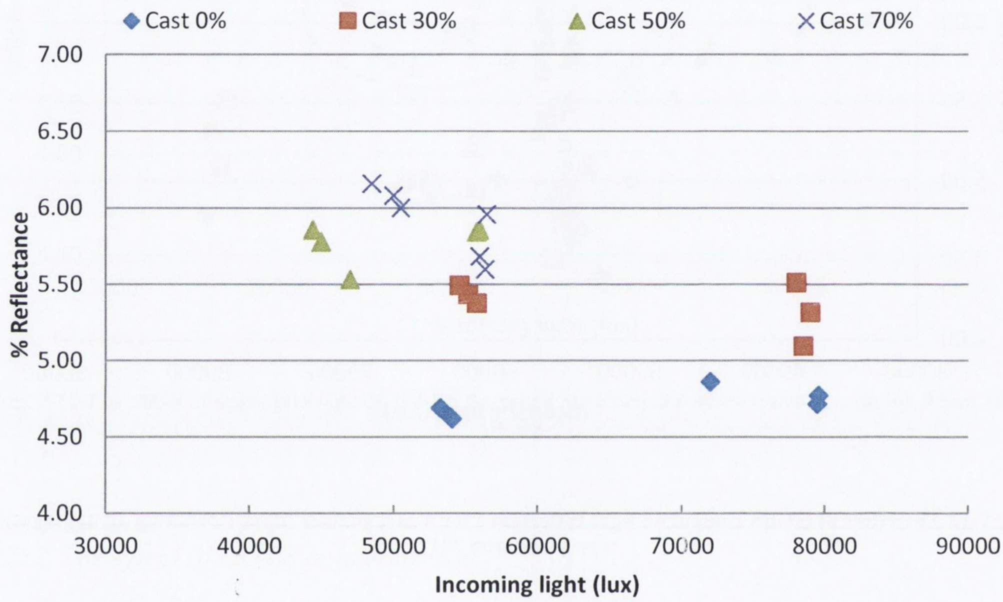

Fig. 7-14 The effect of GGBS content on light reflectance for a cast surface finish (only one aggregate type-LS) – March 2011

Table 7-15 T-test on cast surface finish for March 2011 (one aggregate type included-LS)

DF=11
>1.796
<1.796

	0%		30%		50%		70%
$\mu_{0,6}$	4.72	$\mu_{30,6}$	5.37	$\mu_{50,6}$	5.79	$\mu_{70,6}$	5.91
$\sigma_{0,6}$	0.0911	$\sigma_{30,6}$	0.1538	$\sigma_{50,6}$	0.1287	$\sigma_{70,6}$	0.2234
t(0,30)	8.901	t(30,50)	5.13	t(50,70)	1.14		
t(0,50)	16.62	t(30,70)	4.877				
t(0,70)	12.082						

In conclusion, the GGBS concentration has a significant influence in terms of the resulting lux reflectance, however, by eliminating the effect of aggregate type and focusing on one aggregate in particular, the conclusions on GGBS influence are virtually the same. Therefore, when observing the trends in lux meter results, it is appropriate to combine all three aggregate type results within one scatter plot and t-test, but not the GGBS data.

A scatter plot for the brush surface finish is displayed in Fig. 7-15 and this includes all aggregate type results. Again, there is a progression from 0 to 70% GGBS, however, there is overlapping of some of the results. For the brush finish specimen, where the surface effect would be more important due to the increased dispersion of light, the boundaries between 0 to 70% GGBS are less clear. There is a clear difference between 0 and 70% GGBS but the differences between the adjacent GGBS concentrations (0-30, 30-50 and 50-70%) are smaller. This is as a consequence of having a rougher surface finish.

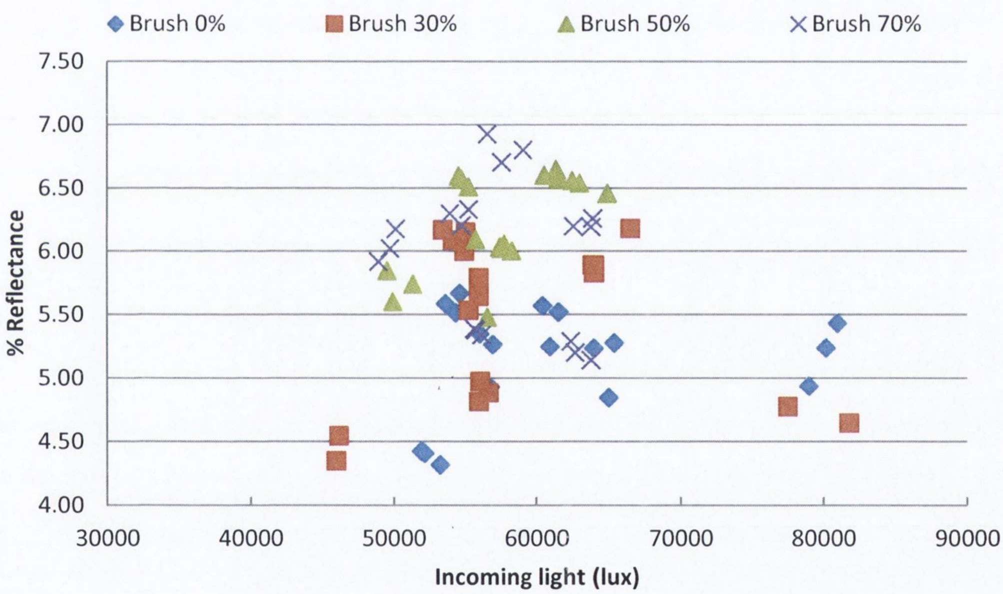

Fig. 7-15 The effect of GGBS content on light reflectance for a brush surface finish (including all aggregate types) – March 2011

The corresponding t-test results for the brush surface finish are presented in Table 7-16. It is evident from the t-test results that one result is highlighted yellow, which indicates that the result lies below the t-test statistic. This implies that there is no statistical difference between the average results for 50 and 70% GGBS. This outcome is confirmed by the scatter plot (Fig. 7-15) as it can be observed that the 50 and 70% specimens have approximately the same percentage light reflectance. The results for screed and tamp can be viewed in Appendix U, and these finishes broadly indicate the same trends. The reader is also referred to Appendix V and Appendix W for the results recorded in July 2011 and March 2012 respectively, which are discussed separately under the ageing section.

Table 7-16 T-test on brush surface finish for March 2011 (all aggregate types included)

DF=35
>1.6905
<1.6905

	0%		30%		50%		70%
$\mu_{0,18}$	5.15	$\mu_{30,18}$	5.49	$\mu_{50,18}$	6.22	$\mu_{70,18}$	5.99
$\sigma_{0,18}$	0.420	$\sigma_{30,18}$	0.651	$\sigma_{50,18}$	0.3865	$\sigma_{70,18}$	0.5687
t(0,30)	1.863	t(30,50)	4.092	t(50,70)	1.419		
t(0,50)	7.953	t(30,70)	2.455				
t(0,70)	5.041						

In conclusion, the effect of GGBS concentration on light reflectance is significant with differences evident from 0 to 70% GGBS, in particular for the cast surface finish. However, when the brush surface finish was considered, the differences between adjacent concentrations of GGBS (such as 0 and 30%, 30 and 50% and 50 and 70% GGBS) are less pronounced. This is due to greater dispersion of light from the brush surface finish.

7.3.2.4 The effect of surface finish

The influence of surface finish on the amount of light reflected from the specimens is presented for both 0 and 70% GGBS in Fig. 7-16 and Fig. 7-17 respectively. The results were recorded in March 2011 and the reader is referred to Appendix X , Appendix Y and Appendix Z for a full set of results, including the results for 30 and 50% GGBS which display broadly similar trends.

The data points in Fig. 7-16 illustrate that there is a clear distinction between light reflectance values for the four surface finishes, with a screed finish having the highest percentage of visible light reflectance. The tamp surface finish is the second most reflective surface, followed by a brush finish and then a cast finish. The brush and cast finish appear to overlap somewhat, having similar light reflectance results. Although there is no GGBS present in these samples, the type of surface finish has a strong influence on the percentage of reflected light.

A t-test was conducted on these results to determine whether there was statistically any difference in light reflectance between each of the surface finish types, with the number of parameters considered being 18 as before. The results from this test are displayed in Table 7-17. The top of the columns denote the surface finish type and the DF is 35 [(18+18) -1], with the t-statistic shown as before. The t-test t(c,s) for example, demonstrates the test is conducted between cast and screed, and if the result is greater than the t-statistic obtained from the percentiles of the t-distribution table, it is highlighted in blue (otherwise it is highlighted in yellow). As evident from the data, each t-test result is highlighted in blue, which confirms the significant difference in the lux reflectance between each of the surface finish types, which is also clearly evident from Fig. 7-16. The order of decreasing reflectance in terms of surface finish type is as follows; screed, tamp, brush and cast. It is interesting to note that the two smooth surface finishes (cast and screed) are very different in terms of the amount of light which they reflect. This is due to the colour of these specimens, as cast is visibly the darkest colour and screed the brightest, which was confirmed using the sphere spectrophotometer.

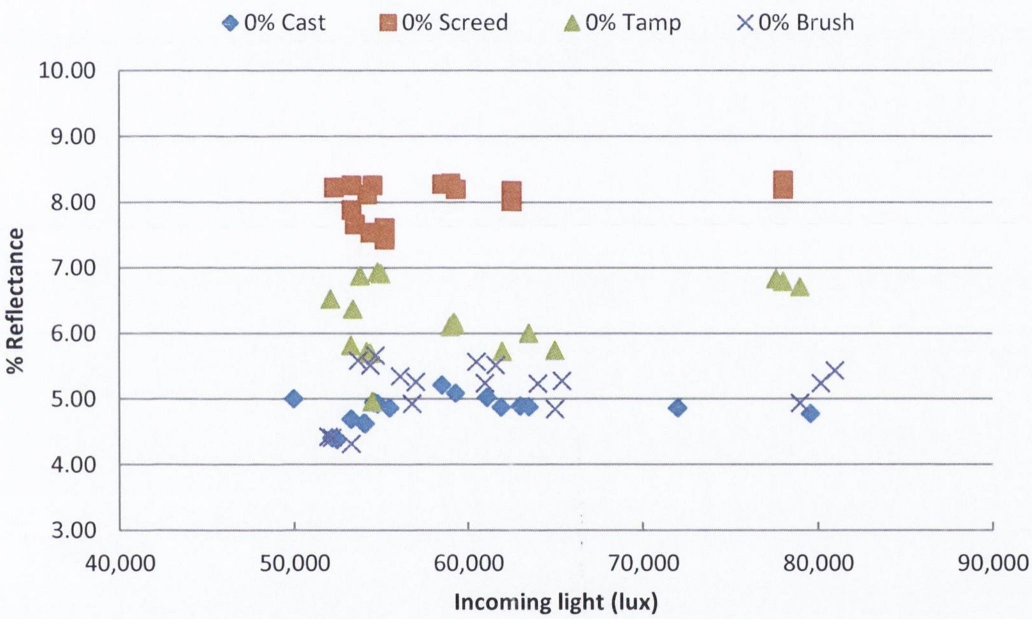

Fig. 7-16 The effect of surface finish type on light reflectance for 0% GGBS (including all aggregate types) – March 2011

Table 7-17 T-test on 0% GGBS specimens for March 2011 (all aggregates included)

DF=35
>1.6905
<1.6905

	Cast		Screed		Tamp		Brush
$\mu_{c,18}$	4.83	$\mu_{s,18}$	8.03	$\mu_{t,18}$	6.22	$\mu_{b,18}$	5.15
$\sigma_{c,18}$	0.224	$\sigma_{s,18}$	0.2952	$\sigma_{t,18}$	0.5589	$\sigma_{b,18}$	0.4429
t(cs)	36.63	t(st)	13.43	t(tb)	6.37		
t(ct)	9.79	t(sb)	24.47				
t(cb)	2.74						

The data presented in Fig. 7-17 represents 70% GGBS specimens containing the four different surface finishes. There is again a clear distinction evident, with screed observing the highest light reflectance as expected. The two least reflective surface finishes are cast and brush, and these have overlapping results. The effect of the smoothness is dominated by the darker colour. A corresponding t-test was produced as before to quantify the differences in light reflectance between the various finish types, and the data is displayed in Table 7-18. The results demonstrate that each of the surface finish types are significantly different from one another, apart from cast and brush (highlighted in yellow). This observation was also noted for the 0% GGBS specimens (see Fig. 7-16).

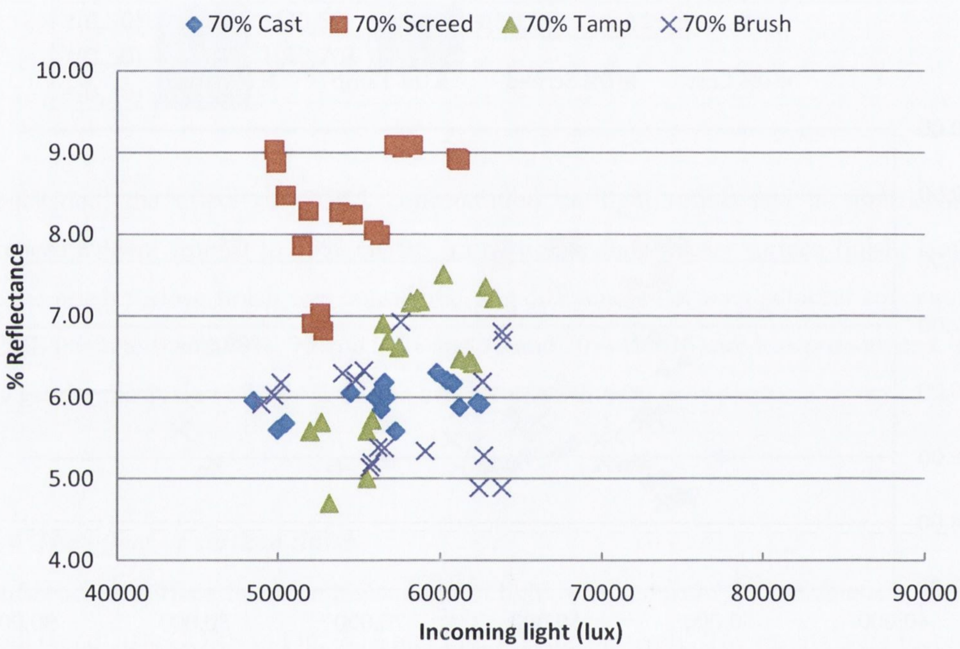

Fig. 7-17 The effect of surface finish type on light reflectance for 70% GGBS (including all aggregate types) – March 2011

Table 7-18 T-test on 70% GGBS specimens for March 2011 (all aggregates included)

DF=35
>1.6905
<1.6905

Cast		Screed		Tamp		Brush	
$\mu_{c,18}$	5.98	$\mu_{s,18}$	8.33	$\mu_{t,18}$	6.41	$\mu_{b,18}$	5.99
$\sigma_{c,18}$	0.204	$\sigma_{s,18}$	0.7656	$\sigma_{t,18}$	0.8472	$\sigma_{b,18}$	0.5687
t(cs)	12.58	t(st)	7.134	t(tb)	1.746		
t(ct)	2.094	t(sb)	10.41				
t(cb)	0.07						

In conclusion, the effect of surface finish type on visible light reflectance is significant, with differences evident between each of the surface finish types, apart from cast and brush which overlap somewhat. Although both parameters are important, the effect of surface finish would appear to have a greater influence on the amount of light reflected when compared to the effect of GGBS concentration, as the differences between the different finish types is greater.

7.3.2.5 The effect of ageing

In March 2012, one year after the first set of readings were recorded, almost every t-test result was above the t-test statistic which is evident by the sample set of results for 0% GGBS displayed in Table 7-19. The reader is referred to Appendix P for a complete set of results. The calculated t-value is highlighted in the table to indicate whether the value is greater (red) or less (green) than the t-value statistic as before.

Table 7-19 Sample of duplicate t-test March 2012 – 0% GGBS

DF=5
>2.015
<2.015

GGBS	0%	Cast	Screed	Tamp	Brush
L	μ_{a3}	5.27	7.60	6.12	6.37
	σ_{a3}	0.03	0.04	0.02	0.03
(a)	μ_{a3}	5.34	8.05	7.46	6.55
	σ_{a3}	0.02	0.02	0.02	0.01
	t(aa)	4.16	20.65	89.44	11.63
PCL	μ_{b3}	5.25	7.47	6.83	6.64
	σ_{b3}	0.02	0.03	0.01	0.02
(b)	μ_{b3}	5.38	7.65	6.44	6.43
	σ_{b3}	0.03	0.01	0.03	0.03
	t(bb)	5.43	9.88	24.73	12.36
SS	μ_{c3}	5.18	6.96	5.64	5.62
	σ_{c3}	0.02	0.02	0.02	0.01
(c)	μ_{c3}	5.23	6.93	5.68	5.32
	σ_{c3}	0.03	0.05	0.01	0.02
	t(cc)	2.65	0.72	3.10	25.24

This change in results when compared with the initial readings recorded in March 2011 (see Table 7-11) would suggest that with time, the slab duplicates are wearing at different rates, therefore, they are giving statistically different results of visible light reflectance. This may also be due to the location of the two slabs being compared as the duplicate slabs are never beside one another on the roof. It was observed visually that the duplicate slabs are not the same, in particular for the rough surface finishes more so than the smooth surface finishes. A possible reason for this result is that the slab surfaces were finished by hand, and that no two rough surface finishes are physically identical. In conclusion, the duplicate specimens are moving away from one another in terms of the amount of light reflected off the surface. This is due to the surface of each of the specimens ageing at different rates. However, it should be noted that the standard deviation is low for the data set, which reduces the possibility of the t-value being less than the t-statistic.

Similarly, a sample of the aggregate t-test conducted on the results for March 2012 is displayed in Table 7-20, with the complete data set displayed in Appendix S. The calculated t-value is highlighted, indicating whether the value is greater (blue) or less (yellow) than the t-value statistic as before. The majority of the results are significant (highlighted in blue) which suggests that the aggregate type does make a difference after the specimens have been exposed to the environment. This table may be compared with results from one year previous (Table 7-12). The standard deviation value is low for each of the individual data sets and this affects the resulting t-test value quite significantly despite the individual results being close to one another. The t-test conducted on the aggregate types shows that this parameter becomes more significant with time.

In conclusion, as the aggregate type has an influence on the amount of light reflected after the specimens were exposed to the environment, the subsequent discussion on the influence of ageing with respect to the GGBS concentration and surface finish type will focus on one aggregate type so as not to hide the true trends.

Table 7-20 Sample aggregate t-test March 2012 – 0% GGBS

DF=11
>1.796
<1.796

GGBS	0%	Cast	Screed	Tamp	Brush
L	μ_6	5.30	7.83	6.79	6.46
	σ_6	0.04	0.25	0.73	0.10
	t(L,PCL)	0.38	2.38	0.50	1.16
PCL	μ_6	5.32	7.56	6.63	6.53
	σ_6	0.07	0.10	0.21	0.12
	t(PCL,SS)	3.45	13.83	11.14	12.77
SS	μ_6	5.20	6.95	5.66	5.47
	σ_6	0.03	0.04	0.03	0.17
	t(SS,L)	4.46	8.48	3.79	12.58

The influence of age on specimens containing different GGBS concentrations will be discussed for a smooth surface finish (cast) and a contrasting rough surface finish (brush). The reader is referred to Appendix AA for the supplementary results for screed and tamp which demonstrate broadly similar results. One aggregate type was utilised in order to clearly view the trends (LS aggregate). There were three sets of data recorded over the course of the project (March 2011, July 2011 and March 2012) and these are included to demonstrate the effect of ageing on light reflectance for 0 and 70% GGBS.

The results for a cast surface finish are displayed in Fig. 7-18 with the corresponding t-test results shown in Table 7-21. The individual 0-70% data sets are labelled 1, 2 and 3 in the plot and correspond to March 2011, July 2011 and March 2012 respectively. It is evident from the plot that if one observes the difference in light reflectance between 0 and 70% GGBS for each of the data sets, that the difference in light reflectance decreases with time. The final set of readings recorded, in particular, display only a small difference in light reflectance between 0 and 70% GGBS. This would suggest that the results are converging with time due to ageing of the specimens.

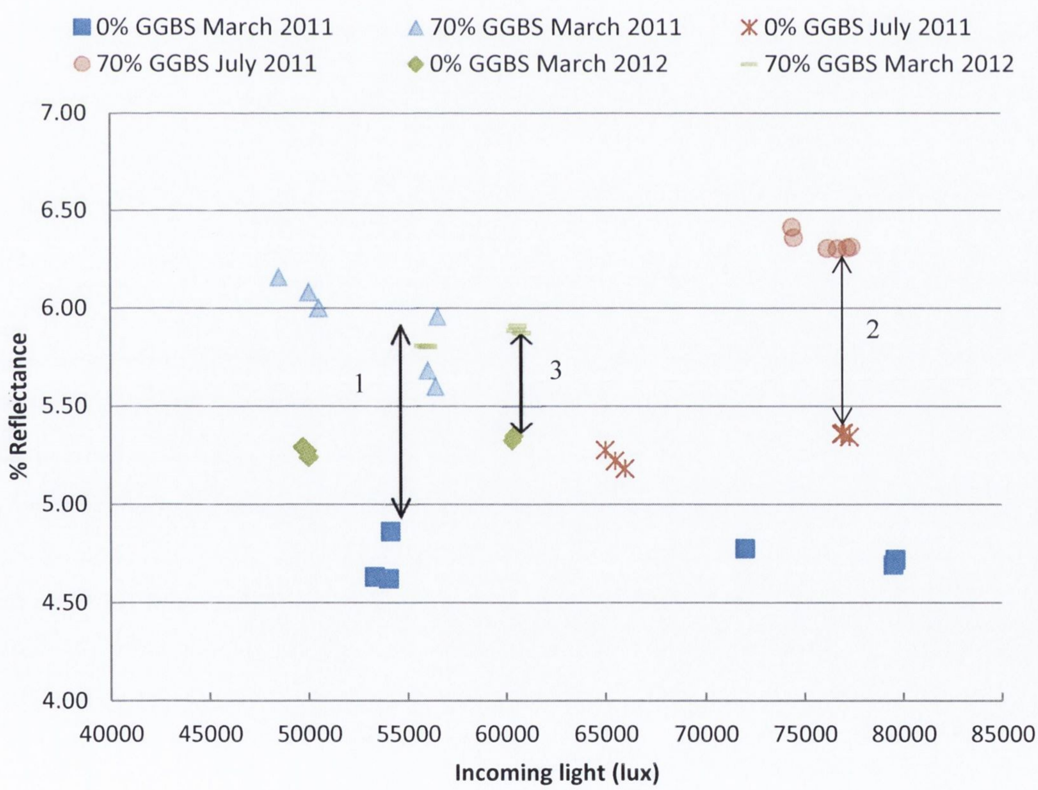

Fig. 7-18 Ageing of 0 and 70% GGBS cast finish slabs between March 2011, July 2011 and March 2012 for LS aggregate only

This outcome is confirmed by the t-test conducted on the individual results between all GGBS concentrations, as before. The majority of the results are highlighted blue suggesting that there is a difference in light reflectance between the GGBS concentrations, however, the result highlighted yellow suggests that there is little or no difference between 30 and 70% GGBS. If one observes the average reading for 30% (5.90) and 70% (5.85) it confirms the result that the 70% GGBS specimens have reduced in light reflectance to that of 30% GGBS. This differs to the initial results from March 2011 (see Table 7-15) whereby the 70% specimens obtained the highest reflectance. This would suggest that the 70% specimens in particular have aged and consequently have a lower percentage of reflected light.

Table 7-21 T-test on cast surface finish for March 2012 to demonstrate ageing (one aggregate type included-LS)

DF=11
>1.796
<1.796

	0%		30%		50%		70%
$\mu_{0,6}$	5.30	$\mu_{30,6}$	5.90	$\mu_{50,6}$	6.14	$\mu_{70,6}$	5.85
$\sigma_{0,6}$	0.04	$\sigma_{30,6}$	0.23	$\sigma_{50,6}$	0.02	$\sigma_{70,6}$	0.05
t(0,30)	6.295	t(30,50)	2.55	t(50,70)	13.2		
t(0,50)	46.01	t(30,70)	0.52				
t(0,70)	21.04						

Similarly, the results for a brush surface finish are displayed in Fig. 7-19 with the corresponding t-test results shown in Table 7-22. The influence of age on the effect of GGBS concentration can be viewed in the scatter plot as the differences between 0 and 70% GGBS decreases with time for the three data sets. The initial readings indicate a significant difference in light reflectance, however, this difference decreases substantially for the final set of results recorded. The t-test results account for the four GGBS concentrations and it may also be observed that the order of increasing light reflectance has changed since the first set of readings recorded in March 2011 (see Table 7-16). The nature of the surface finish contributes significantly to this change due to the dispersion of light off the surface. Although the overall order of GGBS concentration has changed, the difference between specimens containing 0 and 70% GGBS remains evident.

In conclusion, the influence of ageing on the amount of light reflected from a specimen is evident despite there being only one year between the initial and final readings. The specimens containing 70% in particular, appear to decrease in light reflectance at a faster rate. However, irrespective of the surface finish and the incoming light, the concrete slabs have aged and this results in deterioration in the corresponding light reflectance result.

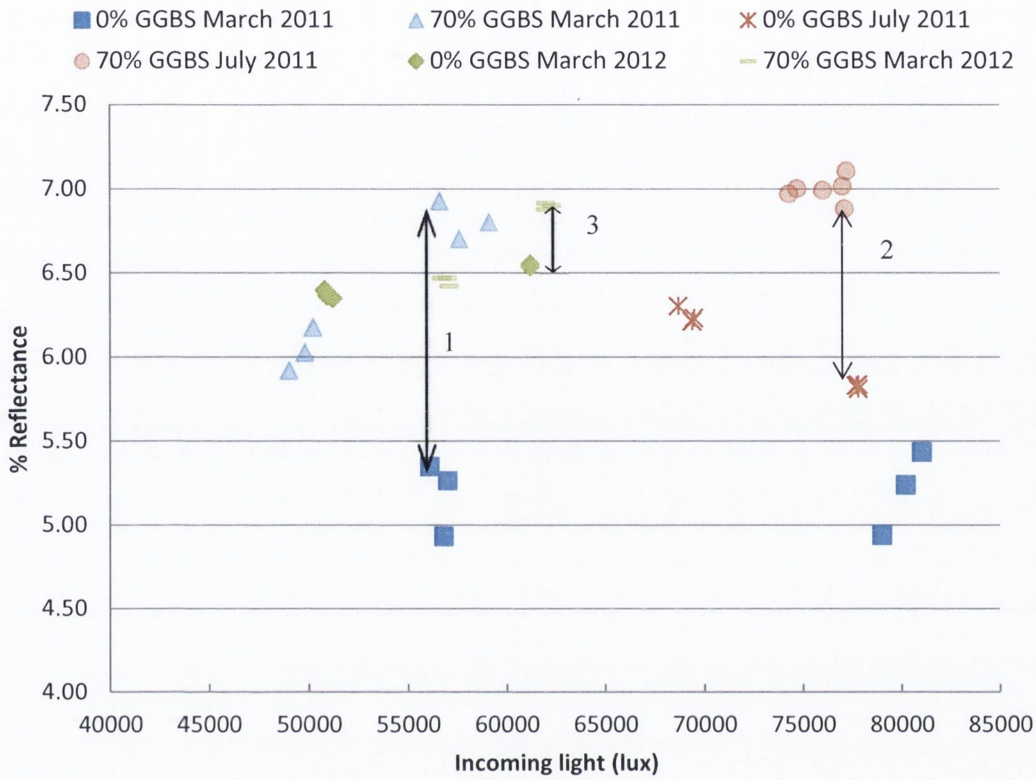

Fig. 7-19 Ageing of 0 and 70% GGBS brush finish slabs between March 2011, July 2011 and March 2012 for LS aggregate only

Table 7-22 T-test on brush surface finish for March 2012 to demonstrate ageing (one aggregate type included-LS)

DF=11
>1.796
<1.796

	0%		30%		50%		70%
$\mu_{0,6}$	6.46	$\mu_{30,6}$	5.46	$\mu_{50,6}$	5.979	$\mu_{70,6}$	6.674
$\sigma_{0,6}$	0.098	$\sigma_{30,6}$	0.35	$\sigma_{50,6}$	0.683	$\sigma_{70,6}$	0.245
t(0,30)	6.739	t(30,50)	1.656	t(50,70)	2.346		
t(0,50)	1.708	t(30,70)	6.96				
t(0,70)	1.987						

The influence of surface finish on light reflectance is presented here for a smooth surface finish (screed) and a contrasting rough surface finish (brush) for 0 and 70% GGBS for the three data sets namely March 2011, July 2011 and March 2012. The supplementary plots for 30 and 50% GGBS are displayed in Appendix BB and present broadly similar results. The corresponding t-test for this scatter plot is displayed in Table 7-23. The three data sets are labelled on the plot from 1 to 3 as before. Although there is a clear reduction evident in light reflectance between these contrasting surfaces with time, the difference in the light reflectance is greater between the surface finishes when compared to the differences between GGBS concentrations (see Fig. 7-19). This is confirmed by the results of the t-test which demonstrate that there is a difference between each of the surface finish types (highlighted in blue), despite the specimens having been exposed for one year following the initial readings taking place. It is interesting to note that the order of decreasing reflectance is screed, tamp, brush and cast. As there is a distinct difference between the smooth surface finishes (cast and screed), this would imply that the colour of the specimen is equally as important as the nature of the surface finish. The cast finish specimen is the least reflective due to its visibly darker colour, and vice versa for the screed finish specimen.

Fig. 7-20 Ageing of screed and brush finish slabs with 0% GGBS between March 2011, July 2011 and March 2012 for LS aggregate only

Table 7-23 T-test on 0% GGBS specimens for March 2012 to demonstrate ageing (one aggregate type included-LS)

DF=11
>1.796
<1.796

Cast		Screed		Tamp		Brush	
$\mu_{c,18}$	5.304	$\mu_{s,18}$	7.825	$\mu_{t,18}$	6.791	$\mu_{b,18}$	6.459
$\sigma_{c,18}$	0.044	$\sigma_{s,18}$	0.251	$\sigma_{t,18}$	0.729	$\sigma_{b,18}$	0.098
t(cs)	25.30	t(st)	3.30	t(tb)	3.00		
t(ct)	4.98	t(sb)	12.45				
t(cb)	26.45						

Similarly, the data for 70% GGBS is presented in Fig. 7-21 for the screed and brush surface finishes also. Once more there is a significant difference in the percentage of light reflected between the two surface finishes, in particular for March 2011 and July 2011. However, this decreases significantly one year later (March 2012).

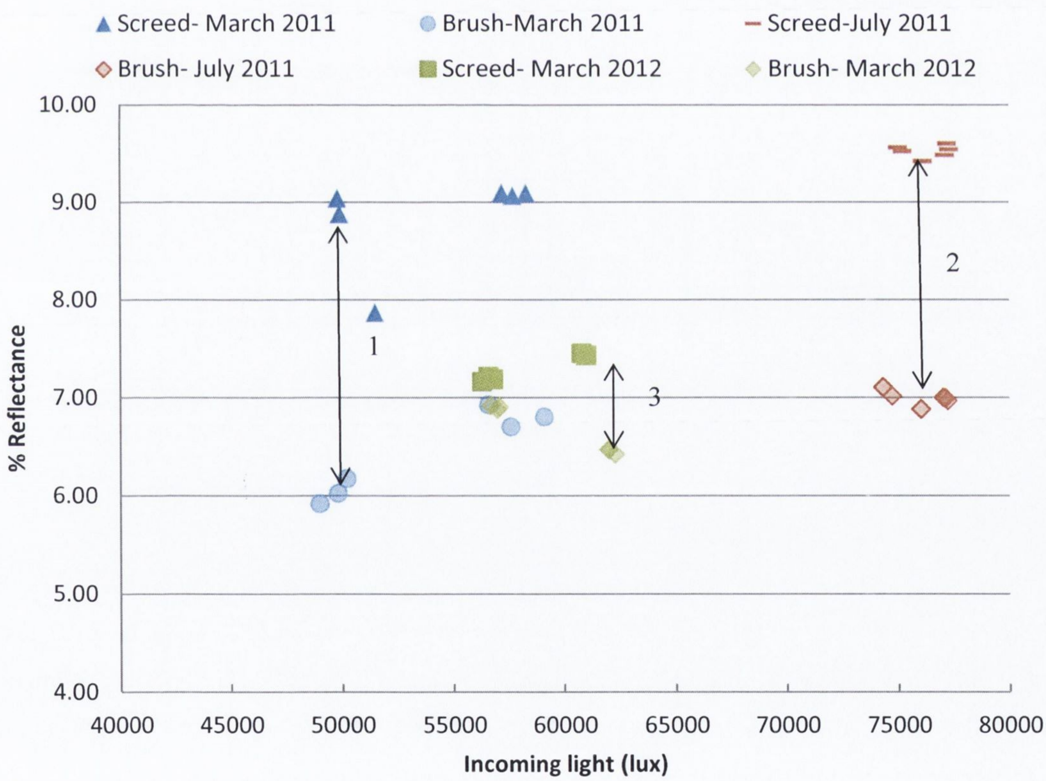

Fig. 7-21 Ageing of screed and brush finish slabs with 70% GGBS between March 2011, July 2011 and March 2012 for LS aggregate only

The corresponding t-test results displayed in Table 7-24 confirm this outcome as they demonstrate that despite the specimens having been exposed for one year following the initial readings, the difference in light reflectance between the individual surface finish types is still significant. One result is highlighted in yellow as there is virtually no difference between the tamp and brush surface finish, however, this was also observed for the initial results recorded in March 2011 (see Table 7-18).

In conclusion, despite the specimens being exposed to the environment for approximately one year, there remains a quantifiable difference in the amount of reflected light between each of the surface finishes. This would suggest that this parameter is the dominating factor over the influence of GGBS concentration. In addition, the 70% GGBS specimen performs quite poorly with age, as it is evident that the lux reading drops to below that of 50% and is similar to 30% GGBS. However, this decrease in light reflectance may be reversed by possible cleaning of the surface of the specimens.

Table 7-24 T-test on 70% GGBS specimens for March 2012 to demonstrate ageing (one aggregate type included-LS)

DF=11
>1.796
<1.796

Cast		Screed		Tamp		Brush	
$\mu_{c,18}$	5.846	$\mu_{s,18}$	7.309	$\mu_{t,18}$	6.770	$\mu_{b,18}$	6.674
$\sigma_{c,18}$	0.047	$\sigma_{s,18}$	0.139	$\sigma_{t,18}$	0.091	$\sigma_{b,18}$	0.245
t(cs)	24.4	t(st)	7.96	t(tb)	0.937		
t(ct)	22.0	t(sb)	5.57				
t(cb)	8.05						

7.3.3 Night-time luminance test

As described in Section 2.3.5, the albedo effect can also be seen at night time with associated advantages, such as the need for reduced lighting and improved road safety. Accordingly, a test to measure night-time luminance was performed in March 2013. A total of four specimens containing 0-70% GGBS with a tamped surface finish were removed from their rooftop location and transported to two different street lamps located in Trinity College (see Fig. 7-22).

Fig. 7-22 Photograph of lamp type used (sodium vapour lamp) in night time luminance test

The test procedure was carried out as follows;

1. The slab was positioned on the stand approximately 3m from the light source and the black box placed over it (see Fig. 7-23).
2. The tunnel of the black box is pointed directly up at the artificial light.
3. The box is propped in position ensuring there is no shadow cast on the surface of the specimen.
4. A reading of incoming and reflected lux are recorded and this is repeated twice.
5. Steps 1-4 are repeated for the three remaining specimens.
6. The four slabs are relocated to a second lamp of the same make where steps 1-5 are repeated.

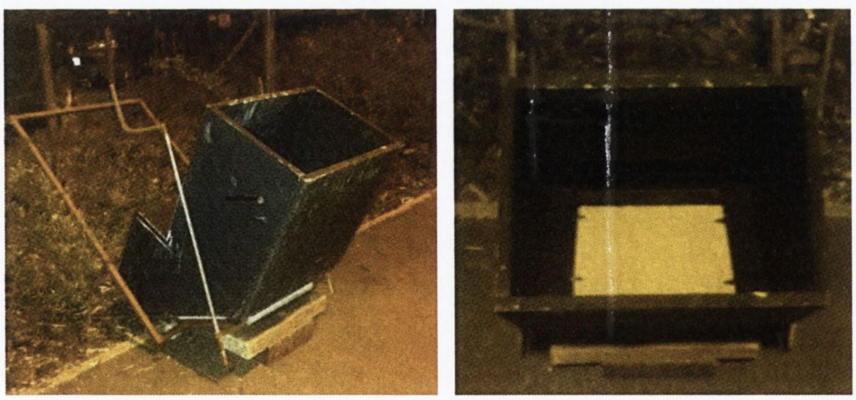

Fig. 7-23 Night-time luminance testing with black box

The data for Lamp 1 is displayed in Table 7-25 where the incoming lux remains reasonably constant at approximately 28 lux. The reflected lux reading was also constant, with only a 0.1 change in the reading for a given GGBS content. The average reflectance's for 0, 30, 50 and

70% GGBS are 4.66, 4.79, 5.35 and 5.04% respectively. The data would suggest that the 70% GGBS specimen is less reflective than the 50% specimen and that there is an increase in light reflectance from 0 to 50% GGBS of approximately 15%. Similarly, the data for Lamp 2 is presented in Table 7-26. The incoming lux is marginally lower at approximately 25 lux. The average reflectance for 0, 30, 50 and 70% GGBS is 4.40, 4.57, 5.0 and 4.66% respectively. There is once more an increase in light reflectance from 0 to 50% GGBS of approximately 15%. The relationship between the level of GGBS and reflected lux is very similar to the result of Lamp 1. It should be noted that if one measures night reflectance for a concrete surface against an asphalt surface, the benefit of using concrete is more significant.

Table 7-25 Night-reflectance data for Lamp 1 at Trinity College

Lamp	Slab	Reading	Incoming	Reflected	Ratio (%)	Average
1	0	1	28.6	1.3	4.55	4.66
		2	28.7	1.3	4.53	
		3	28.6	1.4	4.90	
	30	1	28.6	1.4	4.90	4.79
		2	28.5	1.4	4.91	
		3	28.5	1.3	4.56	
	50	1	28.8	1.5	5.21	5.35
		2	28.4	1.5	5.28	
		3	28.8	1.6	5.56	
	70	1	28.0	1.4	5.00	5.04
		2	28.5	1.5	5.26	
		3	28.8	1.4	4.86	

Table 7-26 Night-reflectance data for Lamp 2 at Trinity College

Lamp	Slab	Reading	Incoming	Reflected	Ratio (%)	Average
2	0	1	25.8	1.1	4.26	4.40
		2	25.6	1.1	4.30	
		3	25.8	1.2	4.65	
	30	1	25.6	1.2	4.69	4.57
		2	25.5	1.2	4.71	
		3	25.4	1.1	4.33	
	50	1	25.9	1.3	5.02	5.00
		2	26.1	1.3	4.98	
		3	26.0	1.3	5.00	
	70	1	25.6	1.2	4.69	4.66
		2	25.8	1.2	4.65	
		3	25.9	1.2	4.63	

The data for the two lamps is illustrated more clearly in Fig. 7-24 which demonstrates that the increase (of approximately 15%) in GGBS content shows an increase in light reflectance up to 50% GGBS. There is a reduction in the light reflectance for 70% GGBS, however, the cause for this is believed to be enhanced ageing. It can be noted that the incoming light for the two lamps is different and this may be due to brighter surfaces nearby or a slightly brighter light, as the measurement of light reflectance was taken at the same distance from each lamp.

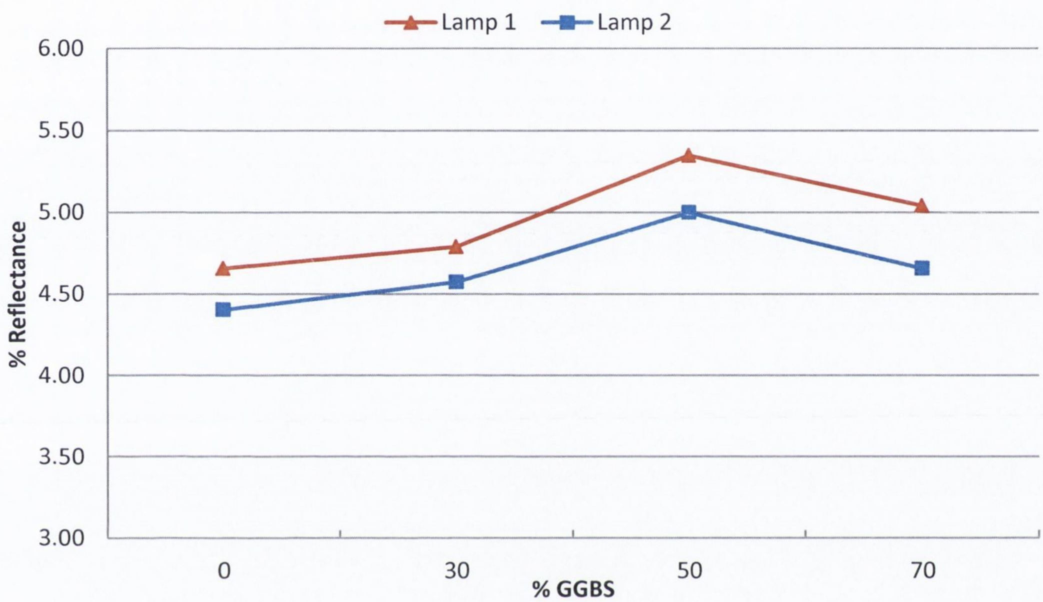

Fig. 7-24 Plot of light reflectance for tamped specimens (0, 30, 50 and 70% GGBS) at night time under two street lamps

7.3.3.1 Conclusions

- The incoming light remains almost constant as it is an artificial light source.
- Although the incoming lux is small (between approximately 25 and 28 lux), the specimens reflect between 4.40-5.35% light.
- The order of increasing reflectance generally corresponds with the increase in GGBS content, however, with 70% having a reduced reflectance due to ageing.
- The trends for both Lamp 1 and Lamp 2 are similar.
- The differences between the percentage reflectance of the different GGBS contents is sufficiently large to make it worthwhile to promote the use of higher GGBS contents in pavements.
- By increasing the level of GGBS from 0 to 50%, there is approximately a 15% increase in the illuminance.

7.3.4 Moisture test on slab specimens

A small test was conducted to illustrate the effect of moisture on the surface of the concrete specimens. The test was conducted on a sunny day where the near surface conditions of the slabs were dry. A lux reading and a greyness scale reading was recorded both when the slab was dry and immediately after wetting the surface of the specimens. The objective of this was to determine how moisture affects the resulting colour and in turn the light reflectance of the specimens. The percentage reduction in lux reflectance and greyness were calculated.

The data obtained (see Table 7-27), would suggest that the presence of moisture strongly affects the colour of the specimen, as expected, with an overall reduction in lux readings ranging between approximately 24 and 40%, and a reduction in greyness ranging between approximately 38-53% (the greyness is a more subjective test method as discussed in detail in Section 7.4). This factor is much more influential than the difference in readings obtained due to a change GGBS content and surface finish type, therefore, it is important that one ensures the near surface of the concrete specimen is dry.

In conclusion, the presence of moisture significantly decreases the light reflectance and colour of concrete, irrespective of the surface finish or level of GGBS present. However, depending on external conditions, the near-surface dries very quickly allowing for readings of reflectance to be recorded. In general, it is sufficient to leave the specimens for one day after there is rainfall, allowing ample time for the surface of the specimens to dry out.

Table 7-27 Lux reading and greyness scale reading for 0 and 70% GGBS specimens for four surface finishes in wet and dry surface conditions

		Dry % Refl Lux	Wet % Refl Lux	Dry Greyness	Wet Greyness	Lux % Red.	Greyness % Red.
0%	Cast	4.28	3.26	0.65	0.35	23.7	46.2
	Screed	4.81	3.00	0.75	0.40	37.6	46.7
	Tamp	4.00	2.72	0.65	0.35	32.0	46.2
	Brush	3.71	2.29	0.65	0.35	38.1	46.2
70%	Cast	4.06	2.71	0.65	0.40	33.1	38.5
	Screed	5.40	3.22	0.75	0.40	40.4	46.7
	Tamp	4.67	3.09	0.70	0.35	33.7	50.0
	Brush	4.76	2.96	0.75	0.35	37.8	53.3

7.3.5 Conclusions

- This series of tests indicates that there is a statistically significant difference between the duplicate specimens, however, this can be attributed to the very low values of standard deviation. The difference between the individual specimens is small in comparison to the differences between GGBS content and surface finish. The data is sufficiently close to enable one to combine the data for the duplicate specimens and compute an average.

- The aggregate type does not have a strong influence on the percentage lux reflectance despite the t-test results showing statistical significance, therefore, this enabled the combining of the three aggregate type results together to compute an average result.
- The effect of GGBS concentration on light reflectance is significant with differences evident from 0 to 70% GGBS, in particular for the smooth surface finishes, for example a cast surface finish. However, where the rough surface finishes are considered, for example, a brush surface finish, the differences between adjacent concentrations of GGBS (such as 0 and 30%, 30 and 50% and 50 and 70% GGBS) are less pronounced. This is due to greater dispersion of light from the brush surface finish.
- The effect of surface finish type on visible light reflectance is significant, with differences evident between each of the surface finish types. Although both parameters are important, the effect of surface finish has a greater influence on the amount of light reflected when compared to the effect of GGBS concentration, as the differences between the different finish types is greater. The general order of decreasing reflectance in terms of surface finish is as follows; screed, tamp, brush and cast.
- The influence of ageing on the amount of light reflected from a specimen is evident despite there being only one year between the initial and final readings. The specimens containing 70% in particular, appear to decrease in light reflectance at a faster rate. The order of reflectance for the rougher surface finish is not well defined, due to the dispersion of light from the surface.
- As there is a distinct difference between the smooth surface finishes (cast and screed), this would imply that the colour of the specimen is equally as important as the nature of the surface finish. The cast finish specimen is the least reflective due to its visibly darker colour, and vice versa for the screed finish specimen.
- Although the specimens were exposed to the environment for approximately one year following the initial readings, there remains a quantifiable difference in the amount of reflected light between each of the surface finishes. This would suggest that this parameter is the dominating factor over the influence of GGBS concentration.
- The order of increasing night time luminance generally corresponds with the increase in GGBS content, however, with 70% having a reduced reflectance due to ageing. By increasing the level of GGBS from 0 to 50%, there is approximately a 15% increase in the illuminance, which would be sufficiently large to make it worthwhile to promote the use of higher GGBS contents in pavements.

- The presence of moisture strongly affects the colour of the specimen, with an overall reduction in lux readings ranging between 24 and 40%, and a reduction in greyness ranging between 38 and 53%. However, depending on external conditions, the near-surface dries very quickly allowing for readings of reflectance to be recorded.
- The order of importance of factors influencing light reflectance are broadly as follows; surface finish type, percentage of GGBS, ageing, aggregate type as determined by the lux meter testing.

7.4 Greyness Index Chart

7.4.1 Introduction

As the colour of a surface has a strong effect on the amount of light reflected off it, it is important to examine and evaluate this parameter. Using a sphere spectrophotometer, which has been shown to be highly accurate, is not always practical or affordable. Therefore, a more accessible method, using a greyness index card as a ready reckoner for colour, is investigated. Thus, characterising the 'greyness' of the concrete slabs surface using a greyness index chart (see Section 4.5) is achieved by placing the colour chart on the surface of the slab in order to determine the colour or greyness index value which it is closest to on the chart (see Fig. 7-25). The greyness index value is accurate to 0.05 and is a subjective test, however, one would aim to categorize the colour of a concrete specimen to within this accuracy range i.e. repeatable to within one band of greyness. The greyness value is then calculated as follows; greyness value = (100-greyness index chart value)/100.

A number of data sets were collected over the duration of this project. These were taken in August 2011, February 2012 and February 2013. The concrete specimens were cast in September 2010. The results are presented in this section and the full set of greyness readings can be found in Appendix CC. The results are presented for the three aggregate types, four different surface finish types and four concentrations of GGBS.

There are many factors which influence the colour of concrete. Some of these factors are as follows;

1. Type of cement: The cements used for this particular test are conventional grey CEM II A-L cement and GGBS, which is known for producing a concrete which is lighter in colour than concrete made with conventional cement.
2. Type of aggregate: The aggregate type used in concrete may influence the colour of the concrete, however, aggregate which is exposed on the surface is usually coated with

cement paste. The effect of aggregate type on colour is more prominent when the aggregate is exposed at the surface. There are three aggregate types used; limestone (L), partially crushed limestone (PCL) and sandstone (SS).

3. Curing time: This factor also has an effect on the end colour of concrete as it affects the surface hydration of the cement paste. Each concrete slab was cured for the same period of time, thus eliminating this additional factor.
4. Moisture content: The amount of moisture present in concrete is measured using a moisture meter to ensure the slab is sufficiently dry before taking a reading. A reading for greyness is taken only when there have been 3 consecutive days of no rainfall to ensure this parameter is eliminated. In general, the smooth surface finishes take longer to dry compared with the rough surface finishes because the surface pores are more closed and so the evaporation rate is slower.
5. Ageing: To study the effect of age on concrete, there was a 6 month period between the first two sets of results taken, and a further year before the final set was taken.

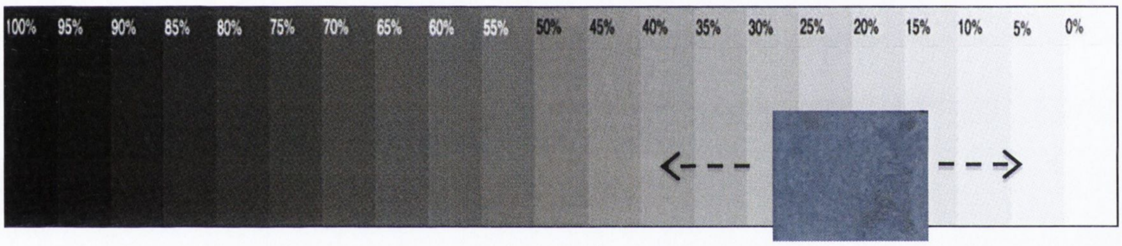

Fig. 7-25 The greyness index chart with a concrete specimen aligned against it to determine the greyness of the specimen

7.4.2 Results of greyness

The results of greyness are displayed in Table 7-28 for each of the three data sets recorded (Aug-11, Feb-12, Feb-13). This data set provides a single value for one particular slab type i.e. an average of the duplicate slab readings were taken (a full set of the individual greyness readings recorded are located in Appendix CC). The GGBS concentration is presented in the first column on the left hand side, followed by the aggregate type in the second column. The surface finish type is displayed at the tops of the columns, with the three data set dates for the different finishes in adjacent columns. The following effects will be discussed in detail;

1. Aggregate type on greyness
2. Surface finish on greyness
3. GGBS content on greyness
4. Ageing of the specimen

Table 7-28 Summary of greyness values for each slab specimen (average values of duplicate specimens)

Surface	Finish	Cast			Screed			Tamp			Brush		
GGBS	Agg.	Aug-11	Feb-12	Feb-13	Aug-11	Feb-12	Feb-13	Aug-11	Feb-12	Feb-13	Aug-11	Feb-12	Feb-13
0	L	0.58	0.58	0.58	0.75	0.75	0.75	0.68	0.68	0.68	0.73	0.73	0.70
	PCL	0.60	0.63	0.58	0.75	0.75	0.73	0.68	0.68	0.68	0.65	0.65	0.60
	SS	0.58	0.58	0.58	0.70	0.70	0.70	0.65	0.65	0.65	0.65	0.63	0.60
30	L	0.65	0.65	0.65	0.83	0.80	0.75	0.78	0.78	0.75	0.75	0.75	0.75
	PCL	0.65	0.65	0.58	0.75	0.75	0.75	0.73	0.73	0.73	0.70	0.70	0.70
	SS	0.58	0.60	0.60	0.80	0.80	0.78	0.75	0.75	0.73	0.78	0.78	0.75
50	L	0.70	0.70	0.68	0.80	0.75	0.70	0.75	0.75	0.73	0.80	0.80	0.75
	PCL	0.70	0.73	0.68	0.78	0.75	0.70	0.73	0.70	0.68	0.80	0.80	0.75
	SS	0.68	0.68	0.68	0.83	0.78	0.73	0.75	0.75	0.73	0.83	0.80	0.80
70	L	0.73	0.73	0.70	0.88	0.83	0.80	0.83	0.78	0.78	0.85	0.83	0.80
	PCL	0.68	0.68	0.68	0.80	0.75	0.75	0.70	0.70	0.75	0.80	0.80	0.78
	SS	0.73	0.70	0.70	0.85	0.78	0.73	0.83	0.78	0.78	0.83	0.80	0.78

7.4.2.1 The effect of aggregate type on greyness

Unlike the data obtained using a spectrophotometer or lux meter, the greyness readings are subjective as they are assessed by the naked eye to the nearest 0.05 (or 5%). Therefore, by studying the results obtained overall for the three different aggregate types in Table 7-28, it appears this method cannot accurately assess the effect of aggregate type on greyness as it is not possible to differentiate between them visually. The coefficient of variation (CoV) between the three aggregate types for any one specimen is no more than 10%. Therefore, in order to assess the influence of GGBS and surface finish type on greyness, the readings for the three aggregate types will be averaged.

7.4.2.2 The Effect of GGBS concentration on Greyness

A summary of the greyness values with averaged aggregate values is displayed in Table 7-29. This data will be utilised to determine the effect of both GGBS content and surface finish on greyness. By observing the general trend from 0 to 70% GGBS, there is an increase in greyness value for each of the GGBS contents which can be viewed more clearly in Fig. 7-26. In addition, there is a consistent trend across the various surface finish types.

The data displayed in Fig. 7-26 is representative of the first set of results recorded in August 2011 for the four surface types. Within each of these surface finish (SF) type results, lie the four GGBS concentrations (0-70%). This chart exhibits a direct correlation between GGBS concentration and greyness for each of the surface finish types, with 0% having the lowest greyness value and 70% the highest. The difference between 0 and 70% GGBS in terms of greyness ranges between 0.11 and 0.16. This can be seen by observing the average greyness value for 0, 30, 50 and 70% which are 0.67, 0.73, 0.76 and 0.79 respectively.

Table 7-29 Summary of greyness values (average value of three aggregate types for duplicate pairs)

SF	Cast			Screed			Tamp			Brush		
GGBS	Aug-11	Feb-12	Feb-13	Aug-11	Feb-12	Feb-13	Aug-11	Feb-12	Feb-13	Aug-11	Feb-12	Feb-13
0	0.59	0.60	0.58	0.73	0.73	0.73	0.67	0.67	0.67	0.68	0.67	0.63
30	0.63	0.63	0.61	0.79	0.78	0.76	0.75	0.75	0.74	0.74	0.74	0.73
50	0.69	0.70	0.68	0.80	0.76	0.71	0.74	0.73	0.71	0.81	0.80	0.77
70	0.71	0.70	0.69	0.84	0.79	0.76	0.79	0.75	0.77	0.83	0.81	0.79

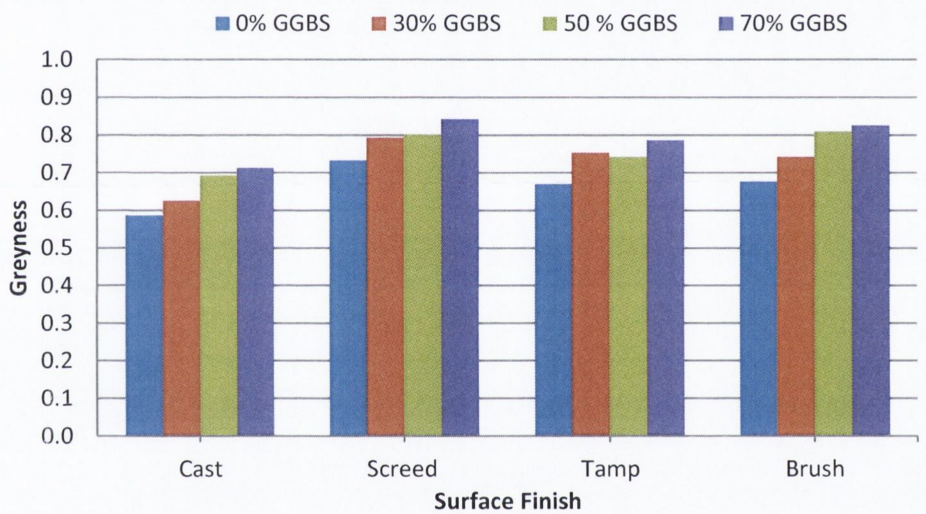

Fig. 7-26 The effect of GGBS concentration on greyness for four surface finish types (Aug-11)

This would suggest that the level of GGBS present in concrete has a significant and measurable effect on the colour or greyness of the concrete produced, with this change being significant enough to be detected easily by the human eye. However, it should be noted that the greyness index result is harder to ascertain for rough surfaces as reading the index is more subjective than for smooth surfaces.

7.4.2.3 The Effect of Surface Finish Type on Greyness

The effect of surface finish on greyness can be studied by observing the average greyness for each of the finish types. The data presented in Fig. 7-27 examines the effect of surface finish type on greyness for the four GGBS concentrations from August 2011. It corresponds directly with the data presented in Fig. 7-26, however, the focus is now on the effect of the surface finish type. There is a strong relationship between greyness and the finish type for each of the GGBS concentrations. The difference in greyness between the two extremes, screed and cast, ranges between 0.11 and 0.16. This range would suggest that the effect of surface finish type on greyness is significant and discernible using the greyness index chart, despite its subjectivity and low accuracy compared to the sphere spectrophotometer. The average greyness for the four finish types screed, brush, tamp and cast are 0.79, 0.77, 0.74 and 0.66 respectively. The results confirm that the surface finish does have a measurable effect on greyness using the greyness index scale, and that this parameter is equally as important, if not more important, than the percentage of GGBS present.

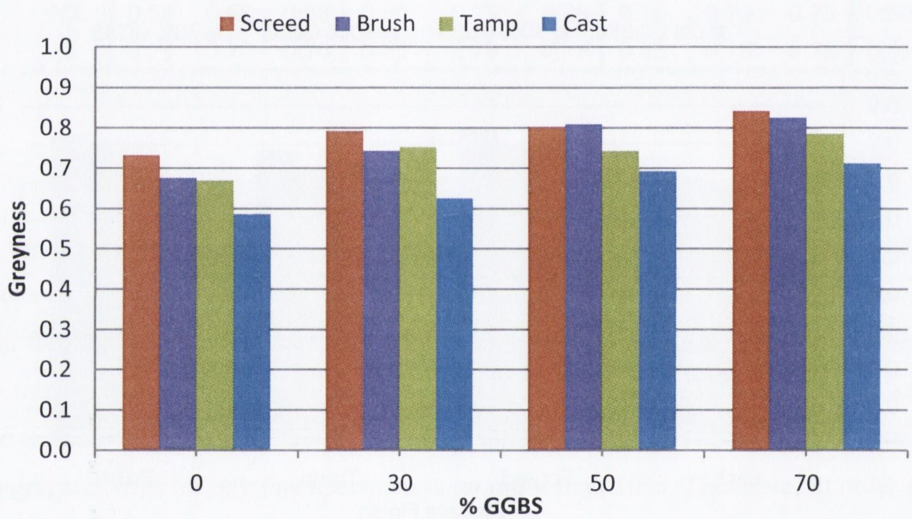

Fig. 7-27 The effect of surface finish on greyness for four GGBS concentrations (Aug-11)

7.4.2.4 Ageing

In order to examine the effects of age, both the second and third data sets recorded in February 2012 and February 2013 will be studied in terms of both GGBS concentration and surface finish type. The data obtained 6 months later (Feb-12) is presented in Fig. 7-28. Already it can be observed that there is a softening of the trend when compared with the first set of results (see Fig. 7-26). However, a detectable correlation between GGBS concentration and greyness remains for the most part. The difference in greyness between the two extremes of 0 and 70% GGBS now ranges between 0.06 and 0.14 which signifies an overall decrease in the range of greyness. Similarly, the average greyness values for 0, 30, 50 and 70% are 0.67, 0.72, 0.75 and 0.76 respectively. Interestingly, it is the 70% GGBS which has reduced in colour most significantly.

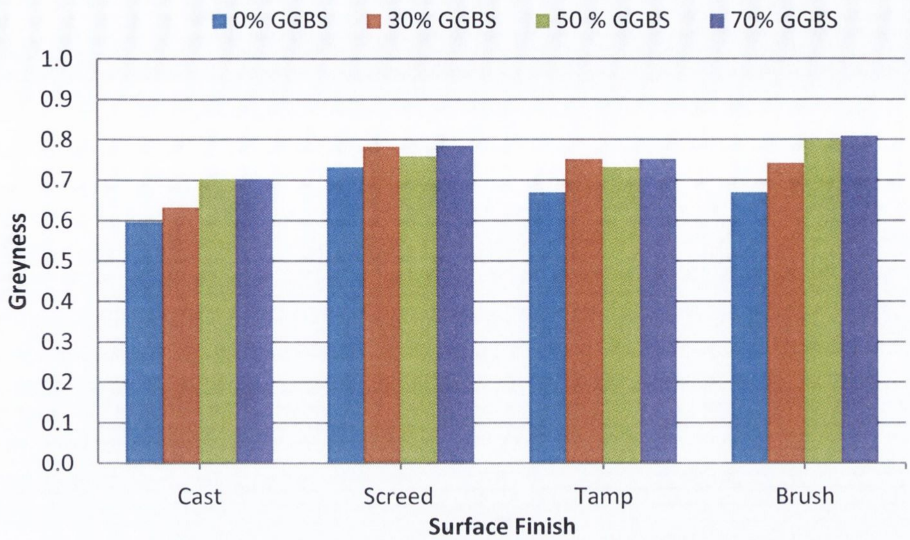

Fig. 7-28 The effect of GGBS concentration on greyness for four surface finish types (Feb-12)

The relationship between greyness and GGBS concentration remains evident in Fig. 7-29 which were recorded in February 2013, however, for the screed and tamp surface finish, the trend of increasing greyness with increased GGBS concentration is not as pronounced. The average greyness for 0, 30, 50 and 70% GGBS contents are 0.65, 0.71, 0.72 and 0.75 respectively. This is a significant change when compared with the results from August 2011 (see Fig. 7-27) where the greyness for 0, 30, 50 and 70% GGBS is 0.67, 0.73, 0.76 and 0.79. The results have somewhat reduced which would suggest that there is deterioration of the samples due to weathering, however, the result would suggest that it is possible to differentiate between the different GGBS content levels throughout, despite the subjectivity of the test.

In terms of surface finish type, this particular parameter is more difficult to differentiate between for the four GGBS concentrations, because rougher surfaces are more subjective than smooth ones. The data recorded in February 2012 (6 months following the first set of results recorded) is displayed in Fig. 7-30. This chart is a re-representation of the data from Fig. 7-28, however, with the primary focus being on the surface finish type and its effect on greyness. Again, there is a definite softening of the trend between greyness and finish type, in particular for 50 and 70% GGBS concentrations, where the screed finish is now lower in greyness than the brushed finish.

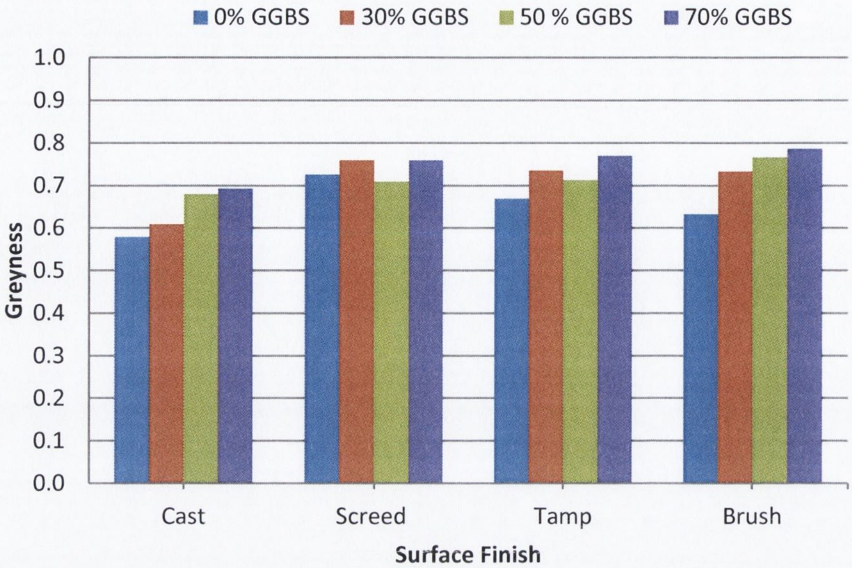

Fig. 7-29 The effect of GGBS concentration on greyness for four surface finish types (Feb-13)

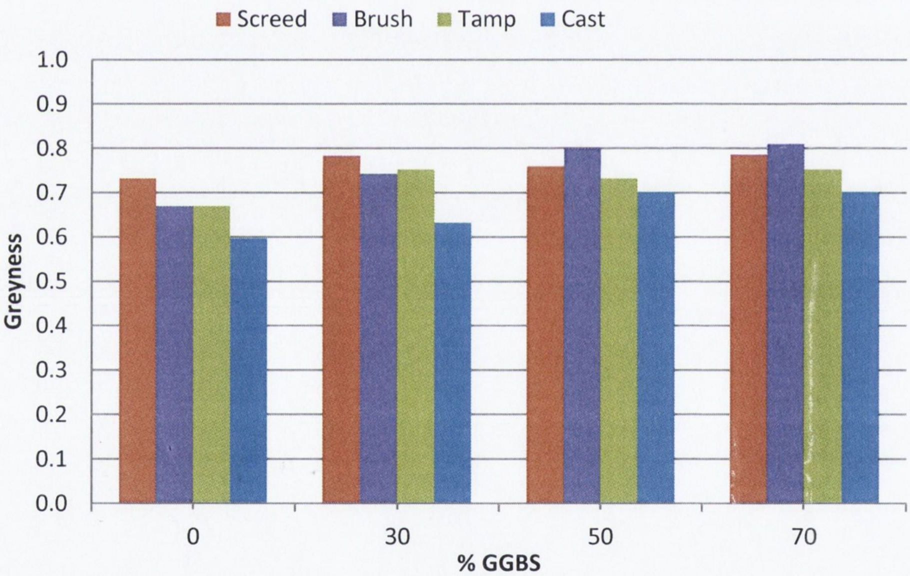

Fig. 7-30 The effect of surface finish on greyness for four GGBS concentrations (Feb-12)

The average greyness for the surface finish types screed, brush, tamp and cast is 0.77, 0.76, 0.73 and 0.66 respectively. An overall reduction of greyness is evident based on these values, however, the order of surface finish type in terms of decreasing greyness remains the same.

The final set of results recorded in February 2013 are displayed in Fig. 7-31. The cast surface finish remains the lowest in terms of greyness, however, there is a detectable overlap of results for the remaining surface finishes which would suggest that there is deterioration of the samples due to weathering to differing degrees. The average greyness for screed, brush, tamp and cast is 0.74, 0.73, 0.72 and 0.64 respectively. On average, the order of surface finish type in terms of decreasing greyness remains unchanged, however, when the individual results are observed in Fig. 7-31, it becomes evident that the effect of surface finish type has diminished with time. In conclusion, the surface finish and GGBS concentration both drop at approximately the same rate and not by a large amount in 18 months, according to the results obtained using the greyness index chart.

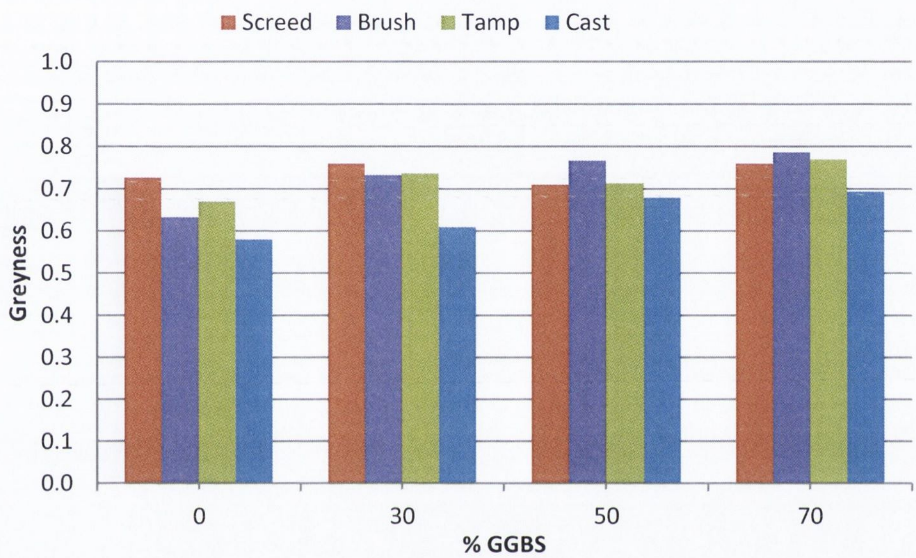

Fig. 7-31 The effect of surface finish on greyness for four GGBS concentrations (Feb-13)

A summary of the average greyness readings is displayed in Table 7-30. The data presents the order of decreasing greyness in terms of both GGBS concentration and surface finish type for the three data sets. The order of decreasing greyness for GGBS is 70, 50, 30 and 0% and the order of decreasing greyness for the various finish types is screed, brush, tamp and cast. This contrasts with the results obtained using the lux meter which seem to indicate that as time progresses, the 70% GGBS specimens deteriorate at a faster rate, however, this former test is very subjective. This outcome will be either verified or dismissed when the results of the thermocouple readings are investigated in Section 7.6.

By observing the average values presented, the greyness has been observed to reduce for each GGBS concentration over time. Similarly, the greyness for each surface finish type has also reduced, with the three surface finishes brush, tamp and screed having almost identical results of greyness in February 2013.

Table 7-30 Summary of data displaying order of decreasing greyness (average) in terms of GGBS and surface finish type

	Order	Aug-11	Feb-12	Feb-13
GGBS	70%	0.79	0.76	0.75
	50%	0.76	0.75	0.72
	30%	0.73	0.72	0.71
	0%	0.67	0.67	0.65
Surface Finish	Screed	0.79	0.77	0.74
	Brush	0.77	0.76	0.73
	Tamp	0.74	0.73	0.72
	Cast	0.66	0.66	0.64

7.4.3 Conclusions

- There are many factors which can influence the colour of concrete such as curing and moisture content for example. These parameters were controlled and monitored so that there was reasonable consistency across all of the specimens, allowing the results for the other variables considered to be comparable.
- The greyness index result is harder to ascertain for rough surfaces as reading the index is more subjective than for smooth surfaces. In addition, there is also the presence of human error when taking a reading.
- A direct correlation between GGBS concentration and greyness for each of the surface finish types was observed for the results recorded in August 2011 when the concrete was 10 months old, with 0% having the lowest greyness value and 70% the highest, as expected.
- There is a strong relationship between greyness and the surface finish type for each of the GGBS concentrations, with the order of decreasing greyness as follows; screed, brush, tamp and cast. This entirely concurs with the results of the lux meter readings but was achieved much more rapidly and cheaply.
- The results confirm that the surface finish type does have a measurable effect on greyness using the greyness index scale, and that this parameter is equally as important, if not more important, than the percentage of GGBS present. The cast surface finish remains the lowest in terms of greyness, however, there is an overlap of results for the remaining surface finishes which would suggest that there are different rates of deterioration of the samples with different surface finishes due to weathering at differing rates.
- In terms of analysing the effect of ageing, the differences between the results are less pronounced which would suggest that there is deterioration of the samples due to weathering, however, the results would also suggest that it is still possible to differentiate clearly between the different GGBS content levels after 18 months, despite the

subjectivity of the test. The greyness index chart shows that the order of GGBS concentration remains the same after 18 months, however, this contrasts with the results obtained using the lux meter. The lux meter results seem to indicate that as time progresses, the 70% GGBS specimens deteriorate at a faster rate, however, the greyness index chart is a very subjective test and thermocouple results will be investigated to clarify this anomaly.

- The data recorded in February 2013 (18 months following the first set of readings) displayed a softening of the trends in terms of GGBS concentration and greyness, however, a detectable correlation remains. There is also a definite softening of the trend between greyness and surface finish type, in particular for 50 and 70% GGBS concentrations, where the screed finish is now lower in greyness than the brushed finish.

7.5 Thermal Imaging

7.5.1 Introduction

An infrared thermal imaging camera is used to measure heat development of the slabs and is an indirect test method. As the slabs absorb sunlight, this is converted into heat which is either reemitted as infrared radiation or is conducted through the slab. The primary objective of this method of testing is to evaluate the two parameters which have an effect on the radiation observed; GGBS content and surface finish. Similar to the lux meter, a high level of sunshine intensity is required, in this case to allow the slabs to heat up sufficiently so that there is a measurable difference between the temperatures of the different slabs. For the most part, a digital image will be presented alongside a thermal image to demonstrate the difference in the colour and radiation of the specimens.

A test was conducted to determine whether the thermal imaging camera detected reflected infrared radiation as well as emitted radiation. This was conducted by recording a thermal image of a concrete specimen when it is firstly in full sunshine, and secondly, when it is immediately removed from the direct sunlight i.e. placed in the shade. The results of these thermal images are presented in Fig. 7-32, where the temperature at the crosshairs is displayed on the top left hand corner of the image. The temperature scale on the bottom of both images is virtually identical, therefore, the two images can be directly compared. From these images, it is observed that the minor difference in the surface temperature (0.8° C) between the two cases is within the accuracy of the device (±2°C). Accordingly, it may be concluded that the influence of reflected infrared radiation is negligible.

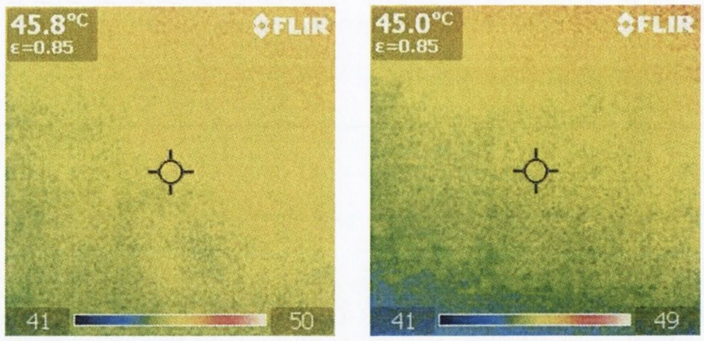

Fig. 7-32 Thermal image of slab in full sunshine (left) and in shade (right)

7.5.2 Results of thermal imaging

7.5.2.1 Surface temperature for cast and screed surface finishes

The following section contains the results obtained from the analysis of surface temperature of cast and screed smooth surface finishes (assuming an emissivity value of 0.93 for concrete (Baehr and Stephan, 2011)). Thermal images of these specimens were recorded on 3rd June 2011 and the sunshine record for this day is displayed in Fig. 7-33. The time at which the images were taken is marked on the chart (approximately 15:00), and this corresponds to a sunshine intensity of approximately 870W/m^2. This plot would suggest that the slab specimens have sufficient time to heat up before the reading was taken. This high value of irradiance confirms that it is both clear and sunny on this particular day.

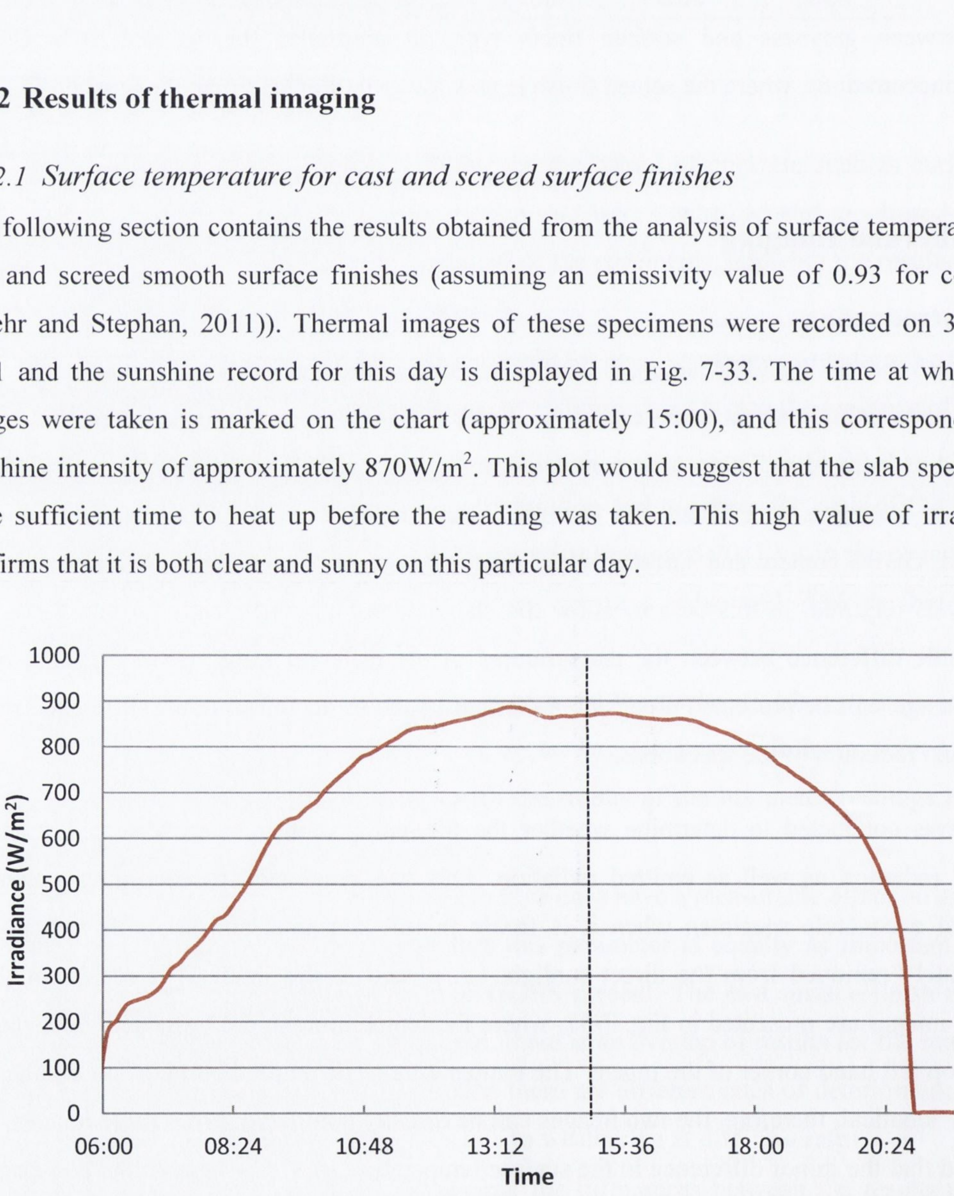

Fig. 7-33 Sunshine intensity on 3rd June 2011 displaying the time the thermal images were recorded at 15:00

The effect of surface finish on the surface temperature is evident in Fig. 7-34 which displays the digital and thermal images for cast and screed finish slabs (with 0 and 70% GGBS photographed together). The advantage of photographing the specimens beside one another is that the specimens can be directly compared with one another using the same temperature scale. On the other hand, the advantage of an individual photograph is that one obtains a better idea of the variation across the surface as well as the individual temperatures, and the image is more sensitive due to the absence of heat sources or sinks. From the digital image of both sets of specimens, it would appear that there is little difference in colour visually, however, the thermal image would suggest otherwise. The cast surface specimens records a temperature of approximately 42.7°C and the screed specimens records a significantly lower temperature of 37.6°C, a difference of approximately 5°C. The thermal image also displays the result in terms of colour, with the darker colour representing a lower surface temperature. The screeded specimens have a cooler surface temperature as they are darker in colour than the cast specimens in the thermal images. This confirms that the screed finish specimens are emitting less radiation than the warmer cast finish specimens. It is interesting to note that there is a bright spot on the thermal image on the left (cast finish), which is the sun being reflected off the smooth timber surface underneath. This suggests that there is some reflected radiation, however, the general image predominately displays emitted radiation. This interference from the sun's reflection suggests that it would be better to photograph the specimens individually so that the temperature recorded is not distorted as a result of this interference.

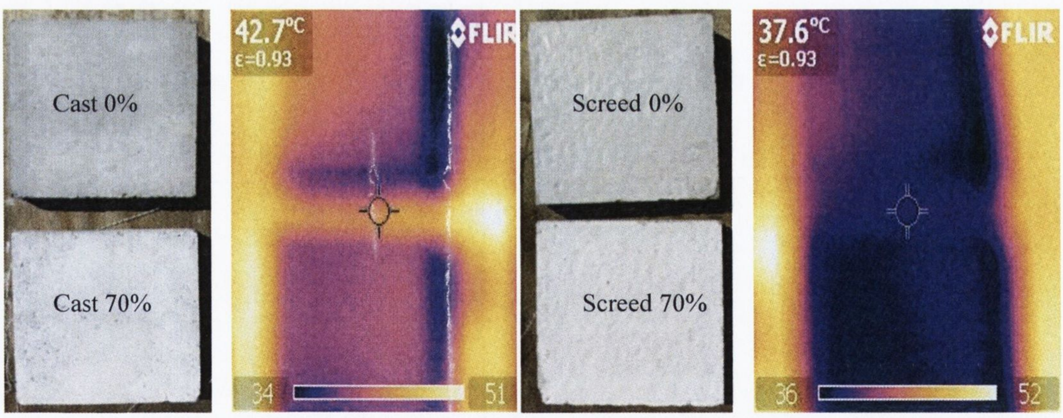

Fig. 7-34 Thermal image displaying the effect of surface finish type on surface temperature (3rd June 2011)

The temperature indicated in the top left hand corner of a thermal image is the surface temperature recorded at the crosshairs based on the assumed emissivity value, therefore, little can be inferred from the reading in this particular case as the image is of two specimens. However, as the temperature scales are almost the same for both images, the thermal images can be directly compared and they indicate that there is a clear difference in the temperature between the 0 and 70% GGBS specimens. The temperature of the surfaces (approximately 40°C) are significantly higher when compared to the ambient temperature of the day (approximately 26.1°C), despite a relatively cold climate and the low intensity of the sun.

These four specimens are examined individually in Fig. 7-35 with the thermal image of the specimen adjacent to the digital image. This set of images demonstrates the effect of both GGBS concentration and surface finish type on the surface temperature of these smooth surface finishes. The cast 0% specimen has a surface temperature of 41.9°C and the 70% specimen has a surface temperature of 40.1°C, a difference of approximately 2.0°C. Similarly, the screed 0% specimen displays a surface temperature of 38.7°C, and screed 70% a temperature of 36.7°C, a difference of 2.0°C also. Therefore, it can be concluded that on this particular day with a sunshine intensity of approximately 870W/m^2, the presence of GGBS with a substitution rate of 70% produces an overall reduction in surface temperature of concrete of 2.0°C.

Similarly, the effect of surface finish is also demonstrated in these results. Where there is no GGBS present, the difference between a cast and screeded finish is 3.2°C, and where there is 70% GGBS present, a difference of 3.4°C between cast and screeded finish is observed. This greater temperature difference would suggest that the effect of surface finish on surface temperature may be greater than the effect of GGBS concentration on surface temperature, though this difference is probably too small to be certain at this stage.

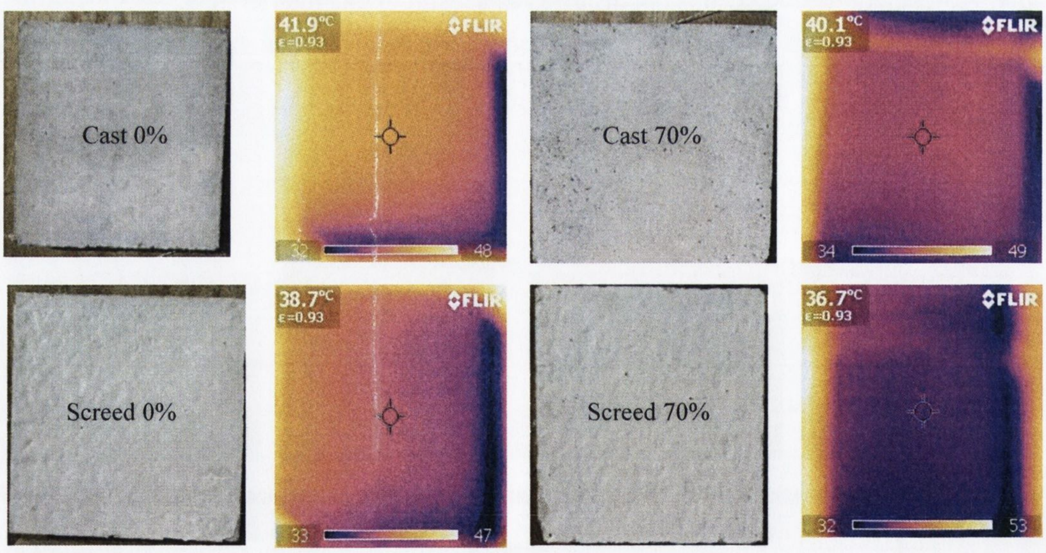

Fig. 7-35 The effect of both GGBS concentration and surface finish type on the surface temperature of cast and screed finish slabs (3rd June 2011)

It is important to note that the thermal imaging camera takes into account the variation of infrared radiation which is within the image when setting the colour contour scale, however, the four scales are very similar (within 2°C of one other) in Fig. 7-35. This enables a reasonable comparison to be made between the four images. It can also be observed that there is a variation in temperature across the surface of one slab. The top left corner of the specimen is warmer as it is directly in sunshine and the bottom right corner is slightly cooler as there is a shadow cast by the slab on the timber below. Therefore, the temperature of the slab is not completely uniform over the entire surface.

7.5.2.2 Surface temperature for tamp and brush surface finishes

The effect of GGBS and surface finish will be examined in this section for the rougher surface finishes, tamp and brush, and these results were also recorded in June 2011. The effect of GGBS concentration for a tamped surface finish in particular, is evident in Fig. 7-36 which is an overview of the four concentrations of GGBS (0, 30, 50 and 70%). The surface temperature recorded is 35.6°C, however, more importantly, the objective of this thermal image is to demonstrate that the presence of GGBS produces less thermal radiation. The two specimens on the bottom of the image (50 and 70%) appear visibly darker in colour than the top two specimens (0 and 30%) which does suggest that the 50 and 70% specimens are marginally cooler on the surface. However, in order to assess each of the specimens, an individual thermal image is required to produce the temperature of one specimen.

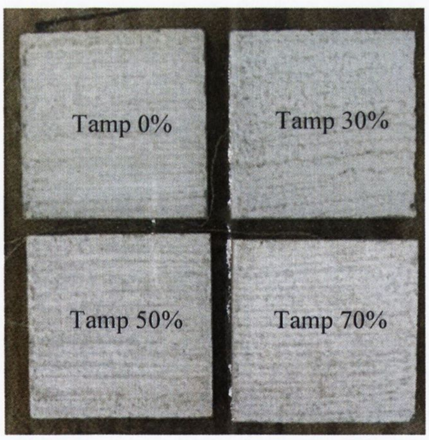

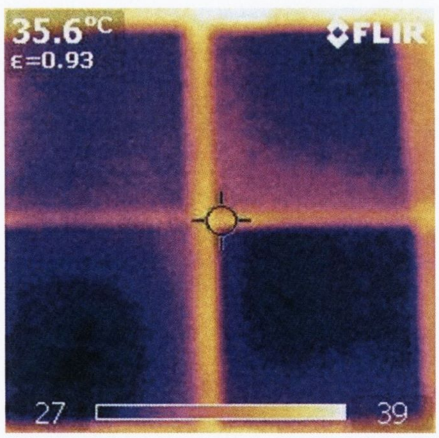

Fig. 7-36 Effect of GGBS concentration on temperature for tamped finish (20th June 2011)

A similar result is observed for the brushed specimens (Fig. 7-37), recording a temperature of 39.2°C, approximately 4.0°C warmer than the tamped specimens. Once again, the 0 and 30% specimens are lighter in colour and the 50 and 70% specimens are darker in colour, suggesting they are cooler. This result is interesting because it suggests that there is a sizeable difference in temperature between 30 and 50% GGBS specimens. This observation will be confirmed by the thermocouple results which will be discussed later in Section 7.6.

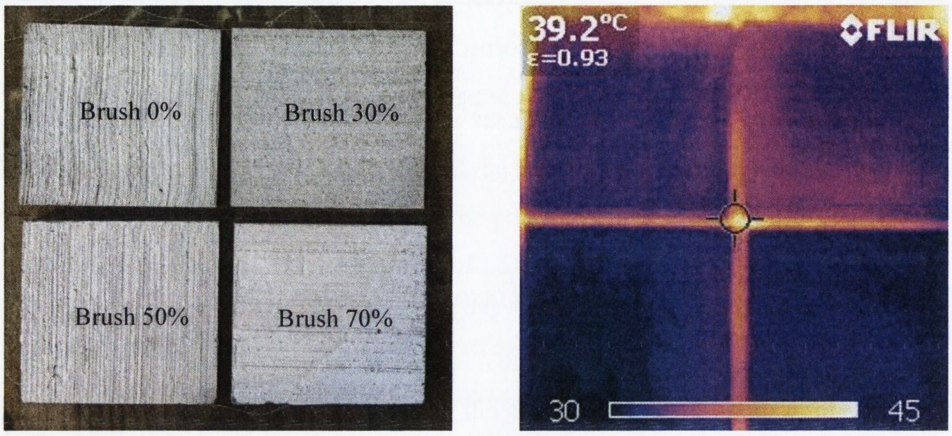

Fig. 7-37 Effect of GGBS concentration on temperature for brushed finish (20th June 2011)

The effect of both GGBS concentration and the surface finish type on the temperature of the tamped and brushed specimens can be seen in Fig. 7-38 which displays a digital and thermal image of both 0 and 70% specimens photographed separately. The tamp 0% specimen produces a surface temperature of 29.0°C, and the 70% tamp specimen displays a surface temperature of 27.5°C which is a difference of 1.5°C. Similarly, the brushed finish with 0% GGBS has a surface temperature of 32.0°C and the 70% GGBS specimen 29.2°C, a difference of 2.8°C. In addition, the 70% GGBS specimens could have aged to some extent, which would also affect the range in temperature reduction of the specimens.

Similarly, the effect of surface finish on the surface temperature can also be determined. The difference in surface temperature between the tamped and brush finish specimens containing no GGBS is 3.0°C, and for 70% GGBS a difference of 1.7°C was noted. This result would reconfirm that the effect of surface finish on the temperature is more important than the effect of GGBS concentration, having a marginally higher range in temperature difference of between 1.7 and 3.0°C.

It should be observed that the temperature scales are quite different in Fig. 7-38, therefore, the colours in the images can only be compared if one checks that the scales are roughly the same. This is the advantage of observing two specimens together in one thermal image. Although one loses some definition in the image, the scales are the same, therefore, the colour contours are relative to one another and can be more easily compared.

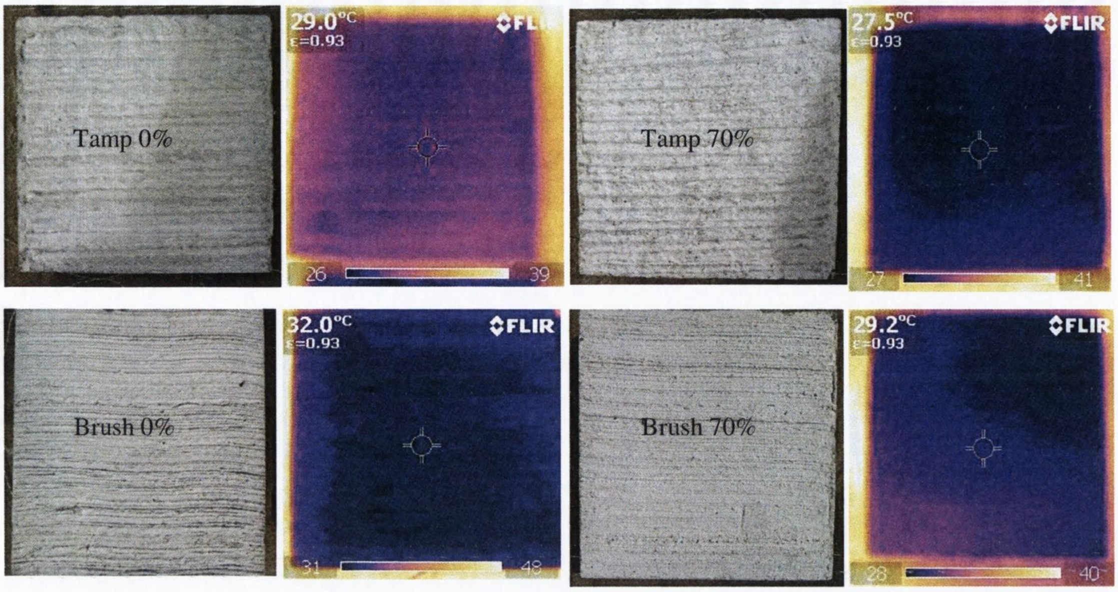

Fig. 7-38 The effect of both GGBS concentration and surface finish type on the temperature of rough surface finish slabs (20th June 2011)

7.5.2.3 The effect of surface finish type and GGBS concentration on surface temperature

The following section contains the results obtained from the analysis of surface temperature of specimens which were recorded on 27th July 2011, with the sunshine record for this day displayed in Fig. 7-39. The time at which the images were taken is marked on the chart (approximately 14:20). At this time, a sunshine intensity of approximately 830W/m^2 was recorded.

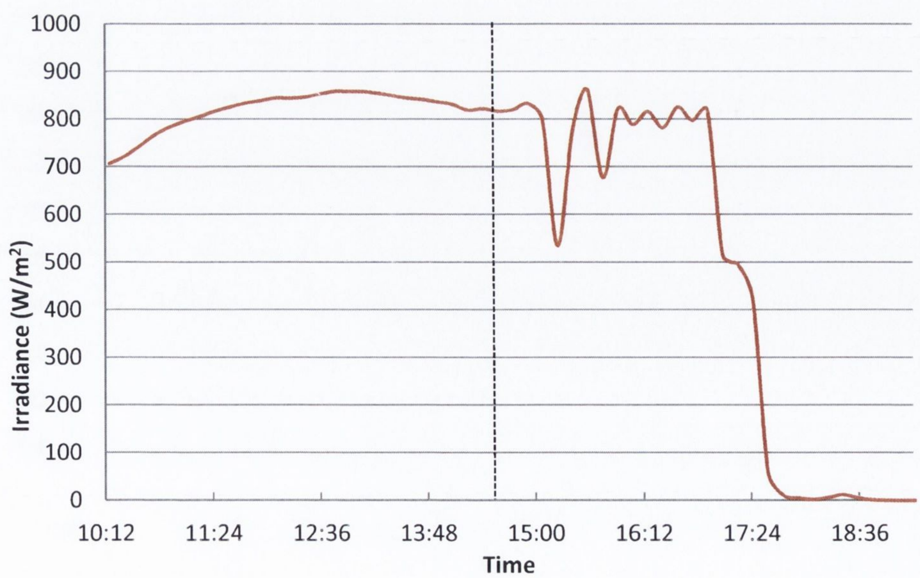

Fig. 7-39 Sunshine intensity for 27th July 2011 displaying the time the thermal images were recorded at 14:20

The thermal images were taken at this time to allow the specimens ample time to heat up, as before. This high value of irradiance confirms that it is both clear and sunny on this particular day. The thermal images displayed in Fig. 7-40 contain a sample set of results for slabs containing no GGBS for different surface finishes with the same aggregate type. It is interesting to note that one can observe differences due to surface undulations as the valleys on the surface may be slightly more in shadow and therefore heat up to a smaller degree. This would imply that the orientation of the striations does have an effect on the temperature variation across the surface. This is only possible to observe as there is no heat source or sink present i.e. the thermal image encompasses the surface of the slab only and excludes the surroundings, thus giving a more sensitive image with a low colour contour range.

It would appear by observing the colour of the thermal images that the tamp and brush finishes are the warmest, however, if one examines the individual temperature scales in addition to the cross-hair temperature (the number on the top left hand corner of each of the images), this is not the case. It can therefore be concluded that one needs to interpret the thermal images carefully as the colour of the images can be misleading.

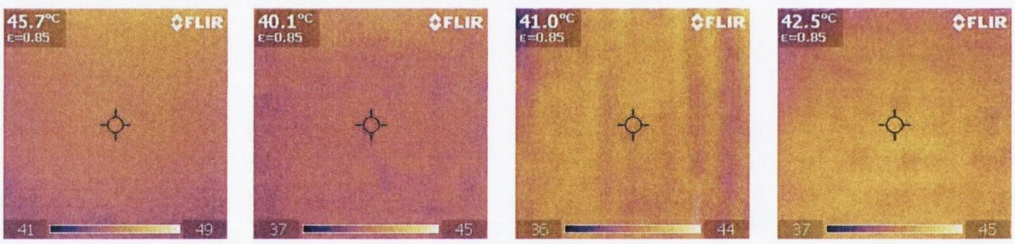

(a) (b) (c) (d)

Fig. 7-40 Thermal image displaying surface temperature of 0% GGBS specimens (27th July 2011) for (a) cast, (b) screed, (c) tamp and (d) brush surfaces

A summary of data is illustrated in Table 7-31 which contains the surface temperature result for each of the 16 specimens from board 2, which contains PCL aggregate. In terms of surface finish, the results show that the cast finish reaches the highest surface temperature in all cases and the screed finish is the lowest, with tamp and brush finishes having similar temperatures. As the cast finish is darker in colour, it is absorbing more radiation, therefore, reaching a higher temperature. The brighter screed finish is reflecting more of the sun's radiation thus experiencing a lower surface temperature. This strongly confirms the outcome from the greyness index chart, which in itself is not an accurate method. It may also be noted that the ambient air temperature is approximately 28°C and the slab surfaces are as high as 45°C, which demonstrates how warm the specimens get even in a temperate climate.

In terms of the effect of GGBS concentration on the surface temperature, this factor does not present as strong a trend as that of surface finish. For the 70% cast and screed slabs, these recorded a higher temperature than the 50% specimens and this may be due to the visible ageing of these slabs which was noted previously using the greyness index chart. In general, there is a reduction in temperature from 0 to 70% GGBS specimens, however, it is possible to conclude that it is more difficult to differentiate between specimens containing different levels of GGBS than by surface finish i.e. the difference between adjacent concentrations such as 0 and 30% for example.

Table 7-31 Surface temperature readings for specimens located on board 2 (July 2011)

% GGBS	Cast	Screed	Tamp	Brush
0	45.7°	40.1°	41.0°	42.5°
30	45.1°	40.4°	39.3°	41.0°
50	41.8°	39.2°	40.9°	41.5°
70	42.8°	40.3°	40.7°	40.7°

A general summary of thermal imaging is displayed for 0 and 70% GGBS in terms of the finish type in Table 7-32. The table was presented in this way as the surface finish type is the dominating factor affecting the surface temperature of the specimens. The order of increasing surface temperature for both 0 and 70% GGBS is screed, tamp, brush and cast, with only a marginal difference in temperature between tamp and brush. This confirms the greyness index chart and the lux meter results.

Table 7-32 Summary of thermal imaging displaying order of increasing surface temperature in terms of surface finish type for 0 and 70% GGBS (Sweeney et al., 2012a)

GGBS (%)	Surface finish
70	Screed Tamp Brush Cast
0	Screed Tamp Brush Cast

7.5.3 Conclusions

- By comparing screed and cast surface finishes directly, the screed finish is darker than the cast finish on the thermal image which confirms that the screed finish is cooler on the surface and therefore emitting less thermal radiation, and it is thus cooler.

- The thermal image displays some bright spots which is the sun being reflected off the timber surface underneath. This suggests that there is some reflected radiation, however, the general thermal image predominately displays emitted radiation. It is therefore recommended that one should take the slab out of the sun just prior to taking a thermal image to get a more accurate temperature reading.
- When a thermal image is taken in isolation (excluding all surroundings beside the slab), the advantage of this is that one obtains a better idea of the variation across the surface as well as the individual temperatures; for example, one can see the striations and differences over the surface, which cannot be seen in the other thermal images due to the contrasting colours given by the contours. In addition, the image is more sensitive due to the absence of heat sources or sinks. However, there is also an advantage to taking a thermal image of the specimens beside one another as the specimens can be directly compared with one another using the same temperature scale. In conclusion, the thermal imaging camera can be used to show variations in the surface temperature provided there are no heat sources or sinks. A more expensive camera may allow one to specify the colour contour scale which would allow more direct comparisons.
- One should be careful when interpreting the thermal images as both the scales on the image as well as the temperature recorded on the top left hand corner need to be considered, as the colour on the thermal image can sometimes be misleading. In addition, the emissivity of the material is required in order to obtain the temperature reading.
- The effect of surface finish for the cast and screed specimens was also analysed, and where there is no GGBS in the specimen the difference between cast and screed finish is 3.2°C, and where there is 70% GGBS present a difference of 3.4°C is recorded. This result would confirm that the effect of surface finish on the surface temperature is as important as the effect of GGBS concentration, if not moreso.
- The overview of the tamp and brush specimens, with the four GGBS specimens on one thermal image, suggested that there is an appreciable difference in surface temperature between 30 and 50% GGBS specimens. This is evident on the thermal image by observing the colour variation, as the 0 and 30% specimens are noticeably lighter in colour than the 50 and 70% specimens. This result would also confirm that the thermal images can differentiate between the extreme GGBS concentrations 0 and 70%, with the adjacent concentrations being more difficult to differentiate.
- The effect of surface finish on the surface temperature for the rough specimens tamp and brush is the dominant factor over the effect of GGBS concentration once more, with a high range in temperature difference between the tamp and brush finish specimens of the same GGBS content.

- The effect of GGBS concentration on the surface temperature demonstrated that this factor is not as strong as that of the surface finish, with weathering occurring in many of the 70% GGBS specimens.
- There is a reduction in temperature from 0 to 70% GGBS specimens which is confirmed by the greyness index chart and lux meter results, however, it is more difficult to differentiate between specimens containing different levels of GGBS using the thermal imaging camera.
- The order of increasing surface temperature/decreasing reflectance for both 0 and 70% GGBS is screed, tamp, brush and cast, with only a marginal difference in temperature between tamp and brush. This is broadly confirmed by the greyness index chart and the lux meter results, with some interchanging between tamp and brush.
- The temperature of the slab surfaces are significantly higher (approximately 40°C) when compared to the ambient temperature of the day (approximately 26°C), despite the temperate climate.
- The thermal imaging camera can be used in isolation to differentiate between differing concentrations of GGBS, however, it is easier to use it to distinguish between different surface finish types as this is the dominant factor.

7.6 Internal Temperature Variation with Sunshine Intensity

7.6.1 Introduction

The following section discusses the data obtained for internal temperature of the concrete slabs at various times of the year. Internal temperature values were recorded at a depth of 20mm from the surface of the slab using a thermocouple wire and the corresponding sunshine intensity was also recorded. Internal temperature data will be discussed in 3 primary subsections (under aggregate type), in each of which two different parameters will be assessed, namely, the effect of surface finish and the effect of GGBS concentration. The ageing aspect of the specimens will also be discussed.

Before beginning to describe the data, it may be useful to recap the observations on the data using the lux meter in Section 7.2. As described previously, in Chapter 4.0, the lux meter was used to measure the surface reflection of visible light from each slab. In general, the highest percentage reflectance was observed for the screed finished samples with the lowest for the cast specimens. The rougher surface finishes had similar reflectance, with the tamped finish typically slightly higher than the brushed finish. Similarly the 70% GGBS specimens had the highest light reflectance and the corresponding 0% slabs the lowest. Based on these trends, it would be expected that the specimens with higher light reflectance would have the lowest internal temperatures, as less light energy is absorbed into the material.

Following placement of the six boards (containing 96 slabs in total) on the roof of the Civil Engineering building in Trinity College, a data logger was installed to record the internal temperature variations in the slabs. At any given time, one board containing 16 specimens could be set up to record real time temperature of the specimens, for a period of approximately one week. The temperatures of the specimens were recorded at various time intervals throughout the course of the project. As the specimens were categorised and placed, primarily by their aggregate types (crushed limestone, partially crushed limestone and sandstone) on the roof, the results of temperature will be studied separately for each of the three aggregate types. Subsequently, the influence of both surface finish type and the concentration of GGBS in the samples will be examined within the aggregate type.

7.6.2 The influence of sunshine intensity on internal temperature

Firstly, it is important to study the influence of sunshine intensity on the internal temperature of the concrete specimens. A sunshine duration sensor (see Section 4.5) was fixed in place on the roof where the slabs are located. The purpose of this device was to measure and record the intensity of sunshine at the same time as the data logger records temperature of the slabs. By taking these measurements in tandem, the effect of sunshine intensity on the internal temperatures within each sample could be assessed.

The data presented in Fig. 7-41 demonstrates the influence of sunshine on the internal temperature of the concrete slabs. These results were obtained from samples on Board 1, comprising of crushed limestone aggregate, and were recorded over a period of three consecutive days in July 2011, indicated using the blue (day 1), red (day 2) and green (day 3) markers. The temperature of the four cast finish specimens together with the intensity of sunshine over time is plotted on the chart, and a strong relationship is evident between these two parameters.

There is no sunshine intensity observed on Day 2 (July 28th) of this particular testing period which would suggest that any change in the temperature of the specimens is as a result of the change in the ambient air temperature, which is between approximately 18 and 20°C. These cloudy conditions have a direct effect on the internal temperature variations of and between the four specimens that reach a peak of approximately 20°C. There is little separation in peak internal temperatures between the four specimens as a temperature range that is slightly greater than 1°C is observed on this day.

There is a small amount of sunshine present on Day 3 (July 29th), with a sunshine intensity of approximately 700W/m^2 and a duration of 2.5 hours. As a consequence, the specimens obtain a temperature of approximately 25°C, having a range in temperature of just 2°C. However, the sunshine intensity on Day 1 is approximately 850W/m^2, which denotes a clear and sunny day, and is observed for approximately 8 hours. The corresponding peak temperature observed in the 0% GGBS sample is approximately 40°C, despite the ambient air temperature being of the order of magnitude of 20°C. There is a distinct difference in the temperature of the four GGBS specimens ranging over approximately 5°C (from 35°C to 40°C) and this temperature differential will be discussed in more detail later in this section. This result differs greatly with the temperature differences observed on Day 2 and Day 3 of the testing period. The reason for the observed differences in both peak temperature and the temperature range between Day 1 and Day 3 are twofold. Firstly, although both days are clear and sunny, Day 3 has a lower peak sunshine intensity by approximately 200W/m^2. Secondly, the duration of this sunshine intensity also contributes to the overall internal temperature of the specimens.

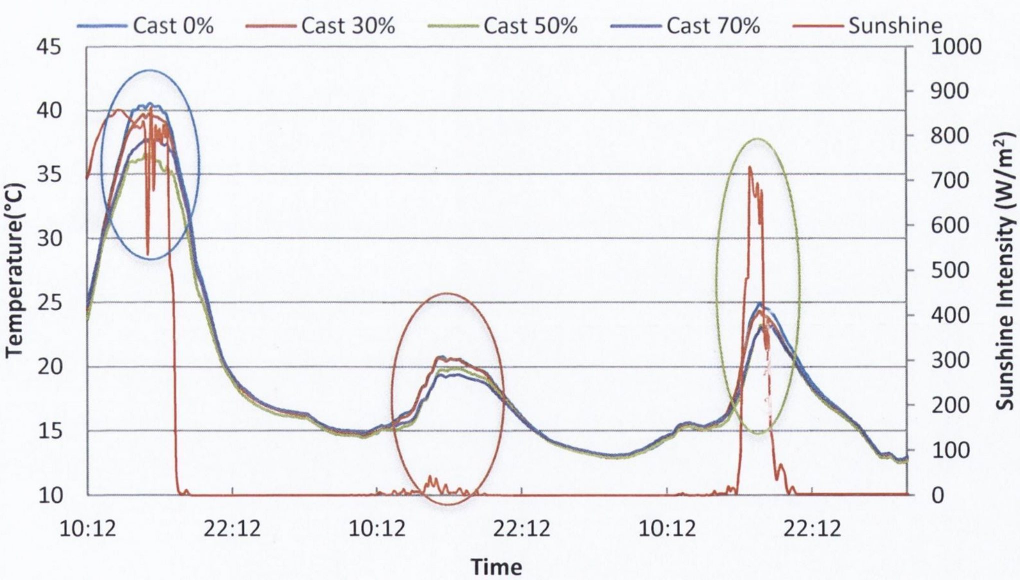

Fig. 7-41 Time vs. temperature and sunshine intensity for cast finish slab (board 1) – 27th-29th July 2011

In conclusion, there are three important factors in relation to sunshine which influence the internal temperature of the specimens, namely whether or not sunshine is present, its intensity and its duration. The temperature variation from 15-20°C during the day (see Day 2 where there is no sunshine present) is due to natural ambient increases and is not due to solar gain, therefore, this is the background change in temperature of the specimens due to the ambient change. The presence of sunshine is of fundamental importance as when there is negligible sunshine, i.e. deemed to be when sunshine intensity is less than $120W/m^2$, there will be little difference between the internal temperatures of the samples as indicated by the results observed on Day 2.

Secondly the intensity of sunshine plays a major role in increasing the internal temperatures of concrete and this indicates whether there are clouds present (between $120\text{-}500W/m^2$) or not (between $500\text{-}1000W/m^2$). When sunshine intensity is high, internal temperatures increase rapidly in the samples as illustrated on Day 1 of the test. Finally, the duration of the sunshine dictates the magnitude of the internal temperature observed as indicated by the data from Day 1 and 3. However, if there is continuous sunshine throughout the day, the slab reaches a particular temperature which is dictated by the intensity and duration of the sunshine, but only up until a certain point. The specimen reaches an equilibrium whereby the convection downwards and the significantly increased radiation from the surface reach a plateau. On Day 1 sunshine intensity remained high for a period of 8 hours compared to just 2.5 hours on Day 3. As a result, the internal temperature is strongly dependant on the presence of sunshine first and foremost, and where this is the case, it is dependant on the intensity and duration of this sunshine.

7.6.3 Results of internal temperature for crushed limestone aggregate

Data analysis carried out on a single aggregate type (crushed limestone) is discussed in this section. Analysis of partially crushed limestone and sandstone samples are analysed in a subsequent section. Results will be considered based on GGBS content as well as finish type. In terms of completeness, when discussing the effect of GGBS content on the samples, all finish types will be discussed individually. Similarly for finish type, data collected from each GGBS concentration will be presented individually. The board numbers from which the data is chosen is selected on a random basis.

7.6.3.1 The Influence of GGBS on Internal Temperature

To identify any relationship between the internal temperature of a concrete slab and the concentration of GGBS used in their construction, it is necessary to eliminate the effect of any other potential parameters. Accordingly, the data illustrated in Fig. 7-42 was recorded on 12th March 2011, using the cast finished samples on Board 1. Despite being recorded in March, the internal temperatures observed in the samples reach a maximum value of approximately 14-

16°C shortly after noon. To aid in the analysis of the results, the sunshine intensity is superimposed on the chart. The sunshine intensity peaks range between approximately 500W/m^2 and 700W/m^2, indicating that it is a clear and sunny day, although conditions are noted as partly clouded around midday. Based on the trends in both sunshine intensity and internal temperature, a relationship between the two is observed as peaks in the temperature in the slabs corresponds with the peaks in sunshine intensity. A lag between the peak in sunshine intensity and the peak in temperature is observed, however, which suggests that the slabs take some time to heat up (as detected 20mm below the surface) from the incoming sunshine, as the surface heat generated by solar rays is conducted through the slab depth. This was also observed and commented upon in the fundamental study on the physical characteristics in Section 6.2. This lag can be verified by observing the time delay between the peaks for sunshine intensity and temperature. For example, the first peak in sunshine intensity occurs at 10:00 and the first peak in temperature occurs at 10:30, 30 minutes after the peak in sunshine. Similarly, the maximum peak in sunshine intensity occurs at 11:20, and the corresponding maximum temperature occurs at 12:00, with a broadly similar lag of 40 minutes.

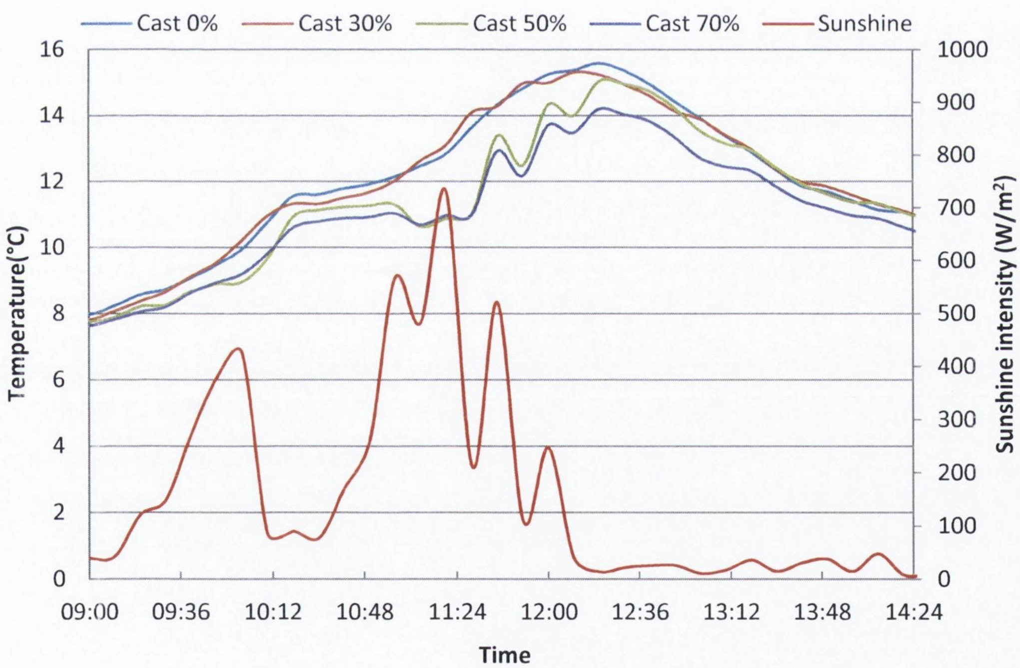

Fig. 7-42 Time vs. temperature and sunshine intensity for cast finish slab – 12th March 2011

The temperature trends give a good representation of diurnal variations observed in the concrete specimens on sunny days. Initially, the internal temperatures of the samples are all very similar, recording a value of approximately 8°C as they increase gradually with the ambient air. At approximately 09:10, sunshine intensity begins to increase whereupon the samples with lower GGBS concentrations, i.e. 0% and 30%, experience an increase in internal temperature at a higher rate than the corresponding temperature change noted in the samples with higher GGBS concentrations, such that the temperature in the former slabs are noticeably higher from 10:00 onwards.

Due to the thermal properties of the concrete, a lag period is also observed between decreasing solar intensity and the internal temperature, as is the case between approximately 10:00 and 10:30 when the solar intensity decreases to 90W/m^2 and conditions are clouded. The rate of temperature gain in the samples decreases in accordance with the clouded conditions and internal temperature plateau at approximately 10:20. During this time period, internal temperatures remain reasonably stable and do not decrease. The internal temperature between the four samples differ slightly in accordance with GGBS content i.e. a 1°C difference exists between 0% (11.9°C) and 70% (10.9°C), which is noteworthy considering that temperatures are reasonably low at the time.

Sunshine intensity begins to increase from 10:40 onwards as the clouds pass, reaching an initial peak at 11:00 (566W/m^2) before fluctuating to reach a maximum diurnal value of 731W/m^2 at 11:20. The corresponding peaks in temperature associated with the maximum sunshine intensity occur at approximately noon. At this point, a relatively large separation occurs between the low and high GGBS concentration. Similar internal temperatures are observed at 0% (15.3°C) and 30% (15.0°C) while a larger difference in internal temperature exists between the 50% (14.3°C) and 70% (13.7°C). This would suggest that a threshold exists above which GGBS dominates the behaviour of the specimens and below which NPC dominates the behaviour of the specimens. There is a 1.6°C temperature difference between the 0% and 70% GGBS samples. Accordingly it can be seen that, as solar intensity increases over the course of the day, the temperature difference increases across all samples, but in particular between 0% and 70% specimens, as the lighter coloured 70% GGBS concrete reflects a larger percentage of light, resulting in consistently lower internal temperatures when compared to the other samples.

When maximum internal temperatures are observed, the difference between the 50% (15.1°C) and 70% (14.2°C) samples increases as the 50% sample approaches temperatures values similar in magnitude to those recorded in the low GGBS concentration specimens. The samples containing 0 and 30% GGBS appear to plateau as relatively small increases in internal temperatures are observed in the 0% (15.3°C to 15.6°C) and 30% (15.0°C to 15.3°C) samples when compared with the 50% (14.3°C to 15.0°C) and 70% (13.7°C to 14.2°C) samples. When clouded conditions occur from approximately noon onwards, the internal temperature of the 0%, 30% and 50% samples converge at a temperature of approximately 14.8°C while the 70%

sample experiences a slightly lower temperature initially. However, as the values reduce, the 70% sample begins to approach the same temperature as the other three samples, which cool down at a marginally quicker rate.

In comparison, data recorded for a screed surface finish slab over the same period in March are displayed in Fig. 7-43. The overall trends in the internal temperatures recorded in the screed sample are similar in nature to those observed in the cast samples as discussed previously. Once more the low concentration GGBS samples appear to attain higher internal temperatures than the high concentration specimens. The maximum temperature for the slabs having a screed finish is approximately 14°C and occurs sometime after the sun is hidden by cloud. The main difference between the cast finish and screed finish specimens is the difference in the maximum temperature, which is approximately 2°C lower for the screed slabs. One would expect that there are equal differences in temperature between the adjacent GGBS concentrations, however, there is a recurring trend whereby the 0 and 30% specimens are closely grouped in temperature, and 50 and 70% specimens behaving similarly. The peak temperature difference between the 0 and 70% specimens is approximately 2°C which is significant considering the maximum temperature reached by the slabs is just 14°C. It is also important to note that the lag between the peak in sunshine intensity and the peak in the temperature of the specimens ranges between approximately 30 and 40 minutes.

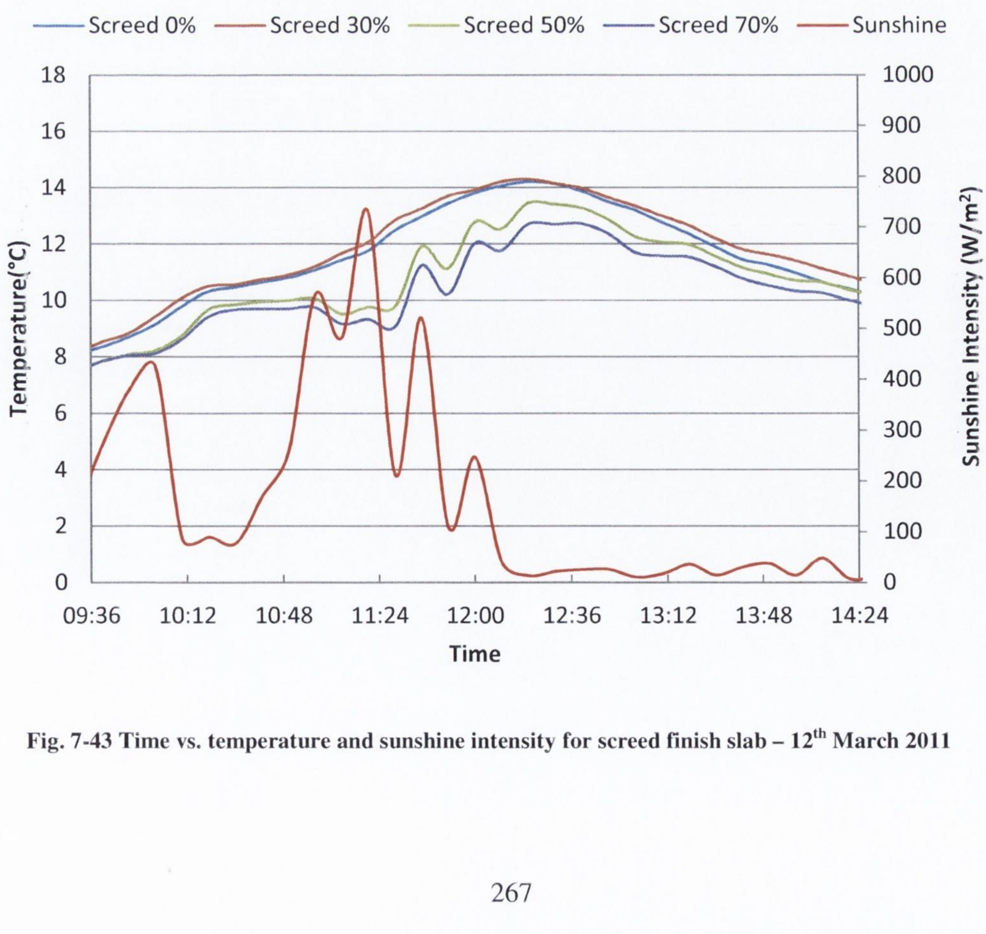

Fig. 7-43 Time vs. temperature and sunshine intensity for screed finish slab – 12th March 2011

To determine whether GGBS content influences rough surfaces in the same manner as the smoother surfaces discussed previously, Fig. 7-44 displays results recorded on April 21st 2011 for a tamped surface finish, with the four specimens ranging from 0 to 70% GGBS. The maximum slab temperature on this particular day is approximately 33°C. Although the sunshine intensity is not recorded on this occasion, the temperature of the specimens is higher than the previous results from Board 1, with the change in temperature being uniform. Therefore, the sunshine intensity and duration are likely to have been consistent and higher during the course of the day, particularly as it is one month later and closer to the summer. There is further evidence for this discussed later on.

As in the previous results for the smooth surface finishes, the specimens containing 0 and 30% GGBS are grouped closely together as are the 50 and 70% samples. The four specimens are at the same temperature at the start of the day, but as the day progresses, there is a distinct difference in the rate of change in temperature. The specimens containing 0 and 30% GGBS have a higher rate of change in temperature than the specimens containing higher levels of GGBS. The maximum temperatures obtained for 0, 30, 50 and 70% GGBS are approximately 33.0, 33.0, 29.5 and 28.0°C respectively and occur at about 15:00. The four specimens have returned to the same temperature by approximately 19:00.

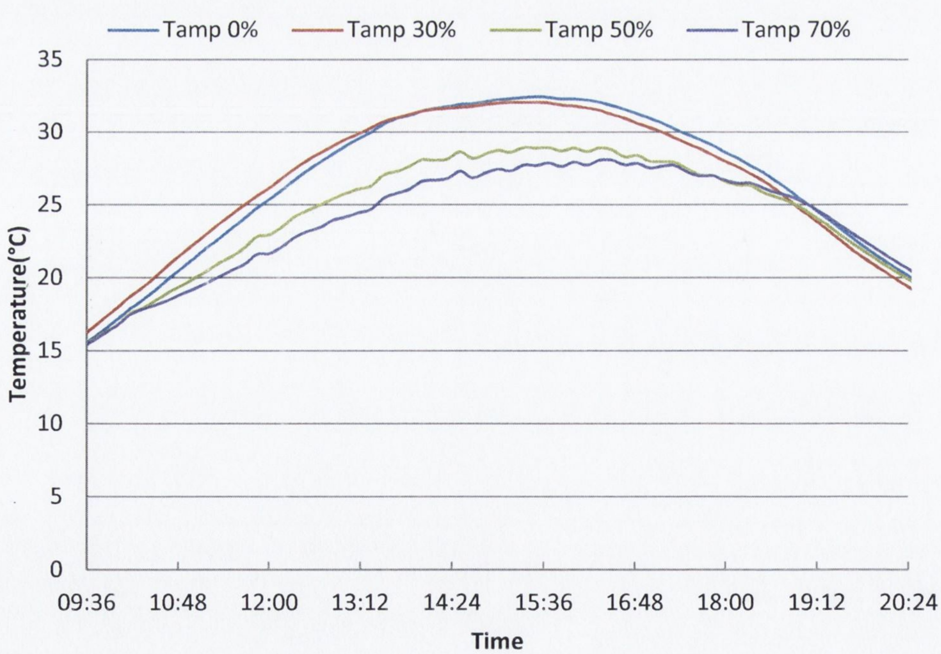

Fig. 7-44 Time vs. temperature for tamp finish slab – 21st April 2011

For completeness, the chart displayed in Fig. 7-45 represent temperature change for a brush finished surface on April 21st 2011 also. As in the aforementioned results for a tamped surface finish, the specimens with a brushed surface finish are displaying similar trends. The slabs containing 0 and 30% GGBS remain closely grouped in temperature. The specimens containing 50 and 70% GGBS, however, have a lower rate of change of temperature, with the slabs having a peak temperature difference of 2°C. The peak temperatures of 0, 30, 50 and 70% GGBS slabs which occur at about 15:00 are approximately 33.0°C, 33.0°C, 30.0°C and 28.0°C respectively, similar to the tamped slabs.

In conclusion, the results for the four different surface finishes would imply that, irrespective of the temperature reached by the specimens, the same trend is observed throughout. The temperature for slabs containing 0 and 30% GGBS are closely grouped, having almost identical temperatures. The temperature of the slabs containing 50 and 70% GGBS follow a similar trend, however, there is a difference in temperature between these specimens. The result overall would imply that the presence of GGBS has a significant influence on the internal temperature of the specimens, with the temperature difference of about 5°C. This can be explained by the simple fact that the addition of GGBS to concrete produces a concrete which is lighter in colour, and this results in increased solar reflectance from the surface of the slab thus reducing the internal temperature.

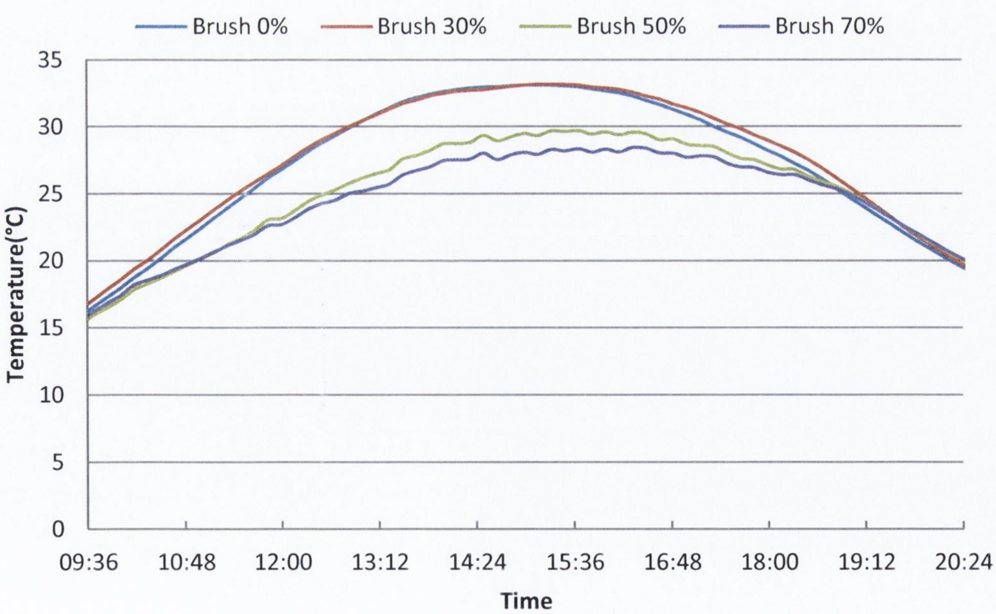

Fig. 7-45 Time vs. temperature for brush finish slab – 21st April 2011

7.6.3.2 *The influence of Surface Finish on internal temperature*

In order to assess more closely the influence of surface finish on internal temperature, two levels of GGBS are chosen from Board 5 (0 and 50%) and two from Board 1 (30 and 70%) which contain the same aggregate type. The data observed for the specimens containing 0% GGBS are displayed in Fig. 7-46. These readings were recorded on 2nd July 2011. The lag between the sunshine intensity and the temperature of the specimens is apparent here once more. In the morning at approximately 09:30, there is already a clear distinction in temperature between the four surface finishes as a result of the sunshine intensity between 07:30 and 09:00, which reaches a peak of approximately 600 W/m^2. The temperature of the specimens reach a peak temperature approximately 30 minutes after the first peak in sunshine intensity occurs. In the order of decreasing temperature they follow the order of cast (21.7°C), brush (20.5°C), tamp (20.0°C) and screed (19.4°C), a range of approximately 2°C.

As the sunshine intensity reaches a maximum of 800W/m^2, there is a corresponding increase in temperature of the four specimens some time later, with a difference in the peak maximum and minimum temperature of approximately 4°C. The temperature of the specimens reach a peak approximately 40 minutes following the peak in sunshine intensity. The cast finish remains the highest in temperature at 33.0°C, followed by the brush finish at 30.3°C. The specimens which are lowest in temperature are screed and tamp, having the same temperatures of approximately 29.0°C in the early afternoon. As the sunshine intensity decreases later on in the day due to cloudy conditions, the difference in temperature between the four surface finishes also decreases, with the cast finish remaining the highest in temperature by approximately 2°C. There is a final increase in the specimen's temperatures around 16:50 corresponding with the increase in sunshine intensity at approximately 16:30 to 700W/m^2, before reducing in temperature once again in the evening. There is a short lag of approximately 20 minutes evident between the peak in sunshine intensity and the peak in the temperature of the specimens.

There is a large fluctuation in the temperature of the specimens during the day, and this is as a result of the change in the sunshine intensity over the course of the day. It can therefore be concluded that the sunshine intensity is considerably more important than the background ambient air temperature. The lag between the peak in sunshine intensity and temperature of the specimens ranged between 20 and 40 minutes.

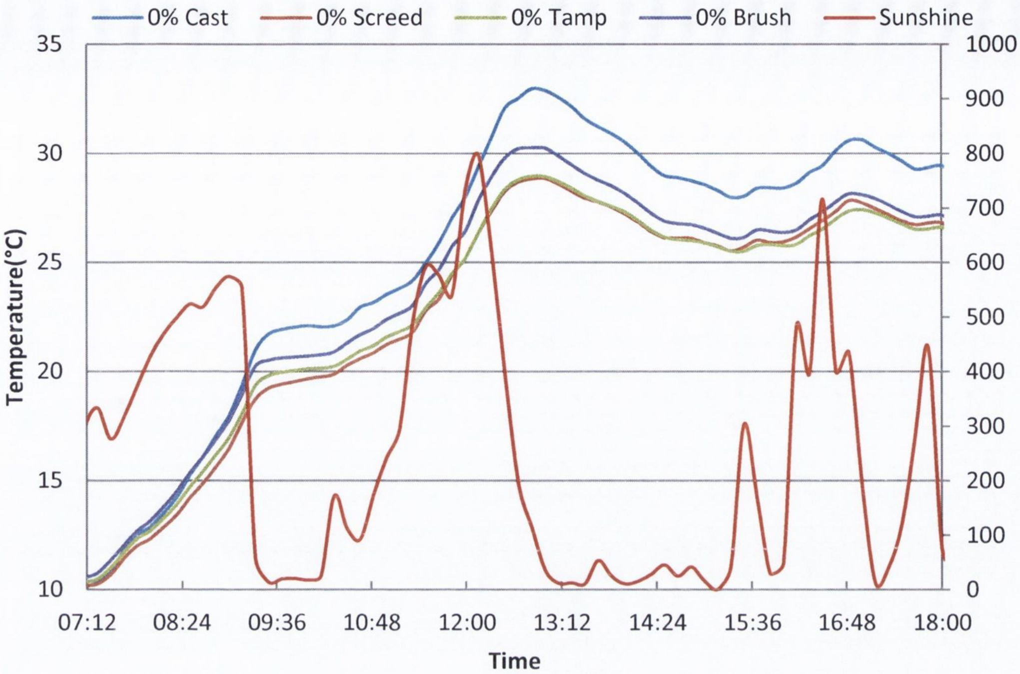

Fig. 7-46 Time vs. temperature and sunshine intensity for 0% GGBS specimens – 2nd July 2011

The results for specimens containing 50% GGBS are displayed in Fig. 7-47, also from 2nd July for Board 5. In general, these results are broadly similar to the 0% GGBS results as they were recorded on the same day. In the morning at approximately 07:00, the sunshine intensity begins to increase and this produces a corresponding separation of the temperatures of the surface finishes at approximately 09:00, with cast having the highest temperature (20.8°C), brushed and tamped having an intermediate temperature (19.6°C) and screed having the lowest temperature (18.6°C), an overall temperature range of approximately 2°C. There is a lag between the peak in sunshine intensity (occurring at 09:00) and the peak in the temperature of the specimens (occurring at 09:30) of approximately 30 minutes. The temperature of the samples continues to increase until it reaches a peak temperature at midday, which is as a direct result of the sunshine intensity reaching a peak at 800W/m^2. The lag evident here is approximately 40 minutes, with the peak in sunshine intensity occurring at 12:10 and the peak in temperature of the specimens occurring at 12:50. The cast sample maintains the highest temperature of 29.3°C, with brush and tamp having identical temperatures of 28.4°C. The screed remains the lowest in temperature at 27.0°C. The overall range in temperature is approximately 2°C. The last peak in sunshine intensity occurs at 16:30 in the afternoon, with the peak in the temperature of the specimens occurring 40 minutes later at 17:10.

At the time of testing, the orientation of the striations in the rough surface slabs were not taken into account, therefore, if the sun is shining parallel to the striations there will be no shadows cast on the slab and it will heat up even more. However, if one turns the slab through 90°, particularly when the sun is low early in the day, there will be shadows cast on the slab by the striations and it is possible that the temperature increase might be slightly different.

This lower temperature range when compared with the same peak temperature range in Fig. 7-46 is as a result of the specimens having 50% GGBS present. The range in the lag period between the sunshine intensity and the temperature is still between approximately 30 and 40 minutes.

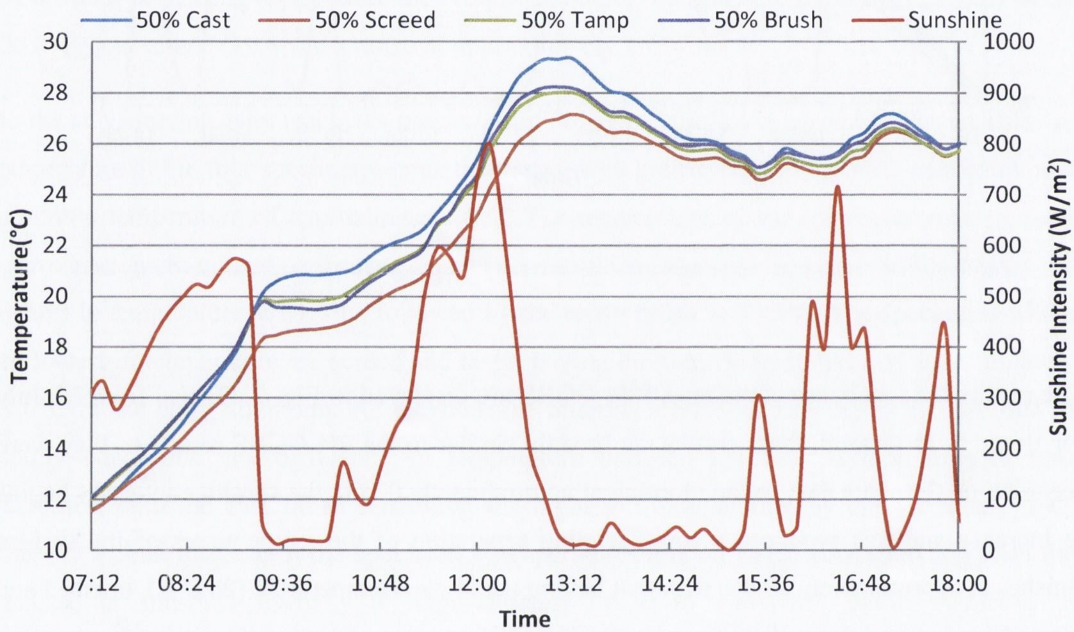

Fig. 7-47 Time vs. temperature and sunshine intensity for 50% GGBS specimens – 2nd July 2011

The plot displayed in Fig. 7-48 represents results for 30% GGBS specimens from 30th July 2011. These results are noticeably different to the previous two plots for 0 and 50% GGBS and the trends are not so clear here, as they were recorded on a different day in July where there was much intermittent sunshine. The four different surface finish types are indicated in the plot. There are two noticeable peaks of sunshine intensity which will be discussed and these are circled on the chart. The first peak occurs at approximately 10:25, which is the maximum sunshine intensity recorded on this particular day (750W/m^2). This first peak in sunshine intensity corresponds to a peak in the temperature of the specimens which occurs at approximately 11:05, a lag of approximately 40 minutes, where the temperature of brush, cast, tamp and screed finishes are 25.6°C, 25.0°C, 24.5°C and 23.1°C respectively. There is a lag present between the peak in the intensity of sunshine and the peak temperature of the specimens due to the low conductivity of the concrete and is outlined in the figure with an arrow illustrating where the lag occurs. The second main peak in sunshine intensity of 570W/m^2 occurs at 12:25. This peak in sunshine intensity corresponds to the maximum peak temperatures of the specimens which occurs at approximately 13:00, a lag of 35 minutes. The maximum temperatures of the brush, cast, tamp and screed finishes are approximately 30.0°C, 30.0°C, 27.7°C and 26.6°C respectively. At this point the cast surface finish remains the highest in temperature of the four specimens.

The lag times for this plot are somewhat unclear due to the nature of the sunshine intensity on this particular day, therefore, it is more difficult to differentiate between the differences in the peak temperatures, however, despite this fact the overall range in the lag periods is between 35 and 40 minutes. The general order of surface finish in terms of increasing reflectance (decreasing temperature) is cast/brush, tamp and screed. Although the sunshine intensity has started to drop off by 14:24, there is still a range of approximately 2°C between the surface finishes at 16:48 and the rate of cooling is slower than the rate of heat gain.

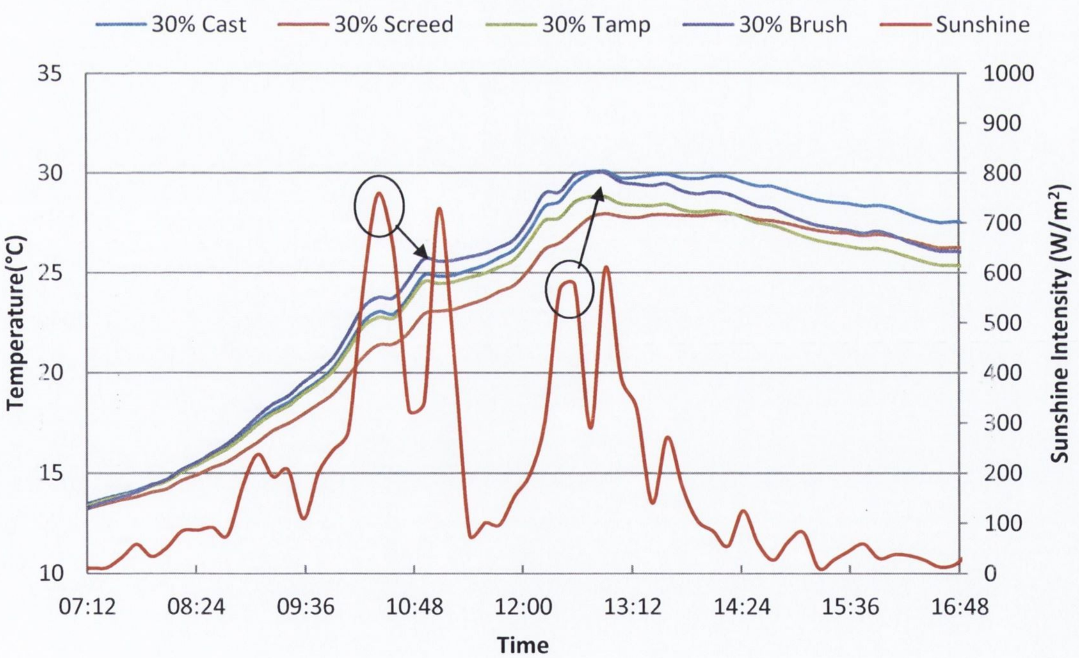

Fig. 7-48 Time vs. temperature and sunshine intensity for 30% GGBS specimens – 30th July 2011

The results for 70% specimens are displayed in Fig. 7-49 also for 30th July 2011. The two primary peaks in sunshine intensity correspond with the peaks in temperature of the specimens as the arrows in Fig. 7-49 indicate, with similar lag times observed here of between 35 and 40 minutes. The results for 70% GGBS concentration are broadly similar to that of 30% GGBS in that the order of surface finishes is the same. The order of increasing reflectance/ decreasing temperature of the four specimens is consistent over the duration of the day. The specimens reach their peak in temperature of 29.3°C, 28.0°C, 26.8°C and 25.7°C for cast, brush, tamp and screed finish slabs respectively.

In conclusion, the type of surface finish has a measurable effect on the temperature of the specimens. The smooth cast finish has the highest temperature, however, the screed surface finish which is also a smooth surface finish, maintains the lowest temperature. This would suggest that not only does the nature of the surface finish (smooth or rough) have an influence on the temperature of the specimens, but also the mechanism by which the surface finishes are achieved. The cast surface finish is attained from the underside of the formwork, therefore it is a more porous and darker finish. This differs from the screeded finish, whereby a steel float is used to close off the surface of the specimen (sealing the pores) while bringing some of the cement fines to the surface, making the concrete visibly brighter in colour. The condition of the pores will mainly affect ageing, discussed presently. The intermittent sunshine is the main reason for the fluctuations in the temperatures of the specimens, however, the temperature differentiation between the specimens is evident despite this fact.

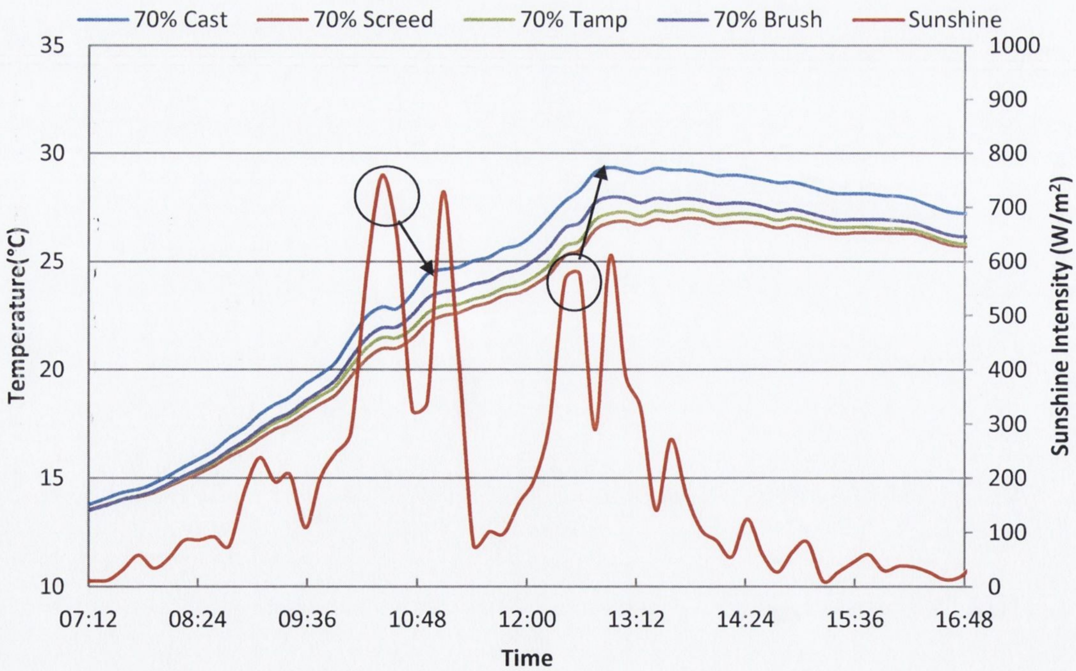

Fig. 7-49 Time vs. temperature and sunshine intensity for 70% GGBS specimens – 30th July 2011

In conclusion, the greatest segregation in the surface finishes is seen where there is a significant amount of sunshine present. The influence of the four different surface finishes on the internal temperature of the slabs is evident for all levels of GGBS replacement, with the level and duration of sunshine intensity greatly affecting the overall temperature difference between the specimens. In general, the order of decreasing temperature in terms of finish type is cast, brush/tamp and screed, with the range in temperature across the finishes being strongly dependant on the properties of the sunshine such as the duration and intensity, in addition to lower temperatures with increasing GGBS percentage, but to a lesser extent than the surface finish. The cast specimen is darker in colour than the others and so this property seems dominant over the roughness or GGBS composition.

7.6.4 Results of internal temperature for partially crushed limestone aggregate

It is difficult to compare different aggregate types to determine whether or not the aggregate type makes a difference as the sunshine intensities are different on different days. However, the trends are generally the same for the different GGBS concentrations and surface finishes. The order in which the surface finish and GGBS content affect the peak temperature will be given in the discussion at the end for all of the plots (including plots in the appendices). For illustrative purposes, one example will be presented to demonstrate the influence of GGBS on internal temperature, and likewise for the influence of surface finish type on internal temperature. The remaining plots for GGBS content and surface finish type can be found in Appendix FF and Appendix GG respectively.

7.6.4.1 The influence of GGBS on internal temperature

The aggregate partially crushed limestone is present in the slabs situated on Board 2 and 6. The results outlined in Fig. 7-50 were recorded in March 2011, and are for cast finish specimens with varying concentrations of GGBS. The duration of sunshine intensity for this day is between approximately 09:00 and 18:00 with few interruptions in the intensity of the sunshine. This plot is somewhat different to the previous plots as there is sunshine all day including the late afternoon. As a consequence, the temperature curve is much more uniform in behaviour. The four cast finish specimens are originally at the same temperature at 08:30, however, this changes once there is sunshine present. The temperature of 0 and 30% GGBS specimens group together, along with 50 and 70% specimens as seen previously. This result is reoccurring and is due to a threshold which exists above which GGBS dominates the behaviour of the specimens and below which NPC dominates the behaviour of the specimens. The 0 and 30% specimens increase in temperature at a higher rate than the 50 and 70% specimens. Also, at 11:00 the temperature of 50 and 70% specimens separate, as the specimen containing the higher level of GGBS (70% GGBS) maintains a lower temperature. This does not occur until approximately 13:00 for the case of the 0 and 30% specimens.

The sunshine intensity reaches a maximum of $900W/m^2$, and as a result, the maximum temperature of 0, 30, 50, and 70% specimens at 15:00 is 21.4°C, 20.5°C, 17.0°C and 15.5°C respectively. There is a temperature difference of almost 6.0°C between 0 and 70% GGBS specimens due to the fact that the sun is out all day, which is very significant considering the temperate climate of Ireland in addition to the time of year the test was conducted. The sunshine intensity drops off at approximately 16:00 as the sun is setting, with the temperature of the four specimens decreasing accordingly. It is difficult to distinguish a lag between the peak sunshine intensity and the peak temperature as there is continuous sunshine for the most part of the day.

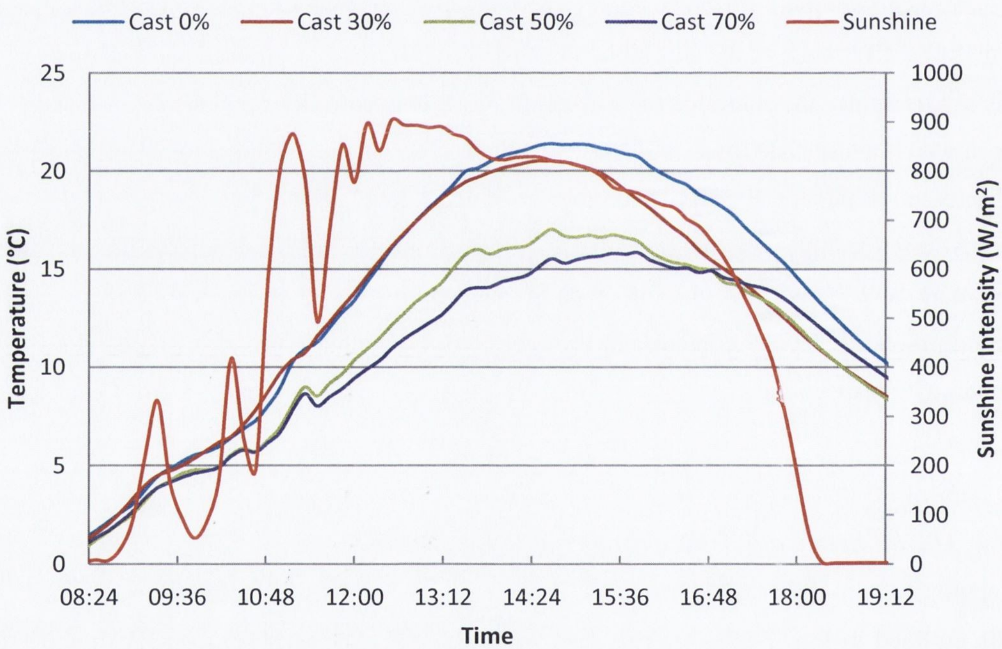

Fig. 7-50 Time vs. temperature and sunshine intensity for cast finish specimens – 16th March 2011

In conclusion, the general trends observed for partially crushed limestone are very similar to that of the trends observed for the specimens containing crushed limestone aggregate in terms of the order of the specimens and the grouping of results, despite the different sunshine intensities on the different days. Thus, possible small differences in thermal conductivity of different aggregates in concrete do not materially affect the results. The order of decreasing temperature corresponds directly with the percentage of GGBS contained in the specimen i.e. 0% GGBS has the highest internal temperature and 70% GGBS the lowest, therefore, it is possible to confirm that GGBS has a strong influence on the internal temperature of the slab. This result can be explained by the simple fact that the addition of GGBS to concrete produces a concrete which is lighter in colour, and this results in increased solar reflectance from the surface of the slab thus reducing the internal temperature. Similarly, the findings for partially crushed limestone correlate with those of crushed limestone, whereby the 0 and 30% specimens are closely grouped in temperature, and the 50 and 70% specimens alike. This separation in the results would suggest that a threshold exists above which GGBS dominates the behaviour of the specimens and below which NPC dominates the behaviour of the specimens.

7.6.4.2 The influence of Surface Finish on internal temperature

The results for 50% specimens from April are presented in Fig. 7-51, with the sunshine intensity included. This particular day shows constant sunshine throughout the day, beginning at 06:00. The intensity of this sunshine increases slowly before reaching a maximum intensity of 900W/m^2 at approximately 11:00, which signifies a clear and sunny day. The sunshine intensity does not drop below 700W/m^2 until 18:30 in the evening where clearly hours of sunshine are longer than in March in Fig. 7-50. There is a separation in the temperature of the four specimens as early as 09:00, with the cast surface finish having a higher rate of increase in temperature, and screed the lowest as expected. The tamped and brushed surface finishes have the same temperature. Once again, unfortunately the orientation of the striations were not taken into account, therefore, this could account for the variation in the peak temperatures for the rough surface finishes. The peak temperature of cast, tamp, brush and screed are 32.3°C, 30.3°C, 29.4°C and 28.4°C respectively, an overall range of approximately 3.5°C. This result is somewhat similar to the previous results, however, the tamped and brushed surface finishes have reversed in temperature. The cast remains at the top in terms of temperature and this is due to the specimen having a visibly darker colour than brush for example. The opposite is the case for the screed surface finish which remains the most reflective and has the lowest temperature due to the specimen having a visibly brighter colour and a smooth surface. This would suggest that the colour of the specimen is clearly more important than the influence of the surface finish on internal temperature.

There is a lag evident between the peak sunshine intensity (occurring at 11:50) and peak temperature of the specimens (occurring at 14:10), which is just over 2 hours. Although for short term peaks as seen previously, which gives rises to undulations in the temperature of the concrete, where there is prolonged amounts of sunshine intensity as in Fig. 7-51, it is the energy that is imparted by that sustained high temperature which causes the temperature to increase. This sustained energy is depicted by the difference between the two occurring peaks, and is indicated by the two dashed lines in the plot.

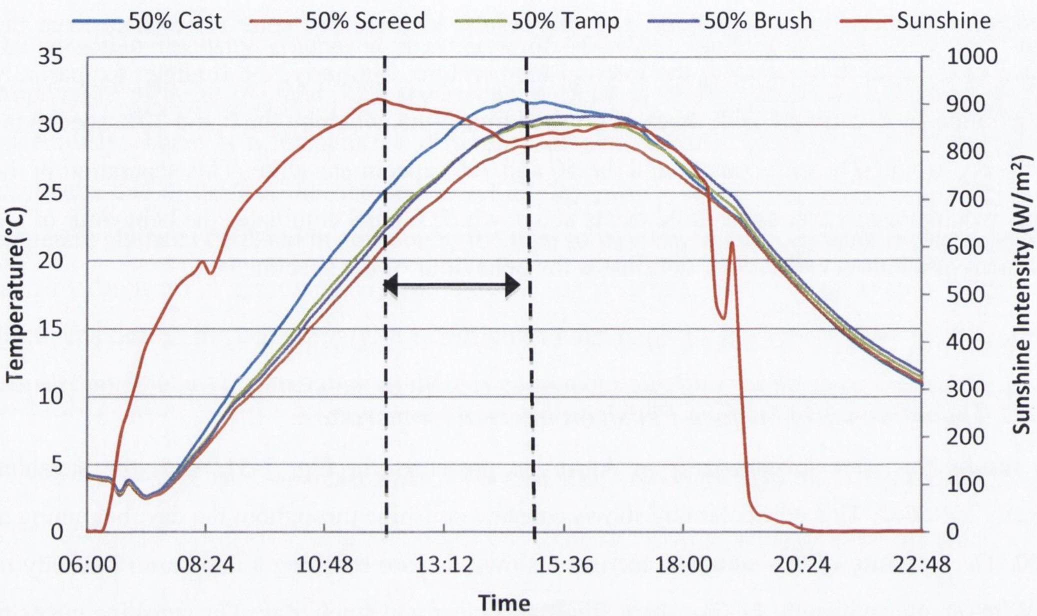

Fig. 7-51 Time vs. temperature and sunshine intensity for 50% specimens – 28th April 2011

In conclusion, the trends for all levels of GGBS for partially crushed limestone are consistent and show little if any difference to the crushed limestone results. Moreover, the nature of sunshine intensity on the test days has added new insights. The order of decreasing temperature/increasing solar reflectance is cast, brush/tamp, screed respectively. The colour of the specimen plays an important part in determining how reflective the specimen is, which was clearly evident by observing the difference in temperature between the two smooth surface finishes cast and screed. The rough surface finishes are identical in temperature except where there is a high level of sunshine intensity. There is some overlap between these specimens which could be accounted for by the orientation of the striations which were not always parallel to the sun's rays at the time of testing.

7.6.5 Results of internal temperature for sandstone aggregate

Similarly for the sandstone aggregate, as the results were recorded under different sunshine conditions compared to the other two aggregate types, it is difficult to determine definitively whether or not the aggregate type has any influence over the reflective properties of the specimens. The order in which the surface finish and GGBS content affect the peak temperature will be given in the discussion at the end for all of the plots (including plots in the appendices). The remaining plots for GGBS content and surface finish type which are not discussed in this section can be found in Appendix HH and Appendix II respectively.

7.6.5.1 The influence of GGBS on internal temperature

The sandstone aggregate is contained in the concrete specimens which are situated on Board 3 and Board 4. Results of internal temperature from these specimens will be presented and analysed in this section. Fig. 7-52 displays the results obtained in June 2011 from Board 3 in particular. These specimens have a cast finish with varying concentrations of GGBS. The plot demonstrates how the sunshine intensity varies on a perfectly sunny day in summer. The maximum specimen temperature was 45°C as evident by the graph which is significant given that the ambient air temperature on this day was approximately 21°C. The sunshine intensity begins to increase at 06:00 on this particularly sunny day and changes linearly until it reaches a peak of 900W/m^2 at approximately 13:00. The specimens begin to increase in temperature following the presence of sunshine at 06:00 and at 10:00 the specimens begin to separate in temperature as the brighter specimens reflect the sunlight and the darker specimens absorb it. A change in the internal temperature of the specimens is evident as a result. There is a lag between the peak in sunshine intensity (occurring at 13:00) and the peak in temperature of the specimens (occurring at 15:00) of approximately 2 hours. A similar lag was previously noted for a day where there was also a high level of sunshine intensity (see Fig. 7-51).

As seen in the previous results in Section 7.6.3 and Section 7.6.4, the specimens containing 0 and 30% GGBS stay in close proximity to one another with 50 and 70% specimens behaving in a similar manner. The sunshine intensity remains constant between 12:00 and 16:30 when it begins to decrease slowly as the sun begins to set. This high level of sunshine has a direct impact on the difference in temperature between 0 and 70% GGBS producing a larger than usual difference of approximately 6°C. The maximum temperature of the four specimens containing 0, 30, 50 and 70% GGBS are 44.6, 42.3, 38.3 and 38.3°C respectively, which occurs at approximately 15:00. There is a minimal temperature difference between 50 and 70% GGBS specimens which is once again a reoccurring trend, indicating possibly some ageing of the high GGBS concentration specimens (see Section 7.6.6). As the results were not recorded until approximately 8 months following the placement of the specimens, this may have been sufficient time for the specimens to age to a small degree.

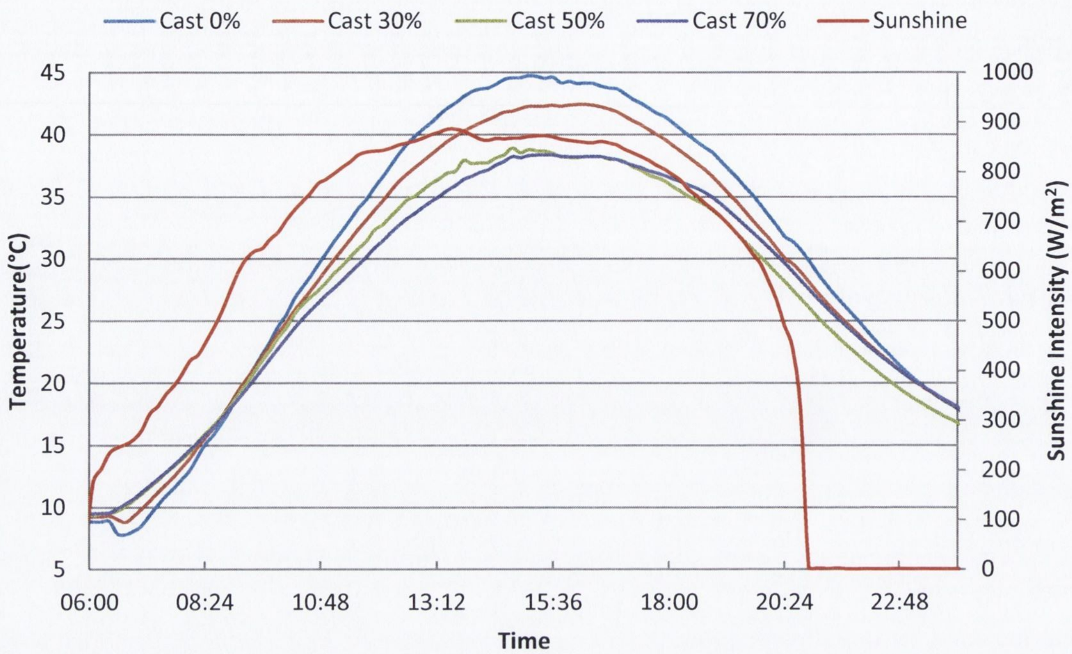

Fig. 7-52 Time vs. temperature and sunshine intensity for cast finish specimens – 3rd June 2011

The data for a brush finish slab are displayed in Fig. 7-53 with the corresponding sunshine intensity included. The specimen containing 0% GGBS has the highest temperature and 70% the lowest. Although the specimens having a brushed finish, the overall result remains the same in terms of the temperature differentiation between the specimens containing different levels of GGBS. The difference between 0 and 70% GGBS is lower when compared with the cast surface finish (see Fig. 7-52) which is due to the dispersion off the undulating surface as the sunshine intensity is the same. The maximum temperature reached by 0, 30, 50 and 70% brushed finish specimens is 41.2, 38.2, 37.2 and 37.2°C respectively, an overall range of 4°C.

In conclusion, the different surface finishes present broadly similar trends to the aforementioned aggregate types (crushed and partially crushed limestone) in terms of the order of the specimens. The addition of the cement replacement GGBS has a significant influence on the temperature gain in the specimens, with a larger substitution rate resulting in a reduced internal temperature in the specimen. The trends in temperature do not change, irrespective of the surface finish type. These trends are as follows; the increase in GGBS substitution results in a reduced temperature in the specimen and also the specimens have a tendency to group together with 0 and 30% being close in temperature, then a significant gap in temperature, then 50 and 70% samples are grouped together, having almost identical temperatures. Where there is a significant amount of sunshine intensity, the behaviour of the temperature is very uniform, and one observes a significant lag between the peak in sunshine intensity and the peak in the temperature of the specimens of approximately 2 hours. The peak temperature of the 0% GGBS specimens of 45°C when the ambient air temperature is 21°C indicates the potential extent of heating due to solar effects leading to the UHI effect, even in moderate climates such as in Ireland.

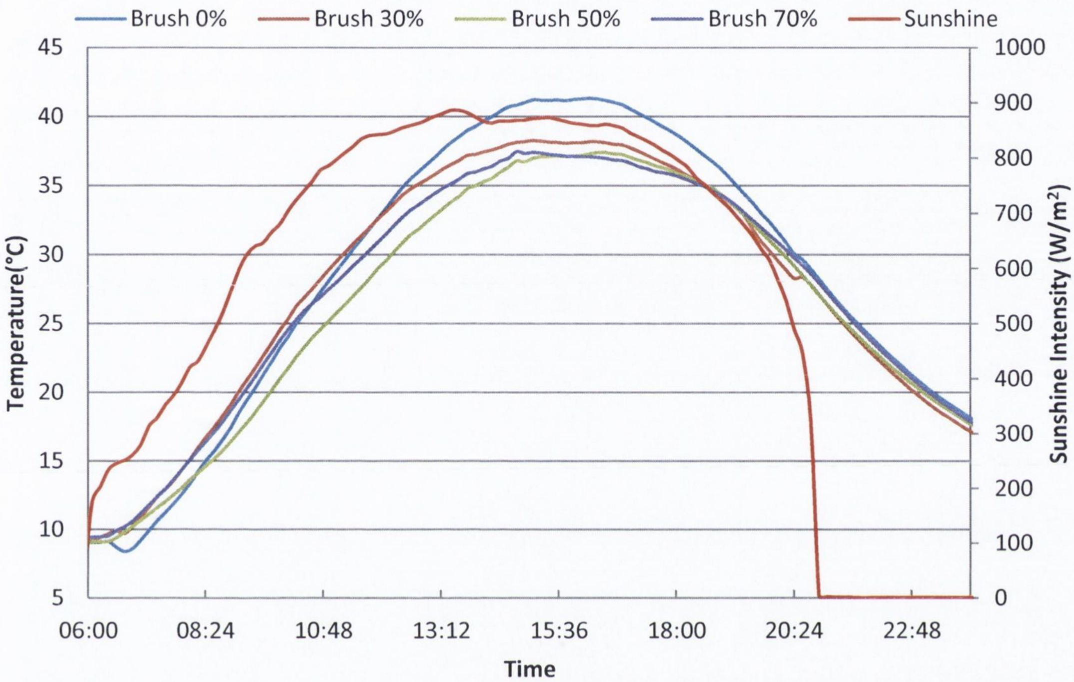

Fig. 7-53 Time vs. temperature and sunshine intensity for brush finish specimens – 3rd June 2011

7.6.5.2 The influence of Surface Finish on internal temperature

The following section focuses on the effect of surface finish on the internal temperature for the sandstone aggregate specimens. The two charts to be discussed are 0% GGBS (April 2011) and 70% GGBS (June 2011). The data for 0 is from Board 4 and the data for 70% GGBS is from the duplicate Board 3. The chart displayed in Fig. 7-54 represents the 0% GGBS specimens with the sunshine intensity included. The sunshine increases from approximately 09:30 to a maximum of 800W/m^2 at 12:30. There is a lag of approximately 2 hours in the temperature of the specimens which reach a peak temperature at 14:30. The order of decreasing temperature for the four surface finishes is as follows, cast (33.0°C), brush (32.4°C), tamp (31.0°C) and screed (30.8°C). This temperature difference maintains a plateau for approximately 2 hours before decreasing in the afternoon due to a dip in the sunshine which occurs between 14:30 and 16:30. The general order of the specimens in terms of surface finish is the same as for the two previous aggregate types. Once again it is difficult to determine whether the sandstone aggregate has any influence on the internal temperature as the trends between the specimens remain broadly similar despite different sunshine intensities.

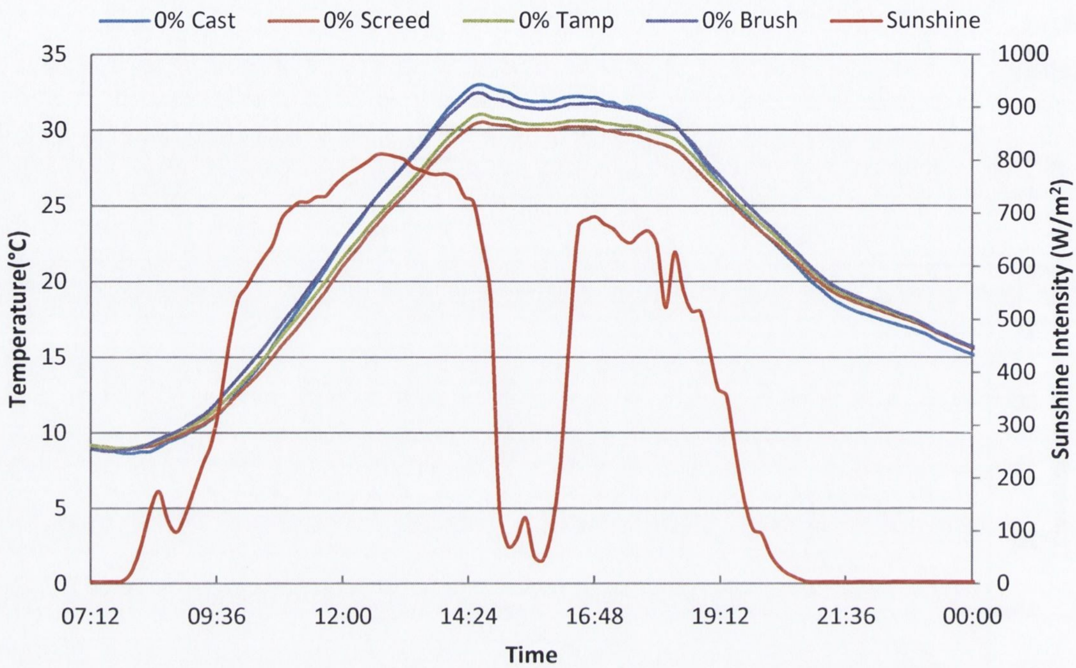

Fig. 7-54 Time vs. temperature and sunshine intensity for 0% GGBS specimens – 10th April 2011

The results for 70% GGBS are displayed in Fig. 7-55 and were recorded on a different day (2nd June 2011). The profile of the sunshine intensity would suggest that it is cloudy until approximately 12:30 where after the sunshine intensity begins to increase. At 13:30 a maximum of 833W/m^2 is obtained, and this level is maintained until approximately 17:30 before beginning to decrease as the sun sets. The peak in the temperature of the specimens for cast is 34.5°C and brush is the second highest at 33.0°C. The screed and tamp finishes have identical peak temperatures of 32.0°C, occurring at approximately 15:15. The cast finish maintains the highest temperature due to the visibly darker colour of the surface, however, there is an overlap between the screed and tamp finishes. As previously mentioned, the orientation of the striations was not taken into account during this testing, which could have affected the peak temperature reached by the rough surface finish specimens.

In conclusion, the two plots of GGBS for sandstone aggregate present the same trends as for the aforementioned crushed limestone and partially crushed limestone aggregates. The cast surface finish remains the highest in temperature and screed the lowest which is primarily due to the colour of these specimens as well as the nature of the surface finish, however, the rough surface finishes are not always consistent in their temperature profile. This inconsistency may be due to the dispersion of light by the rough surfaces in addition to the orientation of the striations which were not always parallel to the sun's rays during testing.

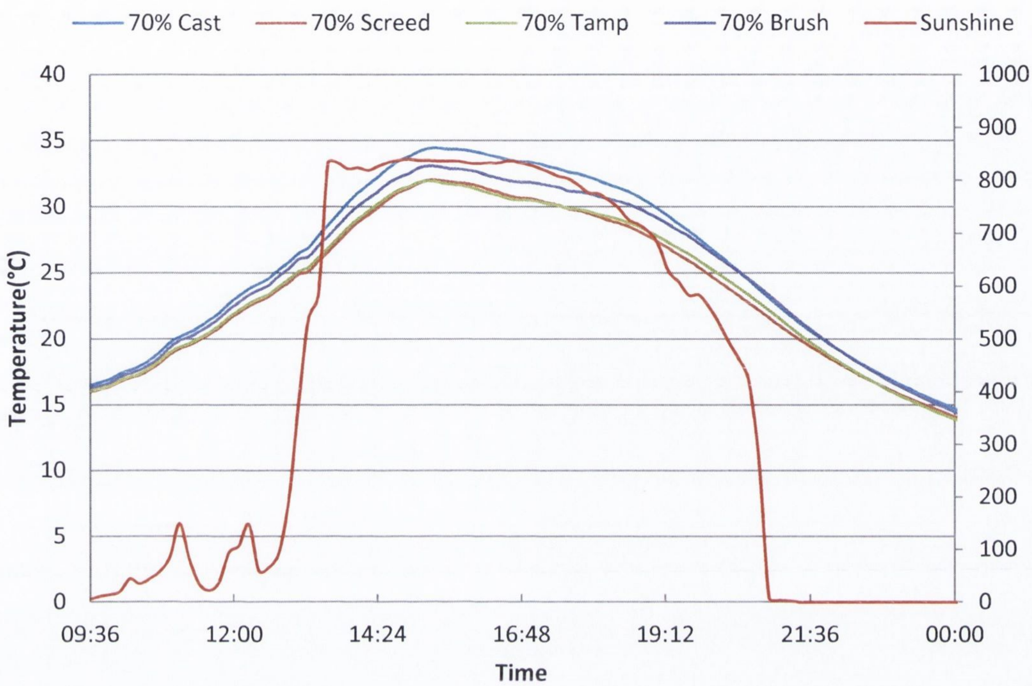

Fig. 7-55 Time vs. temperature and sunshine intensity for 70% GGBS specimens – 2nd June 2011

In terms of the aggregate type, it is not possible to state whether it has a definite influence on the internal temperature of the specimens but it appears to be slight. The plots are not comparable across the aggregate types as there were different sunshine intensities on the different days. Some minor change due to thermal conductivity may exist, giving rise to a slight difference in the lag times. However, it was possible to observe the trends present, in particular the difference in peak temperatures, the order of the specimens in terms of both finish type and level of GGBS, and the grouping of the results. From this it is possible to conclude that the aggregate type does not make any noticeable difference to the temperature observed in the specimens. This means of testing the specimens will be compared with other methods of testing in the discussion at the end of this chapter.

7.6.6 Ageing of the concrete specimens

The concrete specimens were exposed to the environment for over 2 years, therefore, ageing to some degree will have occurred. However, this parameter is more difficult to detect and isolate through thermocouple data as the temperature change in the specimens is dependant on ambient conditions, in particular, sunshine intensity. While this is true to say, there was evidence to suggest through the temperature change, that some level of ageing occurred and these findings will be presented in this section. Results will be presented for a smooth surface finish in addition to a contrasting rough surface finish.

7.6.6.1 Ageing of a smooth surface finish (cast)

There is evidence to show that ageing of the concrete specimens has occurred for a cast surface finish (located on board 1) in particular between the months of March and July 2011 (a period of almost 6 months). The first set of results recorded when the specimens were 6 months old is presented in Fig. 7-56 and as there is intermittent sunshine, there are some fluctuations observed in the resulting temperature. The primary focus in this chart is the peak temperatures occurring between approximately 11:00 and 13:00 of the specimens. As mentioned previously in the analysis of the results, the effect of GGBS on the temperature can be clearly seen, with the decreasing peak temperature correlating with the increased presence of GGBS.

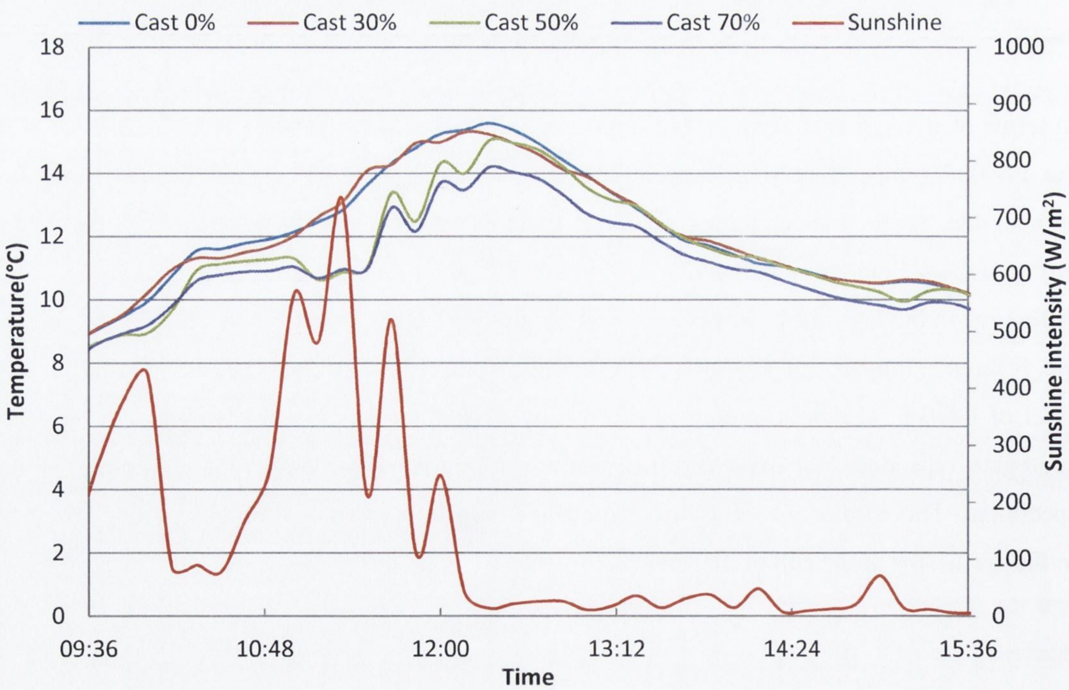

Fig. 7-56 Time vs. temperature and sunshine intensity for cast finish specimens – 12th March 2011

The order of decreasing temperature of the specimens in terms of GGBS concentration is 0, 30, 50 and 70% GGBS as expected, with the peak occurring at approximately 12:20. The peak temperature of 0, 30, 50 and 70% GGBS are 15.6, 15.2, 15.0 and 14.2°C respectively. The peak temperatures of the specimens occurs approximately 60 minutes following the peak in sunshine intensity of 730W/m^2. Once a peak in sunshine intensity occurs at 12:00, there is no sunshine from this time onwards for this particular day.

When one observes the results for these exact specimens two months later (see Fig. 7-57), it is clear from the plot that there is virtually no difference in the temperature between 50 and 70% GGBS specimens. The maximum temperature recorded from the specimens on this particular day in July was approximately 24°C which is significantly higher than for the first set of readings recorded in March (see Fig. 7-56). This peak occurred in the afternoon at 16:45 as it is determined directly by the sunshine intensity. The temperature of 0, 30, 50 and 70% GGBS specimens is approximately 23.8, 23.2, 21.7 and 21.7°C respectively. There remains a measureable difference between all adjacent concentrations apart from 50 and 70% GGBS. As there is increased sunshine duration in May on this particular day, it would be expected that there is a discernable difference in the temperature between the 50 and 70% GGBS specimens. It can be concluded from this observation that ageing of the specimens is occurring to some extent.

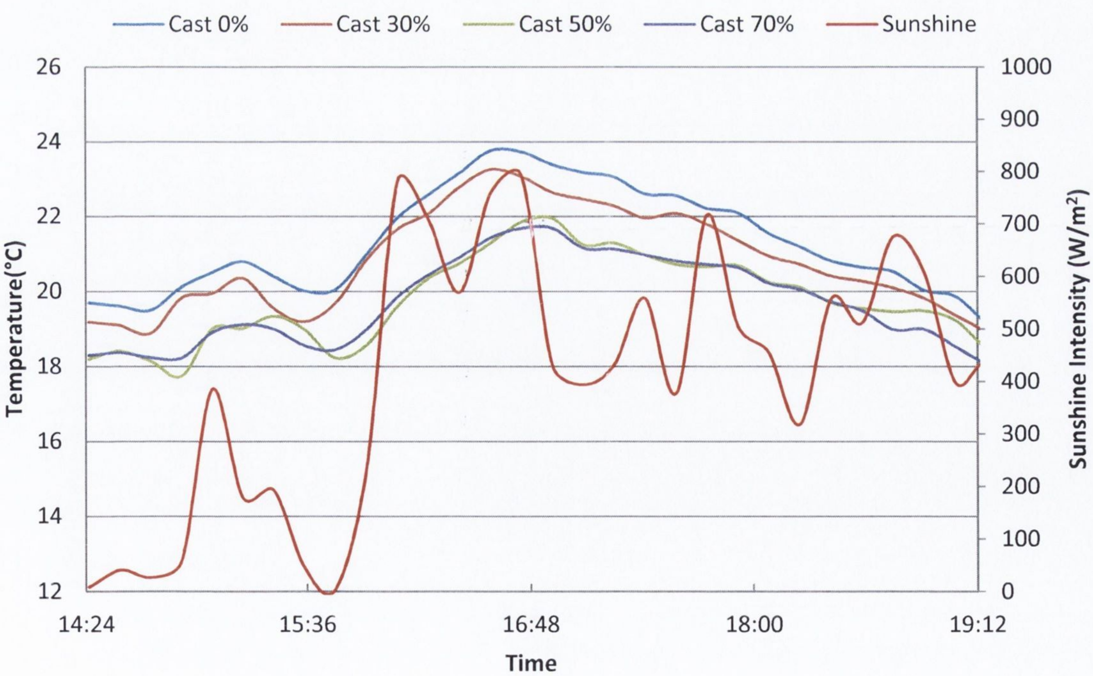

Fig. 7-57 Time vs. temperature and sunshine intensity for cast finish specimens – 9th May 2011

The results recorded after a further 2 months for the same specimens (July 2011) are displayed in Fig. 7-58. This particular day recorded a high sunshine intensity of 850W/m^2 which was broadly constant between 12:00 and 17:00. Consequently the specimens reached an unusually high peak temperature at 14:00 of approximately 40°C. This peak temperature remained at a plateau before beginning to decrease at 17:00. The peak temperature of 0, 30, 50 and 70% GGBS is approximately 40.3, 39.5, 36, 37.6°C respectively. The peak temperature profile shows a change in the order of the specimens in terms of decreasing temperature. The 70% GGBS specimen has now shifted and lies between 30 and 50% GGBS specimens. This change in the order would suggest that ageing of the 70% specimen is occurring with the surface becoming less reflective and ultimately being warmer in temperature than the 50% GGBS specimen. This may be due to different surface characteristics in the higher GGBS concentration specimens and this is a potential avenue for further research.

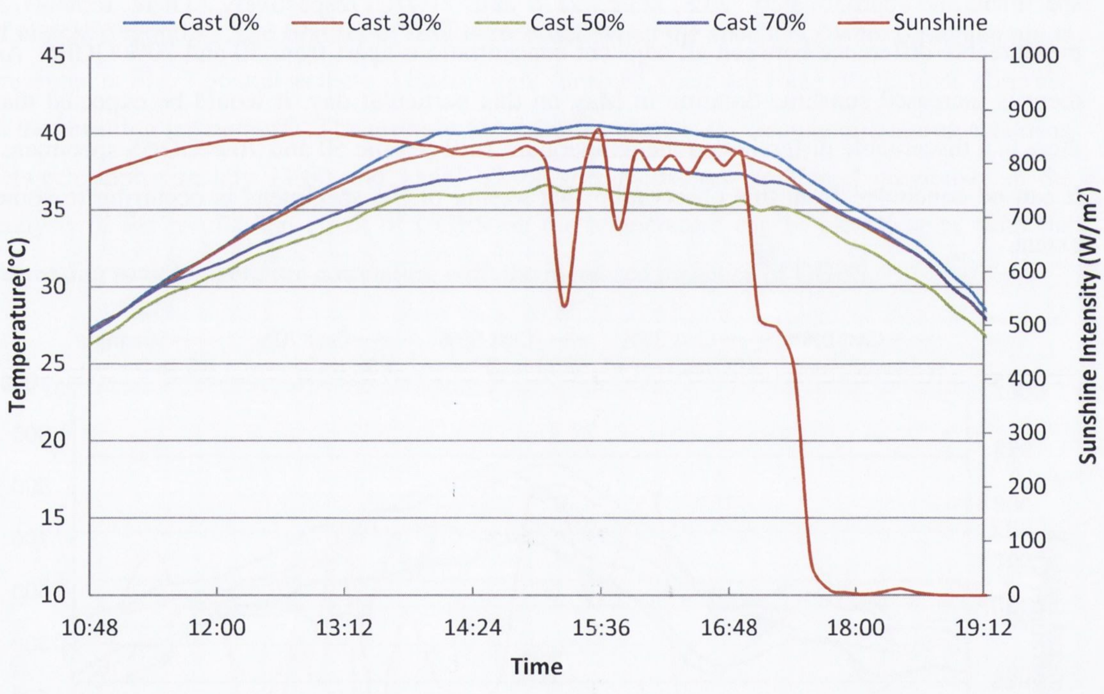

Fig. 7-58 Time vs. temperature and sunshine intensity for cast finish specimens – 27th July 2011

In conclusion, there is some ageing of the smooth cast finish specimens occurring as evident by the aforementioned trends. The original temperature profile (in terms of GGBS concentration) demonstrated that the increase in GGBS content resulted in a decrease in internal temperature i.e. the order of decreasing temperature was 0, 30, 50 and 70% GGBS. However, only 2 months after the first set of readings, it was observed that there was virtually no difference in temperature between 50 and 70% GGBS specimens. Furthermore, after another 2 months the

70% GGBS specimen has surpassed the 50% GGBS specimen and now lies between 30 and 50% GGBS. This trend clearly indicates that the 70% GGBS specimen is ageing and has become less reflective on the surface therefore reaching a higher internal temperature. This trend was also observed using other methods of testing such as the lux meter results and the results for greyness. The surprising results earlier in the lux meter section with regard to the deterioration of the 70% GGBS specimens is strongly confirmed by the trends here in the thermocouple results, despite this being an indirect test method.

7.6.6.2 Ageing of a rough surface finish (tamped finish)

Similarly, the results for a rough surface finish demonstrating ageing will be discussed in this section, in particular for tamp surface finish specimens located on board 4. The first set of readings were recorded in October 2010, and are displayed in Fig. 7-59. The sunshine intensity is shown along with the four specimens containing 0, 30, 50 and 70% GGBS. There is intermittent sunshine on this particular day, not exceeding 700W/m^2. In addition the duration of this sunshine is particularly short, therefore, the specimens reach a peak temperature at 16:15 of 13.0, 13.0, 11.2 and 10.8°C corresponding to 0, 30, 50 and 70% GGBS specimens respectively. It is clear from the plot that there is less difference in temperature between the adjacent GGBS specimens for the rough surface finishes when compared with the smooth finish discussed in the previous section. It should be noted that the orientation of the striations were not taken into account at the time of testing, therefore, this could have an influence on the temperature observed by the specimens. In addition, the undulating surface finish would result in more light being dispersed off the surface.

The results obtained 6 months later in April 2011 are displayed in Fig. 7-60 with the four specimens reaching higher peak temperatures overall. The sunshine intensity is significantly higher at 900W/m^2 in the afternoon and a longer duration of sunshine is observed for this particular day. The temperature of the specimens as a consequence are much more uniform. The peak temperature of 0, 30, 50 and 70% GGBS specimens occurring at 16:30 are 22.5, 21.8, 20.5 and 20.5°C respectively. This result is no different from the first set of results recorded 6 months previously (see Fig. 7-59) as 50 and 70% GGBS specimens are practically the same temperature.

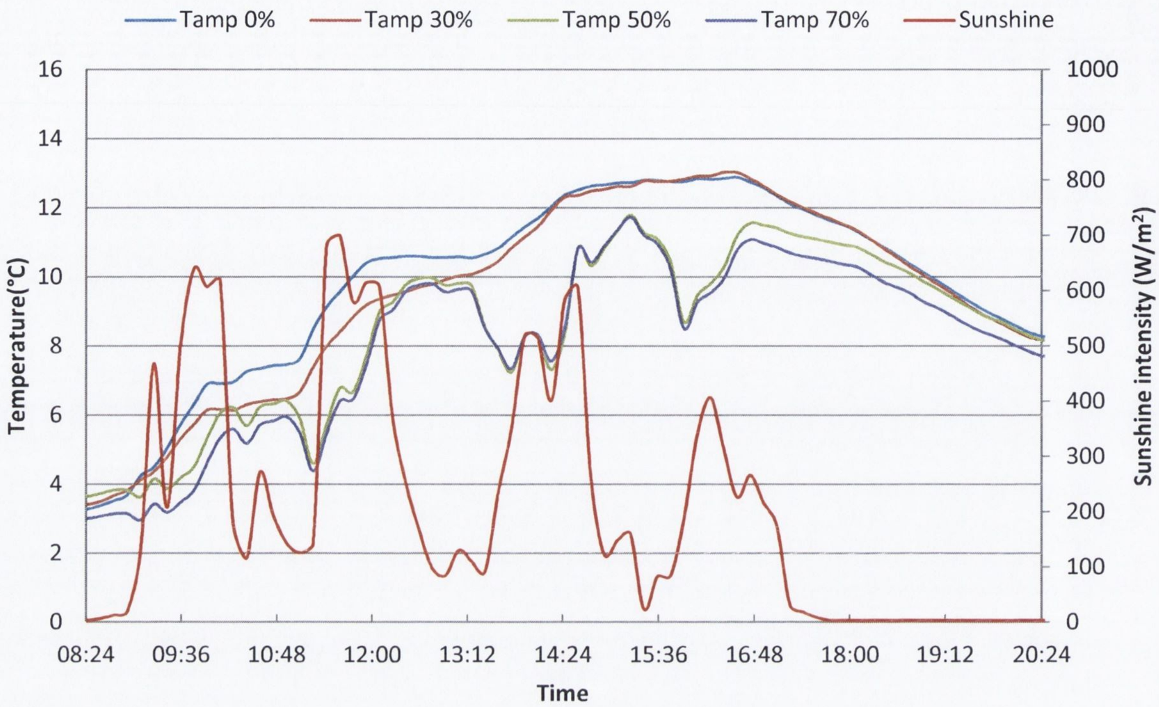

Fig. 7-59 Time vs. temperature and sunshine intensity for cast finish specimens – 30th October 2010

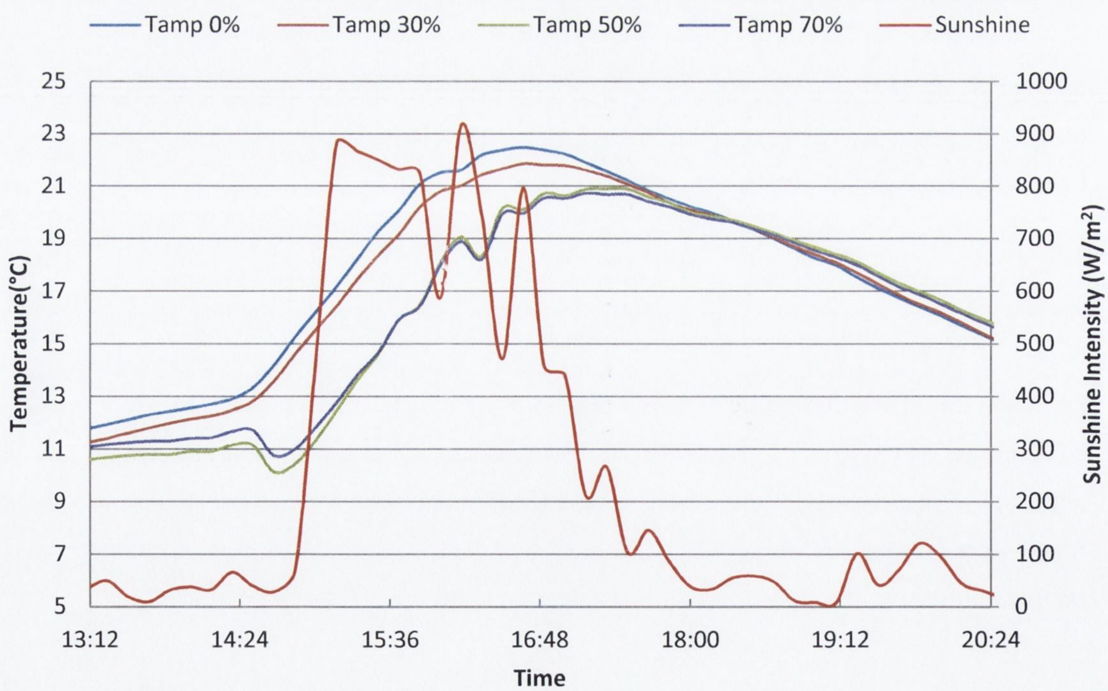

Fig. 7-60 Time vs. temperature and sunshine intensity for tamp finish specimens – 12th April 2011

The final set of results recorded a further 2 months later in June 2011, however, are presented in Fig. 7-61 and demonstrate a somewhat different result. The peak temperature profile shows a change in the order of the specimens in terms of decreasing temperature. The peak temperature of the specimens occurs at 13:30 in the afternoon, with 0, 30, 50 and 70% GGBS recording maximum temperatures of 31.3, 30.3, 28.2, 28.8°C respectively. The sunshine intensity reaches a maximum of 800W/m^2. The 70% GGBS specimen has now changed and lies between 30 and 50% GGBS specimens, as observed for the cast finish specimen discussed in the previous section. This change in the order would suggest that ageing of the 70% specimen in particular, is occurring.

It should be noted that the trend of ageing is a little more difficult to ascertain for a rough surface finish, when one observes the order of the specimens over time. This is due to the presence of the striations on the surface of the specimens, which have an influence on the resulting internal temperature (see Table 5-13 and Table 5-14 for results).

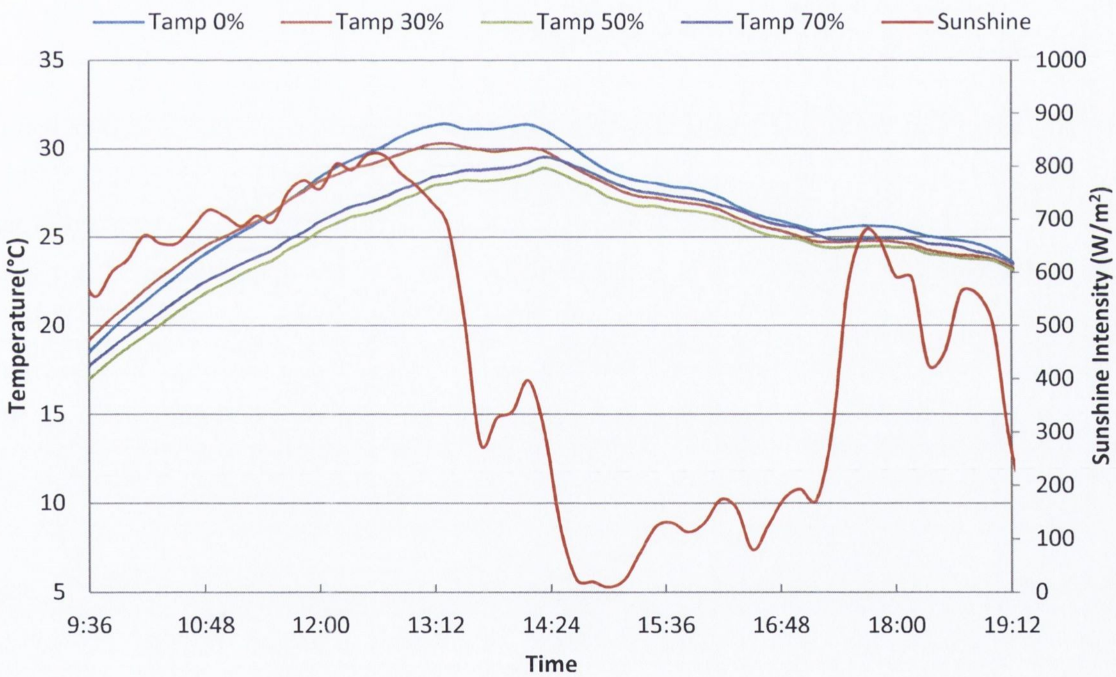

Fig. 7-61 Time vs. temperature and sunshine intensity for tamp finish specimens – 14th June 2011

In conclusion, there is some ageing of the rough tamped finish specimens occurring as evident by the aforementioned trends. However, there is less differentiation evident between the adjacent GGBS concentration specimens which is due to the nature of the surface finish in addition to the orientation of the striations. When the final set of temperature readings were recorded, the 70% GGBS specimen had surpassed the 50% GGBS specimen and now lies between 30 and 50% GGBS. This trend was also noted for the smooth surface finish as previously discussed. This trend clearly indicates that the 70% GGBS specimen is ageing and has become less reflective on the surface, and is reconfirmed by additional methods of testing such as the lux meter results and the results for greyness as discussed previously in Section 7.3 and Section 7.4 respectively.

7.6.7 Summary of thermocouple results

As there were graphs included in the appendices (see Appendix DD to Appendix II) but not discussed in detail in the main text of this discussion on thermocouple results, a summary of these graphs will be presented for the three different aggregate types, demonstrating the effect of GGBS on internal temperature (see Table 7-33) and the effect of surface finish type on internal temperature (see Table 7-34). It should be noted that the temperatures obtained are difficult to cross compare as they were recorded on different days with quite different sunshine intensities.

The results in Table 7-33 are in order of decreasing temperature, with the maximum temperature of the specimens attained on the particular day of testing (T_{max}) in addition to the difference between the maximum and minimum temperatures recorded (ΔT) displayed. The aggregate type (L, PCL and SS) are displayed in the first column, with the surface finish types displayed on the top of each of the subsequent columns. Where there is negligible difference in temperature between the specimens, they are placed in the same row e.g. 50/70 which demonstrates that there is little difference in temperature between the specimens containing 50 and 70% GGBS. The date on which the test took place is also indicated in the summary table of results.

These temperatures are strongly dependant on the sunshine intensity and duration, however, the value for ΔT in Table 7-34 ranges between 1.5°C and 6.3°C. In general, it can be observed that where there is a higher T_{max} result, there is a higher range in ΔT as expected. This result reconfirms the need for a sufficiently high level of sunshine in order to obtain a reasonable difference in temperature between the different specimens. In general, the order of decreasing temperature in terms of GGBS concentration is 0, 30, 50 and 70% GGBS, however, there is some overlapping between some of the specimens particularly as they age.

Table 7-33 Summary of results for thermocouples demonstrating trends evident for the effect of GGBS on the internal temperature of the concrete specimens (March 2011)

Effect of GGBS				
Aggregate	Cast	Screed	Tamp	Brush
LS	0/30 50 70	0/30 50 70	0/30 50 70	0/30 50 70
Date T_{max} ΔT (0-70%)	12th March 15.3 1.5	12th March 14.3 1.6	21st April 33.0 5.0	21st April 33.0 5.0
PCL	0 30 50 70	0 30 50 70	0 30 50 70	0 30 50/70
Date T_{max} ΔT (0-70%)	16th March 21.4 5.9	6th July 22.0 3.0	16th March 19.5 5.5	6th July 23.1 2.1
SS	0 30 50/70	0 30 50/70	0 30 70 50	0 30 50/70
Date T_{max} ΔT (0-70%)	3rd June 44.6 6.3	14th June 31.0 2.6	14th June 31.4 3.4	3rd June 41.2 4.0

Similarly, a summary of the effect of surface finish type on internal temperature (see Table 7-34) results in ΔT ranging between 1.5°C and 4.0°C. The aggregate type is displayed in the first column, with the GGBS concentrations displayed on the top of each of the subsequent columns. The order of decreasing temperature in terms of finish type is cast, brush, tamp and screed, however, there is overlapping between some of the finish types which is indicated where they are placed in the same row e.g. Brush/Tamp which demonstrates that there is little difference in temperature between the specimens containing a brushed or tamped surface finish.

In conclusion, the summary of results demonstrate that there is a correspondence between the maximum temperature observed by the specimen with the value of ΔT for a particular day depending on GGBS content and surface finish. In general, where T_{max} is high, there is a high corresponding value for ΔT. The order in which the specimens lie in terms of GGBS concentration and surface finish type were broadly the same across all of the plots. The order of decreasing temperature in terms of GGBS concentration is 0, 30, 50 and 70% GGBS and the order of decreasing temperature in terms of finish type is cast, brush, tamp and screed. This order is broadly verified by previous methods of testing such as thermal imaging, greyness and lux meter results.

Table 7-34 Summary of results for thermocouples demonstrating trends evident for the effect of surface finish type on the internal temperature of the concrete specimens (March 2011)

Effect of surface finish				
Aggregate	0	30	50	70
LS	Cast Brush Tamp/Screed	Cast/Brush Tamp Screed	Cast Brush Tamp Screed	Cast Brush Tamp Screed
Date T_{max} ΔT (finishes)	2nd July 33.0 4.0	30th July 30.0 3.4	2nd July 29.3 2.3	30th July 29.3 3.6
PCL	Cast Brush/Tamp Screed	Cast Brush Tamp Screed	Cast Brush Tamp Screed	Cast Tamp Brush Screed
Date T_{max} ΔT (finishes)	19th March 20.7 2.5	19th March 21.7 2.8	28th April 32.3 3.9	28th April 32.3 4.5
SS	Cast Brush Tamp Screed	Cast Brush/Tamp Screed	Cast Brush Tamp/Screed	Cast Brush Tamp/Screed
Date T_{max} ΔT (finishes)	10th April 33.0 2.2	10th April 32.3 1.5	2nd June 35.0 3.0	2nd June 34.5 1.5

7.6.8 Conclusions

- There are three important factors in relation to sunshine intensity which influence the internal temperature of the specimens, namely whether or not the sunshine is present, the sunshine intensity and the duration of the sunshine. The intensity and duration of the sunshine is the key determinant in the resulting peak temperature difference obtained between the different specimens containing varying GGBS and surface finish types.
- Slab temperatures as high as 45°C in an ambient condition of 21°C were experienced, even in Irelands temperature climate, indicating the strong thermal gains from solar rays.
- There is a correlation between the internal temperature of the specimens recorded using thermocouple wires and colour or the light reflectance of the specimens i.e. there is less light energy absorbed into the material depending on the GGBS concentration and surface finish employed.
- In general, a lag between the peak in sunshine intensity and the peak in temperature of the specimens is observed, which suggests that the specimens take time to heat up from the incoming sunshine due to the low thermal conductivity of concrete. The lag ranges between approximately 20 minutes and 2 hours. Where there are short peaks in sunshine

intensity, the lag period was between approximately 20 and 40 minutes, however, where there was a sustained amount of sunshine for the entire day, a longer lag period of 2 hours was observed as the specimens absorbed a significant amount of energy due to the prolonged sunshine intensity, whereby an accumulation of energy occurred.

- The specimens containing 0 and 30% GGBS have a higher rate of change in temperature than the specimens containing 50 and 70% GGBS i.e. the 0 and 30% specimens are grouped closely in temperature and 50 and 70% behaving likewise. One would expect an even temperature profile between the different GGBS concentrations. This would suggest that a threshold exists above which GGBS dominates the behaviour of the specimens and below which NPC dominates the behaviour of the specimens.
- The results for the four surface finishes for the crushed limestone aggregate would confirm that the presence of GGBS has a significant influence on the internal temperature of the specimens, with the order of decreasing temperature as follows; 0, 30, 50 and 70%. This is expected as the specimens containing higher concentrations of GGBS are brighter in colour, and therefore reflect more sunlight, resulting in a lower temperature.
- The influence of surface finish on the internal temperature of the slabs is evident for all levels of GGBS replacement for crushed limestone aggregate. The order of decreasing temperature in terms of finish type is cast, brush, tamp and screed. This order is as much to do with the surface finish as it is to do with the colour of the specimen. The cast finish specimen is visibly darker in colour and vice versa for the screed finish. As a consequence the cast slabs absorb the most sunlight obtaining the highest internal temperature and the screed reflects the most sunlight therefore obtaining the lowest temperature.
- There is some overlap in peak temperature for the surface finishes brush and tamp, and also for tamp and screed. The irregular nature of the rough finish types result in different amounts of light being dispersed off the surface. In addition to this, the orientation of the striations was not taken into account and this may have an effect on the resulting internal temperature of the individual specimens.
- The trends observed for the four different surface finishes containing partially crushed limestone are very similar to that of the trends observed for the specimens containing crushed limestone and sandstone. The order of decreasing temperature corresponds directly with the increase in percentage of GGBS contained in the specimen. The order of decreasing temperature in terms of surface finish type is cast, brush, tamp and screed, with some overlapping of temperatures. Once again, the rough surface finishes are not as consistent in the order in which they fall in terms of peak temperatures.

- It is difficult to determine whether the aggregate type has any influence on the internal temperature recorded by the specimens as the sunshine intensity recorded was different depending on the day, therefore, they cannot be directly compared. However, the overall results are broadly the same in terms of the order of the specimens. It would also be true to state that it is difficult to determine whether the surface finish type is more influential on the resulting temperature over the influence of GGBS concentration, as both parameters have a significant influence on the temperature recorded.
- Some ageing of the specimens has occurred as they have been exposed to the environment for an extended period of time. The 70% specimens have gradually become less reflective as they surpassed the 50% specimen and now lie between 30 and 50% GGBS specimens, for both the smooth and rough surface finishes. This deterioration may be due to different surface characteristics in the higher GGBS concentration specimens. It may therefore be concluded that the optimum GGBS substitution rate is 50%.

7.7 Discussion

The colour of the raw cement material was measured with a sphere spectrophotometer using a number of different cement blends in various proportions (0-100%). These cement blends comprised of three different mixes, namely WPC and CEM II A-L, WPC and GGBS, and CEM II A-L with GGBS, and a range of L* values between 63.6 to 90.7 were obtained. It was concluded from this testing that the L* of GGBS and WPC are of similar magnitude, with WPC having a higher L* value by only 2.8%. The results also confirmed that there is little difference in the colour produced by using GGBS with CEM II A-L or WPC with CEM II A-L. This test demonstrated the range in colour between some typical Irish cement powders which have a significant influence on the resulting colour and consequently the albedo of concrete. In particular, it demonstrates that there is only a slight difference in the colour between WPC and GGBS, where WPC is considerably more expensive to purchase.

The primary method used to measure the albedo of a surface is an instrument known as an albedometer, and this instrument was utilised in the project to assess whether it would be a viable means of accurately determining the albedo of small concrete specimens that were manufactured for the purpose of testing. Through a number of sensitivity tests conducted using the instrument, it could be concluded that although it is a very sensitive and accurate instrument, it is difficult to calibrate as there are a number of factors which affect the albedo value. These include the height of the instrument, the time of day at which albedo is recorded, and also the reduction in the field view of the lower dome (sensor). The device could not be calibrated for use on the small concrete specimens as the presence of a restriction on the lower dome results in the sensor becoming so insensitive. It was, however, used on a number of large sites to measure the albedo and consequently the S.R.I of the surface was calculated, to determine whether the surface would qualify for LEED credits (under the heat island category).

The first site at St. James' Gate Brewery (30% brush and 12 months old) obtained an albedo of 0.25 which corresponds to an S.R.I of 28, however, this is below the LEED requirement of 29. A second site was tested at St. James' Gate where a new slab (brush 30%) was tested only one week after casting. The albedo of this surface was approximately 0.29 corresponding to an S.R.I value of 32, exceeding the LEED requirement. This result demonstrates that the requirement for LEED can be met with a 30% GGBS concentration level in the short term and also verifies the negative effect that ageing has on the albedo of a surface. The third site located at Fr. Collins park (24 months old) yielded an albedo of 0.25 for 0% GGBS and 0.34 for 70% GGBS, both on an exposed aggregate surface finish. The corresponding S.R.I for both 0 and 70% GGBS surfaces is 28 and 39 respectively. Once again, the presence of GGBS in a concrete surface demonstrates a positive affect on surface albedo, with a higher concentration resulting in a higher albedo.

In conclusion, the albedometer is a very accurate instrument and can be used to measure the albedo of large surfaces, however, it could not be calibrated to be used on the small concrete specimens for this project. As a consequence, alternate methods of testing were utilised/devised to determine the light reflectance properties of the 96 fabricated specimens, containing different concrete constituents. These five methods comprise of a sphere spectrophotometer, lux meter, greyness scale, thermal imaging and thermocouple wire. The key parameters assessed by each test method on the resulting light reflectance are as follows; the effect of aggregate type, GGBS concentration and surface finish (age will be discussed within each of these parameters).

1. Aggregate type

Testing the concrete specimens using the sphere spectrophotometer confirmed that although there is a difference in L* between two of the aggregate types, with sandstone typically having a lower value, on a whole the aggregate type does not have a significant effect on the colour of the concrete. Similarly, the results from the lux meter testing concluded that initially there is no discernable difference between the slab specimens containing different aggregate types, however, the difference between the aggregates becomes more discernible with age as the concrete weathers. The specimens containing sandstone aggregate were marginally less reflective, also suggesting that the colour of the aggregate type used may contribute to the resulting light reflected in the long-term.

A more subjective method of testing involved using a greyness index card to visually assess the concrete specimens and as there was virtually no means of accurately assessing the effect of aggregate type on greyness. Therefore, this parameter was eliminated and only the effect of GGBS concentration, surface finish and age on the greyness of the specimens were evaluated. This is also the case for the thermal imaging camera as the device is not sensitive enough to detect a difference in the surface temperature of specimens containing different aggregate types. The resulting internal temperature of the specimens was measured through the use of a thermocouple wire, and the effect of aggregate type on the internal temperature could not be determined accurately as only 16 specimens could be tested at any one time, all containing the same aggregate type. However, it was possible to evaluate the trends observed for the specimens containing different aggregate types in terms of GGBS concentration and surface finish, and as these trends were identical for each aggregate type, this parameter was one again excluded from analysis.

In conclusion, the two test methods which were sensitive enough to measure the effect of aggregate type were the sphere spectrophotometer and the lux meter. Both of the test methods concluded that the aggregate type does not have a significant influence on the light reflectance, therefore, the specimens may be studied together instead of focusing on each of the individual aggregate types.

2. GGBS concentration

Testing using the sphere spectrophotometer indicates that there is a general increase in L* with increasing concentration of GGBS, with the order of increasing reflectance as follows; 0, 30, 50 and 70% GGBS. This influencing parameter, however, is not as strong as that of surface finish type. Since ageing would have occurred when the L* was recorded, there is only a difference in the colour between non-adjacent concentrations of GGBS such as 0 and 50%, 0 and 70% and 30 and 70%. However, this instrument is very sensitive as it detects very small differences in colour between the specimens, even after they have been exposed to the environment for 24 months. Similarly, the level of GGBS present in a specimen also has a significant and measurable effect on greyness of the concrete, measured using the greyness index scale. This test method demonstrated that there is a direct correlation between GGBS concentration and greyness achieved for each of the surface finish types, with this change being significant enough to be detected by the human eye. The order of increasing reflectance for the greyness index is as follows; 0, 30, 50 and 70% GGBS. The trend of increasing greyness with increased GGBS concentration is not as pronounced upon the final readings of greyness, with the 70% GGBS specimen having reduced in colour quite significantly. This method of assessing reflectance is a good ready reckoner and is cost neutral thus it can be used quickly and cheaply in the field.

Similarly, the use of a lux meter has also shown that the addition of GGBS to concrete increases the solar reflectance of the specimen, however, the benefit of this is reduced over time as the surface of the slabs become weathered. The results demonstrated that the addition of GGBS to concrete gives increased amounts of light reflectance with increased levels of cement replacement and verified that the device is sensitive enough to detect the difference in light reflectance between adjacent levels of GGBS concentration for the most part. The general order of initial increasing reflectance is 0, 30, 70 and 50% GGBS on aged concrete. One year after the initial lux meter readings, it could be concluded that there was virtually no difference between the light reflectance for all levels of GGBS which strongly suggests that ageing has occurred. An explanation as to why the 70% GGBS specimen is not the most reflective is due to the fact that lux meter readings were not taken until 6 months after the specimens had been placed on the roof, providing a possible window for weathering to occur. This trend is reaffirmed in the testing of night-time luminance, where 70% GGBS reflects less light than the 50% GGBS specimen. The order of increasing reflectance is 0, 30, 70 and 50% GGBS for night-time luminance testing.

By using a thermal imaging camera, the effect of GGBS concentration on the surface temperature is not as strong a trend as that of the surface finish. In general, there is a reduction in temperature from 0 to 70% GGBS, however, it is difficult to differentiate between the specimens containing intermediate rates of substitution. The 70% GGBS specimens recorded a higher temperature than the 50% specimens which would also indicate that ageing of the 70% GGBS specimen has occurred. This was previously noted using a lux meter and greyness index. An overview of the tamp and brush specimens (containing the four GGBS specimens on one thermal image) suggest that there is an appreciable difference between 30 and 50% GGBS specimens. This is evident by observing the colour variation as the 0 and 30% GGBS specimens are noticeably lighter in colour in the thermal image than the 50 and 70% GGBS specimens. This is an interesting result as it coincides directly with the result of internal temperature of the specimens. The main objective of using the thermal imaging test method is to demonstrate that there is an general reduction in the surface temperature through the addition of GGBS, as this technique is a form of UHI mitigation, and for the most part, the presence of GGBS in sufficiently high levels does reduce the surface temperature, however, it is also strongly dependent on the surface finish.

Testing using the thermocouple wire demonstrated that the order of increasing reflectance is as follows; 0, 30, 50 and 70% GGBS, however, there is some overlap between 0 and 30%

specimens and also 50 and 70% specimens. In general, the specimens containing 0 and 30% GGBS have a higher rate of change in temperature than 50 and 70% GGBS specimens, therefore, the 0 and 30% specimens are closely grouped together in temperature and 50 and 70% GGBS specimens behaving likewise. This outcome would suggest that there is little to be gained by using a GGBS substitution rate higher than 50%. Furthermore, ageing of the specimens has occurred as they have been exposed to the environment for over 2 years and it was observed that the 70% GGBS specimen is less reflective and lies between the 30 and 50% GGBS specimens in terms of temperature, which is a reoccurring trend.

In conclusion, the five test methods demonstrate a common trend, that the increase in GGBS replacement in concrete produces a brighter coloured concrete with a corresponding reduction in temperature (see Table 7-35 for summary of results). Although certain test methods cannot detect the temperature difference between two adjacent levels of GGBS concentration, each of the methods demonstrate that there is a significant reduction in temperature/increase in colour between a specimen containing no GGBS and a brighter specimen containing 70% GGBS.

3. Surface finish

The surface finish has a definite and discernable influence on the L* of the concrete specimens, with the decreasing order of L* as follows; screed, brush/cast and tamp. The t-test conducted between the surface finish types demonstrated that there is no difference in colour between the cast and brush finish. It was noted that the L* of the rough specimens is more difficult to obtain in comparison with the smoother surface finishes due to the presence of the undulating surface. It remains clear that the screed surface finish is the brightest specimen. The remaining order of decreasing reflectance, however, is not on par with the other four test methods (see Table 7-35 for summary of results).

The lux meter results conclude that effect of surface finish on light reflectance is the primary factor affecting light reflectance as the t-test demonstrates that there is still a discernible difference between each of the four finish types even after one year of the initial test being carried out. The general order of decreasing reflectance is as follows; screed, tamp, brush and cast. Similarly, a strong relationship between greyness and the surface finish type for each of the GGBS concentrations was obtained. The trend observed for the four finish types in terms of decreasing reflectance is screed, brush, tamp and cast. The results confirm that the surface finish has a measurable effect on greyness by using the greyness index scale, and this parameter is equally as important, if not more important, than the percentage of GGBS present. The ageing of the specimens evaluated through measuring greyness found that the results have somewhat converged with time, which would suggest that there is deterioration of the samples due to weathering, however, the order of decreasing greyness in terms of the surface finish type remains unchanged.

The thermal imaging camera results demonstrated in terms of surface finish, that the cast finish reached the highest surface temperature and the screed the lowest, with tamp and brush finishes having similar intermediate temperatures. The brushed finish had a marginally higher temperature, therefore the order of decreasing reflectance is as follows; screed, tamp, brush and cast. The surface finish type is the dominating factor once more, affecting the surface temperature of the specimens. The influence of surface finish on the internal temperature of the slabs is evident for all levels of GGBS replacement, as measured by the thermocouple wires. The order of decreasing temperature in terms of finish type is screed, tamp, brush and cast. Although ageing of the specimens will have occurred, as the surface finish is the dominating parameter affecting the resulting light reflectance, there is virtually no change in the order of the specimens (see Table 7-35 for summary of results).

Table 7-35 Summary of trends produced by five main testing methods on the fabricated concrete specimens

Testing method	GGBS	Surface finish
Sphere spectrophotometer	70	Screed
	50	Brush/Cast
	30	Tamp
	0	
Lux meter	70	Screed
	50	Tamp
	30	Brush
	0	Cast
Greyness scale	70	Screed
	50	Brush
	30	Tamp
	0	Cast
Thermal imaging	70	Screed
	0	Tamp
		Brush
		Cast
Thermocouple wire	70	Screed
	50	Tamp
	30	Brush
	0	Cast

In conclusion, the five test methods demonstrate a universal outcome, that the effect of surface finish on temperature and light reflectance is the dominating factor over the effect of GGBS concentration. In general, the most reflective surface finish is that of screed and the least reflective surface is that of cast. This outcome is due to the colour of the latter specimen in addition to the surface finish itself, as a cast finish is visibly darker in colour when compared with a screed finish which has the brightest colour.

4. Ageing

The concrete specimens were cast in September 2010 and were placed on site in October 2010, with testing carried out from October 2010 up until about February 2013, therefore, ageing of the specimens would be expected to some extent. Due to its restricted availability, the sphere spectrophotometer was used to measure the specimens colour on a once off basis, after the specimens were exposed to the environment for approximately 2.5 years, thus it is not possible to determine the effect of ageing using this particular test method. Similarly, the thermal imaging camera was used to detect differences between different GGBS concentrations and surface finish types and was not used over a prolonged period of time to determine the effect of ageing on infrared emissions. However, the effect of ageing was detected by the other testing methods, namely the lux meter, greyness index chart and thermocouples.

The influence of ageing on the amount of light reflected from a specimen, as detected by the lux meter, is evident despite there being only one year between the initial and final readings. It was found that irrespective of the surface finish and the incoming light, the concrete slabs have aged and this results in deterioration in the light reflectance result, and a convergence of the results with time i.e. the differences in the light reflectance values are less pronounced with time. There remains a quantifiable difference in the amount of reflected light between each of the surface finishes after one year and this would suggest that this parameter is the dominating factor over the influence of GGBS concentration. In terms of GGBS concentration, the 70% GGBS specimen performs quite poorly with age, as it is evident that the lux reading drops to below that of 50% and is similar to 30% GGBS. This decrease may be due to different surface characteristics in the higher GGBS concentration specimens whereby the slabs with higher GGBS dosages may allow more dirt penetration on the surface. The lux meter was also used to measure night time luminance, and it was also found here that the older 70% GGBS specimen recorded a light reflectance lower than the 50% specimen.

In terms of analysing the effect of ageing using the greyness index chart, the differences between the results are less pronounced with time which would suggest that there is deterioration of the samples due to weathering, however, the results would also suggest that it is still possible to visibly differentiate clearly between the different GGBS content levels after 18 months, despite the subjectivity of the test, with the general order of decreasing reflectance as follows; 70, 50, 30 and 0% GGBS. This contrasts with the results obtained using the lux meter, however, the greyness index chart is a subjective test method. In terms of surface finish type, this particular parameter was more difficult to differentiate between for the four GGBS concentrations, because rougher surfaces are more subjective than smooth ones. On average, the order of surface finish type in terms of decreasing greyness remains unchanged. The order of decreasing greyness for the various finish types is screed, brush, tamp and cast, however, the greyness for each surface finish type has reduced, with the three surface finishes brush, tamp and screed having almost identical results of greyness when the final readings were recorded. In conclusion, according to the results obtained using the greyness index chart, the surface finish and GGBS concentration both drop at approximately the same rate and not by a significant amount in 18 months.

The use of thermocouple wire in the specimens is an indirect means of testing and demonstrated that ageing of the slabs had occurred by virtue of the change in internal temperature. The original temperature profile (in terms of GGBS concentration) for smooth slabs demonstrated that the increase in GGBS content resulted in a decrease in internal temperature i.e. the order of decreasing temperature was 0, 30, 50 and 70% GGBS as expected. However, only 2 months after the first set of readings, it was observed that there was virtually no difference in temperature between 50 and 70% GGBS specimens. Furthermore, after another 2 months the 70% GGBS specimen had surpassed the 50% GGBS specimen and now lay between 30 and 50% GGBS. This trend clearly indicates that the 70% GGBS specimen is ageing and has become less reflective on the surface, therefore reaching a higher internal temperature. This surprising result of the deterioration of the 70% GGBS specimens is strongly confirmed by the trends in the lux meter test method.

Similarly, there is some ageing of the rough surface finish specimens occurring. However, there is less differentiation evident between the adjacent GGBS concentration specimens which is due to the nature of the surface finish in addition to the orientation of the striations. When the final set of temperature readings were recorded, the 70% GGBS specimen had surpassed the 50% GGBS specimen and now lay between 30 and 50% GGBS, as noted for the smooth surface finish. This trend clearly indicates that the 70% GGBS specimen is ageing faster and has become less reflective on the surface, and is reconfirmed by the results for the lux meter.

In conclusion, the three test methods demonstrate a universal outcome, that the exposure of the specimens to the environment for over two years resulted in measurable ageing of the specimens. In general, the higher concentration of GGBS (70%) was found to age at a faster rate, as confirmed by the lux meter and thermocouple data. This outcome is most likely due to the surface characteristics of GGBS compared with NPC. It was also concluded that it is more difficult to assess the effect of ageing on the rough surface finishes due to the nature of the surface finish.

8 The Environmental Impact of Increasing Urban Albedo

8.1 Fundamental Background Theory

8.1.1 The global radiation budget of the earth

The earth's global mean energy budget is displayed in Fig. 8-1, with the incoming sunlight consisting of ultraviolet, visible and a limited portion of infrared energy (shortwave radiation) on the left and the outgoing infrared (longwave) radiation displayed on the right. The earth's atmosphere receives an average 341W/m^2 of incoming solar radiation which is approximately one quarter of the solar constant (1367W/m^2), and 102W/m^2 of this radiation is reflected or scattered back into space by clouds and the atmosphere (79W/m^2) and the surface (23W/m^2). This ratio is known as the global albedo which is close to 31% or 0.31 (Zdunkowski et al., 2007). In order to have a balanced radiation budget, the net gain (341-102=239W/m^2) of short wave solar radiation must be balanced by the emission of longwave radiation to space to achieve an equilibrium. Of this remaining 239W/m^2, 78W/m^2 of the incoming energy is absorbed by the atmosphere and 161W/m^2 is absorbed by the earth's surface. When energy is absorbed, it raises the temperature of the substance which absorbs it i.e. the earth, and this causes the earth to radiate this heat in the form of infrared radiation.

Assuming that the ground emits black body radiation at the temperature of 15°C (which is typical of the surface temperature of soil) an amount of 396W/m^2 of infrared energy is radiated upwards from the ground. However, 90% of this energy is trapped by greenhouse gases (356W/m^2) and the remaining 10% (40W/m^2) is released through the atmospheric window (where the atmosphere is transparent to certain wavelengths). Some of the infrared radiation escapes into space as it is emitted by the atmosphere (169W/m^2 emitted by the atmosphere and 30W/m^2 emitted by the clouds), however, most of the radiation is directed back towards the earth's surface which is denoted by back radiation (333W/m^2). This downward flow of radiation is the cause of increasing the surface temperature to the point where it can radiate 396W/m^2 Therefore, the total energy gain is 161 + 333 = 494W/m^2, however, this exceeds the longwave loss of 396W/m^2 by 98W/m^2. This is accounted for by the thermal loss of 17W/m^2 (the conductive heat flux from the earth's surface to the atmosphere), evapotranspiration of 80W/m^2 and net absorption of 1W/m^2.

By considering the earth's budget of the atmosphere itself, it gains the following energy;

- 78W/m^2 by absorption of solar radiation
- 98W/m^2 by thermals, evapotranspiration and net absorption (17W/m^2+ 80W/m^2 + 1W/m^2)

- $356W/m^2$ from long wave radiation emitted from the surface of the earth

This is a total of $532W/m^2$, which must be reemitted by the atmosphere and is accounted for as follows;

- $169W/m^2$ by atmospheric greenhouse gases
- $30W/m^2$ by clouds
- $333W/m^2$ as back radiation

In conclusion, there is $341W/m^2$ of incoming solar radiation and approximately one third of this is reflected by the earth which is defined as the global albedo ($79W/m^2$ by clouds and atmosphere and $23W/m^2$ by the earth's surface). In so far as improving the albedo of the earth's surfaces are concerned, the objective is to increase the radiation reflected off the surface (currently $23W/m^2$) and to reduce the absorbed radiation by the surface ($161W/m^2$) which is relevant as it would reduce the amount of infrared radiation emitted from the surface.

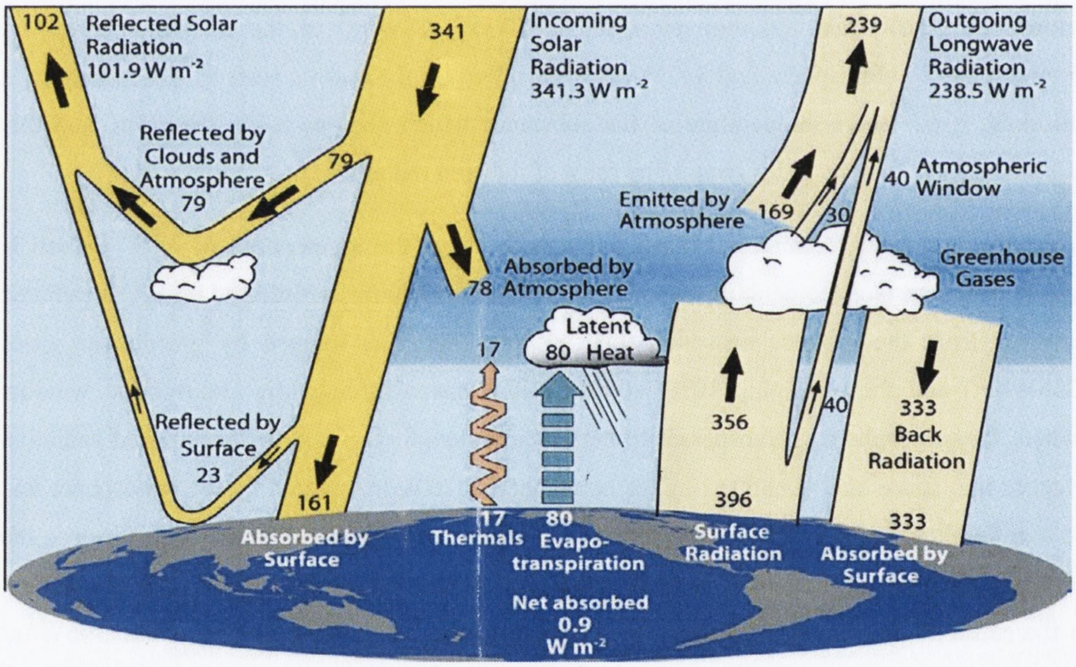

Fig. 8-1 The earth's annual global mean energy budget (Kiehl et al., 2009)

8.1.2 Theory of radiative forcings and offset CO_2

8.1.2.1 Definition of a 'climate forcing'

Climate change is driven by perturbations to the energy balance of the earth's system and these perturbations are called climate forcings. A climate forcing is an energy imbalance imposed on the climate system either externally or by human activities. Climate forcings are subdivided into direct radiative forcings, indirect radiative forcings and non-radiative forcings. Radiative forcing is reported in the climate change scientific literature as a change in energy flux in the tropopause (the boundary between the troposphere and stratosphere) and is calculated in units of W/m^2 (National_Research_Council, 2005). The concept of radiative forcing provides a way to quantify and compare the contributions of different agents that affect surface temperature by modifying the balance between incoming and outgoing radiative energy fluxes (National_Research_Council, 2005). Direct radiative forcings directly affect the radiative budget of the earth, for example, added CO_2 absorbs and emits infrared radiation. Direct radiative forcings may be due to a change in concentration of radioactively active gases, a change in solar radiation reaching the earth or changes in surface albedo.

1. Indirect radiative forcings create a radiative imbalance by first altering climate system components which immediately lead to changes in radiative fluxes, for example, the affect of aerosols (small particles in the atmosphere) on the precipitation efficiency of clouds.

2. A non-radiative forcing is a climate forcing that creates an energy imbalance that does not immediately involve radiation, for example, increasing evapotranspiration flux resulting from agricultural irrigation (IPCC, 2001).

Radiative forcings can be positive or negative. A positive radiative forcing (corresponding to more incoming energy) warms the climate system and a negative radiative forcing (corresponding to more outgoing energy) cools the climate system (Casper, 2009, Dessler, 2011).

The radiative forcing of the various factors which have influenced the climate over the past few centuries are displayed in Fig. 8-2. Radiative forcings are generally calculated as a change from a reference climate. The values plotted are radiative forcings caused by changes since 1750. The atmospheric abundance of CO_2 increased by 100ppm between 1750 and 2005. Since 1750, the increase in greenhouse gases has imposed a radiative forcing of $+3W/m^2$ and of this, CO_2 was responsible for approximately $+1.66W/m^2$.

As globally averaged CO_2 concentrations have increased from 280ppm in 1750 to 380ppm in 2005, it is important to estimate the global temperature response to greenhouse gas forcings. This response is called the earth's climate sensitivity to radiative forcing caused by CO_2 and other greenhouse gases. Sensitivity is expressed as the change in global temperature (T) due to doubling of atmospheric CO_2 concentrations (280ppm to 560ppm), or ΔT_{2xCO2}. For this doubling of CO_2, the climate sensitivity is likely to range between 2.0-4.5°C, with a best estimate of approximately 3.0°C (Cronin, 2010, Dessler, 2011). Doubled CO_2 corresponds to a radiative forcing of approximately $4W/m^2$. Therefore, the climate sensitivity is 0.5-1.12°C/(W/m^2) [(2.0/4) and (4.5/4)], with a best estimate of 0.75°C/(W/m^2) (Dessler, 2011).

In relation to this work, one is interested in the $2xCO_2$ radiative forcing for a doubling of CO_2 in the atmosphere (W/m^2) as this is required to calculate the radiative change per tonne of atmospheric CO_2 (kW/tonne CO_2).

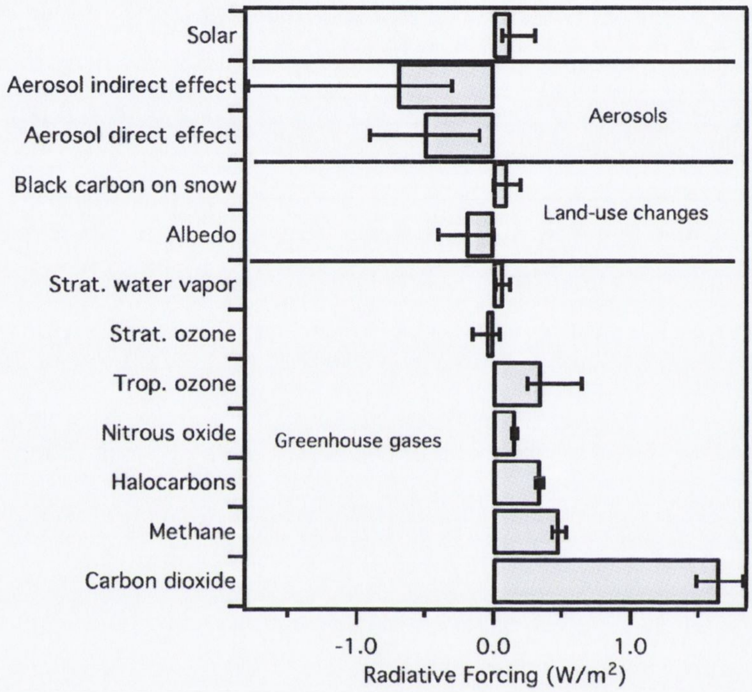

Fig. 8-2 Radiative forcing caused by changes in the climate between 1750 and 2005. The error bars indicate the uncertainty of the estimate (Dessler, 2011)

8.1.3 Previous research on radiative forcing and potential emitted offset CO_2

8.1.3.1 Study 1: Akbari et al. (2008b)

Akbari et al. (2003) suggest that the albedo of roofs and pavements can be increased by at least 0.25 and 0.15 respectively, resulting in an increase of 0.1 in the albedo of urban surfaces. In order to estimate the benefit in terms of CO_2 emission offset, Akbari et al. (2008b) derived an equivalency relationship between the radiative forcing of CO_2 versus the radiative forcing obtained if the albedo of all urban land areas were increased by 0.1.

1. Firstly, they estimated the increase in radiative forcing arising from increasing the atmospheric CO_2 by 1 tonne.
2. Secondly, by using a model they estimate the decrease in radiative forcing by increasing the albedo of roofs and pavements in an urban area.

By comparing these two radiative forcings, it allowed them to relate the changes in solar reflectance of urban areas to the changes in atmospheric CO_2 content.

Akbari et al. (2008b) use a number of different sources which give CO_2 forcings for a doubling of CO_2 in the atmosphere in units of W/m^2. Hansen et al. (1997) estimate a $2xCO_2$ adjusted radiative forcing to be $3.95W/m^2$ and this yields a radiative forcing of 0.93kW/tonne CO_2. Estimates used in IPCC (2007) (based on Myhre et al. (1998)) obtain a $2xCO_2$ adjusted radiative forcing of $3.71W/m^2$ and this yields a radiative forcing of 0.88kW/tonne CO_2. Akbari et al. (2008b) estimate a radiative change per tonne of atmospheric CO_2 of 0.91kW/tonne CO_2 which is based on Myhre's equation and on the current atmospheric concentration of 385ppm. For the calculations, Akbari et al. (2008b) use the average value of 0.91kW/tonne CO_2.

Akbari et al. (2008b) use the data presented in Fig. 8-1 to estimate the sensitivity of radiative forcing to the solar reflectance of the surface. They calculated the change in radiative forcing per 0.01 (1%) change in solar reflectance to be $-1.27W/m^2$. Using the estimated kW/tonne radiative forcing of atmospheric CO_2, they calculate an equivalency of (-1.27/0.91)= $-1.40kg/m^2$ CO_2 of urban areas for a 0.01 change in albedo. The IPCC (2007) state that the observed increase in atmospheric CO_2 does not reveal the full extent of human emissions in that it accounts for only 55% of the CO_2 released by human activity. The rest has been absorbed by the plants on the land. Therefore, assuming 55% of emitted CO_2 stays in the atmosphere, the emitted CO_2 equivalent offset is (-1.40/0.55) = $-2.55kg/m^2$ urban area for a 0.01 increase in albedo.

From this value, they found that increasing the albedo of a roof area by 0.25 could offset $64kg/m^2$ CO_2 (i.e. 16 m^2 of cool roof area to offset 1 tonne of emitted CO_2). For cool pavements with a proposed albedo change of 0.15, the emitted CO_2 offset is equal to $38kg/m^2$ CO_2 (i.e. 26 m^2 of cool paved area to offset 1 tonne of emitted CO_2). The estimate of the global emitted CO_2 offset potential for cool roofs and cool pavements is calculated at 24Gt CO_2 and 20Gt CO_2 respectively. Therefore, the total global emitted CO_2 offset potential is 44Gt CO_2. This offset is greater than 1 year of the 2025 projected world-wide emissions of 37Gt CO_2. The assumptions for the calculations in this research are summarised as follows;

1. The study was only concerned with short term effects (25-50 years), and ignores any time dependence and economics, such as the carbon cost of increasing surface albedo on such a large scale.
2. The study uses existing short-wave radiation balance models for the earth-atmosphere system. The calculations are performed for the entire globe combining the effects of

clouds and atmospheric scattering and absorption into two components, atmospheric absorption and atmospheric reflection.

3. Research has shown that shadows from all sources reduce the annual incidence of sunlight on residential roofs by about 10-25% depending on tree cover, therefore, this tends to reduce the equivalent potential of cool surfaces by a similar 10-25%.

This calculation applies for the average cloud cover over the earth. The radiative forcing for albedo change is a strong function of the cloud cover, therefore, depending on the location of the urban area considered, the radiative forcing value would need to be adjusted. The cloud cover in Ireland lies within the global average as will be discussed in Section 8.2, therefore, this is not an issue.

8.1.3.2 *Study 2: Menon et al. (2010)*

Following on from the work of Akbari et al. (2008b), Menon et al. (2010) performed simulations using the catchment land surface model (CLSM) of the NASA GEOS-5 climate model using the same methodology i.e. the model was designed to allow an understanding of the effect of a 0.1 increase in surface albedo over urban areas on radiative forcings and temperature over all global land areas.

Based on the radiative flux changes obtained from CLSM, Menon et al. (2010) examined the CO_2 offsets that may be expected. It was found that the global reduction in land surface temperature was 0.008K for a global average increase of 0.003 in surface albedo. An average increase in total outgoing radiation of 0.5W/m^2 was obtained from the model for all global land areas, for the average increase in surface albedo of 0.003. These values represent the change estimated from the CLSM for all global land areas. The adjusted radiative forcing value obtained (based on the radiative forcing for a 0.01 increase in the surface albedo) is [(0.5W/m^2)x(0.01)/(0.003)], that is, -1.63W/m^2. Similarly, as before, a value of 0.91kW/tonne CO_2 was also used for the radiative change per tonne of atmospheric CO_2 (Akbari et al., 2008b). Therefore, the atmospheric CO_2 equivalence for a 0.01 increase in urban albedo is obtained from the ratio of -1.63W/m^2 to the radiative change per tonne of atmospheric CO_2 (-1.63/0.91) which equals -1.79kg/m^2. Assuming 55% of emitted CO_2 stays in the atmosphere (IPCC, 2007), the emitted CO_2 equivalent offset is calculated as (-1.79/0.55) = -3.26kg/m^2 urban area for a 0.01 (1%) increase in albedo. The assumptions for the calculations in this research are summarised as follows;

1. The results represent all global land areas for the boreal summer (June-August). The CLSM simulations were performed for 3 months for 12 years.
2. A more meaningful evaluation of the impacts of urban albedo increase on global climate and the expected CO_2 offsets would require simulations which represent the full annual cycle. For annual changes, a lower value would be expected since winter offsets could be lower in some locations.
3. The results are based on the Northern hemisphere summer averages for global land locations only.

Based on this calculation, Menon et al. (2010) found that increasing the albedo of a roof by 0.25 could offset 82kg/m^2 CO_2 (i.e. only 12 m^2 of cool roof area is needed to offset 1 tonne of emitted CO_2). For cool pavements with an increase of 0.15 in albedo, the emitted CO_2 offset is equal to 49kg/m^2 of pavement area (i.e. 26 m^2 of cool paved area is needed to offset 1 tonne of emitted CO_2). Therefore, based on radiative forcings obtained in this study, the potential global emitted CO_2 offset for a 0.25 and 0.15 increase in roof and pavement albedo in urban areas is 31Gt CO_2 and 26Gt CO_2 respectively. This amounts to a total of 57Gt CO_2 which could potentially be offset as a result of the change in the albedo of roof and pavement areas (neglecting the CO_2 expenditure).

Table 8-1 Summary of potential emitted CO_2 offset for a 0.25 and 0.15 increase in albedo of roofs and pavements in urban areas

Source	Roof (0.25 increase)	Pavement (0.15 increase)	Total (Global)
Akbari et al. (2008b)	64kg CO_2/m^2 (= 16m^2 to offset 1 tonne CO_2) 24Gt CO_2	38kg CO_2/m^2 (= 26m^2 to offset 1 tonne CO_2) 20Gt CO_2	44Gt CO_2
Menon et al. (2010)	82kg CO_2/m^2 (= 12m^2 to offset 1 tonne CO_2) 31Gt CO_2	49kg CO_2/m^2 (= 20m^2 to offset 1 tonne CO_2) 26Gt CO_2	57Gt CO_2

8.1.3.3 *Study 3: Akbari et al. (2012)*

The current estimates of CO_2 offset are based on a constant (short-term: 50-100years) radiative forcing of approximately 0.91kW/t of atmospheric CO_2. However, Akbari et al. (2012) state that radiative forcing resulting from a given CO_2 emission will decrease with time, owing to the gradual removal of CO_2 by natural carbon sinks. Therefore, research was carried out by Akbari et al. (2012) where they conducted a series of transient model simulations (using the University of Victoria Earth System Climate Model- Uvic ESCM) in which they estimated the long-term effects of urban surface albedo modification on the global temperature. In addition, they also calculated the equivalent CO_2 emission offset corresponding to the simulated temperature change from albedo modification, using recent estimates of the anticipated temperature change per unit CO_2 emitted.

Firstly they increased the surface albedo by 0.1 over all land areas between ±20 latitude and secondly they applied the same albedo increase over all land areas between ±45 latitude. In addition to this, Akbari et al. (2012) used two global datasets of urban areas to generate a more realistic estimate of the effect of urban surface albedo change, namely GRUMP (Global Rural and Urban Mapping Project) and MODIS (Moderate Resolution Imaging Spectroradiometer). Akbari et al. (2012) incorporated both datasets of urban areas into Uvic ESCM, and increased surface albedo by 0.1. The results from the simulations demonstrated that increasing the albedo by 0.1 for the case of ±20° and ±45° latitude resulted in a temperature decrease of approximately 1K and 2K in 20 years, increasing to 1.3K and 3K after 200 years. Akbari et al. (2012) show that by increasing the albedo of $1m^2$ of a surface by 0.01, it decreases the long-term global temperature by about $3x10^{-15}K$.

Matthews et al. (2009) showed that global average temperature changes linearly as a function of total CO_2 emissions and that this temperature change per unit CO_2 emitted is approximately a constant with time, therefore, they estimate that each 3,700Gt CO_2 emitted results in 1.75K of a global temperature change (with an uncertainty range of 1-2.5K). Based on this estimation, Akbari et al. (2012) calculate that 21Gt CO_2 emitted increases global temperature by approximately 0.01K [(3,700Gtx0.01K)/1.75K]. By using this constant ratio, they calculated the offset in CO_2 emissions in terms of the effect of temperature reduction for changing the albedo of $1m^2$ surface area. The results show that increasing the albedo of $1m^2$ of a surface by 0.01 would have the same effect on global temperature as decreasing emissions by approximately 7kg of CO_2 $[(-3x10^{-15})(21x10^{9})(10^{3})]/0.01]$.

In global terms, they estimate cooling ranging from 0.01-0.07K (based on simulations performed using GRUMP and MODIS datasets), corresponding to a CO_2 equivalent emission reduction of 25-30Gt CO_2 using the GRUMP estimate and 130-150Gt CO_2 using the MODIS estimate of urban areas. There is a significant difference between these estimates, however, per unit of area, the global cooling effect and CO_2 equivalent offset was the same for both cases; $3x10^{-15}K$ and 7kg CO_2 respectively, per m^2 of a surface that its albedo increased by 0.01.

The assumptions for the calculations in this research are summarised as follows:

1. There is a significant difference between estimates of urban land areas in the two global data sets (GRUMP and MODIS) which were used and this represents the largest source of uncertainty in their simulations, however, the global cooling effect and CO_2 equivalent offset was the same for both cases.
2. They estimate a long term global temperature change of 1.75K (uncertainty range of 1-2.5K) resulting from the emission of 3,700 Gt CO_2. Accounting for this uncertainty, the equivalent CO_2 offset is estimated to be in the range of 4.9-12kg/m^2 for an albedo increase of 0.01, assuming no negligible CO_2 increase to achieve this albedo increase in the long term.

8.1.3.4 Conclusions

A summary of the three studies into the potential emitted CO_2 offset is presented in Table 8-2. By increasing the albedo of a surface by 0.01 (1%), the potential emitted CO_2 for urban areas ranges between 2.55-7.0kg/m^2. Akbari et al. (2008b) and Menon et al. (2010) use the same methodology in their calculations, therefore, the resulting offset values are similar. Akbari et al. (2012) examine the long term effects (200 years) of urban surface albedo modification and consequently obtained a significantly higher potential offset of approximately -7.0 kg/m^2 CO_2.

These estimates are based on a number of aforementioned assumptions, therefore, care should be taken as it is an estimation. The minimum potential emitted offset will be calculated for a case study using the conservative value of 2.55kg/m^2 CO_2 for an increase of 0.01 in albedo to demonstrate the minimum amount of CO_2 which could potentially be offset.

Table 8-2 Summary of potential emitted CO_2 offset per m^2 of surface area for three different studies

Source	Albedo increase	Offset kg/m^2 CO_2
Akbari et al. (2008b)	0.01	-2.55
Menon et al. (2010)	0.01	-3.26
Akbari et al. (2012)	0.01	-7.0

8.2 A case study of the topography of Trinity College Dublin

8.2.1 Introduction

Trinity College Dublin, corporately designated as the Provost, Fellows and Scholars of the College of the Holy and Undivided Trinity of Queen Elizabeth near Dublin, was founded in 1592 by Queen Elizabeth I as the "mother of a university", and is the only constituent college of the University of Dublin. Trinity College is located in the centre of Dublin, containing many buildings, both old and new, ranged around large courts (known as "squares") and two playing fields (see Fig. 8-3). It is the oldest university in Ireland and one of the older universities of the world. Standing on a self-contained site in the heart of Dublin, the College covers some 40 acres of cobbled squares and green spaces around buildings which represent the accumulated architectural riches of nearly three centuries.

An example of a classic old building within the campus is the Rubrics, which is the oldest surviving college building (circled in red in Fig. 8-3). The Rubrics is a redbrick range of college residences which was completed in *c.*1700. This is an example of a building which could not be altered in any way to accommodate an increase in albedo for a couple of reasons. This building has a pitched roof which is highly visible and it is one of the oldest buildings in college located in Front Square. In contrast to this, the arts building was completed in 1979 and has a surface area of approximately 4,000m^2 which is relatively large (circled in yellow in Fig. 8-3). It contains flat roofs which are ideal for implementing an albedo change.

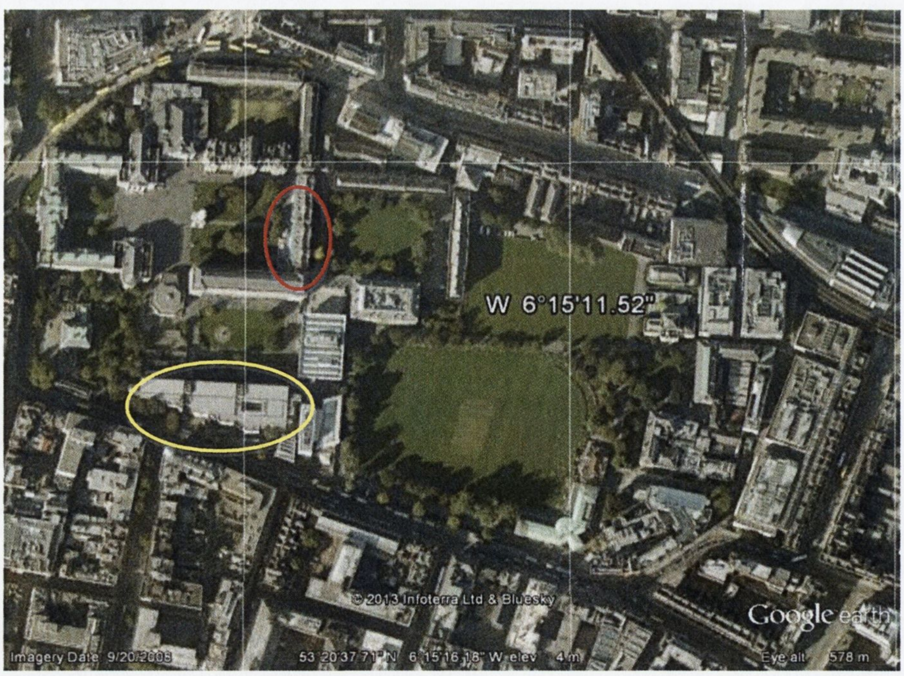

Fig. 8-3 Aerial Photograph of Trinity College Dublin (Google_Earth, 2008)

The primary objectives of this case study are as follows;

1. To quantify and assess the various surface types in the college with the aide of maps and photographs.
2. To determine possible areas within the college where the albedo could be increased.
3. To calculate the potential emitted CO_2 which could be offset from the increase in albedo and to compare this to the current emissions from the campus.

8.2.2 Methodology

8.2.2.1 Outline of Trinity College

The map displayed in Fig. 8-4 presents a detailed overview of Trinity College Dublin which was obtained from the college and is drawn to scale. The area of the map to be studied is enclosed by the heavy black line on the map. The study has been confined to those parts of the campus which are contained within the island.

A walk around the campus was completed first so that all of the surface areas on the map could be identified and marked out. The green areas of the campus were marked green on the map, however, there were slight inaccuracies on the map as not all of the green areas on campus were marked. Similarly, any area that is marked white on the map is effectively a pavement or a footpath with the exception of the railway line. Each of these areas were assessed to determine whether they were concrete or asphalt and were noted. Once the plan had been updated and verified, the area of each of the surface types which have potential for their albedos to be changed, could be calculated from the map directly.

The five main categories were

1. Concrete areas (including all paving slab areas)
2. All roof areas
3. Asphalt footpaths
4. Asphalt car parks
5. Asphalt pavements

A photograph of a typical asphalt car park area and a concrete area are displayed in Fig. 8-5 and were taken at a similar time of day. Although the concrete surface only contains ordinary Portland cement and has aged considerably, there is still a significant difference in brightness between the two surface types.

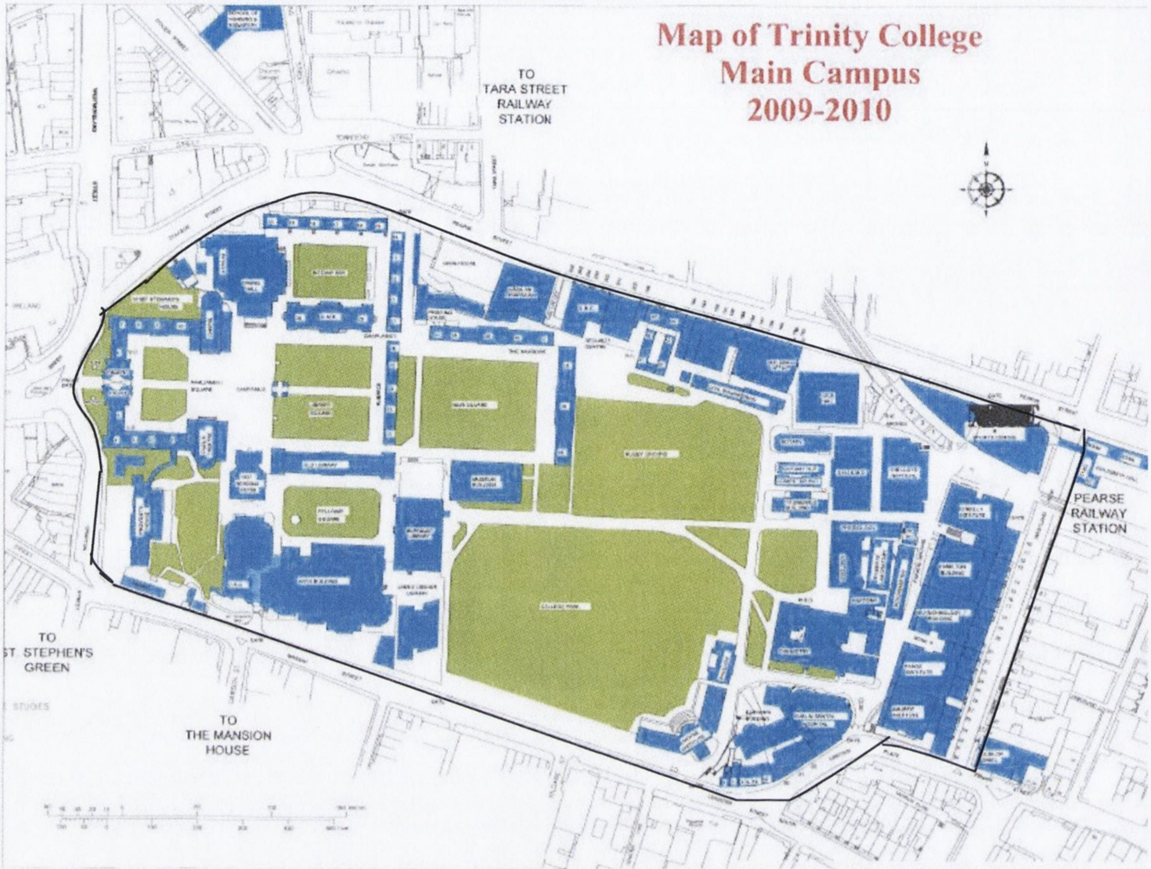

Fig. 8-4 Scaled map of Trinity College Dublin to calculate surface areas

Fig. 8-5 Asphalt car park (left) and concrete path (right) within Trinity College

8.2.2.2 *Calculation of surface areas*

In order to calculate the roof areas, a large aerial photograph was obtained from the college and from this it was possible to analyse the roof areas of each of the buildings. The slanted roof tops and front square buildings could be eliminated immediately as possible roof areas that could be changed because the albedo changes are not effective on slanted roofs and as the college is a protected structure, one is not permitted to change the colour of the roofs in front square. The possible roof tops for albedo modification were examined separately and the surface area of these were calculated, excluding areas such as glass on the roofs.

A breakdown of each area within Trinity College can be found in Appendix JJ. The total area of the campus was calculated as approximately 165,390m^2 and of this area almost one third is occupied by green space (50,705m^2). The roof area also occupies one third, with pavements, footpaths and car parks making up the remaining one third of the campus. The cobbled areas were found to be a small percentage of the campus in addition to the excluded areas (e.g. Provosts house) as outlined in Appendix JJ. The total asphalt area (pavements, car parks and footpaths) comprise approximately 16% of the total area (26,850m^2) while concrete areas constitute for approximately 3.7% (6,089m^2) of the total area. The asphalt areas and the concrete/paving slabs together make up approximately 20% (32,939m^2) of the campus area. This area in conjunction with the total roof area in college (55,491m^2) makes up approximately 53% of the campus area (88,430m^2).

8.2.3 Possible areas to increase albedo in Trinity College

As the albedo effect is most effective on horizontal surfaces, and taking into account the historical characteristics of buildings on campus such as Front Square, the roof areas displayed in Table 8-3 have been selected as possible areas in which the surface could be altered to increase the albedo value. This amounts to a total area of approximately 21,495m^2. Of the surface area available for albedo change, 40% is accounted for by the roof area of the buildings (21,495m^2), 50% is due to pavements, footpaths and car parks (32,939m^2) and 10% is due to the concrete paving slabs (6,089m^2).

The areas indicated in Fig. 8-6 display the possible surfaces on the campus which could be used to increase the albedo of the college, including existing concrete areas and asphalt areas such as carparks, pavements and footpaths. The 'other' section denotes the remainder of the college which cannot be used for certain reasons, such as the presence of cobble stones, a green area or simply due to the fact that the surface is not horizontal. As can be seen from this chart, there is approximately 33% of surface area within Trinity College Dublin where the surface reflectance could be increased.

Table 8-3 Possible horizontal roof locations in Trinity College where albedo could be increased

Buildings	Area (m^2)
Douglas Hyde Gallery	1,390
Arts Building	4,120
Long Room Hub	460
James Ussher Library (excluding glass)	770
Aras an Phiarsaigh	1,350
Simon Perry building	600
Security Centre	500
Museum	200
Buildings Office	900
Luce Hall	1,360
Sami Nasr Institute of advanced materials	880
The Lloyd Institute	1,200
Botany and Computer Hut	415
Naughton institute	690
O Reilly Institute	1,260
Science Buildings (excluding glass)	3,300
Parsons Building	700
Roberts Laboratory	500
Chemistry	900
Total	**21,495**

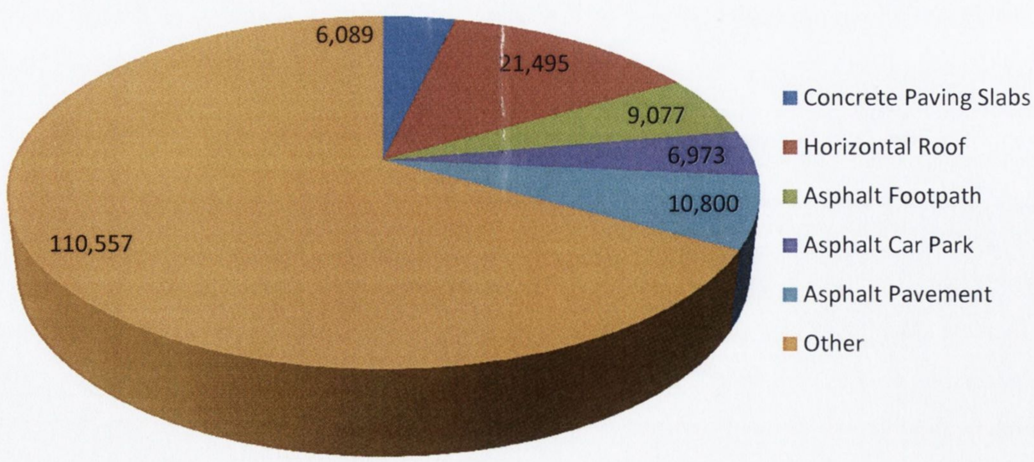

Fig. 8-6 Potential areas to increase albedo in the college (approximately 33%)

8.3 Potential emitted CO_2 offset for Trinity College

8.3.1 Estimated current albedo for existing surfaces on campus

Following the calculation of the surface areas in Trinity College, the potential emitted CO_2 offset could be determined based on the research conducted in the three studies summarised in Table 8-2. In order to calculate the potential emitted CO_2 offset, the current albedo value of the surface in addition to the expected increase in albedo are also required. The five categories of surfaces along with their estimated current albedo based on published albedo values are displayed in Table 8-4.

The albedo of existing roofs does not exceed 0.20 according to Akbari et al. (2008b), therefore, an estimated value of 0.20 will be used for this surface (see Table 8-4). New traditional concrete has an albedo of between 0.35-0.40, however, as most of the concrete on campus has aged, a reduced albedo value of 0.20-0.30 is expected. A value of 0.20 will be assumed for this surface (see Table 2-3 for typical albedo values of urban materials). The three asphalt categories (footpath, car park, pavement) have been assigned an albedo of 0.15 as they comprised of aged asphalt. The area of each category is also presented in Table 8-4. It should be noted that these estimated values of current albedo are conservative in some cases (marginally higher surface albedo than may be expected), to demonstrate the minimum potential emitted CO_2 which could be offset.

Table 8-4 Surface area and current albedo of the five categories of surface areas in Trinity College

	Area (m^2)	Current albedo
Horizontal roof area	21,495	0.20
Concrete paving slabs	6,089	0.20
Asphalt footpath	9,077	0.15
Asphalt car park	6,973	0.15
Asphalt pavement	10,800	0.15

8.3.2 Calculation procedure of potential emitted CO_2 offset

Akbari et al. (2008b) estimate in their research that approximately 206W/m^2 of short wave radiation is incident on the surface, however, they use a lower estimate of 172W/m^2 in their calculations which they obtained from Hatzianastassiou et al. (2005). They then calculate the change in radiative forcing per 0.01 change in solar reflectance of a surface to be -1.27W/m^2 (equating to -2.55kg/m^2 CO_2). However, their calculation applies for the average cloud cover

over the earth. Depending on the location of the urban area considered, the radiative forcing would need to be adjusted for variations in local cloud cover as the radiative forcing for albedo change is a strong function of cloud cover (the larger the cloud cover, the lower the radiative forcing value).

NASA's Ice, Cloud and Land Elevation Satellite (ICESat) measures the height of dynamic features such as glaciers, rivers and clouds with the use of lasers. ICESat has provided the most accurate figure of cloud cover to date, stating that 70% of the world is cloud covered. Previous estimates ranged from 50-75% (NASA, 2006). Similarly, cloud amounts (reported as the number of eight (okta)) show that the mean cloud amount each hour for Ireland ranges between five (62.5%) and six (75%) okta (Met_Eireann, 2013). This would suggest that the cloud cover in Ireland lies within the global average of 70%. Research into the analysis of sunshine records in Ireland over the period 1894 and 1994 also conclude that the satellite cloud factors over Ireland correlated well with cloud factors globally (Palle and Butler, 2001). Based on this knowledge, the radiative forcing value estimated by Akbari et al. (2008b) of -1.27W/m^2 will not be adjusted.

In order to calculate the potential emitted CO_2 offset for a given surface of area A, and increase in albedo Δa, Equation (8-1) is applied.

$$\frac{\Delta a}{0.01} \times \frac{2.55}{1000} \times A = CO_2\ (tonnes) \qquad \textbf{(8-1)}$$

where Δa = the increase in albedo, 2.55 is the offset of CO_2 (kg/m^2) for a 0.01 increase in albedo, and A is the area of the surface (m^2).

8.3.2.1 Potential emitted CO_2 offset based on published albedo values

The potential emitted CO_2 offset was calculated for Trinity College campus using Equation (8-1), applying published values of albedo for 0, 30, 50 and 70% GGBS which are 0.25, 0.36, 0.48 and 0.58 respectively (note that the albedo value for 50% GGBS was attained by interpolating between the albedo values of 30 and 60% GGBS presented in Table 2-10). The resulting CO_2 offset (in tonnes) is displayed in Table 8-5, showing a breakdown of each of the areas and a the total potential offset for each of the four GGBS concentrations (0, 30, 50 and 70%). The initial albedo ($A_{initial}$) and final albedo (A_{final}) are presented in Table 8-5, in addition to the increase in the albedo (ΔA). The areas as calculated previously, are also displayed here. The range of offset emissions ranges between 1,036 tonnes for 0% GGBS (albedo = 0.25) to 5,617 tonnes for 70% GGBS (albedo = 0.58).

This resulting offset is based on the most conservative value of -2.55kg/m^2 CO_2, therefore, the resulting offset is the minimum amount which could be expected. However, if the average of the three studies (see Table 8-2) is calculated [(2.55kg/m^2+3.26kg/m^2+7.0 kg/m^2)/3], this equals an equivalent CO_2 offset of 4.27kg/m^2. By assuming this is a more reasonable offset result which could be expected given that the location of Ireland is within the location boundary of each of the aforementioned studies, the emissions which could be offset are noticeably higher. The offset emissions were calculated using the same values for ΔA and are as follows: 1,740 tonnes (0% GGBS), 4,290 tonnes (30% GGBS), 7,080 tonnes (50% GGBS) and 9,410 tonnes (70% GGBS).

Table 8-5 Potential equivalent CO_2 offset by virtue of an increase in albedo corresponding to the published values for 0, 30, 50 and 70% GGBS (Akbari et al. 2008) for albedo A

% GGBS	Surface	$A_{initial}$	A_{final}	ΔA	Area (m^2)	CO_2 (t)
0	Horizontal roof	0.20	0.25	0.05	21,495	274
	Concrete paving	0.20	0.25	0.05	6,089	78
	Asphalt footpath	0.15	0.25	0.10	9,077	231
	Asphalt car park	0.15	0.25	0.10	6,973	178
	Asphalt pavement	0.15	0.25	0.10	10,800	275
					Total	**1,036**
30	Horizontal roof	0.20	0.36	0.16	21,495	877
	Concrete paving	0.20	0.36	0.16	6,089	248
	Asphalt footpath	0.15	0.36	0.21	9,077	486
	Asphalt car park	0.15	0.36	0.21	6,973	373
	Asphalt pavement	0.15	0.36	0.21	10,800	578
					Total	**2,563**
50	Horizontal roof	0.20	0.48	0.28	21,495	1,535
	Concrete paving	0.20	0.48	0.28	6,089	435
	Asphalt footpath	0.15	0.48	0.33	9,077	764
	Asphalt car park	0.15	0.48	0.33	6,973	587
	Asphalt pavement	0.15	0.48	0.33	10,800	909
					Total	**4,229**
70	Horizontal roof	0.20	0.58	0.38	21,495	2,083
	Concrete paving	0.20	0.58	0.38	6,089	590
	Asphalt footpath	0.15	0.58	0.43	9,077	995
	Asphalt car park	0.15	0.58	0.43	6,973	765
	Asphalt pavement	0.15	0.58	0.43	10,800	1,184
					Total	**5,617**

8.3.2.2 Potential emitted CO_2 offset based on measured albedo values

The albedos of a selection of surfaces were measured during the project, with the results outlined and discussed in Section 5.2. The albedo values correspond to a 0% cast finish, 30% brush finish and 70% cast finish, each of varying ages, as displayed in Table 8-6 for the conservative offset value of 2.55kg/m^2. The measured albedo values are also outlined, and differ somewhat to the published albedo values. The CO_2 offset was calculated for each of these surfaces as per Equation (8-1). The range of potential CO_2 offset is between 1,040 and 2,290 tonnes.

Table 8-6 Potential emitted CO_2 offset (@2.55kg/m^2) for Trinity College using measured albedo values

Surface	Age	Albedo	CO_2 offset (t)
0% GGBS (exposed aggregate finish)	24 months	0.25	1,040
30% GGBS (brush)	12 months	0.25	1,040
30% GGBS (brush)	1 week	0.29	1,590
70% GGBS (exposed aggregate finish)	24 months	0.34	2,290

Similarly, by assuming that the offset equivalent is higher than the minimum value of -2.55kg/m^2, by taking the average of the three studies (-4.27kg/m^2), the potential maximum offset of CO_2 is substantially higher at 1,740 tonnes where the albedo is 0.25, and 3,830 tonnes where the albedo is 0.34. This is a sizeable offset of CO_2 considering the relatively low albedo value of 0.34.

Table 8-7 Potential emitted CO_2 offset (@4.44kg/m^2) for Trinity College using measured albedo values

Surface	Age	Albedo	CO_2 offset (t)
0% GGBS (exposed aggregate finish)	24 months	0.25	1,740
30% GGBS (brush finish)	12 months	0.25	1,740
30% GGBS (brush finish)	1 week	0.29	2,670
70% GGBS (exposed aggregate finish)	24 months	0.34	3,830

In conclusion, by assuming that an average offset of 4.27kg/m^2 is a reasonable offset, the potential emitted CO_2 which could be offset as a result of increasing the possible roof, car park and pavement surfaces to a universal albedo of 0.25 could be as much as 1,740 tonnes. This value is even higher if an albedo of 0.34 could be attained, which would result in approximately 3,830 tonnes of emitted CO_2 being offset.

8.3.2.3 *CO_2 cost of implementation of concrete*

There is a carbon cost associated with placing the concrete in these areas within the campus. As there is approximately 32,000m^2 of the college which could be paved with concrete (assuming a slab thickness of 150mm), the total volume of concrete required would be 4,800m^3 (32,000m^2 x0.150m). As 1m^3 of concrete contains approximately 400kg of cement, a volume of 4,800m^3 would require 1,920 tonnes of cement. One tonne of cement produces approximately 800kg

CO_2, therefore, 1,920 tonnes of cement would produce approximately 1,536 tonnes of CO_2. If one chose 50% GGBS, however, this would significantly reduce the amount of CO_2 produced to 768 tonnes CO_2.

In conclusion, if one chose to implement the albedo changes within the college to the selected areas using 50% GGBS concrete (as 70% GGBS ages quickly), the cost of placing the concrete in terms of CO_2 is approximately 768 tonnes. However, if the concrete achieves an attainable albedo of approximately 0.34, the amount of potential CO_2 which could be offset (assuming 4.27kg/m^2) is as high as 3,830 tonnes which is approximately 5 times that of the carbon cost to implement the changes. Therefore, the potential CO_2 savings are approximately 3,062 tonnes (3,830-768 tonnes).

8.3.3 Comparison of potential offset CO_2 with current CO_2 emissions

8.3.3.1 Current CO_2 emissions from the College

In order to operate all of the facilities in the college over 24 hours, 7 days a week, there is a large amount of kilowatt hours (kWh) used per annum. For the academic year 2010/2011, Trinity College consumed approximately 35,697,000kWh of electricity, 38,000,000kWh of natural gas and 330,000m^3 of water, amounting to just under €7m in cost. To convert this energy into equivalent CO_2 emissions, emission factors sourced from SEAI (2013) are used from the year 2011, which are presented in Table 8-8. The CO_2 emissions are calculated by multiplying the usage (kWh) by the individual emission factor (kgCO_2/kWh) and this is then converted from kg to tonnes.

Thus the estimated total CO_2 emissions for the academic year 2010/2011 is approximately 26,900 tonnes, of which approximately 25,220 tonnes are accounted for by electricity and natural gas usage. The remaining 1,646 tonnes CO_2 is for the small quantity of oil for heating.

Table 8-8 Energy consumption and resulting CO_2 emissions for Trinity College for the academic year 2010/2011 (excluding renewable energy used)

Source	kWh	Emission factor (kg CO_2/kWh)	CO_2 emissions (tonnes)
Electricity	35,697,081	0.4886	17,442
Natural gas	38,000,000	0.2047	7,779
Other	---	---	1,646
Total			**26,867**

Trinity College are currently trying to increase the amount of renewable energy used each year in order to reduce the production of CO_2. Since 2007, a substantial amount of the electricity has been generated from renewable energy sources. Taking into account that 83% of the electricity is provided by one supplier where half of the energy is renewable (2010/2011), this would reduce the overall output of CO_2 emissions to approximately 19,628 tonnes.

Since 2004, Trinity College is working together with three other colleges in Dublin (DCU, DIT and UCD) to reduce energy use for a better environment and a stronger economy and the initiative is called e3. The participation of Trinity in this initiative since 2004 has resulted in the college achieving accumulative savings of just under €1m and 5,000 tonnes of greenhouse gas emissions through reduced energy consumption.

8.3.3.2 Comparison of potential offset CO_2 with current CO_2 emissions

The current CO_2 emissions from Trinity College is approximately 26,867 tonnes (academic year 2010/2011). However, there is potential for some of this emitted CO_2 to be offset by increasing the solar reflectance of surface areas within college (car parks, foot paths and pavements). A reasonable universal albedo of 0.34 could be achieved for these surfaces and this would equate to an additional saving of approximately 3,060 tonnes of CO_2 (including the carbon cost of placing the concrete using 50% GGBS), which would be a substantial contribution to the greening of the college community.

8.3.3.3 List of recommendations for Trinity College

If the modification of albedo within the college was to be considered for implementation, the following procedures would be recommended:

1. Take accurate measurements of the current albedo of the areas within the college which have potential for albedo improvement. An ageing model should be taken into account with regard to different percentages of GGBS and applied it to the different and appropriate surfaces.
2. The potential CO_2 offset should be calculated for a range of values (2.55-4.27kg/m^2), with the CO_2 cost of implementing the strategy taken into account i.e. 50% GGBS concrete will contain half of the CO_2 cost of 0% GGBS concrete.
3. The roofs should be painted white only, as the cost of implementing concrete roofs would outweigh the benefits of offsetting CO_2. Pavements, footpaths and car parking areas should be overlaid or replaced with concrete containing 50% GGBS.

4. Determine when the surfaces need to be cleaned in order to maintain the albedo value, say every 5 years.
5. Compare the CO_2 savings to be made with other CO_2 savings already made from the college.

8.4 Conclusions

- By increasing the albedo of a surface by 0.01, the potential emitted CO_2 offset for urban areas ranges between 2.55-7.0kg/m^2 (based on 3 studies conducted by others). Two of these studies use the same methodology in their calculations, therefore, their resulting offset values are similar. They estimate that the global potential emitted CO_2 offset for a 0.25 and 0.15 increase in roof and pavement albedo is 44Gt (Akbari et al. (2008b)) and 57Gt (Menon et al. (2010)) respectively, but this needs to be set against the CO_2 cost of implementing such a change and maintaining the albedo over time.
- The third study by Akbari et al. (2012) examined the long term effects of urban albedo modification and consequently obtain a higher potential offset of approximately 7.0kg/m^2 CO_2.
- The case study into the topography of Trinity College demonstrated that approximately 33% of the total surface area within the campus (54,434m^2) had the potential to be utilised to increase albedo. This potential area comprises of existing concrete paving slabs (6,089m^2), horizontal roof area (21,495m^2), asphalt footpaths (9,077m^2), asphalt car parks (6,973m^2) and asphalt pavements (10,800m^2). Therefore, of the surface area available for albedo change, 40% is accounted for by the roof area of the buildings (21,495m^2), 50% is due to pavements, footpaths and car parks (32,939m^2) and 10% is due to the concrete paving slabs (6,089m^2).
- The potential for emitted CO_2 to be offset was calculated based on the most conservative value (2.55kg/m^2), and the average value from the three studies (4.27kg/m^2) for comparison. By using published albedo values for 0, 30, 50 and 70% GGBS, the potential emitted CO_2 which could be offset ranged between 1,040 and 5,620 tonnes for the campus. However, this value was significantly higher when the higher average equivalent offset was used. The range of potential CO_2 offset was between 1,740 and 9,410 tonnes of CO_2.
- By using 50% GGBS concrete for the selected areas in the college (as 70% GGBS ages more quickly), the cost of placing the concrete in terms of CO_2 is approximately 768 tonnes and if the concrete achieves an attainable albedo of approximately 0.34, the

amount of potential CO_2 which could be offset (assuming 4.27kg/m^2) is as high as 3,830 tonnes, therefore, the potential CO_2 savings are approximately 3,062 tonnes (3,830-768).

- The measured albedo values from testing on site (see Section 5.2.3 for example) were applied to calculate a reasonable potential offset of emitted CO_2 for the campus and this was found to be in the range of 1,040 and 2,290 tonnes CO_2 using the conservative offset value (2.55kg/m^2) and between 1,740 and 3,830 tonnes using the average offset value (4.27kg/m^2).
- The total CO_2 emissions from Trinity College for the year 2010/2011 was 26,867 tonnes. However, there is potential for an offset of CO_2 by increasing the albedo of surface areas within the college. If an albedo of 0.34 could be achieved for the surface areas calculated (33% of the campus), this would result in an approximate offset of 3,060 tonnes CO_2. This is a very significant amount when the total accumulative savings in the last 9 years (5,000 tonnes) and the current emissions per annum (26,900 tonnes) are taken into account.

9 Conclusions and Recommendations

9.1 Summary of work done

Based on the limited research carried out to date on the effect of concrete constituents on the albedo of concrete, the key parameters to be evaluated were determined, namely the aggregate type, cement type, surface finish and age. A rigorous experimental design was undertaken which factored in these parameters to be tested, resulting in extensive laboratory work being carried out. In order to examine the influence of these parameters on the light reflectance and temperature change in the specimens, the methods of testing were determined, which included measuring the internal temperature of the concrete specimens by means of thermocouple wire. A total of 96 concrete specimens (300x300x60mm) were fabricated comprising 3 different aggregate types (crushed limestone, partially crushed limestone and sandstone), four concentration levels of the cement replacement GGBS (0, 30, 50 and 70%), four different surface finishes to represent varying applications (cast, screed, tamp and brush) and a duplicate of each specimen, with the thermocouple wire placed during the casting of all specimens. Once positioned on the flat rooftop of the civil engineering building in Trinity College, the concrete slabs were connected to data loggers so that the temperature changes could be logged. A sunshine duration sensor was mounted on the parapet of the rooftop so that simultaneous monitoring of sunshine intensity and duration could be recorded .

Some preliminary testing was conducted in order to assess the influence of parameters such as sunlight and air temperature on the surface and internal temperature of the specimens. Subsequently, the chosen test methods for assessing the albedo of the specimens were both direct (albedometer, sphere spectrophotometer, lux meter and greyness scale) and indirect (thermal imaging camera, thermocouple wire). A significant part of the test methods involved determining the sensitivity and accuracy of the aforementioned devices, as much of the testing was influenced by external parameters such as ambient temperature, the incoming sunlight and its intensity.

The albedometer test method involved assessing and quantifying the parameters which have an influence on it, in addition to determining the albedo of a number of site locations containing different concrete surfaces. The lux meter test method developed as part of this research is a unique means of testing which was devised as part of the project, and involves the use of a lux meter to measure the visible light reflectance from the surface of the small scale slab specimens. The instrument was used in conjunction with a box apparatus, which was specifically designed for the task, whose purpose was to eliminate any background light and to measure only the reflectance off the slabs. A sphere spectrophotometer was also employed to measure the colour of the concrete specimens (on a scale of black to white), in addition to measuring the colour of a number of cement powders available on the Irish market. A greyness index chart was used to visually assess the colour of the specimens. The indirect test methods, on the other hand, measure the temperature gain of the specimens when subjected to sunlight. The internal temperature of the specimens were monitored at different stages over the course of the project, in addition to thermal images recorded where there was sufficient sunshine present. By comparing these test methods for determining the influence of the key parameters on both the light reflectance and colour, the findings are summarised in this chapter.

On a global scale, research has shown that by increasing the world wide albedo of urban roofs and paved surfaces, if this were practical, will induce a negative radiative forcing on the earth equivalent to offsetting significant quantities of carbon dioxide emissions. Consequently, a case study was conducted in Trinity College Dublin, whereby each of the horizontal surface areas on the campus were evaluated and measured to determine the potential surface area which could be altered to increase the albedo of these surfaces so as to offset, to some extent, the campus' carbon emissions. The potential emission offset was estimated, and furthermore, was compared to the current annual emissions from the campus and recent savings in such.

9.2 Principal conclusions

The principal findings of this thesis may be summarised as follows:

- From the physics test conducted on three different materials, it can be concluded that it is both the paint and the material underneath which are responsible for the temperature change on the surface. This is because, depending on the nature and colour of the material, solar generated heat is dissipated by infrared emissions from a surface and by conductivity through the material. If the thermal conductivity value is small, the material is a good conductor (e.g. aluminium) while if this value is large the material is a good insulator (e.g. timber).
- The external air temperature is consistently higher than the temperature of the slabs by between 2 and 3°C at night time due to a radiation inversion and the internal temperature of the slabs lags behind the air temperature due to the low thermal conductivity value of concrete.
- The albedometer was used to measure albedo of large surface areas at a number of different site locations. The albedo on the first site at St James Gate Brewery containing aged 30% GGBS concrete with a brush surface finish is 0.25 with a corresponding S.R.I value of 28 which does not meet the LEED criterion of 29. The average albedo value

obtained for the second site at St James Gate Brewery containing new 30% GGBS concrete is 0.285, with a corresponding S.R.I value of 32, which exceeds the minimum S.R.I requirement for LEED accreditation. The albedo of 0% GGBS surface at Father Collins park ranges between 0.24-0.25 which is typical of an aged concrete surface and the 70% GGBS surface is significantly more reflective having an albedo ranging between 0.32-0.34. These albedo readings correspond to S.R.I values on average of between 27.2 and 38 respectively.

- The albedometer is a very sensitive instrument which is difficult to calibrate for limited specimen sizes. The results from the sensitivity tests performed indicate that there is a number of parameters which affect the albedo value, including the height of the instrument, the time of day and season at which the albedo is recorded and also the reduction in field view of the lower dome. Thus, surprisingly, the albedo is not an inherent constant value for a surface. The albedometer does not work with small specimens. The device cannot be calibrated using a restriction on the lower dome given that its presence results in the sensor becoming much less sensitive. However, the albedometer can be used for calculating the approximate albedo of a large surface, such as was carried out at the site locations (St. James Gate Brewery and Father Collins Park).
- The sensitivity tests conducted on the lux meter and black box demonstrated four key points; it is a reliable test method as there is little error as a result of the instrument or in the process of taking a reading; the orientation of the rough surface finish of a slab is important as it effects the percentage of light reflected; the time of day at which the reading is recorded will not affect the overall percentage of reflected lux and similarly the time of year at which the specimen is tested does not affect the result significantly unlike the albedometer results. If the lux meter box is not used, the apparent percentage of reflected lux from a surface is significantly higher, however, considerably less accurate, as background reflected light interferes with the result.
- Preliminary testing using the lux meter on concrete specimens demonstrated some key findings; readings cannot be taken in overcast conditions as they are extremely variable, therefore, testing during sunshine with no clouds present is a requirement; the size of the surface area must be a constant in order to be able to directly compare results of reflected lux; any shadow cast upon the slab surface significantly reduces the reflected lux; the results of ‘relative albedo’ were not consistent with published albedo values, due largely to the size of the testing surface; however, relative values are useful in small scale experiments for comparison purposes.
- Night time luminance testing using the lux meter demonstrated that the order of increasing night time luminance generally corresponds with the increase in GGBS

content, however, with 70% having a reduced reflectance due to ageing. By increasing the level of GGBS from 0 to 50%, there is approximately a 15% increase in the illuminance, which would be sufficiently large to make it worthwhile to promote the use of higher GGBS contents in pavements.

- The L* value of some typical cements displayed a range of values from 63.6 to 90.7. The CEM I and CEM II cements available in Ireland have L* values in the order of 63.6 to 65.7. The L* values of GGBS and white cement are of similar magnitude (87.9 and 90.7 respectively), with white cement having a higher L* than GGBS by approximately 2.8%. The test results of L* for the cement blends indicate that the cement mixes were well blended and uniform across the surface.
- The two test methods that were sensitive enough to measure the effect of aggregate type on light reflectance, which was slight, were the sphere spectrophotometer and the lux meter. Both of these test methods concluded that the sandstone aggregate is marginally less reflective than the limestone aggregates. In addition, as the lux meter was used a number of times to test the specimens at different stages, it was possible to observe a gradual increase in the affect of aggregates on the light reflectance, which signifies that there is a difference between the specimens due to weathering of the surface.
- The five principal test methods which were cross compared (sphere spectrophotometer, lux meter, greyness scale, thermal imaging and thermocouple wire) demonstrate to what degree an increase in GGBS replacement in concrete produces a brighter coloured concrete, with a corresponding reduction in temperature when exposed to solar rays. Although certain test methods, such as thermal imaging, cannot always detect the temperature difference between two adjacent levels of GGBS concentration (i.e. 0 and 30%, 30 and 50%, 50 and 70%), each of the methods demonstrate that there is a significant reduction in temperature/increase in colour between a specimen containing no GGBS and a specimen containing 70% GGBS. It was also concluded that the optimum substitution level of GGBS is 50% as excessive ageing of the 70% specimen was noted by each test method.
- The five test methods demonstrate a universal outcome, that the effect of surface finish on temperature and light reflectance is the dominating factor over the effect of GGBS concentration. In general, the most reflective surface finish is that of screed and the least reflective surface is that of cast. Where there is a rough surface finish such as brush, for example, dispersion on the surface takes place, and based on the review of literature, one would expect these surfaces to gain the highest temperature. However, it was concluded that the colour of the specimen is most important and explains why a smooth surface finish such as cast has the highest temperature - it is visibly darker in colour than the

other specimens, therefore, absorbing more of the solar rays. This fact is clearly more relevant than the surface finish type.

- In order to ascertain the influence of the key parameters on light reflectance, the internal temperature change of the specimen is first and foremost strongly dependant on the presence of clear sunshine, and where this is the case, it is dependant on the intensity and duration of this sunshine. Even peripheral cloud cover can reduce the albedo effect.
- The order of importance in terms of the influential parameters on the light reflectance of concrete is colour, surface finish, GGBS concentration, age and aggregate type. This was confirmed by correspondences between the principal test types, namely L* value, greyness index chart, lux meter and thermocouple data.
- It was estimated that there is a surface area of approximately 33% ($54,434m^2$) within Trinity College Dublin, where the surface reflectance could be increased. The potential for emitted CO_2 to be offset was calculated based on the most conservative value ($2.55kg/m^2$) from one study conducted by Akbari et al. (2008b), and also by using the average value from three published studies ($4.27kg/m^2$) for comparison. By using published albedo values for 0, 30, 50 and 70% GGBS, the potential emitted CO_2 which could be offset ranged between 1,040 and 5,620 tonnes for the campus. However, this value was significantly higher when the higher average equivalent offset of $4.27kg/m^2$ was used. In this case, the range of potential CO_2 offset was between 1,740 and 9,410 tonnes of CO_2.
- By using 50% GGBS concrete for the selected areas in the college (as 70% GGBS ages quickly), the cost of placing the concrete in terms of CO_2 is approximately 768 tonnes and if the concrete achieves an attainable albedo of approximately 0.34, the amount of potential CO_2 which could be offset (assuming $4.27kg/m^2$) is as high as 3,830 tonnes, therefore, the potential CO_2 savings are approximately 3,062 tonnes (3,830-768).
- The total CO_2 emissions from Trinity College for the year 2010/2011 was 26,867 tonnes. The current albedo of the surfaces was assumed to be 0.15 for asphalt surfaces and 0.20 for concrete paving and horizontal roof areas. If an albedo of 0.34 could be achieved for the surface areas calculated (33% of the campus), this would result in an approximate offset of 3,060 tonnes CO_2 (taking into account the carbon cost of implementing the change). This is a very significant amount when the total accumulative savings in the last 9 years (5,000 tonnes) and the current emissions per annum (26,900 tonnes) are taken into account.

9.3 Achievement of objectives

In order to discuss the achievement of the objectives which were set out in the introduction, they are restated here and examined individually. The five principal objectives are as follows;

1. To investigate the present knowledge surrounding all relevant aspects of physics and engineering to understand the phenomenon of solar reflectivity.
2. To evaluate the sensitivity of an albedometer and determine whether it is possible to measure the albedo of small concrete specimens, thus calibrating the instrument.
3. To design a unique and reliable test method of measuring the light reflectance off individual concrete specimens.
4. To investigate the effect of concrete constituents such as aggregate type, GGBS content, surface finish and age on light reflectance and colour of concrete by utilising a number of instruments to measure either directly or indirectly, the effect of the key parameters on the light reflectance or colour of concrete, and as a consequence, compare the various test methods.
5. To conduct a case study at Trinity College Dublin to assess the possible areas where the albedo of surfaces could be improved, and following this, to calculate the possible emitted CO_2 which could be offset against existing values and compared to existing savings.

The first objective of this project was to investigate the present knowledge surrounding all relevant aspects of physics and engineering in order to understand the phenomenon of solar reflectivity. This was carried out by conducting an extensive literature review which encompassed research into the physics of light and its interaction with materials i.e. how light impacts on a surface and the subsequent transfer of energy. It was important to understand the thermal properties of a material, namely how heat is transferred through a material by virtue of conductance and the amount of energy which a material can store. Following this research, there were a number of key physical questions which remained unanswered in relation to the absorption of light and the consequence of painting a material, therefore, there were some preliminary tests conducted in relation to material properties. These tests involved measuring the top and bottom surface temperature of three different materials, namely aluminium, concrete and timber, when subjected to a light source. There were additional specimens (also aluminium, concrete and timber) which were painted black (to represent an albedo of 0), and white (to represent an albedo of 1). There were a number of important conclusions drawn from these tests, one of which was that the colour of a material is important in terms of white and grey, but equally if not more important is the thermal behaviour of the material i.e. its emissivity or ability to shed heat from the surface, and the thermal conductance allowing the transfer of heat down through the depth of the material. These tests conducted on the different materials provided a basis to aide the understanding and interpretation of results from primary test methods.

The second objective involved evaluating the sensitivity of an albedometer and to determine whether it is possible to measure the albedo of small concrete specimens, thus calibrating the instrument. In addition, it was used to measure the albedo of a number of large surface areas. An albedometer is used typically to measure the albedo of large surface areas (approximately 10x10m). Therefore, in order to determine the sensitivity of the device, a number of sensitivity tests were devised, with the aim of using the instrument on the small fabricated concrete specimens containing varying concrete constituents. Before these tests were conducted, a stand was designed for the instrument so that it could be fixed in position over the surface to be tested, at a recommended height of 1.5m and remain level. The five sensitivity tests performed were as follows; to assess the change in albedo over time, to measure the albedo on different days, to determine the effect of altering the height of the instrument, the use of a black cone to restrict the field view of the lower sensor and to assess the relationship between using the cone and the absence of the cone. By determining these key questions, it was then possible to assess whether an albedo result is dependant on these key factors. Once these tests were performed, it was concluded that there are a number of parameters which affect the albedo value, including the time of day and the time of year at which the albedo is recorded, the height of the instrument, and also the reduction in field view of the lower dome. By restricting the lower dome, the sensor becomes much less sensitive, so it was concluded that the device could not be calibrated in this way. The albedometer was, however, used to estimate the albedo of large surfaces and proved to be a very accurate instrument, when used as recommended. The SRI of the surface could also be determined to assess whether the surface qualified for LEED points under the heat island category.

The third objective involved designing a unique and reliable test method of measuring the light reflectance off individual concrete specimens. A lux meter measures light in units of lumens/m^2 and is an inexpensive and reasonably sensitive instrument, therefore, it was chosen as a method of measuring the reflectance off the concrete specimens. However, it could not be used simply by holding it in place over a small specimen to take measurements; thus, a box device was designed, for the purposes of testing, in order to eliminate background light and to obtain a reading solely from the concrete specimens. A number of prototypes were designed, however the final design comprised of a black box which sits on the surface of the slab which is rotated horizontally and vertically, allowing incoming light to reach the slabs surface at an angle of 45°. The sun rays are reflected off the slab's surface and hit the lux meter sensor orthogonal to its axis. To determine whether this test method was accurate and reliable, a number of sensitivity tests was carried out on the prototype which demonstrated that it is a reliable test method as it is not dependant on factors such as the time of day or measuring on a different day. It was concluded, however, that the presence of clouds affect the readings significantly. Preliminary testing was carried out on the lux meter box to verify its reliability, before being used on the fabricated concrete specimens. This objective was met as a result of the outcome from the preliminary tests which concluded that as long as the testing surface area remains constant, with no shadow cast upon the surface of the specimen, and no clouds present when the readings are being taken, the test method is reliable and sensitive enough to differentiate between two slab types with minor reflectivity differences.

The fourth objective of the project is to investigate the effect of aggregate type, GGBS concentration, surface finish and age on the colour and light reflectance of concrete, by virtue of a number of different testing methods. This objective was met by firstly conducting extensive laboratory work to manufacture 96 concrete slabs containing 3 different aggregate types, 4 different GGBS levels and 4 different surface finishes. During this process, one of the test methods (thermocouple wire) was set up so that the internal temperature of the specimens could be monitored. The specimens were then placed on the rooftop of the Civil Engineering building in Trinity College. Five primary test methods were employed on the specimens (excluding the albedometer) which involved the use of a sphere spectrophotometer to measure the colour of the specimens (L* value), a lux meter to measure the reflectance of visible light from the surface, a greyness scale to visually assess the colour of the specimens, a thermal imaging camera to determine the infrared emissions given off by the specimens relative to one another, and the thermocouple wire to log the internal temperature of the specimens.

The sensitivity of the test methods were determined firstly to ensure the method was providing accurate and reliable results. Subsequently, when the various test methods were employed on the specimens, the effect of the concrete constituents were evident. Two test methods which were sensitive enough to measure the effect of aggregate type were the sphere spectrophotometer and the lux meter. It was concluded that the aggregate type does not have a significant influence on the colour of the concrete in the short term, however, as ageing starts to occur, dirt accumulates to different degrees and the aggregates become more exposed at the surface, this factor becomes more influential. The five test methods demonstrate that the increase in GGBS replacement in concrete produces a brighter coloured concrete with a corresponding reduction in temperature. Although certain test methods cannot detect the temperature difference between two adjacent levels of GGBS concentration, each of the methods demonstrate that there is a significant reduction in temperature/increase in colour between a specimen containing no GGBS and a brighter specimen containing 70% GGBS. It was also concluded that the optimum substitution rate of GGBS is 50% as there is little or no difference between 50 and 70% GGBS, with the solar reflectance of the 70% GGBS specimens decreasing with time at a faster rate when compared with the 50% samples. The five test methods also demonstrate that the effect of surface finish on temperature and light reflectance is the dominating factor over the effect of GGBS concentration. In general, the most reflective surface finish is that of screed and the least reflective surface is that of cast. Where there is a rough surface finish such as brush, for example, light dispersion on the surface takes place, and based on the review of literature, one would expect these surfaces to gain the highest temperature, which emerged as not being the case consistently. However, it was concluded that the colour of the specimen is most important and explains why a smooth surface finish such as cast has the highest temperature as it is visibly darker in colour than the other specimens, therefore, absorbing more solar radiation.

Following the testing of the specimens using the various instrumentation as outlined earlier, the final aim of the project was to conduct a case study of Trinity College Dublin to examine whether there were possible areas within the campus to improve the surface albedo, and subsequently, calculate the possible CO_2 emissions which could be offset as a result of this improvement. This was carried out by firstly obtaining a breakdown of the various surface types in the college through the aide of maps and photographs. The area of each of these surface types were divided under the headings of concrete areas, roof areas, asphalt footpaths, asphalt car parks and asphalt pavements. As there were certain areas which could not be used to increase albedo, such as green areas and cobbled areas, the total estimated area which could be utilised was approximately 55,000m^2 equating to 33% of the college campus. Secondly, a review of the current research conducted on the potential offset of CO_2 due to increased albedo of surfaces was carried out and it verified that there were 3 specific studies which estimate the potential offset of CO_2 as a consequence of increasing the albedo of urban areas. Subsequently, the potential for emitted CO_2 to be offset from the campus was calculated based on these studies, using the most conservative value (2.55kg/m^2) from one study, and also by using the average value from the three studies (4.27kg/m^2) for comparison. By using published albedo values for 0, 30, 50 and 70% GGBS, the potential emitted CO_2 was calculated, and this was also conducted for the measured albedo values from three site visits carried out. The total CO_2 emissions from Trinity College for the year 2010/2011 was 26,867 tonnes. The current albedo of Trinity College was assumed to be approximately 0.15 for the asphalt surfaces and 0.20 for the concrete paving areas and roof areas based on published albedo values. However, if a reasonable albedo of 0.34 could be achieved for the surface areas calculated, this would result in an approximate offset of 3,000 tonnes CO_2. This potential CO_2 offset takes into account the carbon cost of implementing these albedo changes, which is approximately 770 tonnes of CO_2 (using 50% GGBS). This saving compares very favourably with hard-won savings made in the last 9 years and taking into account the current CO_2 emissions from the campus. In addition, the albedo changes could be made at no incremental cost to the college, as the new surfaces could be implemented over a number of years once the surfaces require replacing.

9.4 Recommendations for future work

This study has made a contribution towards understanding the effect of concrete constituents on the light reflectance and colour of concrete. However, there is much room for further research in this area. As much of the testing is dependant on sunshine, in particular, where there are no clouds present, there is scope for research to be conducted using artificial light though care in the wavelength of the light to stimulate heat must be taken. Moreover, testing could also be conducted in a country with consistent sunshine and less cloud cover. In such countries, the benefits of reducing UHI effect and air conditioning costs are likely to be much more substantial.

The key testing parameters chosen for this research included a substitution rate of up to 70% GGBS, however, by using an even higher rate, say 85%, this may produce a specimen which is even brighter than a 70% specimen. Furthermore, the use of white cement as a substitution could be carried out, with the results being compared to specimens containing GGBS. Moreover, the use of white aggregates could be implemented so that if ageing occurs and the aggregates become exposed at the surface, they will not significantly reduce the overall colour or light reflectance of the specimen. However, by producing an even brighter material with lighter coloured constituents such as concrete with high levels of GGBS, the effect of glare is one area which would need to be carefully considered, in particular for roads. This is an area where further research could be conducted. Furthermore, by using a high levels of GGBS such as 70% replacement, it was found that the specimen reduced in albedo faster than the other specimens i.e. at a faster rate. As a consequence, research could be carried out into the surface characteristics of the different GGBS specimens, in particular, with relation to the absorption of dirt on the surface.

There is scope for further research in relation to the testing methods used throughout this project. Another possibility could involve cleaning the current slab specimens, to assess whether there is increased light reflectance as a result, and there is also the option of painting the surfaces white to determine its influence on the temperature of the specimens. Furthermore, the effect of GGBS concentration over time could be studied. This could be conducted by monitoring the specimens on roof for several years to determine whether there are trends between the GGBS concentrations and on that basis decide at which stage the cleaning of the surface should be carried out. Moreover, research could be carried out into the various methods of cleaning the surfaces of the specimens in terms of their effectiveness and how often it should be performed.

There is further scope for research by conducting this research in India where the climate would be a distinct advantage. Cool roofs could be implemented (by virtue of white toppings or paint) to sample buildings with on-going monitoring of before and afterwards, to determine the heat differences on upper floors during the summer months. The carbon cost of implementing a high albedo solution should be determined and compared to the carbon saving.

There is also further scope for research into the benefits of high albedo surfaces at night-time, in relation to safety and security and the savings attained by virtue of the need for reduced lighting. With further research, high albedo surfaces could be a positive recommendation for reducing energy consumption in buildings, and in turn, creating more sustainable cities. However, as the research area is relatively new within Europe, more scientific evidence of its potential for improving the urban environment is necessary.

References

ACKERMAN, S. & KNOX, J. 2012. *Meteorology: Understanding the Atmosphere*, Jones and Bartlett Learning.

AHRENS, C. D., JACKSON, P. L., JACKSON, C. E. J. & JACKSON, C. E. O. 2012. *Meteorology Today: An Introduction to Weather, Climate, and the Environment*, Nelson Education.

AKBARI, H. 2003. Measured energy savings from the application of reflective roofs in two small non-residential buildings. *Energy,* 28, 953-967.

AKBARI, H., BELL, R. & TAHA, H. E. A. 2008a. Reducing Heat Islands: Compendium of Strategies- Urban Heat Island Basics.

AKBARI, H., DAVIS, S., DORSANO, S., HUANG, J. & WINNETT, S. 1992. *Cooling Our Communities: A Guidebook on Tree Planting and Light-Colored Surfacing*, United States Environmental Protection Agency.

AKBARI, H., LEVINSON, R. & RAINER, L. 2005. Monitoring the energy-use effects of cool roofs on California commercial buildings. *Energy and Buildings,* 37, 1007-1016.

AKBARI, H., MATTHEWS, H. D. & SETO, D. 2012. The long-term effect of increasing the albedo of urban areas. *Environmental Research Letters,* 7.

AKBARI, H., MENON, S. & ROSENFELD, A. 2008b. Global cooling: increasing world-wide urban albedos to offset CO_2.

AKBARI, H., POMERANTZ, M. & TAHA, H. 2001. Cool surfaces and shade trees to reduce energy use and improve air quality in urban areas. *Solar Energy,* 70, 295-310.

AKBARI, H., ROSE, L. S. & TAHA, H. 2003. Analyzing the land cover of an urban environment sing high-resolution orthophotos. *Landscape and Urban Planning,* 63, 1-14.

AKBARI, H., ROSENFELD, A. & TAHA, H. Summer heat islands, urban trees, and white surfaces. Proceedings of the 1990 ASHRAE Winter Conference, 1990.

AL-AZZAWI, A. 2007. *Light and optics principles and practises*, CRC Press.

ANDERSON, B. 2006. Chapter 3: Thermal properties of Building Structures. *CIBSE Guide A: Environmental Design.* Norwich: Chartered Institute of Building Services Engineers (CIBSE).

ASKELAND, D. R. & PHULE, P. P. 2006. *The science and engineering of materials,* Toronto, Thomson Canada Ltd.

ASTM 1997. E1918 - 06 Standard Test Method for Measuring Solar Reflectance of Horizontal and Low-Sloped Surfaces in the Field. West Conshohocken, PA: ASTM International.

ASTM 2006. E490 - 00a Standard Solar Constant and Zero Air Mass Solar Spectral Irradiance Tables. ASTM International.

ASTM 2008. E408 - 71 Standard Test Methods for Total Normal Emittance of Surfaces Using Inspection-Meter Techniques. ASTM International.

ASTM 2009. C1549 - 09 Standard Test Method for Determination of Solar Reflectance Near Ambient Temperature Using a Portable Solar Reflectometer. West Conshohocken, PA: ASTM International.

ASTM 2010. C1371 - 04a Standard Test Method for Determination of Emittance of Materials Near Room Temperature Using Portable Emissometers. ASTM International.

ASTM 2011. E1980 - 11 Standard Practice for Calculating Solar Reflectance Index of Horizontal and Low-Sloped Opaque Surfaces.

ASTM 2012. G173 - 03 Standard Tables for Reference Solar Spectral Irradiances: Direct Normal and Hemispherical on 37° Tilted Surface. ASTM International.

BAEHR, H. H. D. & STEPHAN, K. 2011. *Heat and Mass Transfer*, Springer.

BEESON, S. & MAYER, J. W. 2008. *Patterns of Light - Chasing the spectrum from Aristotle to LED's,* New York, Springer.

BERDAHL, P., AKBARI, H., LEVINSON, R. & MILLER, W. A. 2008. Weathering of roofing materials – An overview. *Construction and Building Materials,* 22, 423-433.
BERDAHL, P. & BRETZ, S. E. 1997. Preliminary survey of the solar reflectance of cool roofing materials. *Energy and Buildings,* 25, 149-158.
BERGMAN, T. L., LAVINE, A. S., INCROPERA, F. P. & DEWITT, D. P. 2011. *Introduction to Heat Transfer*, Wiley.
BHATTA, B. 2010. *Analysis of Urban Growth and Sprawl from Remote Sensing Data*, Springer.
BOIXO, S., DIAZ-VICENTE, M., COLMENAR, A. & CASTRO, M. A. 2012. Potential energy savings from cool roofs in Spain and Andalusia. *Energy,* 38, 425-438.
BORIBOONSOMSIN, K. & REZA, F. 2007. Mix Design and Benefit Evaluation of high Solar Reflectance Concrete for Pavements.
BRAZEL, A., SELOVER, N., VOSE, R. & HEISLER, G. 2000. The tale of two climates—Baltimore and Phoenix urban LTER sites. *Climate Research,* 15, 123-15.
BRE-GLOBAL. 2012. *BREEAM for communities* [Online]. Available: http://www.breeam.org/ [Accessed 13-02 2013].
BRETZ, S., AKBARI, H. & ROSENFELD, A. 1998. Practical issues for using solar-reflective materials to mitigate urban heat islands. *Atmospheric Environment,* 32, 95-101.
BRETZ, S. E. & AKBARI, H. 1997. Long-term performance of high-albedo roof coatings. *Energy and Buildings,* 25, 159-167.
CASPER, J. K. 2009. *Greenhouse Gases: Worldwide Impacts*, Facts On File, Incorporated.
CHAO, J. 2010. Global Model Confirms: Cool Roofs Can Offset Carbon Dioxide Emissions and Mitigate Global Warming. Available: http://newscenter.lbl.gov/news-releases/2010/07/19/cool-roofs-offset-carbon-dioxide-emissions/ [Accessed 26th August 2013].
CLEVELAND, C. J. & MORRIS, C. 2009. *Dictionary of Energy*, Elsevier Ltd.
CRONIN, T. M. 2010. *Paleoclimates*, COLUMBIA University Press.
DEEGAN, P., O' CONNOR, A. & ARCHBOLD, P. 2010. Measurement of time-dependant colour variation in concrete. BCRI, 2012 Dublin. 247-251.
DESSLER, A. 2011. *Introduction to Modern Climate Change*, Cambridge University Press.
ECOCEM 2009. GGBS and Reducing Global Warming - The Albedo Effect. *worldcement.com*.
EMMANUEL, R. 2005. *An Urban Approach To Climate Sensitive Design: Strategies for the Tropics,* NY, Spon Press.
G.B.I. 2013. *Green Globes: The Practical Building Rating System* [Online]. Available: http://www.greenglobes.com/ [Accessed 13-02 2013].
GARTLAND, L. 2008. *Heat Islands*, earthscan.
GHOSHDASTIDAR, P. S. 2004. *Heat Transfer: Includes CD-ROM*, Oxford University Press.
GIANCOLI, D. C. 2009. *Physics for scientists and engineers with modern physics*, Pearson Education, Inc.
GOOGLE_EARTH. 2008. *Trinity College Dublin 53°20'37.71"N 6°15'16.18"W, elevation 4m* [Online]. Dublin: Google Earth 6.0. Available: http://www.google.com/earth/index.htm [Accessed 09/03/2013.
GOOGLE_EARTH. 2009. *Father Collins Park, Donaghmeade 53°24'15.78"N 6°09'35.55"W, elevation 10m* [Online]. Dublin: Google Earth 6.0. Available: http://www.google.com/earth/index.htm [Accessed 09/03/2013.
GUPTA, R. P. 2003. *Remote Sensing Geology*, Springer.
HANSEN, J., SATO, M. & RUEDY, R. 1997. Radiative forcing and climate response. *Journal of Geophysical Research: Atmospheres,* 102, 6831-6864.
HATZIANASTASSIOU, N., MATSOUKAS, C., FOTIADI, A., PAVLAKIS, K. G., DRAKAKIS, E., HATZIDIMITRIOU, D. & VARDAVAS, I. 2005. Global distribution of Earth's surface shortwave radiation budget. *Atmospheric Chemistry and Physics,* 5, 2847-2867.

HIGGINS, O. & WEST, R. 2010. The design and manufacture of a lux meter instrument which will be used to determine the Albedo effect in concrete. Dublin: Department of Civil, Structural and Environmental Engineering, Trinity College Dublin.

HOLMAN, J. P. 2010. *Heat transfer,* NY, McGraw-Hill.

HUTCHINS, M. 2009. Progress report of the EU cool roofs council technical committee.

IPCC 2001. Climate change 2001-the scientific basis, contribution of working group 1 to the third assessment report of the IPCC. Chapter 6. *Radiative Forcing of Climate Change.* Intergovernmental Panel on Climate Change.

IPCC 2007. Climate change 2007-the physical science basis, contribution of working group 1 to the fourth assessment report of the IPCC. Chapter 7, Figure 7.4 and Section 7.3.2.1.

JACOBSON, M. Z. 2012. *Air Pollution and Global Warming: History, Science, and Solutions*, Cambridge University Press.

KAVIANY, M. 2011. *Essentials of Heat Transfer: Principles, Materials, and Applications,* New York, Cambridge University Press.

KIEHL, J., TRENBERTH, K. E. & FASULLO, J. T. 2009. Earth's Annual Global Mean Energy Budget. *Bulletin of American Meteorological Society,* 90, 311-323.

KINGSLAKE, R. & THOMPSON, B. J. 2011. *Reflection of Light [Art]* [Online]. Chicago: Encyclopædia Britannica Online Academic Edition. Available: http://www.britannica.com/EBchecked/media/165415/In-the-reflection-of-light-the-angle-of-incidence-is [Accessed 7th November 2012].

KIPP_AND_ZONEN. 2013. *CSD3 Sunshine Duration Sensor- Instruction Sheet* [Online]. Available: http://www.kippzonen.com/?product/35132/CSD+3.aspx [Accessed 06/06/2013 2013].

KLINENBERG, E. 2002. *Heat wave: a social autopsy of disaster in Chicago*, The University of Chicago.

LEMAIRE, G., ESCADEILLAS, G. & RINGOT, E. 2005. Evaluating concrete surfaces using an image analysis process. *Construction and Building Materials,* 19, 604-611.

LEVINSON, R. & AKBARI, H. 2002. Effects of composition and exposure on the solar reflectance of portland cement concrete. *Cement and Concrete Research,* 32, 1679-1698.

LEVINSON, R., AKBARI, H. & BERDAHL, P. 2010a. Measuring solar reflectance—Part II: Review of practical methods. *Solar Energy,* 84, 1745-1759.

LEVINSON, R., AKBARI, H., BERDAHL, P., WOOD, K., SKILTON, W. & PETERSHEIM, J. 2010b. A novel technique for the production of cool colored concrete tile and asphalt shingle roofing products. *Solar Energy Materials and Solar Cells,* 94, 946-954.

LEVINSON, R., BERDAHL, P., AKBARI, H., MILLER, W., JOEDICKE, I., REILLY, J., SUZUKI, Y. & VONDRAN, M. 2007. Methods of creating solar-reflective non-white surfaces and their application to residential roofing materials. *Solar Energy Materials and Solar Cells,* 91, 304-314.

LI, H., HARVEY, J. & KENDALL, A. 2013. Field measurement of albedo for different land cover materials and effects on thermal performance. *Building and Environment,* 59, 536-546.

MALPAS, P. 2007. *Basics Photography 03: Capturing Colour*, Bloomsbury Academic.

MANLEY, G. 1958. On the frequency of snowfall in metropolitan England. *Quarterly Journal of the Royal Meteorological Society,* 84, 70-72.

MARTIEN, P., AKBARI, H. & ROSENFELD, A. 1989. Light- colored surfaces to reduce summertime urban temperatures: benefits, costs, and implementation issues. *9th Miami International Congress on Energy and Environment.* Florida.

MATTHEWS, H. D., GILLETT, N. P., STOTT, P. & ZICKFELD, K. 2009. Proportionality of global warming to cumulative carbon emissions. *Nature,* 459, 829-832.

MCMULLAN, R. 2007. *Environmental Science in Building*, Palgrave Macmillan.

MENON, S., AKBARI, H., LEVINSON, R., MAHANAMA, S. & SEDNEV, I. 2010. Radiative forcing and temperature response to changes in urban albedos and associated CO_2 offsets. *Environmental Research Letters,* 5.

MET_EIREANN. 2013. *Sunshine and Solar Radiation: Cloud amounts* [Online]. Dublin: The Irish Meteorological Service Online. Available: http://www.met.ie/climate-ireland/sunshine.asp?prn=1 [Accessed 17th April 2013].

MULVANEY, D. 2011. *Green Technology: An A to Z Guide*, Sage.

MYERS, R. L. 2006. *The basics of physics*, GREENWOOD Publishing Group Incorporated.

MYHRE, G., HIGHWOOD, E. J., SHINE, K. P. & STORDAL, F. 1998. New estimates of radiative forcing due to well mixed greenhouse gases. *Geophysical Research Letters,* 25, 2715-2718.

NASA. 2006. *NASA's ICESat Satellite Sees Changing World Affecting Many - Capturing the Clouds for Clues on Climate and Weather* [Online]. National Aeronautics and Space Administration. Available: http://www.nasa.gov/vision/earth/lookingatearth/icesat_light.html [Accessed 17th April 2013].

NATIONAL_RESEARCH_COUNCIL 2005. *Radiative Forcing of Climate Change: Expanding the Concept and Addressing Uncertainties*, National Academies Press.

NEVILLE, A. M. 1995. *Properties of Concrete*, Longman Group Ltd.

NEWMAN, J. & CHOO, B. S. 2003. *Advanced Concrete Technology 1: Constituent Materials*, Elsevier Science.

NEWTON, R. E. I. 1990. *Wave Physics,* New York, Edward Arnold.

NOLAN, P. J. 2012. Physics for Science and Engineering Students. *Calculus-Based Introductory Physics Textbook.* 1st ed. Lakeville, Minnesota: Physics Curriculum & Instruction.

NSAI 2009a. I.S EN 12390-2 Testing hardened concrete- Making and curing specimens for strength tests. Dublin: National Standards Authority of Ireland (NSAI).

NSAI 2009b. I.S EN 12390-3. Testing hardened concrete - Part 3: Compressive strength of test specimens. National Standards Authority of Ireland (NSAI).

NSAI 2009c. I.S. EN 12350-2 Testing fresh concrete - Part 2: Slump-test. Dublin: National Standards Authority of Ireland (NSAI).

NSAI 2011. I.S EN 197-1 Cement. Composition, specifications and conformity criteria for common cements. Dublin: National Standards Authority of Ireland (NSAI).

O'HARE, G., SWEENEY, J. & WILBY, R. L. 2005. *Weather, Climate, and Climate Change: Human Perspectives,* Essex, Pearson Education Ltd.

OKE, T. R. 1987. *Boundary layer climate*, Taylor and Francis.

PALLE, E. & BUTLER, C. J. 2001. Sunshine Records from Ireland: Cloud Factors and Possible Links to Solar Activity and Cosmic Rays. *International Journal of Climatology,* 21, 709-729.

PEDROTTI, F. L., PEDROTTI, L. S. & PEDROTTI, L. M. 2007. *Introduction to Optics,* San Francisco, Pearson Education :td.

PIRARD, P., VANDENTORREN, S., PASCAL, M., LAAIDI, K., LE TERTRE, A., CASSADOU, S. & LEDRANS, M. 2005. Summary of the mortality impact assessment of the 2003 heat wave in France. Eurosurveillance.

POSTELL, J. & GESIMONDO, N. 2011. *Materiality and Interior Construction*, Wiley.

RACUSIN, J. D. & MCARLETON, A. 2012. *The Natural Building Companion: A Comprehensive Guide to Integrative Design and Construction*, Chelsea Green Publishing.

REAGAN, J. A. & ACKLAM, D. M. 1979. Solar reflectivity of common building materials and its influence on the roof heat gain of typical southwestern U.S.A. residences. *Energy and Buildings,* 2, 237-248.

RESNIK, R. 2013. *Greyness Reference Chart* [Online]. Available: http://www.digital-images.net/temp/Greyscales_ColorChart/GreyRefTool.jpg [Accessed 7th June 2013].

ROHRER, F. 2013. *The Filthy Air Conundrum* [Online]. BBC News. Available: http://news.bbc.co.uk/2/hi/uk_news/magazine/7532603.stm [Accessed 7th June 2013].

ROSE, L. S., AKBARI, H. & TAHA, H. 2003. Characterizing the Fabric of the Urban Environment: A Case Study of Greater Houston, Texas. Heat Island Group,Environmental Energy Technologies Division Lawrence Berkeley Laboratory.

ROSENFELD, A. H., AKBARI, H., BRETZ, S., FISHMAN, B. L., KURN, D. M., SAILOR, D. & TAHA, H. 1995. Mitigation of urban heat islands: materials, utility programs, updates. *Energy and Buildings,* 22, 255-265.

ROSENFELD, A. H., ROMM, J. J., AKBARI, H. & LLOYD, A. C. 1997. Painting the town white and green. *MIT's Technology Review,* 100, 52-59.

SABNIS, G. M. 2012. *Green Building With Concrete: Sustainable Design and Construction*, CRC Press.

SANTAMOURIS, M. 2001. *Energy and climate in the urban built environment, Volume 1,* London, James and James Ltd.

SANTAMOURIS, M. 2006. *Environmental Design of Urban Buildings: An Integrated Approach*, Earthscan LLC.

SANTAMOURIS, M. 2007. *Advances in Passive Cooling*, Earthscan.

SANTAMOURIS, M. 2009. *Advances in Building Energy Research,* 3, 148.

SANTAMOURIS, M., SYNNEFA, A. & KARLESSI, T. 2011. Using advanced cool materials in the urban built environment to mitigate heat islands and improve thermal comfort conditions. *Solar Energy,* 85, 3085-3102.

SCA. 2003. Slag Cement and the Environment. *Slag Cement in Concrete* [Online].

SEAI. 2013. *Emission Factors* [Online]. Sustainable Energy Authority of Ireland. Available: http://www.seai.ie/Publications/Statistics_Publications/Emission_Factors/ [Accessed 15th April 2013].

SHAHMOHAMADI, P., CHE-ANI, A. I., ETESSAM, I., MAULUD, K. N. A. & TAWIL, N. M. 2011. Healthy Environment: The Need to Mitigate Urban Heat Island Effects on Human Health. *Procedia Engineering,* 20, 61-70.

SIDDIQUE, R. & KHAN, M. I. 2011. *Supplementary Cementing Materials*, Springer.

SOLANKI, C. S. 2008. *Renewable Energy Technologies: Practical Guide For Beginneers*, Prentice-Hall Of India Pvt. Limited.

SOLECKI, W. D., ROSENZWEIG, C., PARSHALL, L., POPE, G., CLARK, M., COX, J. & WIENCKE, M. 2005. Mitigation of the heat island effect in urban New Jersey. *Global Environmental Change Part B: Environmental Hazards,* 6, 39-49.

STELLARNET_INC. 2013. *Black comet spectrometer series for UV-VIS and NIR* [Online]. Available: http://www.stellarnet.us/products_spectrometers_BLACK-Comet-SR.htm [Accessed 11/06/2013 2013].

STULL, R. B. 2000. *Meteorology for Scientists and Engineers*, Gary Garlson.

SWEENEY, A. & WEST, R. The use of a greyness index chart as an indicator of surface albedo of concrete. Innovations in Concrete Construction, 2013 India.

SWEENEY, A., WEST, R. & O CONNOR, C. 2010. Parameters affecting the albedo effect in concrete. BCRI, 2010 Cork. 513-520.

SWEENEY, A., WEST, R. & O CONNOR, C. 2012. Measuring the albedo of concrete slabs for different slag contents and surface finishes. Concrete in the low carbon era, 2012a Dundee.

SWEENEY, A., WEST, R. & SEYMOUR, P. 2012. Factors affecting the measurement of solar reflectance using an albedometer. BCRI, 2012b Dublin. 241-245.

SYNNEFA, A., SALIARI, M. & SANTAMOURIS, M. 2012. Experimental and numerical assessment of the impact of increased roof reflectance on a school building in Athens. *Energy and Buildings*.

SYNNEFA, A., SANTAMOURIS, M. & LIVADA, I. 2006. A study of the thermal performance of reflective coatings for the urban environment. *Solar Energy,* 80, 968-981.

TAHA, H. 1997a. Modeling the impacts of large-scale albedo changes on ozone air quality in the South Coast Air Basin. *Atmospheric Environment,* 31, 1667-1676.

TAHA, H. 1997b. Urban climates and heat islands: albedo, evapotranspiration, and anthropogenic heat. *Energy and Buildings,* 25, 99-103.

TAHA, H., AKBARI, H., ROSENFELD, A. & HUANG, J. 1988. Residential cooling loads and the urban heat island--the effects of albedo. *Building and Environment,* 23, 271-283.

TAHA, H., SAILOR, D. & AKBARI, H. 1992. High Albedo Materials for Reducing Building Cooling Energy Use. Energy and Environment Division Lawrence Berkeley Laboratory.

TEYCHENNE, D. C., FRANKLIN, R. E. & ERNTROY, H. C. 1997. *Design of normal concrete mixes*, BREPress.

THE_CONCRETE_SOCIETY 2011. *Cementitious Materials: The Effect of GGBS, Fly Ash, Silica Fume and Limestone Fines on the Properties of Concrete : Report of a Concrete Society Working Party*, Concrete Society.

THIRUMALESHWAR, M. 2006. *Fundamentals of Heat and Mass Transfer,* India, Pearson Education.

THORPE, G. S. 2009. *AP environmental science,* N.Y, Barron's Educational Series.

TILLEY, R. J. D. 2004. *Understanding Solids The Science of Materials*, John Wiley and Sons.

TOMMERUP, H. & SVENDSEN, S. 2006. Energy savings in Danish residential building stock. *Energy and Buildings,* 38, 618-626.

UNFCCC. 2013. *Kyoto protocol* [Online]. United Nations Framework Convention on Climate Change. Available: http://unfccc.int/kyoto_protocol/items/2830.php [Accessed 25th April 2013].

USGBC. 2013a. *Buildings and Climate Change* [Online]. Sacramento, CA: U.S Green Building Council. Available: http://www.documents.dgs.ca.gov/dgs/pio/facts/LA%20workshop/climate.pdf.

USGBC. 2013b. *U.S. Green Building Council* [Online]. Available: www.usgbc.org [Accessed 13-02 2013].

WAN, W. C., HIEN, W. N., PING, T. P. & ALOYSIUS, A. J. W. 2009. A study on the effectiveness of heat mitigating pavement coatings in Singapore. *Second International Conference on Countermeasures to Urban Heat Islands.* Berkeley, California.

WANG, Y. C., BURGESS, I., WALD, F. & GILLIE, M. 2012. *Performance Based Fire Engineering of Structures*, Taylor & Francis Group.

WEISS, N. A. 2008. *Introductory Statistics*, Pearson.

WILSON, J. D., BUFFA, A. J. & LOU, B. 2007. *College Physics*, Pearson Prentice Hall.

XU, T., SATHAYE, J., AKBARI, H., GARG, V. & TETALI, S. 2012. Quantifying the direct benefits of cool roofs in an urban setting: Reduced cooling energy use and lowered greenhouse gas emissions. *Building and Environment,* 48, 1-6.

ZDUNKOWSKI, W., TRAUTMANN, T. & BOTT, A. 2007. *Radiation in the Atmosphere: A Course in Theoretical Meteorology*, Cambridge University Press.

Appendix A Concrete mix design form (Teychenne et al., 1997)

Job title ....

Stage	Item		Reference or calculation	Values
1	1.1	Characteristic strength	Specified	35 N/mm² at 28 days; Proportion defective ...... %
	1.2	Standard deviation	Fig 3	...... N/mm² or no data 8 N/mm²
	1.3	Margin	C1 or Specified	(k = 1.64) 1.64 × 8 = 13.12 N/mm²; ...... N/mm²
	1.4	Target mean strength	C2	35 + 13.12 = 48.12 N/mm²
	1.5	Cement strength class	Specified	42.5/52.5
	1.6	Aggregate type: coarse Aggregate type: fine		Crushed/uncrushed Crushed/uncrushed
	1.7	Free-water/cement ratio	Table 2, Fig 4	0.55 } Use the lower value $\boxed{0.55}$
	1.8	*Maximum free-water/ cement ratio*	*Specified*	......
2	2.1	Slump or Vebe time	Specified	Slump 60-180 mm or Vebe time ...... s
	2.2	Maximum aggregate size	Specified	20 mm
	2.3	Free-water content	Table 3	$\boxed{225}$ kg/m³
3	3.1	Cement content	C3	225 ÷ 0.55 = 409 kg/m³
	3.2	*Maximum cement content*	*Specified*	...... kg/m³
	3.3	*Minimum cement content*	*Specified*	...... kg/m³
				use 3.1 if ≤ 3.2 use 3.3 if > 3.1 $\boxed{409}$ kg/m³
	3.4	Modified free-water/cement ratio		......
4	4.1	Relative density of aggregate (SSD)		2.6 known/assumed
	4.2	Concrete density	Fig 5	2390 kg/m³
	4.3	Total aggregate content	C4	2390 - 409 - 225 = 1756 kg/m³
5	5.1	Grading of fine aggregate	Percentage passing 600 µm sieve	60 %
	5.2	Proportion of fine aggregate	Fig 6	35 %
	5.3	Fine aggregate content	C5	0.35 × 1756 = $\boxed{614.6}$ kg/m³
	5.4	Coarse aggregate content	C5	1756 - 614.6 = $\boxed{1141.4}$ kg/m³

Quantities	Cement (kg)	Water (kg or litres)	Fine aggregate (kg)	Coarse aggregate (kg) 10 mm	20 mm	40 mm
per m³ (to nearest 5 kg)	410	225	615	380	760	
per trial mix of 0.0543 m³	22.26	12.24	33.40	20.60	41.24	

Items in italics are optional limiting values that may be specified (see Section 7).
Concrete strength is expressed in the units N/mm². 1 N/mm² = 1 MN/m² = 1 MPa. (N = newton; Pa = pascal.)
The internationally known term 'relative density' used here is synonymous with 'specific gravity' and is the ratio of the mass of a given volume of substance to the mass of an equal volume of water.
SSD = based on the saturated surface-dry condition.

Appendix B Schedule of mixing

	Monday	Tuesday	Wednesday	Thursday	Friday
August	**2nd**	**3rd**	**4th**	**5th**	**6th**
Morning	**Bank Holiday**	Pour 1: Agg- Limestone 0% Crushed- Cast 0% Crushed- Screed 0% Crushed-Tamp 0% Crushed-Brush	Pour 2: Agg: PC Limestone 0% Partially Crushed-Cast 0% Partially Crushed-Screed 0% Partially Crushed-Tamp 0% Partially Crushed-Brush	Pour 3: Agg Sandstone 0% Sandstone-Cast 0% Sandstone-Screed 0% Sandstone-Tamp 0% Sandstone-Brush	Strip and clean moulds
Afternoon			Strip and clean moulds	Strip and clean moulds	
August	**9th**	**10th**	**11th**	**12th**	**13th**
Morning	Pour 4: Agg- Limestone 30% Crushed -Cast 30% Crushed-Screed 30% Crushed-Tamp 30% Crushed-Brush	Pour 5: Agg: PC Limestone 30% Partially Crushed-Cast 30% Partially Crushed-Screed 30% Partially Crushed-Tamp 30% Partially Crushed-Brush	Pour 6: Agg Sandstone 30% Sandstone-Cast 30% Sandstone-Screed 30% Sandstone-Tamp 30% Sandstone-Brush	Pour 7: Agg- Limestone 50% Crushed-Cast 50% Crushed-Screed 50% Crushed-Tamp 50% Crushed-Brush	Strip and clean moulds
Afternoon	Strip and clean moulds	Strip and clean moulds	Strip and clean moulds	Strip and clean moulds	
August	**16th**	**17th**	**18th**	**19th**	**20th**
Morning	Pour 8: Agg: PC Limestone 50% Partially Crushed-Cast 50% Partially Crushed-Screed 50% Partially Crushed-Tamp 50% Partially Crushed-Brush	Pour 9: Agg Sandstone 50% Sandstone-Cast 50% Sandstone-Screed 50% Sandstone-Tamp 50% Sandstone-Brush	Pour 10: Agg- Limestone 70% Crushed-Cast 70% Crushed-Screed 70% Crushed- Tamp 70% Crushed-Brush	Pour 11: Agg: PC Limestone 70% Partially Crushed-Cast 70% Partially Crushed-Screed 70% Partially Crushed-Tamp 70% Partially Crushed-Brush	Strip and clean moulds
Afternoon	Strip and clean moulds	Strip and clean moulds	Strip and clean moulds	Strip and clean moulds	
August	**23rd**	**24th**			
Morning	Pour 12: Agg Sandstone 70% Sandstone-Cast 70% Sandstone-Screed 70% Sandstone-Tamp 70% Sandstone-Brush	Strip and clean moulds			
Afternoon	Strip and clean moulds				

Appendix C Fresh concrete (slump test) and hardened concrete (compressive strength) test results

Pour no.	Cube no.	GGBS	Aggregate	Water (L)	Slump (mm)	Slump type >150mm = collapsed	Strength at 28 days (MPa)	Average strength at 28 days (MPa)
1	1	0	Crushed LS	10.4	≥160	Collapsed	46.7	47.4
	2	0	Crushed LS				48.1	
2	1	0	PC Limestone	11.2	140	Shear	44.0	43.4
	2	0	PC Limestone				42.8	
3	1	0	Sandstone	10.9	90	True	42.9	43.7
	2	0	Sandstone				44.4	
4	1	30	Crushed LS	10.4	110	True	40.9	47.5 (discard result)
	2	30	Crushed LS				54.1	
5	1	30	PC Limestone	11.17	150	Shear	46.3	46.2
	2	30	PC Limestone				46.2	
6	1	30	Sandstone	10.9	45	True	42.3	43.1
	2	30	Sandstone				43.8	
7	1	50	Crushed LS	10.4	144	Shear	45.8	46.8
	2	50	Crushed LS				47.8	
8	1	50	PC Limestone	11.17	≥160	Collapsed	42.1	41.4
	2	50	PC Limestone				40.7	
9	1	50	Sandstone	10.9	55	True	42.6	43.4
	2	50	Sandstone				44.1	
10	1	70	Crushed LS	10.4	≥160	Shear	41.8	42.9
	2	70	Crushed LS				44.0	
11	1	70	PC Limestone	11.17	≥160	Collapsed	34.3	35.4
	2	70	PC Limestone				36.4	
12	1	70	Sandstone	10.9	25	True	35.9	36.8
	2	70	Sandstone				37.6	

Appendix D Results of Albedo at St James Gate Brewery

Site 1

Cycle	Location	Reading	Pyr (Upper)	Pyr*	Alb(Lower)	Alb*	Albedo	Average
1	A	1	21.5	2.563	5.4	0.619	0.242	0.241
		2	21.6	2.574	5.4	0.619	0.241	
		3	21.6	2.574	5.4	0.619	0.241	
	B	1	22.2	2.646	5.3	0.608	0.230	0.231
		2	22.4	2.670	5.4	0.619	0.232	
		3	22.5	2.682	5.4	0.619	0.231	
	C	1	23.8	2.837	5.6	0.642	0.226	0.227
		2	23.8	2.837	5.6	0.642	0.226	
		3	24.0	2.861	5.7	0.654	0.229	
	D	1	23.2	2.765	5.9	0.677	0.245	0.245
		2	23.4	2.789	5.9	0.677	0.243	
		3	23.4	2.789	6.0	0.688	0.247	
2	A	1	22.8	2.718	6.0	0.688	0.253	0.253
		2	22.8	2.718	6.0	0.688	0.253	
		3	22.9	2.729	6.0	0.688	0.252	
	B	1	23.1	2.753	5.8	0.665	0.242	0.241
		2	23.1	2.753	5.8	0.665	0.242	
		3	23.2	2.765	5.8	0.665	0.241	
	C	1	24.6	2.932	6.0	0.688	0.235	0.233
		2	24.6	2.932	5.9	0.677	0.231	
		3	24.6	2.932	6.0	0.688	0.235	
	D	1	24.4	2.908	6.3	0.722	0.248	0.248
		2	24.5	2.920	6.3	0.722	0.247	
		3	24.5	2.920	6.3	0.722	0.247	

Site 2(a)

Cycle	Location	Reading	Pyr (Upper)	Pyr*	Alb(Lower)	Alb*	Albedo	Average
1	A	1	25.9	3.087	6.7	0.768	0.249	0.246
		2	26.1	3.111	6.6	0.757	0.243	
		3	25.9	3.087	6.6	0.757	0.245	
	B	1	26.1	3.111	6.8	0.780	0.251	0.252
		2	26.2	3.123	6.9	0.791	0.253	
		3	26.2	3.123	6.9	0.791	0.253	
	C	1	26.1	3.111	7.1	0.814	0.262	0.261
		2	26.2	3.123	7.1	0.814	0.261	
		3	25.9	3.087	7.0	0.803	0.260	
	D	1	25.0	2.980	6.6	0.757	0.254	0.254
		2	25.2	3.004	6.6	0.757	0.252	
		3	25.2	3.004	6.7	0.768	0.256	
2	A	1	25.5	3.039	6.4	0.734	0.241	0.241
		2	25.5	3.039	6.4	0.734	0.241	
		3	25.5	3.039	6.4	0.734	0.241	
	B	1	26.1	3.111	6.7	0.768	0.247	0.248
		2	26.1	3.111	6.7	0.768	0.247	
		3	25.9	3.087	6.7	0.768	0.249	
	C	1	25.6	3.051	7.0	0.803	0.263	0.264
		2	25.6	3.051	7.1	0.814	0.267	
		3	25.6	3.051	7.0	0.803	0.263	
	D	1	25.1	2.992	6.6	0.757	0.253	0.254
		2	25	2.980	6.6	0.757	0.254	
		3	24.9	2.968	6.6	0.757	0.255	

Site 2(b)

Cycle	Location	Reading	Pyr (Upper)	Pyr*	Alb(Lower)	Alb*	Albedo	Average
1	A	1	25.3	3.015	6.3	0.722	0.240	0.240
		2	25.3	3.015	6.3	0.722	0.240	
		3	25.3	3.015	6.3	0.722	0.240	
	B	1	25.5	3.039	6.0	0.688	0.226	0.226
		2	25.5	3.039	6.0	0.688	0.226	
		3	25.6	3.051	6.0	0.688	0.226	
2	A	1	25.1	2.992	6.3	0.722	0.241	0.241
		2	25.1	2.992	6.3	0.722	0.241	
		3	25.2	3.004	6.3	0.722	0.241	
	B	1	25.6	3.051	6.0	0.688	0.226	0.227
		2	25.5	3.039	6.0	0.688	0.226	
		3	25.3	3.015	6.0	0.688	0.228	

Appendix E Percentiles of the t-distribution

Entry is $t(A;\nu)$ where $P\{t(\nu) \le t(A;\nu)\} = A$

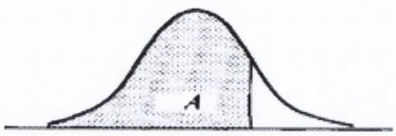

$t(A;\nu)$

	A						
ν	.60	.70	.80	.85	.90	.95	.975
1	0.325	0.727	1.376	1.963	3.078	6.314	12.706
2	0.289	0.617	1.061	1.386	1.886	2.920	4.303
3	0.277	0.584	0.978	1.250	1.638	2.353	3.182
4	0.271	0.569	0.941	1.190	1.533	2.132	2.776
5	0.267	0.559	0.920	1.156	1.476	2.015	2.571
6	0.265	0.553	0.906	1.134	1.440	1.943	2.447
7	0.263	0.549	0.896	1.119	1.415	1.895	2.365
8	0.262	0.546	0.889	1.108	1.397	1.860	2.306
9	0.261	0.543	0.883	1.100	1.383	1.833	2.262
10	0.260	0.542	0.879	1.093	1.372	1.812	2.228
11	0.260	0.540	0.876	1.088	1.363	1.796	2.201
12	0.259	0.539	0.873	1.083	1.356	1.782	2.179
13	0.259	0.537	0.870	1.079	1.350	1.771	2.160
14	0.258	0.537	0.868	1.076	1.345	1.761	2.145
15	0.258	0.536	0.866	1.074	1.341	1.753	2.131
16	0.258	0.535	0.865	1.071	1.337	1.746	2.120
17	0.257	0.534	0.863	1.069	1.333	1.740	2.110
18	0.257	0.534	0.862	1.067	1.330	1.734	2.101
19	0.257	0.533	0.861	1.066	1.328	1.729	2.093
20	0.257	0.533	0.860	1.064	1.325	1.725	2.086
21	0.257	0.532	0.859	1.063	1.323	1.721	2.080
22	0.256	0.532	0.858	1.061	1.321	1.717	2.074
23	0.256	0.532	0.858	1.060	1.319	1.714	2.069
24	0.256	0.531	0.857	1.059	1.318	1.711	2.064
25	0.256	0.531	0.856	1.058	1.316	1.708	2.060
26	0.256	0.531	0.856	1.058	1.315	1.706	2.056
27	0.256	0.531	0.855	1.057	1.314	1.703	2.052
28	0.256	0.530	0.855	1.056	1.313	1.701	2.048
29	0.256	0.530	0.854	1.055	1.311	1.699	2.045
30	0.256	0.530	0.854	1.055	1.310	1.697	2.042
40	0.255	0.529	0.851	1.050	1.303	1.684	2.021
60	0.254	0.527	0.848	1.045	1.296	1.671	2.000
120	0.254	0.526	0.845	1.041	1.289	1.658	1.980
∞	0.253	0.524	0.842	1.036	1.282	1.645	1.960

Appendix F Spectrophotometer results for typical Irish cements

Sample	Reading	L*	a*	b*		
CEM II A-V (Quinn)	1	63.4	-0.05	6.45		
	2	63.7	-0.27	6.41		
	3	63.18	-0.18	6.34	μ_{L*}	**63.57**
	4	63.59	-0.22	6.43	σ_{L*}	0.306
	5	63.99	-0.14	6.36	CoV (%)	0.4814
CEM 1 (Spain cement)	1	65.05	-0.23	6.12		
	2	65.47	-0.21	5.8		
	3	65.57	-0.28	5.59	μ_{L*}	**65.32**
	4	65.31	-0.45	5.87	σ_{L*}	0.211
	5	65.18	-0.44	5.94	CoV (%)	0.3225
CEM II A-L (Irish cement)	1	66.26	-0.11	6.95		
	2	66.07	-0.15	7.04		
	3	65.99	-0.04	7.03	μ_{L*}	**65.65**
	4	65.04	-0.15	6.91	σ_{L*}	0.632
	5	64.90	-0.06	7.00	CoV (%)	0.9629
CEM II A-V (Lagan)	1	65.28	-0.27	6.33		
	2	66.15	-0.35	6.39		
	3	65.32	-0.3	6.26	μ_{L*}	**65.71**
	4	66.28	-0.19	6.35	σ_{L*}	0.473
	5	65.51	-0.28	6.29	CoV (%)	0.7201
CEM II A-L (60:40)	1	76.41	-0.08	5.35		
	2	77.85	-0.19	5.23		
	3	77.40	-0.19	5.28	μ_{L*}	**77.06**
	4	76.89	-0.15	5.32	σ_{L*}	0.569
	5	76.74	-0.18	5.28	CoV (%)	0.7380
GGBS (Sweden)	1	82.06	0.09	5.69		
	2	81.34	0.12	5.58		
	3	80.65	0.16	5.90	μ_{L*}	**81.39**
	4	81.16	0.14	5.70	σ_{L*}	0.543
	5	81.75	0.11	5.82	CoV (%)	0.6677
GGBS (Ecocem sample 1)	1	88.40	0.03	4.65		
	2	88.06	0.04	4.64		
	3	88.43	0.01	4.68	μ_{L*}	**88.07**
	4	87.45	0.00	4.81	σ_{L*}	0.395
	5	88.03	0.00	4.71	CoV (%)	0.4486
GGBS (Ecocem sample 2)	1	88.53	0.07	4.39		
	2	88.51	0.12	4.39		
	3	88.79	0.04	4.36	μ_{L*}	**88.66**
	4	88.42	0.07	4.45	σ_{L*}	0.250
	5	89.03	0.04	4.39	CoV (%)	0.2824
GGBS (Ecocem sample 3)	1	88.37	0.02	4.61		
	2	88.61	0.13	4.41		
	3	87.06	0.01	4.71	μ_{L*}	**88.15**
	4	88.45	0.03	4.65	σ_{L*}	0.622
	5	88.25	0.04	4.44	CoV (%)	0.7058
White cement	1	90.86	-1.72	5.87		
	2	90.50	-1.69	5.97		
	3	90.91	-1.69	5.86	μ_{L*}	**90.72**
	4	91.17	-1.71	5.89	σ_{L*}	0.397
	5	90.15	-1.07	6.04	CoV (%)	0.4380

Appendix G Sphere spectrophotometer results for cement blends containing GGBS and CEM II A-L powders in various quantities

GGBS	CEM II	Reading	L*	a*	b*		
100%	0%	1	87.81	0.26	4.03		
		2	87.33	0.28	4.10		
		3	88.04	0.25	4.06	μ_{L*}	**87.92**
		4	88.27	0.26	3.97	σ_{L*}	0.371
		5	88.15	0.30	4.01	CoV (%)	0.4218
70%	30%	1	76.66	-0.05	5.06		
		2	76.18	-0.07	5.10		
		3	76.48	-0.05	5.19	μ_{L*}	**76.308**
		4	76.07	-0.04	5.19	σ_{L*}	0.251
		5	76.15	-0.07	5.2	CoV (%)	0.3286
50%	50%	1	72.01	-0.05	5.66		
		2	73.35	-0.09	5.36		
		3	73.29	-0.06	5.41	μ_{L*}	**72.798**
		4	72.38	-0.08	5.57	σ_{L*}	0.585
		5	72.96	0.00	5.52	CoV (%)	0.8035
30%	70%	1	68.45	0.00	5.98		
		2	68.87	-0.08	5.92		
		3	67.72	-0.03	5.99	μ_{L*}	**68.28**
		4	67.94	-0.06	5.98	σ_{L*}	0.454
		5	68.42	-0.03	5.97	CoV (%)	0.6654
0%	100%	1	65.20	-0.09	6.16		
		2	64.85	-0.18	6.15		
		3	64.87	-0.05	6.35	μ_{L*}	**64.782**
		4	64.33	0.00	6.34	σ_{L*}	0.319
		5	64.66	-0.04	6.26	CoV (%)	0.4920

Appendix H Sphere spectrophotometer results for cement blends containing GGBS and WPC powders in various quantities

GGBS	WPC	Reading	L*	a*	b*		
100%	0%	1	87.81	0.26	4.03		
		2	87.33	0.28	4.10		
		3	88.04	0.25	4.06	μ_{L*}	**87.92**
		4	88.27	0.26	3.97	σ_{L*}	0.371
		5	88.15	0.30	4.01	CoV (%)	0.4218
70%	30%	1	88.49	-0.19	4.51		
		2	88.19	-0.27	4.70		
		3	87.31	-0.20	4.74	μ_{L*}	**87.958**
		4	87.69	-0.20	4.87	σ_{L*}	0.461
		5	88.11	-0.17	4.72	CoV (%)	0.5246
50%	50%	1	89.30	-0.54	4.72		
		2	89.34	-0.59	4.82		
		3	89.20	-0.58	4.82	μ_{L*}	**88.942**
		4	88.43	-0.48	4.91	σ_{L*}	0.466
		5	88.44	-0.49	4.93	CoV (%)	0.5235
30%	70%	1	89.66	-1.03	5.22		
		2	89.38	-0.98	5.35		
		3	89.55	-1.04	5.26	μ_{L*}	**89.586**
		4	89.64	-1.03	5.25	σ_{L*}	0.128
		5	89.70	-1.07	5.31	CoV (%)	0.1424
0%	100%	1	90.86	-1.72	5.87		
		2	90.50	-1.69	5.97		
		3	90.91	-1.69	5.86	μ_{L*}	**90.718**
		4	91.17	-1.71	5.89	σ_{L*}	0.397
		5	90.15	-1.07	6.04	CoV (%)	0.4380

Appendix I Sphere spectrophotometer results for cement blends containing WPC and CEM II A-L powders in various quantities

WPC	CEM II	Reading	L*	a*	b*		
0%	100%	1	65.20	-0.09	6.16		
		2	64.85	-0.18	6.15		
		3	64.87	-0.05	6.35	μ_{L*}	**64.78**
		4	64.33	0.00	6.34	σ_{L*}	0.319
		5	64.66	-0.04	6.26	CoV (%)	0.4920
30%	70%	1	68.64	-0.12	6.10		
		2	68.47	-0.08	5.93		
		3	68.44	-0.13	6.10	μ_{L*}	**68.55**
		4	69.00	-0.15	5.89	σ_{L*}	0.296
		5	68.20	-0.1	5.92	CoV (%)	0.4325
50%	50%	1	71.79	-0.18	5.88		
		2	71.69	-0.25	5.89		
		3	71.34	-0.26	5.89	μ_{L*}	**71.65**
		4	71.72	-0.26	5.74	σ_{L*}	0.179
		5	71.73	-0.25	5.77	CoV (%)	0.2502
70%	30%	1	75.06	-0.39	5.66		
		2	75.88	-0.42	5.63		
		3	75.97	-0.44	5.68	μ_{L*}	**75.61**
		4	75.86	-0.42	5.61	σ_{L*}	0.413
		5	75.27	-0.47	5.76	CoV (%)	0.5466
100%	0%	1	90.86	-1.72	5.87		
		2	90.50	-1.69	5.97		
		3	90.91	-1.69	5.86	μ_{L*}	**90.72**
		4	91.17	-1.71	5.89	σ_{L*}	0.397
		5	90.15	-1.07	6.04	CoV (%)	0.4380

Appendix J L* value readings for concrete specimens

GGBS	Agg.	Cast		Screed		Tamp		Brush	
0	L	μ_{18}	58.59	μ_{18}	64.06	μ_{18}	55.00	μ_{18}	61.08
		σ_{18}	1.25	σ_{18}	1.51	σ_{18}	2.12	σ_{18}	2.14
		CoV_{18}	2.14	CoV_{18}	2.36	CoV_{18}	3.85	CoV_{18}	3.50
	PCL	μ_{18}	60.00	μ_{18}	64.51	μ_{18}	51.69	μ_{18}	57.52
		σ_{18}	1.66	σ_{18}	1.56	σ_{18}	1.86	σ_{18}	2.61
		CoV_{18}	2.77	CoV_{18}	2.41	CoV_{18}	3.60	CoV_{18}	4.54
	SS	μ_{18}	58.84	μ_{18}	61.17	μ_{18}	46.57	μ_{18}	52.07
		σ_{18}	1.14	σ_{18}	1.26	σ_{18}	2.19	σ_{18}	2.64
		CoV_{18}	1.93	CoV_{18}	2.05	CoV_{18}	4.71	CoV_{18}	5.06
30	L	μ_{18}	60.44	μ_{18}	65.64	μ_{18}	54.26	μ_{18}	56.31
		σ_{18}	0.59	σ_{18}	1.28	σ_{18}	2.47	σ_{18}	1.88
		CoV_{18}	0.97	CoV_{18}	1.95	CoV_{18}	4.56	CoV_{18}	3.34
	PCL	μ_{18}	59.18	μ_{18}	62.72	μ_{18}	57.71	μ_{18}	54.70
		σ_{18}	1.00	σ_{18}	1.39	σ_{18}	2.49	σ_{18}	2.29
		CoV_{18}	1.70	CoV_{18}	2.22	CoV_{18}	4.32	CoV_{18}	4.19
	SS	μ_{18}	57.52	μ_{18}	62.01	μ_{18}	49.41	μ_{18}	58.32
		σ_{18}	1.03	σ_{18}	1.06	σ_{18}	3.32	σ_{18}	1.19
		CoV_{18}	1.79	CoV_{18}	1.71	CoV_{18}	6.73	CoV_{18}	2.05
50	L	μ_{18}	59.88	μ_{18}	64.48	μ_{18}	58.12	μ_{18}	60.16
		σ_{18}	0.82	σ_{18}	1.29	σ_{18}	3.24	σ_{18}	2.43
		CoV_{18}	1.37	CoV_{18}	1.99	CoV_{18}	5.58	CoV_{18}	4.04
	PCL	μ_{18}	59.47	μ_{18}	67.01	μ_{18}	57.56	μ_{18}	62.10
		σ_{18}	1.28	σ_{18}	1.28	σ_{18}	2.35	σ_{18}	1.29
		CoV_{18}	2.15	CoV_{18}	1.92	CoV_{18}	4.08	CoV_{18}	2.07
	SS	μ_{18}	57.28	μ_{18}	64.36	μ_{18}	56.40	μ_{18}	62.99
		σ_{18}	1.36	σ_{18}	1.67	σ_{18}	3.60	σ_{18}	0.90
		CoV_{18}	2.37	CoV_{18}	2.60	CoV_{18}	6.39	CoV_{18}	1.42
70	L	μ_{18}	60.83	μ_{18}	66.71	μ_{18}	61.79	μ_{18}	65.31
		σ_{18}	1.34	σ_{18}	1.28	σ_{18}	2.14	σ_{18}	1.26
		CoV_{18}	2.20	CoV_{18}	1.92	CoV_{18}	3.47	CoV_{18}	1.94
	PCL	μ_{18}	61.91	μ_{18}	66.89	μ_{18}	58.81	μ_{18}	61.65
		σ_{18}	0.97	σ_{18}	1.56	σ_{18}	3.72	σ_{18}	2.25
		CoV_{18}	1.57	CoV_{18}	2.33	CoV_{18}	6.33	CoV_{18}	3.66
	SS	μ_{18}	57.76	μ_{18}	64.62	μ_{18}	55.84	μ_{18}	60.87
		σ_{18}	1.28	σ_{18}	1.40	σ_{18}	2.66	σ_{18}	1.17
		CoV_{18}	2.21	CoV_{18}	2.17	CoV_{18}	4.76	CoV_{18}	1.93

Appendix K Lux meter results March 2011

GGBS	Agg.	Cast		CoV(%)	Screed		CoV(%)	Tamp		CoV(%)	Brush		CoV(%)
0	L	4.77	μ_{a3}	4.81	8.21	μ_{a3}	8.25	6.83	μ_{a3}	6.78	4.94	μ_{a3}	5.20
	(a)	4.86	σ_{a3}	0.05	8.22	σ_{a3}	0.07	6.71	σ_{a3}	0.06	5.24	σ_{a3}	0.25
		4.79	CoV_3	0.98	8.33	CoV_3	0.81	6.79	CoV_3	0.90	5.43	CoV_3	4.75
		4.62	μ_{a3}	4.65	8.26	μ_{a3}	8.21	6.91	μ_{a3}	6.91	5.26	μ_{a3}	5.18
		4.63	σ_{a3}	0.04	8.12	σ_{a3}	0.08	6.88	σ_{a3}	0.03	5.35	σ_{a3}	0.22
		4.69	CoV_3	0.81	8.26	CoV_3	0.98	6.93	CoV_3	0.36	4.93	CoV_3	4.27
	PCL	5.00	μ_{b3}	4.60	8.22	μ_{b3}	7.92	6.53	μ_{b3}	6.24	5.59	μ_{b3}	5.59
	(b)	4.38	σ_{b3}	0.35	7.66	σ_{b3}	0.28	6.37	σ_{b3}	0.37	5.51	σ_{b3}	0.08
		4.41	CoV_3	7.61	7.88	CoV_3	3.56	5.82	CoV_3	5.97	5.67	CoV_3	1.43
		5.09	μ_{b3}	5.11	8.27	μ_{b3}	8.25	6.10	μ_{b3}	6.14	5.57	μ_{b3}	5.45
		5.21	σ_{b3}	0.10	8.29	σ_{b3}	0.05	6.14	σ_{b3}	0.04	5.52	σ_{b3}	0.17
		5.02	CoV_3	1.88	8.20	CoV_3	0.57	6.17	CoV_3	0.57	5.25	CoV_3	3.16
	SS	4.89	μ_{c3}	4.88	8.13	μ_{c3}	8.11	5.73	μ_{c3}	5.82	5.28	μ_{c3}	5.12
	(c)	4.88	σ_{c3}	0.01	8.18	σ_{c3}	0.08	5.74	σ_{c3}	0.15	4.85	σ_{c3}	0.24
		4.88	CoV_3	0.12	8.02	CoV_3	1.01	6.00	CoV_3	2.63	5.23	CoV_3	4.59
		4.93	μ_{c3}	4.91	7.61	μ_{c3}	7.53	5.72	μ_{c3}	5.46	4.42	μ_{c3}	4.38
		4.95	σ_{c3}	0.05	7.43	σ_{c3}	0.09	5.70	σ_{c3}	0.44	4.41	σ_{c3}	0.06
		4.86	CoV_3	0.96	7.54	CoV_3	1.21	4.95	CoV_3	8.04	4.32	CoV_3	1.26
30	L	5.51	μ_{a3}	5.31	8.40	μ_{a3}	6.78	6.54	μ_{a3}	6.52	4.77	μ_{a3}	4.66
	(a)	5.32	σ_{a3}	0.21	6.48	σ_{a3}	1.49	6.51	σ_{a3}	0.02	4.65	σ_{a3}	0.11
		5.10	CoV_3	3.86	5.47	CoV_3	21.94	6.52	CoV_3	0.23	4.55	CoV_3	2.37
		5.49	μ_{a3}	5.43	7.96	μ_{a3}	7.78	7.02	μ_{a3}	7.04	4.81	μ_{a3}	4.89
		5.43	σ_{a3}	0.06	7.95	σ_{a3}	0.30	7.02	σ_{a3}	0.03	4.88	σ_{a3}	0.08
		5.38	CoV_3	1.01	7.43	CoV_3	3.90	7.07	CoV_3	0.41	4.97	CoV_3	1.64
	PCL	4.78	μ_{b3}	4.77	7.75	μ_{b3}	7.99	7.55	μ_{b3}	7.29	6.09	μ_{b3}	6.09
	(b)	4.74	σ_{b3}	0.03	8.24	σ_{b3}	0.25	7.01	σ_{b3}	0.27	6.17	σ_{b3}	0.09
		4.79	CoV_3	0.55	7.99	CoV_3	3.07	7.30	CoV_3	3.71	6.00	CoV_3	1.40
		4.95	μ_{b3}	5.13	8.80	μ_{b3}	8.71	8.17	μ_{b3}	8.11	5.53	μ_{b3}	5.95
		5.21	σ_{b3}	0.16	8.64	σ_{b3}	0.08	8.06	σ_{b3}	0.06	6.15	σ_{b3}	0.37
		5.24	CoV_3	3.11	8.70	CoV_3	0.93	8.09	CoV_3	0.70	6.18	CoV_3	6.16
	SS	5.01	μ_{c3}	4.97	8.10	μ_{c3}	8.17	6.75	μ_{c3}	6.74	5.72	μ_{c3}	5.78
	(c)	4.92	σ_{c3}	0.05	8.19	σ_{c3}	0.06	6.77	σ_{c3}	0.03	5.79	σ_{c3}	0.06
		4.97	CoV_3	0.91	8.21	CoV_3	0.72	6.71	CoV_3	0.45	5.83	CoV_3	0.96
		5.09	μ_{c3}	4.85	8.01	μ_{c3}	8.00	5.32	μ_{c3}	5.36	5.89	μ_{c3}	5.81
		4.95	σ_{c3}	0.30	8.17	σ_{c3}	0.18	5.07	σ_{c3}	0.31	5.89	σ_{c3}	0.14
		4.51	CoV_3	6.24	7.82	CoV_3	2.19	5.69	CoV_3	5.82	5.64	CoV_3	2.49

GGBS	Agg.	Cast		CoV(%)	Screed		CoV(%)	Tamp		CoV(%)	Brush		CoV(%)
50	**L**	5.53	μ_{a3}	5.72	8.12	μ_{a3}	8.20	6.61	μ_{a3}	6.64	5.85	μ_{a3}	5.73
	(a)	5.78	σ_{a3}	0.17	8.21	σ_{a3}	0.07	6.65	σ_{a3}	0.03	5.60	σ_{a3}	0.13
		5.86	CoV_3	3.01	8.26	CoV_3	0.87	6.67	CoV_3	0.46	5.74	CoV_3	2.19
		5.86	μ_{a3}	5.85	8.98	μ_{a3}	8.91	6.32	μ_{a3}	6.59	6.02	μ_{a3}	6.02
		5.84	σ_{a3}	0.01	8.85	σ_{a3}	0.07	6.75	σ_{a3}	0.24	6.00	σ_{a3}	0.02
		5.86	CoV_3	0.20	8.89	CoV_3	0.75	6.70	CoV_3	3.57	6.03	CoV_3	0.25
	PCL	5.71	μ_{b3}	5.56	9.04	μ_{b3}	8.74	5.95	μ_{b3}	6.06	6.59	μ_{b3}	6.56
	(b)	5.30	σ_{b3}	0.23	8.07	σ_{b3}	0.58	6.13	σ_{b3}	0.09	6.51	σ_{b3}	0.04
		5.68	CoV_3	4.11	9.11	CoV_3	6.65	6.09	CoV_3	1.56	6.57	CoV_3	0.63
		5.90	μ_{b3}	5.98	9.19	μ_{b3}	9.20	6.05	μ_{b3}	6.02	6.57	μ_{b3}	6.60
		6.00	σ_{b3}	0.08	9.23	σ_{b3}	0.03	5.97	σ_{b3}	0.05	6.64	σ_{b3}	0.04
		6.05	CoV_3	1.28	9.18	CoV_3	0.29	6.05	CoV_3	0.77	6.60	CoV_3	0.53
	SS	5.77	μ_{c3}	5.76	8.62	μ_{c3}	8.65	7.01	μ_{c3}	6.98	6.46	μ_{c3}	6.52
	(c)	5.78	σ_{c3}	0.03	8.64	σ_{c3}	0.03	6.91	σ_{c3}	0.06	6.54	σ_{c3}	0.05
		5.72	CoV_3	0.56	8.68	CoV_3	0.35	7.03	CoV_3	0.92	6.56	CoV_3	0.81
		5.09	μ_{c3}	5.39	8.33	μ_{c3}	8.16	6.20	μ_{c3}	6.16	5.48	μ_{c3}	5.88
		5.56	σ_{c3}	0.26	8.23	σ_{c3}	0.21	6.10	σ_{c3}	0.06	6.06	σ_{c3}	0.34
		5.52	CoV_3	4.83	7.93	CoV_3	2.55	6.19	CoV_3	0.89	6.09	CoV_3	5.85
70	**L**	5.68	μ_{a3}	5.75	9.04	μ_{a3}	8.59	4.70	μ_{a3}	5.32	5.92	μ_{a3}	6.04
	(a)	5.60	σ_{a3}	0.19	7.86	σ_{a3}	0.64	5.69	σ_{a3}	0.54	6.02	σ_{a3}	0.13
		5.96	CoV_3	3.29	8.88	CoV_3	7.45	5.58	CoV_3	10.19	6.18	CoV_3	2.17
		6.00	μ_{a3}	6.08	9.06	μ_{a3}	9.08	7.18	μ_{a3}	7.19	6.93	μ_{a3}	6.81
		6.08	σ_{a3}	0.08	9.09	σ_{a3}	0.02	7.22	σ_{a3}	0.03	6.80	σ_{a3}	0.12
		6.16	CoV_3	1.32	9.09	CoV_3	0.19	7.16	CoV_3	0.43	6.70	CoV_3	1.69
	PCL	5.58	μ_{b3}	5.87	6.82	μ_{b3}	6.92	5.00	μ_{b3}	5.44	6.33	μ_{b3}	6.28
	(b)	6.18	σ_{b3}	0.30	6.91	σ_{b3}	0.11	5.59	σ_{b3}	0.38	6.20	σ_{b3}	0.07
		5.85	CoV_3	5.12	7.03	CoV_3	1.52	5.72	CoV_3	7.06	6.30	CoV_3	1.08
		6.21	μ_{b3}	6.23	8.93	μ_{b3}	8.92	6.46	μ_{b3}	6.45	6.19	μ_{b3}	6.22
		6.17	σ_{b3}	0.07	8.92	σ_{b3}	0.01	6.47	σ_{b3}	0.03	6.26	σ_{b3}	0.04
		6.30	CoV_3	1.07	8.92	CoV_3	0.06	6.42	CoV_3	0.41	6.20	CoV_3	0.61
	SS	5.92	μ_{c3}	5.91	8.27	μ_{c3}	8.35	7.21	μ_{c3}	7.36	5.29	μ_{c3}	5.21
	(c)	5.94	σ_{c3}	0.03	8.29	σ_{c3}	0.12	7.36	σ_{c3}	0.15	5.14	σ_{c3}	0.08
		5.88	CoV_3	0.52	8.48	CoV_3	1.39	7.51	CoV_3	2.04	5.20	CoV_3	1.45
		6.06	μ_{c3}	6.03	8.24	μ_{c3}	8.09	6.90	μ_{c3}	6.73	5.39	μ_{c3}	5.37
		6.00	σ_{c3}	0.03	8.05	σ_{c3}	0.13	6.61	σ_{c3}	0.15	5.38	σ_{c3}	0.03
		6.03	CoV_3	0.50	7.99	CoV_3	1.61	6.69	CoV_3	2.22	5.34	CoV_3	0.49

Appendix L Lux meter results July 2011

GGBS	Agg.	Cast		CoV(%)	Screed		CoV(%)	Tamp		CoV(%)	Brush		CoV(%)
0	L	5.28	μ_{a3}	5.23	8.45	μ_{a3}	8.50	7.30	μ_{a3}	7.33	6.21	μ_{a3}	6.25
	(a)	5.18	σ_{a3}	0.05	8.57	σ_{a3}	0.06	7.34	σ_{a3}	0.03	6.23	σ_{a3}	0.05
		5.22	CoV_3	0.96	8.49	CoV_3	0.72	7.35	CoV_3	0.36	6.30	CoV_3	0.76
		5.36	μ_{a3}	5.35	9.05	μ_{a3}	9.11	8.15	μ_{a3}	8.12	5.81	μ_{a3}	5.83
		5.36	σ_{a3}	0.01	9.19	σ_{a3}	0.07	8.12	σ_{a3}	0.04	5.83	σ_{a3}	0.02
		5.34	CoV_3	0.22	9.09	CoV_3	0.79	8.08	CoV_3	0.43	5.84	CoV_3	0.26
	PCL	5.40	μ_{b3}	5.38	8.71	μ_{b3}	8.69	7.55	μ_{b3}	7.50	6.05	μ_{b3}	5.98
	(b)	5.40	σ_{b3}	0.03	8.69	σ_{b3}	0.02	7.48	σ_{b3}	0.04	5.96	σ_{b3}	0.06
		5.35	CoV_3	0.54	8.68	CoV_3	0.18	7.47	CoV_3	0.58	5.93	CoV_3	1.04
		5.55	μ_{b3}	5.54	8.55	μ_{b3}	8.57	6.94	μ_{b3}	6.92	5.92	μ_{b3}	5.91
		5.55	σ_{b3}	0.01	8.59	σ_{b3}	0.02	6.96	σ_{b3}	0.05	5.93	σ_{b3}	0.02
		5.53	CoV_3	0.21	8.57	CoV_3	0.23	6.86	CoV_3	0.76	5.89	CoV_3	0.35
	SS	5.11	μ_{c3}	5.12	7.79	μ_{c3}	7.83	6.32	μ_{c3}	6.28	5.42	μ_{c3}	5.40
	(c)	5.11	σ_{c3}	0.02	7.72	σ_{c3}	0.13	6.26	σ_{c3}	0.03	5.39	σ_{c3}	0.02
		5.14	CoV_3	0.34	7.97	CoV_3	1.65	6.27	CoV_3	0.51	5.38	CoV_3	0.39
		5.47	μ_{c3}	5.48	7.96	μ_{c3}	7.90	6.26	μ_{c3}	6.22	4.85	μ_{c3}	4.84
		5.49	σ_{c3}	0.01	7.88	σ_{c3}	0.05	6.21	σ_{c3}	0.04	4.83	σ_{c3}	0.01
		5.48	CoV_3	0.18	7.86	CoV_3	0.67	6.18	CoV_3	0.65	4.84	CoV_3	0.21
30	L	5.79	μ_{a3}	5.79	9.25	μ_{a3}	9.13	7.26	μ_{a3}	7.22	4.94	μ_{a3}	5.00
	(a)	5.83	σ_{a3}	0.04	9.07	σ_{a3}	0.10	7.22	σ_{a3}	0.04	5.13	σ_{a3}	0.11
		5.76	CoV_3	0.61	9.08	CoV_3	1.11	7.18	CoV_3	0.55	4.94	CoV_3	2.19
		6.06	μ_{a3}	6.10	9.09	μ_{a3}	9.08	8.21	μ_{a3}	8.19	5.75	μ_{a3}	5.78
		6.14	σ_{a3}	0.04	9.02	σ_{a3}	0.06	8.21	σ_{a3}	0.04	5.82	σ_{a3}	0.04
		6.10	CoV_3	0.66	9.13	CoV_3	0.61	8.14	CoV_3	0.49	5.78	CoV_3	0.61
	PCL	5.74	μ_{b3}	5.74	9.25	μ_{b3}	9.12	8.29	μ_{b3}	8.28	6.63	μ_{b3}	6.60
	(b)	5.78	σ_{b3}	0.05	9.07	σ_{b3}	0.11	8.27	σ_{b3}	0.01	6.63	σ_{b3}	0.05
		5.69	CoV_3	0.79	9.05	CoV_3	1.21	8.28	CoV_3	0.12	6.54	CoV_3	0.79
		5.66	μ_{b3}	5.74	8.91	μ_{b3}	8.86	8.58	μ_{b3}	8.61	6.52	μ_{b3}	6.50
		5.81	σ_{b3}	0.08	8.74	σ_{b3}	0.11	8.73	σ_{b3}	0.11	6.42	σ_{b3}	0.07
		5.74	CoV_3	1.31	8.94	CoV_3	1.22	8.51	CoV_3	1.31	6.56	CoV_3	1.11
	SS	5.45	μ_{c3}	5.46	8.22	μ_{c3}	8.17	6.82	μ_{c3}	7.01	6.22	μ_{c3}	6.23
	(c)	5.44	σ_{c3}	0.02	8.16	σ_{c3}	0.04	7.16	σ_{c3}	0.17	6.22	σ_{c3}	0.02
		5.48	CoV_3	0.38	8.14	CoV_3	0.51	7.05	CoV_3	2.47	6.26	CoV_3	0.37
		5.72	μ_{c3}	5.74	8.60	μ_{c3}	8.62	6.57	μ_{c3}	6.55	6.61	μ_{c3}	6.59
		5.74	σ_{c3}	0.02	8.59	σ_{c3}	0.04	6.55	σ_{c3}	0.02	6.56	σ_{c3}	0.03
		5.76	CoV_3	0.35	8.67	CoV_3	0.51	6.53	CoV_3	0.31	6.60	CoV_3	0.40

GGBS	Agg.	Cast		CoV(%)	Screed		CoV(%)	Tamp		CoV(%)	Brush		CoV(%)
50	**L**	6.36	μ_{a3}	6.34	8.72	μ_{a3}	8.62	7.32	μ_{a3}	7.39	6.20	μ_{a3}	6.24
	(a)	6.31	σ_{a3}	0.03	8.51	σ_{a3}	0.11	7.41	σ_{a3}	0.06	6.18	σ_{a3}	0.08
		6.34	CoV_3	0.40	8.64	CoV_3	1.23	7.44	CoV_3	0.85	6.33	CoV_3	1.31
		6.55	μ_{a3}	6.53	9.29	μ_{a3}	9.28	6.96	μ_{a3}	6.97	6.78	μ_{a3}	6.77
		6.52	σ_{a3}	0.02	9.26	σ_{a3}	0.02	6.98	σ_{a3}	0.01	6.77	σ_{a3}	0.01
		6.52	CoV_3	0.27	9.30	CoV_3	0.22	6.96	CoV_3	0.17	6.77	CoV_3	0.09
	PCL	6.10	μ_{b3}	6.09	9.54	μ_{b3}	9.61	6.51	μ_{b3}	6.57	7.06	μ_{b3}	7.06
	(b)	6.09	σ_{b3}	0.01	9.67	σ_{b3}	0.07	6.58	σ_{b3}	0.06	7.06	σ_{b3}	0.01
		6.08	CoV_3	0.16	9.63	CoV_3	0.69	6.63	CoV_3	0.92	7.07	CoV_3	0.08
		6.32	μ_{b3}	6.34	8.39	μ_{b3}	8.44	5.97	μ_{b3}	5.89	6.97	μ_{b3}	6.99
		6.32	σ_{b3}	0.03	8.51	σ_{b3}	0.06	5.86	σ_{b3}	0.07	7.00	σ_{b3}	0.02
		6.38	CoV_3	0.55	8.42	CoV_3	0.74	5.85	CoV_3	1.13	6.99	CoV_3	0.22
	SS	5.94	μ_{c3}	5.97	8.48	μ_{c3}	8.49	7.36	μ_{c3}	7.39	6.74	μ_{c3}	6.74
	(c)	5.98	σ_{c3}	0.03	8.54	σ_{c3}	0.05	7.34	σ_{c3}	0.06	6.75	σ_{c3}	0.01
		5.99	CoV_3	0.44	8.44	CoV_3	0.59	7.46	CoV_3	0.87	6.74	CoV_3	0.09
		6.10	μ_{c3}	6.09	8.55	μ_{c3}	8.53	6.84	μ_{c3}	6.87	6.87	μ_{c3}	6.92
		6.08	σ_{c3}	0.01	8.51	σ_{c3}	0.02	6.91	σ_{c3}	0.04	6.97	σ_{c3}	0.05
		6.10	CoV_3	0.19	8.54	CoV_3	0.24	6.85	CoV_3	0.55	6.92	CoV_3	0.72
70	**L**	6.31	μ_{a3}	6.31	9.54	μ_{a3}	9.54	8.11	μ_{a3}	8.12	7.01	μ_{a3}	7.00
	(a)	6.30	σ_{a3}	0.01	9.60	σ_{a3}	0.06	8.16	σ_{a3}	0.03	7.11	σ_{a3}	0.12
		6.31	CoV_3	0.09	9.48	CoV_3	0.63	8.10	CoV_3	0.40	6.88	CoV_3	1.65
		6.30	μ_{a3}	6.36	9.42	μ_{a3}	9.50	7.49	μ_{a3}	7.50	7.00	μ_{a3}	6.99
		6.41	σ_{a3}	0.06	9.52	σ_{a3}	0.07	7.49	σ_{a3}	0.01	6.97	σ_{a3}	0.02
		6.36	CoV_3	0.87	9.56	CoV_3	0.76	7.51	CoV_3	0.15	6.99	CoV_3	0.22
	PCL	6.64	μ_{b3}	6.63	7.15	μ_{b3}	7.17	5.85	μ_{b3}	5.83	6.74	μ_{b3}	6.67
	(b)	6.68	σ_{b3}	0.06	7.20	σ_{b3}	0.03	5.79	σ_{b3}	0.03	6.67	σ_{b3}	0.07
		6.57	CoV_3	0.84	7.15	CoV_3	0.40	5.85	CoV_3	0.59	6.60	CoV_3	1.05
		6.54	μ_{b3}	6.56	8.52	μ_{b3}	8.54	6.39	μ_{b3}	6.34	6.41	μ_{b3}	6.47
		6.56	σ_{b3}	0.02	8.53	σ_{b3}	0.02	6.31	σ_{b3}	0.04	6.52	σ_{b3}	0.06
		6.57	CoV_3	0.23	8.56	CoV_3	0.24	6.33	CoV_3	0.66	6.47	CoV_3	0.85
	SS	6.08	μ_{c3}	6.07	8.30	μ_{c3}	8.34	7.61	μ_{c3}	7.63	5.81	μ_{c3}	5.82
	(c)	6.06	σ_{c3}	0.01	8.37	σ_{c3}	0.04	7.62	σ_{c3}	0.03	5.82	σ_{c3}	0.01
		6.08	CoV_3	0.19	8.36	CoV_3	0.45	7.66	CoV_3	0.35	5.82	CoV_3	0.10
		6.16	μ_{c3}	6.12	8.75	μ_{c3}	8.71	6.78	μ_{c3}	6.72	5.97	μ_{c3}	5.94
		6.10	σ_{c3}	0.03	8.70	σ_{c3}	0.04	6.74	σ_{c3}	0.07	5.95	σ_{c3}	0.03
		6.11	CoV_3	0.52	8.68	CoV_3	0.41	6.65	CoV_3	0.99	5.91	CoV_3	0.51

Appendix M Lux meter results March 2012

GGBS	Agg.	Cast		CoV(%)	Screed		CoV(%)	Tamp		CoV(%)	Brush		CoV(%)
0	L	5.24	μ_{a3}	5.27	7.56	μ_{a3}	7.60	6.10	μ_{a3}	6.12	6.40	μ_{a3}	6.37
	(a)	5.29	σ_{a3}	0.03	7.60	σ_{a3}	0.04	6.14	σ_{a3}	0.02	6.35	σ_{a3}	0.03
		5.27	CoV_3	0.48	7.63	CoV_3	0.46	6.13	CoV_3	0.34	6.37	CoV_3	0.39
		5.35	μ_{a3}	5.34	8.04	μ_{a3}	8.05	7.46	μ_{a3}	7.46	6.55	μ_{a3}	6.55
		5.35	σ_{a3}	0.02	8.05	σ_{a3}	0.02	7.47	σ_{a3}	0.02	6.55	σ_{a3}	0.01
		5.32	CoV_3	0.32	8.07	CoV_3	0.19	7.44	CoV_3	0.20	6.54	CoV_3	0.09
	PCL	5.23	μ_{b3}	5.25	7.50	μ_{b3}	7.47	6.82	μ_{b3}	6.83	6.64	μ_{b3}	6.64
	(b)	5.26	σ_{b3}	0.02	7.47	σ_{b3}	0.03	6.83	σ_{b3}	0.01	6.62	σ_{b3}	0.02
		5.27	CoV_3	0.40	7.44	CoV_3	0.40	6.83	CoV_3	0.08	6.65	CoV_3	0.23
		5.42	μ_{b3}	5.38	7.66	μ_{b3}	7.65	6.41	μ_{b3}	6.44	6.40	μ_{b3}	6.43
		5.36	σ_{b3}	0.03	7.64	σ_{b3}	0.01	6.46	σ_{b3}	0.03	6.45	σ_{b3}	0.03
		5.36	CoV_3	0.64	7.66	CoV_3	0.15	6.45	CoV_3	0.41	6.43	CoV_3	0.39
	SS	5.16	μ_{c3}	5.18	6.97	μ_{c3}	6.96	5.66	μ_{c3}	5.64	5.61	μ_{c3}	5.62
	(c)	5.19	σ_{c3}	0.02	6.93	σ_{c3}	0.02	5.62	σ_{c3}	0.02	5.63	σ_{c3}	0.01
		5.19	CoV_3	0.33	6.97	CoV_3	0.33	5.64	CoV_3	0.35	5.63	CoV_3	0.21
		5.25	μ_{c3}	5.23	6.89	μ_{c3}	6.93	5.67	μ_{c3}	5.68	5.34	μ_{c3}	5.32
		5.20	σ_{c3}	0.03	6.92	σ_{c3}	0.05	5.68	σ_{c3}	0.01	5.31	σ_{c3}	0.02
		5.23	CoV_3	0.48	6.99	CoV_3	0.74	5.69	CoV_3	0.18	5.31	CoV_3	0.33
30	L	5.68	μ_{a3}	5.69	8.27	μ_{a3}	8.29	6.56	μ_{a3}	6.56	5.18	μ_{a3}	5.14
	(a)	5.69	σ_{a3}	0.02	8.29	σ_{a3}	0.02	6.55	σ_{a3}	0.01	5.14	σ_{a3}	0.04
		5.71	CoV_3	0.27	8.30	CoV_3	0.18	6.57	CoV_3	0.15	5.11	CoV_3	0.68
		6.13	μ_{a3}	6.12	7.92	μ_{a3}	7.90	7.16	μ_{a3}	7.15	5.79	μ_{a3}	5.78
		6.09	σ_{a3}	0.02	7.91	σ_{a3}	0.03	7.17	σ_{a3}	0.02	5.77	σ_{a3}	0.01
		6.13	CoV_3	0.38	7.87	CoV_3	0.33	7.13	CoV_3	0.29	5.78	CoV_3	0.17
	PCL	5.84	μ_{b3}	5.85	7.45	μ_{b3}	7.42	7.28	μ_{b3}	7.32	6.01	μ_{b3}	6.01
	(b)	5.85	σ_{b3}	0.02	7.41	σ_{b3}	0.02	7.35	σ_{b3}	0.04	6.02	σ_{b3}	0.01
		5.87	CoV_3	0.26	7.41	CoV_3	0.31	7.33	CoV_3	0.49	6.01	CoV_3	0.10
		5.58	μ_{b3}	5.44	7.41	μ_{b3}	7.43	7.03	μ_{b3}	6.97	6.05	μ_{b3}	6.08
		5.38	σ_{b3}	0.13	7.41	σ_{b3}	0.04	6.96	σ_{b3}	0.05	6.10	σ_{b3}	0.03
		5.35	CoV_3	2.30	7.48	CoV_3	0.54	6.93	CoV_3	0.74	6.08	CoV_3	0.41
	SS	5.25	μ_{c3}	5.22	7.10	μ_{c3}	7.06	6.00	μ_{c3}	5.95	6.21	μ_{c3}	6.25
	(c)	5.20	σ_{c3}	0.03	7.03	σ_{c3}	0.04	5.93	σ_{c3}	0.04	6.23	σ_{c3}	0.05
		5.20	CoV_3	0.55	7.05	CoV_3	0.51	5.93	CoV_3	0.68	6.31	CoV_3	0.85
		6.17	μ_{c3}	6.17	7.31	μ_{c3}	7.31	5.74	μ_{c3}	5.74	5.05	μ_{c3}	5.03
		6.16	σ_{c3}	0.01	7.32	σ_{c3}	0.01	5.77	σ_{c3}	0.04	5.02	σ_{c3}	0.02
		6.17	CoV_3	0.09	7.31	CoV_3	0.08	5.70	CoV_3	0.61	5.02	CoV_3	0.34

GGBS	Agg.	Cast		CoV(%)	Screed		CoV(%)	Tamp		CoV(%)	Brush		CoV(%)
50	**L**	6.16	μ_{a3}	6.13	7.29	μ_{a3}	7.27	6.31	μ_{a3}	6.28	5.36	μ_{a3}	5.36
	(a)	6.11	σ_{a3}	0.03	7.29	σ_{a3}	0.03	6.25	σ_{a3}	0.03	5.39	σ_{a3}	0.04
		6.13	CoV_3	0.41	7.24	CoV_3	0.40	6.29	CoV_3	0.49	5.32	CoV_3	0.66
		6.14	μ_{a3}	6.14	6.89	μ_{a3}	6.85	5.79	μ_{a3}	5.77	6.65	μ_{a3}	6.60
		6.16	σ_{a3}	0.02	6.84	σ_{a3}	0.03	5.75	σ_{a3}	0.02	6.58	σ_{a3}	0.04
		6.13	CoV_3	0.25	6.83	CoV_3	0.47	5.77	CoV_3	0.35	6.57	CoV_3	0.66
	PCL	6.75	μ_{b3}	6.74	6.75	μ_{b3}	6.74	6.28	μ_{b3}	6.28	6.70	μ_{b3}	6.70
	(b)	6.73	σ_{b3}	0.01	6.73	σ_{b3}	0.01	6.30	σ_{b3}	0.03	6.69	σ_{b3}	0.01
		6.75	CoV_3	0.17	6.75	CoV_3	0.17	6.25	CoV_3	0.40	6.70	CoV_3	0.09
		5.90	μ_{b3}	5.95	6.08	μ_{b3}	6.09	5.91	μ_{b3}	5.93	6.83	μ_{b3}	6.81
		5.95	σ_{b3}	0.05	6.10	σ_{b3}	0.01	5.95	σ_{b3}	0.02	6.80	σ_{b3}	0.02
		5.99	CoV_3	0.76	6.10	CoV_3	0.19	5.94	CoV_3	0.35	6.81	CoV_3	0.22
	SS	5.52	μ_{c3}	5.52	7.14	μ_{c3}	7.14	5.89	μ_{c3}	5.87	6.16	μ_{c3}	6.24
	(c)	5.52	σ_{c3}	0.01	7.14	σ_{c3}	0.01	5.86	σ_{c3}	0.02	6.30	σ_{c3}	0.07
		5.53	CoV_3	0.10	7.13	CoV_3	0.08	5.87	CoV_3	0.26	6.27	CoV_3	1.18
		5.76	μ_{c3}	5.79	6.04	μ_{c3}	6.00	5.81	μ_{c3}	5.71	6.58	μ_{c3}	6.58
		5.81	σ_{c3}	0.03	6.00	σ_{c3}	0.04	5.67	σ_{c3}	0.09	6.59	σ_{c3}	0.02
		5.79	CoV_3	0.43	5.96	CoV_3	0.67	5.64	CoV_3	1.59	6.56	CoV_3	0.23
70	**L**	5.81	μ_{a3}	5.80	7.16	μ_{a3}	7.18	6.71	μ_{a3}	6.69	6.91	μ_{a3}	6.90
	(a)	5.80	σ_{a3}	0.01	7.21	σ_{a3}	0.03	6.68	σ_{a3}	0.02	6.88	σ_{a3}	0.02
		5.80	CoV_3	0.10	7.18	CoV_3	0.35	6.67	CoV_3	0.31	6.90	CoV_3	0.22
		5.87	μ_{a3}	5.89	7.45	μ_{a3}	7.44	6.84	μ_{a3}	6.85	6.47	μ_{a3}	6.45
		5.91	σ_{a3}	0.02	7.43	σ_{a3}	0.01	6.85	σ_{a3}	0.02	6.47	σ_{a3}	0.03
		5.88	CoV_3	0.35	7.43	CoV_3	0.16	6.87	CoV_3	0.22	6.42	CoV_3	0.45
	PCL	5.89	μ_{b3}	5.90	6.49	μ_{b3}	6.51	5.97	μ_{b3}	5.97	6.72	μ_{b3}	6.70
	(b)	5.90	σ_{b3}	0.01	6.51	σ_{b3}	0.02	5.99	σ_{b3}	0.02	6.71	σ_{b3}	0.03
		5.90	CoV_3	0.10	6.52	CoV_3	0.23	5.95	CoV_3	0.34	6.67	CoV_3	0.39
		5.80	μ_{b3}	5.82	6.82	μ_{b3}	6.83	6.14	μ_{b3}	6.10	6.16	μ_{b3}	6.22
		5.84	σ_{b3}	0.02	6.83	σ_{b3}	0.01	6.08	σ_{b3}	0.04	6.26	σ_{b3}	0.06
		5.81	CoV_3	0.36	6.83	CoV_3	0.08	6.07	CoV_3	0.62	6.25	CoV_3	0.88
	SS	5.02	μ_{c3}	5.01	7.08	μ_{c3}	7.08	6.43	μ_{c3}	6.42	6.02	μ_{c3}	5.98
	(c)	5.00	σ_{c3}	0.01	7.09	σ_{c3}	0.01	6.40	σ_{c3}	0.02	5.97	σ_{c3}	0.04
		5.02	CoV_3	0.23	7.07	CoV_3	0.14	6.42	CoV_3	0.24	5.94	CoV_3	0.68
		5.10	μ_{c3}	5.06	6.93	μ_{c3}	6.90	6.02	μ_{c3}	6.00	5.61	μ_{c3}	5.58
		5.05	σ_{c3}	0.04	6.98	σ_{c3}	0.09	6.00	σ_{c3}	0.02	5.57	σ_{c3}	0.03
		5.02	CoV_3	0.80	6.80	CoV_3	1.35	5.98	CoV_3	0.33	5.56	CoV_3	0.47

Appendix N Duplicate T-Test March 2011

DF=5
>2.015
<2.015

			Cast	Screed	Tamp	Brush
0	L	μ_{a3}	4.81	8.25	6.78	5.2
		σ_{a3}	0.05	0.07	0.06	0.25
	(a)	μ_{a3}	4.65	8.21	6.91	5.18
		σ_{a3}	0.04	0.08	0.03	0.22
		t(aa)	4.58	0.66	3.41	0.12
	PCL	μ_{b3}	4.6	7.92	6.24	5.59
		σ_{b3}	0.35	0.28	0.37	0.08
	(b)	μ_{b3}	5.11	8.25	6.14	5.45
		σ_{b3}	0.1	0.05	0.04	0.17
		t(bb)	2.44	2.02	0.48	1.31
	SS	μ_{c3}	4.88	8.11	5.82	5.12
		σ_{c3}	0.01	0.08	0.15	0.24
	(c)	μ_{c3}	4.91	7.53	5.46	4.38
		σ_{c3}	0.05	0.09	0.44	0.06
		t(cc)	1.09	8.27	1.37	5.28
30	L	μ_3	5.31	6.78	6.52	4.66
		σ_3	0.21	1.49	0.02	0.11
	(a)	μ_3	5.43	7.78	7.04	4.89
		σ_3	0.06	0.3	0.03	0.08
		t(aa)	1.01	1.14	27.22	2.92
	PCL	μ_3	4.77	7.99	7.29	6.09
		σ_3	0.03	0.25	0.27	0.09
	(b)	μ_3	5.13	8.71	8.11	5.95
		σ_3	0.16	0.08	0.06	0.37
		t(bb)	3.89	4.83	5.14	0.61
	SS	μ_3	4.97	8.17	6.74	5.78
		σ_3	0.05	0.06	0.03	0.06
	(c)	μ_3	4.85	8	5.36	5.81
		σ_3	0.3	0.18	0.31	0.14
		t(cc)	0.66	1.56	7.64	0.3

			Cast	Screed	Tamp	Brush
50	**L**	μ_{a3}	5.72	8.2	6.64	5.73
		σ_{a3}	0.17	0.07	0.03	0.13
	(a)	μ_{a3}	5.85	8.91	6.59	6.02
		σ_{a3}	0.01	0.07	0.24	0.02
		t(aa)	1.31	12.64	0.39	3.93
	PCL	μ_{b3}	5.56	8.74	6.06	6.56
		σ_{b3}	0.23	0.58	0.09	0.04
	(b)	μ_{b3}	5.98	9.2	6.02	6.6
		σ_{b3}	0.08	0.03	0.05	0.04
		t(bb)	3.02	1.37	0.55	1.48
	SS	μ_{c3}	5.76	8.65	6.98	6.52
		σ_{c3}	0.03	0.03	0.06	0.05
	(c)	μ_{c3}	5.39	8.16	6.16	5.88
		σ_{c3}	0.26	0.21	0.06	0.34
		t(cc)	2.42	3.98	16.78	3.2
70	**L**	μ_{a3}	5.75	8.59	5.32	6.04
		σ_{a3}	0.19	0.64	0.54	0.13
	(a)	μ_{a3}	6.08	9.08	7.19	6.81
		σ_{a3}	0.08	0.02	0.03	0.12
		t(aa)	2.81	1.32	5.94	7.64
	PCL	μ_{b3}	5.87	6.92	5.44	6.28
		σ_{b3}	0.3	0.11	0.38	0.07
	(b)	μ_{b3}	6.23	8.92	6.45	6.22
		σ_{b3}	0.07	0.01	0.03	0.04
		t(bb)	2.01	32.89	4.56	1.33
	SS	μ_{c3}	5.91	8.35	7.36	5.21
		σ_{c3}	0.03	0.12	0.15	0.08
	(c)	μ_{c3}	6.03	8.09	6.73	5.37
		σ_{c3}	0.03	0.13	0.15	0.03
		t(cc)	4.72	2.51	5.12	3.46

29
19

Appendix O Duplicate T-Test July 2011

DF=5
>2.015
<2.015

			Cast	Screed	Tamp	Brush
0	**L**	μ_{a3}	5.23	8.5	7.33	6.25
		σ_{a3}	0.05	0.06	0.03	0.05
	(a)	μ_{a3}	5.35	9.11	8.12	5.83
		σ_{a3}	0.01	0.07	0.04	0.02
		t(aa)	4.25	11.12	30.99	14.65
	PCL	μ_{b3}	5.38	8.69	7.5	5.98
		σ_{b3}	0.03	0.02	0.04	0.06
	(b)	μ_{b3}	5.54	8.57	6.92	5.91
		σ_{b3}	0.01	0.02	0.05	0.02
		t(bb)	8.91	8.49	14.65	1.75
	SS	μ_{c3}	5.12	7.83	6.28	5.4
		σ_{c3}	0.02	0.13	0.03	0.02
	(c)	μ_{c3}	5.48	7.9	6.22	4.84
		σ_{c3}	0.01	0.05	0.04	0.01
		t(cc)	31.18	0.91	2.24	41.75
30	**L**	μ_{a3}	5.79	9.13	7.22	5
		σ_{a3}	0.04	0.1	0.04	0.11
	(a)	μ_{a3}	6.1	9.08	8.19	5.78
		σ_{a3}	0.04	0.06	0.04	0.04
		t(aa)	9.98	0.8	29.45	11.73
	PCL	μ_{b3}	5.74	9.12	8.28	6.6
		σ_{b3}	0.05	0.11	0.01	0.05
	(b)	μ_{b3}	5.74	8.86	8.61	6.5
		σ_{b3}	0.08	0.11	0.11	0.07
		t(bb)	0	2.92	5.01	1.95
	SS	μ_{c3}	5.46	8.17	7.01	6.23
		σ_{c3}	0.02	0.04	0.17	0.02
	(c)	μ_{c3}	5.74	8.62	6.55	6.59
		σ_{c3}	0.02	0.04	0.02	0.03
		t(cc)	17	12.83	4.56	17.59

			Cast	Screed	Tamp	Brush
50	**L**	μ_{a3}	6.34	8.62	7.39	6.24
		σ_{a3}	0.03	0.11	0.06	0.08
	(a)	μ_{a3}	6.53	9.28	6.97	6.77
		σ_{a3}	0.02	0.02	0.01	0.01
		t(aa)	10.96	10.58	11.55	11.38
	PCL	μ_{b3}	6.09	9.61	6.57	7.16
		σ_{b3}	0.01	0.07	0.06	0.01
	(b)	μ_{b3}	6.34	8.44	5.89	6.99
		σ_{b3}	0.03	0.06	0.07	0.02
		t(bb)	12.01	22.26	13.11	8.13
	SS	μ_{c3}	5.97	8.49	7.39	6.74
		σ_{c3}	0.03	0.05	0.06	0.01
	(c)	μ_{c3}	6.09	8.53	6.87	6.92
		σ_{c3}	0.01	0.02	0.04	0.05
		t(cc)	7.4	1.48	12.07	6.08
70	**L**	μ_{a3}	6.31	9.54	8.12	7
		σ_{a3}	0.01	0.06	0.03	0.12
	(a)	μ_{a3}	6.36	9.5	7.5	6.99
		σ_{a3}	0.06	0.07	0.01	0.02
		t(aa)	1.56	0.74	31.78	0.2
	PCL	μ_{b3}	6.63	7.17	5.83	6.67
		σ_{b3}	0.06	0.03	0.03	0.07
	(b)	μ_{b3}	6.56	8.54	6.34	6.47
		σ_{b3}	0.02	0.02	0.04	0.06
		t(bb)	2.2	66.67	16.42	3.95
	SS	μ_{c3}	6.07	8.34	7.63	5.82
		σ_{c3}	0.01	0.04	0.03	0.01
	(c)	μ_{c3}	6.12	8.71	6.72	5.94
		σ_{c3}	0.03	0.04	0.07	0.03
		t(cc)	2.54	12.15	21.92	7.06

39
9

Appendix P Duplicate T-Test March 2012

DF=5
>2.015
<2.015

			Cast	Screed	Tamp	Brush
0	L	μ_{a3}	5.27	7.6	6.12	6.37
		σ_{a3}	0.03	0.04	0.02	0.03
	(a)	μ_{a3}	5.34	8.05	7.46	6.55
		σ_{a3}	0.02	0.02	0.02	0.01
		t(aa)	4.16	20.65	89.44	11.63
	PCL	μ_{b3}	5.25	7.47	6.83	6.64
		σ_{b3}	0.02	0.03	0.01	0.02
	(b)	μ_{b3}	5.38	7.65	6.44	6.43
		σ_{b3}	0.03	0.01	0.03	0.03
		t(bb)	5.43	9.88	24.73	12.36
	SS	μ_{c3}	5.18	6.96	5.64	5.62
		σ_{c3}	0.02	0.02	0.02	0.01
	(c)	μ_{c3}	5.23	6.93	5.68	5.32
		σ_{c3}	0.03	0.05	0.01	0.02
		t(cc)	2.65	0.72	3.1	25.24
30	L	μ_{a3}	5.69	8.29	6.56	5.14
		σ_{a3}	0.02	0.02	0.01	0.04
	(a)	μ_{a3}	6.12	7.9	7.15	5.78
		σ_{a3}	0.02	0.03	0.02	0.01
		t(aa)	26.48	21.92	44.5	30.2
	PCL	μ_{b3}	5.85	7.42	7.32	6.01
		σ_{b3}	0.02	0.02	0.04	0.01
	(b)	μ_{b3}	5.44	7.43	6.97	6.08
		σ_{b3}	0.13	0.04	0.05	0.03
		t(bb)	5.73	0.37	9.57	4.25
	SS	μ_{c3}	5.22	7.06	5.95	6.25
		σ_{c3}	0.03	0.04	0.04	0.05
	(c)	μ_{c3}	6.17	7.31	5.74	5.03
		σ_{c3}	0.01	0.01	0.04	0.02
		t(cc)	55.89	12.02	7.01	37.95

			Cast	Screed	Tamp	Brush
50	**L**	μ_{a3}	6.13	7.27	6.28	5.36
		σ_{a3}	0.03	0.03	0.03	0.04
	(a)	μ_{a3}	6.14	6.85	5.77	6.6
		σ_{a3}	0.02	0.03	0.02	0.04
		t(aa)	0.59	16.84	24.35	38.47
	PCL	μ_{b3}	6.74	6.74	6.28	6.7
		σ_{b3}	0.01	0.01	0.03	0.01
	(b)	μ_{b3}	5.95	6.09	5.93	6.81
		σ_{b3}	0.05	0.01	0.02	0.02
		t(bb)	29.64	68.94	18.21	12.37
	SS	μ_{c3}	5.52	7.14	5.87	6.24
		σ_{c3}	0.01	0.01	0.02	0.07
	(c)	μ_{c3}	5.79	6	5.71	6.58
		σ_{c3}	0.03	0.04	0.09	0.02
		t(cc)	17.66	48.71	3.14	7.67
70	**L**	μ_{a3}	5.8	7.18	6.69	6.9
		σ_{a3}	0.01	0.03	0.02	0.02
	(a)	μ_{a3}	5.89	7.44	6.85	6.45
		σ_{a3}	0.02	0.01	0.02	0.03
		t(aa)	6.68	15.85	11.18	23.51
	PCL	μ_{b3}	5.9	6.51	5.97	6.7
		σ_{b3}	0.01	0.02	0.02	0.03
	(b)	μ_{b3}	5.82	6.83	6.1	6.22
		σ_{b3}	0.02	0.01	0.04	0.06
		t(bb)	6.41	33.94	5.12	13.51
	SS	μ_{c3}	5.01	7.08	6.42	5.98
		σ_{c3}	0.01	0.01	0.02	0.04
	(c)	μ_{c3}	5.06	6.9	6	5.58
		σ_{c3}	0.04	0.09	0.02	0.03
		t(cc)	1.79	3.27	28.68	14.22

44
4

Appendix Q Aggregate Type T-Test March 2011(DF=11)

DF=11
>1.796
<1.796

			Cast	Screed	Tamp	Brush
0	L	μ_6	4.73	8.23	6.84	5.19
		σ_6	0.10	0.07	0.08	0.21
		t(L,PCL)	0.82	1.35	6.23	3.15
	PCL	μ_6	4.85	8.09	6.19	5.52
		σ_6	0.36	0.26	0.24	0.14
		t(PCL,SS)	0.31	1.58	3.11	4.13
	SS	μ_6	4.90	7.82	5.64	4.75
		σ_6	0.03	0.33	0.36	0.43
		t(SS,L)	4.14	3.03	8.05	2.25
30	L	μ_6	5.37	7.28	6.78	4.77
		σ_6	0.15	1.10	0.28	0.15
		t(L,PCL)	3.82	2.22	4.02	10.46
	PCL	μ_6	4.95	8.35	7.70	6.02
		σ_6	0.22	0.43	0.48	0.25
		t(PCL,SS)	0.35	1.46	4.38	2.07
	SS	μ_6	4.91	8.08	6.05	5.79
		σ_6	0.20	0.15	0.78	0.10
		t(SS,L)	4.48	1.76	2.14	13.76
50	L	μ_6	5.79	8.55	6.62	5.87
		σ_6	0.13	0.39	0.15	0.18
		t(L,PCL)	0.12	1.72	8.43	9.55
	PCL	μ_6	5.77	8.97	6.04	6.58
		σ_6	0.28	0.45	0.07	0.04
		t(PCL,SS)	1.29	2.58	2.86	2.24
	SS	μ_6	5.57	8.41	6.57	6.20
		σ_6	0.26	0.30	0.45	0.42
		t(SS,L)	1.81	0.73	0.22	1.76
70	L	μ_6	5.91	8.84	6.26	6.43
		σ_6	0.22	0.48	1.08	0.44
		t(L,PCL)	0.93	1.87	0.62	0.99
	PCL	μ_6	6.05	7.92	5.94	6.25
		σ_6	0.28	1.10	0.61	0.06
		t(PCL,SS)	0.66	0.66	3.81	19.99
	SS	μ_6	5.97	8.22	7.05	5.29
		σ_6	0.07	0.18	0.37	0.10
		t(SS,L)	0.61	2.93	1.7	6.21

Appendix R Aggregate Type T-Test July 2011(DF=11)

DF=11
>1.796
<1.796

			Cast	Screed	Tamp	Brush
0	L	μ_6	5.29	8.81	7.72	6.04
		σ_6	0.08	0.34	0.43	0.23
		t(L,PCL)	3.60	1.24	2.34	0.92
	PCL	μ_6	5.46	8.63	7.21	5.95
		σ_6	0.09	0.07	0.32	0.06
		t(PCL,SS)	1.84	15.79	7.25	6.54
	SS	μ_6	5.30	7.86	6.25	5.12
		σ_6	0.20	0.10	0.05	0.31
		t(SS,L)	0.12	6.58	8.31	5.87
30	L	μ_6	5.95	9.11	7.7	5.39
		σ_6	0.17	0.08	0.53	0.43
		t(L,PCL)	2.86	1.46	3.21	6.43
	PCL	μ_6	5.74	8.99	8.44	6.55
		σ_6	0.06	0.17	0.19	0.08
		t(PCL,SS)	2.04	4.84	12.13	1.6
	SS	μ_6	5.60	8.40	6.78	6.41
		σ_6	0.16	0.25	0.28	0.20
		t(SS,L)	3.68	6.69	3.78	5.24
50	L	μ_6	6.43	8.95	7.18	6.51
		σ_6	0.11	0.37	0.24	0.30
		t(L,PCL)	3.04	0.24	5.21	4.22
	PCL	μ_6	6.22	9.03	6.23	7.03
		σ_6	0.14	0.65	0.38	0.04
		t(PCL,SS)	2.89	1.96	4.61	4.28
	SS	μ_6	6.03	8.51	7.13	6.83
		σ_6	0.07	0.04	0.29	0.10
		t(SS,L)	7.66	2.93	0.34	2.54
70	L	μ_6	6.33	9.52	7.81	6.99
		σ_6	0.04	0.06	0.34	0.07
		t(L,PCL)	9.13	5.42	9.47	7.18
	PCL	μ_6	6.59	7.85	6.09	6.57
		σ_6	0.05	0.75	0.28	0.12
		t(PCL,SS)	18.79	2.13	4.66	11.7
	SS	μ_6	6.1	8.53	7.18	5.88
		σ_6	0.03	0.20	0.50	0.07
		t(SS,L)	10.11	11.42	2.56	26.41

Appendix S Aggregate Type T-Test March 2012 (DF=11)

DF=11
>1.796
<1.796

			Cast	Screed	Tamp	Brush
0	L	μ_6	5.30	7.83	6.79	6.46
		σ_6	0.04	0.25	0.73	0.10
		t(L,PCL)	0.38	2.38	0.50	1.16
	PCL	μ_6	5.32	7.56	6.63	6.53
		σ_6	0.07	0.10	0.21	0.12
		t(PCL,SS)	3.45	13.83	11.14	12.77
	SS	μ_6	5.20	6.95	5.66	5.47
		σ_6	0.03	0.04	0.03	0.17
		t(SS,L)	4.46	8.48	3.79	12.58
30	L	μ_6	5.91	8.09	6.86	5.46
		σ_6	0.23	0.21	0.33	0.35
		t(L,PCL)	1.90	7.58	1.88	4.06
	PCL	μ_6	5.65	7.43	7.15	6.05
		σ_6	0.24	0.03	0.19	0.04
		t(PCL,SS)	0.20	4.12	13.87	1.48
	SS	μ_6	5.69	7.19	5.85	5.64
		σ_6	0.52	0.14	0.12	0.67
		t(SS,L)	0.92	8.71	7.12	0.58
50	L	μ_6	6.14	7.06	6.03	5.98
		σ_6	0.02	0.23	0.28	0.68
		t(L,PCL)	1.16	3.72	0.56	2.78
	PCL	μ_6	6.35	6.42	6.11	6.76
		σ_6	0.44	0.36	0.19	0.06
		t(PCL,SS)	3.67	0.51	3.54	4.24
	SS	μ_6	5.66	6.57	5.79	6.41
		σ_6	0.15	0.62	0.11	0.19
		t(SS,L)	8.08	1.82	1.92	1.49
70	L	μ_6	5.85	7.31	6.77	6.68
		σ_6	0.05	0.14	0.09	0.24
		t(L,PCL)	0.43	7.02	15.17	1.45
	PCL	μ_6	5.86	6.67	6.03	6.46
		σ_6	0.05	0.18	0.07	0.26
		t(PCL,SS)	34.64	3.81	1.78	4.88
	SS	μ_6	5.04	6.99	6.21	5.78
		σ_6	0.04	0.11	0.23	0.22
		t(SS,L)	33.35	4.33	5.57	6.70

Appendix T The effect of aggregate type on light reflectance for a screed surface finish (top) and tamp surface finish (bottom) for March 2011

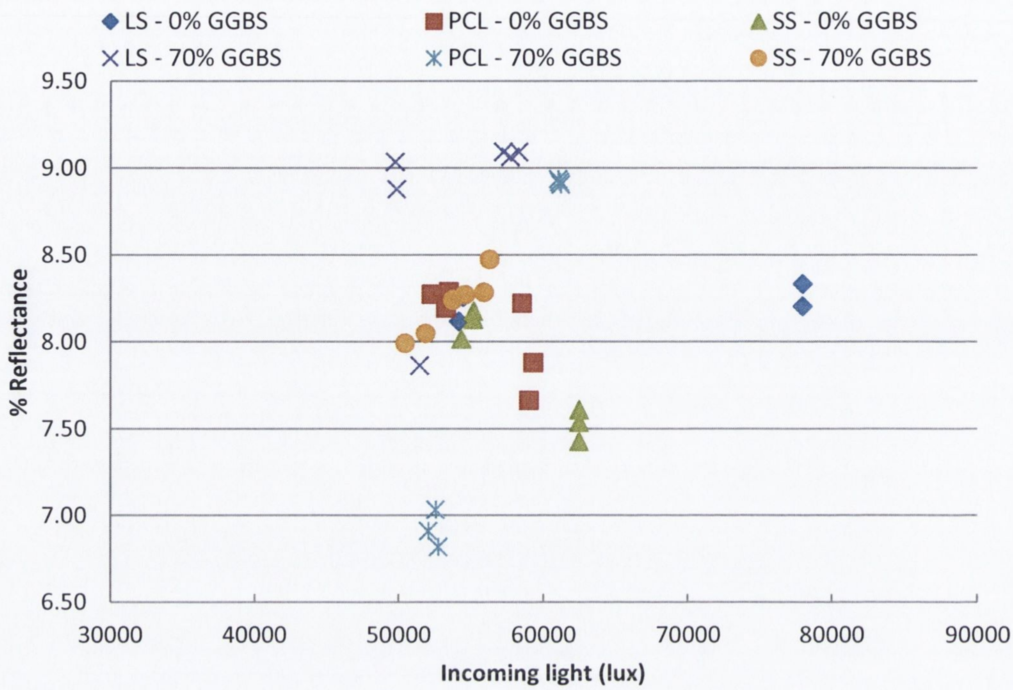

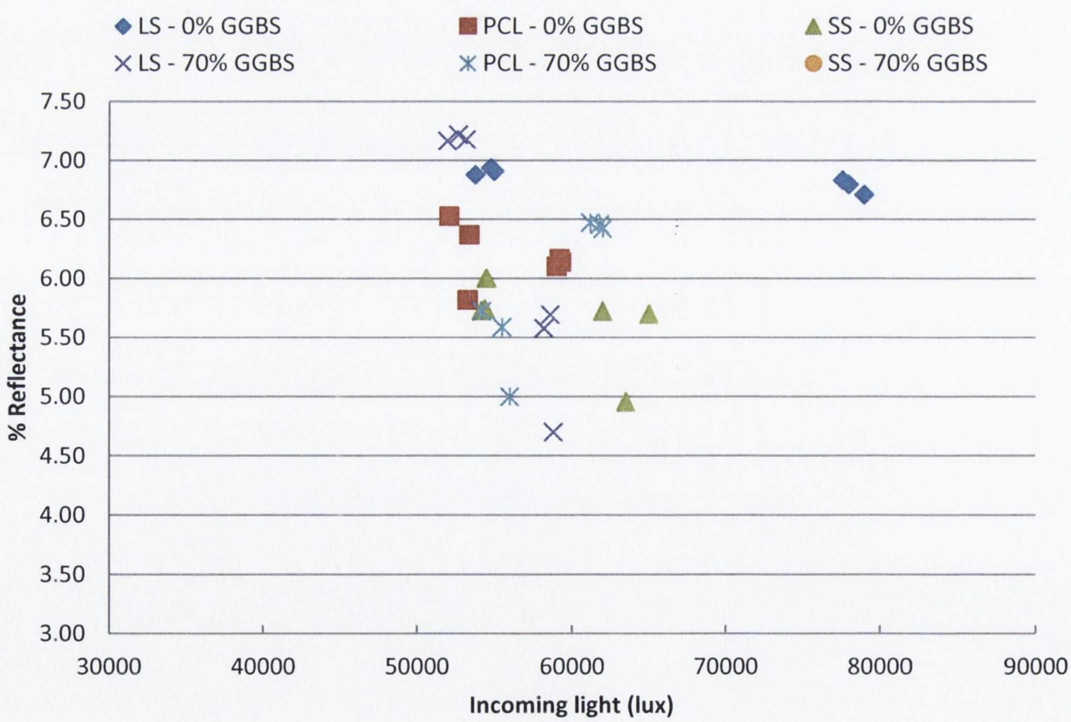

Appendix U The effect of GGBS concentration on light reflectance for March 2011

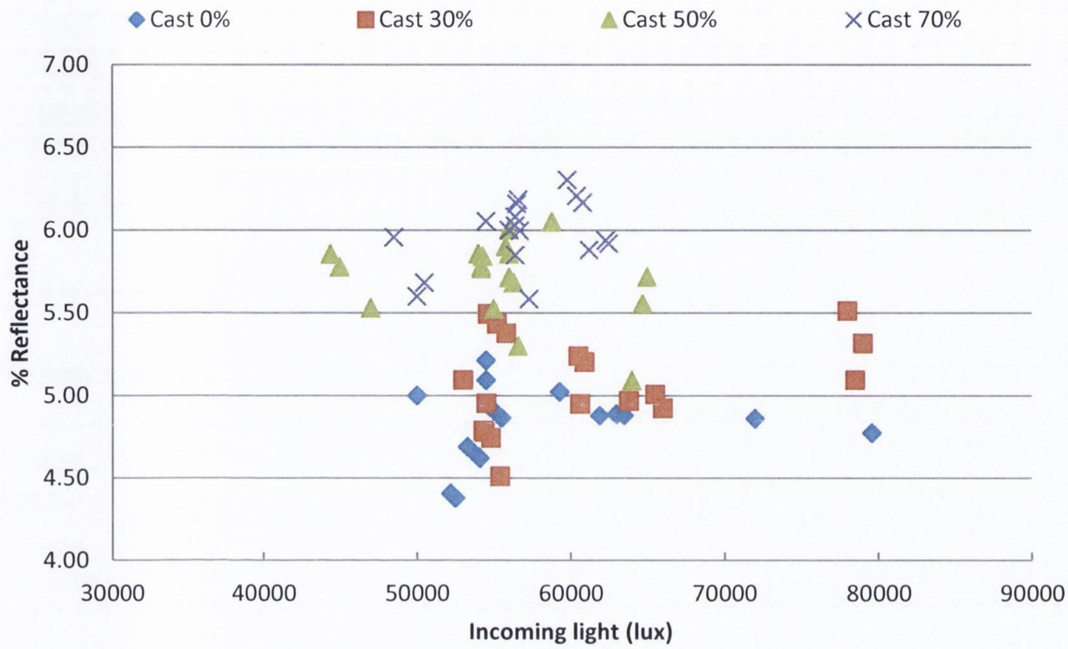

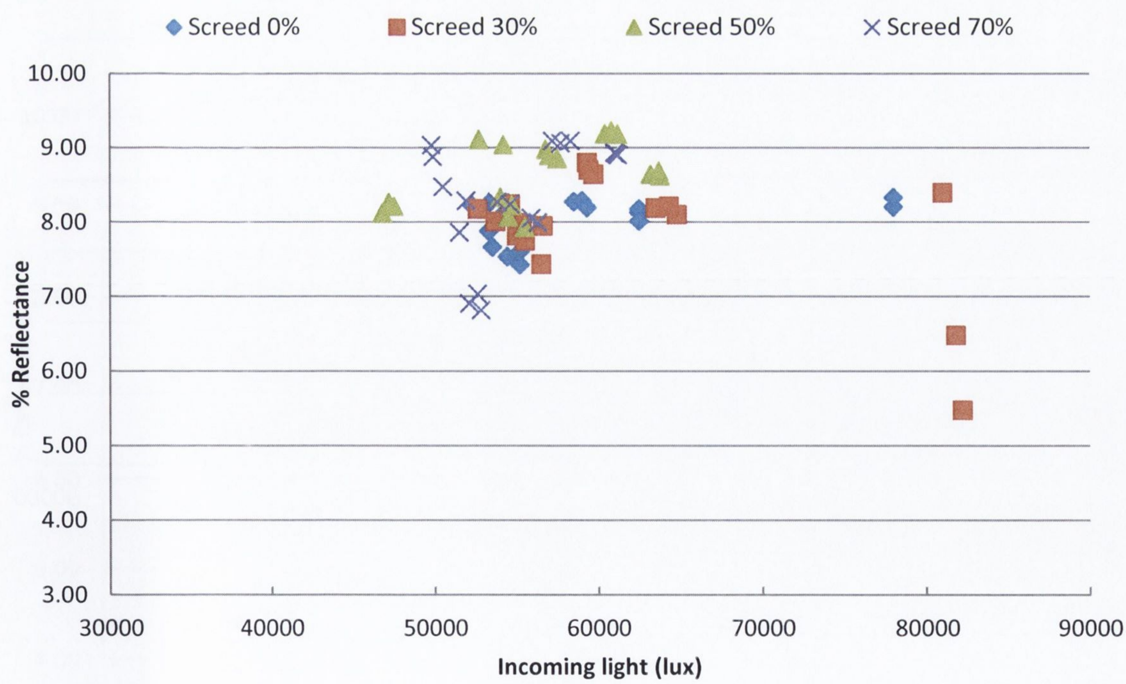

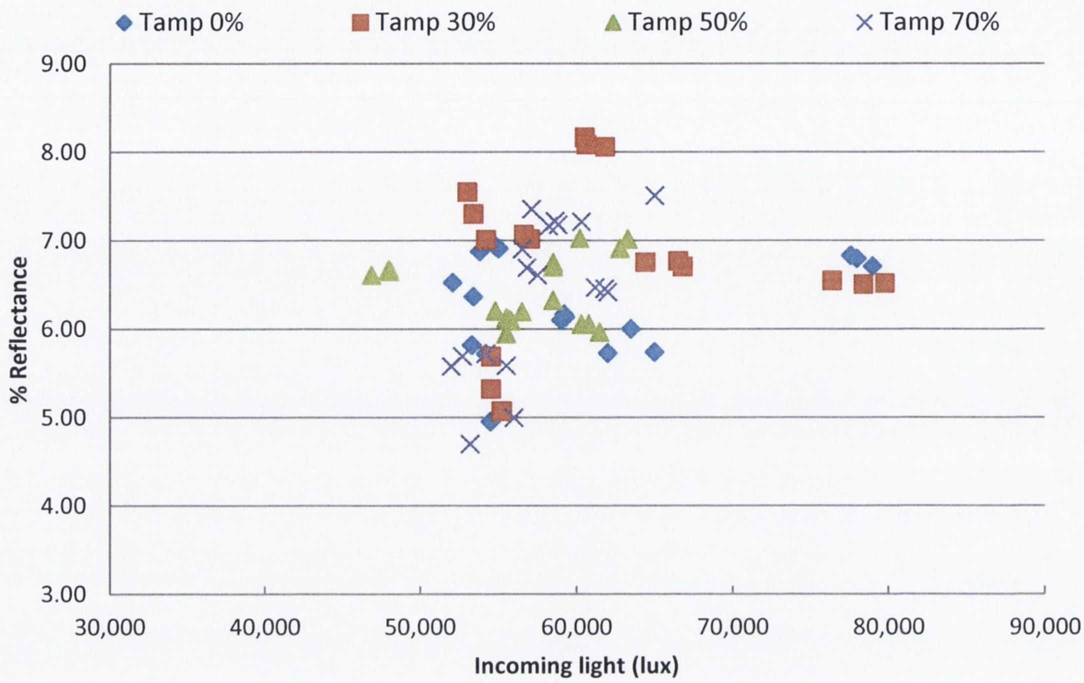
Tamp 0%
Tamp 30%
Tamp 50%
Tamp 70%
9.00
8.00
7.00
6.00
5.00
4.00
3.00
% Reflectance
30,000
40,000
50,000
60,000
70,000
80,000
90,000
Incoming light (lux)

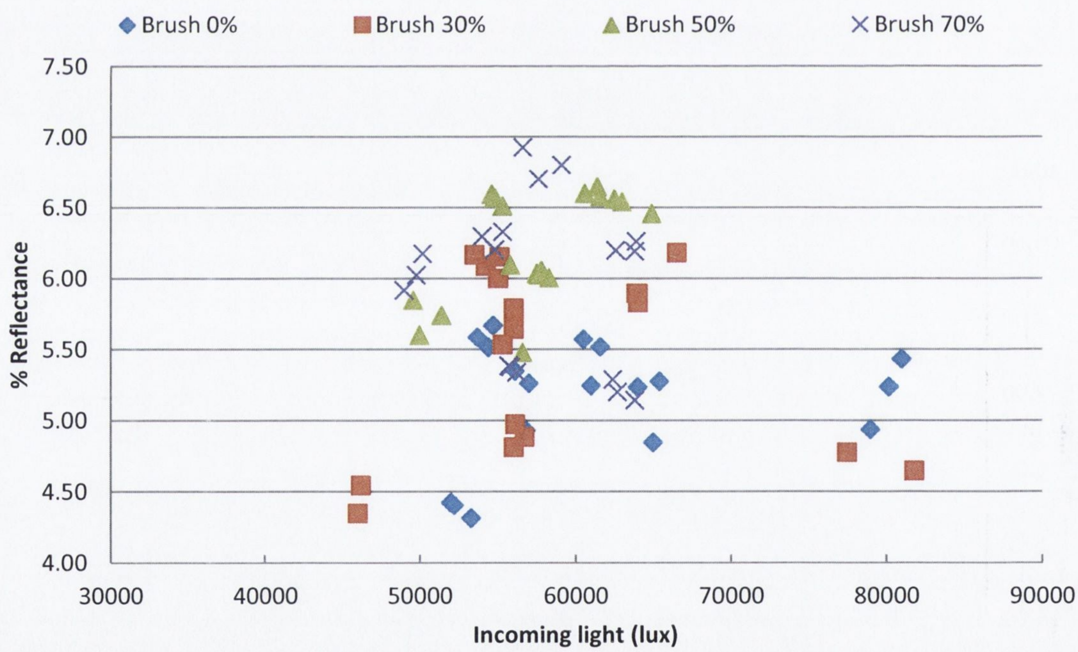
Brush 0%
Brush 30%
Brush 50%
Brush 70%
7.50
7.00
6.50
6.00
5.50
5.00
4.50
4.00
% Reflectance
30000
40000
50000
60000
70000
80000
90000
Incoming light (lux)

Appendix V The effect of GGBS concentration on light reflectance for July 2011

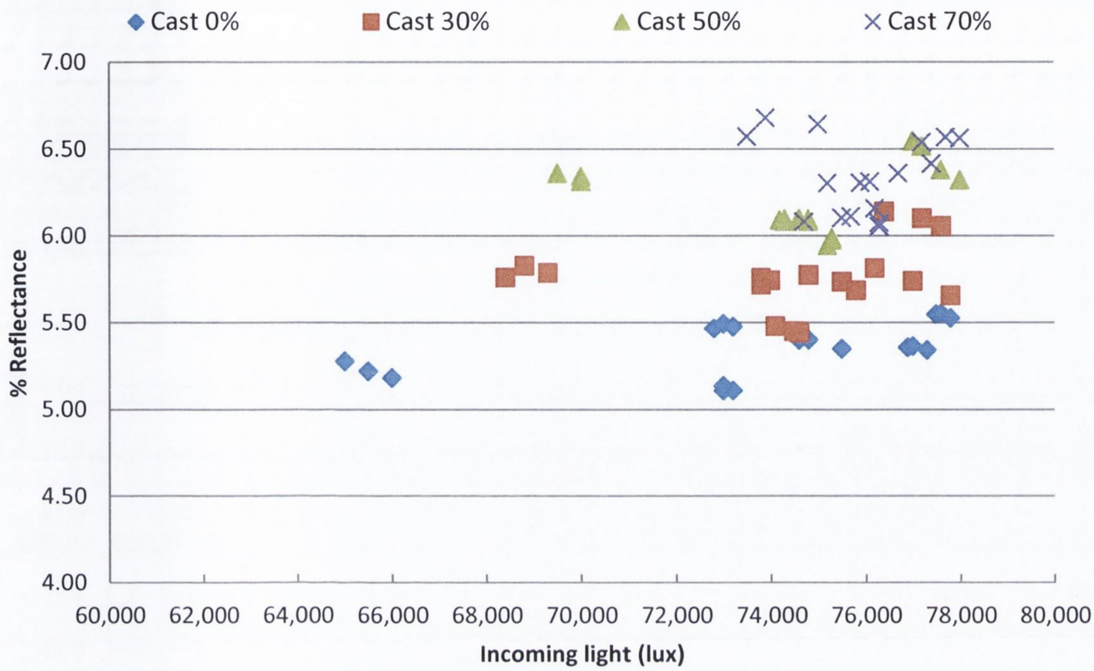

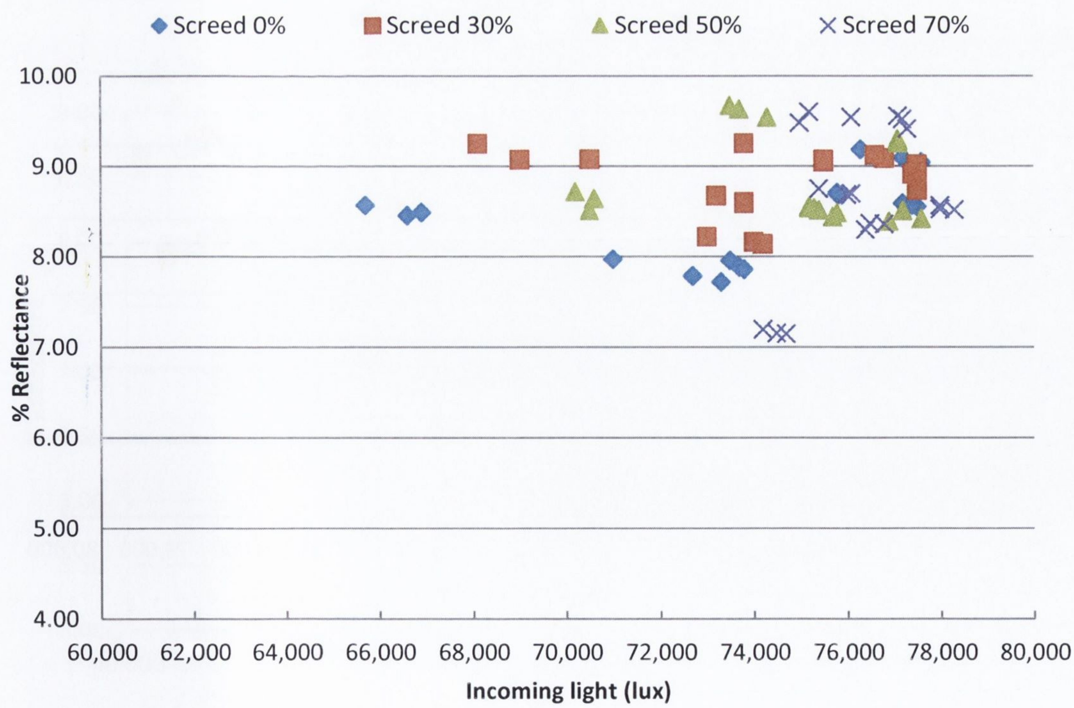

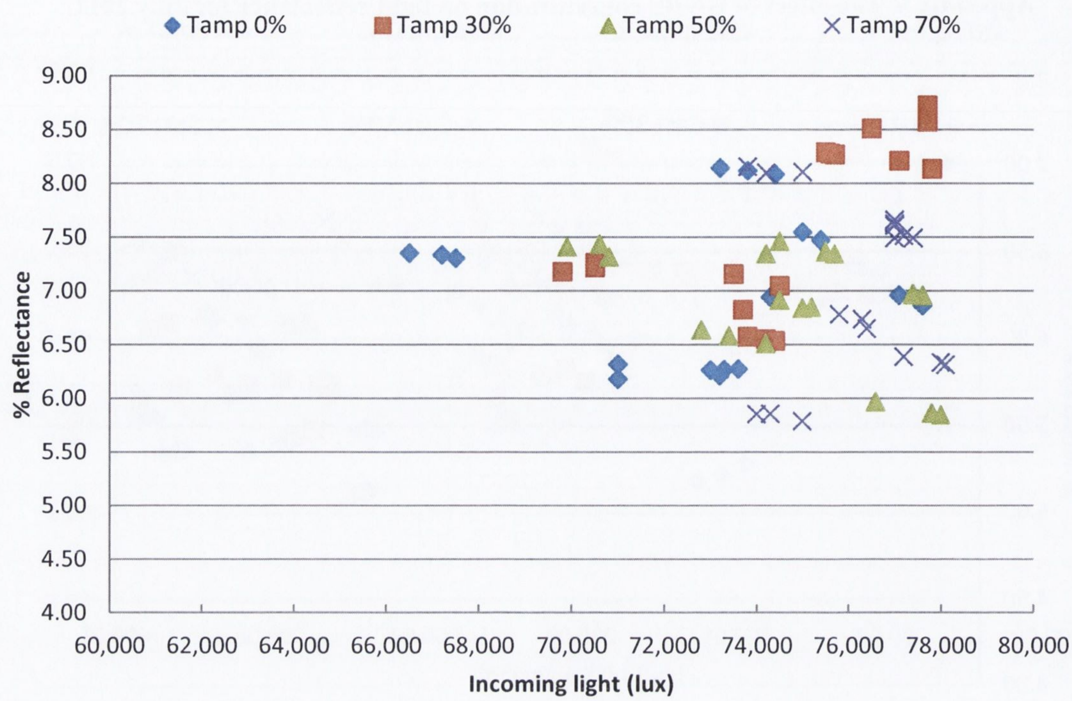

Tamp 0%
Tamp 30%
Tamp 50%
Tamp 70%
9.00
8.50
8.00
7.50
7.00
6.50
6.00
5.50
5.00
4.50
4.00
% Reflectance
60,000
62,000
64,000
66,000
68,000
70,000
72,000
74,000
76,000
78,000
80,000
Incoming light (lux)

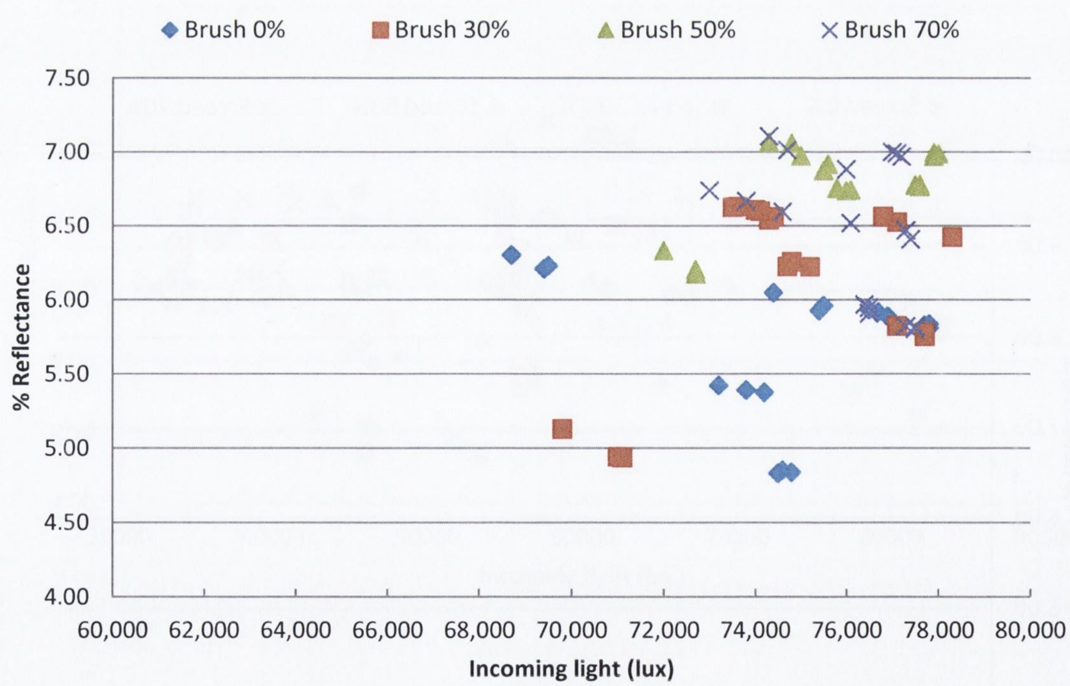

Brush 0%
Brush 30%
Brush 50%
Brush 70%
7.50
7.00
6.50
6.00
5.50
5.00
4.50
4.00
% Reflectance
60,000
62,000
64,000
66,000
68,000
70,000
72,000
74,000
76,000
78,000
80,000
Incoming light (lux)

Appendix W The effect of GGBS concentration on light reflectance for March 2012

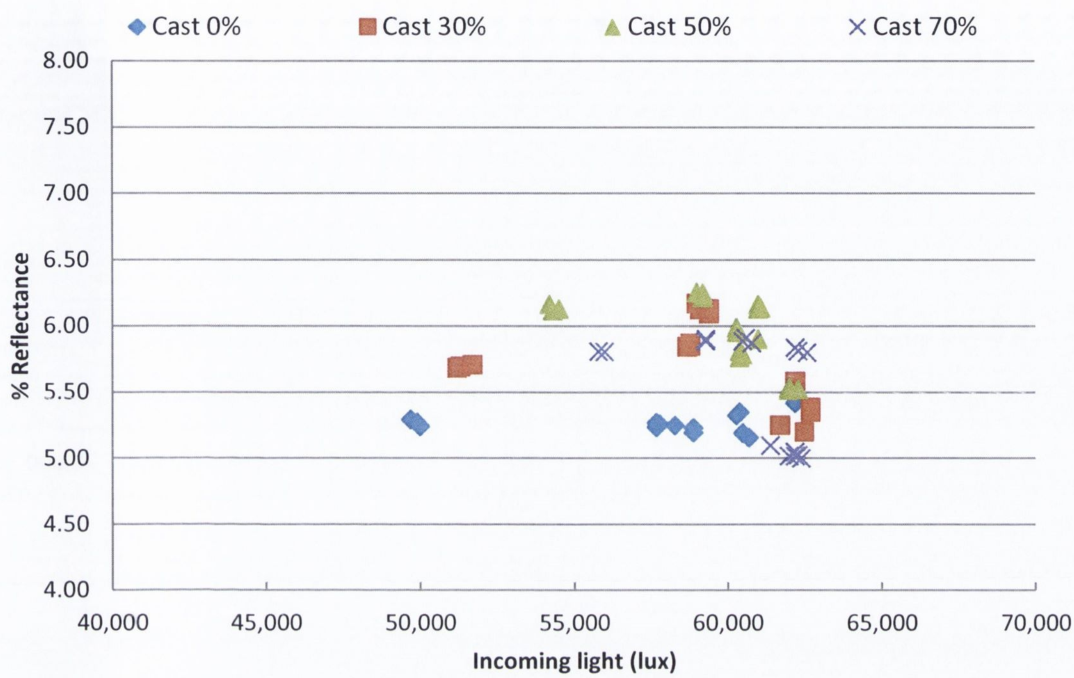

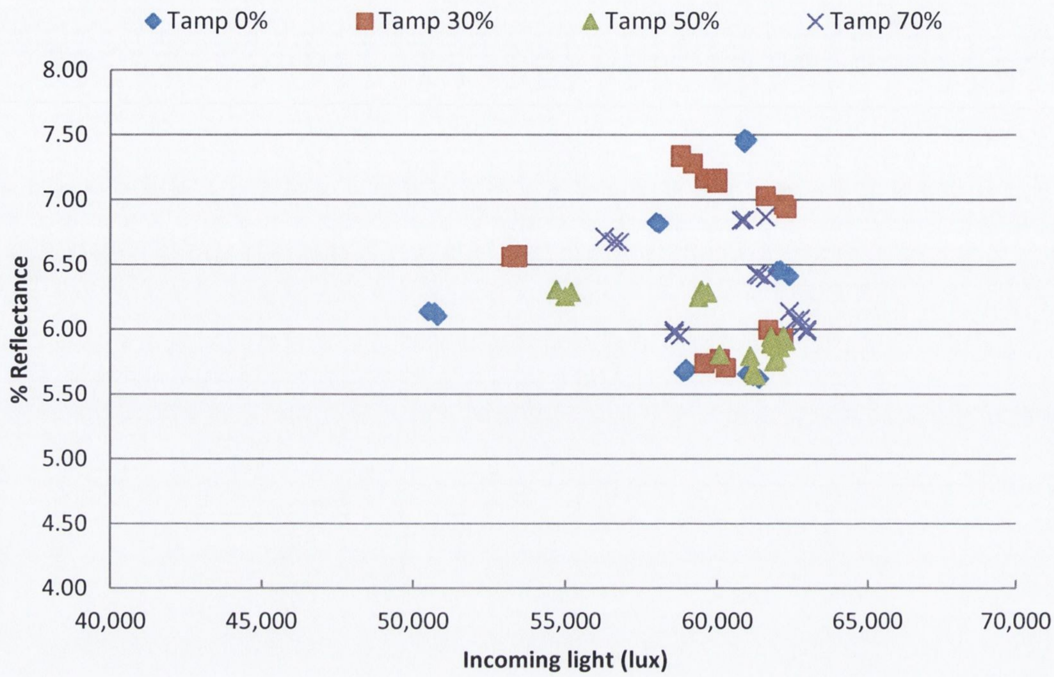
Tamp 0%
Tamp 30%
Tamp 50%
Tamp 70%
8.00
7.50
7.00
6.50
6.00
5.50
5.00
4.50
4.00
% Reflectance
40,000
45,000
50,000
55,000
60,000
65,000
70,000
Incoming light (lux)

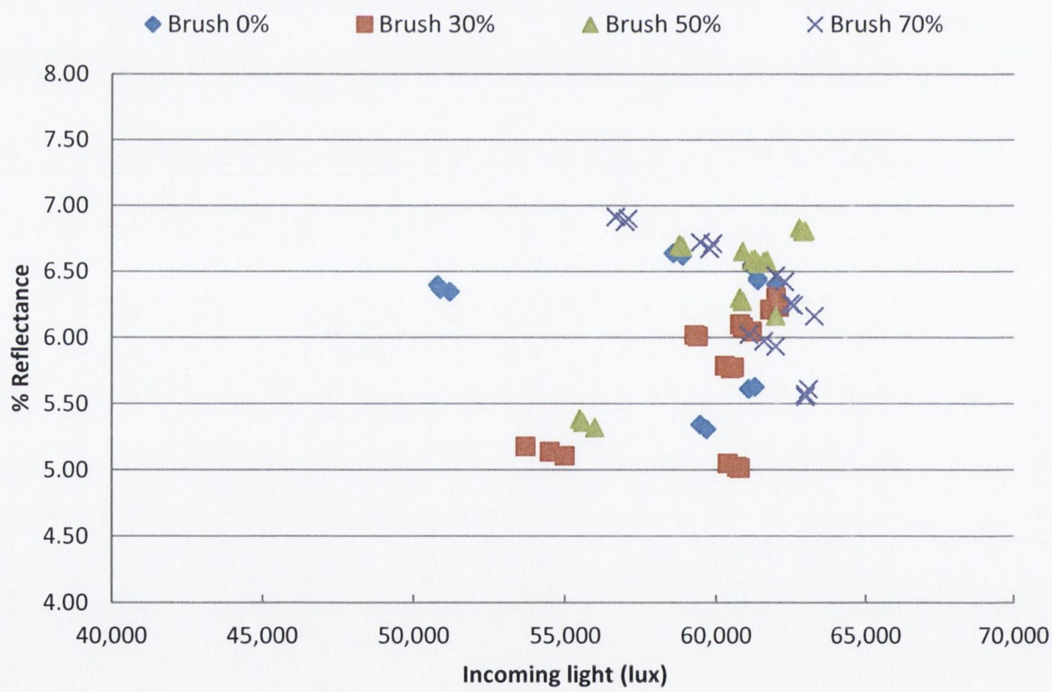
Brush 0%
Brush 30%
Brush 50%
Brush 70%
8.00
7.50
7.00
6.50
6.00
5.50
5.00
4.50
4.00
% Reflectance
40,000
45,000
50,000
55,000
60,000
65,000
70,000
Incoming light (lux)

Appendix X The effect of surface finish type on light reflectance – March 2011

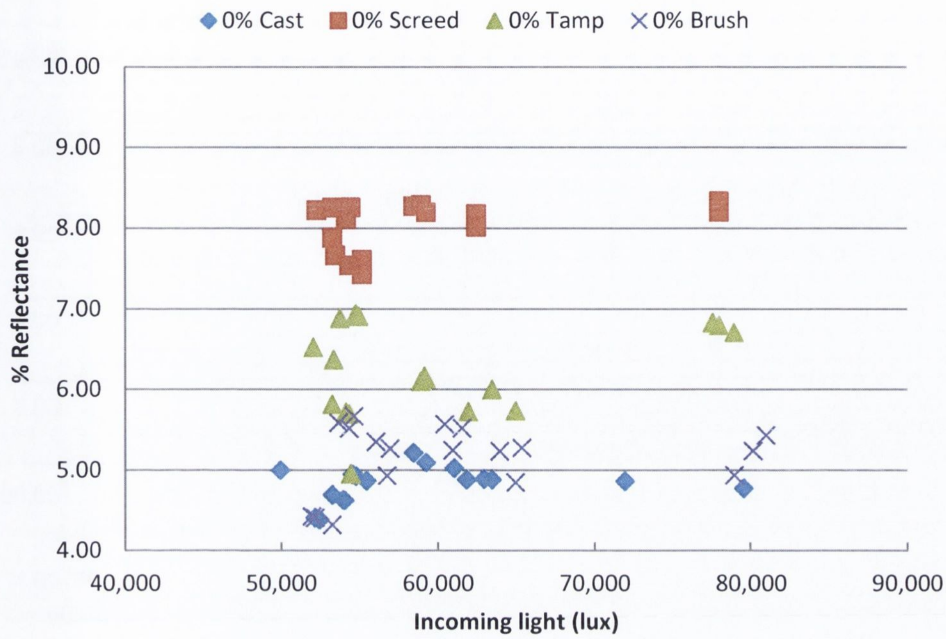

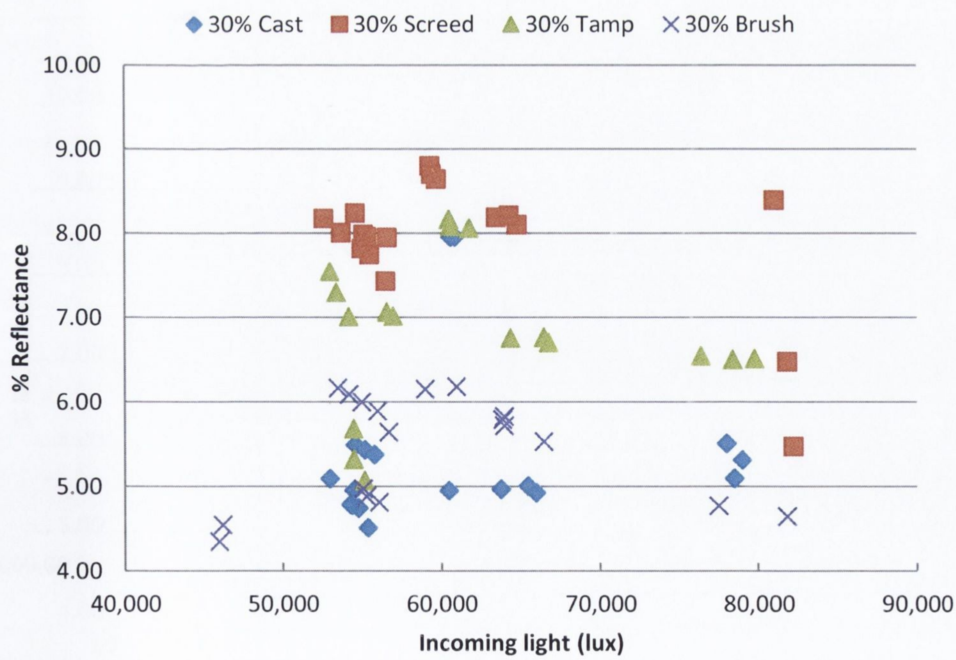

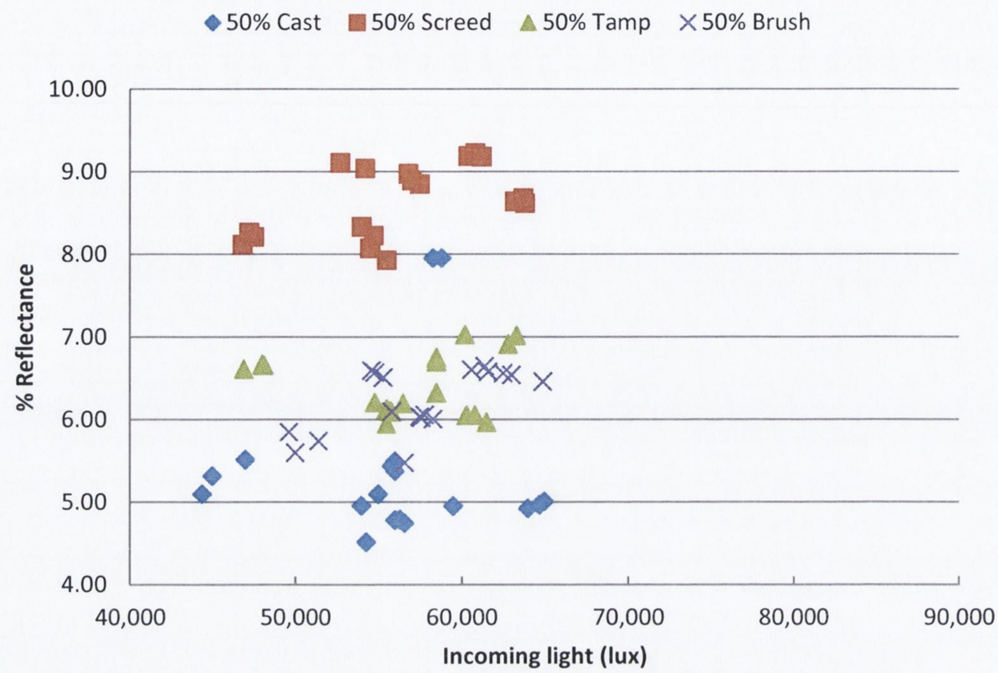
50% Cast
50% Screed
50% Tamp
50% Brush
10.00
9.00
8.00
7.00
6.00
5.00
4.00
% Reflectance
40,000
50,000
60,000
70,000
80,000
90,000
Incoming light (lux)

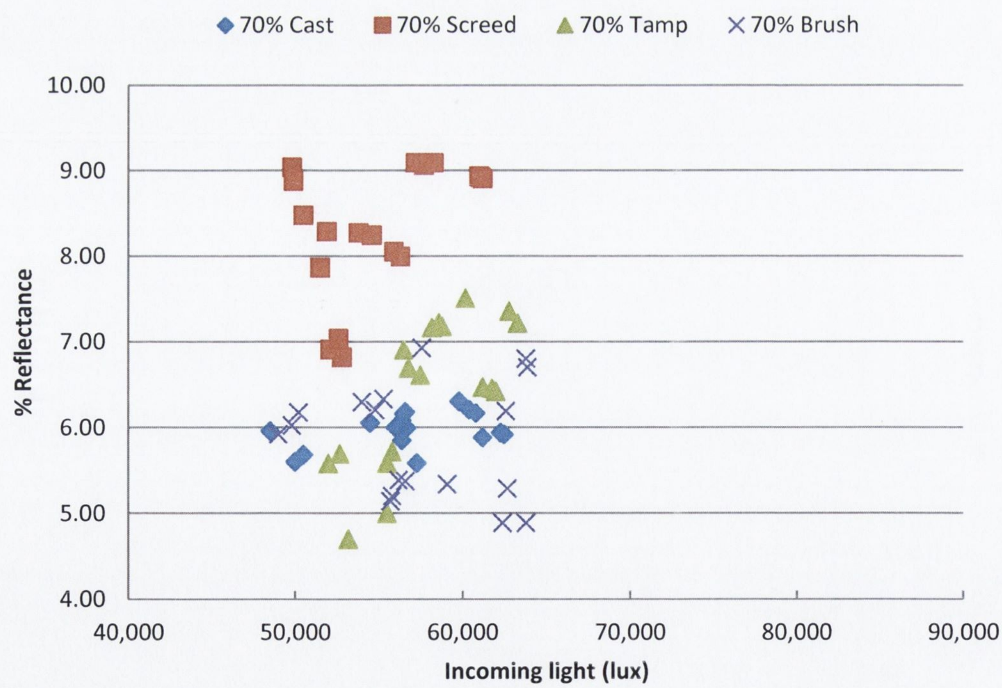
70% Cast
70% Screed
70% Tamp
70% Brush
10.00
9.00
8.00
7.00
6.00
5.00
4.00
% Reflectance
40,000
50,000
60,000
70,000
80,000
90,000
Incoming light (lux)

Appendix Y The effect of surface finish type on light reflectance –July 2011

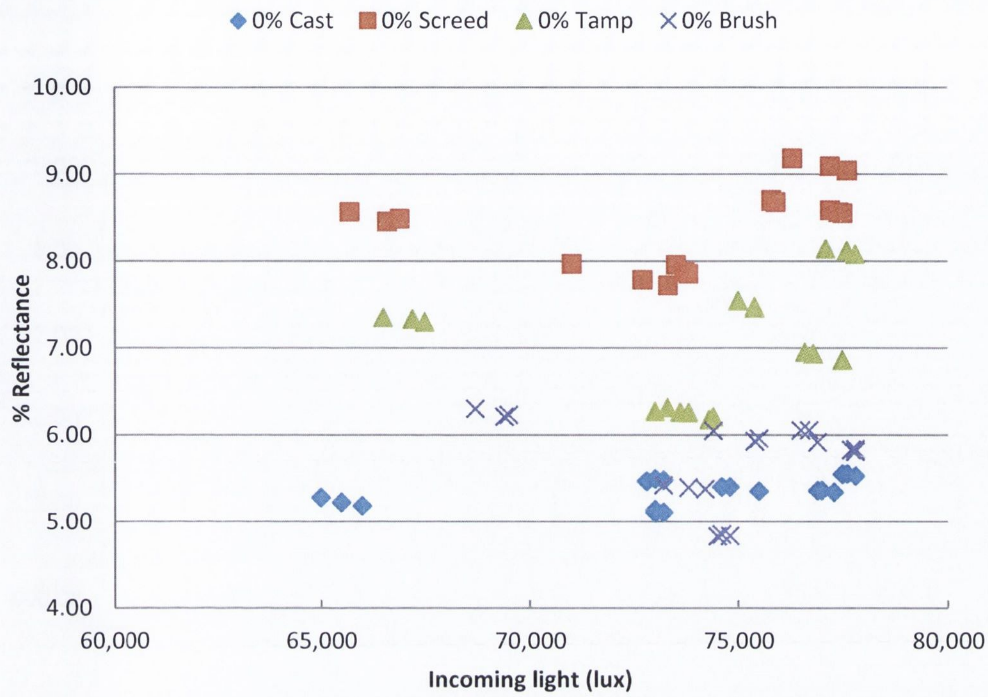

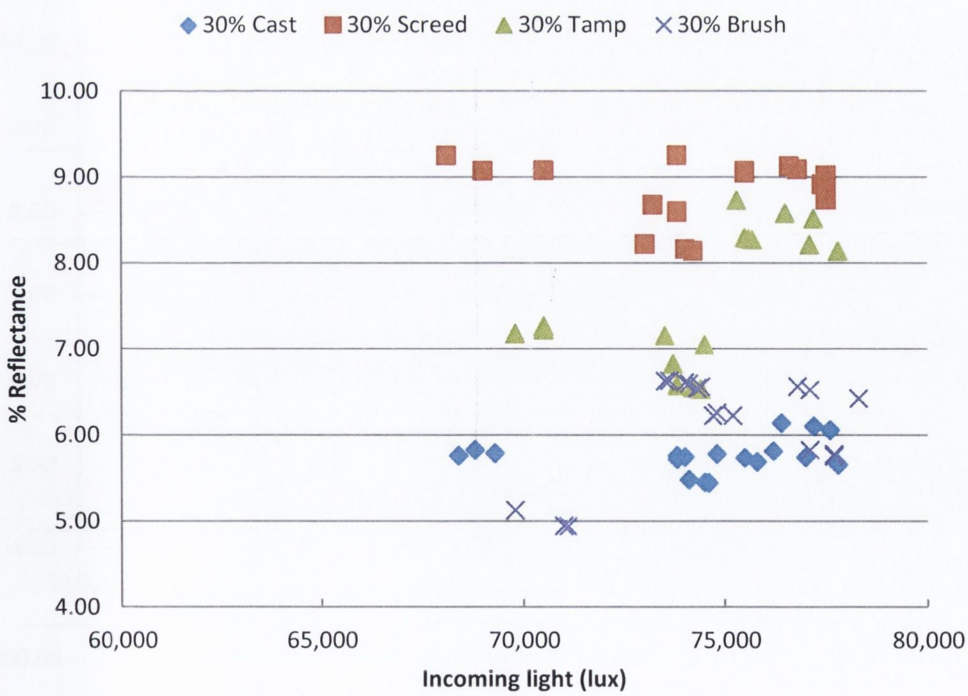

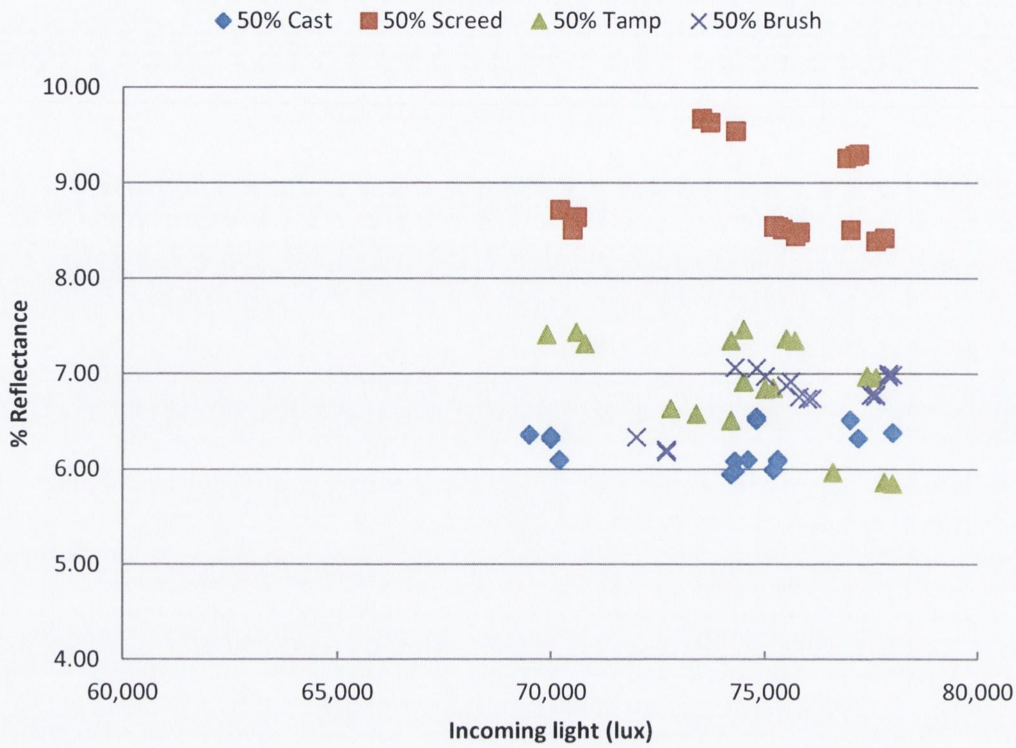

50% Cast
50% Screed
50% Tamp
50% Brush
10.00
9.00
8.00
7.00
6.00
5.00
4.00
% Reflectance
60,000
65,000
70,000
75,000
80,000
Incoming light (lux)

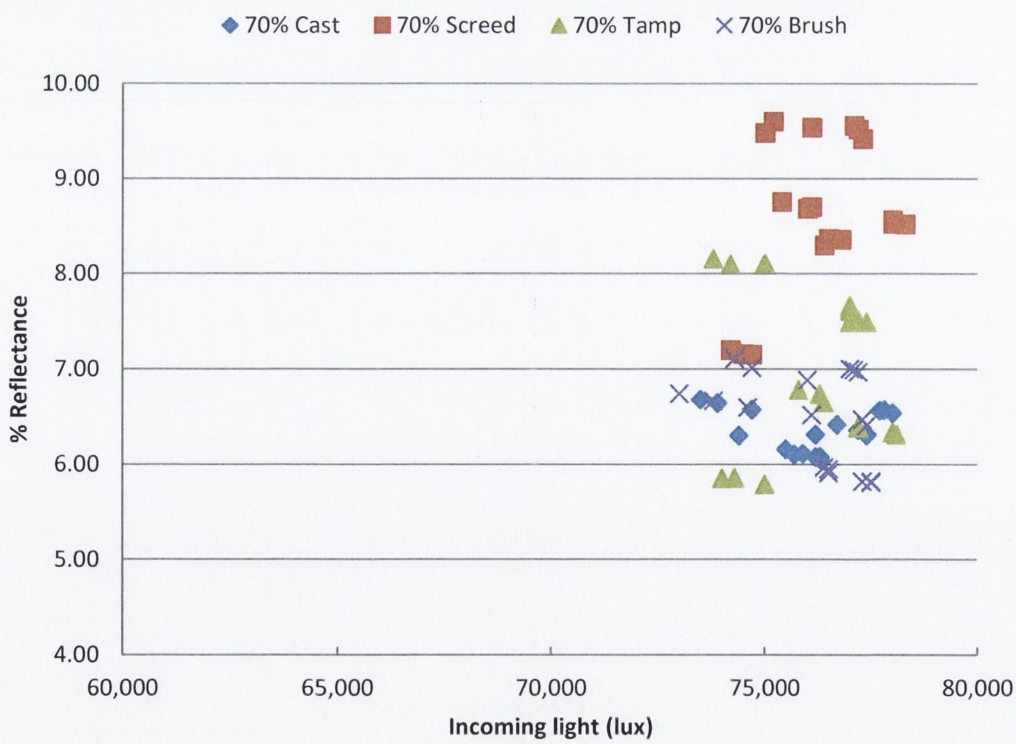

70% Cast
70% Screed
70% Tamp
70% Brush
10.00
9.00
8.00
7.00
6.00
5.00
4.00
% Reflectance
60,000
65,000
70,000
75,000
80,000
Incoming light (lux)

Appendix Z The effect of surface finish type on light reflectance – March 2012

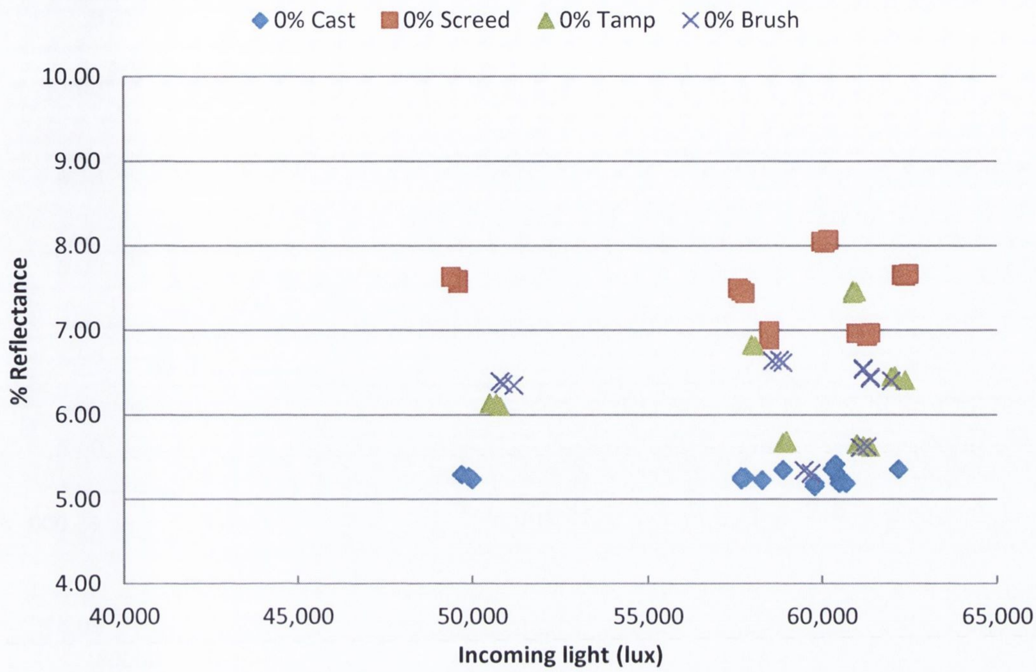

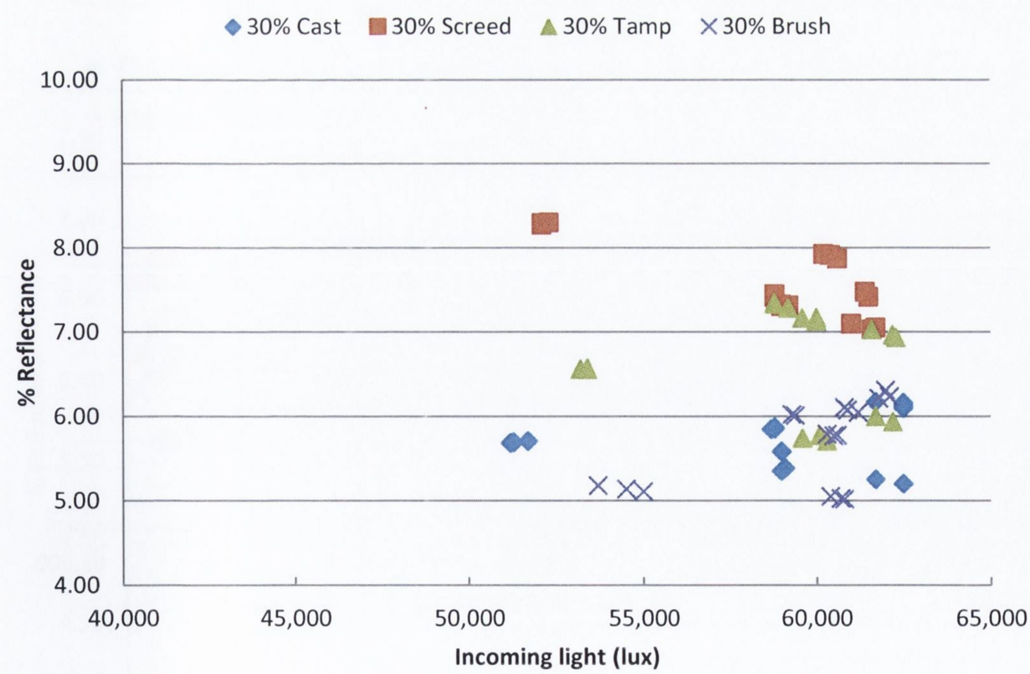

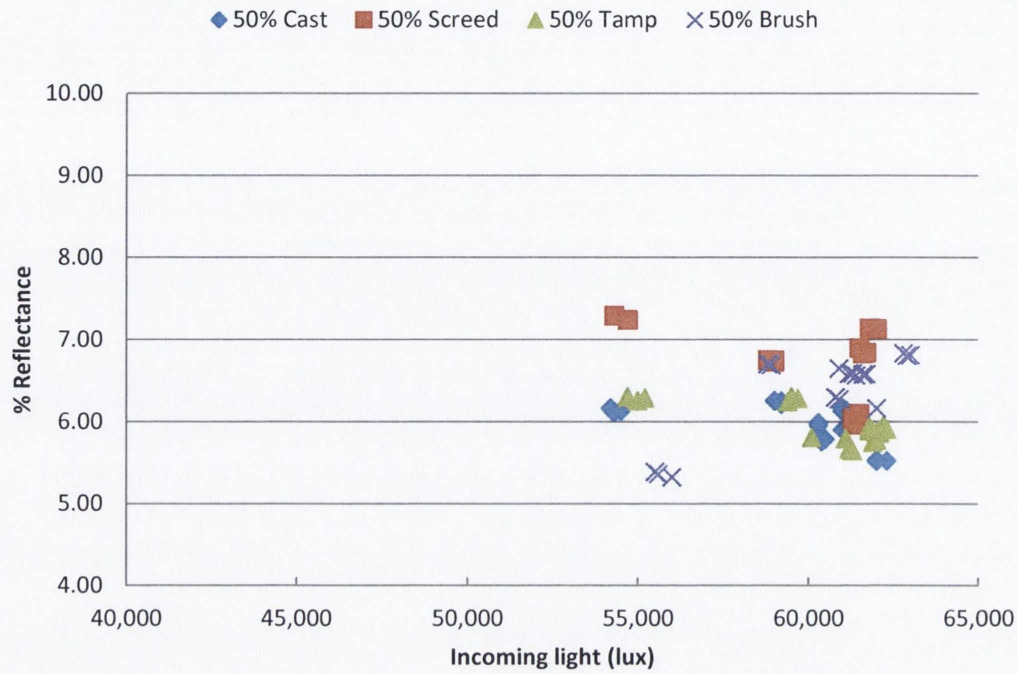

50% Cast
50% Screed
50% Tamp
50% Brush
% Reflectance
10.00
9.00
8.00
7.00
6.00
5.00
4.00
40,000
45,000
50,000
55,000
60,000
65,000
Incoming light (lux)

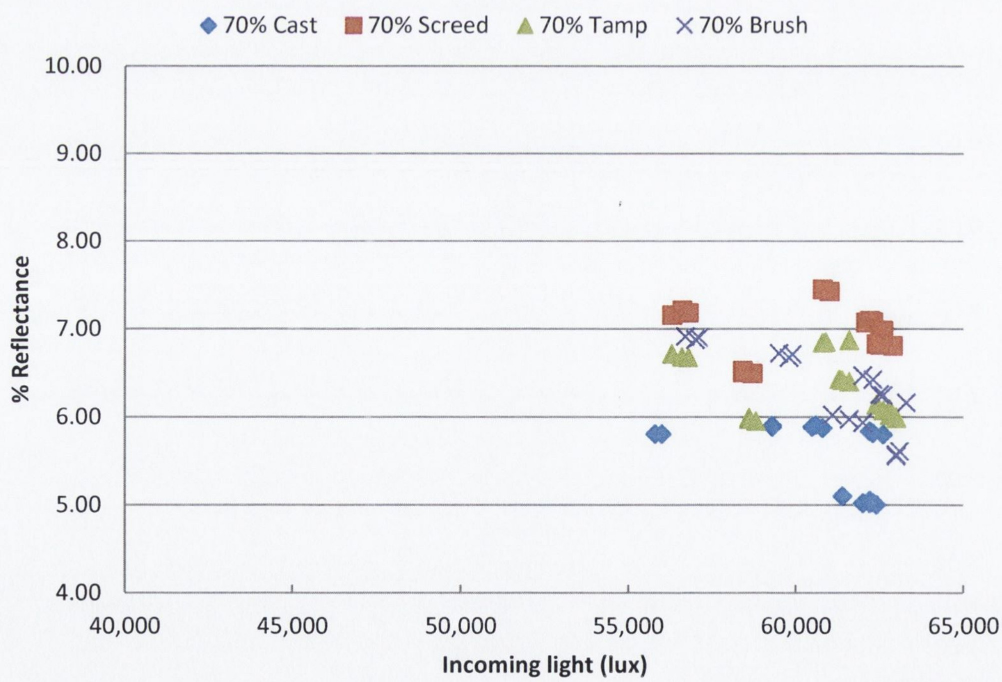

70% Cast
70% Screed
70% Tamp
70% Brush
% Reflectance
10.00
9.00
8.00
7.00
6.00
5.00
4.00
40,000
45,000
50,000
55,000
60,000
65,000
Incoming light (lux)

Appendix AA The effect of GGBS concentration with age on light reflectance for cast, brush, screed and tamp finishes (in order)

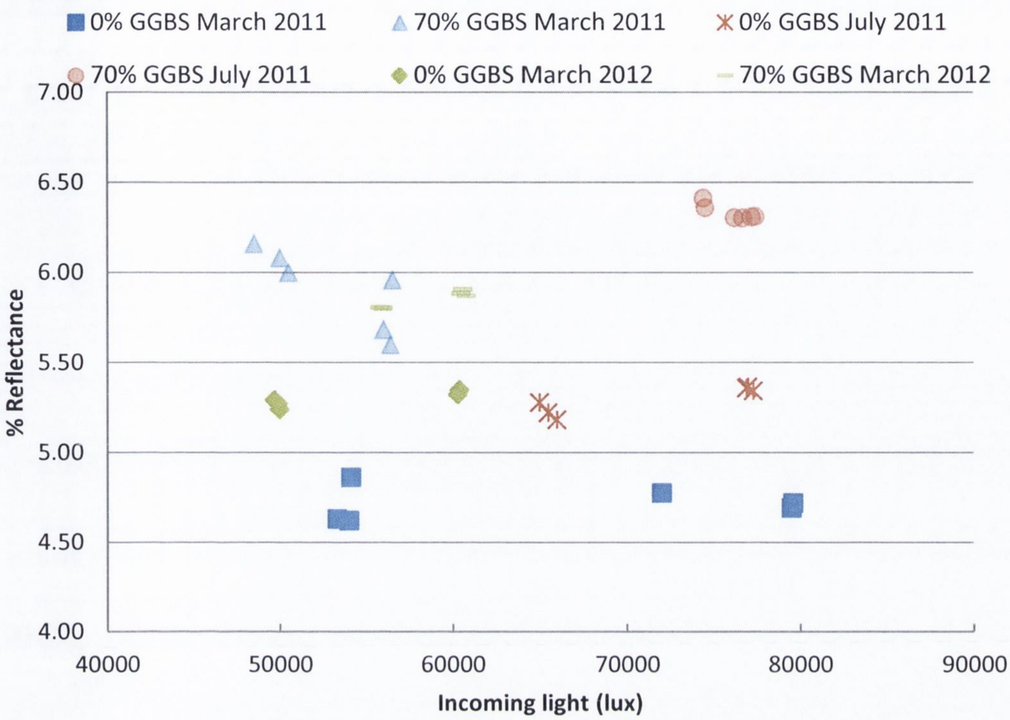

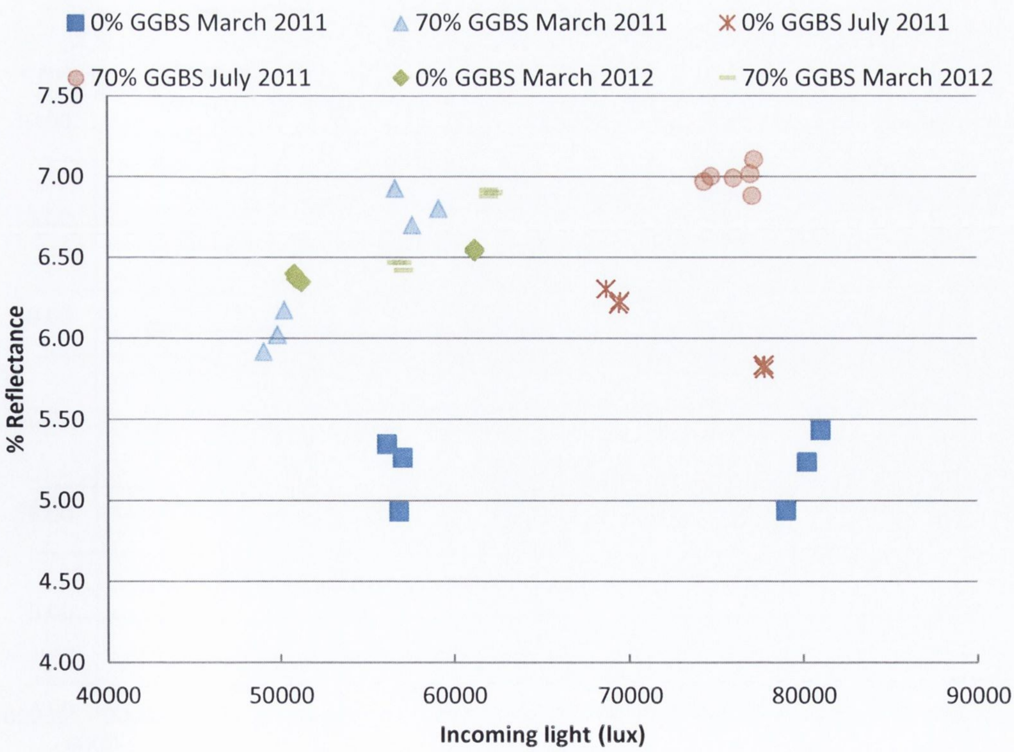

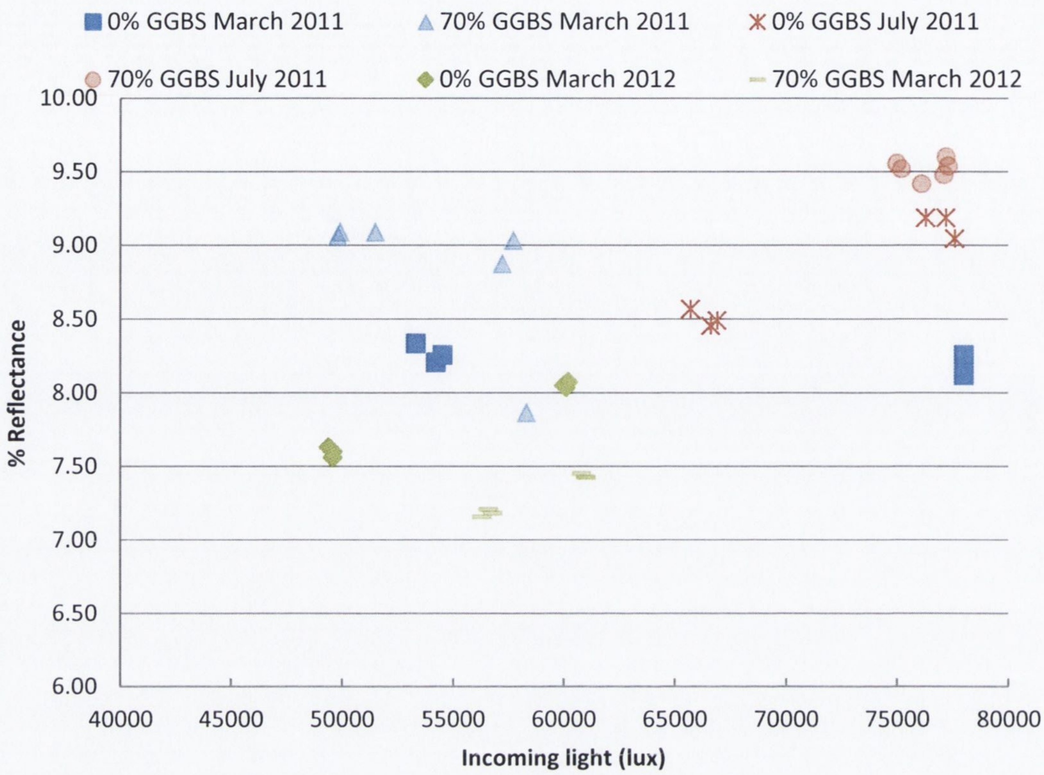

0% GGBS March 2011
70% GGBS March 2011
0% GGBS July 2011
70% GGBS July 2011
0% GGBS March 2012
70% GGBS March 2012
% Reflectance
10.00
9.50
9.00
8.50
8.00
7.50
7.00
6.50
6.00
40000
45000
50000
55000
60000
65000
70000
75000
80000
Incoming light (lux)

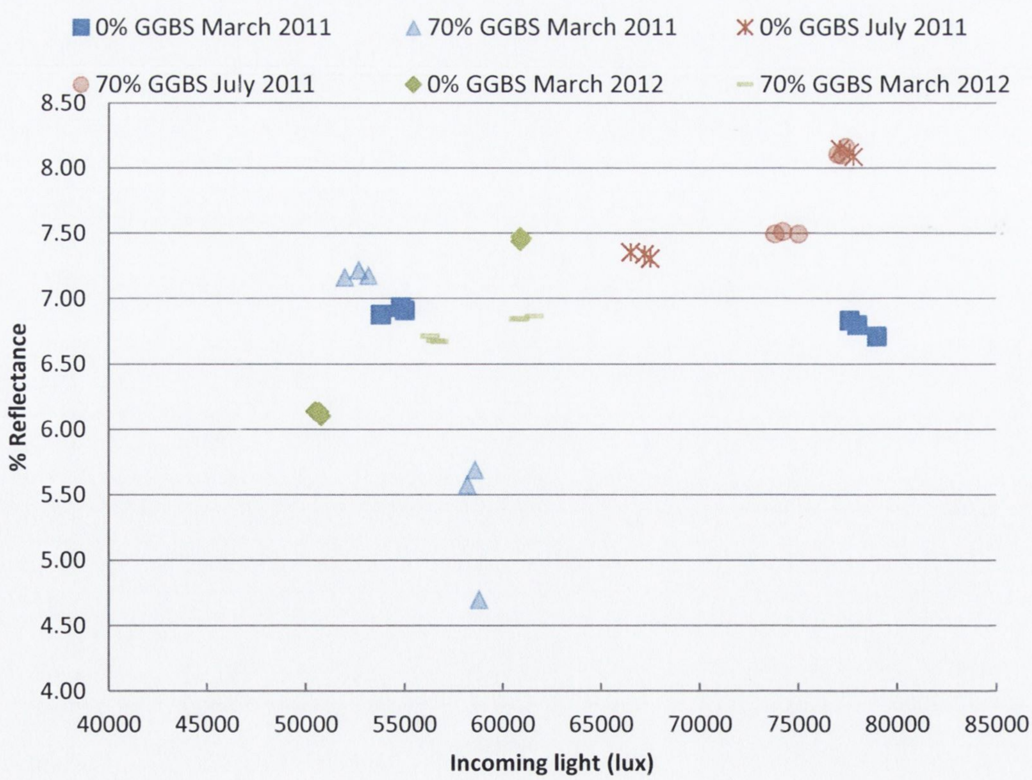

0% GGBS March 2011
70% GGBS March 2011
0% GGBS July 2011
70% GGBS July 2011
0% GGBS March 2012
70% GGBS March 2012
% Reflectance
8.50
8.00
7.50
7.00
6.50
6.00
5.50
5.00
4.50
4.00
40000
45000
50000
55000
60000
65000
70000
75000
80000
85000
Incoming light (lux)

Appendix BB The effect of surface finish with age on light reflectance for 0, 30, 50 and 70% GGBS (in order)

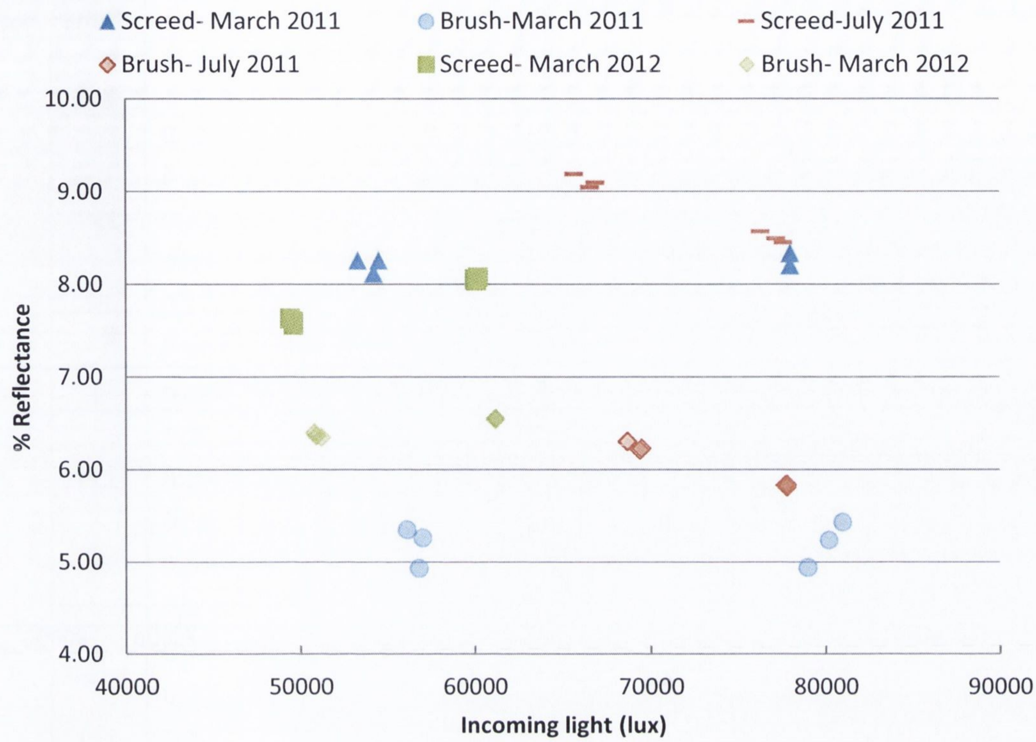

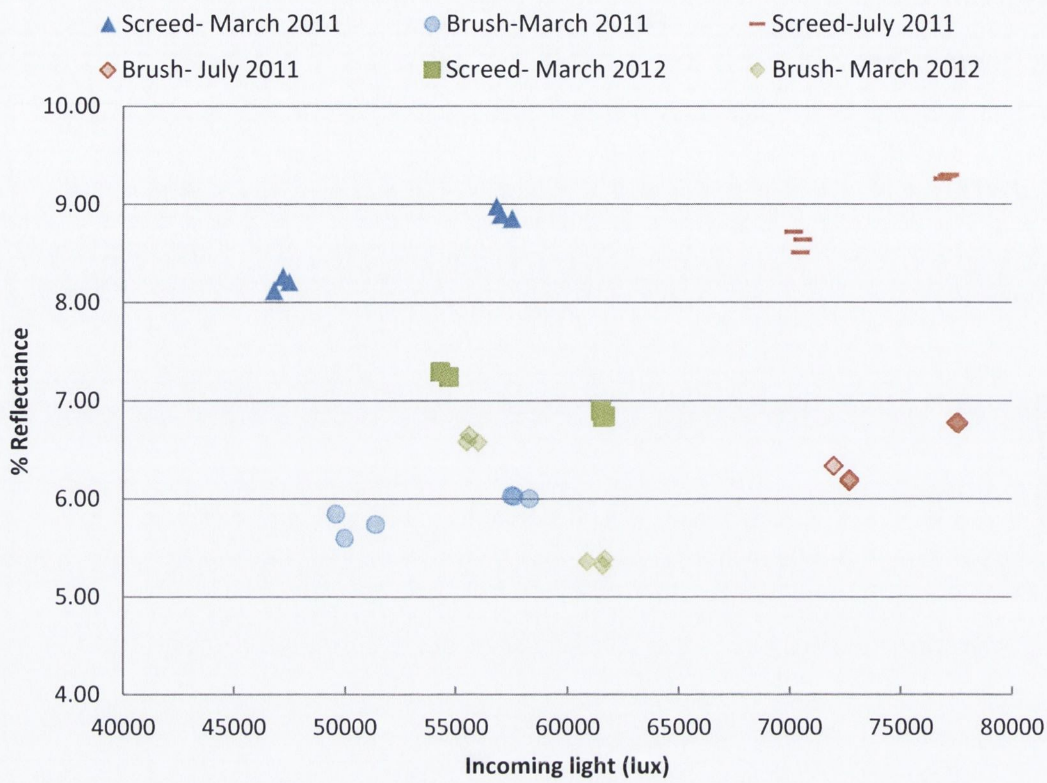
Screed- March 2011
Brush-March 2011
Screed-July 2011
Brush- July 2011
Screed- March 2012
Brush- March 2012
10.00
9.00
8.00
7.00
6.00
5.00
4.00
% Reflectance
40000
45000
50000
55000
60000
65000
70000
75000
80000
Incoming light (lux)

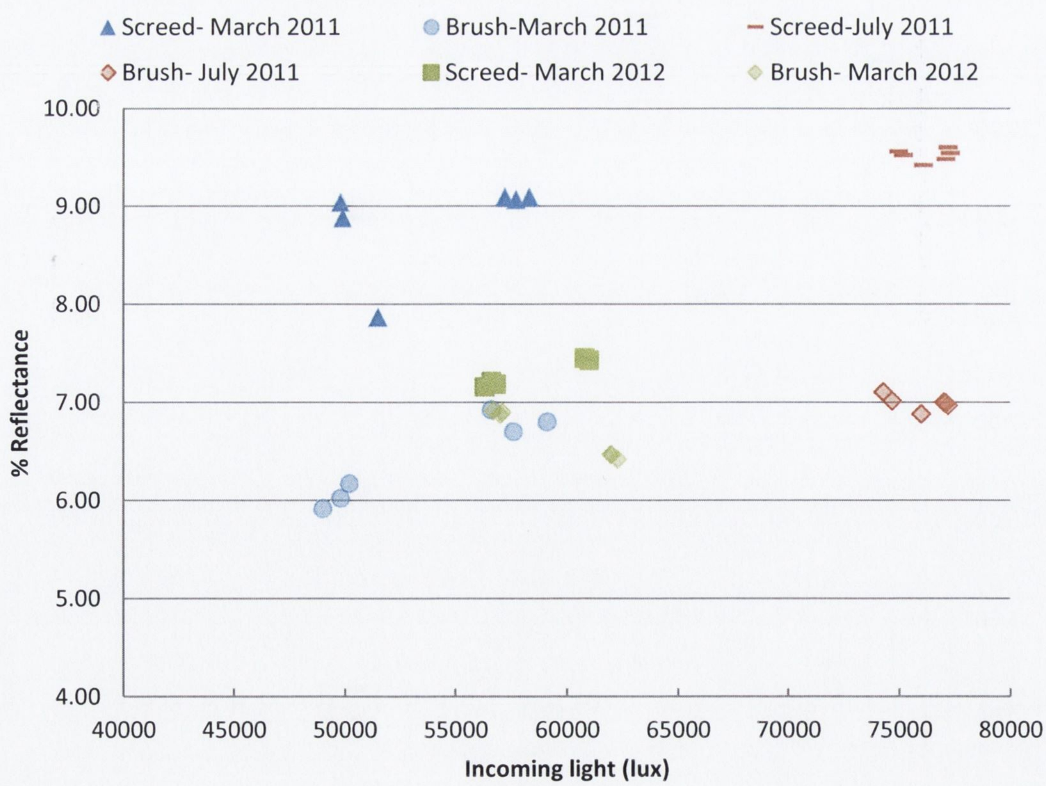
Screed- March 2011
Brush-March 2011
Screed-July 2011
Brush- July 2011
Screed- March 2012
Brush- March 2012
10.00
9.00
8.00
7.00
6.00
5.00
4.00
% Reflectance
40000
45000
50000
55000
60000
65000
70000
75000
80000
Incoming light (lux)

Appendix CC Results of greyness for each specimen for three data sets

Surface	Finish	Cast			Screed			Tamp			Brush		
GGBS	Agg.	Aug-11	Feb-12	Feb-13	Aug-11	Feb-12	Feb-13	Aug-11	Feb-12	Feb-13	Aug-11	Feb-12	Feb-13
0	L	0.55	0.55	0.55	0.75	0.75	0.75	0.65	0.65	0.65	0.70	0.70	0.70
		0.60	0.60	0.60	0.75	0.75	0.75	0.70	0.70	0.70	0.75	0.75	0.70
	PCL	0.60	0.65	0.55	0.70	0.70	0.70	0.65	0.65	0.65	0.70	0.70	0.60
		0.60	0.60	0.60	0.80	0.80	0.75	0.70	0.70	0.70	0.60	0.60	0.60
	SS	0.55	0.55	0.55	0.70	0.70	0.70	0.65	0.65	0.65	0.65	0.65	0.60
		0.60	0.60	0.60	0.70	0.70	0.70	0.65	0.65	0.65	0.65	0.60	0.60
30	L	0.60	0.60	0.60	0.80	0.75	0.70	0.75	0.75	0.75	0.75	0.75	0.75
		0.70	0.70	0.70	0.85	0.85	0.80	0.80	0.80	0.75	0.75	0.75	0.75
	PCL	0.70	0.70	0.55	0.75	0.75	0.80	0.75	0.75	0.75	0.75	0.75	0.75
		0.60	0.60	0.60	0.75	0.75	0.70	0.70	0.70	0.70	0.65	0.65	0.65
	SS	0.50	0.55	0.55	0.80	0.80	0.80	0.75	0.75	0.75	0.75	0.75	0.75
		0.65	0.65	0.65	0.80	0.80	0.75	0.75	0.75	0.70	0.80	0.80	0.75
50	L	0.70	0.70	0.65	0.80	0.75	0.70	0.75	0.75	0.70	0.80	0.80	0.75
		0.70	0.70	0.70	0.80	0.75	0.70	0.75	0.75	0.75	0.80	0.80	0.75
	PCL	0.70	0.75	0.65	0.80	0.80	0.70	0.75	0.75	0.70	0.85	0.85	0.80
		0.70	0.70	0.70	0.75	0.70	0.70	0.70	0.65	0.65	0.75	0.75	0.70
	SS	0.65	0.65	0.65	0.80	0.75	0.70	0.75	0.75	0.70	0.80	0.80	0.80
		0.70	0.70	0.70	0.85	0.80	0.75	0.75	0.75	0.75	0.85	0.80	0.80
70	L	0.75	0.75	0.70	0.90	0.85	0.80	0.85	0.80	0.80	0.85	0.80	0.80
		0.70	0.70	0.70	0.85	0.80	0.80	0.80	0.75	0.75	0.85	0.85	0.80
	PCL	0.70	0.70	0.70	0.75	0.70	0.75	0.70	0.70	0.80	0.80	0.80	0.80
		0.65	0.65	0.65	0.85	0.80	0.75	0.70	0.70	0.70	0.80	0.80	0.75
	SS	0.70	0.70	0.70	0.90	0.80	0.75	0.85	0.80	0.80	0.80	0.80	0.80
		0.75	0.70	0.70	0.80	0.75	0.70	0.80	0.75	0.75	0.85	0.80	0.75

Appendix DD The influence of GGBS concentration on internal temperature for LS aggregate for cast and screed surface finishes (12th March 2011) and tamp and brush surface finishes (21st April 2011)

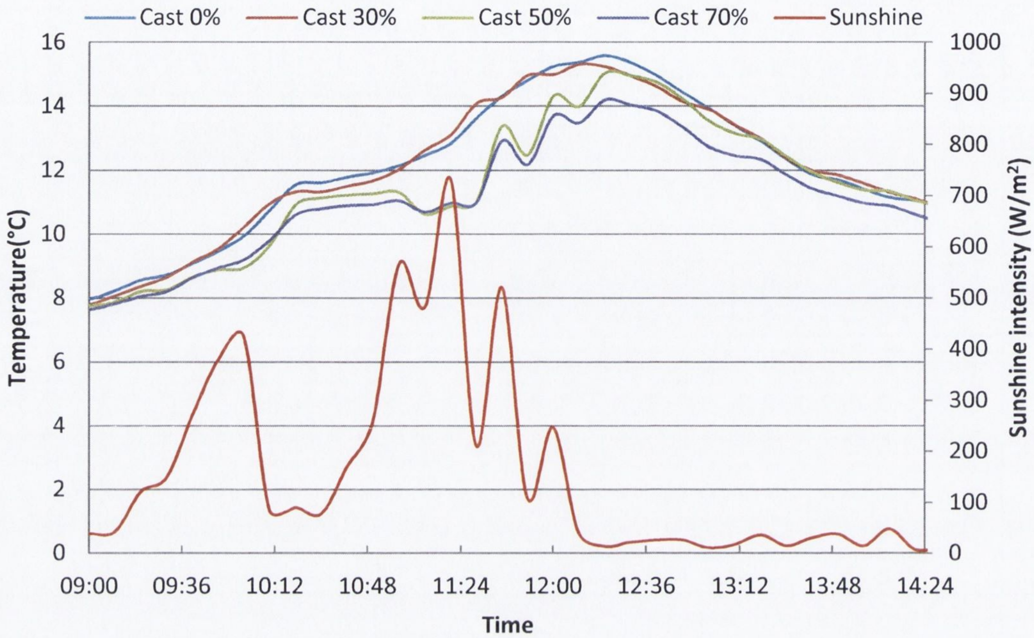

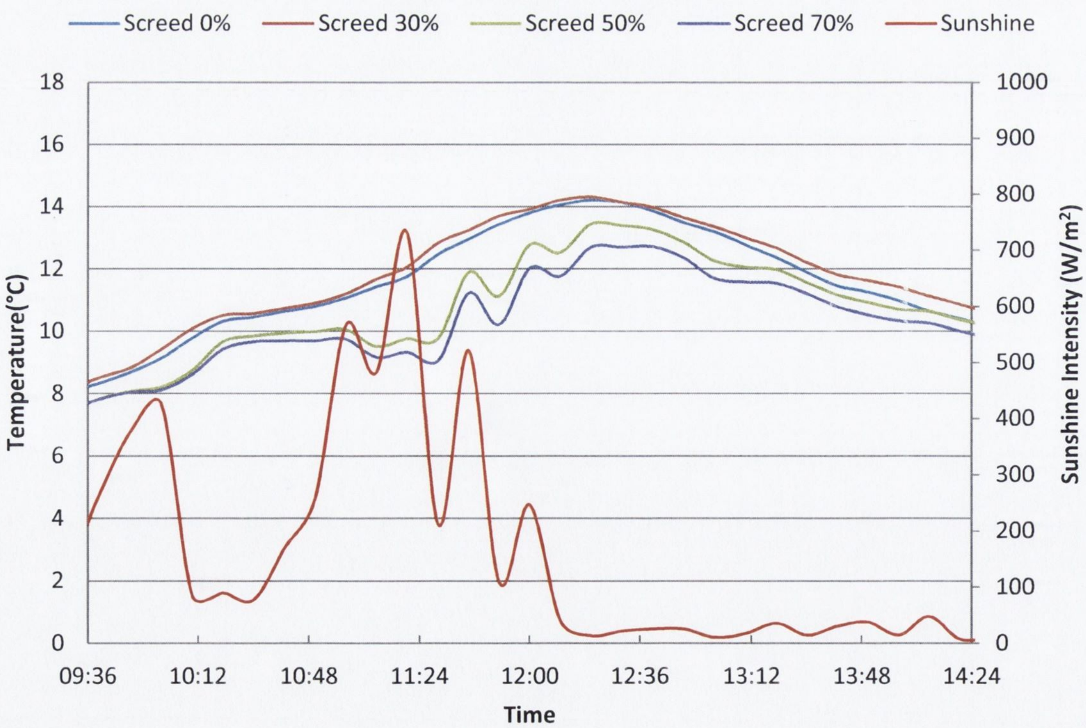

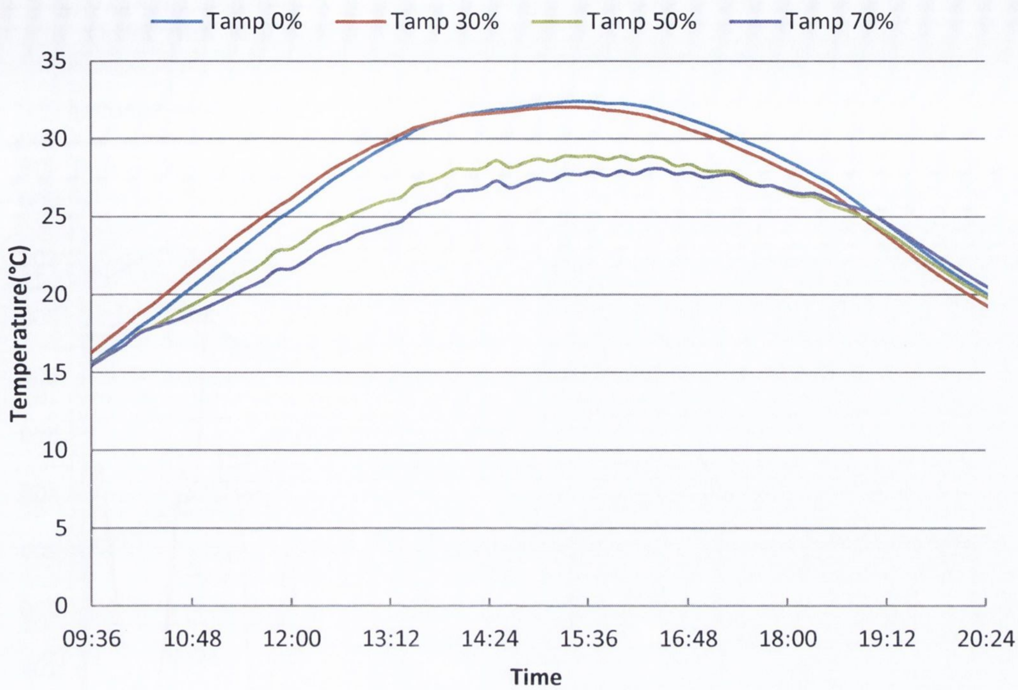
Tamp 0%
Tamp 30%
Tamp 50%
Tamp 70%
35
30
25
20
15
10
5
0
Temperature(°C)
09:36
10:48
12:00
13:12
14:24
15:36
16:48
18:00
19:12
20:24
Time

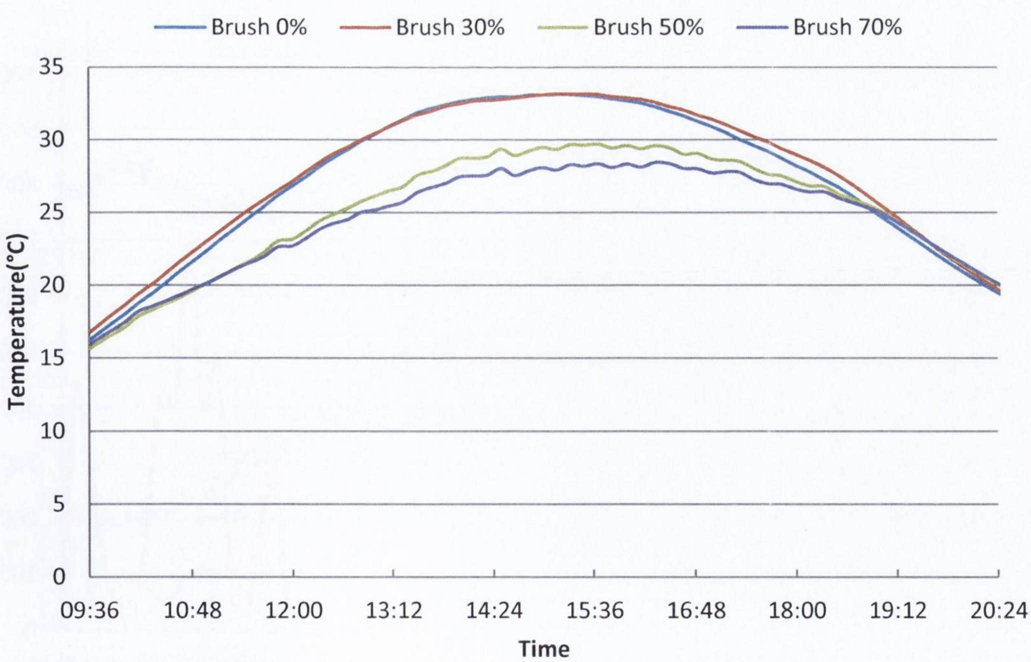
Brush 0%
Brush 30%
Brush 50%
Brush 70%
35
30
25
20
15
10
5
0
Temperature(°C)
09:36
10:48
12:00
13:12
14:24
15:36
16:48
18:00
19:12
20:24
Time

Appendix EE The influence of surface finish on internal temperature for LS aggregate for 0 and 50% GGBS (2nd July 2011) and 30 and 70% GGBS (30th July 2011)

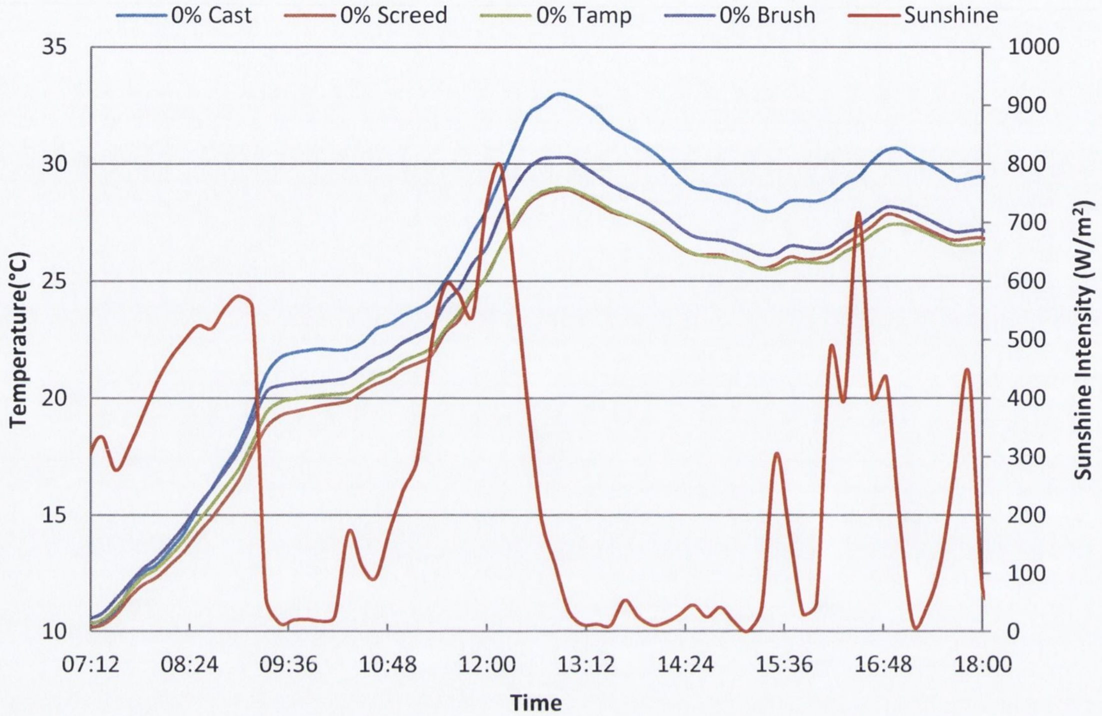

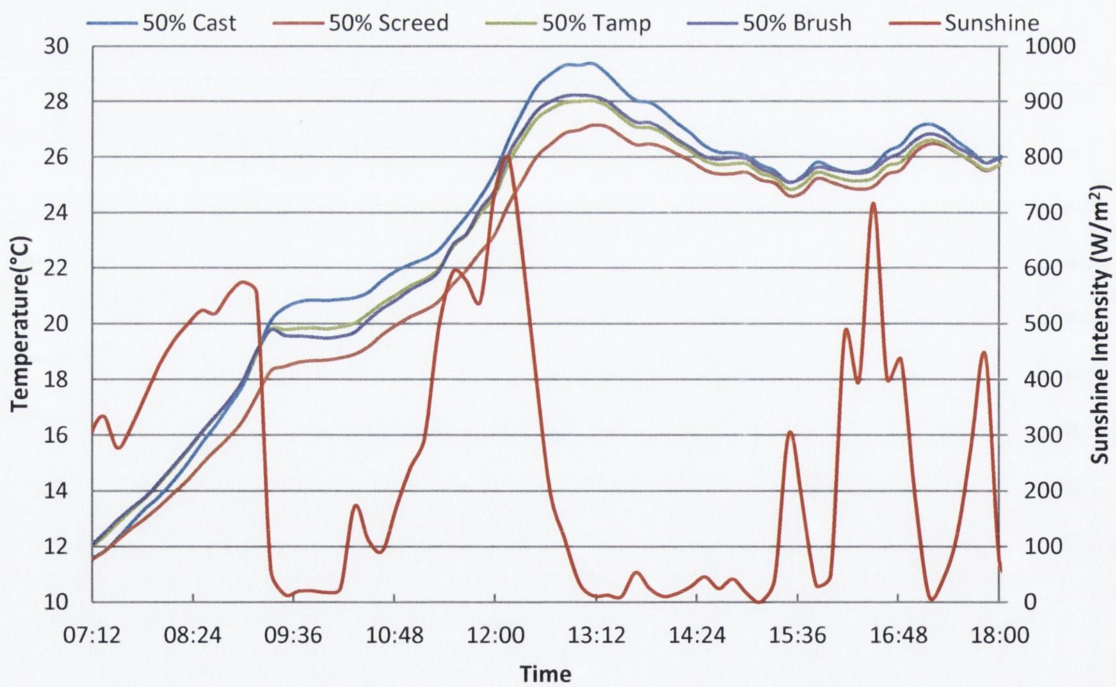

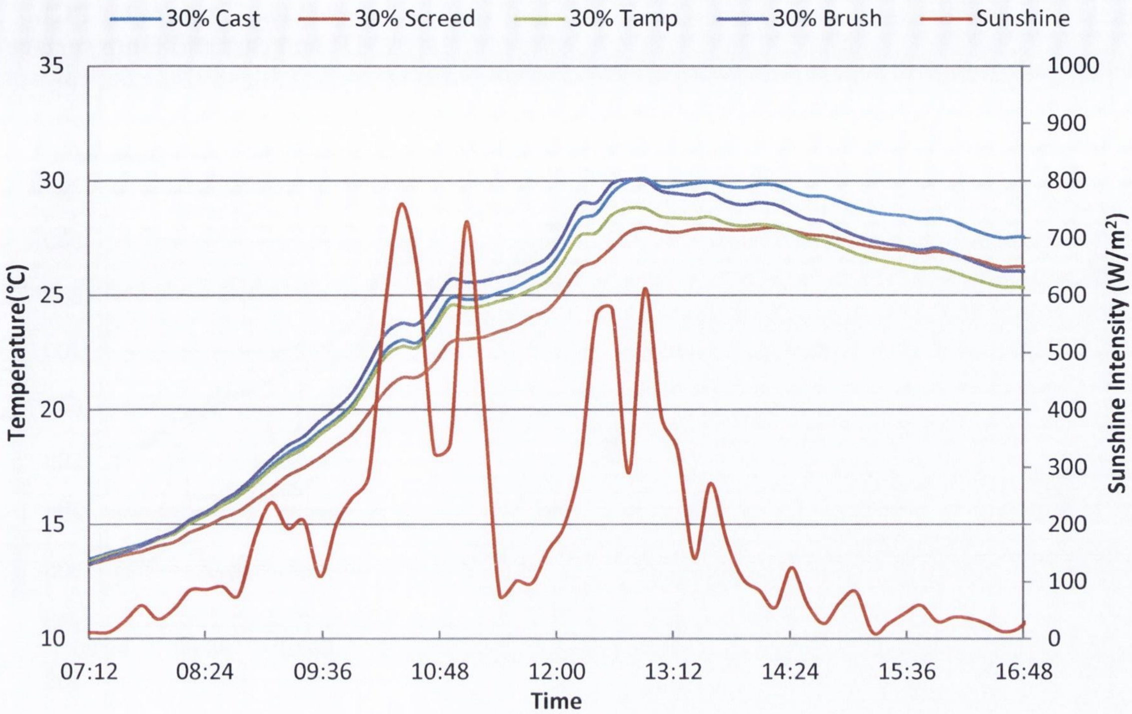
30% Cast
30% Screed
30% Tamp
30% Brush
Sunshine
Temperature(°C)
Sunshine Intensity (W/m²)
35
30
25
20
15
10
1000
900
800
700
600
500
400
300
200
100
0
07:12
08:24
09:36
10:48
12:00
13:12
14:24
15:36
16:48
Time

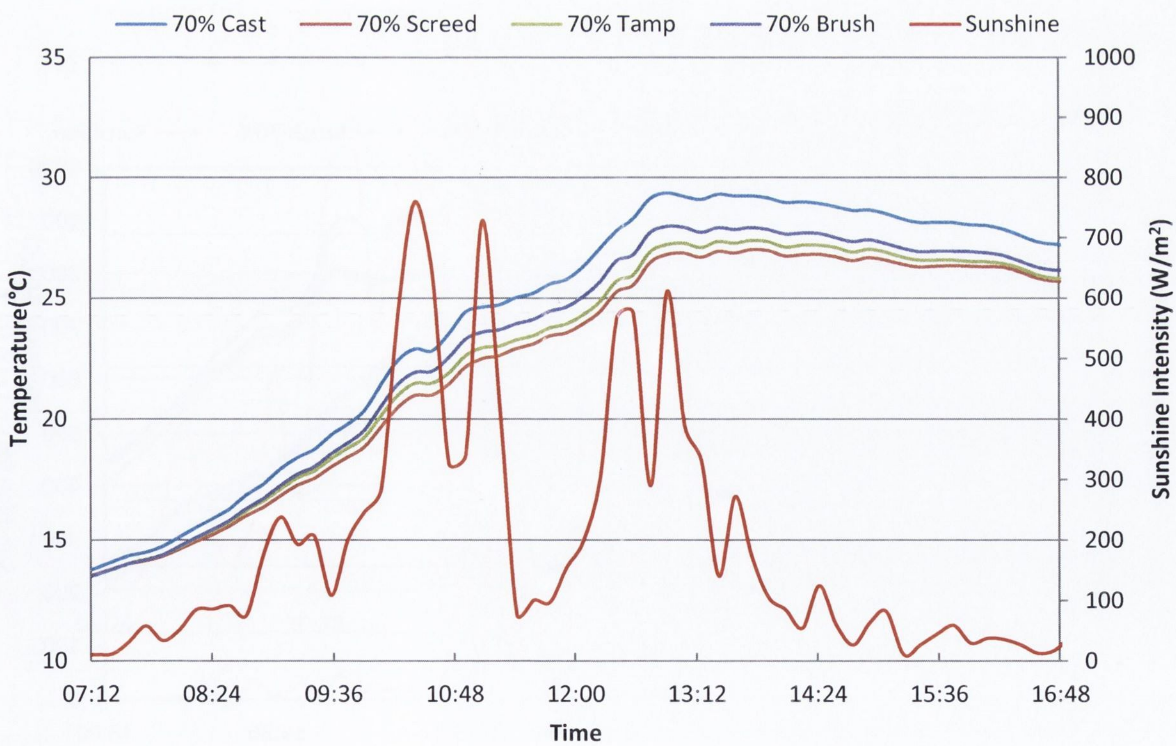
70% Cast
70% Screed
70% Tamp
70% Brush
Sunshine
Temperature(°C)
Sunshine Intensity (W/m²)
35
30
25
20
15
10
1000
900
800
700
600
500
400
300
200
100
0
07:12
08:24
09:36
10:48
12:00
13:12
14:24
15:36
16:48
Time

Appendix FF The influence of GGBS concentration on internal temperature for PCL aggregate for screed and brush surface finishes (6th July 2011) and cast and tamp surface finishes (16th March 2011)

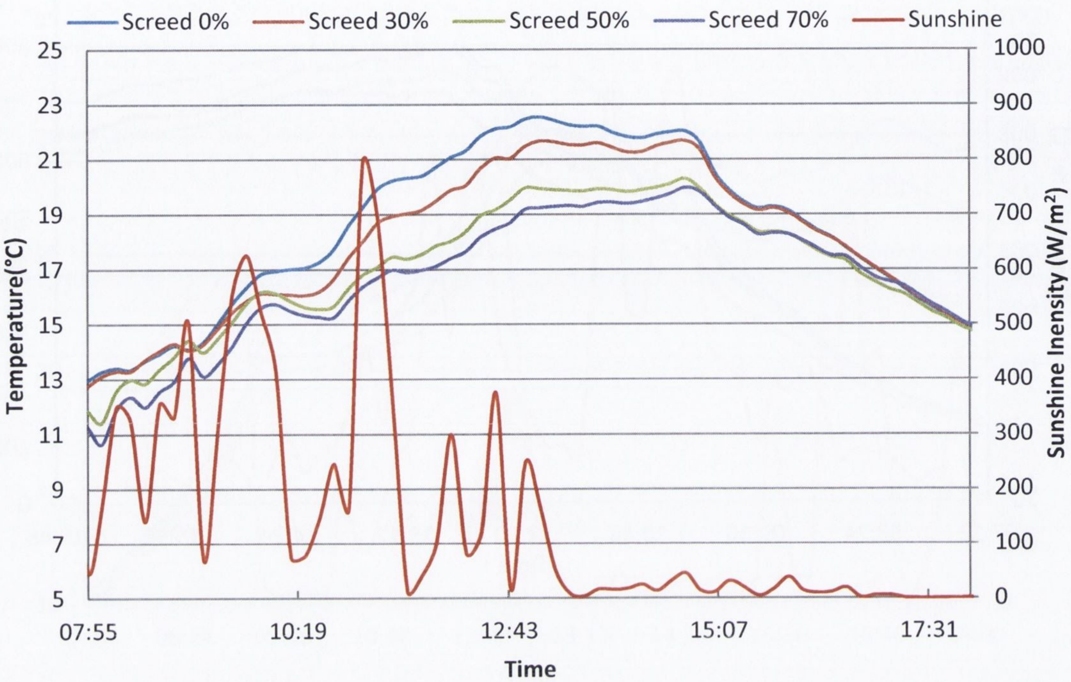

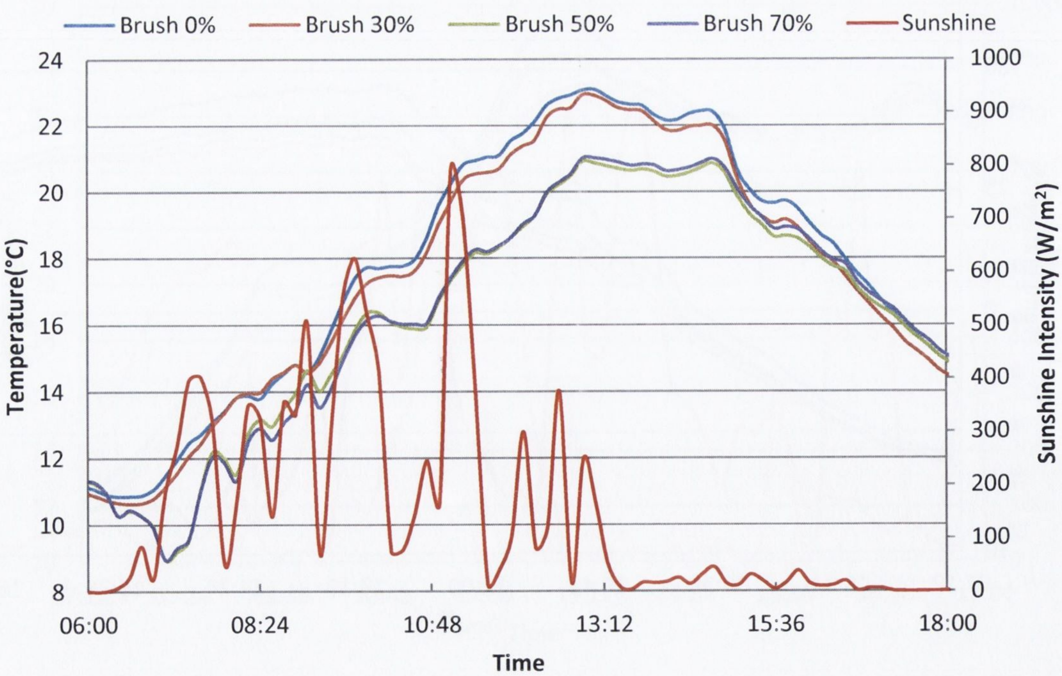

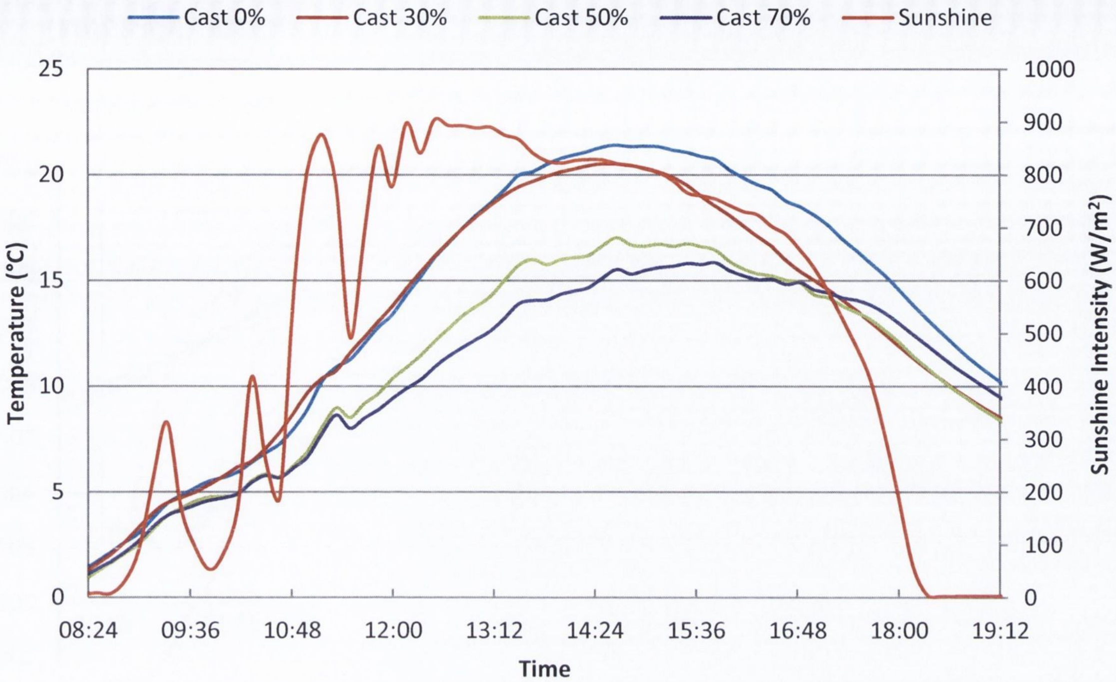

Cast 0%
Cast 30%
Cast 50%
Cast 70%
Sunshine
Temperature (°C)
Sunshine Intensity (W/m²)
Time
0
5
10
15
20
25
0
100
200
300
400
500
600
700
800
900
1000
08:24
09:36
10:48
12:00
13:12
14:24
15:36
16:48
18:00
19:12

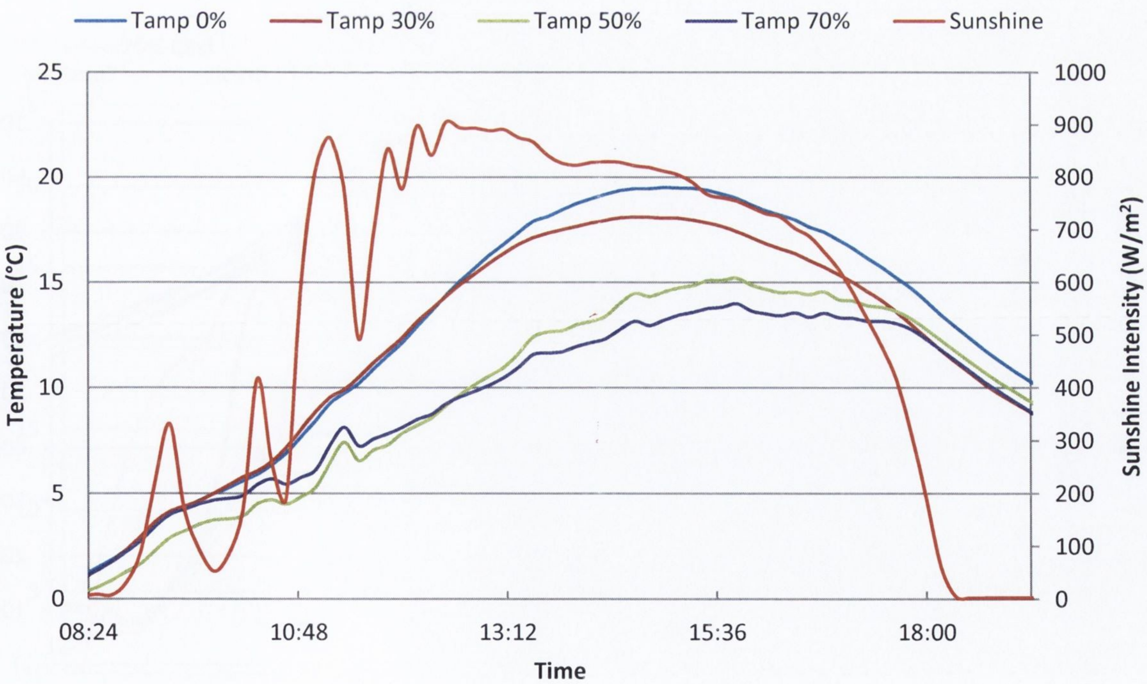

Tamp 0%
Tamp 30%
Tamp 50%
Tamp 70%
Sunshine
Temperature (°C)
Sunshine Intensity (W/m²)
Time
0
5
10
15
20
25
0
100
200
300
400
500
600
700
800
900
1000
08:24
10:48
13:12
15:36
18:00

Appendix GG The influence of surface finish on internal temperature for PCL aggregate for 0 and 30% GGBS (19th March 2011) and 50 and 70% GGBS (28th April 2011)

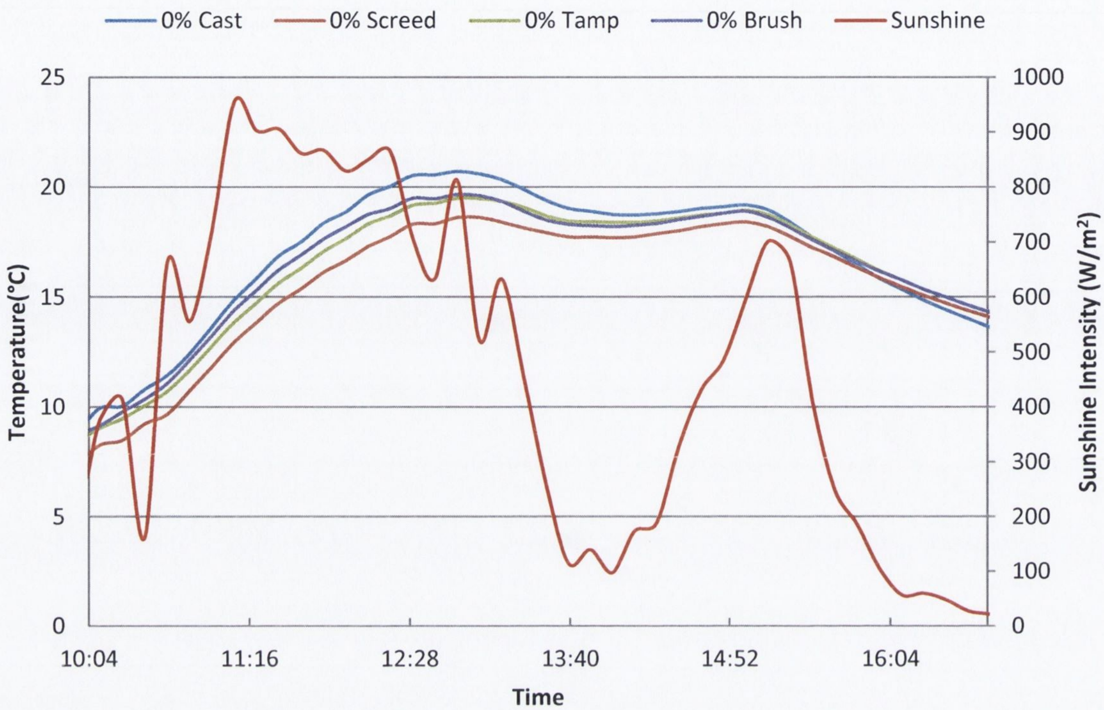

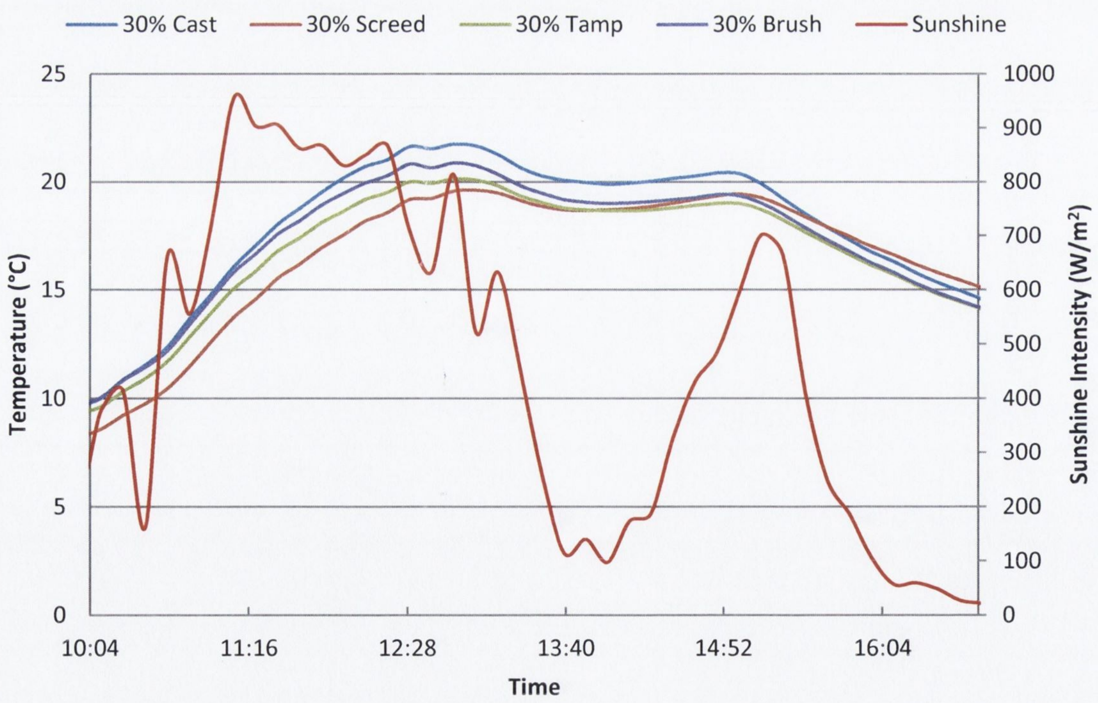

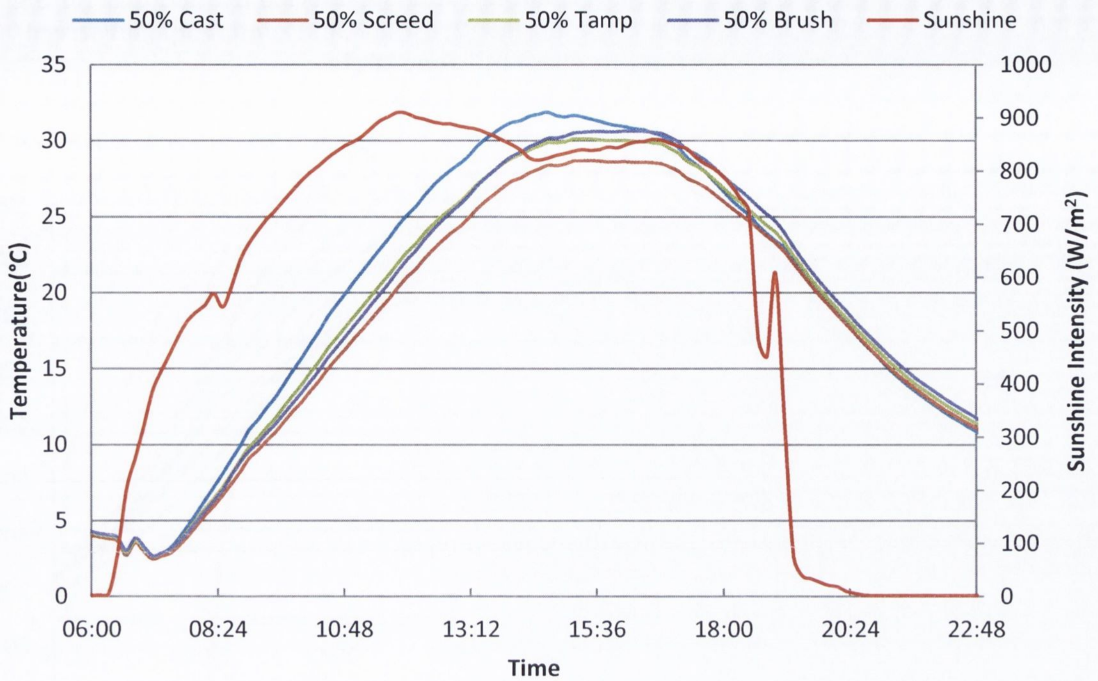
50% Cast
50% Screed
50% Tamp
50% Brush
Sunshine
Temperature(°C)
Sunshine Intensity (W/m2)
Time
06:00
08:24
10:48
13:12
15:36
18:00
20:24
22:48
0
5
10
15
20
25
30
35
0
100
200
300
400
500
600
700
800
900
1000

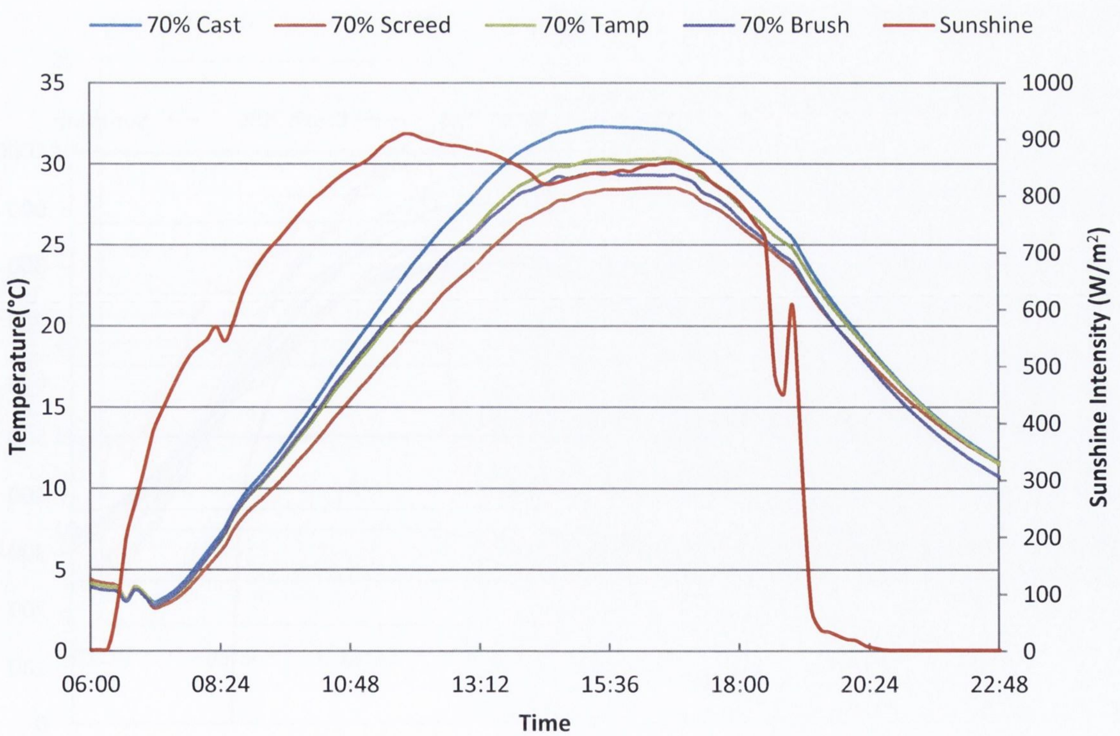
70% Cast
70% Screed
70% Tamp
70% Brush
Sunshine
Temperature(°C)
Sunshine Intensity (W/m2)
Time
06:00
08:24
10:48
13:12
15:36
18:00
20:24
22:48
0
5
10
15
20
25
30
35
0
100
200
300
400
500
600
700
800
900
1000

Appendix HH The influence of GGBS concentration on internal temperature for SS aggregate for cast and brush surface finishes (3rd June 2011) and tamp and screed surface finishes (14th June 2011)

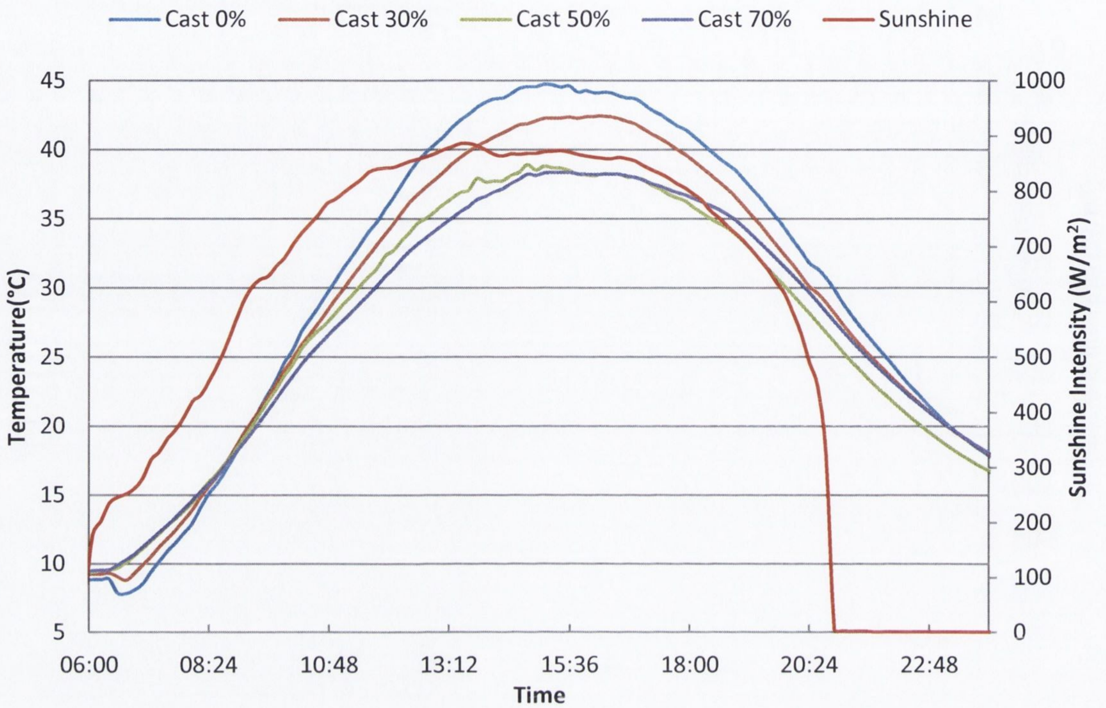

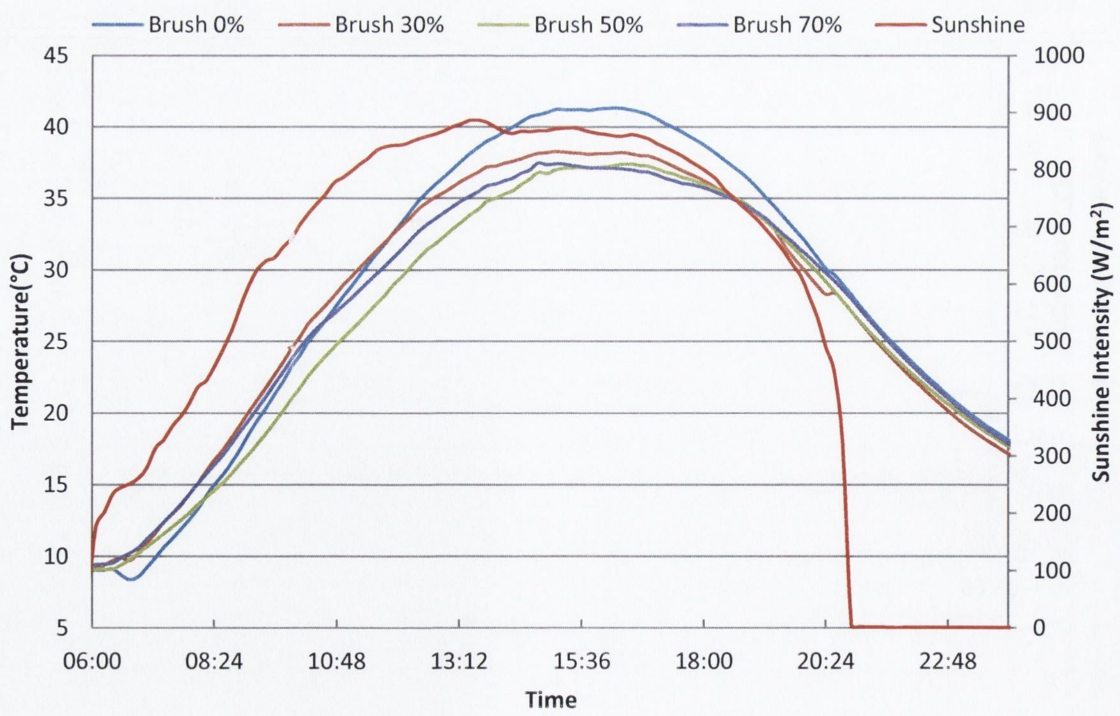

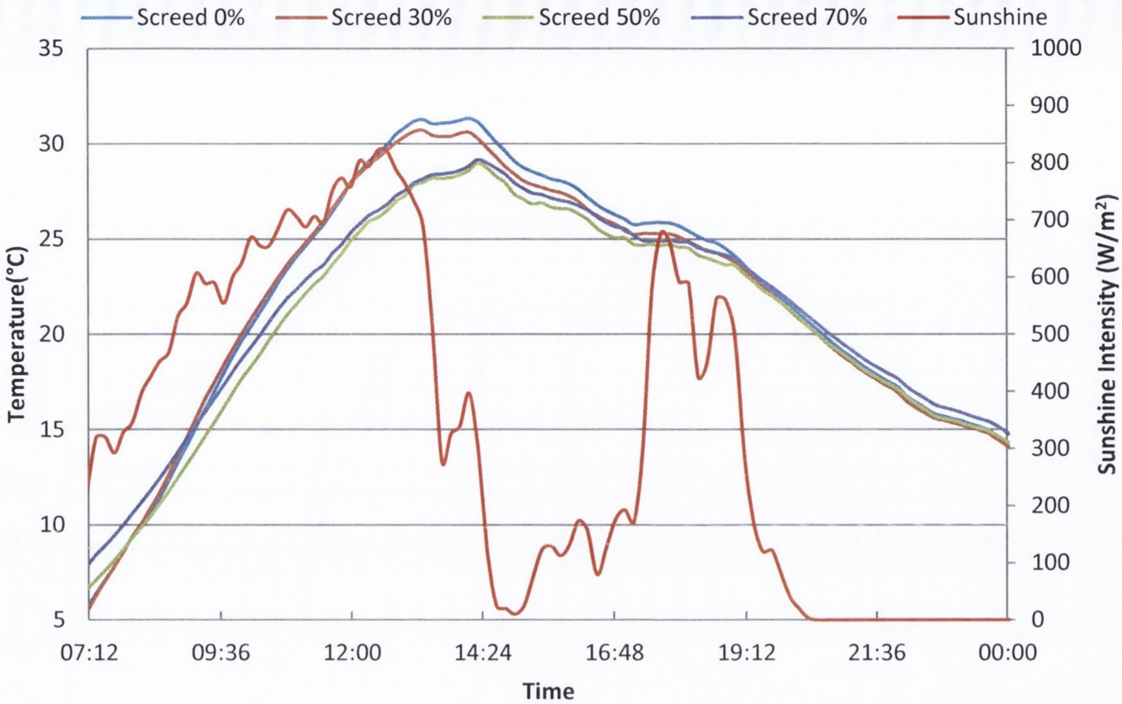

Screed 0%
Screed 30%
Screed 50%
Screed 70%
Sunshine
Temperature(°C)
Sunshine Intensity (W/m²)
Time
35
30
25
20
15
10
5
1000
900
800
700
600
500
400
300
200
100
0
07:12
09:36
12:00
14:24
16:48
19:12
21:36
00:00

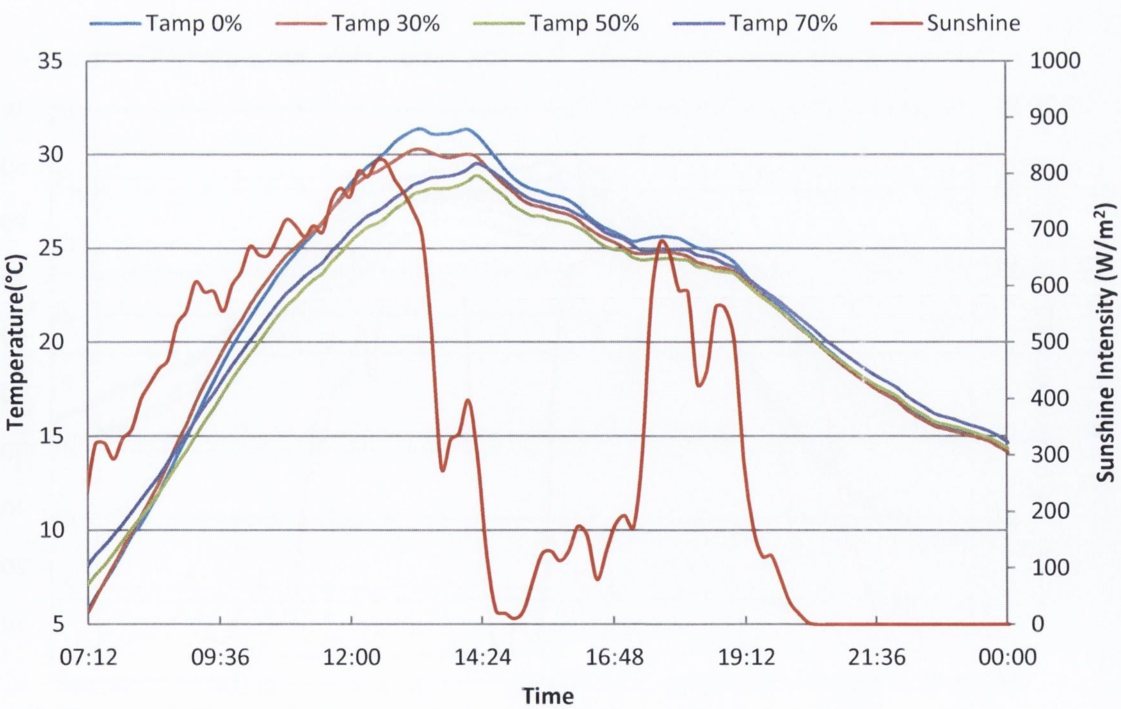

Tamp 0%
Tamp 30%
Tamp 50%
Tamp 70%
Sunshine
Temperature(°C)
Sunshine Intensity (W/m²)
Time
35
30
25
20
15
10
5
1000
900
800
700
600
500
400
300
200
100
0
07:12
09:36
12:00
14:24
16:48
19:12
21:36
00:00

Appendix II The influence of surface finish on internal temperature for SS aggregate for 0 and 30% GGBS (10th April 2011) and 50 and 70% GGBS (2nd June 2011)

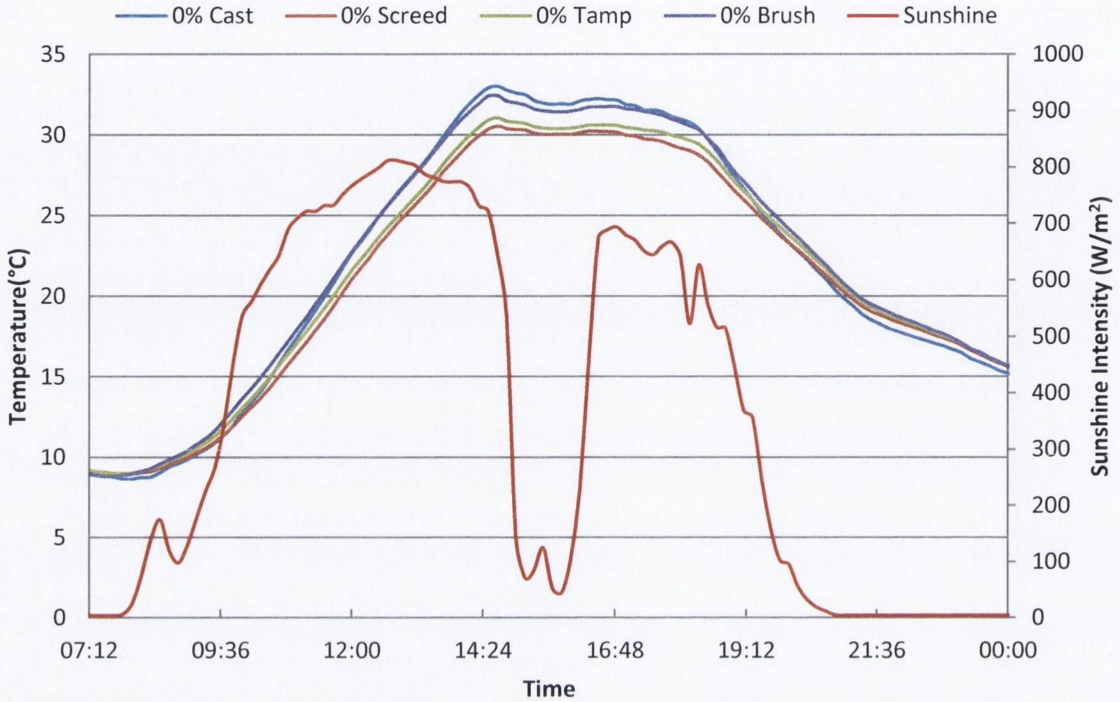

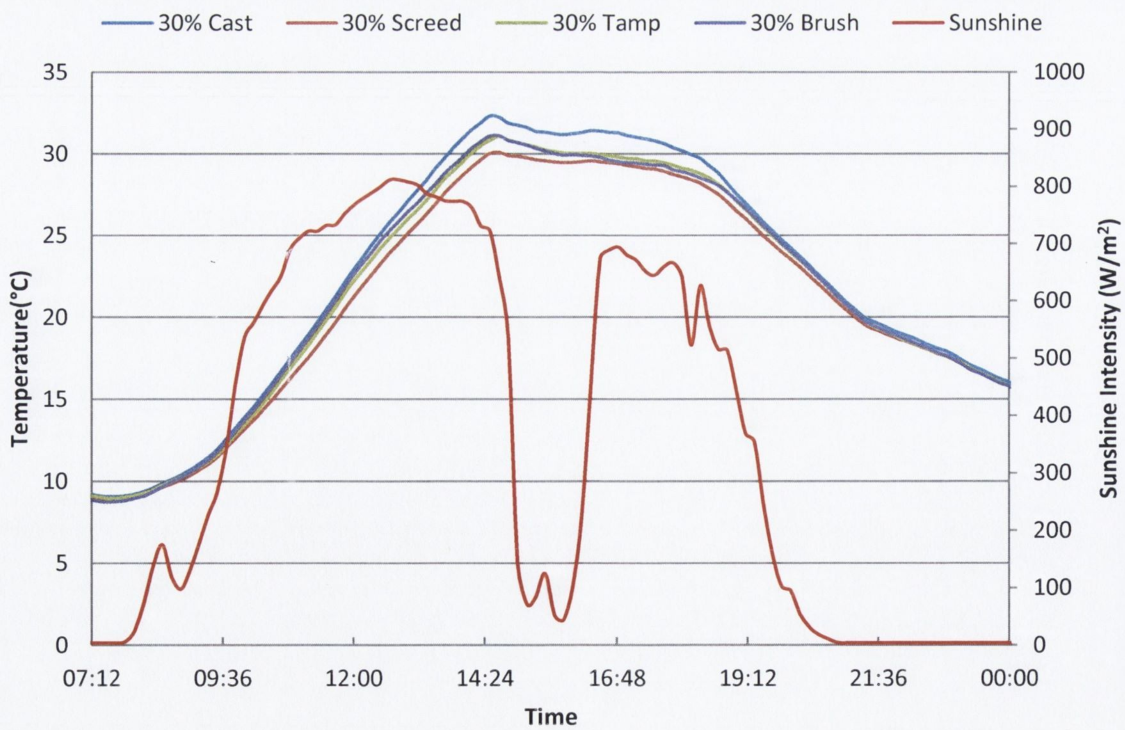

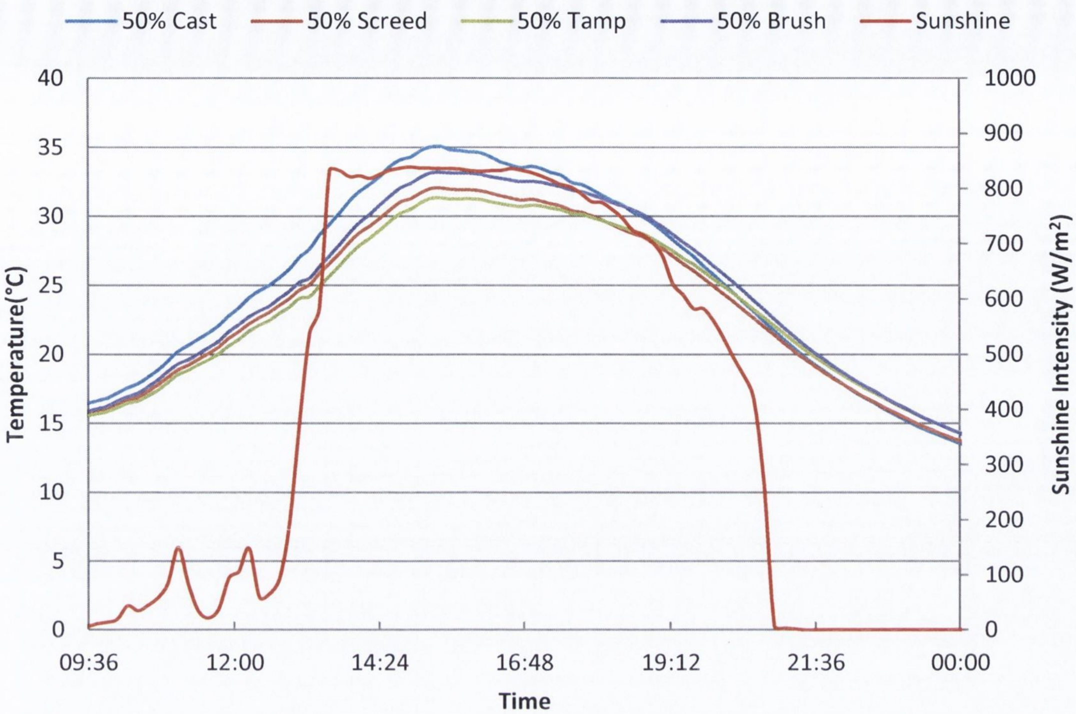
50% Cast
50% Screed
50% Tamp
50% Brush
Sunshine
Temperature(°C)
Sunshine Intensity (W/m²)
Time
09:36
12:00
14:24
16:48
19:12
21:36
00:00

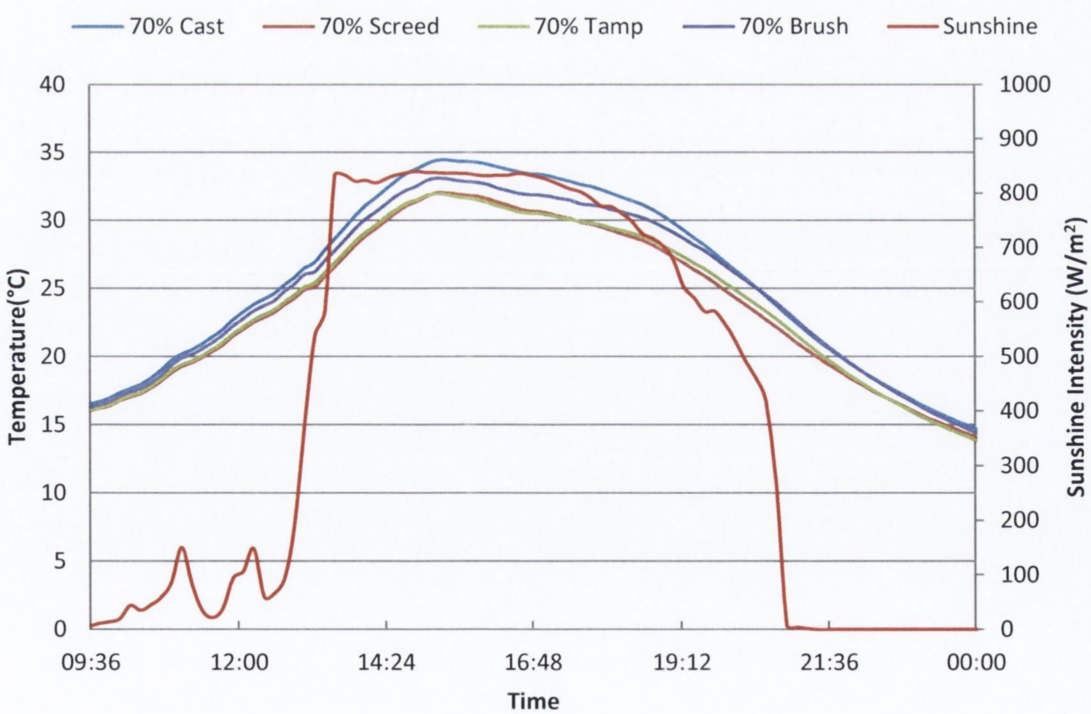
70% Cast
70% Screed
70% Tamp
70% Brush
Sunshine
Temperature(°C)
Sunshine Intensity (W/m²)
Time
09:36
12:00
14:24
16:48
19:12
21:36
00:00

Appendix JJ Breakdown of areas in Trinity College Dublin

Cobbled Areas	Area (m^2)
Front Square	8,202
Total	8,202

Excluded Areas	Area (m^2)
Chief Stewards House	1,355
Provosts House	7,572
Oisin House	1,700
Park Lane East	385
Total	11,012

Green Areas	Area (m^2)
Front Arch	650
Front Square	1,227
Library Square	3,640
Botany Bay	1,698
Fellows Square	2,000
Rubrics	692
New Square	4,620
Museum	1,218
College Park	20,920
Rugby Ground	9,460
Miscellaneous Areas	4,580
Total	50,705

Arts Block Roof	Area (m^2)
Houses 1-5	803
Houses 6-10	928
Public Theatre	740
Chapel	425
Regent House	300
Atrium & Dining Hall	2,400
Reading Room	700
New Site	460
D.H.G	1,390
Old Library	1,230
Arts Building	4,120
Houses 11-14 & 27	670
Houses 15-20	790
GMB & Houses 28+30	1,000
Rubrics 22-26	550
Berkeley Library	1,600
Ussher Library	1,090
Miscellaneous	390
Houses 33-37	870
Houses 38-40	880
Houses 47-52	730
Nassau St Entrance	290
Campanile	110
Total	22,466

Science End Roof	Area (m^2)
Museum	1,300
Printing House	600
Aras an Phiarsigh	1,350
SBC	730
Security Centre	940
Buildings Office	2,360
Civil Eng Building	650
Luce Hall	1,360
Botany	410
Botany Hut	225
Computer Hut	190
SNIAMS	1,280
LLOYD	1,435
Fitzgerald	460
Physiology	460
Zoology	720
Roberts Lab	500
Biochemistry	545
Anatomy	360
Chemistry	2,400
Dental Hospital	3,260
Moyne Institute	1,040
Pavillion	370
Science Block	7,930
Naughton institute	2,000
Misc (PC Hut)	150
Total	33,025

Asphalt Pavements	Area (m^2)
Arts Building	1,620
GMB Front Area	670
Oisin House Lane	870
Civil Engineering Building Front	1,484
MSO & Fitzgerald Building	2,646
Parade Ground-Nassau St Carpark	3,510
Total	10,800

Main Asphalt Carparks	Area (m^2)
Nassau St	2,000
Botany Bay	1,320
New Square	2,536
Rugby Ground	1,117
Total	6,973

Miscellaneous	Area (m^2)
Chemistry	210
Red Brick Areas	1,000
Behind Luce Hall	400
Behind Parsons Building	500
Beside Luce Hall	510
The Arches	1,175
Areas between Anat & PC Hut	300
Paving between O'Reilly and Naughton	1,375
Miscellaneous	1,571
Total	7,041

Concrete Areas	Area (m^2)
Nassau St (Ussher Library)	250
Arts Block Ramp	65
Berkeley Library Square	1,026
Paving Slabs-behind housese 15-20	583
Paving Slabs Atrium Corner	460
Paving Slabs (House 14)	115
SBC	410
Civil Engineering Rear	636
Luce Hall	58
SNIAMS and LLOYD	300
Smurfit Institute	367
Science Entrances (Panoz + Hamilton)	374
Parsons entrance + footpaths	672
Moyne Institute and Pavillion	611
O Reilly Institute	162
Total	6,089

Asphalt Footpaths	Area (m^2)
James Ussher Library	1,510
Fellows Square	755
Botany Bay	603
Campanile	300
New Square	422
College Park-Berkeley Side	810
House 49-50	70
Boardwalk	1,988
Surrounding Huts	590
Luce hall	359
Moyne and Pavillion	365
Naughton Institute	1,305
Total	9,077

Total Area of Trinity	165,390

Appendix KK Paper publications

1. Sweeney, A. & West, R. (2013) The use of a greyness index chart as an indicator of surface albedo of concrete. In: Innovations in Concrete Construction, India.
2. Sweeney, A., West, R. & O Connor, C. (2012) Measuring the albedo of concrete slabs for different slag contents and surface finishes. In: Concrete in the low carbon era, Dundee.
3. Sweeney, A., West, R. & Seymour, P. (2012). Factors affecting the measurement of solar reflectance using an albedometer. In: Bridge and Concrete Research in Ireland, Dublin pp. 241-245.
4. Sweeney, A., West, R. & O Connor, C. (2011) The effects of slag content and surface finish on concrete albedo. In: SB11 World Sustainable Building Conference, Helsinki pp. 58-59.
5. Siddall et al. (2011), 'Personas as a user-centred design tool for the built environment', Proceedings of the Institution of Civil Engineers, Energy sustainability volume 164, issue ES1 pp. 59-69.
6. Sweeney, A., West, R. & O Connor, C. (2010) Parameters affecting the albedo effect in concrete. In: Bridge and Concrete Research in Ireland, 2010 Cork pp. 513-520.